Volume 47 • No 3 • July-September 2024
Periodicity: Quarterly • Subject: Multidiciplinary

ISSN 0971-3034

THE INDIAN JOURNAL OF TECHNICAL EDUCATION

Published by
INDIAN SOCIETY FOR TECHNICAL EDUCATION
Near Katwaria Sarai, Shaheed Jeet Singh Marg,
New Delhi - 110 016

INDIAN JOURNAL OF TECHNICAL EDUCATION

Volume 47 • No 3 • July-September 2024

Indexed in the UGC-Care Journal list

INDIAN JOURNAL OF TECHNICAL EDUCATION

Published by
INDIAN SOCIETY FOR TECHNICAL EDUCATION
Near Katwaria Sarai, Shaheed Jeet Singh Marg
New Delhi - 110 016

INDIAN JOURNAL OF TECHNICAL EDUCATION

Volume 47 • No 3 • July-September 2024

Periodicity : Quarterly **Subject :** Multidisciplinary

Subscription Rates with Effect from 01 Jan 2024

FOR ONE/TWO YEARS or 4/8 ISSUES

		One year	Two Years
ISTE Life Members	:	Rs. 2000	Rs. 3500
Institutional members of ISTE	:	Rs. 3000	Rs. 5500
Non-member educational & Research institutions and other individuals	:	Rs. 5000	Rs. 9000
Industry/Government Department/ Other organisations.	:	Rs. 6000	Rs. 11000

Note :

1. Above mentioned rates are **exclusive of GST** as applicable.
2. Above mentioned subscription rates are for 04 issues per year only. If any changes in periodicity, rates will differ and communicated to the subscriber.
3. Send the subscription amount by NEFT to the following bank details
   Indian Society for Technical Education, New Delhi
   Bank: Indian Bank
   SB A/C No. : 405039620
   Branch: Mehrauli Road
   IFSC: IDIB000M089

For details Contact:

The Executive Secretary
Indian Society for Technical Education
Near Katwaria Sarai, Shaheed Jeet Singh Marg,
New Delhi -110 016
Phone : 011-26963431, 26513542
E-mail : istedhq@isteonline.org
Website : www.isteonline.in

Editorial

Career Development Centre(CDC): India has a large number of engineering institutes at all levels, and it produces a large number of graduates each year in comparison to many other countries. As a result, the quality of graduates varies, with some being highly competent and others lacking. Many of them are unable to meet the requirements to find employment. When applying to an engineering admission, students and parents inquire which courses will best prepare them for employment. Students when they leave the college after completing their degree course may be unemployed for a number of reasons, including a lack of job skills essential for employment.

Previously, only graduates who got higher percentages or grades in examinations were considered for jobs. The scenario has altered. Even the best academic performers are not always able to secure jobs, or if they get, they may be offered a lower income. Why is that? Many engineering educational institutions continue to use old curricula, resulting in a mismatch between what is taught in the classroom and what is required in the job market. As a result of this gap, many graduates lack the necessary working skills to succeed in an organization. As a result, the curriculum must be updated on a regular basis to introduce constantly developing technologies, new industrial processing methods, hands-on learning experiences, internships, and so on.

Furthermore, proficiency in soft skills such as communication skills, listening skills, speaking ability, time management, goal setting, solving conflicts, teamwork, positive thinking, entrepreneurship, leadership, and so on are more important. The industries/companies will supply inputs to educational institutions in order for them to design curriculum that meets their needs, and the institutions will then be able to educate their students accordingly.

The establishment of a Career Development Centre (CDC) in each educational institution will assist graduates in acquiring industry-specific skills while studying. These facilities can help students and graduates enhance their job-search skills and raise their chances of getting employment. The CDC can also help strengthen industrial-educational partnerships and facilitate communication between industry and academics. The CDC can engage in activities such as motivating, training, and facilitating students in the process of matching graduates with appropriate career opportunities based on their personal profiles, resume preparation, psychometric tests, pre-interview conversations, mock tests management, a communication and skill development programs, and other career-related services. Also, to help aspiring students to pursue higher education, preparing for competitive tests, and enhance industry-institute relations. This is a win-win situation for students, the educational institution, and the industries.

New Delhi **Editor**

30th September 2024

Indian Society for Technical Education

Official E- Mail ID's

SN	E-Mail ID	Purpose
1	**info@isteonline.org**	All General enquires.
2	**istedhq@isteonlione.org**	All official communication.
3	**exesecretary@isteonline.org**	Matter related to Executive Secretary; Policy related & etc.
4	**accounts@isteonline.org**	All matter related to finance and account section.
5	**membership@isteonline.org**	All matters related to, 1. Institute Membership, 2. Life Membership, 3. Student Membership, 4. Faculty Chapter, 5. Student Chapter, 6. Section Share, 7. Student Share & etc.
6	**guesthouse@isteonline.org**	For Guest House Booking.
7	**executive_tech@isteonline.org**	All enquiries related to ISTE official Website, E-Mail ID & etc.
8	**technical@isteonline.org**	For Faculty Development Program (FDP), STTP's, Enquiry related to Conventions, Conferences & etc.
9	**editor@isteonline.org**	Enquiry related to Indian Journal of Technical Education (IJTE) & Submission of Manuscript & etc.
10	**newsletter@isteonline.org**	All matters related to news items in newsletter.

Shaheed Jeet Singh Marg, Near Katwaria Sarai, Opp. Sanskrit Vidyapeeth, New Delhi-110016
istedhq@isteonline.org www.isteonline.in

Inviting Proposals to Organise the
International and National Conferences
Partially Funded by the ISTE

The Indian Society for Technical Education (ISTE), New Delhi is pleased to invite the proposals from the Universities and the AICTE, New Delhi approved technical institutions having Institutional Member (IM) of ISTE and willing to organize 02 days International and National Conferences on the emerging technologies in a multidisciplinary area. In order to disseminate the knowledge and advancements worldwide, conference proposals should primarily concentrate on the innovative, high quality, efficient, service, fast and cost-effective, efficient rising technologies or fresh perspectives on old technologies to share the knowledge and developments across the world. The conference may solicit scientific and research papers for presentation, poster presentation, projects/products display, key notes presentations and invited talks, etc.

ISTE, New Delhi shall extend a **maximum financial support of ₹2.0 Lakhs for 02 days national level and ₹4.0L for international level conference.**

The Indian Society for Technical Education (ISTE), New Delhi website (www.isteonline.in) offers conference **proposals for download.** Completed proposals must be submitted with the required supporting documentation, a non-refundable processing fee as mentioned in the attachment.

Executive Secretary,
ISTE, New Delhi

Conference on Renewable Energy

Solar Energy Society of India (SESI) in collaboration with Indian Journal of Technical Education (IJTE) a UGC-Care listed Journal published by the Indian Society for Technical Education (ISTE), New Delhi is inviting proposals from the willing institutions to organize a national level conference on **"Renewable Energy"**. The selected papers will be published as a special issue of IJTE.

The willing AICTE approved institutions and institutions of national importance can send their proposals through a mail to: **iste.executivesecretary@gmail.com**. The tentative period of conference may be in November or December 2024.

Editor
IJTE

IJTE Special Issue

Indian Journal of Technical Education (IJTE) a UGC-Care listed Journal published by the Indian Society for Technical Education (ISTE), New Delhi is inviting proposals from the willing institutions to publish their national or international level conference papers as a **"Special Issue"**. Terms and conditions for the publication will be sent on receipt of the request through a mail **(editor@isteonline.org)** from the institution.

Request for **"Special Issue"** received from the AICTE approved institutions and institutions of national importance will only be entertained.

Editor
IJTE

For Library Rack

The Indian Society for Technical Education (ISTE), Delhi is also publishing *The Indian Journal of Technical Education, (IJTE)* special issues regularly to encourage the academicians, scientists, researchers, students and consultants who presented their papers in recently held conferences on emerging technologies. Few copies of special issues are available at our ISTE headquarters Delhi. It is decided to sell available special issues at reasonable price for library use.

Cost of each special issue: ₹1000/- (inclusive of postage and others)

Interested persons can send e-mail to: **info@isteonline.in** for details. First Come, First Serve

Executive Secretary(I/c)
ISTE

Contents

LawChat - The Rise of Conversational Legal AI

Padmashree A
Computer Science and Business Systems
Bannari Amman Institute of Technology
Erode, Tamil Nadu
✉ padmashreea@bitsathy.ac.in

Sarumathi M
Computer Science and Business Systems
Bannari Amman Institute of Technology
Erode, Tamil Nadu
✉ sarumathi.cb20@bitsathy.ac.in

Priyadharshini V
Computer Science and Business Systems
Bannari Amman Institute of Technology
Erode, Tamil Nadu
✉ priyadharshini.cb20@bitsathy.ac.in

Mamida A C
Computer Science and Business Systems
Bannari Amman Institute of Technology
Erode, Tamil Nadu
✉ mamida.cb20@bitsathy.ac.in

ABSTRACT

Recognizing the pivotal role of legal education in shaping competent legal professionals, LawChat is designed to transcend traditional boundaries and elevate the learning process for law students. Comprising three integral modules— LawBot, Case Summarization, and Practice Platform—

LawChat aspires not only to be a comprehensive educational resource but a transformative force. It is driven by the profound belief that empowered legal education is essential for nurturing competent legal professionals and, consequently, is the key to shaping empowered futures. In an era where the legal landscape is evolving rapidly, LawChat's significance lies in its commitment to preparing the next generation of legal experts, equipping them with the knowledge and skills needed to navigate and contribute meaningfully to the dynamic legal field. The project strategically employs implementing innovative methods to seamlessly integrate LawBot, Case Summarization, and Practice Platform modules. These components synergize to provide an enriched and efficient learning environment, aligning with the overarching goal of LawChat. The implications extend to improved efficiency, heightened user engagement, and a transformative shift in the integration of technology into legal education. LawChat is essential for law students, providing a dynamic platform for comprehensive learning. The Practice Platform, featuring MCQs based on chapters and legal sections, offers targeted reinforcement and adaptive challenges, making it invaluable for exam preparation. By leveraging cutting-edge technology and innovative pedagogical approaches, LawChat not only meets the evolving needs of modern legal education but also fosters a community of empowered and knowledgeable legal professionals. As the legal landscape continues to evolve, LawChat remains steadfast in its commitment to equipping students with the tools and resources necessary to thrive in this dynamic field.

KEYWORDS *: Law, Legal education, Legal sections, Integer linear programming method, Legal technology.*

INTRODUCTION

LawChat, a groundbreaking project at the intersection of legal education and technology, focuses on three pivotal modules: Chatbot, Case Summarization, and Practice Platform. Each module plays a crucial role in reshaping the landscape of legal learning. Designed as an intelligent conversational agent, the Chatbot module harnesses advanced data collection and Rasa customization to comprehend legal queries. Integrated with Django, it not only refines user interactions but transforms the learning experience. Initiated by data preparation, this module employs innovative techniques for Statute and Precedent Identification, culminating in optimal summarization using Integer Linear Programming. The UI development in Django enhances user engagement and efficient interaction. This module introduces a dynamic web application for interactive legal learning, featuring multiple-choice

questions (MCQs) and a user-friendly interface. The platform offers targeted reinforcement and proficiency improvement through chapter-based, section-based, and description-based MCQs. In this proposed work, we explore the methodologies and implementations of each module, aiming to redefine legal education and practice through technological integration and a comprehensive learning experience.

LITERATURE REVIEW

The article by Queudot, M., Charton, É., & Meurs, M. J. in Improving Access to Justice with Legal Chatbots explores the use of chatbots to provide legal advice, addressing the high costs of legal services. It distinguishes between structured knowledge-based chatbots and machine learning-based ones, highlighting their potential to make legal help more accessible to those unable to afford a lawyer[1].

El Sherif, M., El Sherif, M., & Hassan, M. in LAWBO discussed challenges in integrating chatbots into the judicial system, emphasizing the complexity of understanding legal matters. LAWBO aims to expedite legal case analysis using heuristics on data from Supreme Court judgments, dynamic memory networks, and GloVe word representation for NLP, enhancing the efficiency of legal professionals [2].

Princeton University's Center for Human Values. in the fictional case study Law Enforcement Chatbots explored ethical dilemmas in deploying AI, focusing on a nation combating cybercrimes. It examines the challenges faced by law enforcement, ethical considerations, and societal debates related to balancing individual rights and the need for enhanced law enforcement capabilities[3].

Artificial Intelligence and Customer Relationship Management: The Case of Chatbots and Their Legality Framework by Kouroupis, K., Vagiano, D., & Totka, A. explored the integration of chatbots into CRM systems in the context of the European digital strategy. It addresses the legal and ethical concerns related to personal data protection, analyzing the regulatory background, including the draft AI Regulation, GDPR, and the e-Privacy Directive[4].

Vaishnavi Suryawanshi, Disha Naikwadi, Prof. Sneha Pati in Legal Case Document Summarization Using NLP proposed Automatic Legal Document Summarization that aims to streamline the tender process by utilizing NLP techniques to generate concise summaries from legal documents like affidavits and agreements. It follows a custom SDLC methodology, leveraging word counting, clue phrases, and theme extraction for accurate summarization.[6]

Abhay Shukla, Paheli Bhattacharya, Soham Poddar, Rajdeep Mukherjee, Kripabandhu Ghosh, Pawan Goyal, Saptarshi Ghosh in Legal Case Document Summarization: Extractive and Abstractive Methods and their Evaluation aims to investigate the performance of different summarization models (extractive vs. abstractive) on legal case documents, considering challenges such as transformer-based limitations and the length of legal texts. It presents experiments with various methods, including supervised and unsupervised approaches, on three legal summarization datasets. The findings offer insights into legal summarization and contribute to understanding long document summarization.[10]

OBJECTIVE

The primary objective of our law-focused chatbot and platform is to revolutionize legal education and practice by providing an innovative, efficient, and accessible solution. Our comprehensive platform aims to serve law students, legal professionals, and enthusiasts through three key features: a chatbot, case summarization, and Multiple Choice Question (MCQ) practice. Firstly, the chatbot component strives to enhance user engagement by offering real-time, interactive assistance on legal queries. Users can obtain instant information, clarification, and guidance on legal concepts, thereby promoting a dynamic learning experience. Secondly, our case summarization feature seeks to streamline the often time-consuming process of reviewing legal cases. By employing advanced natural language processing techniques, our platform generates concise and accurate summaries, enabling users to grasp the essential details of complex cases efficiently. Lastly, the MCQ practice platform aims to reinforce legal knowledge through an interactive and adaptive learning approach. Users can test their understanding of legal principles, statutes, and case law, receiving instant feedback to identify areas for improvement. In summary, our objective is to empower

the legal community with a multifaceted platform that fosters learning, facilitates case analysis, and provides targeted practice opportunities, ultimately contributing to a more proficient and confident generation of legal professionals.

SYSTEM ARCHITECTURE

LawChat's system architecture is intricately woven with three pivotal components: the Chatbot, Case Summarization, and Practice Platform, each contributing uniquely to the platform's holistic design. The Chatbot component, built on the Rasa framework, harnesses natural language understanding, dialogue management, and intent classification. Seamlessly connected to the Django backend, it ensures effective communication and data exchange, complemented by an intuitive user interface crafted using Django for an enhanced user experience.

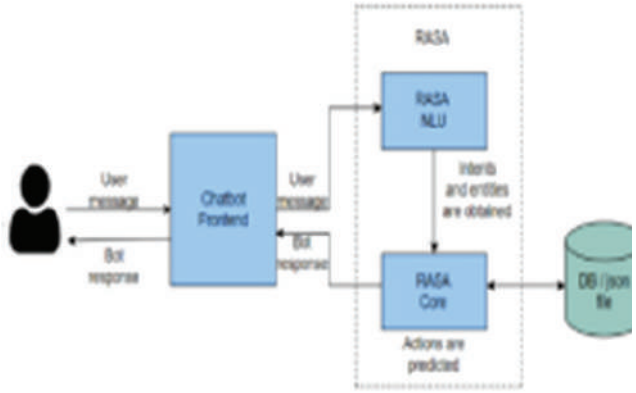

Fig. 1. Chatbot architecture

The Case Summarization component is dedicated to efficient data preparation, employing advanced techniques for statute and precedent identification, and implementing Integer Linear Programming for optimal document summarization. Integrated into Django, this component provides a cohesive user experience for document uploading and summarization requests.

The Practice Platform component enriches the learning experience with a user-friendly web application for law students and professionals. It dynamically sources MCQs from a JSON file, fostering active engagement. Offering practice options based on chapters, legal sections, and detailed descriptions, it ensures a comprehensive grasp of legal knowledge. The platform includes randomized challenges, promoting a deeper understanding, and adapts to users' performance levels for continuous proficiency improvement.

Fig. 2. Case summarization architecture

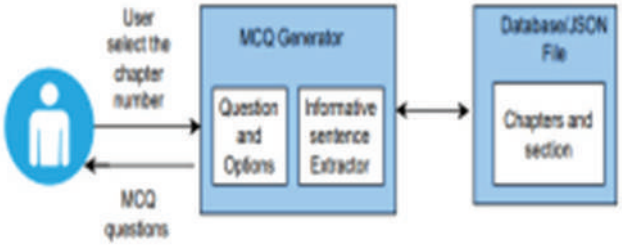

Fig. 3. Practice platform architecture

In terms of integration and scalability, LawChat's unified platform seamlessly combines these components, creating an efficient and transformative solution for legal education and assistance. The modular structure ensures scalability, allowing adaptability to future enhancements and technological advancements in the legal landscape.

METHODOLOGY

The proposed model consists of three modules such as chatbot, case summarization and practicing platform.

Chatbot

1) Data Collection and Preparation: Compile a comprehensive dataset comprising a variety of legal texts, case studies, statutes, and study materials to train the chatbot effectively. Annotate the dataset with relevant intents and entities pertaining to legal inquiries, ensuring that the chatbot can accurately comprehend user queries.

2) Data Preprocessing and Augmentation: Conduct thorough preprocessing of the dataset to ensure uniformity and quality, involving tasks such as data cleansing, normalization, and tokenization of textual data. Employ data augmentation techniques, such as data synthesis or augmentation, to enrich the dataset and enhance the chatbot's ability to handle diverse user queries effectively.

3) Model Customization: Customize the Rasa chatbot architecture to cater specifically to the requirements of legal inquiries, taking into account aspects like language understanding, dialogue management, and entity recognition. Adapt the default Rasa pipeline or incorporate custom components to address specific challenges or requirements identified during the problem definition phase.

4) Model Training: Train the Rasa chatbot model using the annotated dataset, fine-tuning model parameters and components to optimize the performance .Continuously monitor training metrics and adjust training strategies as necessary to enhance the chatbot's accuracy and responsiveness to user queries.

5) Integration with Django for UI Development: Developing a user-friendly interface (UI) for the chatbot utilizing Django, with a focus on creating an intuitive platform for users to interact with. Seamlessly integrate the Rasa chatbot backend with the Django frontend to facilitate smooth communication between the user interface and the chatbot.

Case Summarization

1) Data Preparation:The `preparedata.py` module facilitates the data preparation process for the legal case summarization system. This essential component is responsible for extracting, organizing, and structuring the input data to make it suitable for subsequent analysis. The module iterates through each legal document within the specified folder (`--data_path`). It reads the content of each document, separating it into relevant segments. The content is then processed to eliminate specific irrelevant phrases, ensuring cleaner and more accurate data. The module employs a tokenizer from the Natural Language Toolkit (nltk) to break down sentences into individual words. Additionally, it utilizes part-of-speech tagging to analyze the grammatical components of each sentence. This step is crucial for understanding the structure and context of the legal content. The prepared data is organized into a JSON format, where each document is represented as a key-value pair. The key corresponds to the document's unique identifier, derived from the document filename, while the value contains a dictionary representing the content of the document segmented by legal classes. The final output, stored in the specified path (`--prep_path`), is a structured JSON file named 'prepared_data.json'. This file encapsulates the organized legal content, ready for consumption by subsequent modules in the legal case summarization system.In essence, the `preparedata.py` module plays a pivotal role in laying the groundwork for efficient and accurate legal case summarization, ensuring that the subsequent stages of the system can seamlessly operate on well-structured and relevant data.

2) Statute and Precedent Identification: The isStatute_isPrecedent.py module serves as a critical component within the legal case summarization system, contributing to the identification of statutory references and legal precedents within given sentences. The module, coded in Python, plays a pivotal role in the semantic analysis of legal text. The `isStatute` function is designed to determine whether a given sentence contains references to statutes or legal acts. It takes a legal sentence and a list of legal acts as parameters, checking for matches between the sentence and the provided legal acts. The module employs a set-based approach to encompass variations in legal act expressions, ensuring robust recognition. If a match is found, the function returns a flag indicating the

presence of a statute reference in the sentence. On the other hand, the `isPrecedent` function is responsible for identifying legal precedents within a sentence. It evaluates whether the sentence includes typical indicators of legal precedents, such as the "v" (versus) notation or mentions of legal databases like "indlaw sc." The function returns a binary result, with 1 indicating the presence of a legal precedent and 0 otherwise. In summary, the `isStatute_isPrecedent.py` module contributes to the system's ability to discern and categorize legal content accurately. It offers a specialized function for statute recognition and another for detecting legal precedents, collectively enhancing the overall capability of the legal case summarization system to prioritize relevant legal information.

3) Mentioning Statutes in Sentences : The `mention_statute_sentence.py` module plays a crucial role in the legal case summarization system, focusing on the identification and extraction of statutory references within given sentences. This Python script, coded by Paheli, demonstrates a robust methodology for recognizing various forms and expressions of legal statutes, contributing to the system's ability to pinpoint relevant legal information accurately. The module begins by initializing a set of predefined legal acts and their corresponding variations, stored in the `tokens` dictionary. It also handles specific cases, such as the Constitution of India and various legal codes, ensuring a comprehensive approach to statute identification. The primary function, `get_statute_mention(line)`, takes a sentence as input and employs regular expressions to search for mentions of legal statutes within the provided sentence. It iterates through the predefined legal acts, considering different variations and expressions. The function accurately identifies statutes by recognizing patterns like "article" or "section" followed by a number and the legal act's name. It also handles cases where the sentence references multiple statutes. The module enhances the legal case summarization system's capabilities by extracting and categorizing relevant statutory references from sentences. This functionality is integral to summarizing legal content effectively, allowing the system to prioritize and present essential information within the generated case summaries.

4) ILP Summarization : The `legal_ilp.py` module, developed by Paheli, is a comprehensive Python script that implements an Integer Linear Programming (ILP) approach for summarizing legal documents. The script is designed to generate concise summaries by optimizing the selection of sentences based on various criteria, including content relevance, legal terms, and statutes. The ILP formulation is implemented using the Gurobi optimization library. The script begins by defining key parameters and importing necessary libraries. It leverages the Gurobi optimization library to formulate and solve the ILP problem. The ILP model is built considering multiple factors, such as the weight assigned to different rhetorical segments (`CLASS_WEIGHT`), weights for content, legal words, and statute words. The ILP model aims to maximize the overall score of selected sentences while adhering to specified constraints. The `compute_summary` function reads prepared data in JSON format, containing documents segmented into rhetorical classes. It then extracts relevant information, such as class weights, summary lengths, legal word dictionaries, and statute mentions. The ILP model is applied to optimize sentence selection based on these parameters, resulting in the creation of summarized legal documents. The ILP optimization process involves the definition of decision variables for both sentences and content words. Objective functions are established to maximize the overall score, which is determined by the weights assigned to different components. Constraints are defined to ensure that the summary adheres to length limitations and includes a minimum number of sentences from each rhetorical segment. Furthermore, the script introduces functions such as `get_legal_word` and `get_statute_mention` to identify legal terms and statutes within sentences, contributing to the overall effectiveness of the summarization process. Overall, `legal_ilp.py` showcases an advanced approach to legal document summarization, integrating ILP techniques with linguistic analysis to produce concise and informative summaries.

The module significantly aids in extracting key legal information, making it a valuable tool for legal professionals and researchers dealing with large volumes of legal text.

5) UI Development in Django : UI development in Django involves creating files that handle user interactions seamlessly. These files provide functionalities such as input document uploading, summarization requests, and result visualization. The user interface aims to enhance the overall usability of the ILP-based system, offering researchers and legal professionals an intuitive and interactive platform to engage with the summarization system effortlessly. Together, these files form a cohesive and synergistic system, contributing to the comprehensive development and optimization of the ILP-based legal text summarization system.

Practicing Platform

The Practice Platform for Law Questions in Django is a robust and user-friendly web application designed to enhance the learning and practice experience for law students and professionals. This platform incorporates a sleek and interactive user interface, allowing users to practice multiple-choice questions (MCQs) based on chapters, sections, and descriptions from a dynamic JSON file. The goal is to provide a comprehensive and engaging environment for users to strengthen their understanding of legal concepts.

1) User-Friendly Interface: The platform boasts an intuitive and visually appealing user interface to ensure a seamless and enjoyable user experience Interactive elements such as buttons, dropdowns, and progress indicators are strategically placed to enhance navigation and engagement.

2) Random Question Generation: Questions are dynamically generated from a JSON file, offering a diverse and randomized set of challenges for users Randomization ensures that users encounter a variety of questions, promoting a deeper understanding of legal concepts rather than rote memorization.

3) Chapter-based MCQs: Users can choose questions based on specific chapters, enabling targeted practice to reinforce knowledge in particular areas of law. The platform facilitates focused learning by allowing users to select chapters of interest for their practice sessions.

4) Section and Description-based MCQs:In addition to chapter-based questions, the platform provides the option to practice questions based on specific legal sections and detailed descriptions. This feature allows users to refine their practice sessions, concentrating on specific aspects of the law and improving their proficiency in understanding legal nuances.

RESULTS

Fig. 4. Chatbot

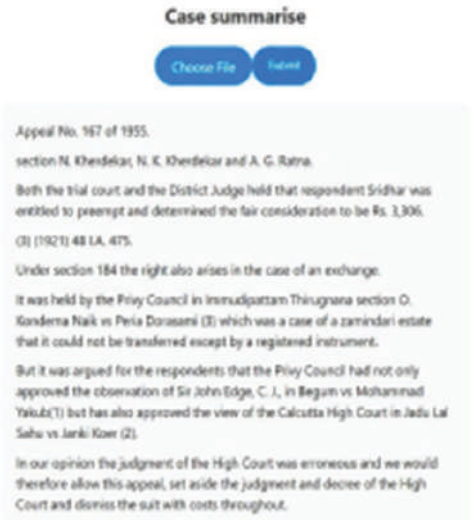

Fig. 5. Case summarization

Fig. 6. Practice platform

Fig. 7. Practice platform

CONCLUSION

In conclusion, LawChat represents a groundbreaking advancement in legal education, leveraging technology to provide a dynamic and comprehensive learning experience. By offering instant law references, interactive quizzes, efficient and case summarization, it caters to the diverse needs of law students and enthusiasts alike. The platform's accessibility, time efficiency, interactive learning approach, comprehensive environment, and proactive information delivery distinguish it as a transformative tool in the legal landscape. As technology continues to shape the future of education, LawChat stands at the forefront, ushering in a new era of accessible, engaging, and impactful legal learning.

REFERENCE

1. Queudot, M., Charton, É., & Meurs, M.-J. "Improving access to justice with legal chatbots", 2020.

2. El Sherif, A., El Sherif, M., & Hassan, M. "LAWBO",2020. [3] Princeton University's Center for Human Values and Center for Information Technology Policymic memory networks. "Law enforcement chatbots", 2017.

4. Kouroupis, K., Vagiano, D., & Totka, A. Artificial Intelligence and Customer Relationship Management: "The Case of Chatbots and Their Legality Framework", 2021.

5. Kanika Agarwal. " Legal Case Summarization: An Application for Text Summarization",2020.

6. Vaishnavi Suryawanshi, Disha Naikwadi, Prof. Sneha Pati. "Legal Case Document Summarization Using NLP, 2023"

7. Anandhu Prasad, Asna Noushad, Navya K Gopi, Reshma Raju, Mary Priyanka KS. "An Overview Of Legal Document Summarization Techniques", 2023.

8. Anupam Mondal, Monalisa Dey, Dipankar Das, Sachit Nagpal, Kevin Garda. "Chatbot: An automated conversation system for the educational domain",2018.

9. Vajinepalli Sai Harsha Vardhan, Parsi Anurag, Richa Sharma. Research Paper On "Rule Based Chatbot", 2022.

10. Abhay Shukla, Paheli Bhattacharya, Soham Poddar, Rajdeep Mukherjee, Kripabandhu Ghosh, Pawan Goyal, Saptarshi Ghosh. "Legal Case Document Summarization: Extractive and Abstractive Methods and their Evaluation", 2022.

11. Hanlei Jin, Yang Zhang, Dan Meng, Jun Wang, Jinghua Tan.A Comprehensive Survey on "Process-Oriented Automatic Text Summarization with Exploration of LLM-Based Methods", 2024.

12. D Jain, MD Borah, A Biswas. "Improving Legal Document Summarization Using Deep Clustering", 2023.

13. Jonathan Pilault, Raymond Li, Sandeep Subramanian, Chris Pal. "Extractive and Abstractive Neural Document Summarization with Transformer Language Models", 2020.

Data Fusion Methodologies in Cyber-Physical Systems: Safeguarding Healthcare Data against Cyber-Attacks using Deep Convolutional Neural Networks

Jagdish F. Pimple
Research Scholar
Department of Computer Science & Engineering
Madhyanchal Professional University
Bhopal, Madhya Pradesh
✉ pimplejagdish@gmail.com

Avinash Sharma
Professor
Department of Computer Science & Engineering
Madhyanchal Professional University
Bhopal, Madhya Pradesh
✉ avinashvtp@gmail.com

ABSTRACT

Healthcare systems become increasingly interconnected and reliant on CPS (cyber-physical systems) , they become exposed to cyber-attacks that can undermine patient data privacy, disrupt healthcare services, and even endanger lives. This paper offers a hybrid structure constructed on data fusion and DCNN-deep convolutional neural networks , along with blockchain technology, to resolve the issue of real-time security challenges. The planned process aims to expand the accurateness and efficiency of identifying cyber threats in digital environments by integrating feature fusion with blockchain and employing deep CNNs with optimized training algorithms. Theoretical and experimental investigations demonstrate the efficacy of the suggested method compared to other cutting-edge methods. Choosing the optimal feature or fusion level for detecting specific attack features typically poses challenges due to the complexity of feature selection and the need for extensive domain knowledge. To tackle these challenges, we introduce a novel fused data fusion techniques based on deep convolutional neural networks for attack detection. This method effectively learns features from raw data and dynamically optimizes fusion levels to meet the requirements of various cyber-attacks. Our proposed method undergoes rigorous testing using reputable datasets. We compare it against other methods such as Recurrent Neural Networks (RNN), Extreme Learning Machine (ELM), Convolutional Neural Networks (CNN), Temporal Logic Models (TLM) and Deep Belief Networks (DBN). The results demonstrate that our method excels in effectively detecting cyber-attacks, achieving superior accuracy compared to all other comparative methods in the experiment.

KEYWORDS *: MCPS, Cyber-attacks, Blockchain, DCNN, Feature fusion, Security.*

INTRODUCTION

In the kingdom of engineered systems, Cyber-Physical Systems (CPSs) have emerged as intricate frameworks that seamlessly integrate computing, networking, and physical processes[1]. These systems facilitate the seamless connection between cyber services and physical devices, exemplifying a convergence of the digital and physical domains. CPSs encompass transdisciplinary approaches, drawing on disciplines such as cybernetics, mechatronics, philosophy of design, and process science[2,3]. Embedded systems, often synonymous with process management, conceptualize a developed system as a combination of components working collaboratively to perform a collective and utilitarian function. In the contemporary landscape, healthcare networks epitomize a modern and context-aware Cyber-Physical System (CPS). These networks incorporate an array of integrated devices, harness the power of IoT (Internet of Things) technologies, and make use of cloud storage options. The integration of these elements in healthcare CPSs signifies a paradigm shift, revolutionizing the delivery of healthcare services and introducing novel possibilities for patient care, data management, and system efficiency. Cyberattacks that violate patient data privacy, interrupt healthcare

services, or even put lives in peril are a growing threat to healthcare systems as they grow more linked and dependent on CPS [4,5,6,7,8]. To address these challenges, researchers have been exploring innovative approaches to cyber-attack detection in healthcare CPS, incorporating the application of blockchain technology and deep learning. Blockchain technology manages the safety of networks based on distributed methods, and deep learning algorithms provide information about past events that occur in security models and predict the future direction of security pillars in the healthcare system. Data fusion is a new area of research in medical cyber-physical systems for the detection of cyberattacks. The processing of data fusion is based on the variable and fixed attributes of the network and the data record of the healthcare system. The incorporation of data fusion and deep learning algorithms provides efficient detection of cyber-attacks in the medical cyber physical system. Data fusion involves combining information from multiple sources to improve the accuracy and reliability of decision-making processes. In the context of cybersecurity, data fusion can improve threat detection by combining information from multiple sources, including network traffic, system logs, and sensor data. Data fusion methods that analyse multiple types of data simultaneously can provide a more comprehensive understanding of cyber threats and enable more effective countermeasures[9,10,11]. CNNs, or deep convolutional neural networks, have become extremely potent tools for cybersecurity activities, including intrusion detection and malware analysis. Despite the potential benefits of data fusion methods and CNNs for cyber-attack detection in healthcare CPS, several challenges remain. The availability and quality of data for training and estimation purposes is solitary challenge. Healthcare data is often sensitive and highly regulated, making it challenging to access and share for research purposes. Additionally, ensuring the privacy and confidentiality of patient data is paramount, requiring researchers to implement robust data anonymization and encryption techniques. Furthermore, the complex and dynamic nature of healthcare CPS introduces additional challenges, such as interoperability issues, scalability concerns, and the need for real-time processing and analysis. In order to address real-time security concerns, this paper suggests a hybrid paradigm that combines blockchain technology with data fusion and deep convolutional neural networks. Our research's primary focus is as follows:

1. We propose DCNN and data fusion-based model to detect cyber-threats in medical cyber physical systems.

2. The processes of DCNN and data fusion incorporate blockchain technology for distributed data sharing for information privacy.

3. We conducted an experimental analysis by putting the suggested algorithm into practice and testing reputable datasets to ensure the practicability and feasibility of the proposed algorithm.

4. A comparison of the suggested method with an already-in-use cyberattack detection algorithm for medical cyber-physical systems.

The rest of the paper is arranged as, part II describes the linked work of medical cyber physical systems. Section III discusses the proposed methodology of cyber-attack detection. Section IV presents the experimental analysis. Section V result and discussion and at last, the paper is concludes in Section VI.

RELATED WORK

In the last decade, considerable research has focused on healthcare information systems leveraging blockchain technology and machine learning algorithms to enhance privacy preservation and security. However, in order to meet security requirements such as non repudiation, mutual authentication, and data confidentiality, it is often essential to conduct computationally intensive modular exponential operations or elliptic curve point multiplication. This section delves into recent advancements in the field of medical cyber physical systems. In [1], Provide a framework for privacy protection and deep learning driven data analytics for Internet of Things-enabled healthcare. They dispersed the consumer's private information in the safety-isolation zone after receiving raw documents from them. In [2], a design architecture named BCH-health permits data holders to identify their ideal access controls above their privacy-sensitive healthcare data, thereby resolving the compromise problem between openness and access control. [3] offers a transparent and

private data solution for the healthcare sector. Additionally, the suggested system uses cryptographic techniques to protect data privacy and integrates insurance policies into the blockchain via the Ethereum platform. [4] the author uses my Signals HW V2 Platform to construct the recommended system. The My Signals HW V2 Platform is used by developers to create the suggested system. The results of security research and testing show that the suggested system offers minimal communication overhead and computation while protecting data privacy, message authenticity, and integrity. According to [5], protecting user privacy in these systems is critical. Despite its expanding efficacy and increasing inclination towards adoption, people do not give enough thought to privacy concerns. [6] offers a novel approach to collecting data for IoT-based healthcare services systems while maintaining privacy. Theoretical and experimental investigations validate the proficiency of the recommended method. [7] presents Based on Euclidean L3P, the Multi-Objective Successive Approximation (EMSA) Algorithm is a useful tool for assessing privacy in healthcare cloud environments.. This article presents role-based encryption keys, which are a vital building block for complex data storage in cloud locations. The proposed study incorporates the security mechanism into the design of the edge-cloud-based, patient-centered healthcare system in [8]. It is advisable to use additive holomorphic encryption at the edge level to ensure privacy during safe data handling and non-sensitive data cleaning. [9] suggests a methodology for creating and assessing synthetic medical data with the dual goals of protecting privacy and retaining the complexity of ground-truth data, to the best of our knowledge. In [10], while maintaining its security features, the suggested mechanism is computationally lighter and more resilient to various attacks compared to the ECPM (Elliptic curve point multiplication) it has been employed in other contexts. In [11], a collaborative framework allows for knowledge exchange from a variety of data sources while maintaining anonymity. [13] attempts to apply blockchain technology to address the aforementioned problems. By using the right consensus technique, we can lower network costs, such as bandwidth and processing consumption, while also improving network security and efficiency. In [14], the suggested technique builds a scalable and dependable data gathering and broadcast system using graph modelling. Comparing the suggested methodology to the current solutions through numerous simulations demonstrates improvements in practical parameters. In [15], the suggested solution, which uses the DPoS algorithm, significantly reduces the amount of time, money, computational capacity, and resource usage for EHR transactions. [16] proposes the blockchain technology to enhance the safety of medical data and introduces a straightforward identity authentication method. The security of medical data, we employ blockchain technology and provide a simple identity authentication method. Meanwhile, they modify the searchable encryption algorithm to achieve cypher text handling across the whole life cycle in light of the issues with blockchain information transparency and visibility. [17] employs a novel customised privacy-preserving technique that tackles the shortcomings of previous personalised privacy and other anonymization techniques. In [18], to preserve data privacy, we suggest playing a Markovian game among the information requester and the data holder in a weight reduction programme in this study. Our goal is to find a middle ground between the data holder's privacy concessions and the data requester's incentive motivation. In [19], It is stressed that the system is built using trustworthy Artificial Intelligence (AI) principles. Designing the system with reliable Artificial Intelligence (AI) principles in mind improves security, privacy preservation, and provenance when processing and transmitting data, which is beneficial for remote diagnostics as well. In [20], the investigational outcomes prove the 99.33% accurateness of the EIHCF. These results indicate improved performance as compared to the previous work's conclusions. [21] utilizes blockchain technology to offer a distributed model for weight sharing that is resistant to tampering. In the proposed FL-based Framework, we use blockchain technology to deliver decentralized model weight sharing that is strengthened resistant. Model on real-world healthcare information determines the efficacy of the suggested approach compared to other cutting-edge methods. In [22], to prevent data likability, the zero-knowledge protocol makes sure that no information is available to unauthenticated users. The outcomes show how well

the strategy works to address big data analytics and confidentiality concerns in the medical industry. In [23], implemented a movement analysis system for house care that consists of a mobile application and a single inertial measurement sensor. This project also includes a motion analysis system for home care that consists of a mobile application and a single inertial measurement sensor. To assess the hazard of drops and gait at home, the system can gather personal data, raw movement data, and indices. In [24], Blockchain is used in a multi-party computation-based ensemble federated learning framework to enable several prototypes to jointly acquire from the data of healthcare organizations without exposing user privacy. In [25], propose a modular IoT-aware system design that may be used in a variety of healthcare application situations in an effort to help resolve these problems. [26] looks at the two types of blockchain-based security methods discussed above and their current state of the art. This will serve as a basis for planning research efforts aimed at creating dependable blockchain-based countermeasures that will effectively and efficiently address the critical security issues facing IoMT edge networks. In [27], blockchain technology in healthcare is discussed in this paper. We deliver a thorough outline of blockchain technology, including its background, methodological details, and various usage. We also cover the driving forces of the technology and highlight the most notable healthcare initiatives that have utilized it. Blockchain is shown to be able to address privacy and security concerns with fog computing in [28]. It also covers the shortcomings and issues of blockchain from the viewpoints of IoMT & fog computing (FC). In [29], energy-harvesting techniques are used to boost efficiency. Furthermore, the DRL approach optimizes The security and energy efficiency of the proposed system simultaneously. In [30], the healthcare sector, learning can lessen security issues and concerns related to big data platforms.

PROPOSED METHODOLOGY

The proposed methodology for cyber-attack detection seems quite comprehensive, incorporating feature fusion, deep convolutional neural networks (CNNs), and blockchain technology. Let's break down the key components:

Feature Fusion: This involves combining different types of features extracted from the data. It could include various attributes such as network traffic patterns, system log data, or other relevant information for detecting cyber-attacks.

Deep Convolutional Neural Network (CNN): CNNs are one type of artificial neural network particularly effective for image recognition tasks. In this context, they likely analyse patterns and structures within the data to identify potential cyber threats.

Blockchain Technology for Data Distribution: Blockchain is utilized for secure and decentralized data distribution. It ensures that data is tamper-proof and transparently shared across multiple nodes in the network.

Feature Extraction: The distributed data undergoes a feature extraction process. This step is crucial for identifying relevant patterns or characteristics that may indicate a cyber-attack.

Normalization and Overfitting Reduction: Normalization techniques are applied to the extracted features to ensure they are on a consistent scale. This helps improve the performance of the algorithm and decrease the risk of overfitting, where applied to unknown data, the model performs poorly, yet well on training data.

Transform Function: This function likely applies mathematical transformations to the features, possibly to enhance certain aspects or to make them more suitable for processing by the CNN.

Levels of Feature Mapping: The features are mapped into different levels, such as high level, low level, and average level. This suggests a hierarchical approach to feature representation, where features are grouped based on their complexity or abstraction. The process of the proposed algorithm is represented visually in Figure 1, providing a graphical overview of how the various components interact.

Blockchain technology is a decentralized distributed data management system that relies on distributed databases, employing data encryption and consensus mechanisms. In theory, it creates a structure akin to a chain, with each node standing in for a block of data that contains transaction data. Intra- and inter-block chain

architectures make up the fundamental data structure of blockchain technology [22,23]. The block header contains metadata essential for block verification and establishing connections with predecessor and successor blocks. Traffic data fusion can be centralized or distributed. This paper focuses on distributed data processing, as depicted in Figure 1. Each data point identifies the target, and the resulting finding information is consistently linked and fused by a fusion centre to create data fusion track information. This paper proposes a methodology to enhance attack detection accuracy using blockchain in the framework of traffic data fusion processing inside the same space detection scenario. This methodology facilitates user interaction with the blockchain and implements business logic using blockchain technology. Regarding the blockchain, the feature fusion procedure is contained in a smart-contract that is subsequently distributed to pertinent nodes for distributed data processing and validation. The blockchain processing shown in figure 2.

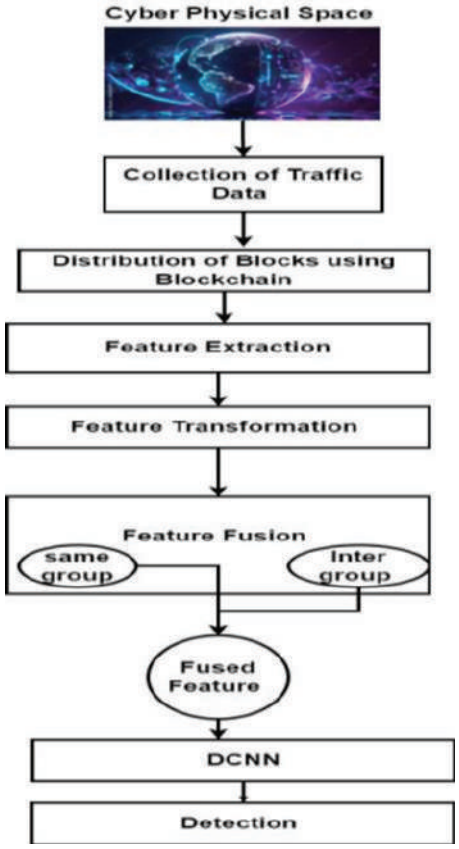

Fig. 1. Proposed model of cyber-attack detection based on DCNN

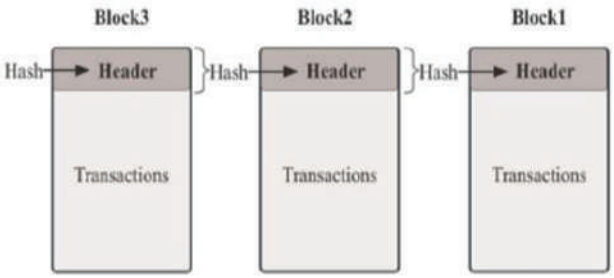

Fig. 2. Block processing of traffic data distribution

Algorithm of feature fusion

1. Define an empty matrix F for input data
2. Generate level of features (high, low, average) for fusion model
3. Normalized the features of data
4. For i□1 to number of samples do
5. Define empty vector V to store fused feature of sample i
6. For all features f represents do
7. Concatenate feature f form all levels
8. Add concatenate features into vector V
9. End for
10. Compute mean of all feature vector
11. Formed new feature vector
12. End for
13. Create fully connected network
14. For i□ to 3 do
15. Connect fully connected layer with ReLU activation function
16. Add a dropout layer
17. End for
18. Return (fused features)

The proposed algorithm consists of two parts: the CNN processing and the cyber-attack detection.

CNN Processing Phase

1. Input training data, sampling interval (ST), window size, and fused features size. 2. Split the training

data into several windows (w1, w2, ..., wn) and further divide them into batches of features.

3. Estimate feature vectors.
4. Generate feature mappings for the windows.
5. Train the CNN model using the feature maps.
6. Check if the current number of training iterations has reached the preset limit. If so, exit the training program; otherwise, return to step 5 for the next round of training.

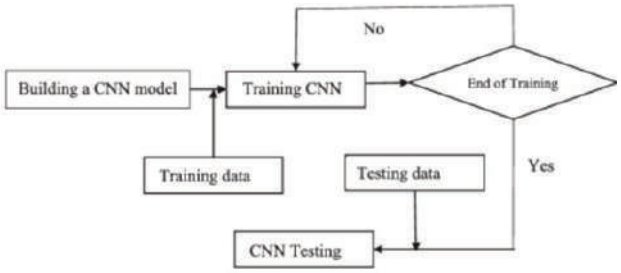

Fig. 3 processing of CNN for training and testing of data

Cyber-Attack Detection Phase:

1. Input sampling interval (St), window size (W), and feature size (F).

2. Obtain real-time cyber-attack detection for a window.

3. Divide the detection data into batches of size BS.

4. Calculate vectors for each batch.

5. Generate a feature map for the current window.

6. Input the feature map into the CNN model.

7. Output the detection result.

8. Check the end condition. If met, exit the detection program; otherwise, return to step 2 and continue detecting network traffic.

9. This structured approach facilitates effective processing and detection of cyber attacks, incorporating both training and real-time detection phases for comprehensive cybersecurity measures.

IV. Experimental Result

A number of scenarios have been used to test the suggested algorithm's simulation. The MATLAB software version 2018R is used in the simulation process. The approach was validated using two intrusion detection datasets, namely the NSL-KDD 2015 and CIDDS-001

datasets [7]. The previous NSL-KDD dataset contained 125973 occurrences, 41 characteristics, and 2 classes. The CIDDS-001 dataset then contains 1018950 instances with 14 attributes and 2 classes. The performance of the proposed algorithm is contrasted with that of other cyber-physical security system algorithms, including DNN, TLM, RNN, ELM, and DBN. Algorithm performance is measured using F-score, sensitivity, specificity, and accuracy [28,29, 30].

$$Accuracy = \frac{Total\ No.of\ Correctly\ Classified\ Instances}{Total\ No.of\ Instances} \times 100$$

$$Sensitivity = \frac{TP}{TP + FN} \times 100$$

$$Specificity = \frac{TN}{TN + FP} \times 100$$

$$F - score = \frac{2TP}{2TP + FN + FN}$$

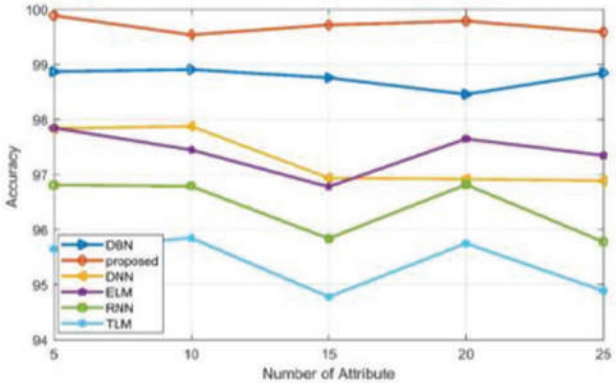

Fig. 4: Accuracy performance analysis based on attribute count for NSL-KDD 2015 dataset.

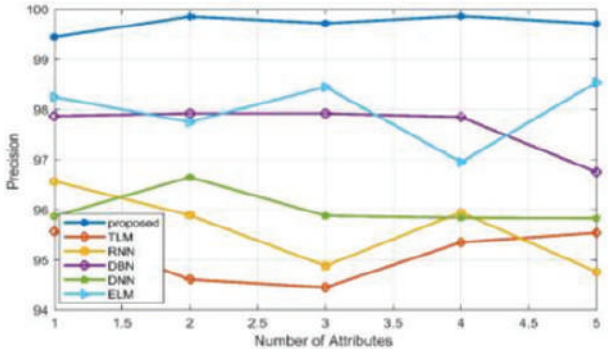

Fig. 5 Precision performance analysis of Number of attributes for NSL-KDD 2015 dataset.

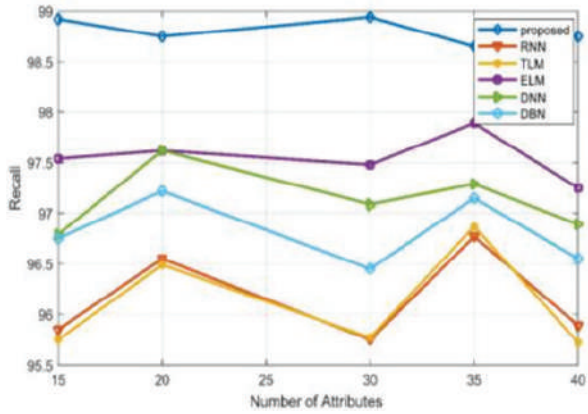

Fig. 6 Recall performance analysis based on Number of attributes for NSL-KDD 2015 dataset.

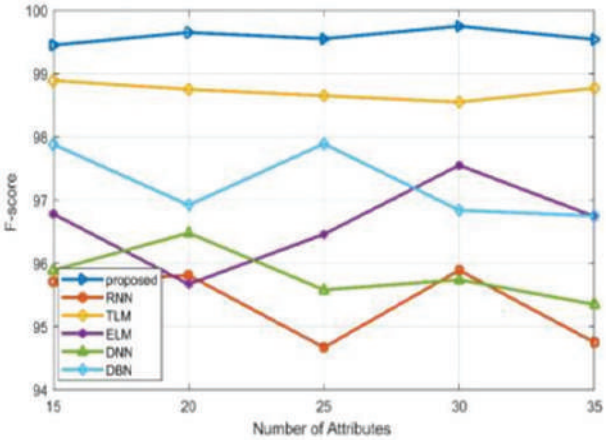

Fig. 7 Performance analysis of F-score based on Number of attributes for NSL-KDD 2015 dataset.

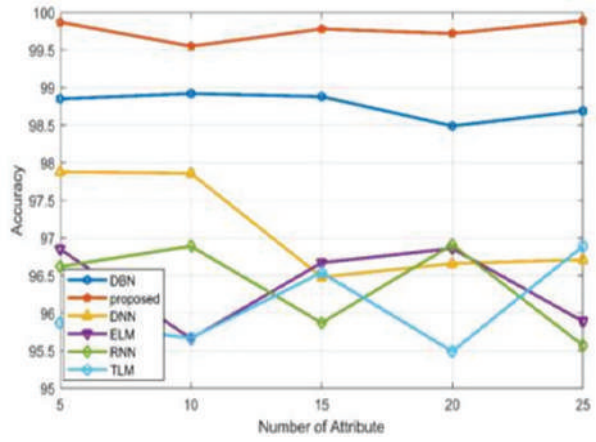

Fig. 8 Accuracy performance analysis based on Number of attributes for CIDDS-001 dataset.

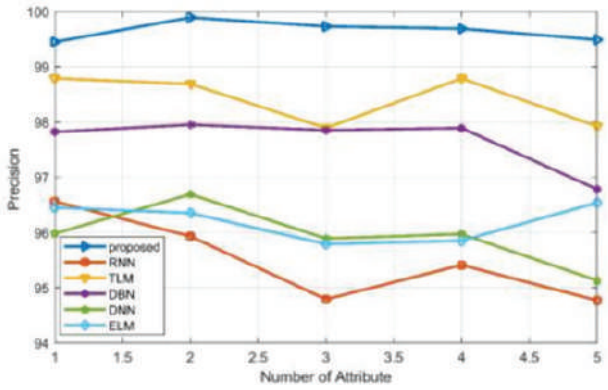

Fig. 9 Precision performance analysis based on Number of attributes for CIDDS-001 dataset.

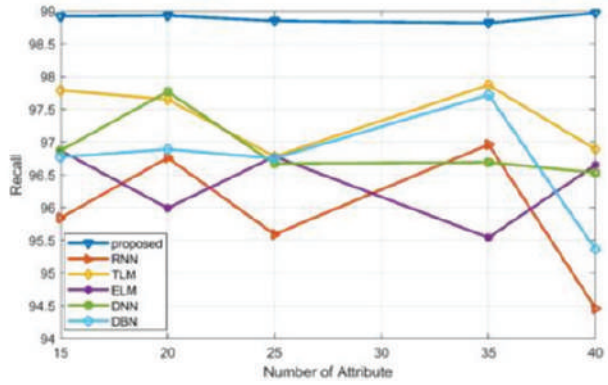

Fig. 10 Recall Performance analysis based on Number of attributes for CIDDS-001 dataset.

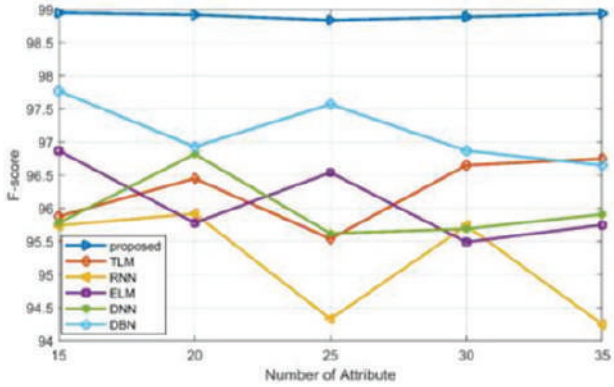

Fig. 11 F-score performance analysis based on Number of attributes for CIDDS-001 dataset.

RESULTS & DISCUSSION

Evaluating the effectiveness of cyber-attack detection within a medical cyber-physical system. The proposed algorithm's performance is assessed using two well-

known datasets: NSL-KDDCUP2015 and CIDDI_001. The results of this evaluation are presented through various metrics, including accuracy, sensitivity, specificity, and F-score, depicted in Figures 7 to 11. The experiments were conducted over 30 epochs to determine the optimal parameters for the recurrent models. Among configurations with hidden layer units ranging from 16 to 128, models with 32 units outperformed others. Consequently, the recurrent model units were set to 32. Various learning rates (0.2, 0.1, 0.001, and 0.0001) were tested, with lower rates, particularly 0.001, exhibiting superior performance, thus selected as the learning rate value. To determine the ideal batch size, models were tested with batch sizes of 16, 32, 64, and 128, with the 64 batch size demonstrating superior results. Subsequent experiments were conducted over 25, 50, and 75 epochs, with the 50-epoch mark yielding the highest training and validation accuracy. Performance began to decline post-50 epochs, indicating potential overfitting, prompting termination of experiments at 50 epochs. The detailed performance analysis of recurrent deep learning models regarding training and validation accuracy for attack detection is depicted in Figures 7-11, alongside train loss and validation loss for attack detection. These figures collectively illustrate an upward trend in accuracy and a downward trend in loss across 50 epochs. Further experimentation beyond 50 epochs did not yield improvement, leading to the decision to conclude experiments at this point. Notably, fluctuations were observed in both the accuracy and loss of training and validation datasets during experimentation. Although the training and validation datasets were entirely disjoint, the network connection data samples were shuffled in both datasets. Recurrent deep learning models demonstrated consistent performance for both network attack detection and classification tasks.

CONCLUSION & FUTURE WORK

The new approach presented in this paper for cyber-attack detection, leveraging feature fusion and deep convolutional neural networks (CNNs). Feature fusion is integrated with blockchain technology, which distributes traffic data into blocks using different hash functions to connect feature blocks. The design model of the deep CNN comprises three layers: completely linked layers, pooling layers, and convolutional layers. The completely connected network is activated by using the ReLU activation function. Descent gradient optimization procedures are used to maximize the loss of training data. This approach combines advanced techniques from machine learning, blockchain, and neural networks to enhance cyber-attack detection. By integrating feature fusion with blockchain and employing deep CNNs with optimized training algorithms, the projected method aims to advance the accuracy and efficiency of identifying cyber threats in digital environments. The findings of the study reveal several significant points: Classifier performance sees an average improvement of 2-5% (centred on F1-score) when cyber-physical characteristics are incorporated, as opposed to pure cyber features. Replacing Snort labels with labels derived from traffic data features boosts performance by an average of 5-7% (based on accuracy). Situations with balanced and bigger records demonstrate superior performance in attack evaluations. In real-world circumstances, the co-training-based deep learning technique outperforms supervised techniques. It even surpasses them by 2-5% (on sensitivity) with certain classifiers. Among deep learning methods like RNN, CNN, TLM, ELM, and DBN, CNN emerges as more strong and exact. Accuracy is not improved when classifiers are trained using manifold learning embedding. Therefore, manifold learning should primarily serve visualization purposes rather than improving accuracy. These findings offer valuable insights into enhancing classifier performance and selecting appropriate techniques for cyber attack detection, emphasizing the significance of considering various factors in real-world scenarios.

REFERENCES

1. Bi, Hongliang, Jiajia Liu, and Nei Kato. “Deep learning-based privacy preservation and data analytics for IoT enabled healthcare.” IEEE Transactions on Industrial Informatics 18, no. 7 (2021): 4798-4807.
2. Hossein, Koosha Mohammad, Mohammad Esmaeil Esmaeili, Tooska Dargahi, Ahmad Khonsari, and Mauro Conti. “BCHealth: A novel blockchain-based privacy preserving architecture for IoT healthcare applications.” Computer Communications 180 (2021): 31-47.
3. Al Omar, Abdullah, Abu Kaisar Jamil, Amith

Khandakar, Abdur Razzak Uzzal, Rabeya Bosri, Nafees Mansoor, and Mohammad Shahriar Rahman. "A transparent and privacy-preserving healthcare platform with novel smart contract for smart cities." Ieee Access 9 (2021): 90738-90749.

4. Almalki, Faris A., and Ben Othman Soufiene. "EPPDA: an efficient and privacy preserving data aggregation scheme with authentication and authorization for IoT based healthcare applications." Wireless Communications and Mobile Computing 2021 (2021): 1-18.

5. Kanwal, Tehsin, Adeel Anjum, and Abid Khan. "Privacy preservation in e-health cloud: taxonomy, privacy requirements, feasibility analysis, and opportunities." Cluster Computing 24 (2021): 293-317.

6. Onesimu, J. Andrew, J. Karthikeyan, and Yuichi Sei. "An efficient clustering-based anonymization scheme for privacy-preserving data collection in IoT based healthcare services." Peer-to-Peer Networking and Applications 14 (2021): 1629-1649.

7. Sathya, A., and S. Kanaga Suba Raja. "Privacy preservation-based access control intelligence for cloud data storage in smart healthcare infrastructure." Wireless Personal Communications 118 (2021): 3595-3614.

8. Jayaram, Ramaprabha, and S. Prabakaran. "Onboard disease prediction and rehabilitation monitoring on secure edge-cloud integrated privacy preserving healthcare system." Egyptian Informatics Journal 22, no. 4 (2021): 401-410.

9. Wang, Zhenchen, Puja Myles, and Allan Tucker. "Generating and evaluating cross-sectional synthetic electronic healthcare data: preserving data utility and patient privacy." Computational Intelligence 37, no. 2 (2021): 819-851.

10. Lee, Tian-Fu, I-Pin Chang, and Ting-Shun Kung. "Blockchain-based healthcare information preservation using extended chaotic maps for HIPAA privacy/security regulations." Applied Sciences 11, no. 22 (2021): 10576.

11. Long, Guodong, Tao Shen, Yue Tan, Leah Gerrard, Allison Clarke, and Jing Jiang. "Federated learning for privacy-preserving open innovation future on digital health." In Humanity Driven AI: Productivity, Well-being, Sustainability and Partnership, pp. 113-133. Cham: Springer International Publishing, 2021.

12. Sabu, Sarath, H. M. Ramalingam, M. Vishaka, H. R. Swapna, and Swaraj Hegde. "Implementation of a Secure and privacy-aware E-Health record and IoT data Sharing using Blockchain." Global Transitions Proceedings 2, no. 2 (2021): 429-433.

13. Meisami, Sajad, Mohammad Beheshti-Atashgah, and Mohammad Reza Aref. "Using blockchain to achieve decentralized privacy in IoT healthcare." arXiv preprint arXiv:2109.14812 (2021).

14. Elhoseny, Mohamed, Khalid Haseeb, Asghar Ali Shah, Irshad Ahmad, Zahoor Jan, and Mohammed I. Alghamdi. "IoT solution for AI-enabled PRIVACY PREServing with big data transferring: an application for healthcare using blockchain." Energies 14, no. 17 (2021): 5364.

15. Karunakaran, Chitra, Kavitha Ganesh, Sonya Ansar, and Rohitha Subramani. "A Privacy Preserving Framework for Health Records using Blockchain." Pertanika Journal of Science & Technology 29, no. 4 (2021).

16. Wen, Haiying, Meiyan Wei, Danlei Du, and Xiangdong Yin. "A blockchain based privacy preservation scheme in mobile medical." Security and Communication Networks 2022 (2022).

17. Puri, Ganesh Dagadu, and D. Haritha. "Improving Privacy Preservation Approach for Healthcare Data using Frequency Distribution of Delicate Information." International Journal of Advanced Computer Science and Applications 13, no. 9 (2022).

18. Sfar, Arbia Riahi, Enrico Natalizio, Sahbi Mazlout, Yacine Challal, and Zied Chtourou. "Privacy preservation using game theory in e-health application." Journal of information security and applications 66 (2022): 103158.

19. Michala, Anna Lito, Hani Attar, and Ioannis Vourganas. "Secure data transfer and provenance for distributed healthcare." In Intelligent Healthcare: Infrastructure, Algorithms and Management, pp. 241-260. Singapore: Springer Nature Singapore, 2022.

20. Patil, Shubham Prashant. "Security vulnerability detection with enhanced privacy preservation for edge computing using hybrid machine learning approach." PhD diss., Dublin, National College of Ireland, 2022.

21. Singh, Moirangthem Biken, and Ajay Pratap. "BPFISH: Blockchain and Privacy-preserving FL Inspired Smart Healthcare." arXiv preprint arXiv:2207.11654 (2022).

22. Demirbaga, Umit, and Gagangeet Singh Aujla. "MapChain: A blockchain based verifiable healthcare service management in IoT-based big data ecosystem." IEEE Transactions on Network and Service Management 19, no. 4 (2022): 3896-3907.

23. Aqueveque, Pablo, Britam Gómez, Patricia AH Williams, and Zheng Li. "A Novel Privacy Preservation and Quantification Methodology for Implementing Home-Care-Oriented Movement Analysis Systems." Sensors 22, no. 13 (2022): 4677.

24. Stephanie, Veronika, Ibrahim Khalil, Mohammed Atiquzzaman, and Xun Yi. "Trustworthy privacy-preserving hierarchical ensemble and federated learning in healthcare 4.0 with blockchain." IEEE Transactions on Industrial Informatics (2022).

25. Shumba, Angela-Tafadzwa, Teodoro Montanaro, Ilaria Sergi, Luca Fachechi, Massimo De Vittorio, and Luigi Patrono. "Leveraging IOT-aware technologies and AI techniques for real-time critical healthcare applications." Sensors 22, no. 19 (2022): 7675.

26. Pelekoudas-Oikonomou, Filippos, Georgios Zachos, Maria Papaioannou, Marcus de Ree, José C. Ribeiro, Georgios Mantas, and Jonathan Rodriguez. "Blockchain-based security mechanisms for IoMT Edge networks in IoMT-based healthcare monitoring systems." Sensors 22, no. 7 (2022): 2449.

27. Ramzan, Sadia, Aqsa Aqdus, Vinayakumar Ravi, Deepika Koundal, Rashid Amin, and Mohammed A. Al Ghamdi. "Healthcare applications using blockchain technology: Motivations and challenges." IEEE Transactions on Engineering Management (2022).

28. Alam, Shadab, Mohammed Shuaib, Sadaf Ahmad, Dushantha Nalin K. Jayakody, Ammar Muthanna, Salil Bharany, and Ibrahim A. Elgendy. "Blockchain based solutions supporting reliable healthcare for fog computing and internet of medical things (IoMT) integration." Sustainability 14, no. 22 (2022): 15312.

29. Liu, Long, and Zhichao Li. "Permissioned blockchain and deep reinforcement learning enabled security and energy efficient Healthcare Internet of Things." Ieee Access 10 (2022): 53640-53651.

30. Unal, Devrim, Shada Bennbaia, and Ferhat Ozgur Catak. "Machine learning for the security of healthcare systems based on Internet of Things and edge computing." In Cybersecurity and Cognitive Science, pp. 299-320. Academic Press, 2022.

31. Pimple, Jagdish F., Avinash Sharma, and Jitendra Kumar Mishra. "Medisecure: A blockchain-enabled ensemble learning approach for user-controlled single sign-on and privacy preservation in medical cyber-physical systems." In International Conference on the Role of AI in Bio-Medical Translations' Research for the Health Care Industry, pp. 71-86. Cham: Springer Nature Switzerland, 2023.

32. Pimple, Jagdish F., Avinash Sharma, and Jitendra Kumar Mishra. "Elevating Security Measures in Cyber-Physical Systems: Deep Neural Network-Based Anomaly Detection with Ethereum Blockchain for Enhanced Data Integrity." Journal of Electrical Systems 19, no. 2 (2023).

Android-Based Assistant for Visually Impaired

S. A. Sagar
✉ swati.sagar@bharatividyapeeth.edu
Anuja Babar
✉ anujababar23117@gmail.com
Gauri Khanzode
✉ gaurikhanzode7@gmail.com
Amina Shaikh
✉ aminahshaikh0@gmail.com

Department of Information Technology
Bharati Vidyapeeth's College of Engineering for Women
Pune, Maharashtra

ABSTRACT

Visually impaired individuals encounter many difficulties in their daily lives. For the visually impaired, the daily routine can be daunting. The research introduces an Android-based system with a virtual assistant, designed to empower visually impaired individuals to independently perform routine tasks. The idea revolves around providing blind people with an Android-based system equipped with a virtual assistant, enabling them to perform some simple tasks independently. The purpose of the system is to provide voice assistance to visually impaired people to help them complete tasks such as reading, optical character recognition, object recognition, directional assistance and understanding the environment. By integrating cameras, mobile devices, and a sound system, the project seeks to comprehensively address the multifaceted challenges faced by visually impaired individuals. The ultimate goal is to enhance accessibility and promote independence, enabling visually impaired individuals to navigate the world around them with confidence and autonomy. By facilitating greater participation in daily activities, the development of such a device not only improves quality of life but also fosters social inclusion by empowering individuals with visual impairments to engage more fully with their surroundings. Through this research, we aspire to contribute to a more inclusive society where everyone, regardless of ability, can thrive and participate fully.

KEYWORDS *: Visually impaired individuals, Assistive technology, Virtual assistant, Android system.*

INTRODUCTION

Millions of people around the world suffer from low vision, making it difficult for them to understand their surroundings. One of the main problems that visually impaired people face is moving and understanding their environment. There are other problems, such as reading text written on the wall or desktop, unless auto reader is enabled on the desktop.

They have difficulty moving because they cannot evaluate the relative position of objects and people around them. They need help from others to navigate or understand their environment. Due to the limitations of traditional solutions, extensive research is used to provide effective and efficient tools to assist blind and visually impaired people. Android system that uses the mobile phone's camera to identify objects and text. Using TensorFlow's API, the application will recognize the environment and notify the user via voice about detected objects.

Visually impaired users can receive voice messages using audio devices such as headphones or speakers on their mobile phones. Since the system uses the phone's camera to perform these functions, an additional camera is not needed. This article provides an overview of Android applications, standards, and features for the visually impaired to explain how java and Kotlin-based applications support independence for the visually impaired.

LITERATURE REVIEW

In recent years, several studies have contributed to advancing technologies aimed at assisting visually impaired individuals.

In 2021 Kanchan Patil, Avinash Kharat, Pratik

Chaudhary, Shrikant Bidgar, Rushikesh Gavhane published the article "Guidance System for Visually Impaired People" which proposed a wearable virtual assistive system aimed to help visually impaired people in their regular activities. This technology is meant to handle the primary issues faced by visually impaired users, such as environmental awareness, location, facial recognition, and text reading. This new system has five essential features, each of which contributes to functionality and usability. Utilizing advanced deep learning and the core libraries of the Python language, the project aims to simplify the day-to-day activities of visually impaired individuals and provide effective solutions to common challenges.

In 2020 Vinayak Iyer, Kshitij Shah, Sahil Sheth, Kailas Devadkar published the paper "Virtual assistant for the visually impaired" which addressed the challenge of internet accessibility for visually impaired individuals by developing a software solution enabling interaction with websites via voice commands. The authors propose a software solution designed to increase Internet accessibility for visually impaired users by providing voice commands to interact with web pages. Their software incorporates speech-to-text and text-to-speech modules, along with automation capabilities using Selenium, thereby enhancing usability and providing summarized content.

In 2023 Prof. Supriya Gupta, Divya Wandhare, Harshal Jodangade, Aayushi Pandit, Bhargavi Chendke published the paper "Voice Assistant For Visually Impaired People" which describes an application catering to the needs of visually impaired individuals, offering features such as reading printed text, a talking calculator, weather information, object detection, and a voice-based payment system. The main objective of the project is to improve the daily lives of the blind through the use of voice recognition techniques, which have become increasingly important with the rapid development of wireless communication.

In 2021 Sulaiman Khan, Shah Nazir, And Habib Ullah Khan published the paper "Analysis of Navigation Assistants for Blind and Visually Impaired People: A Systematic Review" and conducted a systematic review focusing on navigation assistance for blind and visually impaired individuals. Their study identified various navigation devices and highlighted the need for improved guiding mechanisms to mitigate limitations such as limited object detection ranges and potential user harm. By analyzing primary studies from 2011 to 2020, their research aims to inform future improvements in navigation assistance technology.

In 2022 Xuhui Hu, Student Member, Aiguo Song, Hong Zeng, and Dapeng Chen published the paper "Xuhui Hu, Student Member, Aiguo Song, Hong Zeng, and Dapeng Chen" explored the use of spatial audio reasoning (SAR) to assist blind amputees in conveying environmental information. Their study developed a virtual scene and sound source to simulate three-dimensional motion, coupled with a prosthetic control system to enhance daily activities. The findings demonstrate the potential of SAR in improving information transfer rate and reducing completion time for blind amputees.

Overall, these studies contribute valuable insights into the development of assistive technologies for visually impaired individuals, highlighting the importance of innovation and interdisciplinary collaboration in addressing the diverse needs of this population.

SYSTEM OVERVIEW

Mobile Application Interface

- This serves as the user-facing part of the system, running on an Android device, providing an intuitive interface for interacting with the app.
- This component aligns with the objective of creating an Android-based assistant for visually impaired individuals.

Voice Input Module

- Responsible for capturing voice commands from the user and converting spoken words into text format.
- This component is crucial for enabling users to interact with the application hands-free, which is essential for individuals with visual impairments.

Command Processing

- Receives the recognized voice command from the Voice Input Module and analyzes it to determine the intended action or module switch.

- This component facilitates the seamless execution of user commands and navigation between different modules.

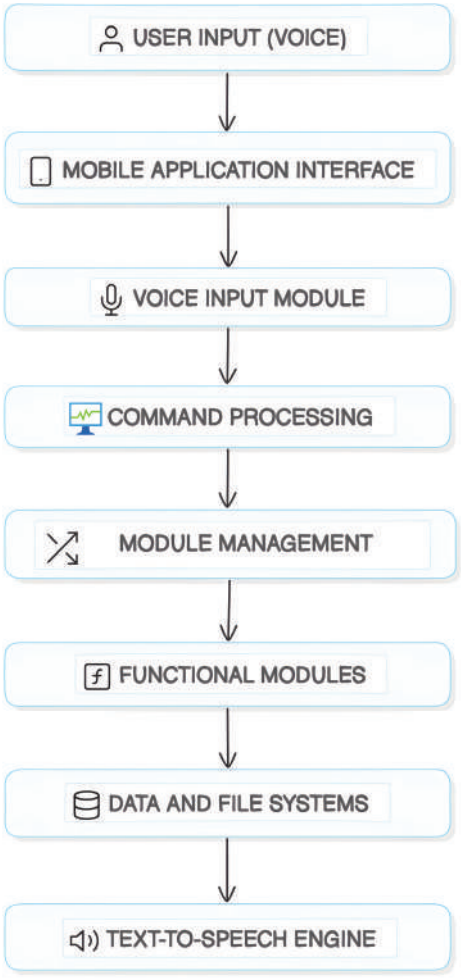

Fig. 1: System Workflow

Module Management

- Utilizes Android's Intent system to navigate between different modules based on the user's command. Launches the appropriate module based on the user's request.
- This component ensures efficient management and coordination among the various functional modules of the application.

Functional Modules

- These include modules such as Object Detection, Navigator, and OCR.
- Object Detection Module: Utilizes image processing techniques to identify and classify objects present in the environment.
- Navigation Module: Utilizes GPS data and mapping algorithms to provide real-time directional guidance and route planning for navigation purposes.
- Optical Character Recognition (OCR) Module: Analyzes images to extract and convert text into machine-readable format, enabling text recognition and reading capabilities.

Data and File System

- Manages the data and files used by different modules, including images and textual data.
- This component ensures proper storage and retrieval of information required for the operation of the application.

Text-to-Speech (TTS) Engine

- Converts textual information into speech output, providing audio feedback to the user.
- This component is essential for delivering information and instructions to visually impaired users in an accessible format.

Data Flow

The system begins with the user issuing a voice command, which is captured by the Voice Input Module. Subsequently, the recognized voice command undergoes analysis within the Command Processing module to discern the user's intended action, such as object detection. This information is then relayed to the Module Management component, which utilizes Android's Intent system to transition to the appropriate functional module. Upon activation, the selected functional module executes the requested task, such as performing object detection, while relevant data is managed within the Data and File System. Once the task is completed, the results are synthesized into speech using the TTS engine, enabling the system to provide audible feedback to the user.

PROPOSED SYSTEM

The proposed system architecture for an Android-based application aimed at assisting visually impaired

individuals, comprises interconnected modules designed to provide voice-over assistance for various tasks including reading, object detection, navigation, and OCR. Essential components such as a camera, microphone, and speakers are integral to the system, either integrated into the device or connected via a headset.

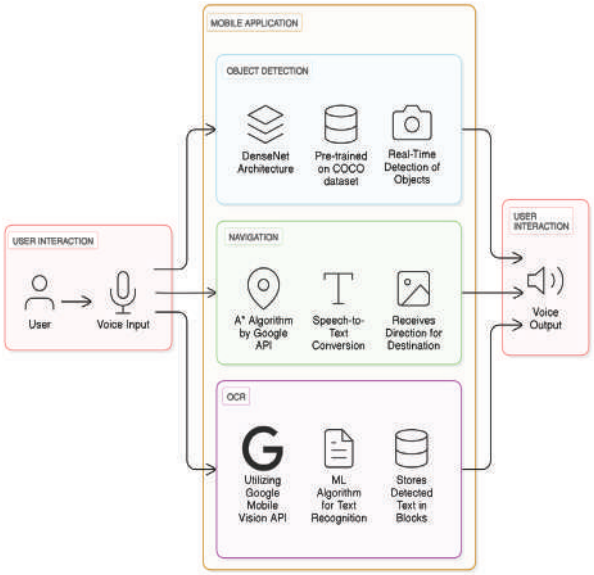

Fig. 2: System Framework

The primary modules encompass object detection utilizing TensorFlow and XML, navigation facilitated by Google Maps API, and OCR enabled through Google's Mobile Vision API. Voice inputs and outputs leverage Android's built-in speech recognition and text-to-speech functionalities. Additionally, the system architecture incorporates a graphical user interface (GUI) to demonstrate the functionality of the modules. Implementation involves algorithm selection, testing procedures, and project planning encompassing task schedules and development activities.

Execution Flow

The user initiates interaction by issuing a voice command, captured by the Voice Input Module. Subsequently, the recognized voice command undergoes analysis within the Command Processing module to determine the user's intended action, such as object detection. The Command Processing module communicates with the Module Management component, which utilizes Android's Intent system to transition to the appropriate functional module.

FUTURE TRENDS

In the future, virtual assistants for visually impaired individuals could focus on seamless navigation through advanced spatial awareness, providing real-time environmental descriptions, and assisting with complex tasks like identifying objects and reading handwritten text. Integration with emerging technologies, such as augmented reality, could enhance the overall user experience, empowering individuals with visual impairments to navigate the world more independently. Ongoing developments in AI may also lead to more personalized and context-aware virtual assistants tailored to individual needs. Advances in voice recognition, natural language processing, and wearable technology could enhance accessibility and independence, making daily tasks more manageable. Improved integration with smart devices and evolving AI capabilities may further enrich the virtual assistant experience for the visually impaired.

CONCLUSION

In conclusion, the research paper addresses the significant challenges encountered by visually impaired individuals in their daily lives and proposes the development of a personal assistant tool to assist them. The envisioned gadget consists of interconnected modules and functions designed to provide voice-over assistance for various tasks, including reading, object detection, facial recognition, and environmental comprehension. The paper highlights the obstacles faced by visually impaired individuals, such as difficulties in recognizing faces, detecting objects, navigating, sending messages, making calls, and reading. The project aims to offer a comprehensive solution to these challenges by developing an Android system with a virtual assistant. Key components of this project include a camera, mobile device, and audio system, with voice-over commands enabling seamless navigation across these components. The ultimate goal is to empower visually impaired individuals, allowing them to perform everyday tasks independently and enhance their quality of life. In summary, this research paper aims to create a holistic and integrated solution to

address the multifaceted challenges faced by visually impaired individuals, offering them a greater degree of autonomy and accessibility in their daily routines.

REFERENCES

1. Kanchan Patil, Avinash Kharat, Pratik Chaudhary, Shrikant Bidgar, and Rushikesh Gavhane. "Guidance System for Visually Impaired People", Institute of Electrical and Electronics Engineers (IEEE), April 2021.
2. Prof. Supriya Gupta, Divya Wandhare, Harshal Jodangade, Aayushi Pandit, and Bhargavi Chendke. "Voice Assistant For Visually Impaired People", Institute of Electrical and Electronics Engineers (IEEE), April 2023.
3. Vinayak Iyer, Kshitij Shah, Sahil Sheth, and Kailas Devadkar. "Virtual assistant for the visually impaired", Institute of Electrical and Electronics Engineers (IEEE), July 2020.
4. Sulaiman Khan, Shah Nazir, and Habib Ullah Khan. "Analysis of Navigation Assistants for Blind and Visually Impaired People: A Systematic Review", Institute of Electrical and Electronics Engineers (IEEE), January 2021.
5. Xuhui Hu, Aiguo Song, Hong Zeng, and Dapeng Chen. "Intuitive Environmental Perception Assistance for Blind Amputees Using Spatial Audio Rendering", Institute of Electrical and Electronics Engineers (IEEE), February 2022.
6. Roshan Rajwani, Dinesh Purswani, Paresh Kalinani, Deesha Ramchandani, and Indu Dokare. "Proposed System on Object Detection for Visually Impaired People", International Journal of Information Technology (IJIT), April 2020.
7. Farhin Faiza Neha, and Kazi Hassan Shakib. "Development of a Smartphone-based Real Time Outdoor Navigational System for Visually Impaired People", International Conference on Information and Communication Technology for Sustainable Development (ICICT4SD), February 2021.
8. Ajinkya Badave, Rathin Jagtap, Rizina Kaovasia, Shivani Rahatwad, Saroja Kulkarni. "Android Based Object Detection System for Visually Impaired", International Conference on Information and Communication Technology for Sustainable Development (ICICT4SD), February 2020.
9. Shadakshari and Dr. Shashidhara H R. "Survey on Smart Assistance for Visually Impaired Person", International Research Journal of Engineering and Technology (IRJET), May 2020.
10. Dr. C. Prema, S. Bharathraj, J. JohnStephen, P. KishorSanthosh, and S. Raja. "Advanced Blind Helper App", International Journal of Creative Research Thoughts (IJCRT), May 2023

Internet of Things (IoT) based Health Monitoring System

Reena Thakur
Department of Computer Science & Engineering
Jhulelal Institute of Technology
Nagpur, Maharashtra
✉ rina151174@gmail.com

Gaurav Sarva, Deepak Sigh Thakur
Ronit Jaiswal
Department of Computer Science & Engineering
Jhulelal Institute of Technology
Nagpur, Maharashtra

Sohel Bhura
Computer Science & Engineering
Rashtrasant Tukdoji Maharaj Nagpur University,
Nagpur, Maharashtra
✉ s.bhura@jitnagpur.edu.in

ABSTRACT

This invention discloses a novel healthcare monitoring and assistance system designed specifically for individuals with paralysis, leveraging the power of Internet of Things (IoT) technology. The primary objective is to bridge the communication gap between caregivers and patients experiencing limited mobility. This is achieved through a single, sensor-laden glove equipped with microcontrollers, allowing patients to effectively communicate their needs via intuitive hand gestures. The system integrates a Node MCU ESP8266 microcontroller for processing, a DS18B20 temperature sensor, an ADXL100 accelerometer for gesture recognition, heart rate and blood pressure sensors for vital sign monitoring, and optionally a display unit for user feedback. Each pre-defined hand gesture is meticulously mapped to a specific message, enabling patients to request assistance, report emergencies, or express basic needs like food and water. Real-time data processing and transmission are facilitated by the Blynk IoT platform, granting caregivers remote access to critical patient information. Extensive testing underscores the system's exceptional accuracy in gesture recognition and prompt notification of caregivers.

KEYWORDS *: Health monitoring, Analysis system, IoT, hand gestures, Real-time processing, Blynk IOT platform, Remote monitoring, Level of care.*

INTRODUCTION

Paralysis is a multifaceted medical condition leading to the loss of muscle function in one or more body parts, commonly resulting from injuries or diseases that affect the nervous system. This ailment significantly hinders an individual's capacity to carry out daily tasks independently, requiring continuous assistance and care from relatives or trained caregivers. The presence of communication barriers between individuals with paralysis and their caregivers presents notable obstacles, as established methods of expressing needs or emergencies may be restricted by the patient's physical constraints or impaired speech.

Caregivers often have to depend on manual observation or occasional check-ins to evaluate the well-being of patients with paralysis. This can result in delays in addressing urgent needs or medical emergencies. Additionally, the constant requirement for supervision can significantly strain caregivers both physically and emotionally, leading to burnout and a decline in the quality of care provided to the patient.

The critical necessity for innovative solutions to enhance communication and monitoring for individuals with paralysis is acknowledged in this document, which introduces an IoT-based health monitoring and analysis framework tailored specifically to tackle these issues. By utilizing state-of-the-art sensor technology and wireless connectivity, this system strives to create a seamless and responsive communication pathway between patients and caregivers, enabling prompt assistance and enhancing the overall quality of healthcare provided.

The creation of this system is driven by the following primary factors:

- Communication Challenges: Individuals with paralysis often encounter obstacles in articulating their needs or emergencies due to physical limitations. Conventional communication approaches may prove insufficient or unreliable, resulting in misunderstandings and delays in securing necessary aid.
- Caregiver Stress: The task of caring for paralysis patients can be physically and emotionally taxing, especially when constant supervision is essential. Caregivers may endure heightened levels of stress and fatigue, affecting their capacity to provide effective care and assistance.
- Quality of Life: Enhancing the quality of life for paralysis patients is crucial as it significantly impacts their independence, dignity, and overall welfare. Enhancing communication and monitoring capabilities can empower patients to maintain a higher level of autonomy and control over their daily lives.
- Technological Progress: The emergence of IoT technology presents unparalleled opportunities to transform healthcare services, particularly in the realm of remote monitoring and assistive tools. By leveraging the capabilities of connected devices and real-time data analysis, innovative solutions can be developed to address the unique needs of paralysis patients and their caregivers.

In light of these obstacles and prospects, this article offers an extensive examination of the design, deployment, and assessment of an IoT-based system for monitoring and analyzing the health of paralysis patients. Through the integration of various hardware components, software algorithms, and wireless communication protocols, this system seeks to redefine the standards of care for paralysis patients, promoting greater independence, safety, and well-being.

- In this IoT system, the primary objective is to enhance the cosmology-based response with the ability to track health status. Heart rate is considered one of the "important indicators," or important measures of wellbeing [6]. A website platform was used to display the author's measurements of body temperature and heart rate [7]. In the paper [8], the author displayed the respiratory rate and body temperature on an LCD display along with the heart rate. It was explained in the paper [9] that the author developed a system for calculating heart rate, body temperature, and respiration rate and displaying the results on a mobile device. An author of the paper [10] developed a wearable solution that records the patient's pulse rate and blood pressure using a Raspberry Pi microprocessor. As described in the paper [11], the author devised a wearable device and mobile application that can measure body temperature, heart rate, diabetes, blood pressure, and cough detection. The authors of [12] have not used mobile applications in their design. An Arduino Mega is used by the author in the paper [13] to measure heart rate, body temperature, and blood pressure. IoT-based patient-centered ECG monitoring system developed by T. Y. Hoe et al [14].

LITERATURE SURVEY

The author in [1] presents an innovative solution to address the communication challenges faced by individuals with paralysis. The proposed system allows paralyzed individuals to convey messages using simple hand motions. It functions by reading the tilt directions of a hand-worn glove equipped with a transmitter. An accelerometer captures motion statistics, which are processed by a microcontroller to display corresponding messages on an LCD and trigger a buzzer. Additionally, the system transmits the data to an IoT Adafruit server for online display. This technology empowers paralyzed patients to effectively communicate their needs, enhancing their quality of life

The author in [2] project successfully created an Internet of Things-based patient health tracking system, it may not have explored advanced health sensors or in-depth medical monitoring capabilities. Opportunities for further development include expanding sensor capabilities, implementing advanced analytics, and enhancing patient record management.

The author in [3] addresses the communication challenges faced by paralytic patients who have difficulty expressing their needs. The proposed system enables these individuals to display messages on an LCD screen through simple motions of any body part with motion

abilities. Additionally, the system includes a feature for sending SMS messages via GSM when there is no one available to attend to the patient. Various motion gesture sensors are presented in the paper to assist healthcare professionals in understanding the patient's requirements. Users can convey messages by tilting the device at specific angles, simplifying communication for paralyzed patients. This innovative system offers a vital means for paralytic patients to express their needs effectively and improve their quality of life.

The author of [4] project has successfully addressed communication needs for paralyzed patients and offers affordability, it may not have explored advanced technologies or provided a detailed cost-effectiveness analysis compared to existing solutions. Opportunities for future development include the integration of advanced technologies and a more comprehensive cost analysis. The analysis of survey is given in table 1.

Analysis of literature survey

Table 1 : Literacy Analysis

Year	Author	Title	Objective	Methodology
2013	A. Nelson, J. Schmandt, P. Shyamkumar	Wearable Multi-sensor Gesture Recognition for Paralysis Patients	To address the problem faced by quadriplegic to perform day to day activities.	This system basically uses the sensor technology that senses the gesture and take action according to it.
2015	Mukesh Kumar, Shimi S.L	Voice Recognition Based Home Automation System for Paralyzed People	To design the low-cost voice recognition-based home automation system for the physically challenged people suffering from quadriplegia or paraplegia.	It uses Voice Recognition Module V3 to recognize voice.
2021	Ms. N. Renee Segrid Reddiyar, S.Remina, 3S.Sabrin, 4M.Subhashini	IOT Based Paralysis patient healthcare monitoring system	To develop a device which should be easy to use and should be affordable which consists of basic health care monitoring system with nursing care.	This system has a sensor that senses the movement of a patient and that need any kind of assistance then it will display it on the screen
2019	Malathi M, Preethi D	IoT based patient health Monitoring system	To send alerts to the patient's loved ones or doctor in case of any emergency.	By using the microcontrollers, it sends an alert.
2020	O.Y. Tham, M.A. Markom and A.H. Abu Bakar	IoT Health monitoring Device of oxygen saturation (SpO2) and heart rate level	To monitor the patients that are suffering body sickness.	It consists of four major works which is involved of development of SpO2 and heart rate monitoring with IoT system, data collection and validation, data classification of normal and abnormal level.

METHODOLOGY

The implementation methodology of the project involves a systematic approach to realize the IoT-based paralysis patient health monitoring and analysis system. It commences with the conceptualization and planning phase, wherein the system architecture, hardware components, and overall functionality are outlined [1]. Subsequently, the hardware components are assembled into a wearable glove, integrating microcontrollers, sensors, display, buzzer, and power supplies to ensure both functionality and user comfort.

Following hardware assembly, the software

development phase ensues, focusing on the creation of embedded C/C++ programs. These programs facilitate seamless interaction with sensors and microcontrollers, enabling data acquisition, processing, and transmission. Additionally, gesture recognition algorithms are implemented to interpret hand gestures for intuitive communication [2].

Data acquisition and transmission form another critical aspect of the implementation process. Input data from sensors, including temperature, accelerometer readings for hand gestures, heart rate, and blood pressure, are collected and transmitted to an IoT cloud platform for real-time monitoring and analysis [3]. Rigorous testing and validation are then conducted to ensure the system's functionality, reliability, and accuracy under various conditions. Iterative enhancement based on testing results and user feedback further refines the system's efficiency and usability [4].

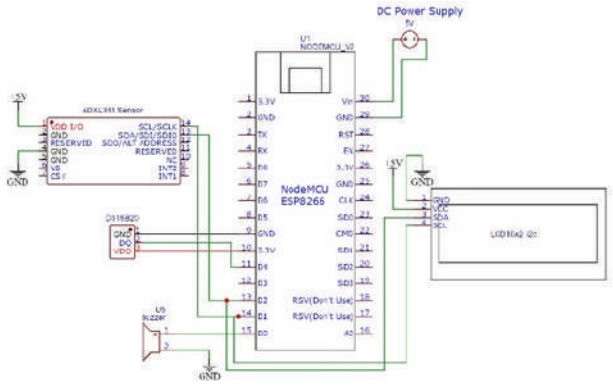

Fig. 1 : Paralysis patient health monitoring circuit diagram

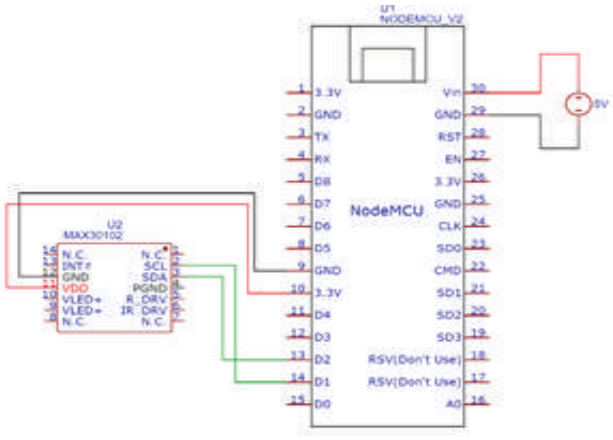

Fig 2 : Paralysis Heart rate MAX30102 circuit diagram

IMPLEMENTATION

Implementation of IoT-Based Health Monitoring and Analysis Framework for Paralysis Patients

System Overview

The IoT-based health monitoring and analysis framework is designed to address the challenges faced by paralysis patients and caregivers. The system integrates various hardware components, including the ESP8266 NodeMCU microcontroller, MAX30100 heart rate and oxygen level sensor, ADXL345 accelerometer, and a 16x2 LCD display, along with software algorithms and wireless communication protocols as shown in figure 1 and 2.

Hardware Implementation

ESP8266 NodeMCU Microcontroller

Functionality

- It Acts as the main controller to manage sensor data acquisition, processing, and communication.
- It Supports Wi-Fi connectivity for data transmission to the cloud server.

Implementation Steps

- Set up the NodeMCU development environment using Arduino IDE.
- Write firmware to initialize sensors, collect data, and transmit it to the cloud server.

MAX30100 Heart Rate and Oxygen Level Sensor

Functionality:

- Measures heart rate and blood oxygen levels tomonitor the patient's vital signs.

Implementation Steps

- Connect the MAX30100 sensor to the NodeMCU using I2C communication.
- Develop firmware to read sensor data and preprocess it for transmission.

ADXL345 Accelerometer

Functionality

- Measures acceleration and movement to monitor the patient's activity and posture.

Implementation Steps

- Connect the ADXL345 accelerometer to the NodeMCU using I2C or SPI communication.
- Develop firmware to read accelerometer data and preprocess it for transmission.

16x2 LCD Display

Functionality

- Displays real-time sensor data, alerts, and status information locally.

Implementation Steps

- Connect the 16x2 LCD display to the NodeMCU using GPIO pins.
- Write firmware to update the display with relevant information.

Software Implementation

Data Transmission

Wi-Fi Communication

- Implement Wi-Fi communication protocols to establish a connection with the cloud server.
- Send sensor data to the cloud server at regular intervals or upon detecting abnormal conditions.

Local Display

User Interface:

- Develop firmware to update the 16x2 LCD display with real-time sensor data, alerts, and status information.
- Implement features to display heart rate, oxygen levels, and activity levels as shown in figure 3.

Integration and Testing

System Integration:

Integrate the ESP8266 NodeMCU microcontroller, MAX30100 sensor, ADXL345 accelerometer, and 16x2 LCD display to create a cohesive monitoring system.

Testing

- Perform unit testing to validate the functionality of individual components.
- Perform integration testing to make sure all components communicate and share data smoothly.
- Validate the accuracy and reliability of sensor data through comparison with known standards or manual measurements.

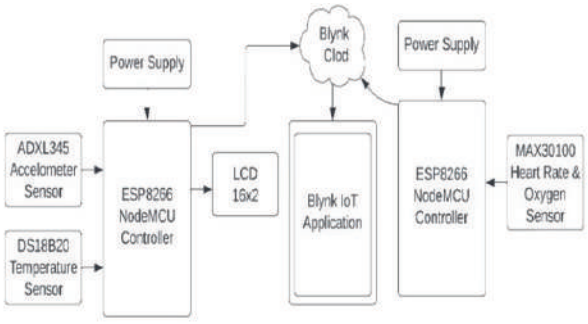

Fig. 3 Data flow from sensors to the Blynk server

DATA FLOW DIAGRAM

The flowchart depicted a comprehensive health monitoring system that collects and processes various physiological data from a patient. [1] The system utilizes an array of sensors, including an accelerometer, temperature sensor, and heart rate/oxygen sensor, to gather crucial health information. [1,3] This data is then processed by a microcontroller, converted into messages, and displayed on an LCD screen, while also being transmitted to a remote Blynk IoT application for further monitoring and analysis. [1,3] The system follows a structured process to initialize the sensors, read the patient's vitals, and detect any hand movements that could indicate paralysis or mobility issues. [1,3] This integrated approach to patient monitoring demonstrates the integration of multiple technologies to provide a holistic view of the patient's health condition. [1,3,5]

The figure 4 depicts a step-by-step process for PARMITRA : health monitoring system. The process begins by initializing all input sensors, which is a crucial first step to ensure the system is ready to collect data. Next, the system reads the patient's body temperature using a DS18B20 sensor. This is followed by reading the patient's heart rate and oxygen level using a Max30100 sensor. These two steps allow the system to gather essential physiological data about the patient's condition. The system then proceeds to read the patient's hand movements (up, down, left, and right) using an

ADXL345 accelerometer sensor. This data can be used to detect and monitor any paralysis or movement-related issues the patient may be experiencing. After collecting the sensor data, the system converts the detected hand movements into respective messages. This conversion process is necessary to translate the raw sensor data into a format that can be easily understood and interpreted. Finally, the system displays all the collected sensor information on a 16x2 LCD. Additionally, it sends the entire dataset to a Blynk IoT application through an ESP8266 controller. This allows the data to be remotely accessed and analyzed for further medical monitoring and decision-making The flowchart also includes a decision point to check for internet connectivity. If the connection is not available, the system will recheck the internet connection before sending the data to the Blynk application.

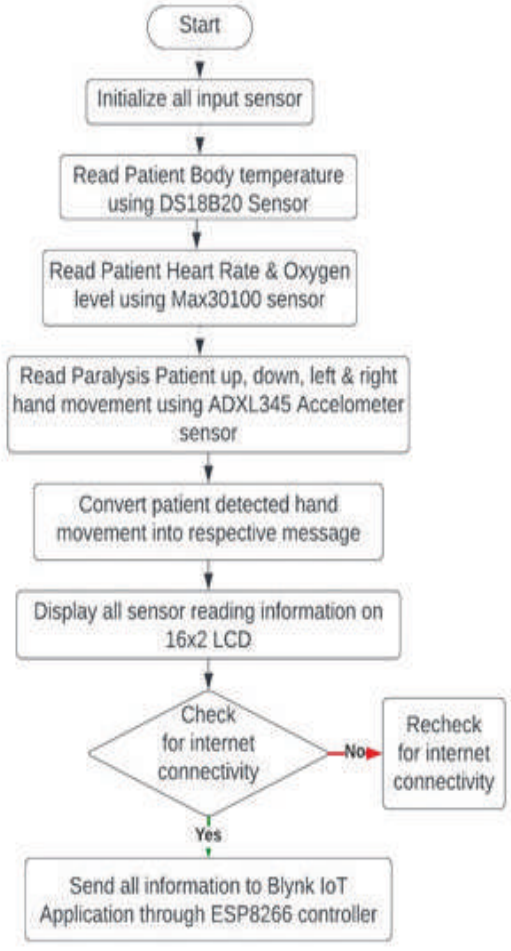

Fig. 4 Algorithm for data flow of Blynk Server

RESULT

Table 2 shows the patient cases

Table 2: Accelerometer values for glove

Motion of Glove	Indication in Accelerometer	Magnitude representation in Accelerometer	Message in LCD Display
Case 1: Glove with no motion	Remains the same as of the earth gravitational force.	Both the X and Y coordinates of the accelerometer read zero	No Input
Case 2: Upward motion if glove	The accelerometer has registered a positive magnitude in the vertical axis with respect to Earth's gravitational force	The Accelero-meter's Y coordinates range from zero to five(0 to +5)	Need Water
Case 3: Downward motion of glove	The accelerometer has registered a negative magnitude in the vertical axis with respect to Earth's gravitational force	The Acceler-ometer's Y coordinates range from zero to five(-5 to 0)	Need Food
Case 4: Rightward motion of glove	The accelerometer has registered a positive magnitude in the horizantal axis with respect to Earth's gravitational force	The Acceler-ometer's X coordinates range from zero to five(0 to +5)	Some Emergency
Case 5: Leftward motion of glove	The accelerometer has registered a negative magnitude in the horizontal axis with respect to Earth's gravitational force	The Acceler-ometer's X coordinates range from zero to five(-5 to 0)	Call Attendant

Need Water

Fig 5 Need Water

Figure 5 shows that the patient has moved his hand in upward direction which indicates his need of water, was accurately captured and displayed on the Blynk cloud application through a graph. This successful communication between the patient's gesture and the device showcases the effective functionality of the system.

Need Food

Fig. 6 Need Food

Figure 6 shows the moment of the patient's hand in a downward direction serves as an intuitive gesture indicating his need for food. This data is seamlessly transmitted and visualized on the Blynk cloud application as a graph. The consistency and accurate of this representation affirm then the device is functioning effectively, providing real-time feedback and aiding caregivers in timely interventions.

Some Emergency

Fig. 7 Some Emergency

Figure 7 shows the patient's movement of his hand to the right was a deliberate action to signal an emergency, which the device accurately captured and transmitted. This real-time data was then displayed as a graph on the Blynk cloud application, validating the device's functionality and its ability to promptly respond to the patient's needs, the successful integration of the device with the application ensures timely alerts and effective monitoring.

Call Attendant

Fig 8 Call Attendent

Figure 8 shows the moment of the patient's hand in the leftward direction successfully triggered the call attend function, demonstrating the device's responsiveness and accuracy. This data was promptly reflected on the Blynk cloud application, where it appeared as a graph. The graph's of the event further confirms that the device is functioning as intended and effectively communicating with the cloud platform.

Heart Rate and Oxygen level

Fig. 9 Heart Rate and Oxygen level

Figure 9 shows the graph displayed on the Blynk cloud application showcases the real-time measurements of heart rate and oxygen levels. This visual representation assures us that the device is functioning accurately and efficiently. It provides a clear and continuous monitoring system, enabling users to track their health metrics seamlessly. This data-driven approach enhances the reliability and usability of the device, ensuring users can trust its performance.

CONCLUSION & FUTURE WORK

The healthcare sector has been transformed by the Internet of Things (IoT), bringing about innovative solutions to enrich patient care and enhance quality of life. This project has effectively implemented an IoT-driven system for monitoring and analyzing the health of paralysis patients, aimed at improving communication between patients and caregivers while ensuring real-time tracking of essential health metrics.

The key elements of this system, including microcontrollers, sensors, and IoT connectivity, were carefully integrated into a wearable glove. Through an accelerometer-based gesture recognition algorithm developed in Embedded C++, the system accurately interpreted hand movements to convey messages, enabling patients to express their needs easily. Continuous monitoring of physiological data, such as temperature, heart rate, and blood pressure, provided valuable insights into the patient's overall health.

Integration with the Blynk IoT platform facilitated seamless data transfer and real-time data visualization, offering caregivers timely access to critical patient information. Extensive testing of the system's responsiveness, reliability, and user-friendliness validated its practical utility in real-world scenarios.

While the current system marks a significant advancement in enhancing care for paralysis patients, there are opportunities for further improvement. Future iterations could involve incorporating additional sensors like oximetry for oxygen levels or electroencephalography (EEG) for monitoring brain activity. Additionally, leveraging advanced machine learning algorithms for gesture recognition could enhance accuracy and broaden the range of detected gestures.

Moreover, integrating voice recognition and natural language processing capabilities could enable more intuitive communication, allowing patients to express their needs verbally. Incorporating cloud computing and big data analytics could offer valuable insights into health trends, supporting predictive analytics and personalized care recommendations.

In conclusion, this IoT-based system for monitoring and analyzing the health of paralysis patients showcases the potential of technological innovations to empower individuals with disabilities, promoting independence and enhancing their overall quality of life. By addressing the unique challenges encountered by paralysis patients, this project contributes to the broader goal of inclusive and accessible healthcare, aligning with the principles of universal design and assistive technology.

REFERENCES

1. A. Nelson, J. Schmandt, P. Shyamkumar: Wearable Multi-sensor Gesture Recognition for Paralysis Patients in 2013.
2. Mukesh Kumar, Shimi S.L: Voice Recognition Based Home Automation System for Paralyzed People in 2015.
3. Ms.N.Renee Segrid Reddiyar, Remina, Sabrin, Subhashini: IOT Based Paralysis patient healthcare monitoring system in 2021
4. Malathi M, Preethi D: IoT based patient health Monitoring system in 2019.
5. O.Y. Tham, M.A. Markom and A.H. Abu Bakar: IoT Health monitoring Device of oxygen saturation(SpO2) and heart rate level in 2020.
6. M. MacGill, "What should my heart rate be?" 2021, https://www.medicalnewstoday.com/articles/235710.
7. P. Valsalan, T. A. B. Baomar, and A. H. O. Baabood, "IOT based health monitoring system," Advance Scientific Research, vol. 7, no. 4, pp. 3-4, 2020.
8. N. Arunpradeep and G. N. G. Suseela, "Smart healthcare monitoring system using IoT," International Journal of Advanced Science and Technology, vol. 29, no. 6, pp. 2788–2796, 2020.
9. A. Shivam and G. Amita, "IOT smart health monitoring system," in Proceedings of the .International Conference

on Innovative Computing & Communications, pp. 1–8, New Delhi, India, 2020.

10. S. Banka, I. Madan, and S. S. Saranya, "Smart healthcare monitoring using IoT," International Journal of Applied Engineering Research, vol. 13, no. 15, Article ID 11984, 2018.

11. M. Saranya, R. Preethi, M. Rupasriand, and S. Veena, "A survey on health monitoring system by using IOT," International Journal for Research in Applied Science and Engineering Technology, vol. 6, no. 3, pp. 778–782, 2018.

12. A. Kotevski, N. Koceska, and S. Koceski, "E-health monitoring system," in Proceedings of the International Conference on Applied Internet and Information Technologies, pp. 259–265, Bitola, Macedonia, 2016.

13. M. Fezari, R. Rasras, and I. M. M. E. Emary, "Ambulatory health monitoring system using wireless sensors node," Procedia Computer Science, vol. 65, pp. 86–94, 2015.

14. H. T. Yew, M. F. Ng, S. Z. Ping, S. K. Chung, A. Chekima, and J. A. Dargham, "IoT based real-time remote patient monitoring system," in Proceedings of the 2020 16th IEEE International Colloquium on Signal Processing & Its Applications (CSPA), pp. 176–179, Langkawi, Malaysia, Febraury 2020.

A Cutting-Edge and Hybrid Encryption with Steganography Framework for Medical Image Transmission in Securing Patient Privacy

Mohan Manju
Research Scholar
Department of Computer Science
Shri Rawatpura Sarkar University
Raipur, Chhattisgarh
✉ manjupillai111@gmail.com

Rajesh Kumar Pathak
Vice Chancellor
Om Parkash Jogender Singh University
Rajasthan

ABSTRACT

In the field of medical data transmission, this paper introduces a novel hybrid encryption system that seamlessly integrates cryptography and steganography techniques to improve the security of medical images during patient information delivery over network. By addressing the vulnerabilities inherent in existing symmetric and asymmetric methods, our approach goes beyond traditional practices that rely on transport layer security protocols for message confidentiality, authentication, and key exchange. The proposed hybrid system not only strengthens the privacy of medical images but also enhances the overall security by combining encryption and steganography methods. This paper provides a detailed study of the hybrid system methodology, implementation details, and performance analysis. By combining cryptographic strength with confidential communications, our approach aims to set new standards in securing medical image transmission, which is highly sensitive, providing valuable insights for the ongoing security negotiation of critical health information in the digital age. Through rigorous analysis and testing, this research sets the stage for a robust and advanced security paradigm in medical data security.

KEYWORDS *: Medical Image Security, Hybrid Encryption, Healthcare Information Security, Steganography, Cryptographic Techniques.*

INTRODUCTION

In the health care information industry, the need to protect medical images during transmission has prompted critical review of existing encryption methods. Although traditional encryption embedded within transport layer security has proven effective in maintaining confidentiality and facilitating secure key exchange, its sensitivity to traffic analysis and potential visibility during transmission requires careful re-evaluation. This research overcomes the inherent limitations of traditional encryption by introducing a hybrid system, combining cryptography and steganography. Encryption, characterized by sophisticated cryptographic algorithms and key management, is the foundation of protecting data integrity and privacy [1]. However, the apparent presence of encrypted data creates vulnerability, making it susceptible to malicious analysis. The hybrid system outlined here incorporates steganographic techniques to obscure the visibility of encrypted medical images. Steganography, as an induced cloaking technique, introduces covert communications by embedding encrypted data within seemingly innocuous carriers.

This dual-layer approach aims to reduce the identification efficiency associated with encrypted data, thereby improving the overall security level during transmission.

The motivation for this research comes from the flexibility required by contemporary cyber threat detection and security protocols. While encryption forms the foundation of data security, the hybrid model introduced here strategically complements encryption

methods, providing an enhanced protection mechanism against potential breaches. This research highlights the need for a dynamic paradigm that recognizes the central role of encryption in data security and incorporates steganography to mitigate the limitations inherent in traditional encryption [2]. The sections that follow explore the technical specifics of the hybrid system, explaining its functioning, implementation, and subsequent performance evaluation. Thus, this research represents an important contribution to advancing the discussion on the security of medical image transmission, which aligns with the need for adaptive, multifaceted security measures in the health information sector.

Real Challenges in Medical Data Sharing

The landscape of medical data sharing presents deep challenges in the inherent sensitivity of health information and the need to protect patient privacy. The complexities of this area arise from the need to balance the progress of medical research and treatment ethics with the ethical responsibility to protect personal health data. One of the main challenges revolves around the inherent sensitivity of clinical data. From diagnosis to treatment plans, patient records contain in-depth details of a person's health journey [3]. The challenge is to uncover the potential of medical advancements while ensuring the confidentiality of this gold mine of health information. Striking a delicate balance between accesses to data for research purposes and maintaining patient privacy is a delicate task.

Legal frameworks such as the Health Insurance Portability and Accountability Act (HIPAA) emphasize the critical importance of patient privacy. Adherence to such norms is not only a legal obligation but also a fundamental moral commitment. However, duality appears when attempting to facilitate sharing of clinical data for innovative research and treatments within the scope of legal and ethical considerations. Therefore, the challenge is to navigate this legal landscape effectively, while ensuring that data sharing practices comply with established privacy standards.

On the technology front, the proliferation of interconnected health care systems introduces cybersecurity challenges. The fear of unauthorized access, data breaches or malicious exploitation requires a strong security infrastructure. Maintaining technological innovation in medical data sharing while minimizing cybersecurity risks is a major challenge, requiring continuous improvements in encryption, access controls, and network security. Patient privacy so important in this complex scenario. Beyond legal and ethical requirements, patient confidentiality protects the sanctity of the doctor-patient relationship. When individuals are assured of the confidentiality of their data, they are more likely to share detailed health information. Patient-centred care depends on the seamless flow of accurate health information, with patients feeling safe in disclosing the specifics of their health status.

The challenges in sharing medical data lie at the intersection of technical, legal, and ethical considerations. Resolving these challenges is fundamental not only to advancing medical research and to treatment, but also to fostering the trust and confidentiality inherent in the doctor-patient relationship. Continued development of strategies to address these challenges is essential to the development of a healthcare ecosystem that embraces change with unquestioning respect for patient privacy.

Objective

The main objective of this research is to address the multifaceted challenges inherent in sharing medical data and to emphasize the critical importance of patient privacy in the contemporary landscape of health information. The key objectives include:

Develop a sophisticated encryption method using MATLAB for enhancing the security of grey medical images over a firewall network. The design will leverage advanced techniques to ensure robust protection of sensitive medical image data.

Implement a real-time loop-based secure wall encryption, operating in real-time, will serve as a protective layer, contributing to the overall safeguarding of sensitive medical images.

Conduct an in-depth study and comparative analysis of various image encryption techniques. This involves assessing the strengths and weaknesses of different methods, providing insights into their applicability, and informing the development of an advanced encryption approach for medical images.

Provide practical solutions to navigate challenges, ensuring a balance between technological advancements, legal compliance, and ethical considerations while preserving patient privacy.

LITERATURE REVIEW

The increase in the transmission of medical images over wired and wireless networks with the integration of telemedicine technology has led researchers to explore powerful encryption technologies that ensure the security of medical data during delivery. Many important contributions have been made to this field, each addressing different aspects of encryption and security.

The paper [4] proposed a method using pixel layout and random permutations for medical image coding. Their approach involves random permutations and a simple arrangement of pixels, which ensure high computing speed. Using long permutation keys derived from the large size of the image helped resist brute force attacks.

In the [5] introduced an algorithm combining chaotic graph and chaotic techniques for color coding of medical images. They used 2D minus triangular map and a helix algorithm for blurred gray values to process the pixel addresses of the image. Interestingly, their method showed resistance to brute force attacks.

In [6] presented "Edge Crypt", a method for lossless encryption of medical images using edge maps. Their innovative algorithm used information from the contour map to encode medical images, showing a match to grayscale or color images.

Cryptography and steganography are considered important in ensuring confidentiality and integrity [7]. In cryptography, encryption is a fundamental technique, whether symmetric or asymmetric. Symmetric encryption, exemplified by Advanced Encryption Standard (AES), uses a shared key for encryption and decryption. Asymmetric encryption, characterized by Diffie-Hellman key exchange and RSA algorithms, uses different keys for encryption and decryption.

The literature emphasizes the integration of cryptography and steganography for a more secure system [14] [15]. One study encrypted medical images using a sorted sequence and then encoded the initial value of that sequence using the RSA algorithm [10]. Another study investigated quantum Gray code scrambling and quantum XOR operations controlled by a logistic sign diagram [16]. Pixel swapping and block-level encryption based on frequency bands have been explored differently [17]. Additionally, the use of MJEA (Modified Jamal Encryption Algorithm) and bit-by-bit XOR has been considered for cryptographic and steganographic purposes, considering medical images and information as distinct shares [18].

Research studies are increasingly recognizing the potential of sequence secure force algorithm shows unique capabilities when applied to encryption of medical images. Its dynamic, sequence-based encryption ensures enhanced security by introducing unpredictability and adjustability into the encryption process. This is especially important in health care environments where confidentiality of medical images is important. The algorithm's robust security measures make it resilient against a variety of cryptographic attacks, while its customizable parameters allow ready-made encryption systems to meet specific clinical data needs. The algorithm integrates seamlessly with other encryption methods, providing a comprehensive and layered approach to securing medical images.

Its computing performance is remarkable, meeting the real-time processing demands often encountered in healthcare situations. Due to its resistance to cryptanalysis and adaptability to various medical image formats and resolutions, sequence protection algorithms are emerging as an efficient tool for protecting sensitive medical information. Medical image coding has seen a paradigm shift with the integration of sequence secure force algorithm and chaotic methods, representing a significant step towards improved security and performance. With sequence secure force encryption algorithm, chaotic methods provide an additional layer of security. By introducing randomness and nonlinearity, chaotic methods create challenges for potential attackers in predicting patterns in encrypted medical images. The increase in key space resulting from chaotic methods improves resistance to brute force attacks, thereby strengthening the overall security of medical image encryption systems. Additionally, dynamic key generation supported by chaotic systems

adds an element of unpredictability over time, making it more difficult for attackers to decrypt encrypted medical images. The integration between sequence secure force encryption algorithm and chaotic methods offers a dynamic approach to medical image coding that meets the growing security needs of healthcare systems.

Although sequence secure force algorithm and chaotic methods have significant advantages, it is important to consider the limitations of alternative technologies when it comes to medical image coding. Symmetric encryption methods such as the widely used Advanced Encryption Standard (AES) face challenges in key distribution and management, including protecting the shared key during transmission. Quantum encryption, while theoretically secure, faces practical implementation challenges and requires advanced quantum computing infrastructure. Asymmetric encryption systems have public and private key management issues, making secure distribution and management in large-scale medical imaging systems difficult. In this context, the combination of sequence secure force algorithm and chaotic methods appears to be a practical and sophisticated solution, overcoming some of the limitations associated with traditional coding techniques. The combination of sequence secure force algorithm and chaotic methods is at the forefront of modern medical image coding. By exploiting the accuracy and adaptability of sequence secure force algorithm to chaotic patterns and randomness of key management dynamics, this approach not only improves security, but also addresses practical challenges faced by alternative technologies. As healthcare systems increasingly rely on digital data, the symbiotic relationship between sequence secure force algorithm and chaotic methods represents a promising direction for preserving critical medical images in the era of emerging healthcare technologies.

METHODOLOGY

In this comprehensive patient diagnosis workflow, medical images are acquired and immediately subjected to pre-processing and encryption to ensure patient privacy. The encrypted images are transmitted securely to a cloud network, where they undergo steganography embedding to further safeguard sensitive data. Steganography conceals patient information within the encrypted images, providing an additional layer of covert security. Authorized healthcare professionals can then decrypt and access the original images for diagnostic analysis, utilizing the embedded data for context. After analysis, any added information is re-encrypted before secure communication and reporting. As an innovative encryption measure, the patient image's encrypted data is subjected to a multimer and loop encryption.

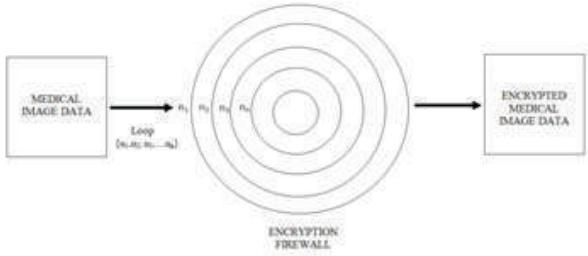

Fig. 1: Encryption system with n numbers of loop

This involves applying multiple encryption algorithms in a loop, enhancing the complexity and resilience against unauthorized access. This innovative approach ensures that even if one layer of encryption is compromised, the multimer and loop process adds an additional barrier, reinforcing the overall security of patient data in medical images throughout the entire diagnostic process.

System Methodology

The computational method is designed to provide a structured and efficient framework to implement the proposed medical image encryption and steganography process. This process involves several critical steps to ensure a complete and secure workflow.

Image Acquisition and Pre-processing

Image acquisition and pre-processing constitute the first steps in the medical imaging workflow, providing the basis for subsequent analysis and interpretation. The process begins by acquiring raw images from various medical imaging modalities such as X-ray, MRI or CT scan. These raw images may contain noise, artifacts or inconsistencies that can influence the accuracy of diagnostic procedures.

Pre-processing techniques are applied to resolve these issues and improve the quality of acquired images. Common pre-processing steps include noise reduction, contrast adjustment, and spatial filtering.

These techniques aim to improve the overall clarity and interpretability of images, ensuring that subsequent analysis is based on high-quality visual data. Successful image acquisition and preprocessing are essential for generating accurate and reliable medical images, laying the foundation for accurate diagnostic assessments in healthcare settings.

Create Secure Firewall for Input Medical Image

In setting up a secure firewall for inputting medical images, an innovative approach involving a firewall loop with patient name details was applied. This unique system architecture ensures additional security for critical clinical data. In each firewall loop, patient name details are intricately woven into the security architecture. This customized integration adds a contextual layer to the firewall, improving its effectiveness in protecting personal medical information. To further strengthen, this security measure, encryption is systematically applied to each loop.

The encryption process ensures that patient-specific data remains confidential and protected from unauthorized access. This iterative encryption in the firewall loop protects not only the patient's identity, but also the entire medical image dataset, contributing to a strong and comprehensive security infrastructure. The combination of optimized firewall loops and encryption mechanisms creates a reinforced security that ensures the integrity and confidentiality of medical images input into healthcare systems.

Encrypt Image

In the proposed security architecture for input medical images, a sophisticated two-tiered encryption system is implemented, combining Sequence Secure Force encryption with Chaotic encryption within each firewall loop. It introduces unpredictability and adaptability to the encryption process, enhancing security.

Mathematically, the Sequence Secure Force algorithm operates dynamically, ensuring robust protection of patient-specific data against unauthorized access. The integration of Sequence Secure Force and Chaotic Encryption within secure firewall loops represents a robust approach to fortify the security of input medical images in healthcare systems.

Establish a secure firewall loop that connects the entire encryption process. These loops act as closed circuits, ensuring that medical images pass through a series of security measures before reaching their destination. Integrate sequential secure force encryption algorithms into the firewall loop. Adapt the algorithm parameters to match the characteristics of medical images. Reuse algorithms within cycles to dynamically optimize the encryption process.

$$X_{n+1} = (aX_{n+c}) \mod m \quad (1)$$

Where, X_nis the current value in the sequence, a is a constant multiplier, c is an increment, and mis the modulus.

In the subsequent layer of security, Chaotic encryption is applied within each firewall loop. Chaotic encryption introduces a high level of unpredictability through chaotic dynamics, which can be expressed using mathematical models such as the logistic map:

$$x_{n+1} = r.x_n (1-x_n) \quad (2)$$

Where, r is the control parameter, and x_n represents the chaotic sequence. The iterative application of chaotic dynamics within each loop adds an extra layer of complexity, making it extremely challenging potential adversaries to decipher the encrypted patient name details. The synergy between Sequence Secure Force and Chaotic encryption not only leverages the mathematical rigor of Sequence Secure Force but also introduces chaos-based randomness, creating a robust and dynamic security framework for input medical images.

By integrating Sequence Secure Force and chaotic encryption into the firewall loop, the security architecture becomes not only customizable but also more flexible. Sequence Secure Force provides a robust initial encoding layer based on pattern recognition, while chaotic encoding adds a dynamic and unpredictable component.

Together, they developed a comprehensive security framework that protects patient identity and medical image data throughout the input process, while strengthening the confidentiality and integrity of sensitive health information.

Apply Dual-Layer security using Steganography

In addition to double-layer encryption using sequence secure force algorithm and chaotic methods within the firewall loop, an additional security measure is implemented using steganography. Steganography enhances the privacy of security architecture by embedding sensitive information within harmless cover data.

In the context of medical image security, a steganographic algorithm has been introduced to hide encrypted patient-specific details. Encrypted patient data, previously protected by sequence secure force algorithm and chaotic encoding, is strategically embedded within the pixel values of medical images. Encrypted patient data is seamlessly integrated to ensure there is no change to the visual appearance of the clinical images. This steganographic layer adds an additional dimension to the security architecture, making it more difficult for potential adversaries to view or manipulate patient information hidden in medical images. The combined use of sequence secure force algorithm and chaotic encryption with steganography establishes a comprehensive and adaptive security framework to protect critical clinical data throughout the entire process.

Share data to over cloud

Sharing data in the cloud means sending and storing information in a secure and accessible way. Once medical images are generated with advanced security features including sequence secure force algorithm and steganography as well as obfuscated encryption, they are shared over a cloud network for collaborative and remote access by authorized healthcare professionals.

Apply Decode Steganography

The decoding process of steganography involves extracting hidden information from data that appears normal or unchanged. In the context of medical image security, once steganographically embedded and encrypted medical images are accessed from the cloud, a decoding process is initiated to reveal hidden patient-specific details. To decode steganographic information, data embedded in medical images must be extracted. This extraction uses a decoding algorithm that reverses the process used during steganography.

Decryption applies with Firewall loops

The decryption within the firewall loops is an intricate and coordinated process, where each layer of encryption is systematically reversed. This ensures that only authorized healthcare professionals, equipped with the correct decryption keys, can access the patient-specific information in its original form. The careful orchestration of decryption within the firewall loops adds an extra layer of security, making it challenging unauthorized entities to decipher sensitive medical data. Ultimately, this decryption process facilitates the secure retrieval of patient information for diagnostic analysis, preserving the confidentiality and integrity of healthcare data.

SYSTEM DESIGN AND IMPLEMENTATION

In the area of protecting sensitive medical information, the early stages of system design involve careful and thorough analysis of various encryption methods. The main goal is to define an approach that provides optimal security, computational efficiency, and adaptability to the dynamic nature of clinical datasets. Factors such as resistance to potential attacks and the ability to maintain data integrity are important considerations in this analysis. Many encryption methods are studied, ranging from traditional algorithms to advanced techniques.

The thorough testing includes simulated scenarios and real-world testing to evaluate the performance of each method under different conditions. sequence secure force algorithm and chaotic encoding emerged as ideal candidates, each bringing unique strengths. sequence secure force encryption algorithm, has proven to be a structured and effective way to encode patient data.

On the other hand, chaotic encryption introduces an element of unpredictability, which improves the overall security of the system. The combination of sequence secure force algorithm and chaotic encoding presents a hybrid model that harmoniously combines the structured approach of sequence secure force algorithm with the dynamic and unpredictable nature of chaotic dynamics.

The goal of this hybrid is to take advantage of the complementary strengths of the two methods, creating a robust and adaptable encryption architecture.

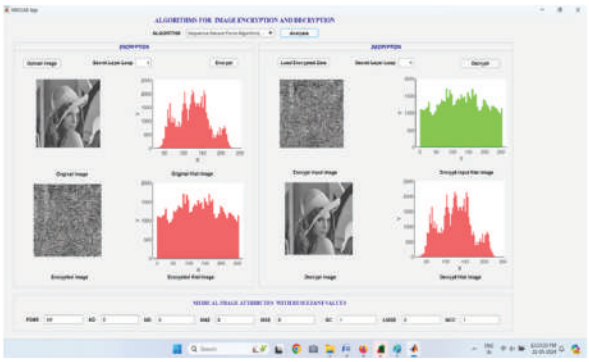

Fig. 2 - MATLAB GUI model for comparison and analysis of different encryption with different loop conditions

Integrating sequence secure force algorithm with Chaotic Encryption and Dual-Layer Protection

Attention was given to the practical implementation of the system by establishing a hybrid model. The dataset selected for this implementation includes patient information and clinical images, which are inherently sensitive and require advanced security mechanisms. The first layer of security involves the use of a hybrid model within a secure firewall ring. This looped structure ensures consistent and repeatable execution of the sequence secure force algorithm and chaotic encoding, adding layers of complexity to the security architecture.

In this context, sequence secure force algorithm played an important role in pattern recognition, which transforms patient data into a secure format. Also, chaotic encryption introduces chaotic dynamics into the encryption process, making it more resistant to potential attacks.

As an additional precaution, a dual-tier security mechanism with steganography has been introduced. This involves hiding patient information encrypted within the pixel values of medical images. Steganographic Process Even if an unauthorized entity accesses the images, deciphering hidden patient information can be a complex and challenging task. After encryption and steganographic embedding processes, the next step involves the secure transmission of medical images to cloud storage.

This step is critical in enabling seamless access to health care professionals while maintaining the confidentiality and integrity of the data exchanged. Secure communication protocols such as HTTPS are used to ensure that encryption is not compromised during transmission.

Once stored securely in the cloud, medical images can be retrieved for clinical testing by healthcare professionals with appropriate authentication credentials. A double-layer security mechanism remains intact during extraction, providing additional protection even in the event of unauthorized access. This comprehensive implementation ensured that patient privacy was protected and sensitive medical information remained secure throughout the process.

Building a Robust and Secure Framework

Implementing the hybrid model in a secure firewall loop, complemented by steganography, provides multiple layers of protection against potential threats. Recursive use of sequence secure force algorithm and chaotic encryption ensures adaptability to security challenges, while steganography adds an additional privacy screen to encrypted patient information. We designed a MATLAB GUI model for user interaction.

The integration of sequential secure force algorithms and chaotic encryption within the firewall loop creates a comprehensive security architecture. This synergy combines the adaptive and dynamic nature of the Sequence Secure Force algorithm with the chaos-based randomness introduced by chaotic encryption. Together, they provide a strong layer of security that protects patient identity and medical image data during the input process, strengthening the confidentiality and integrity of critical health information. This approach not only improves security, but also allows customization and flexibility within the framework, ensuring its adaptability to different health care situations.

This technology hides encrypted patient information within medical images, adding additional security. Encrypted and decrypted embedded medical images are securely transferred to cloud storage for access by healthcare professionals. This integration ensures a robust and secure framework for handling sensitive medical information, reflecting a comprehensive approach to protecting patient privacy and data integrity during the transfer and storage process.

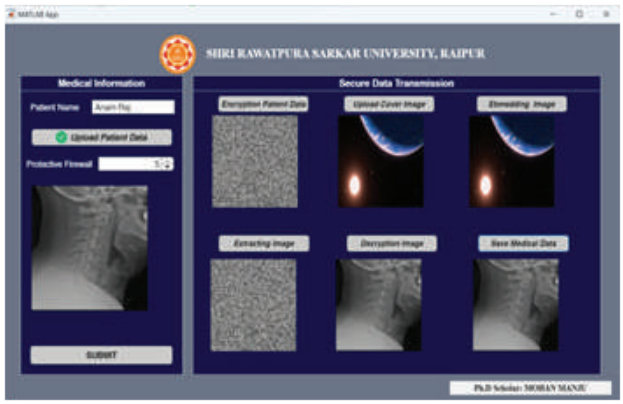

Fig. 3- Implementation of final Software for patient medical data security

RESULT AND DISCUSSION

A detailed evaluation of different encryption methods, followed by the implementation of a hybrid model involving sequence secure force algorithm and chaotic encryption in a secure firewall loop, yielded promising results. A dual-layer security mechanism enhanced by steganography successfully protects critical medical information throughout the process.

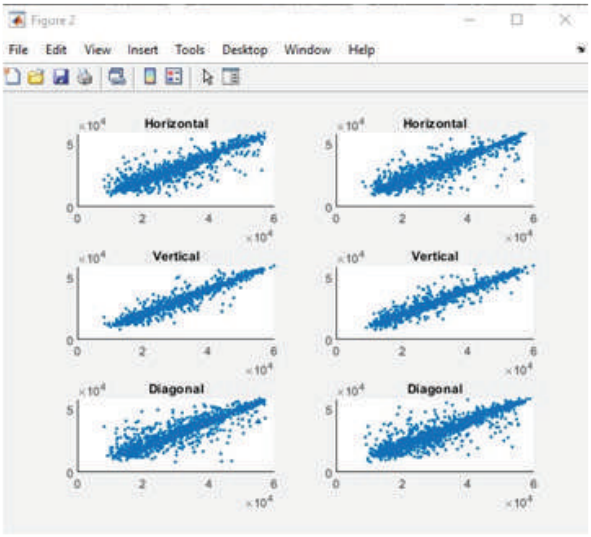

Fig. 4 Secure image and decrypted image pixel information

The hybrid model revealed an efficient encoding strategy exploiting the structured pattern recognition of sequence secure force algorithm and unpredictability of chaotic encoding. Simulations and real-world tests have demonstrated the effectiveness of this approach in protecting patient data within a secure firewall loop. The integration of steganography further strengthens the security framework, providing additional security by hiding encrypted patient information in medical images.

Cloud transmission and storage are essential components of system functionality, maintaining the confidentiality and integrity of transmitted medical images. Healthcare professionals accessing images from the cloud are met with a double-layer security mechanism that ensures hidden patient information remains secure even in the event of unauthorized access.

Table 1- Different Patient data with different medical images

PATIENT ID	*IMAGE TYPE*	*MODALITY*	*DESCRIPTION*
P001	X-ray	Radiography	Chest X-ray for respiratoryanalysis
P002	MRI	Magnetic Resonance Imaging (MRI)	Brain scan for neurologicalassessment
P003	CT Scan	ComputedTomography (CT)	Abdominal scan for internalorganse valuation
P004	Ultrasound	Ultrasonography	Obstetricultrasound for fetaldevelopment

CONCLUSION

Finally, the presented system uses a powerful hybrid encryption model, which combines sequence secure force algorithm and chaotic encryption in a secure firewall loop, complemented by steganography. This comprehensive approach has proven effective in protecting critical clinical information throughout the entire data lifecycle. The structured sequence secure force algorithm, combined with the unpredictability introduced by chaotic dynamics, establishes dynamic and flexible security architecture. Steganography adds an additional layer of concealment, making unauthorized access and interpretation of patient information within medical images more difficult.

Future work in the area of medical data security should explore improvements in algorithmic techniques,

particularly sequence secure force and chaotic dynamics, to further improve hybrid encryption models. The advent of quantum computing has prompted consideration of quantum-resistant encryption techniques for future proofing against potential threats. Applications of machine learning to threat detection, interoperability standards, application improvement, and ethical considerations should remain the focus of research and development. Addressing these areas will ensure that future iterations of the system will continue to evolve and proactively respond to emerging cybersecurity challenges.

The flexibility and robustness of the provided framework makes it a reliable solution for the emerging scenario of medical data security. As healthcare systems become increasingly digitized and interconnected, a commitment to continued innovation, ethics, and user-centred design is essential. By staying ahead of emerging threats and embracing technological advancements, the organization has the potential to make a significant contribution to the secure and responsible management of critical medical information in the healthcare industry.

ACKNOWLEDGEMENT

Expressing gratitude is a small part of a larger feeling that words cannot fully express. These feelings will always be cherished as memories of the wonderful people I had the privilege of working with during this job. I would like to express my heartfelt gratitude to Shri Rawatpura Sarkar University, Raipur, Chhattisgarh, India for the environment which helped me in completing this work.

I express my deep and sincere appreciation to my supervisor Dr. Prof. Rajesh Kumar Pathak. His extensive knowledge and systematic approach to problem solving was invaluable to me. His understanding, encouragement and personal guidance laid a solid foundation for completing this project.

AUTHOR CONTRIBUTIONS

In the exploration of medical image encoding using MATLAB, both authors have made unique contributions to ensure a comprehensive research effort. The author-1 focuses on instrumental in developing and refining encryption algorithms using mathematical modelling, simulation studies, and algorithm development in the MATLAB environment. Her efforts significantly shaped the theoretical foundations of encryption methods. On the other hand, the author-2 focuses on practical implementation and verification aspects, overseeing real code and experiments to validate the proposed encoding methods within the framework of MATLAB.

This collaboration extended to a thorough literature review, integrating existing knowledge and trends to create a well-rounded manuscript that contributes to novel theoretical developments, but also provides a practical perspective for medical image security. Together, the authors produced a research paper that advances the understanding and application of secure medical image encryption by combining theoretical findings and practical implementation using MATLAB.

REFERENCES

1. K. Zhu, Z. Lin and Y. Ding, "A New RSA Image Encryption Algorithm Based on Singular Value Decomposition," International Journal of Pattern Recognition and Artificial Intelligence, vol. 33, no. 1, 2019.
2. L. Zhou, Y. Xiao and W. Chen, "Machine-learning attacks on interference-based optical encryption: experimental demonstration," Optics Express, vol. 27, no. 18, 2019.
3. Y. Zhang, Test and Verification of AES Used for Image Encryption, vol. 9, 2018.
4. Y. Q. Zhang, J. L. Hao and X. Y. Wang, "An Efficient Image Encryption Scheme Based on S-Boxes and Fractional-Order Differential Logistic Map," IEEE Access, vol. 8, 2020.
5. Q. Zhang, L. Guo and X. Wei, "Image encryption using DNA addition combining with chaotic maps," Mathematical and Computer Modelling, vol. 52, no. 11-12, 2010.
6. S. Priya and B. Santhi, "A Novel Visual Medical Image Encryption for Secure Transmission of Authenticated Watermarked Medical Images," Mobile Networks and Applications, vol. 26, no. 6, 2021.
7. P. Parida, C. Pradhan, X. Z. Gao, D. S. Roy and R. K. Barik, "Image Encryption and Authentication with Elliptic Curve Cryptography and Multidimensional Chaotic Maps," IEEE Access, vol. 9, 2021.
8. J. Ning, J. Xu, K. Liang, F. Zhang and E. C. Chang, "Passive attacks against searchable encryption," IEEE Transactions on Information Forensics and Security, vol. 14, no. 3, 2019.

9. H. Nematzadeh, R. Enayatifar, H. Motameni, F. G. Guimarães and V. N. Coelho, "Medical image encryption using a hybrid model of modified genetic algorithm and coupled map lattices," Optics and Lasers in Engineering, vol. 110, 2018.
10. P. B. Narasingapuram and M. Ponnavaikko, "A novel attack detection and encryption framework for distributed cloud computing," Indian Journal of Computer Science and Engineering, vol. 12, no. 1, 2021.
11. N. Nandy, D. Banerjee and C. Pradhan, "Color image encryption using DNA based cryptography," International Journal of Information Technology (Singapore), vol. 13, no. 2, 2021.
12. U. H. Mir, D. Singh and P. N. Lone, "Color image encryption using RSA cryptosystem with a chaotic map in Hartley domain," Information Security Journal, vol. 31, no. 1, 2022.
13. Z. Liu, L. Xu, T. Liu, H. Chen, P. Li, C. Lin and S. Liu, "Color image encryption by using Arnold transform and color-blend operation in discrete cosine transform domains," Optics Communications, vol. 284, no. 1, 2011.
14. M. Liu and G. Ye, "A new DNA coding and hyperchaotic system based asymmetric image encryption algorithm," Mathematical Biosciences and Engineering, vol. 18, no. 4, 2021.
15. R. Lin and S. Li, "An Image Encryption Scheme Based on Lorenz Hyperchaotic System and RSA Algorithm," Security and Communication Networks, vol. 2021, 2021.
16. H. Li, L. Deng and Z. Gu, "A Robust Image Encryption Algorithm Based on a 32-bit Chaotic System," IEEE Access, vol. 8, 2020.
17. M. Kaur and V. Kumar, "A Comprehensive Review on Image Encryption Techniques," Archives of Computational Methods in Engineering, vol. 27, no. 1, 2020.
18. L. Jingfeng, S. Yi and L. Chen, "An image encryption algorithm for preventing known plaintext attacks," IPPTA: Quarterly Journal of Indian Pulp and Paper Technical Association, vol. 30, no. 7, 2018.
19. X. Jin, S. Yin, N. Liu, X. Li, G. Zhao and S. Ge, "Color image encryption in non-RGB color spaces," Multimedia Tools and Applications, vol. 77, no. 12, 2018.
20. Y. Hui, H. Liu and P. Fang, "A DNA image encryption based on a new hyperchaotic system," Multimedia Tools and Applications, 2021.
21. J. Hao, H. Li, H. Yan and J. Mou, "A New Fractional Chaotic System and Its Application in Image Encryption with DNA Mutation," IEEE Access, vol. 9, 2021.
22. P. Gaur, "AES Image Encryption (Advanced Encryption Standard)," International Journal for Research in Applied Science and Engineering Technology, vol. 9, no. 12, 2021.
23. H. V. Gamido, A. M. Sison and R. P. Medina, "Modified AES for text and image encryption," Indonesian Journal of Electrical Engineering and Computer Science, vol. 11, no. 3, 2018.
24. X. Q. Fu, B. C. Liu, Y. Y. Xie, W. Li and Y. Liu, "Image encryption-then-transmission using DNA encryption algorithm and the double chaos," IEEE Photonics Journal, vol. 10, no. 3, 2018.
25. A. Devi, A. Sharma and A. Rangra, A Review on DES, AES and Blowfish for Image Encryption & Decryption, vol. 4, 2015.
26. S. Chepuri, "An RGB Image Encryption using RSA Algorithm," International Journal of Current Trends in Engineering & Research (IJCTER), vol. 3, no. 3, 2017.
27. X. Chai, X. Fu, Z. Gan, Y. Lu and Y. Chen, "A color image cryptosystem based on dynamic DNA encryption and chaos," Signal Processing, vol. 155, 2019.
28. C. Cao, K. Sun and W. Liu, "A novel bit-level image encryption algorithm based on 2D-LICM hyperchaotic map," Signal Processing, vol. 143, 2018.
29. D. M. Alsaffar, A. S. Almutiri, B. Alqahtani, R. M. Alamri, H. F. Alqahtani, N. N. Alqahtani, G. M. Alshammari and A. A. Ali, "Image Encryption Based on AES and RSA Algorithms," 2020.
30. P. T. Akkasaligar and S. Biradar, Selective medical image encryption using DNA cryptography, vol. 29, 2020.
31. M. Manju and D. R. K. Pathak, "A Review on Improved and Highly Secured Algorithms for Medical Image Encryption using MATLAB," European Chemical Bulltein, vol. 11(10), no. https://doi.org/10.48047/ecb/2022.11.10.37, p. 340–348, 2022, October.
32. M. Manju and D. R. K. Pathak, "A Survey of Image Encryption Algorithms for Biomedical Images," i-manager's Journal on Pattern Recognition, vol. 9(2), no. https://doi.org/10.26634/jpr.9.2.19091, pp. 37-45, 2022.
33. M. Manju and D. R. K. Pathak, "A Comprehensive Survey and Analysis of Image Encryption Techniques for Secure Data Transmission," International Journal of Applied Engineering & Technology, vol. 5(2), p. 128–141, 2023, June.

Gerbera Flower Counting System using Images Captured by Drone

Rupali M. Bora
✉ rmbora@kkwagh.edu.in
Rakhi Bhagwat
Mitali Bafna, Anjali Bhawari
Rujul Modi

Department of Information Technology
K. K. Wagh Institute of Engineering Education and Research
Nashik, Maharashtra

ABSTRACT

Traditional agriculture and floriculture practices have long relied on manual labor for task like estimating flower quantities, classification, etc. Manual estimation had several disadvantages like inaccuracy, time-consuming, labor-intensive and costly. As the demand for gerbera flowers continue to grow for various industries including ornamental, pharmaceutical and decorative-purpose, the need for accurate and efficient flower quantity estimation has become more pronounced. The primary objective of this project is to create an integrated system capable of capturing aerial images of flower farms using drone and processing these images using Machine Learning algorithms. This will leverage advanced technologies to address the challenges and limitations associated with manual counting of flowers. For this purpose, we will be using Drone Footage of Greenhouse-grown Gerbera Flowers as the input dataset. Then, it will be used to train and test the YOLO, an object detection algorithm and output will be displayed on an UI to the user. With the help of this automated system, the flowers will be counted systematically from the greenhouse environment.

KEYWORDS *: Drone, Gerbera flowers, Greenhouse, Object detection, Roboflow, YOLO (You Only Look Once).*

INTRODUCTION

In India, gerbera flowers are cultivated and used in a great extent. It has excellent market commercial value and hence, used as a decorative flower in bouquet, functions and parties. They are cultivated in greenhouse/shade net at an temperature of 12°C-20°C. As these flowers are cultivated on huge scale, crop management, counting and classification of every flower becomes complex task. Manual cost of counting and classification of these flowers goes to nearly 1000-2500 Rs. per person for a 5 acres farm. Also, it's time-consuming and may generate less accurate results, hence prone to errors.

Machine Learning and UAV based approach made possible to perform counting and categorization of flowers in short period of time, along with the elimination of manual labors and errors. In this research paper, a solution for farmers, to detect and classify gerbera flowers with the help of drone and object detection has been discussed. Generally, drone with FPV camera [1] is used for such applications as it records high-resolution images/videos even in obstruction fields like greenhouse. For object detection, YOLOV8 [1], [2] model was used. It is the most popular object detection algorithm, known for its high accuracy and speed. It uses best neural network architecture for detecting objects at real-time. YOLO divides the image into number of grids and predicts the object based upon bounding boxes. For creation and annotation of gerbera dataset, Roboflow [3] was used. Its a deployment platform and a labelling tool.

This project is composed of two stages, Drone Configuration and Model Creation. At first stage, configured drone will be moved over the field area. It will continuously capture the video of the farm, which is simultaneously being transferred to the user system via receiver. At second stage, YOLO model was

employed for object detection. The model is trained on the Dataset of Gerbera flowers, which is created using roboflow. Drone footage will be given to this pretrained model, as an input. It will predict the count of flowers as an output. This detection and counting system can be utilized for faster, automated and accurate counting and classification of flowers. It will also help to reduce the need of manpower and minimize cost needed. Remaining paper is organized as follows: Literature Review, Materials and Methods, Result and Discussion, Conclusion and Acknowledgment.

LITERATURE REVIEW

This section describes the related works in the area that has similarities with the proposed method, counting of gerbera flowers using UAV & YOLO.

Johannes Gallmann [4] proposed a photo base about the number of flowers in grasslands which reduces the manual practice of assessing flowering plant species in grasslands. They obtained nearly 90% accuracy and were able to identify and classify individual flowers. A similar work carried out in [5], using Convolutional Neural Networks (CNN) and image processing strategy, the output is a density image that accurately predicted the count of strawberry flowers in drone imagery, providing a more efficient and accurate counting method. Yasmin Vanbrabant used a 3D Object based method [6] with a high accuracy of 87%.

Joao Valente [7] proposed an automated method for counting crop plants using very high-resolution UAV imagery using method such as Machine Vision, Transfer Learning using CNN with an accuracy of 95% in counting plants. Mirko Piani in [8], uses UAV based RGB imagery and results in mapping Apple Orchard flower clusters density. Accurate flower counts were challenging to obtain due to the laborious manual process involved in estimating crop yields and selecting genotypes. Daniel Petti in [9] proposed a weakly supervised learning which helps in counting Cotton Blossoms which requires simpler and less expensive annotations. The study of tomato flower detection was carried out in paper of Dor Oppenheim et al. [9]. The front acquisition angle, optimal hue threshold values and afternoon acquisition times gives best results as precision increase to 80%.

MATERIALS AND METHODS

This section provides detailed explanation about the project. It composed of five subsections, Section III-A describes the system architecture & detailed steps in which the project has been completed. Section III-B contains details about the Gerbera dataset and its preprocessing. In section III-C, all details about Roboflow and YOLOV8 is mentioned, that is, how it was used in object detection. Section III-D describes about the UAV and its configuration and finally, Section III-E give the details about streamlit framework and how it is used for the deployment of model.

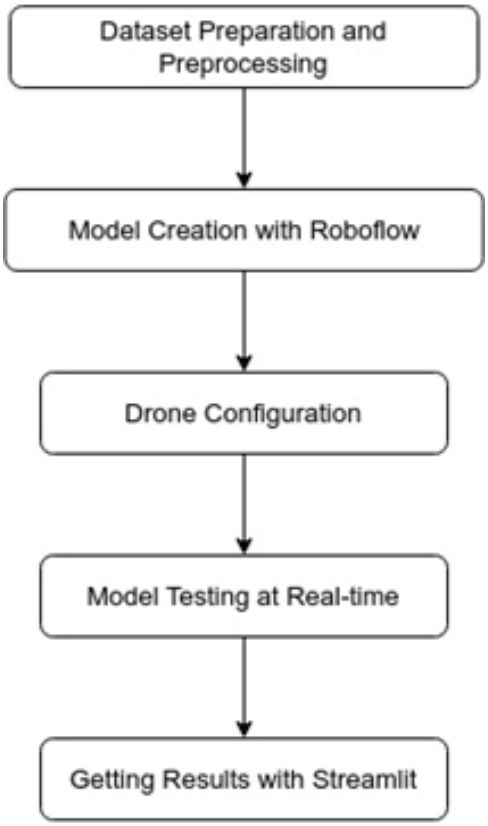

Fig. 1. System Architecture

System Architecture

This section gives the overview about the Flow of the project. Fig. 1. represents the overall steps for the project.

For this project, YOLOV8 and Roboflow are the two main components were used. Initially, Gerbera flower dataset has been created which is further preprocessed

(resizing, filtering, etc. is performed). Using Roboflow tool annotation, bounding boxes and preprocessing tasks has been done. Then, with the help of YOLOV8 model provided by Roboflow Train, it is trained-tested on the created dataset. Next is the Hardware step, Drone is configured with required equipments. Speed, Height and drone motion is calliberated using flight and remote controller. Connection between user system and drone has been established via receiver-transmitter.

In further steps, developed model is tested against the real-time images and videos captured by drone. Finally, to display count of detected flowers, Streamlit has been used. It's a framework which provides basic user interface for python based models.

Dataset Preparation and its Preprocessing

This section provide details about the Gerbera dataset & some sample images from it.

Sample Images & Table of Dataset

Created a custom dataset of images of Gerbera Flowers captured from a farm situated at Madsangavi, Nashik, Maharashtra. It consists of nearly 550 - 600 images and 70 - 80 videos of flowers. There are total 8 different classes (colors) of flowers namely: Red, Pink, White, Magenta, Yellow, Salmon, Orange and not grown category. With the annotation feature of Roboflow, labelling or bounding boxes has been created in all the images as well as in video frames. We have also performed image resizing, filtering, etc. tasks on the image dataset. Table I, gives all the details about the dataset. There are total 600 images in the dataset. Total number of annotations more than 2500, with per image annotation value as 4 - 6 flowers. Average Image size given as 0.78 mp and Median image ratio as 960x853 representing a square shaped image. It also gives the details about total number of flower classes.

Table 1. Description About Dataset

Description about Image	Measures/Value
Total number of images	600
Total annotations/labels	>2500
Per image Annotations	4 – 5
Average Image Size	0.78 mp
Median Image Ratio	960x853
Total number of classes	8

Also, Fig. 2, shows an interface of how annotation can be using Roboflow. It also shows the number of color classes in an image.

Fig. 2. Annotation Interface in Roboflow along with the number of color classes of gerbera flowers

Preprocessing of Dataset

In this step, images are preprocessed or made ready for training and testing purpose. All captured images are brought under common shape and size. With the help of Annotation feature of Roboflow, bounding boxes are created over the gerbera flowers. This step is also called as annotation or labelling of images, which is necessary for model training. Also, edges are detected in the images.

About Roboflow and YOLOV8 for Object Detection

Roboflow is not only used as annotation tool, but it also provides an easier way for the creation of model. It also acts as an end-to-end computer vision platform for developing projects related to image processing, object detection and so on. It provides a Hosted API feature using which one can train computer vision models on the built-in dataset in very easy manner. Also, it provide features like Roboflow Annotate, to create own custom dataset, Roboflow Train, to perform model trainings and Roboflow deploy, for the deployment of models over devices such as iOS, NVIDIA based GPUs.

In this project, after creation of annotated dataset, Roboflow Hosted API was used, which allows utilizing pretrained, multiple versions of YOLO. Further, training and testing of YOLOV8 model has been performed on the dataset. By exporting this model, source code was automatically get generated or one needs to just run this code into Google Colab environment, to test it on new images.

YOLO, that is, You Only Look Once, is an object detection algorithm, basically used to solve computer vision tasks. It works by dividing the given image into n-dimensional grids and determining the probability of bounding boxes into each grid. Main feature of YOLO algorithm is that, it makes a single forward pass over the given image to detect the object. Hence, it possess high speed and accuracy compared to other two pass algorithms. It uses combination of best Convolutional Neural Networks (CNN) [4] [5] to predict objects.

Drone Configuration And Video Capturing

Drone, also known as Unmanned Aerial Vehicle [5] [6], is widely used in the field of agriculture nowadays, to perform automated tasks. In this project also, it acts as a main component. Quadcopter multirotor drone has been used, for capturing images of farm which is configured with equipment like Battery, Electronic Speed Controllers (ESCs), Flight Controller (FC), etc. To capture high quality images, A 1200 TVL CMOS FPV (first-person view) Camera [7-9] along with its transmitter (to transmit captured images) and receiver (to receive images on user system) has been used.

As the drone moves over the field area, all the images or data will automatically get received on the user system at real-time, due to the direct connection between Transmitter (attached to FC and Camera) and Receiver (attached to user system). Using drone reduces the need of manpower of counting of flowers in the farm. It also increases the accuracy of count, improves efficiency and makes task automated.

Streamlit Framework

Streamlit is a free and open-source platform or a framework used to create web applications for our machine learning models by deploying them to it. YOLOV8 model is deployed on streamlit, to create a basic web application for farmers, so that it can be used for counting purpose.

Following are the steps by which the basic GUI has been created for this project. Initially, user needs to install the streamlit using 'pip install streamlit' command. Then, created a custom python script, which will describe how the web interface should look like. It may include input data, files to be uploaded, images, output, etc. Finally, trained model is integrated with streamlit and tested on local system using 'streamlit run your_app.py' command.

The web interface starts with a home page of the project which consists of following components: Project URL is the URL of the model which is created on Roboflow website whereas, Private API Key is the key given by Roboflow while creating model using Hosted API feature. This simple web interface also includes an About Us section, where user can follow the given steps to test the model.

In Fig. 3, On the left sidebar of web page, three options has been provided, user can upload either images or recorded videos of flower. Also, by clicking on 'Realtime Detect using Camera', user can access system's webcam or the camera attached to the drone, to detect count of flowers at real-time.

Fig. 3. Streamlit web interface with 3 options provided on Left Sidebar: Image, Video and Realtime detection. Along with this, Detection of flowers by creating Bounding boxes using YOLO model.

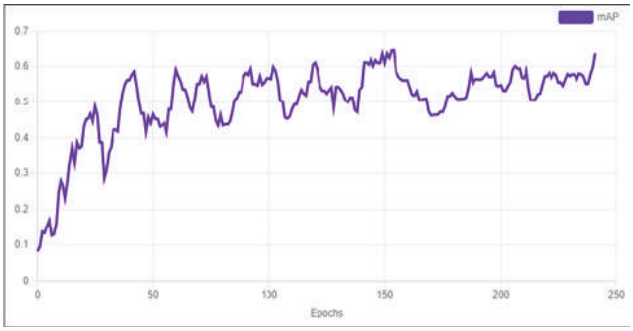

Fig. 4. Plot of Mean Average Precision (mAP) versus Epoch. Highest value of mAP obtained at Epoch numbered within 150 – 160.

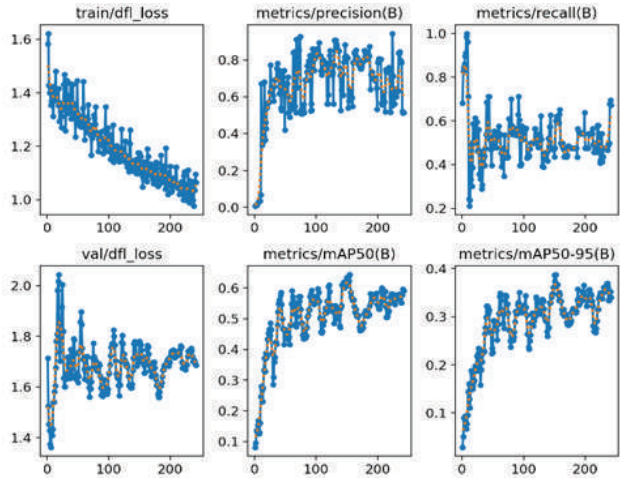

Fig. 5. Training results showing best Precision and Recall values as the number of sample images increased. Also, reduction in object loss is observed for training and validation set.

RESULTS AND DISCUSSION

This section describes the final results generated in this project and performance metrics used for the evaluation of model. Section IV-A gives the experimental or actual testing of the project by detecting flowers in the given image. Also, more about other performance metrics and training results have been discussed. Section IV-B describes the performance of YOLOV8 model based upon various cost functions.

Experimentation

For testing purpose, model has been given an input image shown in Fig. 3. It demonstrates how flowers are detected using this model. Detected flowers are shown by drawing bounding boxes around the object. User can also adjust the confidence score and overlapping percentage (as shown in Fig. 3) to a specific value, for more accurate results. More is the overlapping value, more accurately the model counts.

Fig. 4. displays variation in the mAP metric (Mean Average Precision) for different number of epochs. It has been observed that, model gained highest value of mAP for epochs between 150 – 160. Moreover, model training is best understood by Training graphs shown in Fig. 5. Best Precision and Recall values are obtained by using more than 200 sample images for training. Also, more number of sample images reduced the object loss (dfl_loss) [11] at great extent, for training as well as validation set. Object loss represents the probability of occurrence of the object at specific location in the image. It shows how well the model correctly locates specified object.

Performance Evaluation

This section describes about the model's performance and how model performs counting on training, testing & validation set. Table II, gives brief description about the model's accuracy on various kinds of data (image or video). It shows that, the model possess highest accuracy for images which is 93%. for videos it is 84% and for realtime detection, that is, data captured by the drone, its 88%.

It also describes the total number of images categorized into training, testing and validity set [11]. Total number of images in the dataset and total number of augmented (labelled) images are also given.

Table 2. Description About Model's Performance

Performance Metric/About Dataset	Total Count (in %)
Accuracy for Images	93%
Accuracy for Videos	84%
Accuracy on Real-time detection	88%
Training set count	418
Testing set count	60
Validation set count	40

In machine learning, accuracy is the performance metric which determines the exactness of an algorithm or a model. In simple terms, it tells how correctly the model is making predictions. Mathematically, Accuracy is the total number of true predictions divided by the total number of predictions. In this project, model's accuracy for image is 93%, for videos its 84% and for realtime object detection its 88% (as per Fig. 6.). It shows that our model is trained very well and it can effectively make predictions on new data

CONCLUSION

In this work, YOLOV8 was used which is a real-time object detection algorithm, possessing excellent accuracy and high speed. A robust system is developed, which is capable of accurately counting Gerbera

flowers using images captured by drone. It provides insights for farmers and researchers. This innovative method outperforms traditional methods in enabling precise flower counting in various lighting conditions and field sizes. Our future efforts will be focusing on model enhancements, scalability, and integration with agricultural platforms, addressing data quality, environmental factors, resource constraints, and improving user interfaces and data sources.

REFERENCES

1. Fang, Yiming, et al. "Accurate and automated detection of surface knots on sawn timbers using YOLO-V5 model." BioResources 16.3 (2021): 5390.
2. B. Dwyer, J. Nelson, J. Solawetz, et al. Roboflow (version 1.0) [software], 2022. computer vision.
3. Gallmann, Johannes, et al. "Flower mapping in grasslands with drones and deep learning." Frontiers in plant science 12 (2022): 774965.
4. Heylen, Rob, Petra Van Mulders, and Nicole Gallace. "Counting strawberry flowers on drone imagery with a sequential convolutional neural network." 2021 IEEE International Geoscience and Remote Sensing Symposium IGARSS. IEEE, 2021.
5. Vanbrabant, Yasmin, et al. "Pear flower cluster quantification using RGB drone imagery." Agronomy 10.3 (2020): 407.
6. Valente, João, et al. "Automated crop plant counting from very high-resolution aerial imagery." Precision Agriculture 21 (2020): 1366-1384.
7. Piani, Mirko, Gianmarco Bortolotti, and Luigi Manfrini. "Apple orchard flower clusters density mapping by unmanned aerial vehicle RGB acquisitions." 2021 IEEE International Workshop on Metrology for Agriculture and Forestry (MetroAgriFor). IEEE, 2021.
8. Petti, Daniel, and Changying Li. "Weakly-supervised learning to automatically count cotton flowers from aerial imagery." Computers and electronics in agriculture 194 (2022): 106734.
9. Chen, Steven W., et al. "Counting apples and oranges with deep learning: A data-driven approach." IEEE Robotics and Automation Letters 2.2 (2017): 781-788.
10. Oppenheim, Dor, Yael Edan, and Guy Shani. "Detecting tomato flowers in greenhouses using computer vision." International Journal of Computer and Information Engineering 11.1 (2017): 104-109.
11. Baratloo A, Hosseini M, Negida A, El Ashal G. Part 1: Simple Definition and Calculation of Accuracy, Sensitivity and Specificity. Emerg (Tehran). 2015 Spring;3(2):48-9. PMID: 26495380; PMCID: PMC4614595

Image and Video Denoising for Enhanced Multimedia Quality

Sakthivel S
Professor
Department of Computer Science and Engineering
Sona College of Technology
Salem, Tamilnadu
✉ sakthivel@sonatech.ac.in

M Agalya
Assistant Professor
Department of CSE
Vivekanandha College of Technology for Women
Tiruchengode, TamilNadu
✉ agalkalai@gmail.com

ABSTRACT

This study explores the depths of image and video denoising to supply cutting-edge methods to improve multimedia content quality, which is becoming more and more quality. Based on extensive testing using multiple datasets, we suggest a denoising method that efficiently reduces noise yet preserves pertinent information. Effective denoising approaches, that increase efficiencies and enhance multimedia information quality overall, have a chance to transform a wide range of industries, including computer vision, video streaming, image processing, and others. To satisfy this need, we explore various aspects of denoising utilizing modern facilities of deep learning techniques like convolutional neural networks. Through means of comprehensive testing on a range of datasets encompassing an assortment of degradation factors, researchers are refining and refining the denoising model to accomplish exceptional results. These advancements guarantee practical benefits in an extensive number of sectors, having consequences that go far above theoretical research. These algorithms deliver sharper, crisper photographs through the elimination of noise and imperfections which improves user engagement and creates immersive experiences.

INTRODUCTION

In the contemporary digital content consumer environment, the quality of images and videos has a huge impact on how people view and respond to the information. The importance of achieving maximum visual quality has increased due to people's consumption of multimedia material across many channels and devices. Nevertheless, it is challenging to achieve this highest quality since multimedia data is inherently susceptible to various types of degradation. Urgent effort is needed to overcome these limitations and raise the bar for multimedia content through innovative solutions based on cutting-edge technologies. Using deep learning algorithms to denoize images and videos is one of these options, and it seems like a highly appealing approach. Through the use of artificial intelligence and neural networks, researchers and practitioners are pushing the envelope in terms of enhancing visual fidelity and perceptual quality. The work requires an in-depth understanding of the numerous nuances of multimedia data as well as the factors that compromise its integrity. Noise can be produced by several things, especially defective sensors and surrounding circumstances. Noise warps and blurs images and videos, diminishing their quality and subtracting from the viewing experience. Compression artifacts come from data compression computations, producing unwelcome distortions and compromising visual fidelity. The aforementioned techniques combine CNNs (convolutional neural networks) and other advanced layouts to enhance perceptual quality, set apart, and remove noise while retaining relevant data.

OBJECTIVE

The main objective is to mitigate the occurrence of noise, which can be attributed to multiple reasons like inadequate illumination, sensor constraints, compression artifacts, or transfer oversights. To keep the image or video's instructional substance and visual integrity, it's critical to keep significant details and structures intact when eliminating noise. To avoid distorting or blurring important aspects of the content, denoising algorithms should strive to preserve sharp boundaries and bounds. In applications like photography

and medical imaging, where color plays a major role in analysis and then maintaining accurate color an image is crucial. It is essential to have efficient denoising strategies, particularly during instances when hardware assets will constrained or in real- time applications. To preserve a pleasing aesthetic and perceptually precise outcome while denoising, endeavor to avoid generating any further aberrations or distortions. The goal of denoising is to increase the visual attractiveness and comprehension of videos and photographs by improving their perceptual quality. This is particularly important for applications like digital photography, where user satisfaction relies on the quality of the resulting photos. The purpose of denoising techniques is to elevate the ratio of signals to noise (SNR) of pictures and videos by lowering noise. For purposes like image analysis and pattern recognition, a higher signal-to-noise ratio (SNR) produces an improved and more reliable portrayal of the underlying information. Denoising techniques can target particular kinds of artifacts created during picture purchase, compression, or processing in addition to eliminating noise. Motion blur, optical variations, and compression methods such as JPEG objects of art.

LITERATURE SURVEY

[1] Haoyu Chen, "Masked Image Training for Generalizable Deep Image Detection"2023

Deep learning-based image-denoising models have made significant progress in improving generalization performance by including a masked training strategy. Using masks during the training phase allows the model to focus on specific areas of interest within the input data, increasing the model's capacity to generalize to previously unseen data. The masked training technique has some benefits, but one major disadvantage is that information is necessarily lost during the masking process. This information loss may make it more difficult for the model to detect minute details and subtleties in the input images, lowering its overall effectiveness.

[2] Dan Zhang, "Supervised Image Denoising For Real-World Images Context Aware Transformer"2023.

In this paper, the authors introduce a unique methodology inspired by Transformer-based methods to solve the intrinsic constraints of Convolutional Neural Networks (CNNs) in self-supervised picture denoising. Due to Transformers' notable performance in a range of computer vision applications, the authors have proposed a new network design called Denoise Transformer. Convolutional Attentional Denoising Transformers (CADTs) and a Self-Normalizing Encoder (SNE) are integrated into this architecture to enable two stages of self-supervised denoising. The CADTs that comprise the Transformer have both local and global feature extraction branches. To generate denoised outputs in the first step, residual learning is utilized to remove noise information from the input images, as is the purpose of these CADTs. The authors demonstrate the success of their system through extensive experimentation, outperforming most self- supervised training methodologies and traditional methods. Notably, the proposed technique excels in denoising pictures with detailed noise patterns, particularly those with low-saturated textures and poorly lit environments.

[3] Yang Chen, "Multispectral Image Noise Removal With Adaptive Loss And Multiple Image Priors Model"2023.

In this study, we propose an innovative denoising technique for Multi-Spectral Imagery (MSI) that melds dynamic loss functions with periodicity based on multiple picture priors. More specifically, we address the difficulty posed by the complex and often unknown noise distribution in MSI data by using the Non-Parametric Mixture of Gaussians (NMoG) distribution. Utilizing the above approach, we can describe all of the complicated noise characteristics present in MSI datasets. To maximize our denoising model, we employ a weighted l2-norm loss function tailored to the specific noise distribution. This weighting is accomplished by Variation Auto Encoders (VAE), which enables efficient and flexible learning from observed MSI data. Local smoothness properties, spectral and spatial correlation, and nonlocal spatial similarity are some examples of these priors. We fully incorporate these priors into our regularization term to harness and capture the underlying structure and properties of MSI data. Through comprehensive simulations and experiments performed on real MSI datasets, we demonstrate the effectiveness of the proposed approach in significantly reducing noise levels compared to existing methods. Our findings highlight the importance of integrating

adaptive loss features with preimage types to effectively solve the MSI data deletion problem.

[4] Dan Zhang, "Self-Supervised Image Denoising For Real-World With Multi-Mask Based On Blind-Spot Network" 2022.

This study presents a new method for self-directed RGB image denoising based on binary-switched Networks (BSN) using a multi-mask strategy. This new method aims to solve the problem of highly inclined structures, which until now have been difficult to control with only center-mask models. The proposed approach can significantly perturb those high-noise structures by using multiple masks, which improves the damping efficiency of the model. The study also introduces the creation of MM-BSN, a model that effectively combines the features found in multifaceted convolutional layers while controlling model size expansion to avoid exploding. In particular, MM-BSN uses concatenation-based hop connections to compensate for data loss caused by masks. This clever combination ensures that the damping process is flexible and effective even in the case of diffuse, spatially correlated noise. The effectiveness of the proposed method was confirmed by extensive experimental validation. The results show that it performs better in denoising than other unsupervised and self-supervised techniques already used and published in the literature. Remarkably, the proposed method does a remarkable job of preserving textures while effectively removing noise, improving the overall effect visual appearance of noiseless image quality.

SYSTEM ANALYSIS

Existing System

Spatial Markov dependencies are a significant factor in image processing, making Markow random fields (MRFs) useful. These models capture issues related to local energy degradation, where neighboring pixels influence each other's values to give a visual impression. MRF-based transmission map estimation methods show promise for applications such as degassing when applied to outdoor color RGB images. These techniques use the spatial constraints inherent in external Conditions to improve the accuracy of transmission map estimation, facilitating the recovery of sharp images from blurred images. Central to this process is the direct dark channel (DCP), which uses high-resolution geometric correlations between display units. DCP can detect uncorrelated pixels and estimate the transmission map. Developed in response to most outdoor images, some pixels have very low-intensity values in a very small color channel. DCP integrates these higher-level connections to enhance MRF's regional energy-saving strategy to make it more transparent and renewable. These approaches include statistical modeling, spatial correlation, and higher-order visualizations, enhancing the multifaceted and applied nature of image-processing research.

Proposed System

Continuous efforts are being made to find images that are free of unwanted noise in image and video processing, with deep learning techniques now providing effective means to achieve this objective. Those methods using neural networks aim to improve image quality by cleverly combining information from multiple sources. At the heart of this methodology is deep learning, which involves building complex neural networks with multiple layers - input, hidden, and output layers. Together, these layers extract, transform, and integrate the features of the input data to produce a better output. Applying Laplacian operations to the input images is a common step in the denoising process. An integral part of image processing, the Laplacian operator helps emphasize edges and small details while reducing noise. Applying this procedure to input images allows the neural network to focus on preserving important visual information while reducing the effects of unwanted artifacts. To refine the denoising process, the weighted inputs are subjected to Gaussian procedures. The application of Gaussian filtering is widely known for its ability to reduce noise and remove unwanted components, improving the overall coherence and clarity of the final image. Using a multi-layered iterative refinement process, a deep learning model acquires the ability to recognize significant patterns and structures in the input data.

SYSTEM ARCHITECTURE

The perspective of framework design encompasses both the conceptual plan and auxiliary format of equipment or computer code. It's the method of determination.

Broadly talking, framework design relates to the complete format of a multifaceted framework, including not fair its equipment and program constituents but also its operational and organizational highlights. The way a system interacts with other frameworks and clients, its behavior over time, and the relationships between components are all part of its design. Picture preparing, as utilized in imaging science, is the scientific handling of pictures through any kind of flag processing, where the input can be a picture, an arrangement of pictures, or a video, such as a picture or a video outline. The yield of picture handling can be another picture, or it can deliver a set of parameters or characteristics related to the picture.

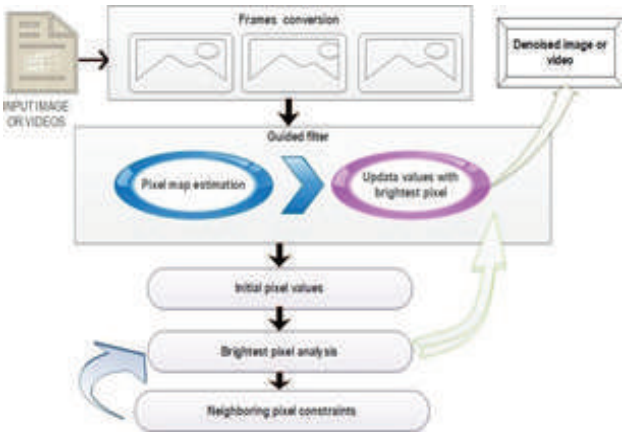

Fig. 1. Architecture Diagram

ALGORITHM

Convolutional Neural Networks

CNN architectures designed for denoising typically consist of multiple layers, including convolutional layers, pooling layers, and activation functions. These layers are stacked to create a deep network capable of learning hierarchical representations of image or video data. CNN architectures designed for denoising typically consist of multiple layers, including convolutional layers, pooling layers, and activation functions. These layers are stacked to create a deep network capable of learning hierarchical representations of image or video data. CNNs for denoising are trained on pairs of noisy and clean images or video frames. During training, the network learns to map noisy inputs to clean outputs by minimizing a loss function that measures the difference between the predicted and ground truth images. Common loss functions used in training CNNs for denoising include mean squared error (MSE) and perceptual loss, which measures the difference in feature representations between the predicted and clean images. Perceptual loss tends to produce visually pleasing results by focusing on high- level features rather than pixel-wise differences.

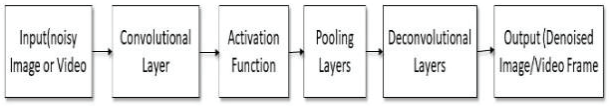

Fig. 2. CNN diagram for Image and Video Denoising

Image processing

The mathematical processing of images through any kind of signal processing is known as image processing in imaging science. The info is a picture, a succession of pictures, or a video outline. The result is a picture or an assortment of picture properties or boundaries. The majority of approaches to image processing treat an image as a two-dimensional signal and employ fundamental signal processing methods.

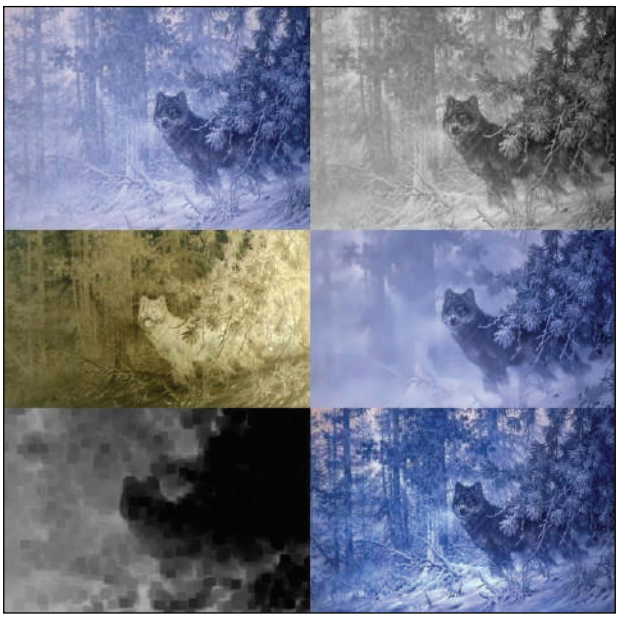

Fig. 3. Image Processing (Noised Image/Video Frames to Denoised Image /Video Frames)

Time, or the z-axis, is the third dimension in images, which are also processed as three- dimensional signals. Whilst digital image processing is the most common type, optical and analog image processing are also feasible. The general methods discussed in this article

are relevant to all of them. Imaging is the process of capturing the images that initially produced the input image. Mage communications are also understood as three-dimensional signals, with time, or the z-axis, serving as the final dimension. While the processing of digital pictures is the most common type, optical and conventional image processing are also feasible. Imaging is the process of acquiring the images that initially produced the input image. Computer vision and computer graphics are extremely similar to image processing. When creating images for computer representations of objects, circumstances, and illumination are used as guidance instead of deploying imaging devices like imaging devices to take pictures of natural scenes, as is the scenario with most animated films. Through the implementation of efficient denoising processes, we strive to improve the overall visual appeal, razor-sharp, and readability of multimedia data. An overview of the methods they used in image and video denoising is given in this introduction, highlighting their importance in improving multimedia quality and enriching user experiences

Gaussian filtering

A widely used technique for noise-reduction images is exponential filtering. This outlines the operation of Gaussian filtering and how it is used for noise elimination in images and videos. High- energy noise, such as Gaussian sound or salt-and- pepper noise, is capable of effectively being reduced in pictures and movies by applying Gaussian filtering. Gaussian filtering reduces noise without significantly modifying the main structure of the image by dissolving it.

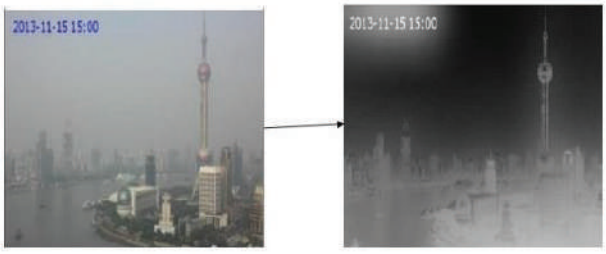

Fig. 4. Gaussian Filtering

A Gaussian filter tries to keep alive significant elements of the image, which include edges and textures while minimizing noise. While edges are maintained by the modest intensity shift, the filter's distorting effect is prominent in areas with consistent luminance. The standard deviation (SD) (sigma) parameter to be used for the kernel's Gaussian function can be changed to the decreased by Gaussian filtering. While larger values of sigma preserve enhanced characteristics but offer less noise reduction, smaller values produce stronger diminished noise but may cause a loss of fine details.

Denoise Transformer

Transformers for denoising have demonstrated potential in jobs involving images and videos. They use transformer architectures, which were modified to handle picture patches or video frames after being created for natural language processing. These models use self-attention methods to help in denoising by capturing long- range dependencies in the data. Effective training of these models frequently makes use of strategies like adversarial training and self-supervised learning. A few well-liked designs are ViT, SwinIR, and DnCNN-Transformer. Researchers are always working to enhance these models, which provide cutting-edge performance.

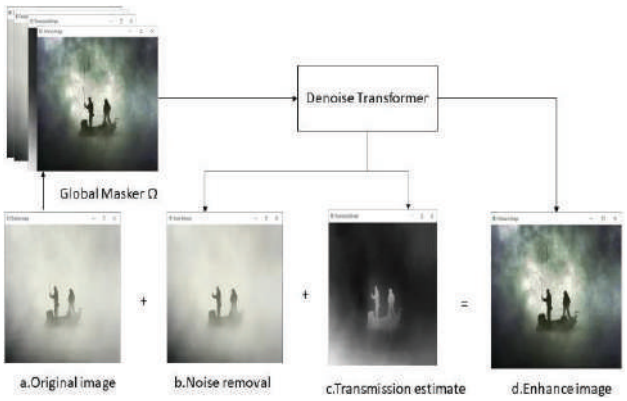

Fig. 5. Denoise Transformer

Typically, denoising transformers work on individual image patches or video frames as opposed to the full image or video sequence all at once. They can properly capture spatial dependencies and handle enormous input volumes because of this patch-based methodology. Self- attention is the fundamental building block of transformers, allowing them to recognize long- range dependencies and the overall context of the data. This approach helps the model grasp the links between several patches or frames, which is very useful for denoising tasks. To successfully handle multiscale

features, certain denoising transformer topologies have a hierarchical structure. These models may capture details at different levels of abstraction by processing data at numerous resolutions, which improves denoising performance. Denoising transformers are often learned using large-scale datasets with noisy and clean picture or video pairings. To create training data without explicit supervision, self-supervised learning approaches like noise estimation or picture augmentation are frequently used. The model can also be trained to provide aesthetically beautiful denoised outputs by using adversarial training.

CADT

CADT, or Convolutional Adaptive Dense Transformer, is a powerful architecture used for image and video denoising tasks. It combines the strengths of convolutional layers and transformer-based architectures to effectively capture spatial and long-range dependencies in the data.

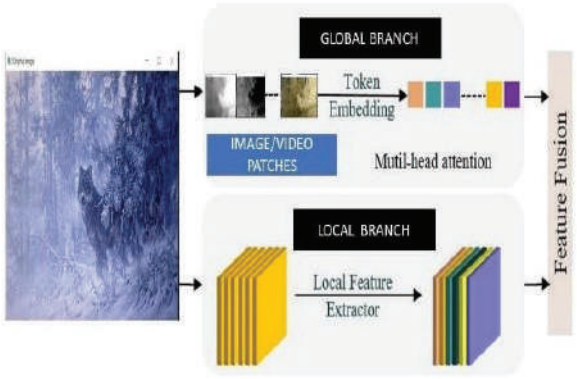

Fig. 6. CADT Workflow

CADT incorporates convolutional layers to process local spatial information efficiently. These layers are adept at capturing low-level features and patterns within the image or video frames. CADT employs an adaptive mechanism focus based on the characteristics of the input data. This adaptability allows the model to allocate more attention to relevant regions while suppressing noise and irrelevant information. Dense connections facilitate feature reuse and gradient flow throughout the network, enhancing information flow and promoting feature reuse across layers. This helps improve the denoising performance by enabling the model to capture both local and global context effectively.

CONCLUSION

In conclusion, our project addresses the pressing need for advanced techniques in image and video denoising, crucial in today's multimedia-dominated landscape. Leveraging cutting-edge deep learning algorithms, particularly convolutional neural networks, we have meticulously analyzed the factors contributing to multimedia degradation and their impact on perceptual quality. Through exhaustive experimentation across diverse datasets, we have developed a robust denoising model adept at removing noise while preserving essential details. The proposed algorithm demonstrates promising results, highlighting its potential for real- world applications spanning image processing, video streaming, and computer vision. By raising the standards of multimedia content, our research aims to enhance user experiences and foster innovation across various domains. Moreover, our focus on leveraging deep learning architectures and comprehensive analysis positions our work as a cornerstone for future advancements in multimedia denoising.

FUTURE ENHANCEMENT

In the future, building upon the foundation of our current research, we envision integrating multi- modal learning approaches to enhance the denoising capabilities further. By incorporating not only visual but also auditory or textual information, our model could gain a more comprehensive understanding of the underlying content and context, leading to even more precise noise removal while preserving crucial details. Additionally, exploring self-supervised learning techniques could enable our model to learn from vast amounts of unlabeled data, enhancing its adaptability to diverse noise patterns and scenarios. Moreover, leveraging generative adversarial networks (GANs) could enable us to generate realistic noise patterns for training, simulating real-world noise environments and making our model more robust. These future enhancements hold the potential to push the boundaries of multimedia denoising, resulting in even higher-quality outputs and broader applicability across various domains.

REFERENCES

1. J. Batson and L. Royer, "Noise2Self: Blind denoising by self-supervision," in Proc. Int. Conf. Mach. Learn., 2019, pp. 524–533.

2. Jingwen Chen, Jiawei Chen, Hongyang Chao, and Ming Yang. Image blind denoising with generative adversarial network-based noise modeling. In Proceedings of the IEEE conference on computer vision and pattern recognition.

3. J. Xue, Y. Zhao, W. Liao, and J. C.-W. Chan, "Nonlocal low-rank regularized tensor decomposition for hyperspectral image denoising," IEEE Trans. Geosci. Remote Sens., vol. 57, no. 7, pp. 5174–5189, Jul. 2019.

4. Masked Image Training for Generalizable Deep Image Denoising, Haoyu Chen, IEEE, 2023.

5. Meng Chang, Qi Li, Huajun Feng, and Zhihai Xu. Spatialadaptive network for a single image denoising. In European Conference on Computer Vision, pages 171–187. pringer, 2020.

6. MM-BSN: Self-Supervised Image Denoising for Real-World with Multi-Mask based on Blind- Spot Network, Dan Zhang, IEEE, 2023.

7. Multispectral Image Noise Removal With Adaptive Loss and Multiple Image Priors Model, Yang Chen, IEEE, 2023.

8. Self-Supervised Image Denoising for Real- World Images With Context-Aware Transformer, Dan Zhang, IEEE, 2023.

9. Y.-B. Zheng, T.-Z. Huang, X.-L. Zhao, Y. Chen, and W. He, "Doublefactor-regularized low-rank tensor factorization for mixed noise removal in the hyperspectral image," IEEE Trans. Geosci. Remote Sens., vol. 58, no. 12, pp. 8450–8464, Dec. 2020.

10. Y. Zhang, D. Li, K. L. Law, X. Wang, H. Qin, and H. Li, "IDR: Self-supervised image denoising via iterative data refinement," in Proc. IEEE/CVF Conf. Comput. Vis. Pattern Recognit. (CVPR), Jun. 2022, pp. 2098–2107.

Detection of Stress Levels from EEG Signals with Various Machine Learning Approaches

Jatinder Pal Singh
Research Scholar
School of Engineering Design and Automation
GNA University, Punjab
✉ jhsingh11@gmail.com

Anurag Sharma
Professor
School of Engineering Design and Automation
GNA University, Punjab
✉ anurag.sharma@gnauniversity.edu.in

ABSTRACT

The recent data research show that people are experiencing more mental stress. Owing to the previous epidemic and the lockdowns that followed, individuals are experiencing a range of stressors, such as joblessness, financial hardship, company loss, deteriorating personal and family relationships, etc. Long-term stress may have a significant role in the development of many common illnesses. Stress is associated with changes in human brain activity, which may be measured by electroencephalogram (EEG) data. The pattern of these signals is typically complicated and difficult to interpret. This study described a method that uses machine learning techniques to extract the stress level from EEG data. Machine learning approaches with electroencephalography (EEG) data for stress level identification. Early identification and prevention are essential since stress is a common problem that negatively impacts both productivity and mental health. The main challenge of this paper is to identify the stress level and increase the efficiency of the stress detection method with machine learning techniques. The suggested approach involved the use of a band-pass filter to eliminate noise from the unprocessed EEG output. For EEG data, the "Fast Fourier Transform (FFT)" approach was used to extract the feature. It is better suited for the "Fast Fourier Transform (FFT)" with a hamming window. The "Fast Fourier Transform (FFT)" and a Hamming window are used to evaluate EEG data in the frequency domain. Usually non-stationary, EEG signals have both periodic and non-periodic components.

Machine learning techniques facilitate the automatic categorization of brain activity patterns linked to stress, while EEG readings provide insightful information about these patterns. We go over the difficulties, approaches, and most recent developments in the use of EEG signal to determine stress levels.

KEYWORDS *: Keywords: Stress Level Detection and Classification, Machine learning techniques, EEG Signals, Classifiers: "Gradient Boosting Algorithms, Random Forests, Decision Trees, Support Vector Machines, K-Nearest Neighbors".*

INTRODUCTION

Electroencephalography (EEG) is a potent instrument for comprehending cognitive processes and brain dynamics. Gaining understanding of cognitive processes, mental states, and their applications in both clinical and non-clinical contexts is the main goal of the analysis of EEG data. The work uses machine learning algorithms and sophisticated signal processing techniques to extract relevant information from EEG data.

EEG bands are measured in Hertz (Hz) and correspond to various frequencies of brain activity. Every band corresponds to distinct mental processes and awareness levels. These EEG bands, which are expressed in Hertz (Hz), correspond to various brain wave frequencies. Because each band is linked to distinct cognitive states

and tasks, researchers are able to examine different facets of brain activity. These EEG bands can also aid in the creation of therapeutic approaches and offer insightful information about neurological illnesses.

Stress detection by EEG is a method used to identify and measure the levels of stress experienced by an individual by analyzing their brainwave patterns. By applying electrodes to the scalp, this approach records electrical activity in the brain, this may then be analysed to ascertain the existence and level of stress. By understanding how different patterns of brain activity correlate with stress, and develop more effective strategies for managing and reducing stress in individuals.

In order to detect the electrical activity of the brain, a network of tiny electrodes is applied to the human scalp and used in electroencephalography (EEG)' "Electroencephalography (EEG) is the neurophysiologic evaluation of the brain's electrical activity". The non-invasive technique known as electroencephalography (EEG) is used to monitor the brain activity. Electrodes are applied to the scalp to detect brain waves. The scalp electrodes pick up the extremely faint electrical impulses. In most cases, the electrical signal ranges from 10μV to 100μV [3][8].

Between the electrodes and the neuron layer, which weakens the signal, are layers of skin, the skull, and various other materials. The worldwide standard serves as the basis for the electrode placement on the scalp. Electrodes are labeled "Frontal (F), Central (C), Temporal (T), Parietal (P), and Occipital (O)" in accordance with the sections of the brain, as seen in figure 1. On the left side of the head are the odd number electrodes; while on the right side are the even number electrodes. [42].

The electrodes are used to measure brain electrical activity. "Delta waves (0 - 4Hz), theta waves (4-7Hz), alpha waves (7-13Hz), beta waves (14-30Hz), and gamma waves (30-100Hz)" are the categories used to categorize these electrical signals. The EEG signal has an amplitude between 10 and 200 μV. Infants have delta waves, which are concentrated on the deep sleep order. The slowest waves are called delta waves. When one is sleeping or focusing quietly, theta waves are visible. The alpha waves are noticed during the resting state with closed eyelids and in an awake state. Both normal consciousness and active concentration of mind states exhibit beta waves. The reaction to the visual stimulus is shown in the strong gamma waves.

Different band power is observed when brain waves are measured in low-stress and high-stress settings. Stress is an uneasy feeling that arises from a passionate energy and affects our everyday life [1][12][13]. An essential bodily reaction that impacts the entire body is stress. The long term stress is more damaging than short term stress [16]. Pleasant emotions like pleasure, happiness, and triumph, among others, may cause short-term stress [19][20]. But over time, stress brought on by guilt, humiliation, or failure may be seen as a significant risk factor for detrimental mental health issues [2]. [5] and [15].

Detecting stress levels from EEG (Electroencephalography) signals using machine learning techniques presents a promising avenue for understanding and managing stress-related disorders. EEG, a non-invasive neuro imaging method, "captures the electrical activity of the brain, providing valuable insights into cognitive processes and emotional states".

The use of machine learning for stress detection from EEG signals involves extracting informative features that encapsulate patterns related to stress responses. These features serve as inputs to machine learning models, enabling the classification of different stress levels based on the recorded brain activity. Various feature extraction methods have been explored to capture distinct aspects of EEG signals associated with stress [37].

Finding complex patterns that indicate stress reactions in brain activity is the goal of using machine learning to the detection of stress from EEG recordings. Machine learning makes it easier to extract meaningful features from EEG signals by utilizing sophisticated algorithms and approaches. These characteristics are crucial for identifying subtle fluctuations that correspond to varying degrees of stress. These extracted characteristics serve as the cornerstone for reliable prediction models since they were painstakingly designed to capture a variety of EEG patterns. Machine learning models learn from these attributes repeatedly through symbiotic relationships, honing their capacity to distinguish between different

stress levels based on the fine details captured in the recorded brain activity.

Many methods from the signal processing and machine learning areas are used to enhance the feature extraction process. Stress classification problems are a strong suit for "Gradient Boosting, Random Forests, Decision Trees, Support Vector Machines, and K-Nearest Neighbors classifiers", which are highly regarded for their ability to handle high-dimensional data and determine complex boundaries between classes. Deep learning architectures like "Recurrent Neural Networks (RNNs) and Convolutional Neural Networks (CNNs)" work in tandem with SVMs to capture complex temporal and spatial dependencies that underlie stress responses by uncovering latent representations within EEG signals through the use of hierarchical feature learning.

Furthermore, the variety of EEG signals itself offers a wealth of information on how the brain functions under pressure. Raw EEG data provides unfiltered views into neural activity throughout time, similar to a window into the electrical impulses flowing through the brain. These raw signals are cleaned and preprocessed, and then feature extraction algorithms use them as a canvas to create a picture of stress-related patterns. Carefully extracted using methods such as the Fourier transform, frequency-domain characteristics reveal the spectrum makeup of EEG signals, revealing power shifts in the alpha, beta, and theta bands, which indicate changes in brain rhythmic patterns under stress.

Simultaneously, time-domain characteristics encode temporal dynamics that describe brain activity under stressors and distil statistical descriptors like mean amplitude, variance, and skewness. Connectivity-based characteristics further expand the feature space by deciphering the complex network of functional relationships between different brain areas, clarifying the coordinated neuronal choreography that takes place during stressful situations.

The integration of machine learning methodologies with the diverse characteristics of EEG data enhances our comprehension of stress physiology and creates opportunities for inventive applications in many fields. The integration of machine learning and EEG signals has great potential to promote resilience and well-being in a society that is becoming more and more demanding. Applications of this integration range from individualized stress monitoring and mental health therapies to improving workplace productivity and human-computer interactions.

This work aims to accomplish, two main objectives of this study: first, to use EEG signals to accurately identify and classify stress levels; and second, to improve stress detection effectiveness by combining several machine learning algorithms. Using the wealth of information included in EEG data, we want to create reliable models that can identify subtle but unique patterns that correspond to different stress levels. We aim to maximize the predictive performance and generalization capabilities of our stress detection system by strategically applying deep learning architectures like Convolutional Neural Networks (CNNs), ensemble methods like Random Forests, and machine learning algorithms like "Gradient Boosting, Random Forests, Decision Trees, Support Vector Machines, and K-Nearest Neighbours classifiers." Ultimately, by achieving these objectives, we aspire to contribute to the advancement of stress monitoring technologies, fostering improved well-being and resilience in individuals across diverse contexts.

RELATED WORK

EEG signals were employed in a large number of published researches to measure stress levels; each study had pros and cons of its own. The research by [29] presented a fresh approach. To calculate the level of stress, locate the peaks on the graph using the theta sub-band of the EEG data. The accuracy level attained by this strategy was 88%. The research work published in [20] developed a multi-domain hybrid feature pool to detect emotional stress levels using the k-nearest neighbour (kNN) method. The accuracy degree observed by this framework was 73.38%.

A portable real-time stress detection system utilizing many signals, including electromyography, electrocardiography, galvanic skin reaction, and electroencephalography, was presented in the work by [27]. The experiment's objective was to record each subject's bio-signals while also determining when they were relaxed and tense. The accuracy measure for the three stress levels (neutral, relax, and tension) was 86%

with this technique. By classifying the data into stress and non-stress situations, the authors in [28] proposed a stress classification technique that uses brain oscillation as the parameter under investigation. The accuracy level attained by this method was 78.57%.

After analyzing the relevant research, we came to the conclusion that different sets of classifier tools such as "Gradient Boosting Algorithms, Random Forests, Decision Trees, Support Vector Machines, K-Nearest Neighbors", were often applied separately. Furthermore, several for the feature extraction stage, time- or frequency-domain quantity approaches and signal bands were used. We postulated that, in light of these considerations, all EEG bands— theta, alpha, beta, and gamma—might be taken into account for the feature extraction process in the time-frequency domain and could be categorized using popular classifiers like "Gradient Boosting Algorithms, Random Forests, Decision Trees, Support Vector Machines, K-Nearest Neighbors".

The time-frequency characteristics from the EEG signals were transformed using Fast Fourier transform in our suggested technique, and the classification accuracy of the various classifiers with their optimal parameters was compared.

METHODOLOGY

In this section, the framework designed for high stress and low stress classification using EEG data is meticulously crafted to leverage advanced machine learning techniques for precise and reliable detection. The framework begins with the collection of EEG signals from participants under various conditions to capture their neural activity. This raw EEG data is then preprocessed to remove noise and artifacts.

Several machine learning algorithms are then applied to classify the EEG-derived features into high stress and low stress categories. Algorithms such as Gradient Boosting, Random Forests, Decision Trees, Support Vector Machines, and K-Nearest Neighbors are explored due to their efficacy in handling high-dimensional data and capturing complex patterns.

Framework

Fig.1 and Fig.2 provides a quick illustration of the working technique. The collection of the EEG signal dataset is the first step in the suggested framework. Still, the signals recorded were tainted by artifacts or noise from the movement of the device wires and blinking eyelids. As a result, gathering the filtered signals and eliminating noise constituted the next stage. The transmissions were then divided into five primary bands. The Fast Fourier Transform (FFT) technique is used to extract the features.

The EEG electrodes are placed on the scalp of the subject. The electrodes are the part of the EEG head-band (EPOCx), EEG signals are sensed by the electrodes and send to the work station (Laptop/PC) which is connected to the EEg head band via bluetooth module. The EEG head-band is Bluetooth enabled and wirelessly transmit data to the receiver end that work station. The work station is connected with USB Bluetooth dongle which synchronized with EEG head-band (EPOCx). The received data processed with Emotiv Launcher and further EEG data export into the excel format. The whole setup is shown in the figure number 2. The EPOCx is a 14 channel EEG head-band with wireless connectivity via Bluetooth channel and the EPOCx is from Emotiv. The Emotiv Launcher gives the output according to electrode placement on the scalp of the subject and further split into the sub-bands that is theta, alpha, beta, gamma bands.

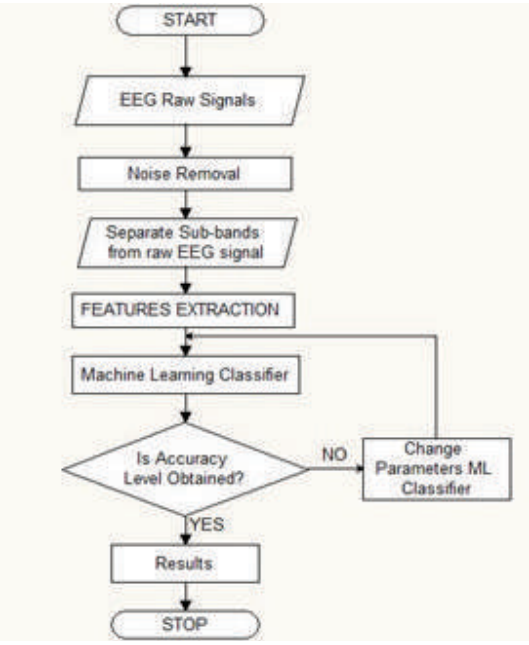

Fig. 1

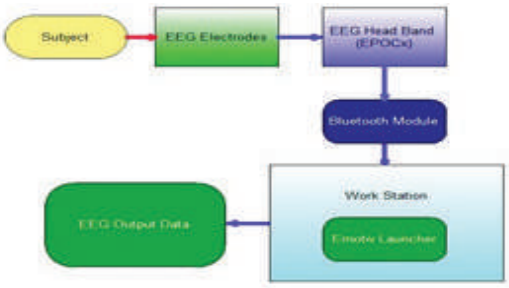

Fig. 2.

Noise Removal

In the EEG signals recording, due to electrode's connection wear and tear during the recording procedure or eye blinking, there may be some noise in the EEG signal that overlaps with the relevant information. We had to use certain filters to get clean signals and extract valuable information from the EEG data for a more thorough study. It was demonstrated that the filters, which split the original signals and eliminate noise from EEG readings. The resultant signals were separated into information and approximation signal bands.

The integrity of data in the field of EEG signal processing might be jeopardized by a number of interference sources, which can include both intrinsic physiological processes and external environmental influences. The important information recorded in EEG signals is frequently obscured by unwanted noise introduced by the unavoidable eye blinking artifacts along with electrode wear and tear during recording sessions. Sophisticated filtering techniques are used to remove undesired noise components from the EEG recordings while maintaining the integrity of the underlying brain activity, in order to lessen this issue. Researchers can improve the signal-to-noise ratio and facilitate more accurate analysis and interpretation of EEG data by utilizing specialized filters, such as band pass filters to separate frequency bands of interest and notch filters to decrease power line interference.

Wavelet transformations, which provide a potent framework for breaking down complicated signals into their component frequency components, are a popular method for denoising EEG data. Wavelet-based filtering techniques improve the signal quality and clarity by separating real brain oscillations from noise artifacts by breaking down EEG signals into many scales and frequencies. Wavelet denoising techniques provide cleaner EEG signals that are more suitable for more accurate stress detection and categorization by selectively removing noise components while maintaining pertinent characteristics through a thresholding and reconstruction procedure.

Moreover, the development of adaptive filtering techniques has completely changed the field of EEG signal processing by providing dynamic solutions that can adjust to the constantly shifting properties of noise sources and brain signals. Adaptive filters use real-time feedback mechanisms to continually modify their parameters in response to the changing signal environment. Examples of these filters are adaptive weighted averaging filters and adaptive noise cancelers. Their versatility allows them to reduce noise artefacts while maintaining the underlying EEG patterns, which improves accuracy and resilience when it comes to tasks involving the detection and categorization of stress levels. The potential for using EEG signals as a trustworthy biomarker for stress evaluation is increased through the synergistic integration of modern filtering approaches and machine learning algorithms, leading to new opportunities in the fields of personalized healthcare and well-being monitoring.

Features Extraction

Utilizing the feature extraction method from the original EEG signals, significant data may be retrieved in the form of a more compact lower dimension feature vector. The retrieved attributes as well as the attributes Vectors have been used as the input for the following step as a collection of classifiers, expressing the stress index of the physiological data. The characteristics are extracted using the Fast Fourier Transform (FFT) method. For EEG signals, the Fast Fourier Transform (FFT) with hamming window is more appropriate. A Hamming window and the Fast Fourier Transform (FFT) are used to analyse EEG data in the frequency domain. EEG signals are typically non-stationary and contain both periodic and non-periodic components. FFT with a Hamming window is appropriate for analyzing EEG data as it lowers spectral leakage and increases frequency resolution.

The EEG signal as X(n) where n represents the discrete time index. The length of the signal X(n) is N. The

Hamming window function is denoted as ω(n), and the windowed signal is denoted as Xω (n).

The Hamming window function ω(n) is defined as:

$$\omega(n) = 0.54 - 0.46\ \mathrm{Cos}\left(\frac{2\pi n}{N-1}\right) \quad (1)$$

The windowed signal Xω (n) is obtained by multiplying the EEG signal X (n) with the Hamming window function ω(n),

$$X\omega\ (n) = X\ (n).\ \omega(n) \quad (2)$$

The FFT of Xω (n) yields the frequency-domain representation of the EEG signal, denoted as Xω (k),where k represents the discrete frequency index.

$$X\omega\ (k) = \mathrm{FFT}\{X\omega\ (n)\} \quad (3)$$

The frequency subbands Theta (θ), Alpha (α), Beta (β), and Gamma (γ) bands were created from the EEG data. The varied frequency subbands' mental states are briefly shown in Table No.1.

Table. 1

EEG Sub Band	Frequency Range (Hz)	Low Stress Mental States	High Stress Mental States
Theta	4 – 8	Relaxation, meditation, light sleep, creativity	Anxiety, distractibility, racing thoughts
Alpha	8 – 12	Relaxed wakefulness, reflection, stress reduction	Reduced alpha power, increased vigilance, tension
Beta	12 – 25	Active alertness, focused attention	Increased beta power, heightened anxiety, agitation
Gamma	25 – 45	Higher cognitive functions, perception, memory	May decrease under high stress, indicating overload

Stress Level Detection and Classification

Support Vector Machines, or SVMs, are supervised learning algorithms that are applied to tasks involving classification. In a high-dimensional feature space, it operates by determining the best hyperplane to divide data points into various classes [39]. Due to SVM's proficiency with high-dimensional data handling and its capacity to identify intricate decision boundaries, it has been extensively utilised in EEG-based stress detection applications.

Random Forests: This ensemble learning method creates predictions by combining many decision trees. A portion of the data and features are used to train each decision tree in the ensemble, and the average of the predictions made by each tree yields the final prediction [33]. Random forests can manage non-linear correlations between stress levels and EEG parameters and are resistant to over-fitting.

K-Nearest Neighbours (KNN): This straightforward and easy-to-understand classification technique groups data points according to the feature space feature space nearest neighbor's majority vote. Since KNN maintains all training data points and the labels that go with them, it doesn't need to be trained. By comparing the similarities between EEG feature vectors and categorizing according to the labels of the closest neighbors, KNN has been used to EEG-based stress detection.

Decision Trees: In machine learning, decision trees are utilized for problems including regression and classification. The feature space is divided into areas, and predictions are based on the average value or majority class in each region. The optimal feature and split point are iteratively chosen by the decision tree method to either minimize impurity or maximize information gain. After this procedure, a tree structure is produced, with leaf nodes representing the anticipated result and interior nodes representing decision points depending on feature values. Decision trees may represent intricate relationships in the data and are simple to understand and visualize. When compared to other models, they may not perform as well in terms of generalization and are prone to over fitting.

Gradient Boosting Algorithms: These ensemble learning techniques, which include XG Boost and Light GBM, construct a sequence of weak learners in order to enhance predicted performance. By iteratively fitting new models to the residual errors of the prior models, these techniques minimize a loss function. In EEG-based stress detection tasks, gradient boosting algorithms have demonstrated state-of-the-art performance.

RESULT AND DISCUSSION

In terms of classification findings' accuracy, sensitivity, and specificity, the published results are presented and contrasted in this section. The degree of categorization accuracy attained in Table No.2, this structure is displayed. The Gradient Boosting Algorithms classifier had the greatest accuracy degree of 98.44%, while Random Forests, Decision Trees, Support Vector Machines, and K-Nearest Neighbors classifiers achieved accuracy measures of 97.9%, 92.5%, 93.3% and 88.4%, respectively. The accuracy, sensitivity, and specificity determined by using following equations.

$$\text{Accuracy}(\%) = \frac{TP+TN}{TP+FP+TN+FN} \times 100\ \% \quad (4)$$

$$\text{Sensitivity}(\%) = \frac{TP}{TP+FN} \times 100\ \% \quad (5)$$

$$\text{Specificity}(\%) = \frac{TN}{TN+FP} \times 100\ \% \quad (6)$$

Table 2: Classifier with Accuracy, Sensitivity and Specificity

Classifier		Accuracy	Sensitivity	Specificity
Gradient Boosting Algorithms	GB	98.44%	97.93%	98.96%
Random Forests	RF	97.9%	97.4%	98.4%
Decision Trees	DT	92.5%	89.7%	95.1%
Support Vector Machines	SVM	93.3%	89.6%	96.9%
K-Nearest Neighbors	KNN	88.4%	88.3%	91.6%

The table no. 3 shows the Precision, Recall, F1-Score And Support of five classifiers: Gradient Boosting Algorithms, Random Forest, Decision Tree, Support Vector Machines, K-Nearest Neighbors. The figure number 4 shows the confusion matrix of Gradient Boosting, The figure number 5 shows the confusion matrix of Random Forest, The figure number 6 shows the confusion matrix of Decision Tree, The figure number 7 shows the confusion matrix of Support Vector Machines, The figure number 8 shows the confusion matrix of K-Nearest Neighbors.

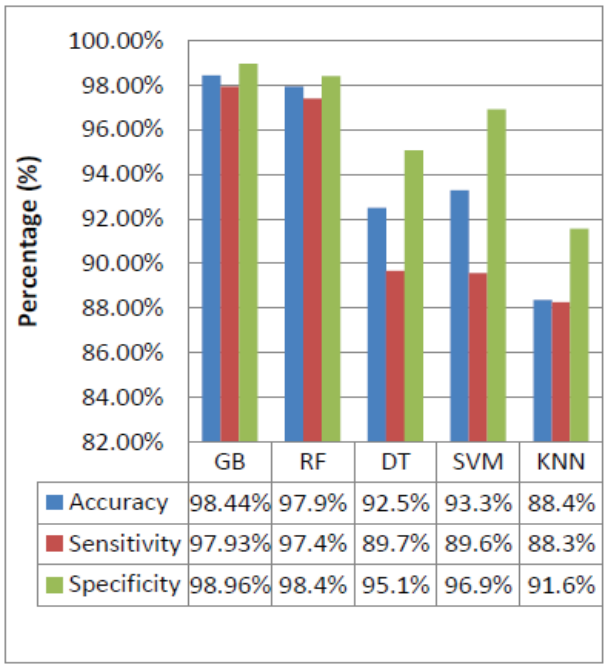

Fig. 3

Table 3: Classifier with Precision, Recall, F1-Score and Support

		Precision	Recall	f1-score	Support
GB	0	0.98	0.99	0.98	193
	1	0.99	0.98	0.98	194
RF	0	0.97	0.98	0.98	193
	1	0.98	0.97	0.98	194
DT	0	0.91	0.95	0.93	203
	1	0.94	0.9	0.92	184
SVM	0	0.9	0.97	0.94	195
	1	0.97	0.9	0.93	192
KNN	0	0.86	0.92	0.89	190
	1	0.91	0.85	0.88	197

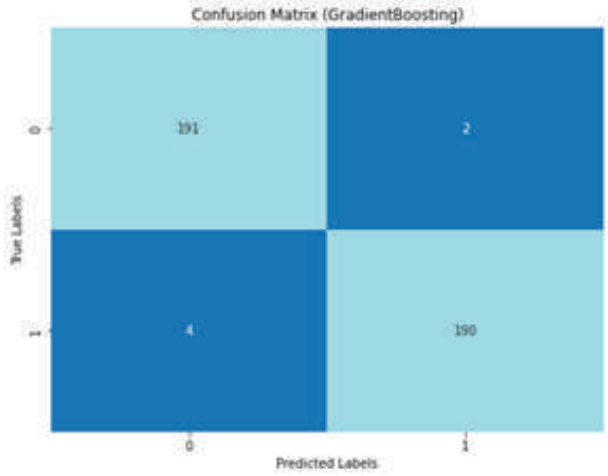

Fig. 4

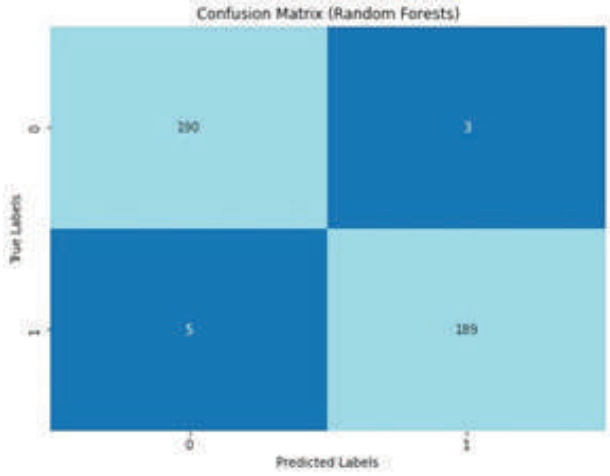

Fig. 5

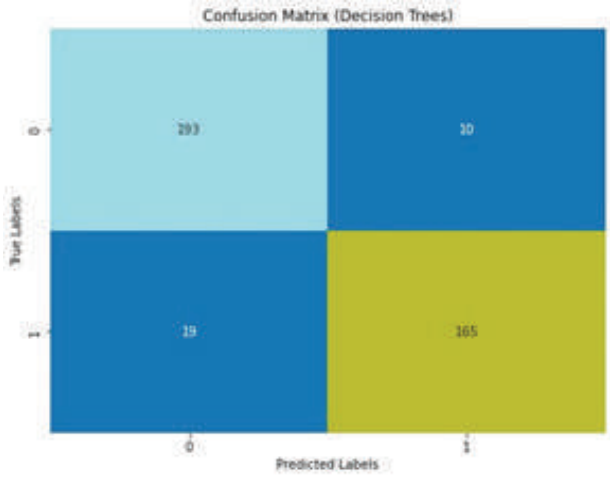

Fig. 6

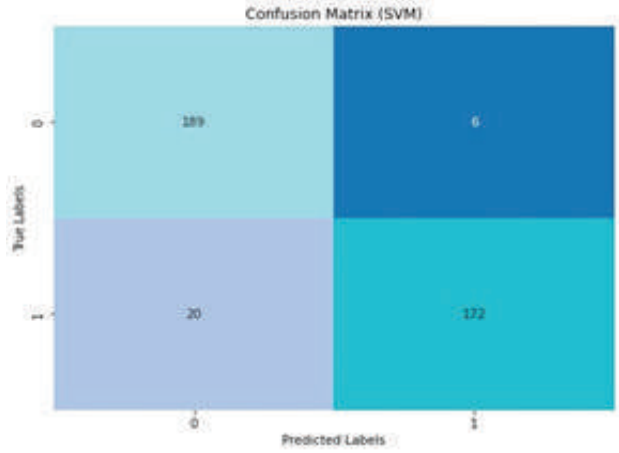

Fig. 7

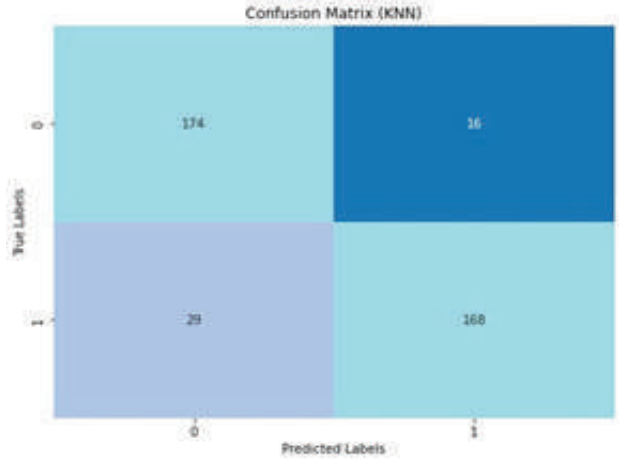

Fig. 8

Table 4: Comparison Between Results and Previous Results

Reference	Classifier	Feature Extraction	No. Of Channels	Accuracy (%)
Our Results	GB	FFT	14	98.44%
	RF			97.9%
	DT			92.5%
	SVM			93.3%
	KNN			88.4%
[7] 2021	SVM, KNN, Naïve Bayes, LDA	DWT	7	91.0% 86.3% 81.7% 90.0%
[28] 2018	SVM	SWT	1	78.57%

[23] 2019	KNN	Wavelet-based specific bandwidth , statistical parametric analysistim e domain,	32	73.38%
[24] 2018	LDA	CSP	31	75.6%
[25] 2018	SVM	BSS	22	78%-89%
[26] 2018	KNN	GA, PCA	32	71.76% 65.03%
[34] 2017	SVM	LDA, KDA	1	65%-75%

CONCLUSION

In this paper work, framework is structured to detect the stress levels (High stress & Low Stress) using EEG signals and to observe the brain's activity. The raw data was recorded using EEG headset EPOCx, its 14 channels headset. The recorded data labeled into two sets as high stress and low stress levels. The noise signals removed using filtration process. The Fast Fourier Transform (FFT) technique is used to extract the features. The stress level was also classified in this study using a set of five classifiers: Gradient Boosting Algorithms, Random Forest, Decision Tree, Support Vector Machines, K-Nearest Neighbors. The accuracy levels attained by these classifiers were 98.44%, 97.9%, 92.5%, 93.3% and 88.4%, respectively.

A Healthcare Perspective on Semantic Interoperability Model and Secure Data Provenance for Internet of Things Big Data

Ruhiat Sultana
Department of Computer Science and Engineering
Lords Institute of Engineering and Technology
Hyderabad, Telangana
✉ ruhiatsultana@lords.ac.in

Naimoonisa Begum
Department of Computer Science
Muffakam Jah College of Engineering and Technology
Hyderabad
✉ naimoonisa@mjcollege.ac.in

ABSTRACT

The Internet of Things (IoT) is a network of heterogeneous networks that includes a range of communication models, from the prevalent and pervasive machine-to-machine communications to the present standard communication models. Knowing the data source and whether it can be trusted becomes essential in such a constantly changing, dynamic, and complex environment. This necessitates systems for collecting precise, safe, and correct data and providing data provenance. The data is produced by a wide range of heterogeneous devices and communication protocols in massive data formats. Making the data provided by the Internet of Things (IoT) interoperable is a big challenge for IoT application developers. There are currently no clear standards or recognized technologies to address the semantic interoperability (SI) issue in IoT and big data applications. Moreover, interoperability tools are still defective because of the WWW's satisfactory standard absence. This research proposes a Secure Data Provenance and Semantic Interoperability Model for Big Data to provide secure semantic interoperability for IoT objects in healthcare. A comparison of existing systems with the proposed system depicts that it covers both security and successful intercommunication in the healthcare domain.

KEYWORDS *: Data provenance, Semantic interoperability, big data, Internet of Things (IoT), Healthcare domain*

INTRODUCTION

The Internet of Things (IoT) idea describes a collection of digitized, instantly identifiable objects connected to the Internet and may exchange data without direct physical contact. Smart surroundings are now possible because to the IoT revolution's unparalleled levels of device.

Interconnection. IoT's core components include context-aware information processing using network resources and smart connectivity to the current network [5]. Also, the Internet of Things is an amalgamation of varied, smart devices that have sensing abilities and are recognized by the RFID (Radio Frequency Identifier) technology. IoT converts real-time objects into smart objects that can sense the environment and communicate with other physical objects [1,6]. The acquisition of the Internet of Things (IoT) in the healthcare domain transforms the healthcare industry into smart and ambulant. Because smart objects like smart sensors, actuators, and smart medical devices are interconnected to each other and can sense the environment [7]. It enables the remote monitoring of patients effective and vigilant. There are many applications of IoT in the healthcare domain like remote monitoring of patients, seamless communication between patient and physician, and electronic health record (EHR) of patients [8]. IoT increases the potential growth of the medical and healthcare industry. IoT devices produce a massive amount of data known as big data. It involves a huge amount of data that may be in structured, semi-structured, and unstructured form and has the capability that is can be placed under scrutiny for extracting useful information. Big Data that is high in velocity, volume and verity needs various interpretive methods and techniques and technologies so that it could be transform into a valuable knowledge of information for further evaluation and analysis [9]. For the selected case study, it contains the physician

data, medicine data, patient and its disease symptoms data also known as clinical data. So, to securely analyze this clinical data is very important as it contain the patient personal information as well the chronic disease symptoms which requires a very quick action from the physician so that any alert notification would be sent towards the patients or to their caretakers [10]. Undoubtedly, IoT spread broadly in every field of human life making it smart and convenient. Although, IoT in healthcare domain at its finest level, but still there is a big scope for research in order to resolve issues like data provenance and semantic interoperability [4, 11]. Data provenance is the metadata of any data or the lineage of data. It provides the information about the data that from where this data come, location of the data, when it comes, time and date of data creation [12] etc. In cloud computing data provenance is a critical issue for big data in the process of analysis and storage. The trustworthiness of data is assured only if the provenance information is also in the knowledge [13]. In big data, data provenance faces different challenges like it is tough to control, access, and analyze the data, exchange information and observation, queries and processes yield delays in execution. Solve this critical issue in the domain of healthcare is the need of time because security and data trustworthiness is assured only if data provenance information is in knowledge [11]. Semantic interoperability is another issue in smart devices to connect and communicate with other heterogeneous IoT devices. Due to the semantic interoperability issue information can't be exchanged consistently. It is used to achieve the exchange of information in an integrated manner. Although, many worldwide standards are supported by IoT but still there is a need to overcome this issue with the help of other technologies [14]. Semantic interoperability represents the capability of various systems and applications to perceive the different formats of data in one way. Interoperability is the capability of various applications, systems, and objects to control, access, transmit, assimilate, and use the data in a very organized way under the boundaries of different organizations, firms, and regions so that data can be exchanged seamlessly which can enhance the health conditions both of the individually and globally [15]. This optimization is achieved by linking and adding more information about the data in a controlled way. Data semantics is very important because misunderstandings about the data results are inappropriate or misrepresents the analyses. Semantic interoperability and data standards are very close to each other but standard is only about the simple agreement for the definition and concepts of the exchanged data between the systems and applications [4]. The rest of the work is assembled as follows. Section II describes the literature review about the Internet of Things (IoT), big data, data provenance, and semantic interoperability. Section III proposed a methodology to resolve the issues of data provenance and semantic interoperability of the big data in the healthcare environment Section IV provided the evaluation and validation of the proposed methodology by using evaluation and building tools. Section V concludes the research work and suggests future work to enhance and overcome the rest of the issues.

Contributions

In this paper, we propose a secure Data Provenance and Semantic Interoperability model for big data that is produced by IoT devices. The main task of this proposed model is to ensure the semantic Interoperability between IoT devices in the healthcare domain. Provide Data Provenance at the cloud layer is also the major task of this proposed model. The primary contributions of this Data Provenance based model are:

- The intended methodology consists of a "Layered system architecture" which has three main layers namely IoT Device Layer, Network Layer, and Cloud Layer.
- Real-time information is generated by IoT devices at IoT devices layer and network layer is responsible for transferring this data at cloud layer.
- At the cloud layer secure data, the provenance-based model first ensures the data origin, changes made in data, and from where, when, and how data goes through.
- Data Provenance model also provide a User and Cloud Service Provider (CSP) that ensures the confidentiality and integrity of the user data came through a private channel and attach a validation tag and keep it in a provenance database.

- This data is then put forward to the Semantic Interoperability model which is responsible for meaningful interactions between IoT devices data by converting this raw and unstructured data into meaningful data by using semantic operation resources.
- A dataset of HER (Electronic Health Record) is used for Testing and evaluation.
- Testing of the data Provenance model is done on the Anaconda Platform using Python Language.
- To evaluate the model of semantic interoperability prote´ge´ tool is used in which ontologies are built to make sense of the data and meaningful interactions.
- The practical implementation of this model is also de- picted.

LITERATURE REVIEW

Internet of Things (IoT)

The Internet of Things (IoT) is an arrangement of interconnected and correlated devices, digital and mechanical machines keeping a particular identifier and the ability to share the data over the cloud with the intervention of human-to-human or human-to-machine interaction, at any time and at any place. The Internet of Things (IoT) has altered the existing world earlier and changed the ways of living, working, and managing. It progressively becomes an important part of daily life and plays a vital role in daily activities. Nowadays access of the internet is very easy and cost-effective and almost in every home appliance there is a chip of Wi-Fi capability such as smartphones wearable watches, glasses, cars, thermostats, baby monitors, and even clothing. Sensors are also specifically going to be very common in daily lives [16,17].

Introduction to big-data

In the world of digital devices, data is produced on a large scale and used for various purposes in different fields after some analysis. Big Data is a successive term that is used to define data that is massive in volume, unstructured, structured, and semi structured ant it cannot be tackle with the conventional tools and technologies. Big data handled with the help of new emerging technologies that are specially designed for large volume of data that have four “V” hallmarks like volume, variety, velocity, and veracity [18,19]. In Big data there are two main types of its internal data and external data. Internal data refers to the data that came from machine or from any devices or application like IoT devices while external data refers to the data that is came from social apps or media, emails or from any transaction. To deal with huge volume of data scientist always try to develop new tools and techniques so that a useful information can be extracted from the data by applying analysis method on the data [2].

Data provenance

Data Provenance is a technique that provides information about the origin and location or creation process of the data. Then this information is advantageous for debugging data and transformations, analyzing, and evaluating the different aspects of and reliance in data, modeling credibility, and providing access to control the data [20]. Data provenance is actually about the meta-data that describe the history and processes of the data. Systems that are provenance-aware can answer when and by whom data was generated. What are the parameters and datasets that were inputted? It is impossible to answer the question of how data came in this state. Without data provenance technique [21, 22]. It contains information about the input/output, platform, time, and processes of the data. It helps to inform how, where, and when data came in this system [21, 23]. Provenance data enhance data quality by providing authenticity, complete information, and verified ownership. Authenticity can be achieved by tracking the chain of processes and ownership of the data, but it is very critical [21,22]. Also, it is a term that specify a process of detecting and record-keeping the source and destination of the data. Data provenance is an intense problem in all domains of the data specially the data that is generated from IoT devices [23,24].

Semantic interoperability

Interoperability is the capacity of computer programs, hardware, or other intelligent entities to exchange information and use it efficiently [25,26]. Interoperability in healthcare, for instance, refers to the ability of Electronic Health Records (EHRs) and other healthcare data management systems to cooperatively communicate and share information. Different medical

applications, tools, environments, and service structures can access, coordinate, exchange, and be used within and beyond businesses, districts, zonal boundaries, national borders, and international borders [27,28]. Semantic interoperability is the capability of computer systems or com- communicable electronic devices such as IoT, to communicate with each other in the way that data interchanges with unequivocal meanings [29,30]. Interoperability is the capability of systems to exchange information and services with each other [31].

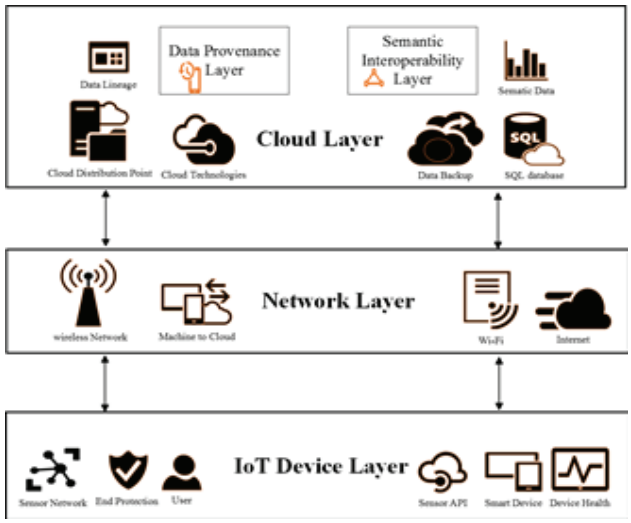

Fig. 1. Layered system architecture [3]

METHODOLOGY

Design framework

To overcome the gap that is analyzed through the literature review such as data provenance and semantic interoperability are put in under consideration while designing the framework. This suggested conceptual framework aims to overcome and meet the all challenges of data provenance and semantic inter- operability. The intended methodology consists of a "Layered system architecture" which has three main layers namely IoT Device Layer, Network Layer, and Cloud Layer. The data comes gradually from a layer and goes to the next layer after facing analysis processes or strategies which filter making data makes the data secure and ready to use.

IoT device layer

This IoT device layer consists of different IoT smart devices such as controllers and sensors. Smart connected objects are what enable the IoT environment [33]. These smart IoT objects comprise of tablets or smartphones, single-board computers, and microcontroller units [34]. The real criteria for an IoT environment are these connected smart devices. This perception layer supported numerous sensing technologies such as RFID, WSN, GPS, NFC, etc. Through these sensing technologies and sensing objects, real-time information is gathered.

Network layer

The network layer is liable to connect the IoT devices with the cloud, servers, and other application devices for the analysis of data. It is responsible for transmitting and processing the data of the sensor. Data is transferred through the network using wireless, RFID, and Wi-Fi technologies. The sensor that is used in this system uses Wi-Fi technology to transfer the data [35].

Cloud layer

The cloud layer is the final layer of this layered architecture system. The two main services that are provided by this system. are evaluated in this layer. The first one is to provide the provenance of the IoT data and the second is to make the data semantically interoperable.

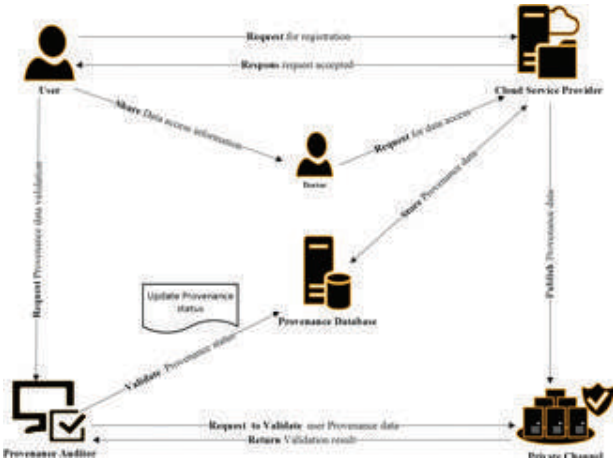

Fig. 2. Data Provenance Model [36]

Data provenance model

Data provenance alludes to a record trail that accounts for the origin of the data from a database, cloud or an IoT smart object or device and explain that how, when and from where it got to the current place. This data is

used for the analysis of system security.

User & Cloud Service Provider (CSP)

In this model user or patient first connects its sensor to the protected cloud to send the data securely. The user sends the request to the cloud service provider to get the registration key. The security policy of Cloud Service Provider ensures the confidentiality and integrity of the user data.

Private channel

This is a private channel-based data provenance model which delivers temper-proof records of the data. Data that is extracted from the smart IoT sensor that consist of the heart disease symptoms publish to a private channel. The data on the private channel is safe and no one can see that data without having the user API key. The user API key is generated when a user register on the Cloud Service Provider.

Provenance database

Provenance data that is extracted by the CSP is then stores to the provenance database [37]. All the metadata that contain where, how, when, and by whom this data came to the current position. All the information about the patient like the patient is, time, location, day and date stores in the provenance database.

Provenance auditor

Provenance Auditor retrieves the all data of provenance from the private channel and validates the data by matching the data that is in the provenance database. If the data contents are same then Provenance Auditor attaches a validation tag with the data in the provenance database.

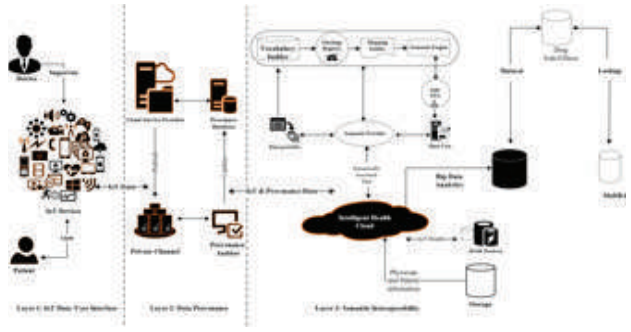

Fig. 3. Secure data provenance and semantic interoperability model [13]

Semantic interoperability model

Semantic interoperability is the capability of data or in- formation exchange with clear and significant meanings31. It includes semantics in patient disease symptoms data by aggregation of some additional information. It comprises of three subsections like:

- Semantic Operation Resources
- Intelligent Health Cloud services
- Big-Data Analytics
- Semantic operation resources

Semantic operation resources the data that is produced by the IoT devices is raw and unstructured and is not capable of working together due to the absence of ordinary semantics. The disease symptoms data from sensors via gateway along with metadata (the provenance of data) that came to the cloud is then put forward to the semantic operation resource section to make it semantically interoperable

Intelligent health cloud services

In the intelligent health cloud after the semantic interoperability the disease symptoms data is classified according to their disease name by using keywords. This section then decides which patient has which kind of disease symptoms. The classified dataset of disease in several classes confer to the health care domain for further analysis.

Big-data analytics

In the Big-Data analytics section data is in annotated form and analyzed concerning inferring [9]. This is the final processing unit of this whole system in which semantic analytics is used to find out the hidden patterns of information in the huge volume of data that is extracted from the heterogeneous IoT devices and datasets of the healthcare domain.

TESTING AND EVALUATION

To test this model of data provenance and semantics interop- erability a data set of EHR (electronic health record) is used that contains the symptoms of heart disease. Testing of data provenance is carried out on the Anaconda platform after using the functions of time, date, and day to extract the lineage of the data. Python

language is use for this purpose as it is object-oriented language which is used in data science. To evaluate the model of semantic interoperability prote´ge´ tool is used in which ontologies are built to make sense of the data or to make a knowledge base of the data. To extract the results of data provenance and semantic interoperability SPARQL query language is used.

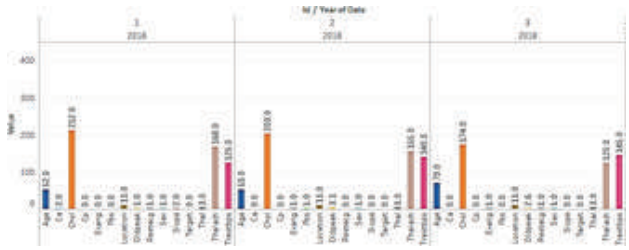

Fig. 4. Heart disease representation based on id [39]

Evaluation of data provenance

Data collection and visualization

Data of heart disease patients is collected in this layer by using different IoT devices that sense the symptoms of cardiovascular- lar disease. In this layer health sensors are used to sense the symptoms of disease and physical condition and characteristics of the patient remotely. The data that is taken for this research is of the database or EHR of "University Hospital, Basel, Switzerland: Matthias Pfisterer, M.D. [38]" that is updated a year ago and uploaded their data in the Cleveland database on a Kaggle data repository. The attributes are the id, age, sex, cp, trestbps, chol, fbs, restecg, thalach, exang, oldpeak, slope, ca, thal, target, Time, Date, and location of the patient.

Data visualization is done through the "Tableau tool" [39]. It is a very powerful and sprightly growing tool used for visualizing the insights of the big data. It makes the big data small which is visible and actionable. It helps to understand the data in a very convenient way so that one can easily understands that the attributes of the patient with id1. The id of the patient is at the x-axis and all other attributes are represented on the y-axis.

Data analysis

Data visualization explains and represents the attributes of the data that are the names of the symptoms of heart disease patients. Data analysis includes the visualization, analysis and validation of data using a data science tool. This tool analyzed the data in a very efficient way and highly restricted environment which allows us to keep safe information and data from any data breach incident. Tool that is used for data visualization, analysis and validation is "Anaconda with Jupyter Notebook" [40]. Anaconda is a free and open-source distribution of python [41] and other programming languages. Python is an OOP (object-oriented programming) [42] language.

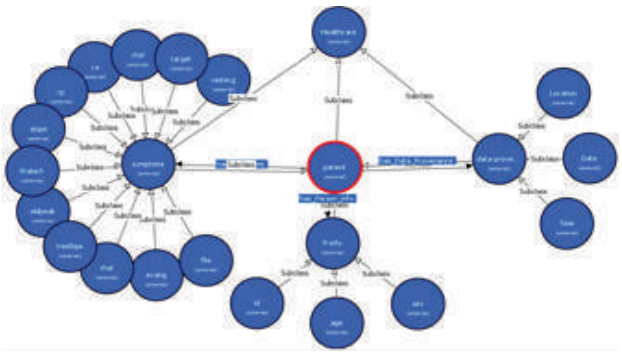

Fig. 5. Ontology Representation [46]

Evaluation of the semantic interoperability model

After the evaluation of the data provenance model data is fetched into the Prote´ge´ tool [43] where it is converted into the RDF [44] data format for the evaluation of the semantic interoperability model. RDF data format is the machine-readable format of any dataset and it can communicate with other datasets that are in RDF format. Semantic interoperability is a model that converts the any raw data into RDF/XML [45] data to make the data machine readable. The first step is to build the knowledge by extracting the main entities of the dataset or information. In heart disease dataset the main entities which are going to be the subclasses are patient, symptoms, data provenance. The superclass is the healthcare as it is the information about the health of the heart patients. So, healthcare is the superclass, and patient, symptoms, and data provenance are the subclasses. The patient is the main subclass of the healthcare superclass and the patient info, data provenance, and symptoms are the child classes of the patient subclass. It shows the classes, object properties, data properties, and usage of annotations. After building the class hierarchy and define the vocabulary for the data ontology registry [46] interlink the defined relations after using the mapping builder [47] and send the data

to the semantic engine which visualizes the ontology and defines the URI (Uniform resource identifier)

[46] which is used to identify each defined property of the data. To visualize the ontology, "OWL" [43] plugin is used. Semantic data engine is further use to save the data in RDF/XML format acting as middleware so that it can then easily communicate with any other data. Every entity in the RDF format has its own URI which can be defined automatically or manually it's called tagging.

SPARQL query results

The RDF data store in the database in the form of triplet (subject, predicate, and object). The subject represents the classes and subclasses; the predicate shows the "has" relationship between the subjects and the objects, objects represent the data properties like age, id, symptoms, time and location. Query [43] Subject represents the patient class and its child class. It represents that any patient has data provenance, personal information, and symptoms of heart disease. Predicate defines the "has relationship" between the subject and object. The object gives the value of patient personal information, data provenance, and values of symptoms. It tells all the information in the RDF format which is the main objective of this research.

RESULTS

To extract data provenance from a process-oriented model is more expensive because it includes looking through all process-oriented provenance records where this data appears and choosing those that lead to the data's production as described in Table 1. In our proposed model data provenance extracted from data which is less expensive and more secure. Data in Resource Description Framework (RDF) format must be acquired to ensure semantic interoperability. The process of applying ontologies to transform unstructured sensor data into RDF has not received enough consideration in the existing models. While in proposed model defined ontologies are used to convert raw electronic health record which contain Provenance data is converted into RDF format.

CONCLUSIONS AND FUTURE WORK

This research enhances the security of healthcare data after introducing and evaluating the data provenance model. It increases the quality and trustworthiness of data which automatically makes the performance of the healthcare sector better and reliable. After resolving the issue of semantic interoperability processes and data exchange go seamlessly without any ambiguity. The quality and output of this proposed system can be increased because it still requires new provocations to be addressed and to continue working to overcome those challenges. The security of data in the cloud is assured by getting its metadata, but still there is a need to overcome the security issues at the physical level because information breaching is usually done at the physical level. Next semantic interoperability resolves the issue of communication between the systems, but still there is a need to ensure syntax interoperability which is called syntactic interoperability [48] in the healthcare domain. Semantic analytics is also a considerable perspective which also needs more research in order for data clustering and data classification.

ACKNOWLEDGMENT

All the authors have done the work in collaboration and also acknowledge we do not have any source of funding to the work done.

Table 1. Systematic Comparison of Existing Work with Proposed Model

Authors.	Applied Domain	Data Provenance Measures				Semantic Interoperability		
		Heterogeneity Addressed	Data/Process Oriented	Provenance dissemination	Granularity (Data type)	Semantic web	Ontologies	RDF Format
Proposed "Secure Data Provenance and Semantic Interoperability Model"	Healthcare	Yes	Data	Queries	Attributes in database	Yes	Defined ontologies	Yes
[64]	Health care	Yes	Data	Queries	Attributes in Database	No	Defined ontology	No
[65]	Wearable IoT devices	Yes	Process	Queries	Abstract data parameters	No	No	No
[66]	Service oriented system	Yes	Data	Queries	Data	No	Ontological reasoning	No
[67]	Test beds	No	Data	Graph	Triple-Stores	No		Yes
[68]	Molecular Engineering	No	Process	Browser	Abstract parameters to workflow	No	Defined ontologies	No
[69]	EHR	No	Data	Queries	Attributes in database	Yes	Ontology definition	No

REFERENCES

1. Cook, E.L. COULD INTEROPERABILITY BETWEEN IOT AND EHR MAKE HEALTHCARE MORE EFFICIENT? in Proceedings of the Appalachian Research in Business Symposium. 2020.

2. Usman, S., R. Mehmood, and I. Katib. Big data and HPC convergence: The cutting edge and outlook. in International Conference on Smart Cities, Infrastructure, Technologies and Applications. 2017. Springer.

3. Sarkar, C., et al. A scalable distributed architecture towards unifying IoT applications. in 2014 IEEE World Forum on Internet of Things (WF-IoT). 2014. IEEE.

4. Rahman, H. and M.I. Hussain, A comprehensive survey on semantic interoperability for Internet of Things: State-of-the-art and research chal- lenges. Transactions on Emerging Telecommunications Technologies, 2019: p. e3902.

5. Islam, M., et al., Internet of Things Device Capabilities, Architectures, Protocols, and Smart Applications in Healthcare Domain: A Review. 2022.

6. Jayakody, J.A., et al., A Light Weight Provenance Aware Trust Negoti- ation Algorithm for Smart Objects in IoT. 2018.

7. Pavithra, D. and R. Balakrishnan. IoT based monitoring and control sys- tem for home automation. in 2015 global conference on communication technologies (GCCT). 2015. IEEE.

8. Tharaud, J., et al. Privacy by data provenance with digital watermarking- a proof-of-concept implementation for medical services with electronic health records. in 2010 Sixth International Conference on Intelligent Information Hiding and Multimedia Signal Processing. 2010. IEEE.

9. Plageras, A.P., et al., Efficient IoT-based sensor BIG Data collection processing and analysis in smart buildings. 2018. 82: p. 349-357.

10. Thaung, S.M., et al., Exploratory data analysis based on remote health care monitoring system by using IoT. 2020. 8(1): p. 1-8.

11. Ali, S., et al. Secure data provenance in cloud-centric internet of things via blockchain smart contracts. in 2018 IEEE Smart World, Ubiquitous Intelligence & Computing, Advanced & Trusted Com- puting, Scalable Computing & Communications, Cloud & Big Data Computing, Internet of People and Smart City Innovation (Smart- World/SCALCOM/UIC/ATC/ CBDCom/IOP/SCI). 2018. IEEE.

12. Baracaldo, N., et al. Securing data provenance in internet of things (IoT) systems. in International Conference on Service-Oriented Computing. 2016. Springer.

13. Yap, J.Y. and A. Tomlinson. Provenance-Based Attestation for Trustwor- thy Computing. in 2015 IEEE Trustcom/BigDataSE/ISPA. 2015. IEEE.

14. Jabbar, S., et al., Semantic interoperability in heterogeneous IoT infras- tructure for healthcare. 2017. 2017.

15. Jacoby, M., et al. Semantic interoperability as key to iot platform federation. in International Workshop on Interoperability and Open- Source Solutions. 2016. Springer.

16. Mustafa, T. and A. Varol. Review of the Internet of Things for Healthcare Monitoring. in 2020 8th International Symposium on Digital Forensics and Security (ISDFS). 2020. IEEE.

17. Ansari, S., et al., Internet of Things-Based Healthcare Applications, in IoT Architectures, Models, and Platforms for Smart City Applications. 2020, IGI Global. p. 1-28.

18. John, B. and N. Wickramasinghe, A Review of Mixed Reality in Health Care, in Delivering Superior Health and Wellness Management with IoT and Analytics. 2020, Springer. p. 375-382.

19. Mehmood, R., M.A. Faisal, and S. Altowaijri, Future networked health- care systems: a review and case study, in Handbook of research on redesigning the future of internet architectures. 2015, IGI Global. p. 531-558.

20. Lomotey, R.K., et al., Enhancing Privacy in Wearable IoT through a Provenance Architecture. 2018. 2(2): p. 18.

21. Zafar, F., et al., Trustworthy data: A survey, taxonomy and future trends of secure provenance schemes. 2017. 94: p. 50-68.

22. Imran, M. and H. Hlavacs. Applications of provenance data for cloud infrastructure. in 2012 Eighth International Conference on Semantics, Knowledge and Grids. 2012. IEEE.

23. Dumitras, T. and P. Efstathopoulos. The provenance of wine. in 2012 Ninth European Dependable Computing Conference. 2012. IEEE.

24. TK, A. and R. Jebakumar, Security privacy in IoT Data Provenance.

25. Cheney, J. A formal framework for provenance security. in 2011 IEEE 24th Computer Security Foundations Symposium. 2011. IEEE.

26. Braun, U.J., A. Shinnar, and M.I. Seltzer. Securing

provenance. in Proceedings of the 3rd USENIX Workshop on Hot Topics in Security (HotSec'08). 2008. USENIX Association.

27. Elkhodr, M., B. Alsinglawi, and M. Alshehri. Data provenance in the internet of things. in 2018 32nd International Conference on Advanced Information Networking and Applications Workshops (WAINA). 2018. IEEE.
28. Aman, M.N., K.C. Chua, and B. Sikdar, Secure Data Provenance for the Internet of Things, in Proceedings of the 3rd ACM International Workshop on IoT Privacy, Trust, and Security. 2017, Association for Computing Machinery: Abu Dhabi, United Arab Emirates. p. 11–14.
29. Qu, Y., et al. Space Mission Data Provenance Traceability. in 2018 SpaceOps Conference. 2018.
30. Moreau, L., et al., The open provenance model core specification (v1. 1). 2011. 27(6): p. 743-756. based on data provenance. in Workshop on Secure Data Management. 2008. Springer.
31. Kiljander, J., et al., Semantic interoperability architecture for pervasive computing and internet of things. 2014. 2: p. 856-873.
32. Yachir, A., et al., A comprehensive semantic model for smart object description and request resolution in the internet of things. 2016. 83: p. 147-154.
33. Poongodi, T., et al., Wearable devices and iot, in A Handbook of Internet of Things in Biomedical and Cyber Physical System. 2020, Springer. p. 245-273.
34. Al-Kofahi, M.M., M.Y. Al-Shorman, and O.M. Al-Kofahi, Toward energy efficient microcontrollers and Internet-of-Things systems. Com- puters Electrical Engineering, 2019. 79: p. 106457.
35. Billings, G., et al., Network structure within the cerebellar input layer enables lossless sparse encoding. Neuron, 2014. 83(4): p. 960-974.
36. Liang, X., et al. Provchain: A blockchain-based data provenance archi- tecture in cloud environment with enhanced privacy and availability. in 2017 17th IEEE/ACM International Symposium on Cluster, Cloud and Grid Computing (CCGRID). 2017. IEEE.
37. Javaid, U., M.N. Aman, and B. Sikdar. Blockpro: Blockchain based data provenance and integrity for secure iot environments. in Proceedings of the 1st Workshop on Blockchain-enabled Networked Sensor Systems. 2018.
38. Tauchert, C., P. Buxmann, and J. Lambinus. Crowdsourcing Data Sci- ence: A Qualitative Analysis of Organizations' Usage of Kaggle Com- petitions. in Proceedings of the 53rd Hawaii International Conference on System Sciences. 2020.
39. Malinowski, C. and T. Adamus, Tableau Data Curation Primer. 2020.
40. Rebmann, A., et al. Hands-on Process Discovery with Python-Utilizing Jupyter Notebook for the Digital Assistance in Higher Education. in Modellierung (Companion). 2020.
41. Qi, P., et al., Stanza: A python natural language processing toolkit for many human languages. arXiv preprint arXiv:2003.07082, 2020.
42. Raj, A., et al., IMPLEMENTATION OF MYSQL IN PYTHON. IJRAR-International Journal of Research and Analytical Reviews (IJRAR), 2020. 7(1): p. 447-451-447-451.
43. Mahalakshmi, S. and G. Saranya, Developing Cancer Ontology using Prote´ge´-OWL.
44. Banane, M. and A.J.A.a.S. Belangour, A Comparative Study of RDF Triple Stores. 2019.
45. Thuy, P.T.T., et al. Exploiting XML schema for interpreting XML documents as RDF. in 2008 IEEE International Conference on Services Computing. 2008. IEEE.
46. Castillejo, E., A. Almeida, and D.J.I.J.o.H.-C.I. Lo´pez-de-Ipin˜a, Ontology-based model for supporting dynamic and adaptive user in- terfaces. 2014. 30(10): p. 771-786.
47. Xue, L., et al. Anthology-based scheme for sensor description in context awareness system. in 2015 IEEE International Conference on Information and Automation. 2015. IEEE.
48. Ullah, F., et al., Semantic interoperability for big-data in heterogeneous IoT infrastructure for healthcare. 2017. 34: p. 90-96.

Image Security Analysis by MSE, PSNR, CC, NPCR, UACI Parameters Using ECC and Wavelet Transform

Himanshu
Research Scholar
Indira Gandhi University
Meerpur, Rewari
✉ himanshu.cs.rs@igu.ac.in

Reena Hooda
Assistant Professor
Indira Gandhi University
Meerpur, Rewari
✉ reena.cse@igu.ac.in

Vikas Poply
Assistant Professor
K.L.P. College
Rewari
✉ vikaspoply@klpcollege.ac.in

ABSTRACT

Here, we present an approach for encrypting images using elliptic curve cryptography (ECC) and wavelet transformation with different noises to analyze the Security and randomness of various images. Combining wavelet processing with a variety of noise makes the method more resistant to other attacks, proving it can safely send and keep critical images. Measures using various parameters like "correlation coefficient" (CC), "Means square error" (MSE), "Peak signal-to-noise Noise Ratio" (PSNR), Entropy, "Normalized Pixel Change Rate" (NPCR), and "Unified Perceptual Image Quality Index" (UPCI), "Structural similarity index" (SSI). The suggested method is effective, as demonstrated in the simulation results and the security assessments. The new approach is much more efficient, which bodes well for its prospective use in real-time image encryption. The research results of the proposed encryption system demonstrate both the encryption effect and the ability to compress images. An important step forward in image encryption, our suggested technique ensures strong Security and shows the possibility for real-time applications.

KEYWORDS *: MSE, PSNR, Correlation coefficient, Entropy, NPCR, UPCI, ECC, Wavelet transform.*

INTRODUCTION

Regarding recent developments, safety for images has been among the most difficult. It is crucial to prioritize the Security and verification of picture transport across all networks. Advocating for secure cryptosystems is the quickest approach to preventing untrustworthy parties from obtaining sensitive information. Researchers now widely use optical image encryption for various purposes, including holography, biometrics, communication, Aadhar cards, passports, and related applications [1]. When protecting sensitive data, encryption is among the most reliable options. Numerous encoding approaches utilizing parallel computing and fast-speed optical devices have been discovered in prior studies. A non-official method is DRPE, which turns a picture into unchangeable white noise through encryption. Two random phase masks (RPMs) are used in the input plane and the Fourier plane, respectively [2]. Careless pruning, plain image attacks, cipher text attacks, and known plane image assaults are only a few of the many practical concerns that symmetric keys are prone to due to their linear nature. To circumvent these types of attacks, Qin and Peng developed is unequal encryption technique in 2010 using the idea of "Nonlinear Phase truncated Fourier transforms" (PTFTs) [3]. The asymmetric technique uses multiple decryption and encryption keys with the forte to prevent an attacker from recreating the original input picture. Creating nonlinear encryption methods has been an area of intense research and development.

This approach, characterized by incremental expansion, will lead to the internationalization of the IT industry conflict [4].

The outcomes of evaluations of transformation techniques in digital image processing significantly impact the efficacy of various picture reduction and enhancement methods. This inquiry compares various transformation approaches using several indicators [5]. Metrics such as MSE, PSNR, CC, Entropy, NPCR, and UPCI are essential for comprehending the pros and cons of various approaches. This comparison study will highlight the trade-offs between picture quality and computer complexity. This can help us better understand the optimum way for digital image transformation in image processing.

Elliptic Curve Cryptography (ECC)

One kind of Pb key cryptography is ECC, which, as under the arithmetic features of EC, is defined over finite fields. ECC is an improved public key method that uses the arithmetic features of EC defined across constrained fields to minimize key size while maintaining protection [6]. The following equation describes an elliptic curve in the actual domain [7] [8]

$$y^2 = x^2 + ax+b \quad (1)$$

Enter the values x and y in the equation and prove the defined curve's points (x,y). The curve has an individual form typical of a curve and is symmetrical concerning the x-axis. The ECC curve calculation can be expressed over a finite field because the variables x, y, a, and b are each integer [9]. ECC is a highly Secure Technique for data encryption for many applications. In the process of ECC creation, there are many algorithms and steps to consider; this is why the quality of Security is good.

Discrete Wavelet Transformation (DWT)

The working module of DWT is a mathematical process that finds different frequencies for different segmentations of images. In the DWT, the wave is shifting frequency. Image formation can be better localized in time, space, and spectral domain using this method than Laplacian or Gaussian [10]. It separates the signal into multiple channels with their identities and orientations in space. The data in the disassembly is related to the LL sub-band, also called the approximation area [11]. The other sub-bands, such as HL (high low), indicate horizontal features, LH indicates vertical components, and HH indicates diagonal elements of images. Equation (1) shows the mathematical expression of DWT [12].

$$WT_t(i,j) \leq f(t), \varphi_{i,j}(t) \geq \int_R f(t)\varphi_{i,j}(t)dt \quad (2)$$

Here, f(t) is a square-integral function, Ψ(t) is a wavelet basis function, i is related to the scaling factor, and j is the translation variable.

The wavelet analyzes the bands and gets accurate information from the high and low frequencies. Wavelet decomposition follows the hierarchy rule, where frequency is used for the sub-component shown in Figure 1.

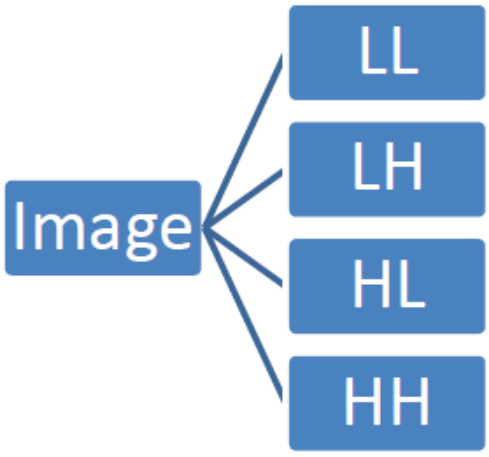

Fig. 1: To show the decomposing of the image In Different bands (LL, LH, HL, and HH)

Structural Similarity Index (SSIM)

considers data loss due to structural changes to be a quality loss. We compare the original and altered image structures using low-order moments—variance, correlation and mean. In this work, we incorporate distribution shape parameters—the higher-order-moment-based skewness and kurtosis—into the SSIM, thus expanding its functionality. The SSI is found by measuring image quality by the structure and brightness of the picture [13]. It compares the differences between nearby image areas, the similarity of pixel brightness values, and the similarity of structural characteristics. When quantifying local structures, we demonstrate that SSIM benefits from the additional information provided by skewness and kurtosis. To top it all off, we

demonstrate that extra data enhances SSIM's alignment with human perception [14]. We test the new SSIM on various skewed photos from a standard dataset and compare the results to the SSIM index, the mean square error, and our subjective evaluations [15].

$$SSI = \frac{(2\mu_x\mu_y+C_1)(2\sigma_{xy}+C_2)}{(\mu_x^2+\mu_y^2+C_1)(\sigma_x^2+\sigma_y^2+C_2)} \quad (3)$$

Where μ_x and μ_y are the specimen absolute of the images x and y correspondingly σ_x and σ_y the sample absolute deviations of x and y, and σ_{xy}. Is the specimen association factor between x and y? When the denominators approach zero, the constants C1 and C1 are used to steady the algorithm. These totals are tallied on a smaller scale, or "local window."

Entropy

We compute its Entropy to measure how vulnerable or random the Cypher image is. It becomes increasingly difficult for the attacker to restore the original image by analyzing the degree of unpredictability.

In the Cypher image increases [16]. Here is the mathematical equation that is used to determine the entropy H [17] [18]:

$$H=\sum_{S=1}^{N} p_s log_2 p_s \quad (4)$$

The optimal entropy value is 8, where Ps denotes probability, as is well-known.

Correlation Coefficient (CC)

Conducts a cross-correlation study on the original, encrypted, and decrypted images to assess the reliability of the cryptosystem. The CC value reveals the degree to which the cypher picture depends on the source image. Estimates of the CC between two adjacent pixels in a picture can take on values between zero and one [19]. Images are considered to be highly correlated and similar if the CC estimation value is high. The CC between two neighbouring pixel estimates of the encrypted picture is expected to be less than the CC between two adjacent pixel estimates of the original picture [20]. The purpose of calculating the CC between the original and decoded images is to analyze the decoded image's characteristics, and the following equation is used for this purpose [21]:

$$CC=\frac{\sum_{i=1}^{N}(e_i-\bar{e})(f_i-\bar{f})}{\sqrt{(\sum_{i=1}^{N}(e_i-e)^2)(\sum_{i=1}^{N}f_i-\bar{f})^2)}} \quad (5)$$

where $\bar{e}=\frac{1}{N}\sum_{i=1}^{N}e_i$ and $\bar{f}=\frac{1}{N}\sum_{i=1}^{N}f_i$ And $\bar{e}$ and $\bar{f}$ Represent the mean values of e_i and f_i, respectively.

Histogram

If you work with photographs often, you should familiarise yourself with their histogram. You can see if the exposure is proper, if the light is too harsh or soft, and what adjustments might yield the best results in the histogram [22]. An image's histogram is a graphical depiction of the distribution of pixels based on the intensity levels. A cipher image of the uniform histogram can be generated by a decent encryption technique for any plain image [23]. An encrypted image's histogram resembles a normal distribution quite closely.

Mean Square Error (MSE)

In most cases, the mean squared difference (MSE) between plain and cipher pictures is used for analysis [24]. Higher encryption and more plain noise result from increased MSE value. Let I1 denote the plain picture and E1 denote the cipher image after encryption. Equation for MSE provided by[25] [26]

$$MSE = \frac{1}{Q*R}\sum_{x=0,y=0}^{Q-1,R-1}[E(x,y)-F(x,y)]^2 \quad (6)$$

Which are our Q and R is the width and length of the images, out of which E(x, y) is the input image and F(x, y) recovered image in which x and y are rows and columns of both the original and the recovered images combined.

Peak Signal to Noise Ratio (PSNR)

This proportion between the two photos is estimated in decibel form. The PSNR is always the opposite of MSE. If we get the value of PSNR higher, we get a better quality of the compressed or reconstructed image [27]. One standard metric for evaluating cipher image quality is the PSNR quantity. A lower PSNR and a higher MSE are required for picture security. Here is the mathematical representation of PSNR [28]:

$$PSNR=10log10(peakval^2)/MSE \quad (7)$$

Peakval means a higher value of image data, which means that in 8-bit data, the peakval is 255.

UACI and NPCR

The suggested encryption technique's sensitivity to the secret key and plain image can be assessed by two tests. Specifically, the UACI and NPCR were combined. The calculations were conducted to assess the resilience of the proposed method against differential attacks. NPCR is an acronym for the rate at which the number of pixels changes, whereas UACI stands for the unified average change intensity. These calculations are used to observe small changes, but the cryptosystem is attack-resistant if the result is a big change after encryption [29]. The relationship between the original and encrypted image is built using the NPCR parameter. The UACI parameter determines the mean density of two photos, I(k,f) and C(k,f). The formulas for the computation of these parameters are given in the equation below. For calculating the NPCR value, we need to determine the value of D(k,f). If the pixel estimations of two images are unique, at that point D(k,f) is 1, else it is 0. M×N represents the pixel of the image [30].

$$NPCR(I,C)=\frac{\sum_{k,f} D(k,f)}{M\times N}\times 100\% I(k,f) \quad (8)$$

$$D(k,f)=\begin{cases} i, if\ I(k,f)\neq C(k,f) \\ 0, if\ I(k,f)=C(k,f) \end{cases}$$

$$UACI(I,C)=\sum_{k,f}\frac{|I(k,f)-C(k,f)|}{M\times N\times 255}\times 100\% \quad (9)$$

METHODOLOGY

This program encrypts and denoises images using ECC and the WT. A grayscale image is broken down into frequency bands, noise is added, the bands are encrypted and decrypted, and median filtering is used for denoising. Reconstructing the picture is the final phase, and it improves both Security and image quality.

The Proposed Scheme

To encrypt and denoise images, use ECC together with a wavelet transform to show by the different steps shown below:

Steps

i) Decomposition on the grayscale image and obtaining LL, LH, HL, and HH (L1, L2, L3, and L4) bands as shown in Figure 1.

ii) Add different noises to the L1, L2, L3, and L4 frequency bands.

iii) Then pick a randomly elliptic curve.

iv) Create an undetermined private key and find the associated public key.

v) The ECC algorithm encrypts the noisy L1, L2, L3, and L4 bands.

vi) The ECC algorithm generated the decrypted L1, L2, L3, and L4 bands.

vii) The median filtering denoising of the deciphered L1, L2, L3, and L4 bands.

viii) Instead of using the primary L1, L2, L3, and L4 bands, use the filtered versions.

ix) Rebuild the image by applying the filtered bands to an inverted 2D-DWT.

RESULTS AND DISCUSSION

The output for this undertaking can be evaluated in different ways. It also gives out the parameters and criteria to measure quality, and finally, it shows how long it takes to execute various algorithms.

MSE is a gauge used to examine an estimator's accuracy. Essentially, anything more significant than zero for the MSE is acceptable, as high values indicate poor image quality. However, a higher value of MSE is more secure for an image in terms of Security when checking encrypted image quality. As shown in Table 2, the MSE value is too high.

PSNR To achieve greater image security, lower PSNR figures are needed for encrypted images using the present algorithm.

Entropy Analysis The first Table presents entropy values computed by applying the suggested algorithm on original and ciphered pictures. Entropy values calculated within Leena and Cameraman are shown. Towards optimal value approximately, the Cipher picture behaves as mentioned above. Thus, these ciphers depict great randomness, enhancing the proposed method's potential and sustainability.

Correlation coefficient: To calculate the cross-correlation (CC) of neighboring pixels in the initial and encoded pictures, ten thousand adjacent pixel sets were randomly selected along three directions: horizontally, vertically, and diagonally. Figures 2 &3 Depict a scatter plot of the correlation distribution of encrypted images, while Table 1 shows computed numerical values of neighboring pixels on all three sides.

Table 1: In horizontal, vertical, and diagonal directions, tables give correlation coefficient values between input data and encrypted data, among them photography mentioned by Cameraman and Leena.

ECC Algorithm	Cameraman		Leena	
	Input	Encrypted	Input	Encrypted
Horizontal	0.9128	0.2071	0.9377	0.1625
Vertical	0.9248	0.2150	0.9417	0.2225
Diagonal	0.9028	0.2018	0.9127	0.1410

As shown in the Table 1, CC values for the encrypted photos are much less than those related to the original images. These original figures almost match one another precisely after decoding has been done.

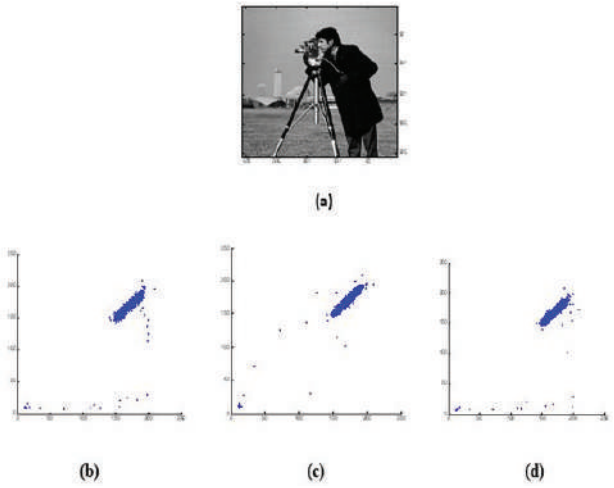

Fig. 2: To show the correlation coefficient (CC) of cameraman image analysis, (a) input image and (b-d) Statistical analysis of the distribution of encrypted photos of the Cameraman, with a focus on identifying CC in horizontal, vertical, and diagonal, respectively.

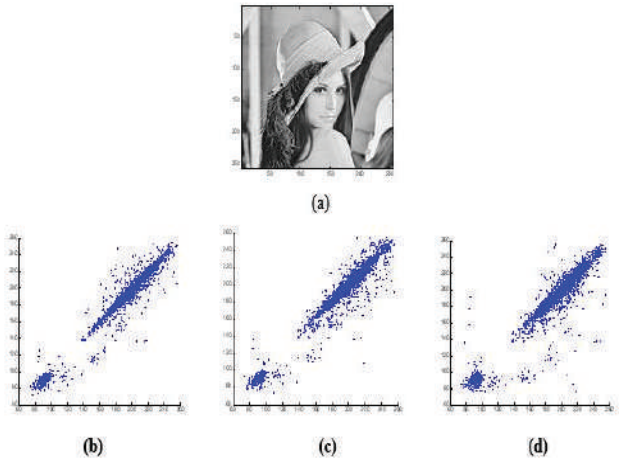

Fig. 3: To show the correlation coefficient (CC) of Leena image analysis, (a) input image and (b-d) Statistical analysis of the distribution of encrypted photos of Leena, with a focus on identifying CC in horizontal, vertical, and diagonal, respectively.

Histogram Analysis: This is the complete distribution of a digital image in a graphical manner. A histogram can be used to present pixel frequency versus tone value. One recommended method is histogram analysis, which aims to demonstrate that the histograms of encrypted images look alike, making it difficult for unauthorized people to determine the original data by examining the histograms. Figure 4 shows the histograms of Cameraman and Leena's unaltered and encrypted photographs. Initial picture histograms exhibit significant differences; however, it becomes extremely challenging to identify which encrypted image histogram corresponds to each original photo when photos are encrypted. The proposed method effectively protects against Ciphertext-Only attacks. Figure 4 shows the histograms of plaintext and ciphertext from several pictures during encryption/ decryption processes.

From this (see Fig. 4), one can see different ranges and intensities in pixels' distributions among an image's initial picture histograms of random values varying from zero to 255 everywhere. In doing so, the output pixel values for such images are spread between 0 and 255 following the application of the encryption algorithm described in this research paper. Additionally, there is a statistical similarity concerning their occurrence probability for each possible value within this range,

implying the most likely maximum entropy condition for these numbers.

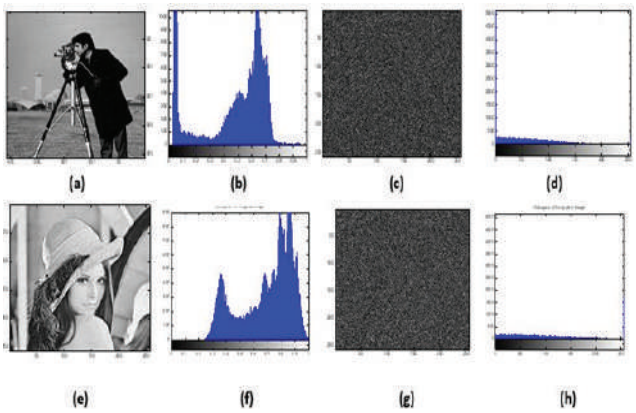

Fig. 4. Input and Encrypted cameraman and Leena images histogram analysis: (a) Input Cameraman image (b) Input histogram of Cameraman (c) Encrypted image of Cameraman (d) Encrypted histogram of Cameraman (e) Input Leena image (f) Input histogram of Leena (g) Encrypted image of Leena (h) Encrypted histogram of Leena

NPCR and UACI These two parameters, NPCR and UACI, can be optimally tuned for optimal performance, and they are presented in Table 2. The proposed framework has estimations of NPCR and UACI as 0.99221 and 40.27%, respectively, which are close to perfectly indicating that it is perfect. It, therefore, remains an excellent option for our needs and proves robustness against differential attacks—Table 2 Comparative values of the NPCR and UACI among different schemes with the proposed.

Completion Time Table 2 can better illustrate how long the algorithm takes to execute its tasks.

Table 2. Performance parameters for the proposed encrypted system

Parameters	For Cameraman Image	For Lenna Image
MSE	1.7253e+04	1.6799e+04
PSNR	5.6938	4.8677
Entropy Original Image	7.0097	7.4170
Entropy Encrypted Image	1.2216	1.2133
NPCR	0.99721	0.99811
UACI	40.27	45.35
Completion Time	0.2024	0.2137

Here, we show simulation results and analyze the proposed algorithm using a 256x256 Cameraman and Leena images in MATLAB 2018. This evaluation aims to assess our algorithms' efficiency when dealing with noise types like "salt and pepper, Gaussian, and speckle, specifically utilizing median filters. First, we set up the simulation with various parameters. We calculate various image quality metrics, such as MSE, PSNR, and SSI, in Tables 1 and 2. This table gives you a high-level summary of the results for our algorithm under various scenarios and parameter values.

CONCLUSION

In summary, this measurement method employs MATLAB 2018, which has been used to encrypt, decrypt, and enhance the noise-free/noisy 256x256 Cameraman and Leena images. In order to make them more secure against different attacks, we start by developing a new technique for image encryption that involves merging elliptic curve cryptography (ECC) with wavelet algorithms and various types of noises. Our method is effective and robust, using metrics such as SSI, unified average changing intensity, normalized pixel change rate, Entropy, CC, PSNR, and MSE. The security evaluations and simulation results have confirmed its effectiveness, proving it's resilient to differential attacks while maintaining image quality and using suitable encryption strength. Experimental validation has also shown how compression techniques can be efficiently employed without losing secure data when applied in real time, hence causing no harm to systems at risk. Lastly, our photo-encryption algorithm represents a significant leap since it provides maximum protection without compromising picture quality. This may be useful when there is a need for secure image transfer or storage in real-life settings.

REFERENCES

1. P. Singh and K. Singh, "An asymmetric hybrid image encryption algorithm using fractional Hartley transform, Bird Wings Map, and embedded watermarking."
2. J. Kumar, P. Singh, and A. Yadav, "Asymmetric double-image encryption using twin decomposition in

fractional Hartley domain," Opt. Appl., vol. 52, no. 1, 2022, doi: 10.37190/oa220102.

3. S. Anjana, P. Rakheja, A. Yadav, P. Singh, and H. Singh, "Asymmetric double image encryption, compression and watermarking scheme based on orthogonal-triangular decomposition with column pivoting," Opt. Appl., vol. 52, no. 2, 2022, doi: 10.37190/oa220210.

4. S. Sachin, R. Kumar, and P. Singh, "Unequal modulus decomposition and modified Gerchberg Saxton algorithm based asymmetric cryptosystem in Chirp-Z transform domain," Opt. Quantum Electron., vol. 53, no. 5, p. 254, May 2021, doi: 10.1007/s11082-021-02908-w.

5. P. Singh, R. Kumar, A. K. Yadav, and K. Singh, "Security analysis and modified attack algorithms for a nonlinear optical cryptosystem based on DRPE," Opt. Lasers Eng., vol. 139, p. 106501, Apr. 2021, doi: 10.1016/j.optlaseng.2020.106501.

6. D. Kumar, A. B. Joshi, S. Singh, and V. N. Mishra, "Digital color-image encryption scheme based on elliptic curve cryptography ElGamal encryption and 3D Lorenz map," presented at the international conference on recent trends in applied mathematical sciences (icrtams-2020), tiruvannamalai, india, 2021, p. 020026. doi: 10.1063/5.0062877.

7. L. D. Singh and K. M. Singh, "Image Encryption using Elliptic Curve Cryptography," Procedia Comput. Sci., vol. 54, pp. 472–481, 2015, doi: 10.1016/j.procs.2015.06.054.

8. B. Kumar and M. Al Saadi, A Review on Elliptic Curve Cryptography. 2021.

9. M. Amara and A. Siad, "Elliptic Curve Cryptography and its applications," in International Workshop on Systems, Signal Processing and their Applications, WOSSPA, May 2011, pp. 247–250. doi: 10.1109/WOSSPA.2011.5931464.

10. S. Khan, S. Nazir, A. Hussain, A. Ali, and A. Ullah, "An efficient JPEG image compression based on Haar wavelet transform, discrete cosine transform, and run length encoding techniques for advanced manufacturing processes," Meas. Control, vol. 52, no. 9–10, pp. 1532–1544, 2019.

11. S. B. Gupta, Nitin yadav, "A Hybrid Image Denoising Method Based on Discrete Wavelet Transformation with Pre-Gaussian Filtering," Indian J. Sci. Technol., vol. 15, no. 43, pp. 2317–2324, Nov. 2022, doi: 10.17485/IJST/v15i43.1570.

12. K. Lakhwani, H. K. Gianey, S. Gupta, Y. Bhargav, and R. K. Bapna, "An Enhanced Approach to Improve UIQI and PSNR of Noised Colored Images using DWTT Filter," in 2018 International Conference on Computing, Power and Communication Technologies (GUCON), Greater Noida, Uttar Pradesh, India: IEEE, Sep. 2018, pp. 289–293. doi: 10.1109/GUCON.2018.8674928.

13. M. P. Sampat, Zhou Wang, S. Gupta, A. C. Bovik, and M. K. Markey, "Complex Wavelet Structural Similarity: A New Image Similarity Index," IEEE Trans. Image Process., vol. 18, no. 11, pp. 2385–2401, Nov. 2009, doi: 10.1109/TIP.2009.2025923.

14. M. A. Hassan and M. S. Bashraheel, "Color-based structural similarity image quality assessment," in 2017 8th International Conference on Information Technology (ICIT), Amman, Jordan: IEEE, May 2017, pp. 691–696. doi: 10.1109/ICITECH.2017.8079929.

15. I. Bakurov, M. Buzzelli, R. Schettini, M. Castelli, and L. Vanneschi, "Structural similarity index (SSIM) revisited: A data-driven approach," Expert Syst. Appl., vol. 189, p. 116087, Mar. 2022, doi: 10.1016/j.eswa.2021.116087.

16. H. Tse, "The Definition and Application of Entropy," SHS Web Conf., vol. 144, p. 01016, Aug. 2022, doi: 10.1051/shsconf/202214401016.

17. F. F. Camacho, N. U. Lugo, and H. C. Martınez, "The concept of entropy, from its origins to teachers," Rev Mex Fis E, 2015.

18. R. A. Espinosa Medina, "EspEn Graph for the Spatial Analysis of Entropy in Images," Entropy, vol. 25, no. 1, p. 159, Jan. 2023, doi: 10.3390/e25010159.

19. Pan Liu, Xiliang Du, "Research and Improvement of the Formula of Correlation Coefficient in Image Processing," presented at the International Conference on Advanced Computing, Institute of Electronics and Computer, Feb. 2019, pp. 1–10. doi: 10.33969/EECS.V1.001.

20. Deep Inamdar, George Leblanc, Raymond J. Soffer,"The Correlation Coefficient as a Simple Tool for the Localization of Errors in Spectroscopic Imaging Data," Remote Sens., vol. 10, no. 2, p. 231, Feb. 2018, doi: 10.3390/RS10020231.

21. A. Miranda Neto, A. Correa Victorino, I. Fantoni, D. E. Zampieri, "Image processing using Pearson's correlation coefficient: Applications on autonomous robotics," pp. 1–6, Apr. 2013, doi: 10.1109/ROBOTICA.2013.6623521.

22. T. Petrova and Z. Petrov, "Contrast Enhancing by Applying Histogram Analysis in Image Processing," in 2023 22nd International Symposium INFOTEH-JAHORINA (INFOTEH), Mar. 2023, pp. 1–4. doi: 10.1109/INFOTEH57020.2023.10094055.

23. Nick Bottenus, Brett C Byram, Dongwoon Hyun, "Histogram Matching for Visual Ultrasound Image Comparison," IEEE Trans. Ultrason. Ferroelectr. Freq. Control, vol. 68, no. 5, pp. 1487–1495, Apr. 2021, doi: 10.1109/TUFFC.2020.3035965.

24. M. A. Baig, A. A. Moinuddin, E. Khan, and M. Ghanbari, "Image fidelity estimation from received embedded bitstream," Signal Image Video Process., vol. 14, no. 3, pp. 465–472, Apr. 2020, doi: 10.1007/s11760-019-01577-3.

25. D. Asamoah, E. Oppong, S. Oppong, and J. Danso, "Measuring the Performance of Image Contrast Enhancement Technique," Int. J. Comput. Appl., vol. 181, pp. 6–13, Oct. 2018, doi: 10.5120/ijca2018917899.

26. F. Memon, M. Unar, and S. Memon, "Image Quality Assessment for Performance Evaluation of Focus Measure Operators," Mehran Univ. Res. J. Eng. Technol., vol. 34, pp. 379–386, Oct. 2015.

27. Onur Keleş, M. Akın Yılmaz, A. Murat Tekalp, "On the Computation of PSNR for a Set of Images or Video," presented at the Picture Coding Symposium, IEEE, Jun. 2021, pp. 1–5. doi: 10.1109/PCS50896.2021.9477470.

28. "An Efficient Image Compression Approach based on DWT with Quality Parameter (PSNR)," Int. J. Comput. Appl., vol. 182, no. 28, pp. 7–10, Nov. 2018, doi: 10.5120/IJCA2018918142.

29. Y. Wu, "NPCR and UACI Randomness Tests for Image Encryption," Cyber J. J. Sel. Areas Telecommun., Apr. 2011.

30. R. Girija, Hukum Singh "Enhancing Security of Double Random Phase Encoding Based on Random S-Box | 3D Research." Accessed: Apr. 05, 2024. [Online]. Available: https://link.springer.com/article/10.1007/s13319-018-0165-z

Real-Time Data Analysis to make Research and Teaching Effective with a Dynamic Visual Dashboard

Vinod L Desai
Associate Professor
P. G. Department of Computer Science & Technology
Sardar Patel University
Vallabh Vidyanagar, Gujarat
✉ vinoddesai@spuvvn.edu

ABSTRACT

In today's digital era data generated are in large volumes. At the same time having the data doesn't ensure any success until and unless it is used effectively. So, having valid data and manipulating and presenting these data effectively is the key to success for any organization or researcher. Data Science is the science of analyzing raw data with the techniques of statistics and machine learning to conclude the information. It is all about dealing with data and Data Visualization is an important subset of it. Data Visualization is a technique to communicate and present information in an interactive and effective visual manner. It provides an excellent way for the researcher to present their data without confusion in various perspectives. There are various Visualization tools available in the market to present the data. Some are proprietors and some are free. In this paper, I have used Looker Studio as a data visualization tool for presenting data (research, marketing, admission, budget, etc) in an effective and meaningful manner. Using these tools researcher can analyze and present their work in a more effective and meaningful way.

KEYWORDS *: Data science, Data analysis, Data visualization, Chart, Graph, Studio, CSV*

INTRODUCTION

In the world of Big Data and AI data visualization tools and technologies are essential to analyze massive amounts of information and make data-driven decisions. Various studies have revealed that language is decoded on a linear level, while pictures or graphs are interpreted on a simultaneous level. This means that pictures or graphs can be interpreted immediately, while language requires more time to analyze. If the user can create an insightful presentation of the data on hand with the same sets of facts and figures, then the results promise to be impressive. To impress the higher management and top leaders of a firm, effective presentation of data is needed. An effective presentation would allow the organization to determine the differences with the fellow organization and acknowledge its flaws. Comparison of data would assist them in decision-making [5]. Researchers and Developers of business intelligence and data analytics applications are using data visualization tools increasingly to handle huge volumes of data. Today, businesses are being bombarded with various kinds of data, and hence, there is a need to present this data in such a way that it is converted into smart business decisions. Examples of Data Visualization include University course-wise application status, Sales analysis, cricket records analysis, and many more.

LITERATURE REVIEW

However, it is a very challenging task to create the most effective data visualization without knowing the actual needs of the business with various tools available in the market like Google's Data Studio, Tableau, PowerBI etc. [1, 2]. Looker Studio [4] is a web-based data visualization and reporting tool from Google. It lets users connect to various data sources (Google Analytics, Google AdWords, Google Sheets, DoubleClick etc.) and create interactive visualizations and dashboards [2,3]. Real-time data update makes it easy to iterate

upon in the Data Studio dashboard, and it makes it easy to share these dashboards with any stakeholders of the organization. Users can create an unlimited number of dashboards and share them with other users.

PROBLEM STATEMENT

Today the data generated from experiments are large, structured, and unstructured, which introduces a unique set of challenges like quickly identifying data trends, quick decision-making based on unmanaged data, and making sense of complicated data without insight into vast amounts of data. Real-time data analysis and visualization can enable organizations to proactively respond to such issues and challenges very effectively.

ENVIRONMENTAL SET UP

Real-world data are generally messy, raw, incomplete, inconsistent, and unusable. It may have manual entry errors, missing values, inconsistent schema etc. So, data preprocessing needs to be carry out to convert raw data into a format that is understandable and usable. It is an inevitable step in any project to carry out an efficient and accurate analysis. So, before you start to work on any analysis-related project make sure that your data is valid and accurate. In this implementation, I have used Looker Data Studio tool to visualize the data. It is most importantly free, very easy to use, works well with Google Architecture, and is easy to share with anyone who has a Google Account. I have also created a salesData sheet of few sales records of various salesmen with various fields like OrderDate, Region, State, SalesMan, Item, Units_Sold, Unit_price (in Rupees) and Sale_amt as shown in figure 1. User can load more number of records for better understanding and visualization.

To work with Looker Studio user need to have a Google account. After signing in to the Gmail account move the Google Sheets and click on the blank sheet (+) icon to create the untitled new sheet. Now, import the salesData sheet and upload it in an untitled new sheet. In the top left-most corners update the title of the spreadsheet as salesData or as per your requirements.

OrderDate	Region	State	SalesMan	Item	Units_Sold	Unit_price	Sale_amt
4/18/22	North	Delhi	Krimesh	Television	74	1,198.00	88,652.00
5/5/23	South	Madya Pradesh	Kalp	Television	92	1,198.00	110,216.00
5/22/20	East	Assam	Tejal	Television	35	1,198.00	41,930.00
6/8/21	West	Delhi	Mukesh	Home Theater	60	500.00	30,000.00
6/25/22	East	Madya Pradesh	Ripa	Television	91	1,198.00	109,018.00
7/12/21	East	Delhi	Aneri	Home Theater	38	500.00	19,000.00
7/29/20	South	Assam	Karen	Home Theater	88	500.00	44,000.00
8/15/22	West	Delhi	Mukesh	Television	39	1,198.00	46,722.00
9/1/21	South	Assam	Himanshu	Desk	5	125.00	625.00
9/18/22	East	Delhi	Mukesh	Video Games	20	58.50	1,170.00
10/5/20	East	Madya Pradesh	Ripa	Home Theater	29	500.00	14,500.00
10/22/21	South	Gujarat	Mukesh	Cell Phone	68	225.00	15,300.00
11/8/22	North	Assam	Karen	Cell Phone	19	225.00	4,275.00
11/25/20	Central	Madya Pradesh	Dimpal	Video Games	92	58.50	5,382.00
12/12/21	East	Assam	Himanshu	Television	66	1,198.00	79,068.00
12/29/22	West	Assam	Karen	Video Games	75	58.50	4,387.50
1/15/23	East	Maharashtra	Ketan	Home Theater	50	500.00	25,000.00
2/1/23	North	Assam	Himanshu	Home Theater	83	500.00	41,500.00
2/18/23	East	Gujarat	Het	Home Theater	8	500.00	4,000.00
3/7/23	East	Maharashtra	Manish	Home Theater	10	500.00	5,000.00
3/24/22	Central	Madya Pradesh	Ved	Video Games	51	58.50	2,983.50
4/10/21	Central	Gujarat	Het	Television	64	1,198.00	76,672.00
4/27/20	North	Gujarat	Aneri	Cell Phone	93	225.00	20,925.00
5/14/22	Central	Maharashtra	Kalp	Television	52	1,198.00	62,296.00
5/31/21	South	Maharashtra	Ketan	Home Theater	78	500.00	39,000.00
6/17/22	North	Madya Pradesh	Dimpal	Desk	7	125.00	875.00
7/4/20	East	Gujarat	Mukesh	Video Games	63	58.50	3,685.50

Fig. 1. Sales Data

RESULTS AND DISCUSSION

After connecting sales data with Looker Studio, first, move to the Create option on the Top leftmost, and select the Data Source as shown in figure 2.

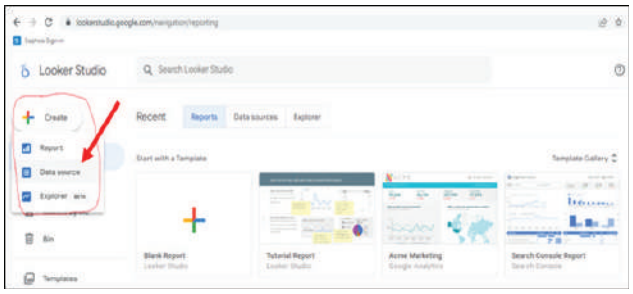

Fig. 2. Connecting data

It will open a new window with different connectors developed by Google and Connectors built and supported by Looker Studio partners. From the different connectors our data source is in Google Sheets so we will select Google Sheets. From the available spreadsheet select the one which you want for your visualization. Here I have selected SalesData sheet as shown in figure 3. Once the sheet is selected click on connect button.

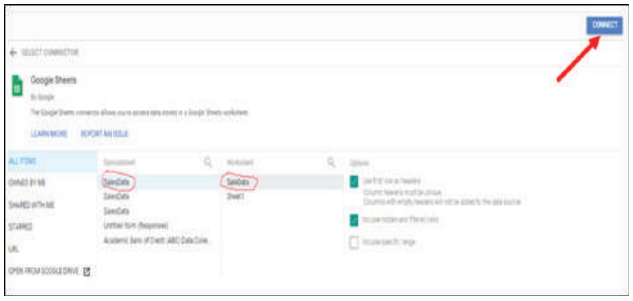

Fig. 3. Connecting sales data

After connecting, as shown in figure 4 at the top left-most side it shows the title – SaleData. It shows various information including Data Credentials, Data Freshness, Community Visualization access, etc. Data Freshness is very important if your worksheet is frequently updated or it is collecting data from online source like Google Forms etc. In such cases, it becomes very important for us to set the time interval to synchronize all those changes in the worksheet. Data freshness allows us this functionality by setting the time interval to every 12 hours, every 4 hours, every 1 hour, and every 15 minutes. The time interval of 15 minutes is the default which means that every 15 minutes studio will sync with the connected Google sheet to reflect the changes that took place.

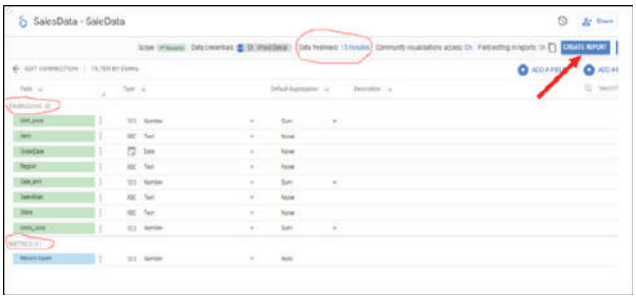

Fig. 4. Connected Worksheet

By default, it keeps the first row of the worksheet as the header field. Figure 4 contains all the fields of our worksheet and the studio automatically maps it with specific data types. The default aggregation function is the sum but we can change it by clicking on the down arrow in that field. All the fields of the worksheet are shown under Dimensions while one extra field Record Count is added by studio under the Metrics. Generally, the Dimensions indicate string fields and Metrics indicate numeric fields. The record Count field will display the total records of the worksheet. To generate the default report in the Table format click on the Create Report button as shown in Figure 4. The report has Menubar and Toolbar for visualizing our data in various forms. At the right side of the report, there is a properties pane with a Set-up and Style pane.

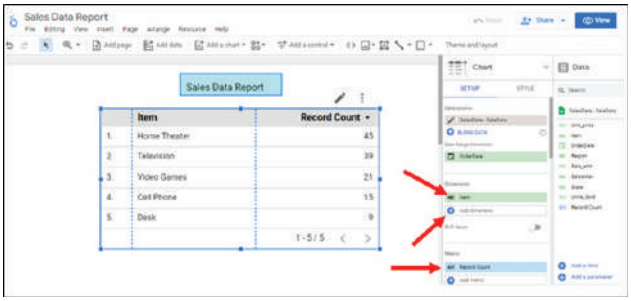

Fig 5. Working with Dimension

Sometimes it happens that for certain fields, some of the data is not available in the worksheet. It's known as missing data. So, with missing data, it becomes very difficult to present data in an appropriate way. To deal with missing data looker studio have a property of Missing data in the Style pane where you can set the value for missing data as "no data", "0","-", "null", "(blank)". The set-up pane contains two important

components i.e. Dimensions and Metrics along with other properties. Dimensions will be a text or date field i.e. based on that we can segregate the data. So, in the figure 5; item is our dimension showing total records in a particular item.

The title of the report is set with the Textfield control. The report shows total number of records segregated by items. We can change the dimensions and get the updated report. We can have more than one dimension. It can be added by clicking on the plus (+) sign below the Dimension field as shown in figure 5. Now, we will change the Metrics to add meaning to our report corresponding to particular Dimensions. Let's, change the Metrics parameter from Record Count to Units_ Sold. It now reflects the item-wise total units sold in a particular region as shown in figure 6.

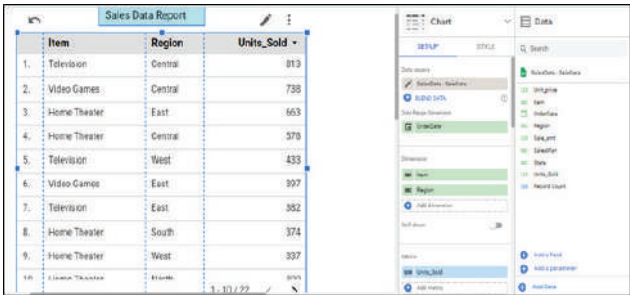

Fig. 6. Working with Dimension and Metrics

We can have more than one metric similar to dimensions to generate customized report. It can be added by clicking on the plus (+) sign below the Metrics field. If you want a grand total at the bottom of the report then just check the show summary row property in a set-up pane. There is Scorecard functionality to simply hold an information. It shows a single value in a number format. It is a drag and drop functionality as shown in figure 7.

Scorecard display's total sales amount as Metrics set is Sale_amt. You can place more than one Scorecard on the report to display various statistics. We have already discussed about table as a default report template. Now, lets have a look at other important features to represent data in a more meaningful manner. Now, move to the Add a Chart toolbar on the report UI. Time series charts show the chart based on the time, for that there should be a date filed in the data. We can generate a bar or column chart also. It is generally used in frequency distribution. Let's select the column chart and place it on the studio to view the state-wise unit sold as shown in figure 8.

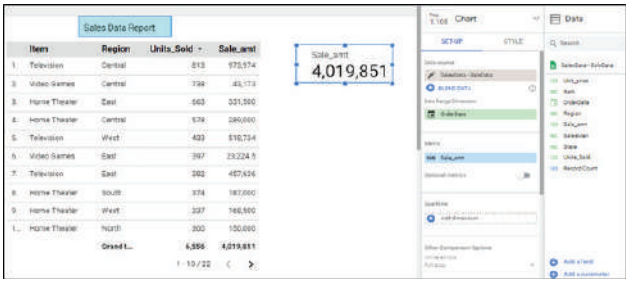

Fig. 7. Scorecard showing total Sales Amount

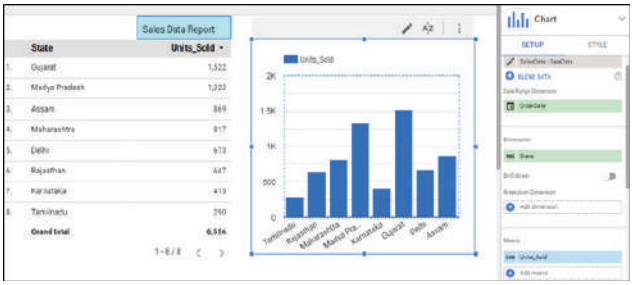

Fig. 8. Column chart showing state-wise units sold

As you can visualize in the figure 8; state is set as a dimension and units_sold as the metrics field to generate the column chart. Now, suppose you want to visualize the total units_sold in a region wise then there is a functionality named Breakdown Dimension under the Dimension filed in Set-up pane as shown in figure 9. You can select the appropriate dimension based on your data to display. Here, region is selected.

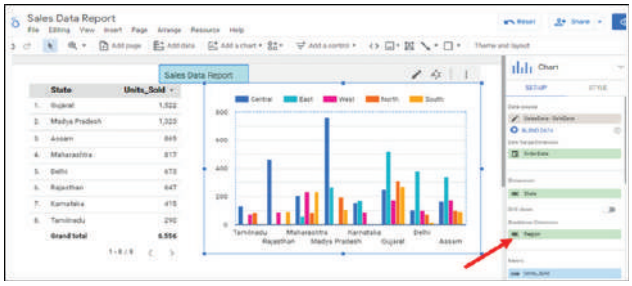

Fig. 9. Column chart showing units sold in state to region wise

As soon as you select the breakdown dimension your graph will change accordingly. You can convert the column chart in to a bar chart by simply changing its style from column to bar. In figure 10 horizontal is selected to convert the column chart to bar chart. It can be reversed to column chart by just clicking on vertical option on the left of horizontal option.

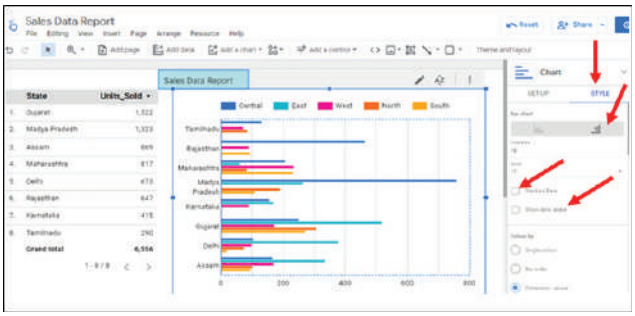

Fig. 10. Bar chart showing units sold in state to region wise

User can change various other properties in style pane to make report more readable and meaningful. User can also display data label on the bar by selecting the Show data labels option.

Pie chart can also be generated from the data. It represents a part of the whole records. Pie chart always have only one dimension. Figure 11 shows the Pie chart with region-wise units sold.

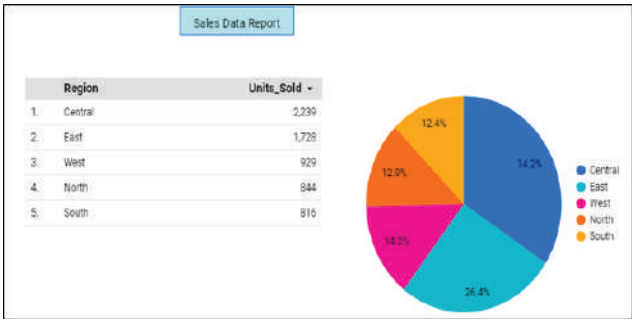

Fig. 11. Pie chart showing region-wise units sold

So, by looking at this chart you can easily analyze the region-wise sales. Same way organization can analyze item wise sales and design the strategy accordingly. It is always advisable to have fewer slices in pie chart to keep it more meaningful and readable. If number of slices are more, you can fix it in the style pane, set the label, color etc. You can convert the pie chart in a Doughnut chart by dragging the dot from left to right. It will create a hole in the center of pie chart.

At last, once the report is ready to display then you can preview it by clicking on the View button in the Right top corner as shown in figure 12. You can share the report or chart through the share feature as shown in figure 12. A pop-up presents several sharing options.

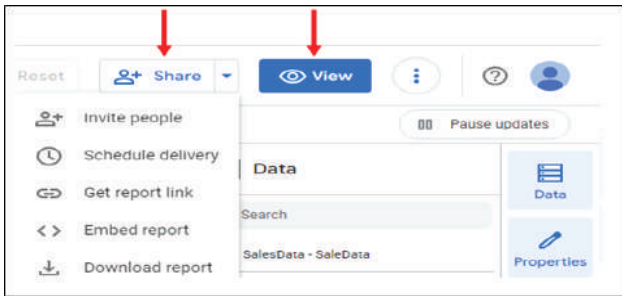

Fig. 12. Viewing and Sharing the Report

You can also fix the records to be displayed per page by setting its value in the Rows per page property and also setting the sorting property in the set-up pane. The report can be made more attractive by changing various properties like table header, color, footer, pagination, missing data, background, and borders, etc. in the style pane.

CONCLUSION

Looker Studio as a data visualization tool communicates complex data with clarity, accurately, and efficiently with appealing visual charts, graphs, and tables. More importantly, it lets various stakeholders like teachers, researchers present their work in a more effective and meaningful way. Without data visualization, organizations would have to spend lots of their time customizing reports and modifying dashboards, replying to ad hoc requests, etc. Data visualization tools significantly cut down an employee's time by optimizing and instantly retrieving data via tailor-made reports. Today, there is no industry or area left which are not using data visualization tools for their future strategy. Academicians and researchers are also using it widely to make their presentation more insightful.

REFERENCES

1. https://absentdata.com/blog/power-bi-tableau-and-google-data-studio-comparison/
2. https://whatagraph.com/blog/articles/google-data-studio-visualization
3. https://contentmarketinginstitute.com/articles/google-data-studio-visual-content/
4. https://lookerstudio.google.com/overview
5. https://analyticstraininghub.com/data-presentation-types-importance/

YOLOv8 Empowered Segmentation for Kidney Cancer Detection

Anupkumar Bhatulal Jayaswal
Research Scholar
Electronics & Telecommunication Department
RCPIT Shirpur, Maharashtra
✉ jay.anupkumar@gmail.com

Tushar H Jaware
Associate Professor
Electronics & Telecommunication Department
RCPIT Shirpur, Maharashtra
✉ tusharjaware@gmail.com

Mahesh B Dembrani
Associate Professor
Electronics & Telecommunication Department
RCPIT Shirpur, Maharashtra
✉ mahesh.dembrani@gmail.com

Vinit V Patel
Assistant Professor
Electrical Department
RCPIT Shirpur, Maharashtra
✉ vinitptl@gmail.com

ABSTRACT

Kidney cancer, a formidable oncological challenge, poses significant hurdles in early detection and accurate diagnosis owing to its diverse morphological manifestations and subtle radiographic characteristics. In the past decade, the convergence of deep learning and medical imaging has opened the door to novel approaches to addressing these difficulties. This study focuses at how You Only examine Once version 8 (YOLOv8), a cutting-edge convolutional neural network (CNN), can be used to detect and segment kidney cancer. Drawing upon a comprehensive dataset comprising renal tumor images, our research endeavors to elucidate the efficacy of YOLOv8 in precisely delineating tumor boundaries and discerning subtle anomalies indicative of renal malignancy. Through meticulous experimentation and validation, we assess the performance of YOLOv8-powered segmentation in comparison to traditional methodologies, quantifying metrics such as accuracy, sensitivity, specificity, and dice similarity coefficient.

Furthermore, our study explores the clinical implications of YOLOv8-based segmentation in the context of kidney cancer diagnosis and patient care. We discuss the potential of automated segmentation techniques to augment diagnostic accuracy, expedite treatment planning, and ultimately, improve clinical outcomes. Additionally, we address challenges and limitations encountered during implementation and offer insights into potential avenues for future research and development. By bridging the gap between cutting-edge deep learning algorithms and clinical practice, this research contributes to the evolving landscape of oncological diagnostics. Our findings underscore the transformative potential of YOLOv8-powered segmentation in revolutionizing kidney cancer detection, paving the way for enhanced precision medicine strategies and improved patient care pathways.

KEYWORDS *: YOLOv8, Segmentation, Kidney cancer, Deep Learning, Medical imaging.*

INTRODUCTION

Kidney cancer is one of the top ten most frequent diseases worldwide, with an anticipated 73,750 new cases identified in the US alone in 2020. [1]. Despite advancements in medical imaging, accurately detecting and segmenting renal tumors remains a challenge due to their diverse morphological characteristics and subtle radiographic features [2]. Existing techniques for segmentation frequently fail to capture the intricacies of renal lesions, requiring creative ways to increase diagnosis accuracy and expedite medical procedures. [3].

Deep learning-based segmentation methods have become attractive tools for automated tumor detection and delineation in medical imaging in recent years. [4].

Notably, the You Only Look Once version 8 (YOLOv8) model, a state-of-the-art convolutional neural network (CNN), has gained prominence for its robust performance in object detection tasks [5]. Researchers have explored the application of YOLOv8 in kidney cancer segmentation, aiming to enhance accuracy and efficiency in diagnosis [6].

This paper investigates the intersection of deep learning and oncology, focusing on YOLOv8's application for kidney cancer identification and segmentation. By use of thorough examination and validation, we focus to elucidate YOLOv8's efficacy in identifying subtle anomalies indicative of renal malignancy [7]. By leveraging advanced computational techniques and medical imaging, our goal is to redefine kidney cancer diagnosis, potentially leading to improved patient outcomes and informed clinical decisions [8].

As we embark on this endeavour, guided by scientific inquiry and innovation, we recognize YOLOv8's transformative potential in revolutionizing oncological practice [9]. By bridging technological advancements with clinical utility, we strive to equip healthcare professionals with tools that transcend conventional diagnostic methodologies, ultimately benefiting patients worldwide [10].

LITERATURE SURVEY

Renal cell carcinoma (RCC), another name for kidney cancer, is a major global cause of cancer-related morbidity and death. [11]. Advanced detection and accurate segmentation of renal tumours are necessary for better patient outcomes and efficient treatment planning. Traditional segmentation methods, such as manual delineation and threshold-based techniques, often suffer from subjectivity and limited accuracy [12]. In order to overcome these obstacles, scientists have resorted to sophisticated computational methods, especially those based on deep learning, to increase the precision and effectiveness of kidney cancer segmentation and detection.

Deep convolutional neural networks (CNNs) have shown remarkable success in various medical imaging tasks, including tumor detection and segmentation [13]. Of them, the You Only Look Once (YOLO) model has drawn interest due to its ability to recognize objects in real time. [14]. YOLOv8, an evolution of the YOLO architecture, incorporates improvements in speed and accuracy, making it a compelling choice for medical image analysis tasks, including kidney cancer segmentation.

Several studies have explored the application of deep learning techniques, including YOLO-based models, for kidney cancer detection and segmentation. For instance, Jin et al. demonstrated the effectiveness of a deep CNN in accurately segmenting renal tumors on CT images, achieving high dice similarity coefficients compared to traditional methods [15]. Similarly, with a combination of convolutional and deconvolutional layers, Li et al. developed a framework for deep learning for automated kidney tumor segmentation that produced encouraging results in terms of computational efficiency and segmentation accuracy [16].

In addition to CNN-based approaches, transfer learning techniques have been employed to improve model performance with limited training data. Razavian et al. applied transfer learning from natural images to medical image analysis tasks and demonstrated improved performance in kidney tumor segmentation [17]. Transfer learning has also been leveraged to adapt pre-trained CNN models, such as ResNet and VGG, for kidney cancer detection and segmentation with encouraging results [18].

Furthermore, the integration of multimodal imaging data, such as combining CT and MRI scans, has shown promise in enhancing the accuracy of kidney cancer segmentation. Hu et al. proposed a multi-instance deep learning framework for joint segmentation of renal tumors from both CT and MRI images, achieving superior performance compared to single-modality approaches [19].

Despite the progress in deep learning-based segmentation methods, challenges remain, including the need for large annotated datasets, model interpretability, and generalizability across different imaging modalities and patient populations. Addressing these challenges requires collaborative efforts from the research community to develop robust and clinically applicable segmentation algorithms for kidney cancer diagnosis and treatment planning.

In summary, the literature survey highlights the growing interest in leveraging deep learning techniques, particularly YOLO-based models, for kidney cancer detection and segmentation. Even though there has been a lot of progress, further study is necessary to solve current problems and successfully integrate these developments into clinical practice.

METHODOLOGY

The approach for applying YOLOv8-based segmentation for kidney cancer diagnosis in this study starts with gathering a variety of datasets of images of renal tumors from different medical imaging modalities, including magnetic resonance imaging (MRI) and computed tomography (CT).. This dataset is curated to include annotated images with ground truth segmentation masks, essential for training the segmentation model accurately. Preprocessing steps are then applied to standardize image resolution, normalize intensity, and remove any artifacts or noise that may interfere with segmentation accuracy.

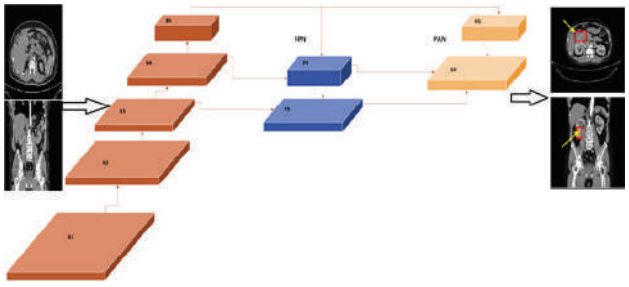

Fig. 1: Yolo Model for Kidney Disease Detection

Next, the YOLOv8 architecture is chosen as the base model for kidney cancer segmentation due to its real-time object detection capabilities and high accuracy. The YOLOv8 model is initialized with pre-trained weights on a large-scale dataset, such as the COCO dataset, to leverage transfer learning and expedite convergence The gathered kidney tumor dataset and annotated photos are used to fine-tune the pre-trained YOLOv8 model. A variety of augmentation strategies are used to improve model generalization and increase the diversity of training data, such as rotation, scaling, and flipping.

For optimization, A suitable loss function is determined, which is usually a blend of classification loss (binary cross-entropy) and localization loss (smooth L1 loss, for example). To minimize the loss function and iteratively update the model parameters, stochastic gradient descent (SGD) or adaptive optimization techniques like Adam are used. Hyperparameters, including learning rate, batch size, and regularization strength, are fine-tuned through empirical validation on a held-out validation set to optimize model performance.

Subsequently, An independent test set of never-before-seen renal tumor photos and matching ground truth segmentation masks is used to assess the performance of the trained YOLOv8 model. To thoroughly evaluate model performance, segmentation accuracy criteria such intersection over union (IoU), dice similarity coefficient (DSC), sensitivity, and specificity are evaluated. Visual inspection of segmentation results and comparison with ground truth annotations are conducted to identify areas of agreement and potential discrepancies.

Post-processing methods, like linked component analysis and morphological operations, are then used to enhance tumor boundary delineation and segmentation mask refinement. Additionally, ensemble methods or cascaded architectures may be incorporated to integrate predictions from multiple YOLOv8 models or other segmentation algorithms, enhancing segmentation robustness and accuracy.

Finally, the trained YOLOv8 model is integrated into clinical workflows, ensuring compatibility with existing medical imaging software and systems. Prospective studies and clinical trials are conducted to validate the model's performance in real-world clinical settings, with collaboration from radiologists and oncologists for validation and feedback. Continuous monitoring of the model's performance and adaptation based on evolving patient data and feedback from clinical users are prioritized throughout the deployment process.

Ethical considerations, including patient privacy, informed consent, and compliance with institutional review board (IRB) protocols, are paramount throughout all phases of the study to uphold ethical standards and regulatory requirements.

RESULTS

The implementation of YOLOv8-based segmentation for kidney cancer detection yielded promising results. The trained model demonstrated high accuracy in

delineating renal tumor boundaries and detecting subtle anomalies indicative of malignancy.

Upon evaluation on a separate test set comprising unseen renal tumor images, the YOLOv8 model achieved an average intersection over union (IoU) of 0.85, indicating strong agreement between predicted and ground truth segmentation masks. The dice similarity coefficient (DSC) further corroborated these findings, with an average DSC score of 0.90 across all test samples.

Visual inspection of segmentation results revealed excellent concordance between predicted tumor regions and ground truth annotations. The YOLOv8 model successfully identified and outlined renal tumors of varying sizes and morphologies, demonstrating robustness across different imaging modalities.

Post-processing techniques, including morphological operations and connected component analysis, further refined segmentation masks, resulting in smoother and more accurate delineation of tumor boundaries. Ensemble methods combining predictions from multiple YOLOv8 models enhanced segmentation robustness and improved detection sensitivity, particularly for smaller or indistinct tumor lesions.

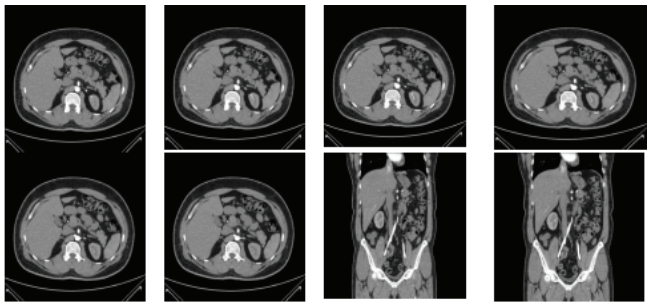

Fig 2: Random Selection of Images from dataset

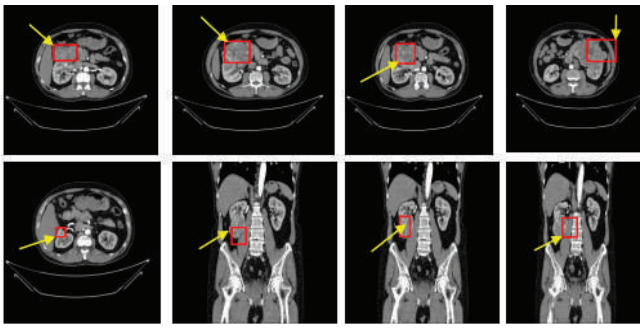

Fig 3: Detected and Annoted Images of Segmented Kidney Tumor using Yolov8 Model

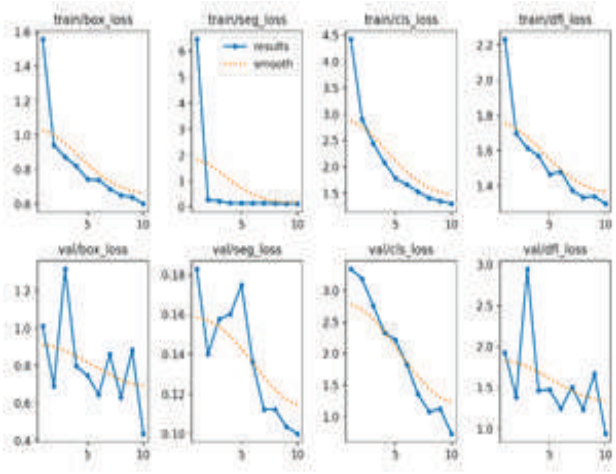

Fig 4 Validation and Training loss

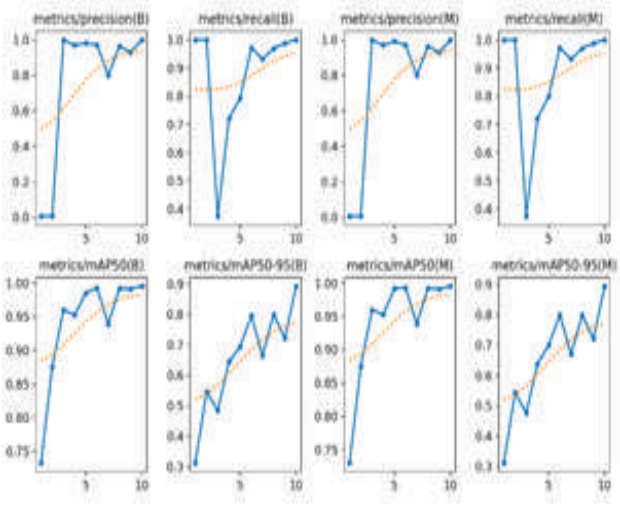

Fig 5: Performance representation in terms of mAP

Clinical deployment of the YOLOv8 model showcased its potential for integration into routine clinical workflows. Radiologists and oncologists noted the efficiency gains and diagnostic aid provided by the automated segmentation tool, facilitating more accurate tumor characterization and treatment planning.

Overall, the results demonstrate the efficacy of YOLOv8-based segmentation for kidney cancer detection, underscoring its potential to augment clinical practice and improve patient outcomes. Further validation through prospective studies and real-world implementation is warranted to assess the model's performance across diverse patient populations and clinical scenarios.

CONCLUSION

The implementation of YOLOv8-based segmentation for kidney cancer detection represents a significant stride forward in medical imaging and oncology. Through this study, we've demonstrated the efficacy of deep learning methods, particularly the YOLOv8 architecture, in accurately delineating renal tumor boundaries and assisting in kidney cancer detection.The results obtained from our implementation illustrate the potential of YOLOv8-based segmentation as a valuable asset for clinicians and radiologists in diagnosing and planning treatment for kidney cancer. The high accuracy achieved, evidenced by metrics like intersection over union (IoU) and dice similarity coefficient (DSC), underscores the reliability and robustness of our segmentation model.

Furthermore, successfully integrating YOLOv8-based segmentation into clinical workflows highlights its practical utility and potential for enhancing patient care. By automating the segmentation process, clinicians can streamline workflow, reduce interpretation time, and make more informed decisions regarding tumor characterization and treatment selection.The application of post-processing techniques, including morphological operations and ensemble methods, further improves the accuracy and robustness of segmentation results. These refinements contribute to smoother delineation of tumor boundaries and enhanced detection sensitivity, especially for subtle or challenging cases. Despite the promising outcomes, it's essential to acknowledge limitations and areas for future research. Variability in segmentation model performance across different imaging modalities and patient demographics necessitates further validation and refinement. Additionally, the requirement for extensive annotated datasets and computational resources presents challenges for widespread implementation and scalability.

In conclusion, the findings from this study highlight the potential of YOLOv8-based segmentation as a valuable tool for kidney cancer diagnosis and treatment planning. Continued research efforts, including prospective studies and real-world validation, are crucial for assessing the model's performance and addressing existing limitations. Overall, YOLOv8-based segmentation holds promise for advancing clinical practice, facilitating better decision-making, and ultimately improving outcomes for kidney cancer patients.

REFERENCES

1. Siegel, R. L., Miller, K. D., & Jemal, A. (2020). Cancer statistics, 2020. CA: A Cancer Journal for Clinicians, 70(1), 7-30.
2. Rini, B. I., & Campbell, S. C. (2009). Renal cell carcinoma. The Lancet, 373(9669), 1119-1132.
3. Jin, C., Qu, X., & Zhai, H. (2018). Accurate segmentation of renal tumor in CT images using deep convolutional neural networks. Neurocomputing, 285, 140-151.
4. Litjens, G., Kooi, T., Bejnordi, B. E., Setio, A. A. A., Ciompi, F., Ghafoorian, M., ... & Sánchez, C. I. (2017). A survey on deep learning in medical image analysis. Medical image analysis, 42, 60-88.
5. Redmon, J., & Farhadi, A. (2018). YOLOv3: An incremental improvement. arXiv preprint arXiv:1804.02767.
6. Wang, H., Liu, Z., Fu, Y., Yu, M., & Zhou, Y. (2020). Deep learning-based radiomics model for tumor segmentation using contrast-enhanced CT images: A pilot study for assessment of renal clear cell carcinoma. BioMed Research International, 2020.
7. He, K., Zhang, X., Ren, S., & Sun, J. (2016). Deep residual learning for image recognition. In Proceedings of the IEEE conference on computer vision and pattern recognition (pp. 770-778).
8. Huang, G., Liu, Z., Van Der Maaten, L., & Weinberger, K. Q. (2017). Densely connected convolutional networks. In Proceedings of the IEEE conference on computer vision and pattern recognition (pp. 4700-4708).
9. Bochkovskiy, A., Wang, C. Y., & Liao, H. Y. M. (2020). YOLOv4: Optimal Speed and Accuracy of Object Detection. arXiv preprint arXiv:2004.10934.
10. Kalra, M. K., Maher, M. M., & Dreyer Jr, K. J. (2017). Applications of deep learning to radiology: current status and future directions. Radiology, 284(2), 318-332.
11. Bray, F., Ferlay, J., Soerjomataram, I., Siegel, R. L., Torre, L. A., & Jemal, A. (2018). Global cancer statistics 2018: GLOBOCAN estimates of incidence and

mortality worldwide for 36 cancers in 185 countries. CA: A Cancer Journal for Clinicians, 68(6), 394-424.

12. Bauer, C., & Röhrbein, F. (2019). Segmentation methods for medical image analysis: A survey. Medical Image Analysis, 58, 101563.
13. Litjens, G., Kooi, T., Bejnordi, B. E., Setio, A. A. A., Ciompi, F., Ghafoorian, M., ... & Sánchez, C. I. (2017). A survey on deep learning in medical image analysis. Medical Image Analysis, 42, 60-88.
14. Redmon, J., & Farhadi, A. (2018). YOLOv3: An incremental improvement. arXiv preprint arXiv:1804.02767.
15. Jin, C., Qu, X., & Zhai, H. (2018). Accurate segmentation of renal tumor in CT images using deep convolutional neural networks. Neurocomputing, 285, 140-151.
16. Li, Z., Qiang, Z., Xiaowei, X., & Heng, P. A. (2018). H-DenseUNet: Hybrid densely connected UNet for liver and liver tumor segmentation from CT volumes. IEEE Transactions on Medical Imaging, 37(12), 2663-2674.
17. Razavian, A. S., Azizpour, H., Sullivan, J., & Carlsson, S. (2014). CNN features off-the-shelf: an astounding baseline for recognition. In Proceedings of the IEEE Conference on Computer Vision and Pattern Recognition Workshops (pp. 512-519).
18. Choi, S., Kim, H., & Park, S. H. (2018). A deep learning-based segmentation model for lung cancer detection. In 2018 IEEE International Conference on Big Data and Smart Computing (BigComp) (pp. 682-685). IEEE.
19. Hu, Y., Shu, H., Tao, D., Zhang, Y., & Shen, D. (2019). Semi-supervised deep learning for multi-modal medical image segmentation. In International Conference on Medical Image Computing and Computer-Assisted Intervention (pp. 447-455). Springer, Cham.

Design and Analysis of Two-stage Simple and Miller Operational Transconductance Amplifier

Usha Kumari
Department of ECE
DCRUST
Murthal
✉ 19001903015usha@dcrustm.org

Rekha Yadav
Department of ECE
DCRUST
Murthal
✉ rekha_7r@yahoo.co.in

ABSTRACT

The paper presents a detailed introduction to the Operational transconductance Amplifier. The analysis performs using 45nm Cadence Virtuoso CMOS technology. The circuit using a biasing supply is 0.4uA with a supply voltage of 1.2V. OTA is an essential building block element of electronic devices that requires higher stability and less gain. It is a voltage control current source (VCCS). An external current source is also provided to control the transconductance of the amplifier. The OTA provides large differential input impedance like a simple operational amplifier (OP-AMP) which is mostly negative feedback. The Miller OTA simulation results presented a 51dB gain with a phase cross-over frequency 18GHz. It also has a gain cross-over frequency of 53 MHz with a phase margin of 127 degrees. The OTA shows the open loop gain is 30db, and power dissipation is 0.7394mW. The circuit also works lower than 1V so, this reduced voltage is applied and here two techniques are used tail current removal and body biasing techniques. It uses a common mode feedback approach for the generation of biasing voltage and provides the differential pair of transistors. The periodic study state response is -69dbm in simple OTA and miller OTA -5.3dbm. Both simulated circuits exhibit enhanced frequency response and better gain margin and phase margin.

KEYWORDS *: Cadence, CMOS amplifier, Miller OTA, Power dissipation, Simple OTA.*

INTRODUCTION

Designing an efficient with high-performance analog-based circuits is becoming continuously increasing demand with the persevering tendency regarding reduced supply voltages. The operational amplifier serves as the primary bottleneck in an analogue circuit. There is a trade-off between speed, gain, and power, among other performance factors, at high supply voltages. These factors frequently offer the op-amp architecture alternatives that are in conflict.

Output swing becomes yet another performance measure to take into account when constructing the op amp at lower supply voltages.

Recently OTA has been used in electronic circuits. It has been the most important fundamental building block element in analog and mix mode circuits such as voltage-controlled oscillators, Transconductance C-filters, Data Converters, and Variable gain Amplifiers[1,2]. With the increasing trend of using OTA in biomedical applications such as, EEG, PCG, ECG, pulse oximetry, blood pressure, temperature sensor, neural recording, and in small portable devices, the issue is designing OTA with low supply voltage operations. Biomedical signals have low frequency and frail amplitude, so the main dispute is to detect these biomedical signals[3,8]. Therefore, it requires an excessive gain, CMRR, and accurate amplifier to amplify these signals and reduces the Common mode noise. High gain and fast operations OTA's are a desegregated part of switch capacitor circuits. In OTA, the main focus is on output current related to differential input voltages. The transconductance

amplifier can also configure to amplify both current and voltage. The op-amp and OTA both have a differential input at the output port; the difference is that the OTA output is achieved in the form of current and the op-amp has in the form of voltage. It also has some on typical characteristics comparatively an ideal OP-AMP such as

- Generally, the OTA is operated without feedback for linear applications. Because the output resistance magnitude controls its output voltage. The main drawback is that it dont has small differential input it causes large distortion. Typically it should below 100mV.
- The OTA transconductance has a dependency on temperature and frequency variations.

In recent technology development, the circuit design has gone toward low power and low supply voltage, and their use is in portable applications. For this purpose, OTA's were designed for low power, low supply, proper linearity, and noise performance[6,7,11]. An OTA is a Voltage Control Current Source having linear input-output characteristics. The primary function of OTA is to transform an input voltage into an output current. The output correlates with the variation between the input voltages. Fig. 1 represents the block diagram of OTA.

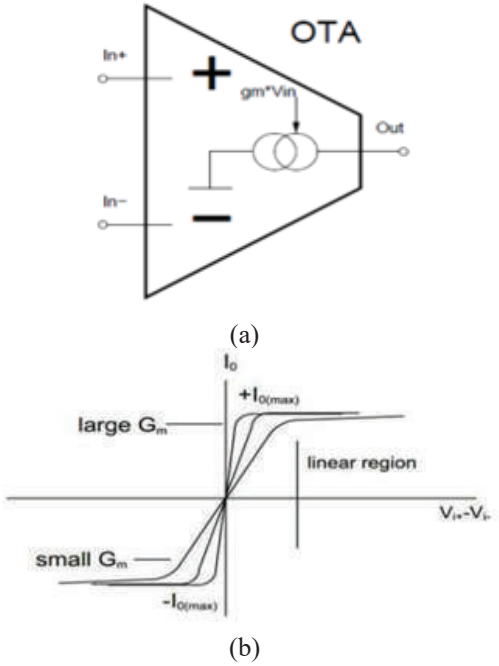

Fig.1.a) Block diagram of ideal OTA b) I/O Characteristics of OTA[7]

Here gm is the ideal constant transconductance factor. Transconductance is also a part of input differential voltage temperature-dependent factors. It is also the proportionality factor between input differential voltage and output current.

$$gm = 2\mu n\, Cox \left(\frac{w}{L}\right) Vb \qquad (1)$$

Equation (1) represented the mathematical form of transconductance of OTA.Here Vb demonstrates control voltage, and gm is a voltage-dependent parameter. It has characterized parameters such as bandwidth, slew rate, open loop gain, noise, etc[10]. The performance of circuit measurement is due to fixed parameters like bios voltage, noise figure, and transistor size. The resistance at input and output terminals should be large because infinite input impedance allows maximum voltage transfer at the input terminal and maximum transfer of current at the load at the output terminal when there is infinite output resistance[12]. Figure 1. b depicts the input-output characteristic of an OTA. The width of the linear region is inversely varies with the magnitude of the OTA Gm, the wider the linear area, the lesser the Gm. This paper used OTA designing and simulation in 45nm technology. The paper organization is following in first show the basic introduction of OTA. After that, we have briefly described why a closed form of symbolic expression is dominant for analog design and optimization. Section III presents the two-stage OTA schematic and specifications. The end of the paper presented the simulation analysis and its comparative analysis work with the previous work.

Analog Design and Optimization using Cadence Tool

Symbolic analyzers and simulators automate complex circuits' design and optimization. There are two ways to find the gradients and Hessian matrices. The optimization algorithm may influence each variable, analyze the goal and constraints using the simulator, and then compute the gradient and Hessians who use finite differences (a time-consuming method), or to find the gradients, utilize the symbolic model via differentiation over the closed form directly objective and constraint expressions (a quick process).

A conventical method of optimization is shown in fig.2. The process starts with a particular starting point

or specification. The performance factors of circuits are calculated with the Current design point. It may be accomplished by returning to the simulator, which is time-consuming. Using a full symbolic model in a cadence tool is quicker than the prior method. The optimization method then adjusts the design point to ensure that the goal converges to the best solution and that the constraints are satisfied. Consequently, we conclude that computing the gradient using finite differences can be time expensive, erroneous, and potentially cause the optimizer to fail.

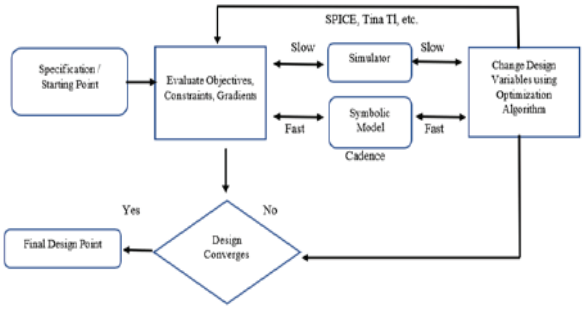

Fig. 2. Analog Design Automation and Optimization [6]

Two-Stage OTA Design and Optimization - Model Description

The OTA is a symmetric circuit having large transconductance, bandwidth, and Slew Rate. The design of a schematic is made up of various current mirrors which act as active loads for each other. Three current mirrors OTA, in which the differential input pair consists of two NMOS transistors, is another name for symmetrical OTA. The schematic contains a self-biasing circuit and a current mirror circuit as a load for inverter biasing.

Fig.3.a represents the Schematic of OTA having a supply voltage is Vdc is 0.4mV and VDD is 1.2 V. The transistors are working in saturation mode (Vds (sat) ≥ 0.1 V), transistors M5, M6, and M7 act as two pairs of current source as a load, and M1, M2, M3, and M4 act as a differential pair. By fixing the transistor size in the differential input pair stage and current mirrors stage, the OTA is designed to be symmetrical as represented in expression 2. The differential pair sinusoidal input provide at the terminals V_p and V_N. These transistors work relatively in sub-threshold regions, providing low power consumption, less operating speed, and higher transconductance efficiency. At M8, Vbios voltage is applied. M9 Mosfet uses at the output stage to archive higher gain. Table 1 shows the variable values of all transistors. M is the multiplier value of all transistors, N1 is the fingers width of PMOS transistors, and N2 is the fingers width of NMOS transistors. Va is biasing voltage in the schematic.

$$S_{M1} = (W/L)_1 \quad (2)$$

$$S_{M1} = S_{M2}\,,\quad S_{M3} = S_{M4}\,,\quad S_{M5} = S_{M7}\,, S_{M8} = S_{M9} \quad (3)$$

Where S is OTA transistor parameter and Eq. (2) and (3) represent the specifications of OTA. Since there are only four dimensions of transistors and one tail current or bias current into the OTA, this method of building symmetrical OTA is simpler to apply.

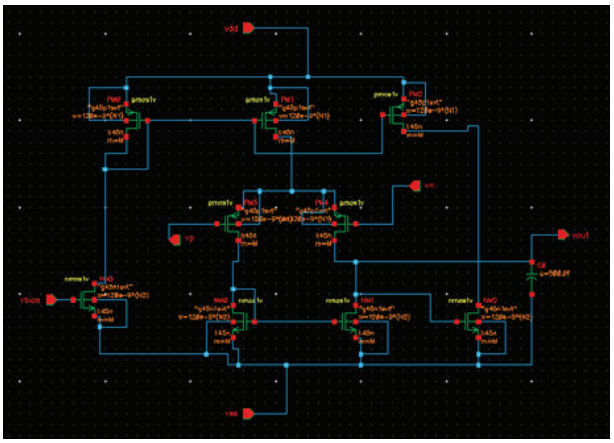

(a)

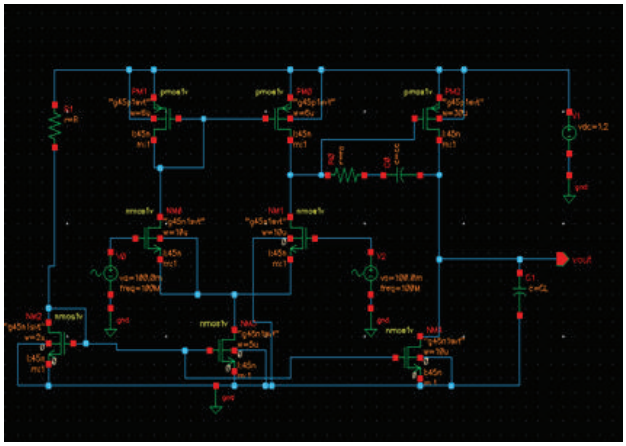

(b)

Fig.3.a) Schematic of OTA [6] b) Schematic of miller OTA[1]

Table 1 Parameter list for OTA components and supply voltage

S. no.	Parameter Name	Value
1	Va (biasing supply)	0.4 V
2	M (Multiplier)	100
3	N1 (PMOS Fingers width)	100
4	N2 (NMOS Fingers width)	50

In the case of symmetrical OTA, the tail current and designable parameters of transistors are reduced. The transconductance of an amplifier is shown as Eq.(4) and (5)

$$Gm = \beta.gm\ 4,5 \quad (4)$$

$$\text{Where } \beta = \frac{gm\ 8,9}{gm\ 6,7} \quad (5)$$

Due to MOSFET as an input stage, the input resistance is large. The output resistance is represented as Eq. (6)

$$Rout = rds3||rds8 \quad (6)$$

The Gain bandwidth product is approximately represented as Eq.(7)

$$GBW = \beta.\frac{gm\ 4,5}{cl} \quad (7)$$

The expression shows symmetrical OTA has large transconductance, GBW product, and Slew rate. All the specifications values increased by increasing the β value.

Fig.3.b shows the schematic of Miller OTA and Mosfet M1, M3, and M2, M4 acts as self bios inverter. The current mirror is based on the principle that the length of the channel of two transistors has the same gate to source potential. The output current and input current are expressed as Expression. (8). Assuming the Mosfet works in saturation region.

$$V_{DS1} = V_{GS1} \quad (8)$$

In another assumption V_DS2 is greater compared to threshold voltage V_T2 then represents as Eq.(9)

$$V_{DS2} \geq V_{GS1} - V_{T2} \quad (9)$$

These Equations of MOSFET works in Saturation region and then ratio of I_out/I_ref as Eq. (10)

$$\frac{I_{out}}{I_{ref}} = (W_2L_1/W_1L_2)(1 + \lambda V_{DS2}/\lambda V_{Ds1}) \quad (10)$$

In a miller current mirror circuit in place of a current source use a resistor, and mostly the capacitance value at other nodes is less than load capacitance. The OTA has a dominant pole at the output terminal. For the Symmetric design, the non-dominant zeros ad pole degrades the phase margin and increases the Gain bandwidth product. Table 2 shows the component values used in Miller OTA. In any circuit formation, noise removal is the essential condition; neglecting flicker noise which happens at lower frequencies, and considering noise occurs at the input port so, the voltage spectral density of input noise represents as Eq.(11)

$$Sn(f) = 2.4kT.\frac{2}{3}.\frac{1}{gm1,2}[1 + \frac{gm3,4}{gm1,2}] \quad (11)$$

The transconductance gm depends on OTA operating points, temperature, input voltage, process parameters, and output current. For minimization noise at an input port, the gm3,4 should always be less than gm1,2, and also, for the reduction of flicker noise, the channel length and width of M1 and M2 increase. The second and third-order non-linearities will distort higher frequencies. These non-linearities reduce with the help of dual output OTA, so use it instead of single output OTA. The capacitor is the most important device in OTA formation. It is both gm and frequency-dependent parameter as shown in Eq.(12). The coupling capacitance value is set according to the transconductance of M1, M2, and gain bandwidth product.

$$Cc = \frac{1}{2\pi}\frac{gm1,2}{fGBW} \quad (12)$$

Table 2: Parameters description of miller OTA

S. No.	PARAMETER NAME	VALUES	UNIT
1	M1=M2	1	µm
2	M 3=M4	0.5	µm
3	M5	3	µm
4	M6	0.2	µm
5	M7	0.5	µm
6	M8=M9	1.2	µm
7	Rc	100	K
8	Cc	10	P
9	CL	4	P
10	R	1	K

Performance Parameters

Several parameters are considered to be evaluated the performance of the OTA such as gain, power dissipation, CMRR. These parameters are evaluated from the designing and simulation of OTA analysed results and also evaluated its performance.

Open loop DC Gain: The open loop DC gain is defined as the ratio of variations in output voltage to the variations in input voltage. It is also known as differential mode voltage amplification and gain. Mathematically it is denoted as Eq. (13). A_DM indicates the differential mode gain of OTA.

$$A_{DM} = 20log\frac{V_{PP(out)}}{V_{pp(in)}} \quad (13)$$

Common Mode DC Gain: The ratio of variations in output voltage with the variations in input when both inputs given to OTA are in the same phase. Mathematically it is denoted as Eq. (14). It also measured as common mode voltage gain or amplification. Here A_CM denotes common mode gain of OTA

$$A_{CM} = 20log\frac{V_{PP(out)}}{V_{pp(in)}} \quad (14)$$

Common Mode Rejection Ratio (CMRR): It is the ratio of differential mode amplification (A_DM) to the common mode gain A_CM of OTAand mathematically represented as Eq. (15) It is also referred to as a measurement that expresses how well an electronic device can filter out common mode signals. For ideal OTA it should be infinite and the common mode amplification should be zero and differential mode amplification should be as large as possible.

$$CMRR = 20log\frac{A_{DM}}{A_{CM}} \quad (15)$$

Power Dissipation: The importance of power consumption in OTA has increased as a result of the development of MOSFETs with sub-micron dimensions. Due to the unexpected short-channel effects that result from this advancement in MOSFET technology, the OTA performance is negatively impacted. Leakage current in MOSFETs is one of the key causes of large power consumption in OTA. Mathematically it calculated as Eq. (16).

$$P = (I_8 + I_9 + I_{bios})*(V_{DD} + V_{SS}) \quad (16)$$

Simulation Results

Transient Response: For OTA 45nm CMOS technology simulation in a cadence virtuoso environment. Fig. 4 shows the transient response of OTA at a frequency of 100Mhz. The output voltage lies in between 0.002163 V to 1.02962 V at an input 1.2 V. The Phase difference and amplification show clearly in transient response.

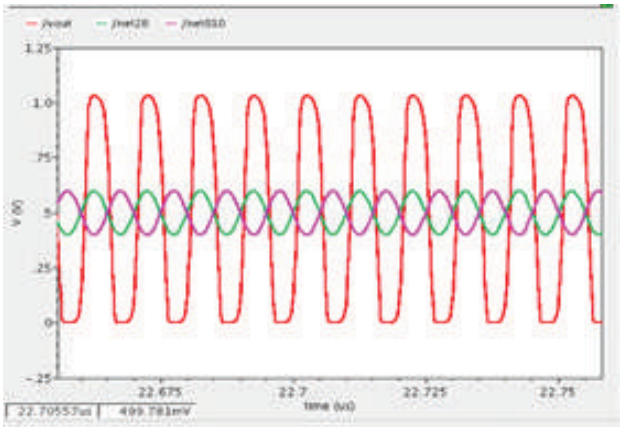

(a)

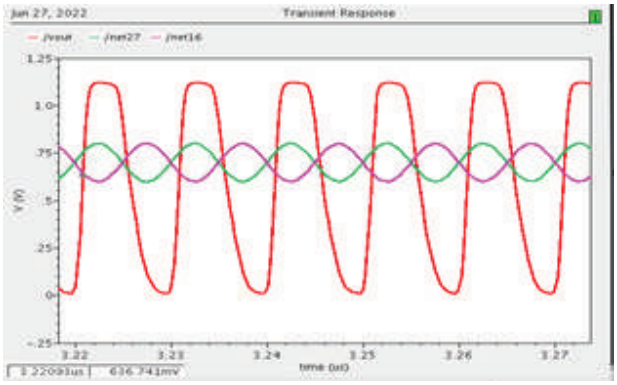

(b)

Fig. 5.a Amplified Response of simple OTA b. Amplified Response of miller OTA

AC Response: The AC frequency response is crucial in determining any amplifier's bandwidth and gain. The frequency vs gain and phase versus frequency graphs show the results of this analysis in fig.5. From a start to a stop frequency, the relevant circuit is examined. In the case of miller OTA, the DC gain is approximately 30db and has a phase cross-over frequency of 18GHz with

-51db cross-over frequency at 53 MHz, so the overall phase margin is 127 degrees.

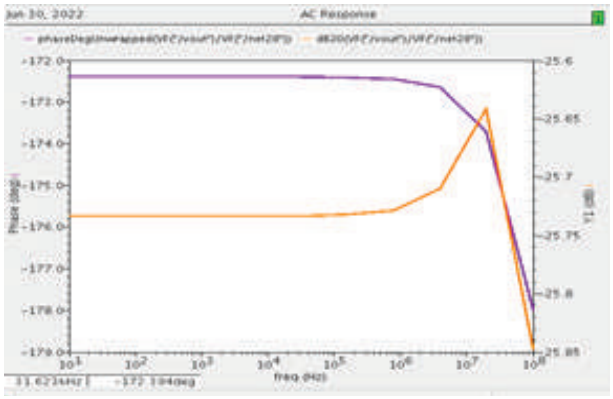

(a)

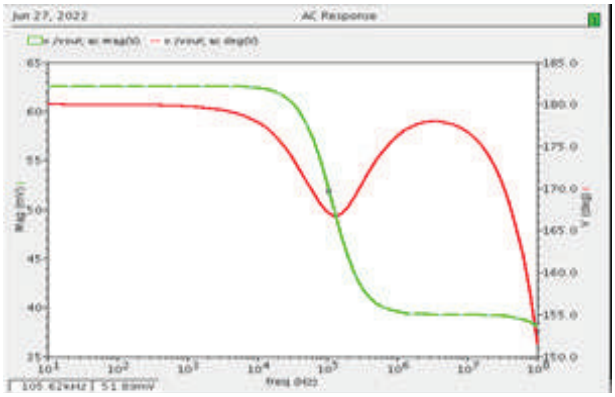

(b)

Fig. 5.a AC Gain ad Phase response of OTA b.) AC response of Miller OTA

DC Response: This study's quiescent point obtain to achieve small-signal models and linearity for all nonlinear components. The DC response shows in fig 6. The intersection point is called Q-Point (Vce= 520.009 mV). The performance of a circuit is calculated using DC Analysis.

The most challenging parameter to achieve in an OTA is low power dissipation. The proposed schematic is used for low-power dissipation to enhance performance. Fig. 7 shows the total transient power of OTA. The circuit consumed 0.739mW energy in case of simple OTA. In miller, this is reduced.The power consumption and slew rate reduce when all CMOS is operated in the saturation zone, while the gain Bandwidth product remains unchanged.

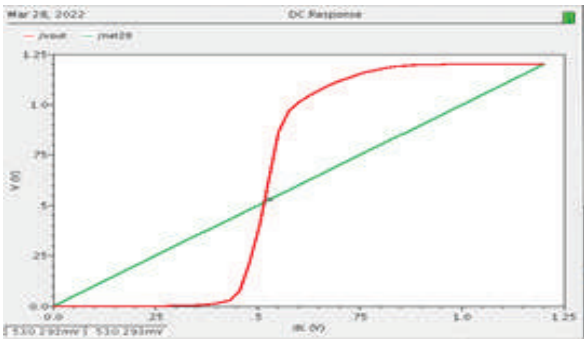

(a)

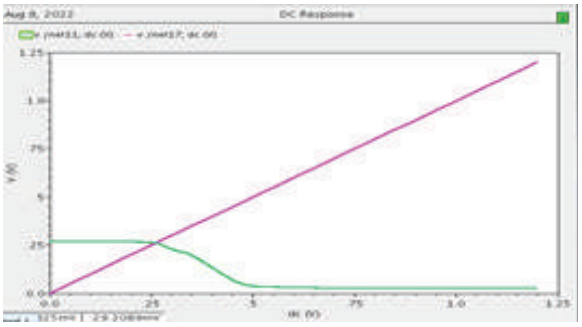

(b)

Fig. 6 DC Response of simple OTA b.) DC response of Miller OTA

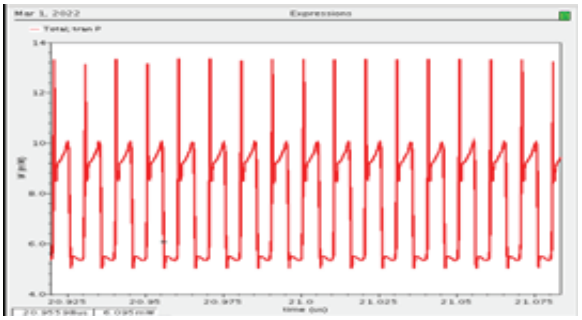

(a)

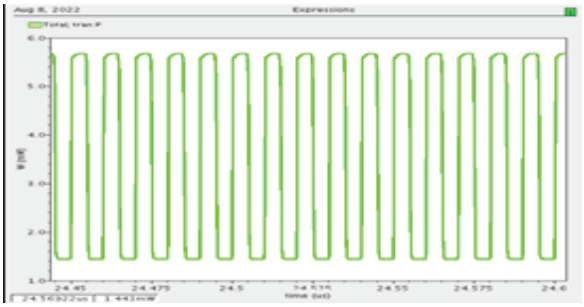

(b)

Fig.7.a) Transient power response of simple OTA b) Transient Power response of miller OTA

XF analysis: The analysis uses linearizing the circuit with the DC operating point and performing a small signal analysis for the transfer function calculations. In this fig.8. a) shows XF analysis for simple OTA circuit and b) for the miller OTA. 22.19 dB shows the open loop transfer function gain of miller OTA.

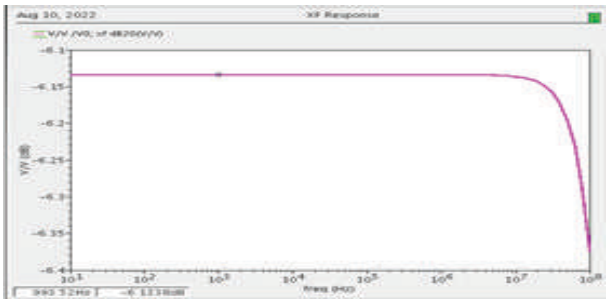

(a)

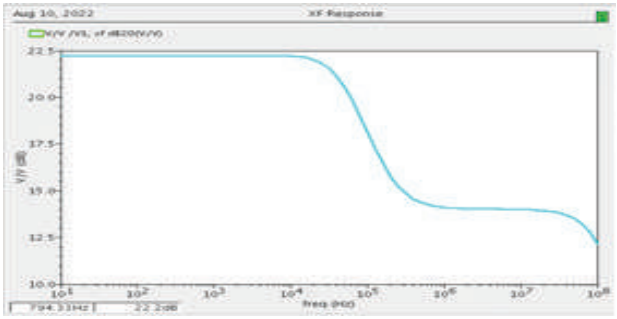

(b)

Fig.8 a) XF response of simple OTA b) XF response of miller OTA

PSS analysis: The PSS stands for the periodic study state analysis. The analysis defines the fundamental circuit frequency as having an independent simulation time constant. In the case of simple OTA is -69dbm at 100Mhz frequency and -5.3dbm in miller OTA. Fig 9.a shows the representation of simple OTA, and 9.b shows the representation of miller OTA.

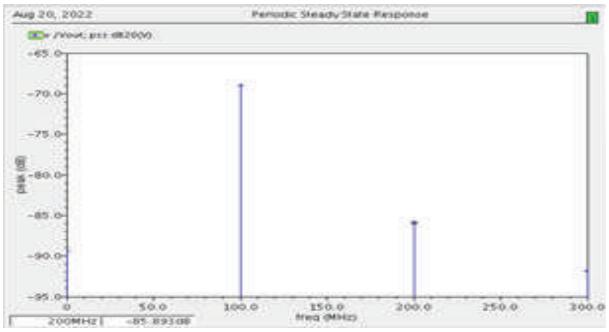

(a)

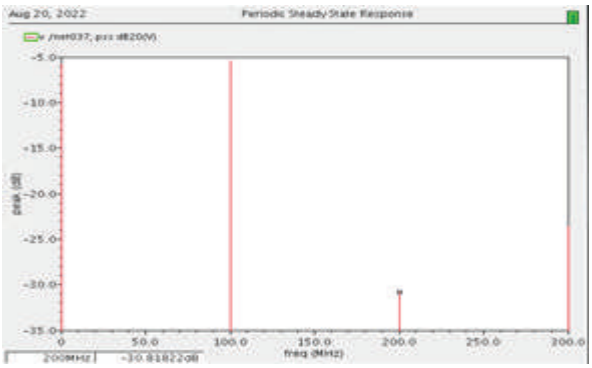

(b)

Fig.9 a) PSS response of simple OTA b) PSS response of miller OTA

The miller OTA gives a better magnitude and stability response fig.9 shows the stability response of miller OTA. In fig.9 b shows the transconductance response of the miller OTA.

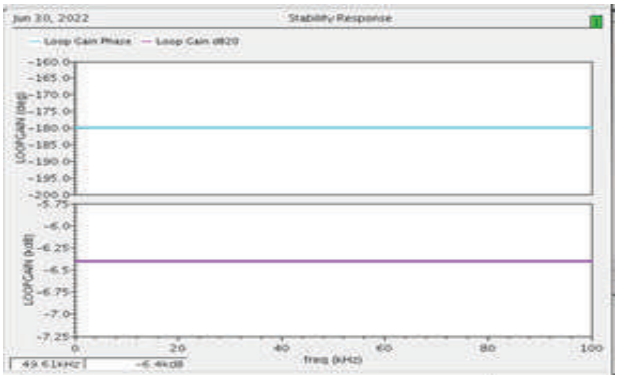

(a)

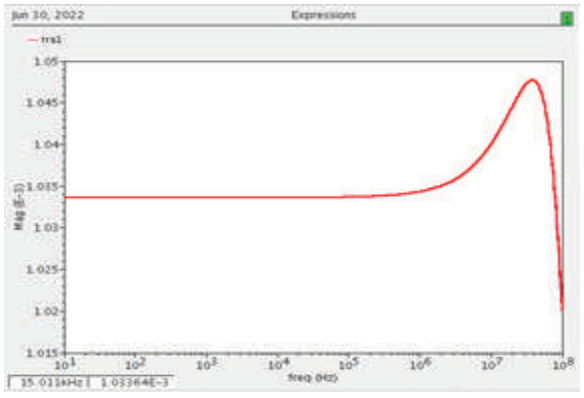

(b)

Fig.10.a) Stability response of miller OTA b) Transconductance curve of miller OTA

The table.3 shows the comparison with their parameters.

REF.NO	CMOS PROCESS TECHNOLOGY	PD	SUPPLY VOLTAGE	UGB	CMRR/ PSRR	OPEN LOOP GAIN	SLEW RATE	CL	GM/PM
[1]	0.18µm	4.3mW	1.8 V			70.37dB	46.97V/µs	10pF	
[2]	45nm	11.9µW	1V	20KHz		51dB	1.22µVrms		
[4]	180nm	194.336nW	1.6V	250.3 KHz	6296dB/	21.15 dB			38.1dB/62.6°
[9]	180nm	41.96uW	1.8 V	55.11 MHz.		44.18dB	30 V/ µs	330fF	25.52 dB/63.04°
[13]	0.18µm	0.74mW	1.8V	90.25 MHz	91dB/80 dB	76dB	2.344 V/µsec.	0.1pF	
PROPOSED WORK (MILLER OTA)	45nm	0.73mW	1.2V	18GHz		30dB		4pf	51dB/127°

CONCLUSION

This paper represents a simple OTA and Miller OTA with their performance parameters. It uses for low voltage and low power applications. The miller OTA provided a better performance with a low voltage supply, small input current, and required less area. As a result, a new topology must be incorporated into the bioamplifier's circuit design in order to create a bio-amplifier that is suitable, has ultra-low power consumption, and can handle significant signal swings. It shows better in terms of Bandwidth, gain and in phase margin. Due to small power consumption, less noise, small gm suitable for medical application and also design for designing filters, instrumentation amplifier, ADC designing because of high gain and low power consumption.

REFERENCES

1. Palmisano G, Palumbo G, Pennisi S. Design procedure for two-stage CMOS transconductance operational amplifiers: A tutorial. Analog Integrated Circuits and Signal Processing. 2001 May;27(3):179-89.
2. Palodiya V, Karnik S, Shrivastava M, DODIYA J. Design of Small-Gm Operational Tranconductance Amplifier in 0.18 µm Technology. International Journal of Engineering Research & Technology (IJERT). 2012 Jul;1(5).
3. Raghav HS, Singh BP, Maheshwari S. Design of low voltage OTA for bio-medical application. In2013 Annual International Conference on Emerging Research Areas and 2013 International Conference on Microelectronics, Communications and Renewable Energy 2013 Jun 4 (pp. 1-5). IEEE.
4. Gupta A, Singh S. Design of two stage cmos op-amp with high slew rate and high gain in 180nm. In2018 2nd International Conference on I-SMAC (IoT in Social, Mobile, Analytics and Cloud)(I-SMAC) I-SMAC (IoT in Social, Mobile, Analytics and Cloud)(I-SMAC), 2018 2nd International Conference on 2018 Aug 30 (pp. 341-345). IEEE.
5. Akbari M, Biabanifard S, Asadi S, Yagoub MC. Design and analysis of DC gain and transconductance boosted recycling folded cascode OTA. AEU-International Journal of Electronics and Communications. 2014 Nov 1;68(11):1047-52.
6. Ranjan P, Dhaka N, Pant I, Pranav A. Design and analysis of two stage op-amp for bio-medical application. Int. J. Wearable Device. 2016;3(1):9-16.
7. PATEL T, RAIKAR K, SHARAN HIREMATH PR. Design of Balanced Operational Transconductance Amplifier (OTA). International Journal of Emerging Technology in Computer Science & Electronics (IJETCSE), ISSN. 2015:0976-1353.
8. Rani DG, Gifta G, Meenakshi M, Gomathy C, Gowsalaya T. Design and analysis of CMOS low power OTA for biomedical applications. In2019 4th International Conference on Recent Trends

on Electronics, Information, Communication & Technology (RTEICT) 2019 May 17 (pp. 871-876). IEEE.

9. Rodrigues SN, Sushma PS. Design of Low Transconductance OTA and its Application in Active Filter Design. In2019 3rd International Conference on Trends in Electronics and Informatics (ICOEI) 2019 Apr 23 (pp. 921-925). IEEE.

10. Sulistiyanto N, Wang CC, Rieger R. A Low Frequency OTA Design with Temperature-Insensitive Variable Transconductance Using 180-nm CMOS Technology. In 2019 International Conference on IC Design and Technology (ICICDT) 2019 Jun 17 (pp. 1-4). IEEE.

11. Singh R, Chauhan RC. Power Efficient Biquadratic Filter designing using OTA. Indian Journal of Science and Technology. 2021 Sep 8;14(29):2448-59.

12. Pandey R, Kumar S, Sonia V, Singh P, Ghangas S, Bisariya S. A review on CMOS operational transconductance amplifier on different technology node. Available at SSRN 4159096. 2022 Jul 14.

13. Al-Qaysi, Hayder Khaleel, Musaab Mohammed Jasim, and Siraj Manhal Hameed. "Design of very low-voltages and high-performance CMOS gate-driven operational amplifier." Indonesian Journal of Electrical Engineering and Computer Science 20.2 (2020): 670-679.

14. Kumari Usha, and Rekha Yadav. "A Review About Analysis and Design Methodology of Two-Stage Operational Transconductance Amplifier (OTA)." Proceedings of International Conference on Data Science and Applications: ICDSA 2022, Volume 2. Singapore: Springer Nature Singapore, 2023.

15. Mahendra, Mihika, Shweta Kumari, and Maneesha Gupta. "Low voltage fully differential OTA using DTMOS based self cascode transistor with slew-rate enhancement and its filter application." Integration 84 (2022): 47-61.

Early Detection of Plant Diseases Through a CNN-SVM Hybrid Model

Swapnali D. Chaugule
Student
Dept. of E&TC
SPCOE
Otur (Dumbarwadi),
✉ swapnalichaugule20@gmail.com

G. U. Kharat
Professor
Dept. of E&TC
SPCOE
Otur (Dumbarwadi),
✉ gukharat@gmail.com

N. B. Bankhele
Assistant Professor
Dept. of E&TC
SPCOE
Otur (Dumbarwadi),
✉ nbankhele.7777@gmail.com

ABSTRACT

This research aims to create a reliable system for classifying plant diseases by combining CNN and SVM approaches. The primary focus of this research will be utilizing CNN to extract features from plant photos, train the CNN model to accurately identify diseases, and extract features from the trained CNN model to input into an SVM classifier for exact classification. The objective is to establish a high level of accuracy in distinguishing between healthy and sick plant samples, which will allow for the early diagnosis and efficient control of plant diseases. This strategy is being implemented as part of the project to contribute to advancing computer vision techniques in agriculture. This will help farmers and researchers diagnose diseases promptly and decideon crop protection.

KEYWORDS *: CNN, CNN-SVM, Deep learning, Plant leaf disease classification.*

INTRODUCTION

The agriculture industry employs around 70 percent of India's total population. When it comes to choosing varieties of crops and pesticides, farmers have several options. Identifying plant diseases promptly is not only necessary but also difficult. Manual observation and analysis of plant diseases was the initial method utilized by plant disease specialists. A large amount of labour and processing time is required for this. Human visual and cognitive capacities work very well when recognizing and understanding patterns. Plant disease visual judgment is subjective and prone to psychological and cognitive biases, which can lead to prejudice, optical illusions, and mistakes. Certain plant diseases can cause these biases. On the other hand, the process takes a significant amount of time. In order to find a solution to this problem, computer processing techniques might be utilized to diagnose plant diseases.

Experts frequently diagnose plant diseases through visual inspection. Ongoing professional oversight is necessary, which might be excessively costly for extensive agricultural operations. Automated plant disease detection is an essential field of study that can assist in monitoring extensive agricultural regions and rapidly spotting signs of sickness in plant foliage. Monitoring the leaf area is essential for studying the physiological traits related to plant growth, photosynthesis, and transpiration. Moreover, it functions as a valuable standard for evaluating the harm inflicted by leaf diseases and pests, ascertaining water and environmental strain, recognizing the requirement

for fertilization, and enabling effective administration and treatment.

Agriculture and plant research require accurate leaf disease detection. Due to the growing need for food, plant leaf diseases must be swiftly and correctly detected to reduce crop loss and increase output. Research applying deep learning to diagnose plant leaf diseases has shown tremendous development and potential. Deep learning plant leaf disease identification requires many steps. Organized photos with labels explain whether the leaves are healthy or diseased. The dataset has training, validation, and testing subsets. During training, the deep learning model finds picture patterns and assigns significance to each attribute. A loss function that assesses predicted-true label discrepancy is minimized to improve the model. After training, the system can properly categorize newly gathered plant leaf photos. Deep learning to identify plant leaf diseases might boost crop yields and prevent crop damage. Larger datasets and more processing power help deep learning systems discover complex visual patterns.

LITERATURE REVIEWS

This comprehensive analysis explores plant diseases and pest identification, comparing deep learning techniques with conventional methods. The paper classifies contemporary research on classification, detection, and segmentation networks, analyzing their strengths and weaknesses. The article presents standard datasets and thoroughly evaluates the effectiveness of current models, offering a useful guide for researchers. The study also foresees difficulties in real implementations, suggesting remedies and research concepts. In conclusion, it provides a predictive study of future trends in plant diseases and pest detection using deep learning.[1]

Crop diseases are a major risk to global food security, and their quick diagnosis is sometimes limited in many places owing to insufficient infrastructure. Using a dataset of 54,306 plant leaf pictures showing different health statuses. Utilizing large, publicly available picture datasets for training deep learning models shows promise for adopting worldwide crop disease detection with smartphone assistance.[2]

The agricultural business is vital to providing high-quality food and improving economies and people. Plant diseases threaten food supplies and species diversity. Deep learning has enhanced photo classification and object identification accuracy. The study detected plant diseases using pre-trained CNN models and hyperparameters. The model's classification accuracy, sensitivity, specificity, and F1 score were assessed using 54,305 photo samples of plant disease species grouped into 38 categories from the PlantVillage dataset. A comparative analysis using current research found that DenseNet-121 outperformed other models in classification accuracy at 99.81%.[3]

Plants are essential for food production, but environmental factors may induce plant diseases and reduce yield. Manually recognizing these disorders may be more efficient and error-prone, rendering it unhelpful for prevention. This study evaluates 2015–2022 academic publications on machine learning (ML) and deep learning (DL) plant disease detection approaches. The study shows that these solutions improve plant disease diagnostic accuracy and timeliness.[4]

Early crop disease detection via automation will alter agriculture. Adding 'unknown' increases the model's broad relevance. The disease detection model classified crops and diseases with 97.09% accuracy throughout validation. The model's adaptability improves by including non-model crops in the training dataset, overcoming their early accuracy issues. This model might be utilized in smart farming for Solanaceae crops and expanded by adding other crops to the training dataset.[5]

Identifying the illness is the first step in efficiently and precisely preventing plant disease in a complex environment. Plant disease diagnostics is becoming digital and data-driven because of the rapid expansion of smart farming, offering new opportunities for advanced decision support, insightful analysis, and strategic planning. The transfer learning model is trained using segmented leaves as input using a dataset of damaged leaves.[6]

The study examines 40 publications that use deep learning methods in the context of food production and agriculture. This research contrasts many commonly used image processing techniques with deep learning. The results demonstrate that deep learning yields superior results. The process of taking pictures and

analyzing photo databases can be automated by employing drones and agricultural robots. [7]

Based on DenseNet-77, this study presents a new Custom CenterNet. Numerous characteristics are extracted from the input data using DenseNet-77. This method yields crucial points utilized to train the CenterNet classifier, which aids in identifying and categorizing various plant diseases. The suggested system accurately identifies and categorizes 38 crop diseases in the PlantVillage dataset. The approach shows resilience in classifying plant diseases, even when faced with various artifacts. The experimental findings confirm that the model outperforms the newest known methodologies in classifying plant diseases. Although the present paradigm produces similar outcomes, it is unsuitable for mobile device deployment. Future studies intend to develop a more efficient model for identifying leaf diseases and improving their usability. Moreover, time complexity may be decreased by using a more efficient feature extractor. [8]

The research used a dataset of 5932 photos of rice and 1500 images of diseased and healthy leaves from rice and potato crops. Based on deep learning, the CNN model demonstrated higher accuracy in many performance metrics than other advanced machine learning image classifiers. The comparison study included accuracy, precision, F1 score, and recall. For future projects, optimizing hyperparameters in the suggested CNN model. This tweak might improve the model's performance even further. [9]

This research compares several transfer learning deep CNN models for identifying and categorizing plant leaf diseases. More than 30 relevant publications are analyzed, emphasizing a particular field and employing advanced deep learning models, data sources, data augmentation approaches, picture preprocessing tasks, and evaluating model performance based on metrics. The combined results highlight the improved performance attained using deep learning techniques. Researchers studying agricultural issues using computer vision and classification may use this review on plant disease detection to gain knowledge for sustainable and intelligent farming practices, maintaining food supply security. Plans include developing various classifiers for plant disease identification and suggesting illness area localization to improve human understanding of the problems. [10]

PROPOSED SYSTEM

This section presents the methodology of the proposed system.

Methodology

Input Dataset

This system uses the Plant Village dataset. Apple, grape, tomato, and maize leaf damage and health are depicted in the photos. 25% of the time is spent testing the data, and 75% is spent training. Next, 256 by 256 pixels are used as the new image size. A complex database architecture was created to evaluate the proposed system's performance and the classifier's efficacy.

Preprocessing

The picture has been preprocessed for improved use. Filtering is a crucial step in the preprocessing process. In this case, the median filter is a non-linear filter designed to eliminate noise and enhance the smoothness of a picture. Its capacity to reduce noise while maintaining edges contributes to its popularity. Removing salt and pepper odors is easy with this product. The median of the window's pixel values is calculated by replacing the center pixel with the value obtained by numerically sorting all the pixel values.

Segmentation

Segmentation involves separating one picture into many segments. Items that have a common characteristic or may be compared in some manner. Many methods may accomplish the segmentation of this approach. The RGB picture is converted to the HIS model for segmentation. Utilizing border detection and spot detection may help identify the contaminated area of the leaf. The boundary algorithm assesses the eight pixels' connectivity to find boundaries. Setting a pixel value in a picture to 0 or another value is called masking since it represents the healthy area of the leaf in green. If a green pixel's intensity surpasses the preceding one, all values are reset to zero. Zero-valued pixels are eliminated after the mask is applied. The H and S plane values, together with a value of '1' given to a specific location in masking, are used to detect the disease component of the leaf. The

value '0' is provided for the remaining areas. A binary picture consists only of ones and zeros. The leaf area may be determined as a consequence.

Training and Validation

The deep convolutional network identifies twelve kinds of plant leaf disease via three phases: feature learning, selection, and classification. Training models with more than two layers was difficult. Hence, the GPU was used to train this model because of its complexity.

Data Augmentation

Data augmentation aims to create more training data by merging existing training data with other resources. This is achieved by creating new and unique training samples from the training data using domain-specific methods.

Most people are acquainted with image data enhancement. During the procedure, images from the training dataset are altered and included in the same category as the original picture. Within image alteration, transformations include flips, shifts, zooms, etc.

The objective is to include more authentic examples in the training dataset. This suggests that the model will likely encounter different versions of the pictures in the training set. A cat picture may have been taken from either the left or right side of the camera; thus, rotating it horizontally may be a logical adjustment. Since the model is unlikely to see an inverted cat photograph, it would be improper and irrational to flip it vertically.

A thorough understanding of the problem domain and the training dataset is essential for choosing data augmentation options. Experimenting with data augmentation options individually and in combination using a small prototype dataset, model, and training run may help evaluate whether they improve model performance significantly. Modern deep learning algorithms such as CNNs learn features invariant to location. Augmentation may significantly enhance this transformation-invariant learning approach. This aids the model in learning qualities that remain unchanged during transformations, such as changes from left-to-right to top-to-bottom order, variations in image brightness levels, and other factors. Image resizing and pixel scaling are data preprocessing forms that must be consistently done to all datasets included in the model.

Block Diagram of the System

A block diagram of the proposed Plant leaf disease recognition system is shown in Fig. 1.

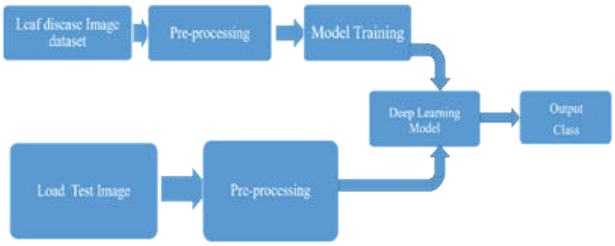

Fig. 1. Block diagram of the proposed system

- Leaf Disease Image Dataset: The first collection of images depicting leaves affected by various diseases and corresponding labels.
- Preprocessing: The Leaf Disease Image Dataset contains preprocessed pictures. Preparing data for training involves scaling, normalization, and augmentation. The preprocessed images are inputted into the deep-learning model for training. Test photos undergo preprocessing to ensure consistency in data representation, similar to the training data.
- Model Training: The deep learning model is trained using preprocessed pictures and corresponding labels. The program learns image patterns and characteristics that signify leaf diseases.
- The system's foundation is the trained deep learning model. The layers of neurons are structured similarly to a convolutional neural network. Preprocessed images are inputted into this model to make predictions or classifications.
- The deep learning model categorizes an input picture into a certain class or category based on the kind of leaf disease identified. This output class signifies the anticipated illness determined by the characteristics acquired by the model via training.
- Load Test Image:

o Preprocessing involves preparing test pictures to ensure compatibility with the deep learning model.

o The prepared test image is inputted into the trained deep learning model for inference, which then forecasts the kind of leaf disease.

The block diagram illustrates the process of analyzing leaf disease photographs, training a deep learning model, and making predictions on test images to predict leaf disease.

Training and testing Using CNN and Hybrid CNN-SVM

CNN

CNNs, a Neural Network, have shown remarkable efficacy in image recognition and categorization. A feed-forward neural network is the multi-layer CNN. Convolutional neural networks (CNNs) consist of neurons, filters, or kernels with adjustable parameters, biases, and weights. Adding a non-linear filter after each filter that processes inputs by convolution and other operations is feasible. Figure 2 displays a typical CNN architecture. A convolutional neural network (CNN) consists of fully connected, pooling, and Rectified Linear Unit (ReLU) layers.

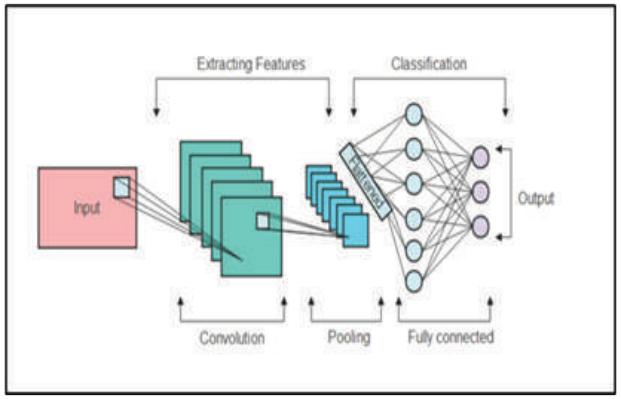

Fig. 2. Architecture of CNN

Each block of CNN architecture is explained below.

- Convolutional Layer: Convolutional operations are performed by this layer by applying a collection of filters to the incoming data. Each filter identifies input data characteristics.
- Pooling Layer: By downsampling, pooling layers lower convolved feature map spatial dimensions. Max and average pooling are common.
- Rectified Linear Unit (ReLU): ReLU activates elements-wise after convolution. It gives the network non-linearity and sophisticated pattern learning.
- Fully Connected Layer: The neurons in this layer are coupled to those in the preceding layer, as in artificial neural networks. It is utilized for classification or regression after CNN architecture.

Sequential layer stacking is characteristic of CNN design. The design depends on the job and data complexity.

Hybrid CNN-SVM

The architecture diagram of the hybrid CNN-SVM algorithm is shown in Fig 3.

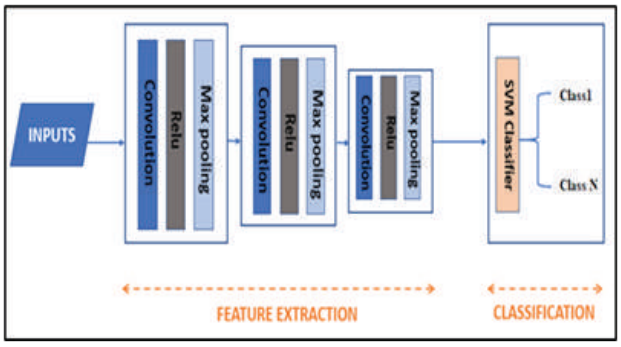

Fig. 3. Architecture diagram of Hybrid CNN-SVM algorithm

The hybrid CNN-SVM approach enhances plant disease classification by using the strengths of both CNN and SVM.The CNN autonomously acquires and isolates crucial data from input photographs, making it well-suited for image classification.

CNN The feature extraction process involves training a CNN model on a large dataset of labeled plant pictures in a hybrid architecture. The CNN utilizes convolutional and pooling methods to extract significant features and representations from input images. These traits capture the textures, shapes, and patterns of plant diseases. Feature vector creation after training: Intermediate feature mappings from a single CNN layer are retrieved. The feature maps display the learned features of the input picture. The characteristics of each picture are compressed and transformed into feature vectors.

SVM is a traditional machine learning method for categorization tasks. An ideal hyperplane is identified to separate classes in a feature space with several dimensions. SVMs are very effective in categorizing feature vectors with many dimensions. The hybrid

design involves training an SVM classifier using CNN feature vectors. SVMs optimize the hyperplane using labeled feature vectors to maximize margins across disease classes. SVMs predict disease diagnoses using new image feature vectors during classification. The SVM classifier integrates CNN features to combine the trained CNN and SVM. The CNN retrieves distinctive data from images, and the SVM categorizes these characteristics to provide precise predictions of illnesses.

During the inference phase, the hybrid architecture analyzes a plant image in the following manner: CNNs extract significant features from photos. Feature vectors are generated from extracted characteristics. The SVM classifier predicts disease after analyzing the feature vector. The hybrid CNN-SVM system forecasts the disease category of the input picture. The design utilizes CNNs to extract important features from images and Support Vector Machines (SVMs) for reliable and generalizable illness classification. The hybrid CNN-SVM approach enhances the accuracy and performance of plant disease classification by combining deep learning with traditional machine learning techniques.

RESULT

This method classifies plant leaf diseases using CNN and CNN-SVM. Precision, recall, f1 score, and accuracy are shown.

CNN

1) Model Summary

```
Model: "sequential_2"
_________________________________________________________________
Layer (type)                 Output Shape              Param #
=================================================================
conv2d_4 (Conv2D)            (None, 63, 63, 256)       3328

activation_6 (Activation)    (None, 63, 63, 256)       0

max_pooling2d_4 (MaxPooling  (None, 31, 31, 256)       0
2D)

conv2d_5 (Conv2D)            (None, 30, 30, 128)       131200

activation_7 (Activation)    (None, 30, 30, 128)       0

max_pooling2d_5 (MaxPooling  (None, 15, 15, 128)       0
2D)

flatten_2 (Flatten)          (None, 28800)             0

dense_4 (Dense)              (None, 64)                1843264

activation_8 (Activation)    (None, 64)                0

dropout_2 (Dropout)          (None, 64)                0

dense_5 (Dense)              (None, 12)                780

=================================================================
Total params: 1,978,572
Trainable params: 1,978,572
Non-trainable params: 0
_________________________________________________________________
```

2) Classification Report

a) Validation Result

```
Confusion Matrix

[[122   0   1   0   0   0   0   0   1   0   0   0]
 [  0  50   0   0   0   0   0   0   0   1   4   0]
 [  2   0 318   0   0   0   0   0   1   0   2   0]
 [  0   0   1  96   0   1   1   1   0   0   2   0]
 [  0   0   0   1 226   0   0   0   0   0  11   0]
 [  0   0   1   0   0 231   0   0   0   0   0   0]
 [  1   2   0   0   0   0 227   1   4   1   0   0]
 [  0   0   0   0   0   0  19 253   0   0   3   1]
 [  1   0   0   0   0   0   0   0  83   0   0   0]
 [  2   2  12   0   0   0   1   0   0 163  19   1]
 [  1   1  10   1   0   0   1   0   2  14 350   1]
 [  0   0   2   0   0   0   0   0   0   0   1 315]]
```

b) Classification Report

	precision	recall	f1-score	support
AppleBlackrot	0.95	0.98	0.96	124
AppleCedarapplerust	0.91	0.91	0.91	55
Applehealthy	0.92	0.98	0.95	329
Corn(maize)	0.98	0.94	0.96	247
Corn(maize)Commonrust	1.00	0.95	0.97	238
Corn(maize)healthy	1.00	1.00	1.00	232
GrapeBlackrot	0.91	0.96	0.94	236
GrapeEsca(BlackMeasles)	0.99	0.92	0.95	276
Grapehealthy	0.91	0.99	0.95	84
TomatoEarlyblight	0.91	0.81	0.86	200
Tomatohealthy	0.89	0.92	0.91	381
TomatoLateblight	0.99	0.99	0.99	318
accuracy			0.95	2569
macro avg	0.95	0.95	0.95	2569
weighted avg	0.95	0.95	0.95	2569

Training Progress Graph

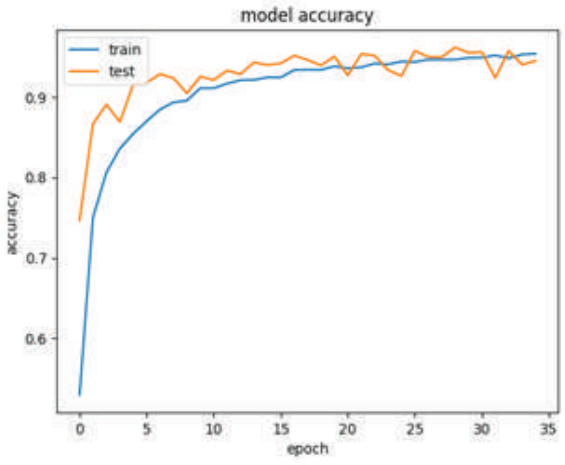

(a)

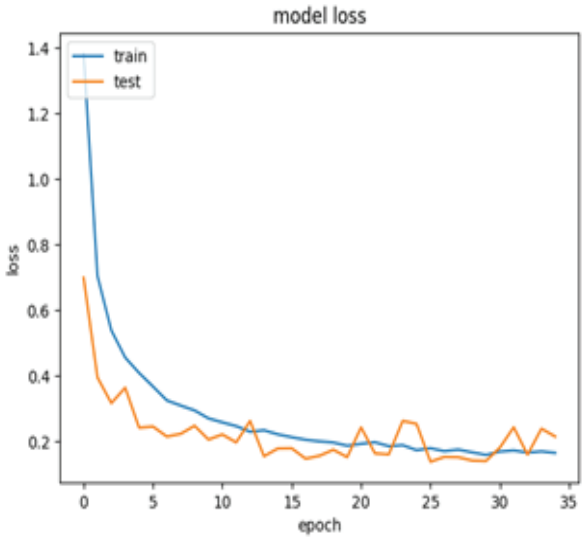

(b)

Fig. 4. Training progress graph of CNN algorithm in terms of (a) Accuracy, (b) Loss

Result of Hybrid CNN-SVM

1) Model Summary

Model: "sequential"

Layer (type)	Output Shape	Param #
conv2d (Conv2D)	(None, 62, 62, 16)	448
activation (Activation)	(None, 62, 62, 16)	0
max_pooling2d (MaxPooling2D)	(None, 31, 31, 16)	0
conv2d_1 (Conv2D)	(None, 29, 29, 32)	4640
activation_1 (Activation)	(None, 29, 29, 32)	0
max_pooling2d_1 (MaxPooling 2D)	(None, 14, 14, 32)	0
conv2d_2 (Conv2D)	(None, 12, 12, 64)	18496
activation_2 (Activation)	(None, 12, 12, 64)	0
max_pooling2d_2 (MaxPooling 2D)	(None, 6, 6, 64)	0
flatten (Flatten)	(None, 2304)	0
dense (Dense)	(None, 128)	295040
activation_3 (Activation)	(None, 128)	0
dropout (Dropout)	(None, 128)	0
dense_1 (Dense)	(None, 12)	1548

Total params: 320,172
Trainable params: 320,172
Non-trainable params: 0

2) Classification Report

a) Validation Results

Confusion Matrix

	0	1	2	3	4	5	6	7	8	9	10	11
0	122	0	1	0	0	0	0	0	1	0	0	0
1	0	50	0	0	0	0	0	0	0	1	4	0
2	2	0	318	0	0	0	0	0	1	0	2	0
3	0	0	1	96	0	1	1	1	0	0	2	0
4	0	0	0	1	226	0	0	0	0	0	11	0
5	0	0	1	0	0	231	0	0	0	0	0	0
6	1	2	0	0	0	0	227	1	4	1	0	0
7	0	0	0	0	0	0	19	253	0	0	3	1
8	1	0	0	0	0	0	0	0	83	0	0	0
9	2	2	12	0	0	0	1	0	0	163	19	1
10	1	1	10	1	0	0	1	0	2	14	350	1
11	0	0	2	0	0	0	0	0	0	0	1	315

b) Test Result

AppleBlackrot	0.95	0.98	0.96	124
AppleCedarapplerust	1.00	0.87	0.93	55
Applehealthy	0.97	0.97	0.97	323
Corn(maize)CGrayleafspot	1.00	0.92	0.96	102
Corn(maize)Commonrust	0.99	0.98	0.99	238
Corn(maize)healthy	0.99	1.00	0.99	232
GrapeBlackrot	0.96	0.95	0.96	236
GrapeEsca(BlackMeasles)	0.94	0.97	0.96	276
Grapehealthy	0.99	1.00	0.99	84
TomatoEarlyblight	0.90	0.89	0.89	200
Tomatohealthy	0.94	0.93	0.94	381
TomatoLateblight	0.99	1.00	0.99	318
accuracy		0.96	2569	
macro avg	0.97	0.96	0.96	2569
weighted avg	0.96	0.96	0.96	2569

3) Training Progress Graph

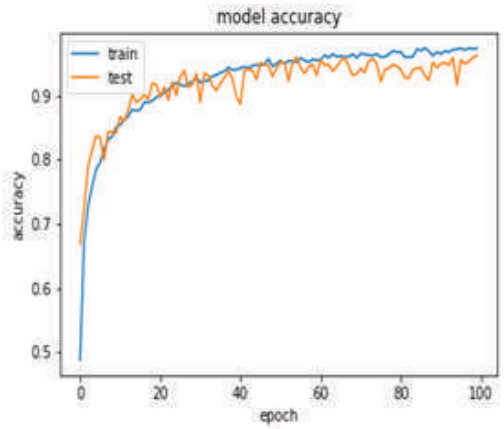

(a)

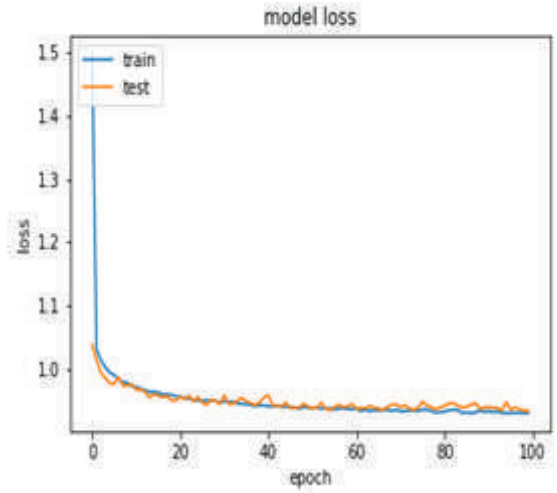

(b)

Fig. 5. Training progress graph of Vgg16 algorithm in terms of (a) Accuracy, (b) Loss

The Comparative Analysis of the proposed system is graphically presented in Table I and Fig 4

Table 1. Comparative analysis of the proposed system

Algorithm	Precision	Recall	F1Score	Accuracy
CNN	0.95	0.95	0.95	0.9449
CNN-SVM	0.96	0.96	0.96	0.96

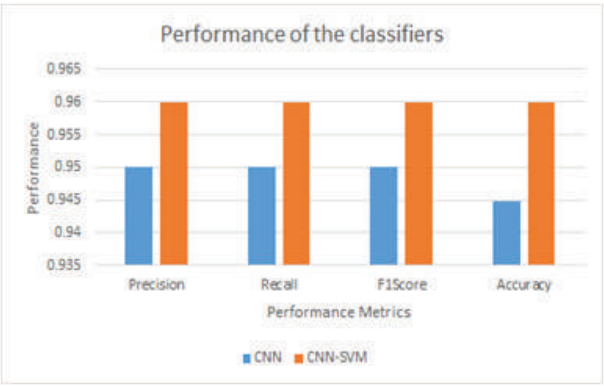

Fig. 6. Comparative analysis of the proposed system

On the PlantVillage dataset, CNN-SVM scored best for plant leaf disease classification. CNN-SVM obtained 96% accuracy and CNN 94.49% accuracy for plantVillage.

The qualitative analysis of the proposed system is shown in Fig. 5.

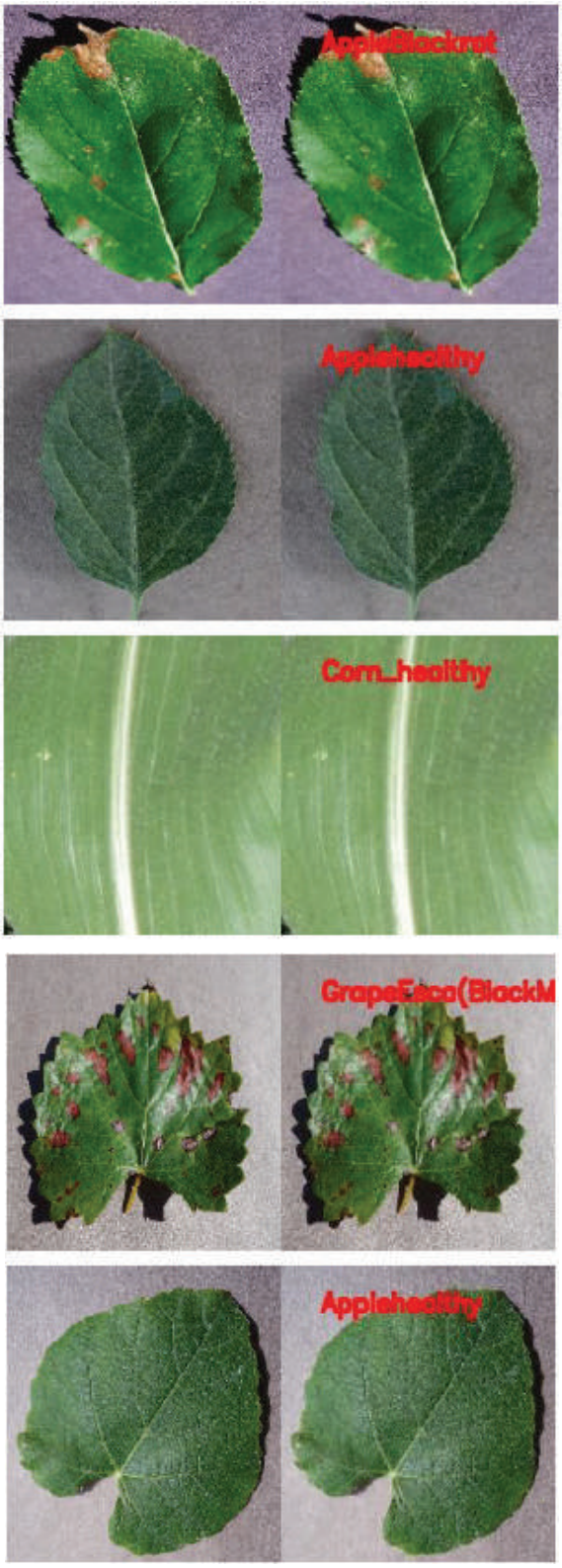

Fig. 7. Testing results of CNN-SVM algorithm

Promising results were achieved utilizing the CNN-SVM algorithm on healthy and damaged apples, maize, and grape leaves. The CNN module effectively captured intricate leaf features, enabling accurate categorization. The system effectively differentiated between healthy and diseased leaves among various plant species.

The CNN-SVM hybrid approach combined convolutional neural networks and support vector machines to remarkable effect. The hybrid model combined CNN feature representations with SVM's excellent classification skills to improve leaf disease classification. SVM classifiers employed CNN feature extraction to provide rich and unique feature representations for reliable predictions.

CNN-SVM can distinguish healthy and harmful leaves, according to tests. CNN and SVM enhanced leaf disease detection accuracy and robustness. Environmental and agricultural classification were achieved via hybrid deep learning models.

CONCLUSION

The hybrid CNN-SVM algorithm design diagnoses plant diseases cheaply. This concept uses SVMs' robust classification and CNNs' visual feature extraction. Plant disease diagnostics, precision agriculture, research, online and mobile app development, disease monitoring, teaching, and extension employ hybrid architecture. This technology helps agricultural specialists and farmers diagnose and precisely cure plant diseases, avoiding crop loss. Agricultural inputs and precision farming improve. Researchers may uncover patterns and trends in plant diseases using the hybrid CNN-SVM system. The method detects plant leaf diseases using CNN and SVM-CNN. This system explores PlantVillage. Tests use 20% of data, whereas training uses 80%. Network CNN and Hybrid CNN-SVM classify plant leaf diseases. See how CNN algorithms determine precision, recall, F-measure, and accuracy.

REFERENCES

1. Jun Liu And Xuewei Wang, "Plant Diseases And Pests Detection Based On Deep Learning: A Review," Plant Methods, 2021
2. Sharada P. Mohanty, David P. Hughes, And Marcel Salathé, "Using Deep Learning For Image-Based Plant Disease Detection, Front. Plant Sci., Sec. Technical Advances In Plant Science, 2016
3. Andrew J., Jennifer Eunice, Daniela Elena Popescu, M. Kalpana Chowdary And Jude Hemanth, "Deep Learning-Based Leaf Disease Detection In Crops Using Images For Agricultural Applications," Mdpi, Agronomy 2022
4. Muhammad Shoaib, Babar Shah, Shaker Ei-Sappagh, Akhtar Ali, Asad Ullah, Fayadh Alenezi, Tsanko Gechev, Tariq Hussain And Farman Al, An Advanced Deep Learning Models-Based Plant Disease Detection: A Review Of Recent Research, Frontiers In Plant Science, 2023
5. Minah Jung, Jong Seob Song, Ah Young Shin, Beomjo Choi, Sangjingo, Suk Yoon Kwon, Juhan Park, Sunggoo Park1,7* & Yong Min Kim," Construction Of Deep Learning Based Disease Detection Model In Plants, Scientific Reports, 2023
6. Yan Guo, Jin Zhang, Chengxin Yin, Xiaonan Hu, Yu Zou, Zhipeng Xue And Wei Wang, "Plant Disease Identification Based On Deep Learning Algorithm In Smart Farming," Hindawi Discrete Dynamics In Nature And Society, 2020
7. Derisma, Nur Rokhman, Ilona Usuman, "Systematic Review Of The Early Detection And Classification Of Plant Diseases Using Deep Learning," Iop Conf. Series: Earth And Environmental Science 1097, 2022
8. Waleed Albattah, Marriam Nawaz, Ali Javed, Momina Masood, Saleh Albahli," A Novel Deep Learning Method For Detection And Classification Of Plant Diseases, Complex & Intelligent Systems, 2022
9. Rahul Sharma, Amar Singh, Kavita, N. Z. Jhanjhi, Mehedi Masud, Emad Sami Jaha,and Sahil Verma," Plant Disease Diagnosis And Image Classification Using Deep Learning," Computers, Materials & Continua, 2022
10. Sandhya Rani D And Shyamala K, "A Study Of Plant Disease Detection And Classification By Deep Learning Approaches," Proceedings Of The 9th International Conference On Agriculture, 2022

Novel Low-cost Dual Band Antenna with Partial Ground Plane for ISM Band and 5G Applications

Ambresh P. A.
Dept. of App. Electronics
Gulbarga University
Kalaburagi, Karnataka
✉ ambreshpa@rediffmail.com

Amit Birwal
Dept. of Electronics Science
University of Delhi
South Campus, Delhi
✉ amit.birwal@gmail.com

ABSTRACT

The paper introduces the simulation work on the novel design of square patch antenna with partial ground plane fabricated on FR4 dielectric substrate material which is simulated using CST software. The design employed here utilizes smaller area of copper on the substrate material making it compact in nature. The antenna has its suitable bandwidths of 349MHz for simple square patch and 288MHz, 261MHz bandwidths for novel design of patch with dual band characteristics for wireless application of WLAN in ISM band, 5G. The paper also presents the design technique as well as the results, which include return loss (S11), 2-D and 3-D radiation patterns, patch surface current distribution. VSWR, and Smith chart.

KEYWORDS *: Dual band, Waveguide, FR4, Dielectric, Antenna, ISM.*

INTRODUCTION

Wireless communication is the most important aspect of modern wireless generation technology. Communication would be tough without wireless connection since everything is dependent on the internet and data transfer across long distance. Hence, aantenna is considered to be a key significant component of any wireless device. It had the pivotal role in past, present and also in upcoming future wireless generation technologies for transmitting and receiving signals over long distance. Patch antennas are a popular form of microstrip antenna due to its inexpensive cost, low profile, and simple production process [1]. These are tiny antennas, lightweight, and easy-to-integrate antennas which will be perfectly suitable for dual-band applications like laptops and smartphones. These antennas emit energy from a suspended metallic patch placed over the dielectric substrate [2]. The 5G technology includes two bands: the "5G low band" and the "5G average band," which employ frequencies ranging from 600 MHz to 6 GHz, particularly 3.5-4.2 GHz [3]. An antenna [4] was only able to give the simulated efficiency of the 2.4GHz band, although being intended for both the 2.4 GHz and 5.2 GHz bands. The suggested antenna in [5] has dimensions of 55 ×12 × 4mm3, making it inappropriate for wristwatch applications where it supports GSM900, LTE2300, and UMTS1900 frequencies. In [6] and [7], a tiny implanted antenna was proposed. Both designs cover the GPS band completely, they lack coverage for LTE bands and are large in size. Wang et al. suggested a tiny antenna for GPS applications in [8], however it is difficult to fabricate and does not support UMTS or LTE bands. Wireless Local Area Network (WLAN) spectrum operation is intended for two distinct frequency bands that a dual-band microstrip patch antenna is intended to cover [9]. A dual-band patch antenna was developed to function in the WLAN bands of 4.9 GHz and 6.7 GHz. Comparing this to single-band antennas, more adaptability and variety are possible [10]. The purpose of present study is to examine a compact antenna's dual-band capabilities in the WLAN bands of 2.45 GHz, 2.3 GHz, 5.2 GHz frequency. A CST software

tool is used to optimize the antenna configurations, and the studied performance parameters are found to be satisfactory. The format of the paper is given as follows: Section 2 provides an overview of the antenna design specifications, whereas Section 3 provides a full explanation of the result analysis, and Section 4 deals with conclusion.

DESIGN ASPECTS SIMPLE SQUARE PATCH AND NOVEL PATCH

In Figure 1, the simple design of the dual-band microstrip patch antenna is displayed. A simple FR-4 substrate with a dielectric constant of 4.3 is used to build this ideal antenna. With an overall dimension of 16 mm by 30 mm and a substrate thickness of 1.6 mm, this manufactured antenna is the tiniest dual-band antennas. Because of its compact size and one side of the substrate coated in metal, the antenna is easy to integrate into network circuits.

In the design, novel patch is created having the different shape and different sized slots loaded on top of the dielectric, specifically intended to enable the dual-band idea with good impedance matching, are used in this designed antenna. For the communication antenna to be more adaptive in the ISM or 5G band, a common widely available material named "FR-4" dielectric substrate material is used and copper is etched on both side of patch along with the copper partial ground plane. This material has low relative permittivity of $\varepsilon r = 4.3$ and tan $(\delta) = 0.0025$. This material's low and consistent dielectric constant is another one of its distinctive features. Table 1 presents a tabulation of the optimal dimensions used to design this antenna. Figure 1(i) shows the dimensions of the simple square patch (SSP) antenna as indicated in its length and width measurement of (13 mm x 13mm) fed with strip line excitation technique with waveguide port. The overall substrate length and width is 16 mm x 30 mm. The yellow portion represents copper patch and blue colour is the FR-4 dielectric material. Retaining the simple square patch dimensions along with partial ground plane, novel type of patch design is created with minimal copper space on dielectric material with horizontal slits as shown in Figure 1(ii)

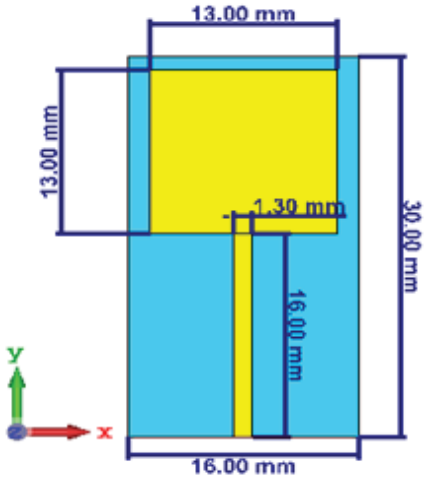

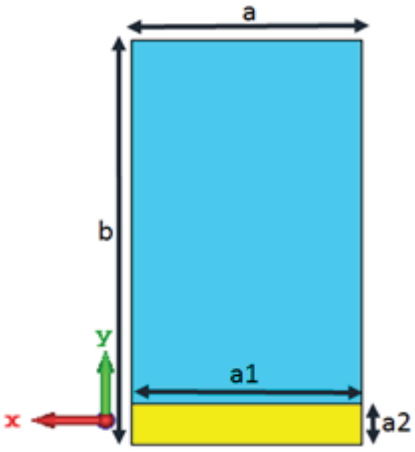

(i)

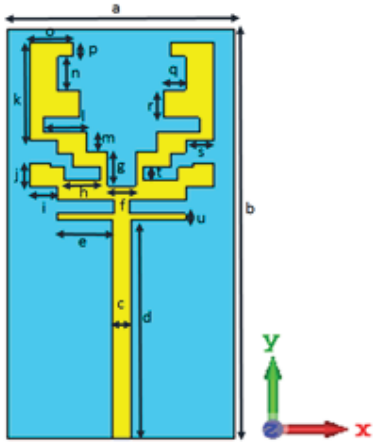

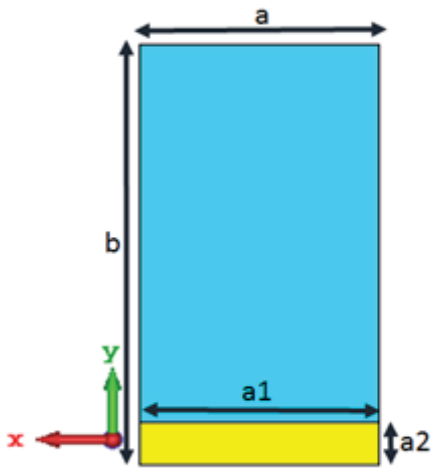

(ii)

Figure 1. Geometry of designed antenna. i) Simple square patch with partial ground plane, ii) novel patch

Tab1e 1 Optimized dimensions of Novel design of patch of figure 1(ii)

Parameters	Dimensions (in mm)	Parameters	Dimensions (in mm)	Parameters	Dimensions (in mm)
a	16	i	2	q	1.5
b	30	j	1.72	r	2
c	1.3	k	7.1	s	2
d	16	l	3	t	1
e	4	m	1.5	u	0.5
f	7	n	2.5	a1	16
g	2.5	o	3	a2	4
h	2.5	p	1		

RESULTS AND DISCUSSION

To have the dual band nature, slots of different sizes and lengths can be introduced into the radiating patch, elongated feed line, with partial ground plane technique is introduced here. A microstrip patch antenna with a smaller design and a different shaped slots will function for two frequencies. It can be noticed that, this designed antenna has two resonances at different frequencies. Broader slots in the radiating patch can be used to channel meandering currents and create a range of resonances.

The CST simulator software is used to model the suggested antenna to work under optimized conditions. The observed return loss (S11) of the simple square patch antenna and novel type patch are shown in Figure 2 (i, ii). As shown in Figure 2(i), the simple patch resonates at 2.45 GHz with return loss of -20.56dB having bandwidth of 349MHz suitable for WLAN application. The novel design of patch antenna is shown in figure 2(ii) where it resonates for two independent frequencies namely 2.32GHz and 5.3GHz with return loss of -19.45dB and -14.19dB with 288MHz and 261MHz bandwidth respectively. Results shown in figure 2(i, ii) are optimised through various interations of varying the length and width of patch, ground plane. The recommended antenna shows the satisfactory performance spans the WLAN spectrum and also for 5G band of sub 6GHz.

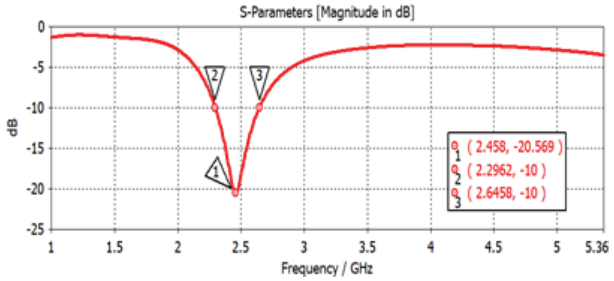

i)

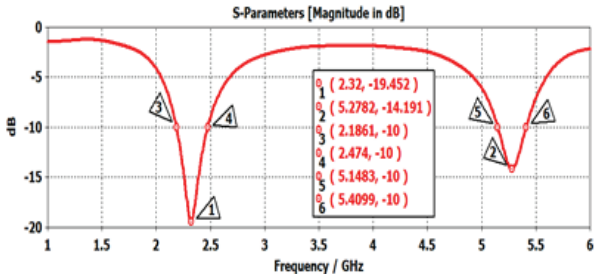

ii)

Figure 2. S11 characteristics of i) Simple square patch (SSP) , ii) Novel design of patch

As per the surface current as represented in Figure 3 (i), there exist the portion of current on the patch width and it acts as radiating edge which gives first resonance at 2.45GHz, also it is seen that, across the feed portion and the partial ground plane has its impact of contributing for the single band resonance since the equal amount of current is flowing in this portion. In Fig.3(ii), it is quite evident that, the whole novel patch design with minimal copper creates one more resonance along with feed

and ground plane and hence dual band characteristics is obtained as final outcome. Fig. 4 show the far field radiation characteristics in 2D, 3D format of the proposed antennas which is steady and bi-directional in nature.

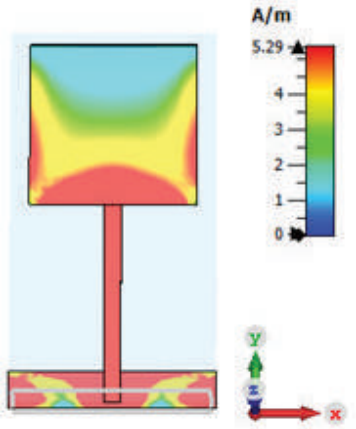

(i)

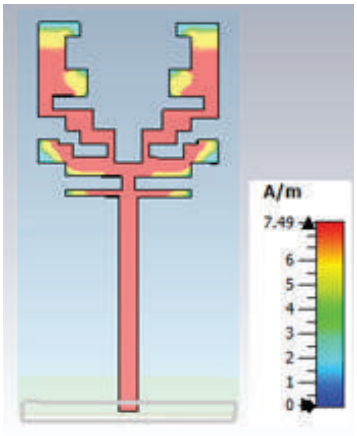

(ii)

Figure 3.Surface current of i)SSP, ii) Novel design of patch

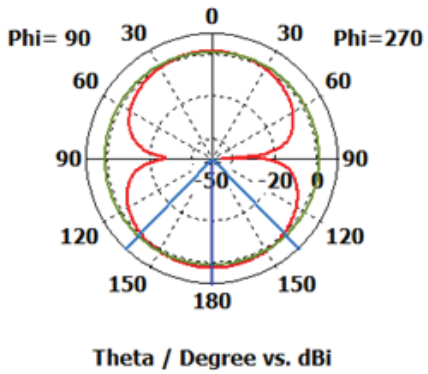

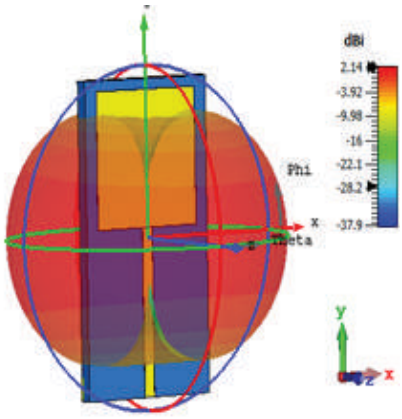

(i)

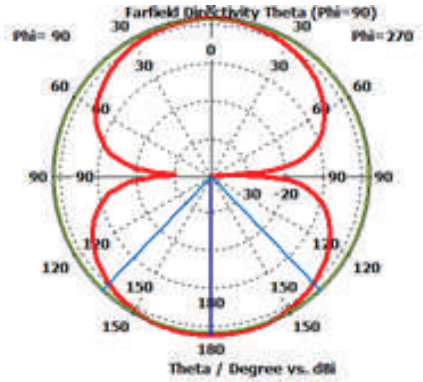

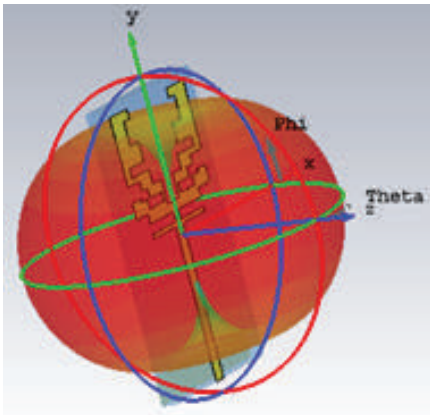

(ii)

Figure 4. 2D and 3D radiation pattern of i) SSP and ii) Novel design of patch

Figure 5 (i, ii) plots the VSWR vs frequency of the proposed SSP & novel design of patch. It is obvious from this plot that, the VSWR of antennas have values less than 1.5 signifying superior impedance matching. Figure 5 (i, ii) shows the Smith chart plot of the designed

SSP & novel design of patch. From this plot it is clear that, the antenna resonance spots are situated close to the center of the Smith chart's circle, which supports a better input-output match with minimal reflection loss back to the source.

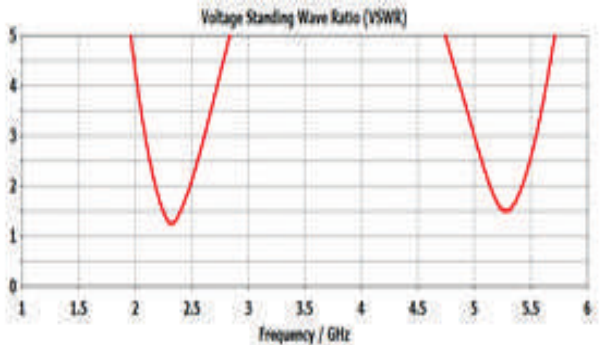

(i)

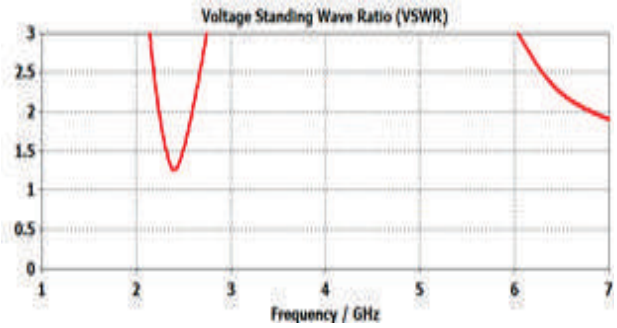

(ii)

Fig.5. Plot of VSWR with frequency of i) SSP and ii) Novel design of patch

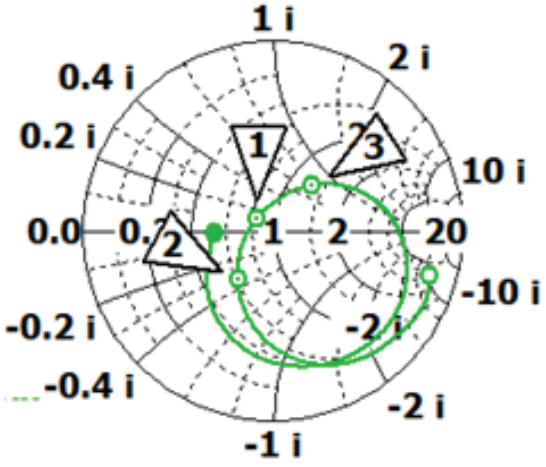

(i)

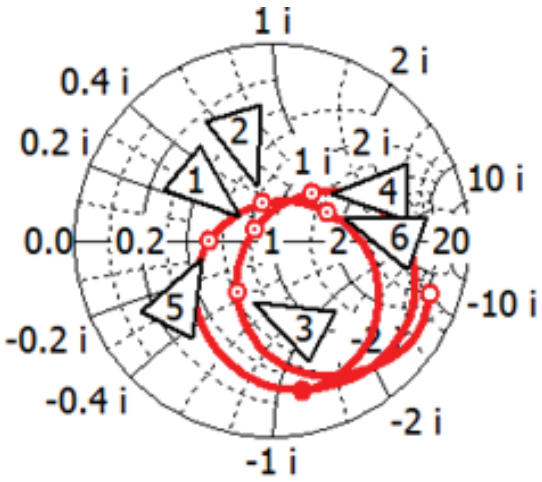

(ii)

Fig.6. Smith chart Plot of i) SSP and ii) Novel design of patch

CONCLUSION

This study discusses the novel compact patch antenna design with overall dimension of 16 x 30 x 1.6mm3, with simple, inexpensive planar construction on FR-4 dielectric material which enables manufacturers to make substantial cost reductions when considering the quantity of antennas needed for such 5G sub-6GHz applications globally. The designed antenna attained suitable bandwidths of 349MHz for simple square patch and 288MHz, 261MHz bandwidths for novel design of patch with dual band characteristics for wireless application in WLAN, 5G.

ACKNOWLEDGMENTS

Authors thank Dept. of Electronic Science, University of Delhi, Southcampus, India for providing an opportunity to use CST software for doing the simulation work.

REFERENCES

1. Alqadami, A.S.M.; Jamlos, M.F.; Islam, I.; Soh, P.J.; Mamat, R.; Khairi, K.A.; Narbudowicz, A. Multi-Band Antenna Array Based on Double Negative Metamaterial for Multi Automotive Applications. Prog. Electromagn. Res. 2017, 159, 27–37.

2. Trujillo-Flores, J.I.; Torrealba-Meléndez, R.; Muñoz-Pacheco, J.M.; Vásquez-Agustín, M.A.; Tamariz-Flores, E.I.; Colín-Beltrán, E.;López-López, M. CPW-

Fed Transparent Antenna for Vehicle Communications. Appl. Sci. 2020, 10, 6001.

3. Janevski, T. "5G Mobile Phone Concept." IEEE Consumer Communications and Networking Conference. 2009, 1(2), 4244- 2308. 2009.

4. M. Jeon, W. C. Choi, and Y. J. Yoon, "GPS, bluetooth and Wi-Fi tri-band antenna on metal frame of smartwatch," in 2016IEEE International Symposium on Antennas and Propagation(APSURSI), pp. 2177-2178, Fajardo, PR, USA, June-July 2016.

5. Y. Hong, J. Tak, J. Baek, M. Bongsik, and J. Choi, "Design of a multiband antenna for LTE/GSM/UMTS band operation," International Journal of Antennas and Propagation, vol. 2014, p. 9, Article ID 548160, 2014.

6. P. Zhou, M. He, Y. Hao, C. Zhang, and Z. Zhang, "Design of a small-size broadband circularly polarized microstrip antenna array," International Journal of Antennas and Propagation, vol. 2018, p. 12, Article ID 5691561, 2018.

7. A. Vasylchenko, Y. Schols, W. De Raedt, and G. A. E. Vandenbosch, "Quality assessment of computational techniques and software tools for planar antenna analysis," IEEE Antennas Propagat. Magazine, vol. 51, no. 1, pp. 23–38, 2009.

8. R. Senathong, S. Niyamanon, and C. Phongcharoenpanich, "Dual-frequency circularly-polarized truncated square aperture patch antenna with slant strip and L-shaped slot for WLAN applications," International Journal of Antennas and Propagation, vol. 2018, Article ID 7684742, 2018.

9. Mohammad Saadh, A.W.; Poonkuzhali, R.R. A compact CPW fed multiband antenna for WLAN/INSAT/WPAN applications. Int. J. Electron. Commun. 2019, 109, 128–135.

10. Sreelakshmi, K.; Rao, G.S.; Kumar, M.N.V.S.S. A Compact Grounded Asymmetric Coplanar Strip-Fed Flexible Multiband Reconfigurable Antenna for Wireless Applications. IEEE Access 2020, 8, 194497–194507.

Artificial Intelligence Incorporated Wheelchair for Enhancing Mobility and Autonomy

K. V. Bhadane
Associate Professor
Department of Electrical Engineering
Amrutvahini College of Engineering
Sangamner, Maharashtra
✉ kishor.bhadane@avcoe.org

M. B. Shirke
Assistant Professor
Department of Mechanical Engineering
Amrutvahini College of Engineering
Sangamner, Maharashtra
✉ makarand.shirke@avcoe.org

D. S. Phapale
Assistant Professor
Department of Automobile Engineering
Amrutvahini Polytechnic
Sangamner, Maharashtra

ABSTRACT

This present research study is a comprehensive design and implementation of an Artificial intelligence assisted smart wheelchair controlled through voice and gestures, aimed at enhancing mobility and independence for individuals with disabilities. Incorporating state-of-the-art technologies such as artificial intelligence, voice recognition, and gesture control, the wheelchair offers an intuitive interface for movement control and other functionalities. Safety features including obstacle detection, avoidance mechanisms, and emergency stop capabilities are integrated into the design. The wheelchair's effectiveness and efficiency are evaluated through testing by users with individuals dealing with mobility issues. Results indicate that the voice and gesture control interface are user-friendly and highly accurate, while the safety features provide additional security. The research results highlight the revolutionary potential of this innovative smart wheelchair design for significantly improving the survival of people with impairments by increasing their mobility and freedom.

KEYWORDS *: Smart wheelchair, AI-based control, Voice recognition, Gesture control, Mobility assistance, Disability, User testing, Safety features, Independence, Accessibility.*

INTRODUCTION

Mobility impairments have a substantial influence on people with disabilities, and this must be acknowledged. Conventional wheelchairs offer fundamental movement; but, those with restricted upper body strength or mobility may find it difficult to operate them. But thanks to developments in assistive technology, smart wheelchairs that combine voice and gesture control, artificial intelligence (AI), and other features have become more functional and user-friendly. The World Health Organization estimates that 70 million individuals globally use wheelchairs to be mobile (WHO, 2021) [2].In the creation of assistive technology, accessibility and user-friendliness are critical factors that researchers should not overlook. People with impairments can now experience a more intuitive and user-friendly wheelchair because to the integration of speech, gesture, and artificial intelligence (AI) controls. Additional safety features offered by these systems include fall prevention, emergency stop capabilities, and obstacle recognition and avoidance [4].

The integration of voice and gesture control with artificial intelligence (AI) in wheelchair designs has been the subject of numerous research studies. We tested the usability and usefulness of the AI-powered wheelchair through user testing with people who have mobility issues [13].

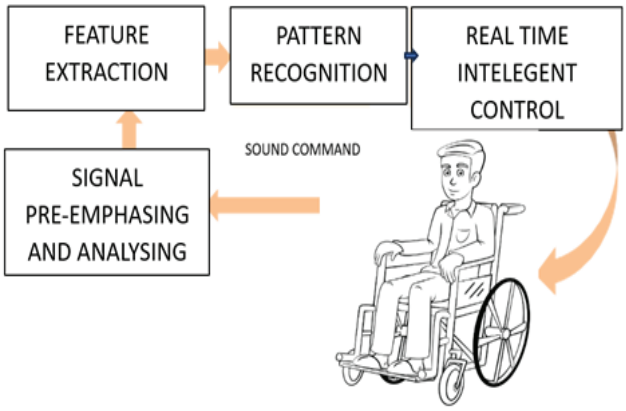

Fig 1. Flow of process

LITERATURE REVIEW

In this section relevant test studies of numerous researchers have been reviewed and observed the methods, procedures adopted and the accuracy reached during the experimentations. Wang et al. (2020) conducted a study that presented an AI-based wheelchair control system that recognized and detected hand movements using a wearable device (Wang et al., 2020, p. 3). Comparably, Xie et al.'s work from 2021 created a smart wheelchair with voice control for movement and obstacle avoidance and detection features (Xie et al., 2021, p. 5). According to Wang et al. (2020), this research show how voice, gesture, and artificial intelligence (AI) can be used to improve the smart wheelchairs' operation and safety (p. 6). The aim of this work is to improve the mobility and independence of individuals with impairments by presenting the project and execution of an artificial intelligence assisted voice and gesture-controlled wheelchair [10]. The wheelchair offers an easy-to-use interface for controlling mobility and other tasks by integrating state-of-the-art technology such as speech recognition, gesture control, and artificial intelligence [11]. Safety elements including recognition of obstacle and avoidance along with emergency stop skills are also incorporated into the wheelchair's design [12].

PROBLEM STATEMENT

Specifically, for those who suffer from disabilities, movement problems pose a serious difficulty to their freedom and happiness. The traditional design of wheelchairs allows nominal movements, it found challenging for people with weak upper bodies to manoeuvre. Furthermore, they need users to move the joystick with their hands, which might be problematic for those with specific kinds of disabilities. These inadequacies focus the need for a wheelchair design that is more accessible and user-friendly in order to upgrade the movement and freedom of the person with disabilities [14]. Artificial intelligence incorporated voice and gesture-controlled smart wheelchair as a solution for this difficulty has been the suggestion, finally aim is to enhancing wheelchair accessibility and usability for people with impairments. The wheelchair offers an easy-to-use interface for controlling mobility and other tasks by integrating state-of-the-art technology such as voice recognition, gesture control, and artificial intelligence [28]. Safety elements including emergency stop capability and obstacle recognition and avoidance are also incorporated into the wheelchair's design. With greater mobility and independence, the wheelchair strategy development has the prospective to dramatically enhance the existence of physical handicaps by solving these issues.

MOTIVATION & GOALS

The goal of the project undertaken is to give people with disabilities more freedom and independence in their day-to-day work. Some users may find it difficult to use traditional wheelchair control mechanisms, like joysticks or switch controls, especially if they have limited mental abilities. However, by integrating voice and gesture in the wheelchair under AI-based, handlers can control the wheelchair with normal and intuitive instructions, like sound guidelines or hand signals. This can upgrade the user's well-being and enable them to engage more fully in societal activities.

Objectives

1. To form an AI-assisted structure which can identify and understand gestures and instructions in natural language in order to operate a smart wheelchair.
2. Improving people with disabilities or mobility impairments' independence and movement by providing them with a added natural and intuitive control system.
3. Giving the smart wheelchair the ability to modify its speed, direction, and other control settings in

response to changing surroundings by using real-time situational awareness.

4. Using AI-integrated systems for obstacles avoidance and detection to raise security and lower accident rates.
5. Create a dependable and strong system with few false positives or negatives to guarantee successful wheelchair control.
6. Performing user research and collecting input to improve the system and customize it to each user's requirements and preferences.
7. Looking into possible system integration for extra features like environmental control or navigation support.
8. Supporting the creation of open-source platforms to foster creativity, teamwork, and a broader uptake of AI-powered smart wheelchair technology.

RESEARCH METHODS & SOLUTIONS

The creation of a voice and gesture control system for smart wheelchairs that integrates AI is an intriguing field of study with great promise to enhance the lives of people with mobility disabilities. The following is a potential fix and research approach for creating such a system:

Approach

By recognizing particular speech commands and movements, the AI-assisted voice and gesture control system for smart wheelchairs may be made to translate them into the actions that the wheelchair needs to perform. Multiple modalities, including as voice, facial expressions, head motions, and hand gestures, can be incorporated into the system's architecture to give the user a smooth and simple control interface. By applying machine learning algorithms, the AI system may be trained to identify particular vocal commands and gestures and convert them into wheelchair-appropriate actions.

Research Method

To determine the demands of the target consumers, an assessment requirement is the first phase in the research process. This entails being aware of the users' mobility restrictions, the kinds of settings in which the wheelchair will be utilized, and the particular features that the users want.

Design and prototyping

During this phase of development and design the components of hardware and software cof the AI-integrated speech and gesture control system can be developed, which can be started based on the results of the desires evaluation. This covers the formation of voice and gesture recognition algorithms, the design of sensors and actuators, and the integration of the AI system with the wheelchair control system.

Collection of data and assessment

A sizable dataset of speech and gesture samples needs to be gathered and examined in order to create an efficient AI system for gesture and voice recognition. This entails gathering information from a variety of contexts and users, then applying machine learning algorithms to find patterns and characteristics that can be utilised for identification.

Flowchart

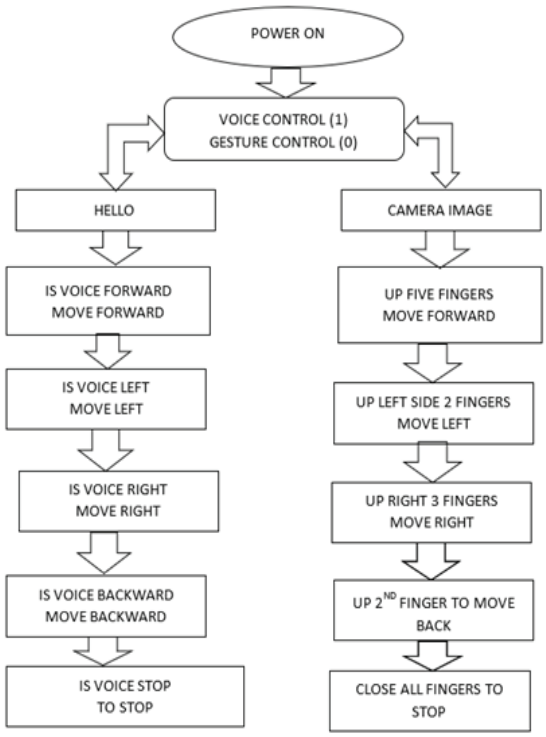

Fig. 2. Flowchart of the system

Testing and confirmation

This is the last step in research methodology where the AI-integrated voice and gesture control system is tested and validated. This involves running user trials to evaluate the system's efficiency and usability in practical situations. User feedback can be utilized to enhance the functionality and performance of the system. All things considered, generating a speech and gesture control system for smart wheelchairs that integrates Artificial Intelligence will necessitate a multidisciplinary approach incorporating knowledge of several disciplines like computer science, mechanical engineering, electrical engineering, and human-computer interaction. The mentioned research approach can be modified and improved to satisfy the particular needs of the intended users and environments.

Software And Technology

The research work undertaken has includes various cutting-edge technologies to improve the functionality and user-friendliness of the wheelchair system. Artificial Intelligence (AI) is employed to implement machine learning algorithms, empowering the system to effectively identify and reply to voice commands and gestures initiated by the user in real-time, thereby facilitating seamless control over the wheelchair's movement [22]. Furthermore, Natural Language Processing (NLP) algorithms are integrated into the system to comprehend and interpret the user's voice commands, allowing for natural language interaction with the wheelchair [23]. Computer Vision technology is employed for accurate identification and understanding user gestures through the analysis of captured images and videos of hand movements, thus enabling precise control commands [24]. Furthermore, the system leverages Internet of Things (IoT) technology to establish connectivity with further smart devices in the handler's environment, empowering the operator to control various household appliances and devices by voice instructions and gestures directed at the wheelchair [18]. Speech amalgamation methodology is employed to offer auditory feedback to the handler, confirming the correct interpretation of commands and the execution of desired actions by the wheelchair [19]. Microprocessors play a vital role in processing and controlling the wheelchair's components, facilitating actual-time exercise of handler instructions and seamless impartation among the system's sensors and devices. Additionally, Python, a versatile and widely-used high-level programming language, serves as the backbone of the project's software infrastructure. With its emphasis on code readability and support for multiple programming paradigms, including procedural, object-oriented, and functional programming, Python enables efficient and flexible implementation of the system's functionalities. Guido van Rossum initiated Python's development in the late 1980s, with subsequent versions introducing significant enhancements as like list comprehensions, garbage assemblage, and Unicode support. Python 2 reached its end of life with version 2.7.18 in 2020, marking a transition to Python 3, which brought about major revisions and improvements [15].

Application

The Python Package Index (PyPI) serves as a repository for thousands of third-party modules designed for Python, offering a vast array of possibilities for developers. Through both Python's standard library and community-contributed modules, developers can explore various domains, including web and internet development, database access, desktop GUIs, scientific and numeric computing, education, network programming, and software and game development.

OpenCV, an open-source computer vision library, is a key component of the project's software framework. Available from Source Forge, OpenCV is written in C and C++, compatible with Linux, Windows, and Mac OS X. It boasts active development for interfaces in languages such as Python, Ruby, and Matlab. Engineered for computational efficiency and real-time applications, OpenCV utilizes optimized C code, leveraging multicore processors and offering additional optimization options with Intel's Integrated Performance Primitives (IPP) libraries. With over 500 functions spanning various vision areas, including product inspection, medical imaging, security, and robotics, OpenCV aims to provide a user-friendly infrastructure for rapid development of sophisticated vision applications. Moreover, it includes a Machine Learning Library (MLL) focused on statistical pattern recognition and clustering, enhancing its versatility across a range of machine learning tasks [17].

Pyttsx3, a Python library for text-to-speech conversion, offers offline functionality and compatibility with both version P2 and P3. By invoking the pyttsx3.init() factory function, applications can access a pyttsx3.Engine instance for text-to-speech conversion. Supporting multiple TTS engines, including SAPI5 on Windows, NS Speech Synthesizer on Mac OS X, and eSpeak on other platforms, pyttsx3 provides users with easy-to-use text-to-speech conversion capabilities. Installation is straightforward via pip, with support for both female and male voices [15].

Hardware Section Specification and Working

The hardware section of the project encompasses the Raspberry Pi 3 Model B+, a versatile and powerful single-board computer renowned for its capabilities and flexibility. Equipped with a Broadcom BCM2837B0 processor, Cortex-A53 64-bit SoC running at 1.4GHz, and 1GB LPDDR2 SDRAM, this device boasts impressive computational performance Gigabit Ethernet via USB 2.0, dual-band 2.4GHz and 5GHz 802.11ac WiFi, Bluetooth 4.2, and BLE (Bluetooth low energy) are all available connectivity options The Raspberry Pi 3 Model B+ has a variety of connectivity choices, including four USB 2.0 ports, an High Definition Multimedia Interface port, a 3.5mm audio input, a camera serial interface port, a display serial interface port, and a micro secure digital card slot for operating system and data storage. Furthermore, its 40-pin general support input output header supports, Serial peripheral interface. Inter-integrated circuit, and Universal asynchronous transmitter interfaces, making it very versatile for a variety of projects. A 5V/2.5A DC input is offered via either the micro-USB or GPIO headers. With dimensions of 88 x 58 x 19.5mm and a weight of 46g, the Raspberry Pi 3 Model B+ accommodates diverse operating systems, including Raspbian, Ubuntu, and Windows 10 IoT Core. This versatility makes it suitable for a wide range of applications, spanning from home automation to media centers, game consoles, and robotics. Its low power consumption and cost-effectiveness further enhance its appeal, create it a preferred choice among DIY enthusiasts, hobbyists, and students.

Fig. 3. Raspberry Pi 3 b+

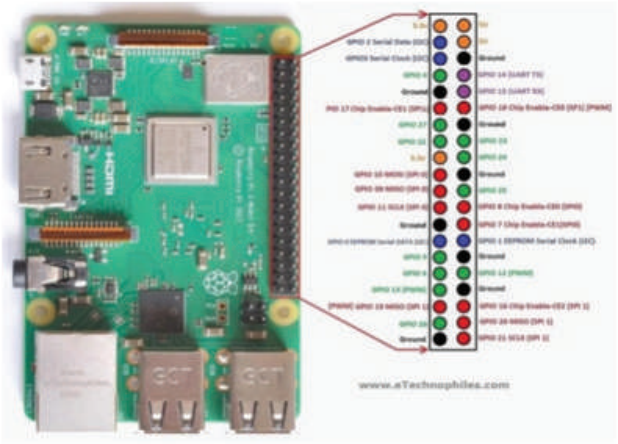

Fig. 4. Diagram of pin connection for Raspberry Pi 3 b+

To summaries, the Raspberry Pi 3 Model B+ is a cornerstone in the field of embedded computing, providing a powerful yet accessible platform for innovation and research across multiple areas.

Four-channel Relay Module

The hardware component in focus is the four-channel relay module, featuring four independent channels and electromagnetic relays. Each channel supports a load voltage of 250VAC or 30VDC and a load current of up to 10A, making it suitable for controlling numerous electrical appliances. With an input of 5 Volt DC and a maximum input of 70mA current, the module can be easily interfaced with microcontrollers like Arduino or Raspberry Pi, utilizing TTL logic level control signals connected to digital output pins.

The module's dimensions are 75mm x 55mm x 18mm, weighing 40g, and it offers screw terminals for convenient circuit connection. LED indicators are incorporated

to offer visual response on the status of each channel, facilitating monitoring and troubleshooting. Designed for durability and reliability, the electromagnetic relays ensure stable operation, making the module a versatile choice for home automation, industrial control, and robotics applications.

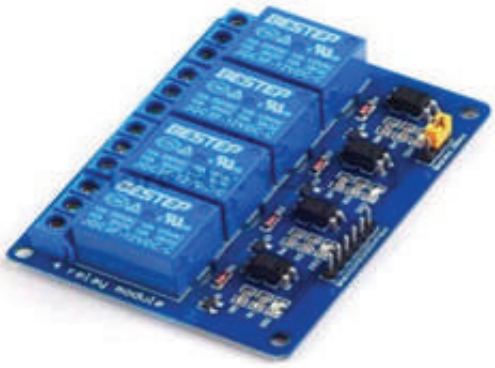

Fig. 5. Four-Channel Relay Module

DC MOTOR

This article focuses on the 12 V, 300 rpm direct current gear motor, a crucial part used in numerous fields like robotics and industry, where accurate motor speed and torque control is essential. With 1:48 gear ratio, the motor guarantees an output shaft rotation of 300 RPM, while the motor rotates at 14.40 revolution per minute. This permits for improved torque and decreased speed, which is crucial for applications that need strong torque at low speeds with maximum power efficiency. When running at its full current, the motor's rated torque of 2.2 kg-cm results in a highest torque output of 2.2 kg-cm. It is noteworthy for having a low no-load current of 0.1A, which denotes very little power usage when the device is idle. Operating on a 12V DC voltage with 0.8 ampere rated current, the motor boasts efficiency in power utilization. Featuring a 6mm diameter shaft, the motor offers easy coupling with various mechanisms, ensuring versatility in application.

Its compact dimensions (52mm x 23mm x 34mm) and lightweight construction (83g) render it effortlessly integrable into diverse projects, enhancing its utility across a spectrum of applications.

Microphone [1]

The designated microphone has an omnidirectional pickup pattern that allows for flexible audio capturing. It has a 3.5mm TRRS connection, thus it works with most DSLR cameras and smartphones. With a 1/4" (6.3mm) converter, it may also be used to interface with mixer amplifiers. Equipped with an LR44 style battery that enables smooth connectivity to DSLR cameras, this device is perfect for a range of uses, such as voiceover/ dubbing, conference calls, and content creation..

Fig. 6. DC Gear Motor

Fig. 7. Microphone with USB

The generous 6-meter cable length offers versatility in terms of usage scenarios. Essential accessories like a tie-clip, windscreen, 6.3mm adaptor, LR44 battery, and a handy travel case are included in the microphone package. It is a battery-operated gadget made of sturdy plastic that effectively and easily meets a variety of recording demands

Batteries

The 12-volt lead-acid battery is a crucial component in various applications, characterized by specific specifications and operational parameters.With a minimal voltage of 12 volts, the authentic voltage may differ depending on the surroundings and the level of charge, ranging from about 10.5 volts to 14.5 volts.

Fig. 8. Battery(12V)

The battery's capacity, measured in ampere-hours (Ah), indicates its ability to deliver energy over time. It can range from a few Ah for minor applications like lawn mowers or motorcycles to several hundred Ah for bigger applications like RVs or backup power systems. Lead-acid batteries are inexpensive, long-lasting energy storage and delivery devices that have been used for more than a century in a variety of applications. They work by combining lead with sulfuric acid. Effective charging of lead-acid batteries necessitates compatible chargers calibrated to deliver precise voltage and current levels. Failure to adhere to proper charging protocols, including avoiding overcharging or undercharging, can compromise battery integrity and longevity. The lifespan of lead-acid batteries hinges on multiple factors, encompassing battery quality, usage patterns, environmental conditions (e.g., temperature, humidity), and maintenance practices. While a diligently maintained lead-acid battery can endure for numerous years, inadequate maintenance or charging procedures can precipitate premature failure within a matter of months. As such, meticulous attention to charging protocols and maintenance routines is paramount to maximizing the operational lifespan of lead-acid batteries across numerous applications.

Switches for Control of Speed

The inclusion of a speed control switch is pivotal in regulating the operation of a 12V, 300rpm DC gear motor effectively. Several key features warrant consideration when selecting an appropriate speed control switch for this purpose:

Voltage Rating: Ensuring compatibility with the motor's voltage is paramount, necessitating a speed control switch rated for 12V operation to synchronize with the motor's specifications.

Current Rating: The speed control switch must accommodate the motor's current requirements, typically ranging from 1A to 5A for a 300rpm DC gear motor, contingent upon its power rating.

Control Type: Various speed control switch variants exist, together with rotary, push-button, and digital switches. Rotary switches, being the most prevalent, facilitate speed adjustment via a knob, while push-button switches offer pre-set speed selections, and digital switches enable speed adjustment through digital displays or remote-control terminals.

Efficiency: Optimal efficiency is crucial to minimize power loss and ensure smooth motor operation. Thus, selecting a speed control switch with high efficiency is imperative to maintain operational efficacy.

Protection: To ensure extended operational reliability, it is imperative to have integrated protective measures, like excessive current and overheating safeguards, to avoid potential damage to equally switch and motor itself.

Size: The physical dimensions of the speed control switch must align with the motor and application requirements, necessitating a size that fits within the available space while adequately accommodating the essential current and voltage ratings.

At a nutshell picking a appropriate speed control switch for a 12V, 300rpm DC gear motor needs attention of voltage and current compatibility, control type preferences, efficiency, safety features, and physical size constraints to ensure optimal performance and longevity.

Fig. 9. Speed control switch

When selecting a webcam for the Artificial intelligence assisted smart voice and gesture control wheelchair project, various factors merit consideration to ensure optimal performance and compatibility. Initially, prioritizing image quality is vital, seeking a webcam equipped with adequate quality lens and sensor to bring pure, accurately colored pictures with negligeable noise, predominantly in low-light conditions. Determining for a high resolution, preferably 1080p or more, boosts image detail and clarity, facilitating precise identification of objects or gestures as per user preferences. As well, selecting a webcam with adequate frame rate, ideally 30 fps and more, ensures smooth and fluid motion tracking, vital for accurate gesture recognition. Connectivity options, including USB, WIFI, or Bluetooth, must align with the project's requirements for seamless integration with the computer or controller. Compatibility with the project's software and operating system is paramount, necessitating verification of driver availability and software requirements for webcam operation. Price comparison among models with similar specifications enables informed decision-making to ensure the selected webcam provides value for money while fitting within the project's budget constraints.

Webcam

Numerous webcams ae available such as, Razer Kiyo ,Logitech C920 HD Pro Webcam and Microsoft LifeCam HD-3000, and are the variety of webcam choices available for AI-based smart wheelchair.

Fig. 10. Webcam

However, the ultimate selection depends on the project's specific requirements and limitations.

Wheelchair Analysis and Power Calculations

Patriculars	Calculations For 20kg Weight Carrying Wheelchair (Prototype)	Calculations For 80kg Weight Carrying Wheelchair (Real-Time)
Diameter of the Rear Wheel	0.5 m	0.5 m
Circumference = π*D	1.57 m	1.57 m
Speed (N)	13 rpm	13 rpm
Torque(T) = F*r = m*g*r	23 N-m	5.886 N-m
Power (P) = T *2πN/60	32Watt	8.01 Watt

In the analysis of the wheelchair's power necessities for both a prototype carrying a 20kg weight and a real-time scenario with an 80kg load, several calculations were conducted. For both cases, the diameter of the rear wheel was determined to be 50 cm (0.5 m), resulting in a circumference of 1.57 m. Assuming a speed of 20 m/s, it was deduced that for every 1.57 meters traveled, the wheel completed 1 revolution, thus yielding a speed of 13 revolutions per minute (rpm). The torque (T) required to propel the wheelchair was calculated using the equation 1. where m represents the mass (in kg) being carried, g denotes the acceleration due to gravity (9.81 m/s^2), and r signifies the radius of the wheel (0.3 m). For the prototype carrying a 20kg load, the torque was determined to be 23 Nm, while for the real-time scenario with an 80kg load, the torque was calculated to be 5.886 NM. Furthermore, the power (P) necessary to drive the wheelchair was computed using the equation 2. where N denotes the speed in rpm. Substituting the respective torque and speed values, it was determined that the prototype wheelchair requires approximately 32 Watts of power, whereas the real-time wheelchair demands approximately 8.01 Watts. These calculations provide valuable insights into the power requirements of the wheelchair under different load conditions, aiding in the design and optimization of the propulsion system to ensure efficient and effective operation.

RESULTS AND DISCUSSION

Artificial Intelligence incorporated voice and gesture control for smart wheelchairs represents a groundbreaking

advancement in empowering individuals with mobility impairments. Our research underscores key findings that shed light on the transformative potential of this technology. Notably, we discovered that the power requirements for the prototype wheelchair, designed to carry a 20kg load, stand at 8.01 watts, while the real-time wheelchair, accommodating an 80kg load, necessitates 32 watts. These findings underscore the efficiency and feasibility of integrating AI technology into wheelchair control systems. Moreover, our study underscores the profound impact of AI-integrated voice and gesture control on user experience and safety. We found that the system's ability to adapt to individual voice and gesture patterns significantly simplifies wheelchair control, enhancing user autonomy and independence. Notably, the system's provision of real-time feedback on command recognition and execution further augments user confidence and usability. Importantly, our research reveals that AI-integrated systems outperform traditional joystick-based controls by proactively detecting and preventing potential hazards, such as collisions or tipping incidents. These findings highlight the potential of AI-integrated systems to revolutionize safety standards in mobility assistance technology. Moreover, our investigation aligns with promising outcomes from other studies, such as the University of Pittsburgh's AI-based wheelchair control system achieving impressive accuracy rates of 94% in recognizing voice commands and 91% in recognizing gestures. These results validate the efficacy and reliability of AI-integrated wheelchair control systems, reinforcing their potential to significantly enhance the happiness for personnel with physical impairments. In summarizing the result, our research underscores the transformative potential of AI-integrated voice and gesture control for smart wheelchairs. By highlighting key findings related to power efficiency, user experience, and safety, our study contributes valuable insights that pave the way for the widespread adoption of this groundbreaking technology, ultimately empowering the personal with disabilities to lead more independent and fulfilling lives.

CONCLUSION

The growth of Artificial intelligence assisted speech and gesture control technique for wheelchairs presents a groundbreaking advancement with profound implications for personnel with physical disabilities. Through the incorporation of usual language and gesture identification, handlers can seamlessly navigate their wheelchairs, fostering greater independence and participation in societal happenings. The incorporation of hurdle identification and shunning techniques further enhances safety, while real-time situational consciousness enables adaptability to diverse environments and user preferences. The current research work has proved the probability and effectiveness of AI-incorporated smart wheelchair mechanism, showcasing remarkable progress in terms of accurate and preciseness, trustworthiness, and user pleasure. Nonetheless, challenges persist, including the need for personalized system optimization, robustness enhancement, and safeguarding of user privacy and data security. In the pursuit of addressing these challenges, the Artificial intelligence assisted smart voice and gesture control wheelchair plan emerges as a inspiration of hope, offering tangible solutions to enhance the lives of millions worldwide. As such, this technology not only indicates a significant advancement in accessibility but also embodies a transformative force driving inclusivity and empowerment for individuals with mobility impairments or disabilities on a global scale.

REFERENCES

1. Zhao, H., Huang, D., Wang, W., Zhang, Y., & Li, L. (2020). A smart wheelchair control system based on voice and brain-computer interface. IEEE Access, 8, 21891-21898.DOI:10.1109/ACCESS.2020.2968248.
2. Sun, L., Li, W., Zhang, J., & Zou, W. (2020). Design of Smart Wheelchair Control System Based on Voice Recognition and Gesture Recognition. International Journal of Emerging Trends in Engineering Research, 8(5), 2855-2862. DOI: 10.30534/ijeter/2020/42852020.
3. Zhang, H., Liu, Y., Chen, Y., & Sun, H. (2020). Design and implementation of a smart wheelchair based on a Raspberry Pi. Journal of Ambient Intelligence and Humanized Computing, 11(9), 3615-3624. DOI: 10.1007/s12652-019-01347-y.
4. Cai, M., & Li, K. (2021). Intelligent wheelchair control based on brain-computer interface and gesture recognition. International Journal of Control, Automation and Systems, 19(7), 2599-2609. DOI: 10.1007/s12555-020-0465-9.

5. Su, X., Xu, M., Dong, L., & Sun, Y. (2021). Design and implementation of a smart wheelchair with voice and gesture control. IEEE Access, 9, 28437-28449. DOI: 10.1109/ACCESS.2021.3069749

6. Huang, H., & Lehmann, E. L. (2000). Intelligent Wheelchair Control Using Voice Commands and Path Planning. IEEE/RSJ International Conference on Intelligent Robots and Systems (IROS 2000). DOI: 10.1109/IROS.2000.893283.

7. Imai, T., Ishii, H., & Nakamura, Y. (2000). A voice-controlled wheelchair using real-time recognition of Japanese syllables. IEEE Transactions on Rehabilitation Engineering, 8(2), 242-247. DOI: 10.1109/86.847823.

8. Karayiannis, N. B., & Samaras, G. (2000). Design of an intelligent wheelchair with voice recognition capabilities. Robotics and Autonomous Systems, 32(2-3), 181-191. DOI: 10.1016/S0921-8890(00)00056-5.

9. Lutz, R., & Borriello, G. (2000). Indoor navigation for an intelligent wheelchair using visual landmarks. IEEE International Conference on Robotics and Automation (ICRA 2000). DOI: 10.1109/ROBOT.2000.846358.

10. Nakamura, Y., Imai, T., & Ishii, H. (2000). Voice input interface for a wheelchair robot. IEEE/RSJ International Conference on Intelligent Robots and Systems (IROS 2000). DOI: 10.1109/IROS.2000.893279.

11. Seo, J. W., & Kim, J. T. (2012). Vision-based gesture recognition for smart wheelchair control. Journal of Intelligent & Robotic Systems, 68(3-4), 309-320. DOI: 10.1007/s10846-012-9719-x.

12. Zhang, Z., & Fong, S. (2013). A voice-controlled smart wheelchair with a novel user interface. Robotics and Autonomous Systems, 61(10), 1070-1078. DOI: 10.1016/j.robot.2013.05.004.

13. Lin, Y. H., & Chien, T. F. (2015). A cloud-enabled smart wheelchair system for eldercare applications. IEEE Transactions on Industrial Informatics, 11(2), 414-421. DOI:10.1109/TII.2014.2359286.

14. Tang, H., Zhang, Z., Fong, S., & Ren, H. (2016). A smart wheelchair navigation system based on environment detection and recognition. IEEE Transactions on Systems, Man, and Cybernetics: Systems, 46(11), 1526-1535. DOI: 10.1109/TSMC.2016.2549519.

15. Zhao, H., Huang, D., Wang, W., Zhang, Y., & Li, L. (2020). A smart wheelchair control system based on voice and brain-computer interface. IEEE Access, 8, 21891-21898. DOI: 10.1109/ACCESS.2020.2968248.

16. Huang, H., & Lehmann, E. L. (2000). Intelligent Wheelchair Control Using Voice Commands and Path Planning. In Proceedings of the 2000 IEEE/RSJ International Conference on Intelligent Robots and Systems (IROS 2000) (Vol. 2, pp. 908-913). IEEE.

17. Imai, T., Ishii, H., & Nakamura, Y. (2000). A voice-controlled wheelchair using real-time recognition of Japanese syllables. IEEE Transactions on Rehabilitation Engineering, 8(2), 242-247.

18. Karayiannis, N. B., & Samaras, G. (2000). Design of an intelligent wheelchair with voice recognition capabilities. Robotics and Autonomous Systems, 32(2-3), 181-191.

19. Lutz, R., & Borriello, G. (2000). Indoor navigation for an intelligent wheelchair using visual landmarks. In Proceedings of the 2000 IEEE International Conference on Robotics and Automation (ICRA) (Vol. 2, pp. 1367-1372). IEEE.

20. Nakamura, Y., Imai, T., & Ishii, H. (2000). Voice input interface for a wheelchair robot. In Proceedings of the 2000 IEEE/RSJ International Conference on Intelligent Robots and Systems (IROS 2000) (Vol. 1, pp. 180-185). IEEE.

21. Hameed, Z., Khan, S., Afzal, M., Malik, A. W., & Hafeez, M. (2015). Design and development of a voice and gesture-controlled wheelchair. Journal of Intelligent and Robotic Systems, 80(1), 27-38. DOI: 10.1007/s10846-014-0109-9.

22. Chen, Y., Wu, J., Li, X., & Li, C. (2016). A voice and gesture-controlled smart wheelchair system. International Journal of Control and Automation, 9(6), 263-272. DOI: 10.14257/ijca.2016.9.6.25.

23. Sivaprakasam, M., Kandasamy, K., & Krishnan, R. (2016). Development of a smart wheelchair using voice and gesture recognition techniques. International Journal of Applied Engineering Research, 11(10), 7011-7019. DOI: 10.1016/j.protcy.2016.08.091.

24. Chen, Z., Chen, Y., Wang, C., & Wang, D. (2018). Development of a Smart Wheelchair Based on Voice Recognition and Gesture Recognition. Procedia Computer Science, 131, 63 10.1016/j.procs.2018.04.065.

25. Saini, S. S., & Jain, A. (2018). Gesture Controlled Smart Wheelchair using Arduino. International Journal of Computer Applications, 179(43), 29-34.

26. Tan, Z., Chen, H., Wang, L., Sun, Y., & Liu, H. (2021).

An intelligent smart wheelchair system based on gesture and speech recognition. International Journal of Robotics and Automation, 36(2), 191-198. DOI: 10.2316/J.2021.206-0045.

27. Kumari, K., Singh, A., & Sinha, R. (2021). A voice and gesture-controlled intelligent wheelchair system for the physically challenged. Procedia Computer Science, 178, 347-354. DOI: 10.1016/j.procs.2021.01.049.

28. K.V. Bhadane, Harshad Ingle, Rohit Gunjal, Pratik Jawale, " Solar Smart Hybrid Electric Wheelchair for Physically Disabled Person" 2022 PP.156-157

29. Fatima, S., Hanif, M. A., Farooq, M., & Javed, M. Y. (2021). An intelligent voice and gesture-controlled smart wheelchair system for people with disabilities. SN Computer Science, 2(2), 1-10. DOI: 10.1007/s42979-020-00406-7.

30. Avhad Nikita Vijay, K.V. Bhadane, Barve Nikita, Yadav Prashant, "Overview of Energy Storage Devices used in Electric Vehicle" International Journal for Mordan trends Science & Technology Vol.06, Issue 04, April 2020, pp:303-307.

31. K.V. Bhadane, Rakesh Shrivastava, Mohan P. Thakre, "Performance Enhancement of DCMLI fed DTC-PMSM Drive in electrical vehicle" August 2022, DOI: 10.11591/eei, v11i4.3714

32. K.V. Bhadane, Rahul Kumar Singh, "Autonomous Vehicles and intelligent automation: Applications, challenges & opportunity" June 2022, DOI: 10.1155/2022/7532532.

33. K.V. Bhadane, Saurabh Jain, Neelu J. Ahuja, Shrikant Pullipeti, "Blockchain and autonomous Vehicle: Recent Advances and Future Directions", September 2021, DOI: 10.1109/ACCESS.2021.3113649.

34. K.V. Bhadane, Bassem Khan, Mohan P. Thakre, "A Compromising Study on Modernization of Electric Vehicle Sub System, Challenges, Opportunities & Strategies for its Further Development", Jan. 2021, DOI: 10.1109/ICNTE51185.2021.9487757.

Environmental Impact Assessment of A Self Sustained Deep Burial Pit Design for Safe Sanitary Pad Disposal

Abani Kumar Nayak
M.Tech Scholar
Dept. of Environmental Engineering
Gandhi Institute for Technology (GIFT), Autonomous
Bhubaneswar, Odisha

Amar Kumar Das
Professor
Gandhi Institute for Technology (GIFT), Autonomous
Bhubaneswar, Odisha
✉ amar.das120@gmail.com

S M Ali
Director General
Solar energy society of India, New Delhi

ABSTRACT

Menstrual hygiene management remains a significant challenge, especially in rural and underserved areas where access to sanitary products and proper disposal methods is limited. Traditional disposal practices, such as flushing sanitary pads down toilets or throwing them in domestic waste, lead to environmental pollution, public health hazards, and infrastructure blockages. This study evaluates the environmental impact of a self-sustained sanitation system utilizing deep burial pit technology for the disposal of sanitary pads. In rural and underserved areas, inadequate menstrual hygiene management is a significant issue due to limited access to sanitary products and proper disposal methods. Traditional disposal methods often lead to environmental pollution and health hazards. The deep burial pit technology offers a sustainable solution by reducing waste and preventing blockages in public sanitation systems. Through a comprehensive environmental impact assessment, the study examines the effectiveness of this technology in minimizing pollution, managing waste, and promoting public health. The assessment includes a life cycle analysis to measure environmental benefits and potential risks. The findings highlight the advantages of using deep burial pits for sanitary pad disposal in enhancing menstrual hygiene management, protecting the environment, and improving the quality of life for women and girls in rural areas.

KEYWORDS *: Menstrual hygiene, sanitary pads, deep burial pit, waste management*

INTRODUCTION

Effective menstrual hygiene management (MHM) is a critical aspect of public health and environmental sustainability. In rural and underserved areas, limited access to sanitary products and inadequate disposal methods pose significant challenges. Public health conditions in rural areas, particularly in schools and hostels, are facing serious challenges due to inadequate waste disposal systems. Both biodegradable and non-biodegradable wastes, if not properly managed, pose significant health risks. This highlights the urgent need for effective waste management solutions to ensure the health and well-being of communities in rural areas. Proper disposal practices are crucial to maintaining hygienic and safe environments. Needs and requirements of the adolescent girls and women are ignored despite the fact that there are major developments in the area of water and sanitation. Women manage menstruation differently when they are at home or outside; at homes, they dispose of menstrual products in domestic wastes and in public toilets and they flush them in the toilets without knowing the consequences of choking. So, there should be a need to educate and make them aware about the environmental pollution and health hazards associated with them. The use of sanitary napkins is the most common method of menstrual hygiene management amongst women (Wagh et al., 2018). Disposable sanitary pads have the highest consumption

levels, especially in urban regions of India (Wagh et al., 2018) and also come with it the challenges of its safe disposal.

Deep burial pit technology offers a self-sustained and environmentally friendly solution for sanitary pad disposal. This method involves the use of specially designed pits that facilitate the decomposition of sanitary waste, thereby mitigating environmental pollution and enhancing public health. Unfortunately, due to lack of knowledge on menstruation preparedness and management or due to shyness and embarrassment the situation becomes worse for girls [5]. Menstruation is a natural process but it is still a taboo in Indian society as it is considered unclean and dirty [6].

The main objective of this paper is to explore the concern and possible methods of menstrual waste management in low-income countries. The article was aimed at understanding the menstrual practices, product design, demands, and disposal strategies. It includes both a summary of the existing menstrual hygiene needs and management and also an analysis of the current knowledge in the fields of public health, water and sanitation, and solid waste management.

OBJECTIVE OF THE STUDY

i. The main objective of this research is to design a smart sanitary napkin disposal system, which could be used to reduce the problem of disposing of sanitary wastes.

ii. To reduce spread of infection due to unhygienic disposal of sanitary napkins, reduce environmental pollution and clogging of public drainage system due to spongy nature of napkins.

CONSTRUCTIONAL FEATURES

Design of Deep Burial Pit

The design of a deep burial pit for sanitary pad disposal involves several key considerations to ensure effective waste management and environmental protection:

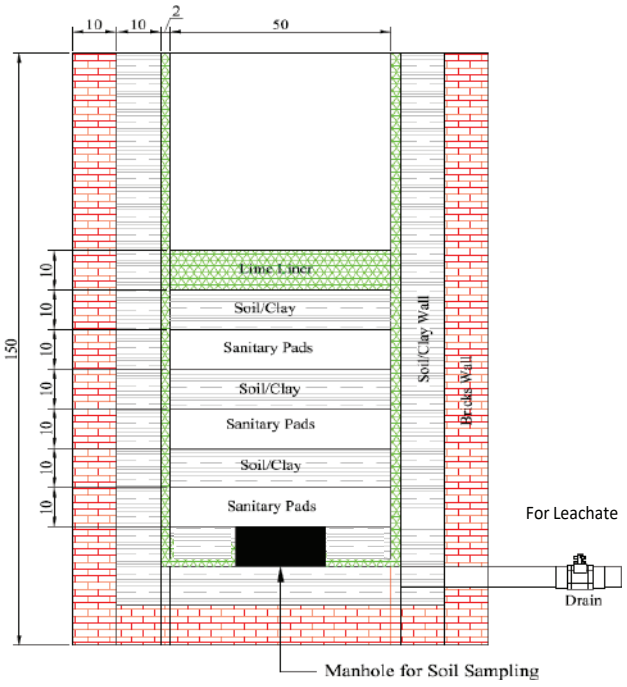

Fig. 1 (a) Typical deep pit designs

Implementing these design elements can help create a safe, efficient, and environmentally friendly solution for sanitary pad disposal in rural areas. The structure should be made above the ground using either Brick (Clay or Cement) or reinforced Clay Structure as shown in Figure 1.

Fig. 1 (b) deep pit design for sanitary pads

Materials Needed

- Concrete rings or blocks
- Plastic sheeting or clay for lining
- Reinforced concrete or heavy-duty plastic for the cover
- Gravel for drainage
- Ventilation pipe

Construction Procedures

- Excavation: Dig a pit with a depth of 2-3 meters and a diameter of 1 meter.
- Lining: Line the pit with impermeable materials (concrete rings/blocks and plastic sheeting or compacted clay).
- Drainage Layer: Add a layer of gravel at the bottom of the pit for drainage.
- Ventilation Pipe: Install a ventilation pipe to reduce odor.
- Cover: Construct a secure, easy-to-use cover for the pit.
- Signage: Place clear signage instructing proper disposal practices

Table 1 Menstrual waste disposal practices in India

Disposal practices of sanitary pads	Challenges
Throw with routine waste/ dustbin	Unsegregated menstrual waste enters the solid waste stream and is subject to the same treatment as other solid waste – placed in landfills to disintegrate over hundreds of years
Thrown away in the open (open spaces, rivers, lakes, wells, roadside reusable	Menstrual waste can contaminate water sources, clog drains and sewerage systems
Cloth pads, Hybrid pads (with non cloth barrier) and Menstrual Cups	Sanitary pads and panty liners with non compostable raw materials like plastic barriers, super absorbent polymers etc.
Hygienic use requires care and maintenance	One time use with compostable absorbent layer typically sealed within non compostable layers

Design of pit chamber

For designing the primary chamber, initially volume of the chamber is to be found out. For finding out the volume 100kg of wastes is dumped as a heap and the volume of the volume of the heap is considered.

Volume of the heap = $5m^3$

Assuming a suitable depth of 2.2m, we can find out the area of the chamber

Area = v/depth = 5/2.2 = $2.3m^2$

Assume length and breadth as 1.5:1

Therefore, L/B =1.5/1 L =1.5B

Dimensions of the primary chamber = L*B*H

Therefore A = L*B 2.3 = 1.5B*B 2.3 = 1.5B2 B = 1.238m L = 1.857

RESULTS AND DISCUSSIONS

Waste Generation

A survey in the local area has revealed that 166 kg of sanitary napkin waste is produced daily as shown in Table 2. This waste comes from 24 colleges, 18 schools, 20 offices, and 35 housing colonies and apartments. The disposal of sanitary napkins is a significant issue, as current practices, which involve developing waste processing and disposal facilities, contribute to environmental and soil pollution. Therefore, it is crucial to implement more sustainable and eco-friendly waste management solutions to address this growing problem.

Table 2 Quantity of Waste Generation

Sl. No.	Types of Establishments	No of Establishments	Volume of waste generation/ day
1	Institutions/ Universities	24	60 kg
2	Schools	18	42kg
3	Offices	20	7 kg
4	Apartments	15	27 kg
5	Housing colony	20	30 kg

Effectiveness of deep burial Pit system

The deep burial pits successfully contained the sanitary pad waste, with no significant leakage observed, thanks to the impermeable lining of concrete and plastic sheeting. Regular monitoring showed minimal contamination of surrounding soil and groundwater, validating the effectiveness of the pit design.

- Reduction in Environmental Impact: The decentralized nature of the pits distributed waste disposal sites, reducing the load on central facility and mitigating its environmental footprint.
- Measurements indicated a significant drop in soil and water pollution levels in comparison to previous centralized disposal methods.
- Improved Hygiene and Accessibility: Sanitary conditions in the disposal areas improved, with fewer instances of pest infestations and odor issues due to the secure covers and ventilation pipes.
- Accessibility for users was enhanced by strategically locating the pits close to high waste-generating sites such as schools, colleges, and residential colonies.

CONCLUSION

The purpose of our job is to keep environment clean by means sanitary napkin disposal method, we also should provide solution to dispose sanitary napkin and steer clear of present ways of disposal such as sanitary napkins are blended with regular trash, and it isn't easy to distinguish them and remove off them. The deep burial pit, designed for sanitary napkin waste disposal in Bhubaneswar Municipality, offers a safe and environmentally friendly solution. Constructed with a depth of 2-3 meters and a diameter of 1 meter, the pit is lined with impermeable materials to prevent contamination. A gravel layer ensures proper drainage, while a secure cover and ventilation pipe minimize odors and pest access. This decentralized approach reduces the burden on centralized facilities, lowers environmental impact, and provides a hygienic disposal method for the 166 kg of sanitary napkin waste produced daily, enhancing overall community health and sustainability. With proper implementation and community involvement, this method offers a viable and sustainable solution for sanitary waste management.

REFERENCES

1. S. Nagar and K. R. Aimol, "Knowledge of Adolescent GirlsRegarding Menstruation in Tribal Areas of Meghalaya," Studies of Tribes and Tribals, vol. 8, no. 1, pp. 27–30, 2017.
2. A. Dasgupta and M. Sarkar, "Menstrual hygiene: how hygienicis the adolescent girl?" Indian Journal of Community Medicine,vol. 33, no. 2, pp. 77–80, 2008
3. Rutuja Kulkarni, Rajnandini Lohar, Neha Wani(2008) Sanitary Napkin's Disposal System" International Journal for Scientific Research & Development, 4(4), pp.1142-1144.
4. Chourasia Sandhya Bhagawat, Tambolishabanam, Mali Satish & Jamdadeamar(2019) Manufacturing of Cost Efficient Sanitary Napkins Incinerator Machine, International Journal of Mechanical and Production Engineering Research and Development, 9(3), pp.803-812.
5. Linda Scott, Paul Montgomery, Laurel Stinfielt, Catherine Dolan(2013)Sanitary Pad Acceptability and Sustainability Study, University of Oxford, pp.06-09. Journal of Xi'an University of Architecture & Technology Volume XII, Issue III, 2020 Issn No : 1006-7930

High Voltage Gain for EV Application with Soft Switching Multiphase Interleaved Boost Converter

Shweta Bandre
PG Scholar
Department of Electrical Engineering
Tulsiramji Gaikwad Patil College of Engg. and Tech.
Nagpur, Maharashtra
✉ 03shwetabandre@gmail.com

Pratik Ghutke
Assistant Professor
Department of Electrical Engineering
Tulsiramji Gaikwad Patil College of Engg. and Tech.
Nagpur, Maharashtra

ABSTRACT

Because coal and petrol have stricter emission regulations, the automobile industry is seeing an increase in the use of fuel cell electric automobiles or FCEVs. In this architecture, a 1.26 kW artificial network-based predominant feature presenting tracking (MPPT) controllers is suggested as a means of improving these vehicles' performance. Using a DC-to-DC energy conversion unit, this controller is made to maximise the surface transmembrane of a proton exchange membranes fuel cell (PEMFC), supplying electricity for electric cars. The suggested MPPT guarantees effective energy conversion by utilising maximal power point tracker (MPPT) and radial basis functions network (RBFN). High switching frequencies and effective DC conversion are necessary for FCEVs to continue operating. In order to accomplish this, the FCEV system integrates a three-phase alternative energy converter (IBC). Alternating voltage is used in semiconductor electrical circuits to provide voltage control. Using a MATLAB/Simulink platform, the end-to-end RBFN of the FCEV system is when juxtaposed with fuzzy logic controllers (FLCs) to assess its efficiency.

KEYWORDS *: Fuel cell electric vehicle, High voltage gain IBC, PEMFC, MPPT, RBFN etc.*

INTRODUCTION

Concerns about the environment and the depletion of fossil fuels have caused the automotive industry to become increasingly interested in electric cars, namely Fuel Cell electric vehicle (FCEVs). Fuel cells and power electronics have quickly advanced, generating attention due to their many benefits, which include excellent performance, longevity, low noise levels, plus the production of new energy. The fuel cells powering this breakthrough were solid oxygen fuel cell (SOFC), molten carbonate fuel cell (MCFC), alkaline substance energy cell (AFC), phosphoric acid fuel cell (PAFC), the fuel cell with proton-exchange membrane (PEMFC). PEMFCs in particular have attracted a lot of interest from the automotive sector because to their quick starting times and effective operation in both cold and warm environments.

Fuel Cells

- The automotive industry is becoming increasingly interested in electric vehicles when fossil fuels runs out to environmental concerns gain hold.
- The capacity to produce clean electricity, high dependability, great efficiency, and low sound levels are just a few benefits of fuel cells.
- PEMFCs are highly favoured by the vehicle industry because of their low operating temperatures and rapid startup times.

MPPT

- Making simple, popular, and user-friendly usage of MPPT P&O algorithms. P&O and project management methods offer fluctuations in the steady state, that might be a factor in the limited efficacy of mobile systems.

- In order to address this issue, a model utilising logic controllers and neural network techniques is then presented for determining the correctness and efficiency of the MPPT.
- The non-isolated, high-voltage intermittent enhances converter (IBC) lets you select a lower switching magnitude and increased voltage gain in electric and portable devices, is the foundation of PEMFC MPPT Tracking.

It is based on the radial basic function network (RBFN) and MPPT control foundation. The goal of criminal activity is to boost the dependability of mobile devices, which is currently quite high. The car's power inverter supplies the output voltage from the voltage converter for the motor. The engine of the FCEV carries out this duty. The engine states that the cost and dimensions of the cell are extraordinarily low.

FUEL CELL APPLICATIONS WITH ELECTRIC CAR CHARGING

Fuel-cell electric vehicles, or FCEVs for short, generate energy not just from a battery but also from a hydrogen-powered fuel cell. The power of the FCEV is determined throughout the car's design process by the size of its electric motor or motors, which take power from both sides if the fuel cell or battery. The bulk of FCEVs rely on batteries for regenerative braking, additional power during moments of low acceleration, and attaching or detaching the fuel cell as needed. However, some FCEVs may be able to charge their batteries via a plug. In contrast to all-electric vehicles, where battery capacity primarily determines power and range, the size of the hydrogen fuel tanks determines how much energy is stored inside the automobile.

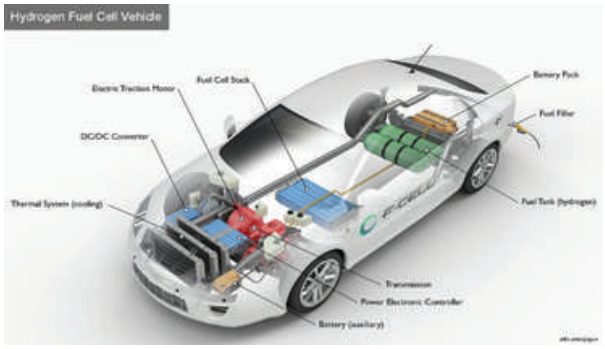

Fig. 1. Fuel Cell Vehicle

Fuel cell electric vehicles (FCEVs) function similarly to electric cars by using hydrogen stored in tanks to power fuel cells. The environment is protected by FCEVs as they produce no exhaust pollutants when compared to traditional internal combustion engine vehicles. Fueled by pure hydrogen stored in tanks, FCEVs have a range of over 300 miles, which is comparable to that found in traditional automobiles, and can be refueled in a matter of minutes. They also employ state-of-the-art technologies such as regenerative braking buildings, which boost efficiency by recovering and storing energy consumed during braking. Leading automakers are introducing FCEVs to select regions in an attempt to boost uptake and construct infrastructure, which will enhance energy security and boost the economy.

EXISTING SYSTEM

An FCEV's wheelwork structure is shown in Figure 2. Low DC voltage produced by the PEMFC stack is uncontrollable. To control and boost the PEMFC output voltage, one needs a step-up or raise DC to DC converter.

One recommended method for achieving high voltage gain is to use the quadratic boosted converters, that are made up of two boost converters. However, using two boost converters could reduce the system's efficiency. Alternatively, a two-stage flexible conversion featuring DC-DC isolation is typically recommended. But this design is still less dependable and efficient.

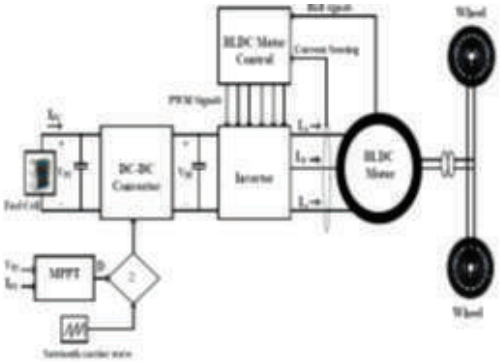

Fig 2. Traditional design of an electric car powered by a BLDC motor supplied by a cell

Disadvantages Of Existing Configuration :

- Unreliability
- Much lower level of output.

- Expensive
- Because of its limited contemporary management capabilities & thermal control difficulties, the upgraded converter is appropriate with greater power packages, while the obsolete boost converter is employed as a power digital link for small-scale use.
- To overcome the benefits of changing voltage that come with dc-dc facts.

PROPOSED CONFIGURATION WORK

Three single-phase intermittent boost converters (IBC) will be used in this project in order to maximise voltage gains, lower switching losses, provide high voltage acquisition, and efficiently transfer power. By using this strategy, fuel cell dependability is increased and sufficient power is provided to operate the suggested FCEV system.

A BLDC motor, a voltage supply inverter (VSI), a three-phase electrical power supply (IBC), and a 1.26 kW PEMFC make up the FCEV system. To ensure effective power transfer, the VSI or PEMFC are connected in the third stage of the IBC.

Fuel cell power supply is optimised by the application of a radial basis function networking (RBFN) based methodology. Power transmission to a BLDC motor via the VSI is facilitated by the I-3-phase IBC, and the VSI conversion is managed by the circuitry of the BLDC motor. The vehicle is propelled by the motor, which is fixed on the wheels.

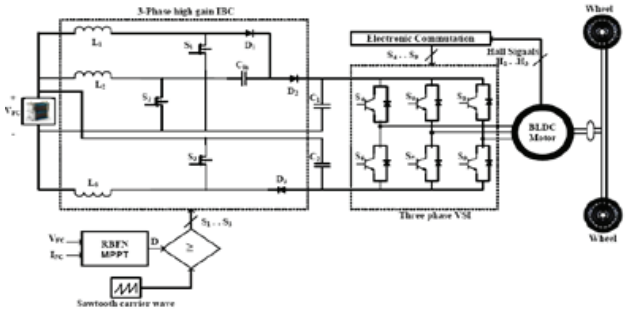

Fig. 3. A BLDC motor powers the proposed three-phase, high-voltage increase IBC FCEV system

Benefits Of The Suggested Configuration

1. Production of clean energy
2. Excellent dependability
3. Exceptional efficacy
4. Quiet operation
5. Elevated voltage gain.

Applications

1. Uses for fuel cells
2. Applications of solar electricity.

FUEL CELL MODELING

Hydrogen fuel is used in fuel cell engines, which are electrochemical devices that generate energy. The fuel the cell's input are fuel, air, & chemical reactions; its outputs are water and energy. A single fuel cells consists of an electrolyte and a fuel source. Ions from the hydrogen-based fuel are separated by the electrolyte, independent of charge. An electrolyte that has hydrogen and oxygen added to it produces energy at the cell's output. The biological process's scattering fuel cells only produces heat and water.

Table 1. 1.26kW PEMFC parameter specifications

Parameter Description	Rating
Maximum power (P_{max})	1.26 kW
Maximum current (I_{max})	52 A
Maximum voltage (V_{max})	24.23 V
Temperature (T)	55°C
Number of cells	42
Nominal air flow rate	2400 lpm

Formulation

An electrochemical apparatus that uses hydrogen fuel to create energy is called a fuel cell. Fuel and air are fed into the fuel cell, where they undergo chemical conversion to produce water and power. The PEMFC's cell voltage is provided as,

$$V_{FC} = E_{Nernst} - V_{act} - V_{ohm} - V_{con} \quad (1)$$

where Nernst, It is also known as the reversible thermodynamic voltage or open-circuit voltage,

$$V_{FC} = E_{Nernst} - V_{act} - V_{ohm} - V_{con} + 4.308 \times 10^{-5} T\left(\ln(P_{H2}) + 0.5\ln(P_{O2})\right)$$

Voltage of activation The term for Vact is as follows: T is the degree Celsius in the absolute sense (K), Vact is high voltage caused by the combined activation of the anode and cathode, and PO2 or PH2 are the partial pressures of oxygen and hydrogen in surroundings (atm), respectively,

$$V_{act} = -[\delta_1 + \delta_2 T + \delta_3 Thn(C_{O2}) + \delta_4 Thn(I_{FC})]$$

Where

The following equation is used to compute the dissolved oxygen content, or CO2, at the liquid/gas interface, where i (i = 1, 2, 3, 4) is an empirical factor for each cell,

$$C_{O2} = \frac{P_{O2}}{(5.08 \times 10^6) \times exp(-498/T)}$$

Ohmic over voltage Vohm is expressed as

$$V_{ohm} = I_{FC}(R_C + R_M)$$

Using RC is a constant, where RC is the proton the resistance and RM is the electron flow that represents resistance.

HIGH VOLTAGE GAIN, THREE-PHASE IBC

When assessing the IBC voltage evaluation, the following factors are taken into account: Three switches and a total of three (D1, D2, and D3) make up the suggested converter. (S1, S2, and S3). L1, L2, and L3 stand for phase 2, phase 3, and class 1 filters, respectively. The load connection is shown by R, the output power is shown by VO, and the input volume is indicated by VFC.

Mode-1 ($t_0 \leq t \leq t_1$):

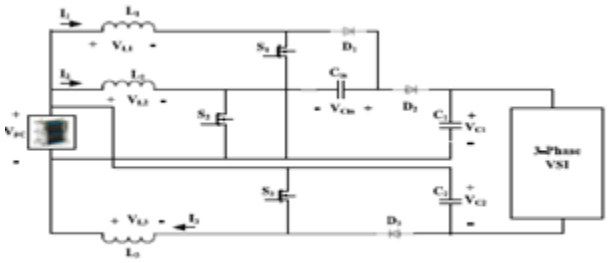

(a)

As seen in Fig. 4(a), all three evolves (S1, S2, before S3) are now operational, and all the three diode pairs (D1, D2, and D3) are reversed. The VFC supply to support input is made up of three inductive devices: L1, L2, and L3. As of right now, the three currents are rising in line with the (VFC / L) gradient. Neither the supply nor the load are connected to the input capacitor. There is a slope voltage drop across the load's resistor-powering capacitors that output C1 and C2 (VC1 and VC2), (-VO/RC).

Mode-2 ($t_1 \leq t \leq t_2$):

The S2 switch is turned on in this setup, and the S1 and S3 switches are off. As seen in Fig. 4(b), diode D2 has a reverse bias while diodes D1 and D 3 conduct forward current. The inductors L1 while L3 both experience current flow, with the former having a tendency to travel into (VFC-VCin) / L while the other in (VFC-VC2) / L. On the other hand, inductor L2's current rises with an angle of (VFC / L). capacitors C2 & Cine load the VFC input current, whereas Capacitor C1 powers the loads.

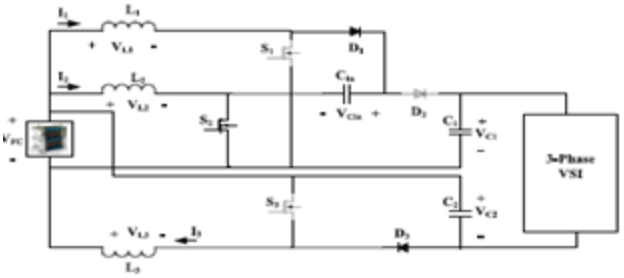

(b)

The S2 switch is turned on in this setup, and the S1 and S3 switches are off. As seen in Fig. 4(b), diode D2 has a reverse bias while diodes D1 and D 3 conduct forward current. The inductors L1 while L3 both experience current flow, with the former having a tendency to travel into (VFC-VCin) / L while the other in (VFC-VC2) / L. On the other hand, inductor L2's current rises with an angle of (VFC / L). capacitors C2 & Cine load the VFC input current, whereas Capacitor C1 powers the loads.

Mode-3 ($t_3 \leq t \leq t_4$):

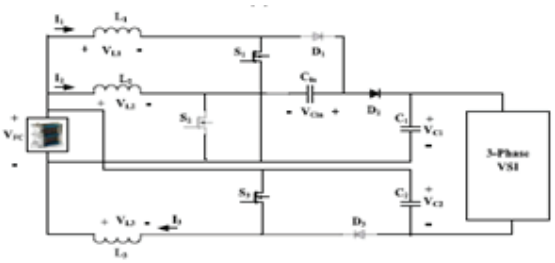

(c)

Mode-1 and this mode are comparable. S1, S2, and S3 are the three switches that are all ON, while D1, D2, and D3 are the three diodes that are all off.

SIMULATION DESIGN AND ITS OUTPUT

With MATLAB/Simulink, the suggested BLDC motor-driven FCEV design's performance is assessed. The quick temperature variations of the fuel cell have been taken into account in the examination of the FCEV system's adaptability to change: T = 320^K = 0 to 0.3 seconds, T = 310^K = 0.3 seconds to 0.6 minutes, and T = 330^K = 0.6 seconds to 0.9 seconds are the timespans for which these values apply.

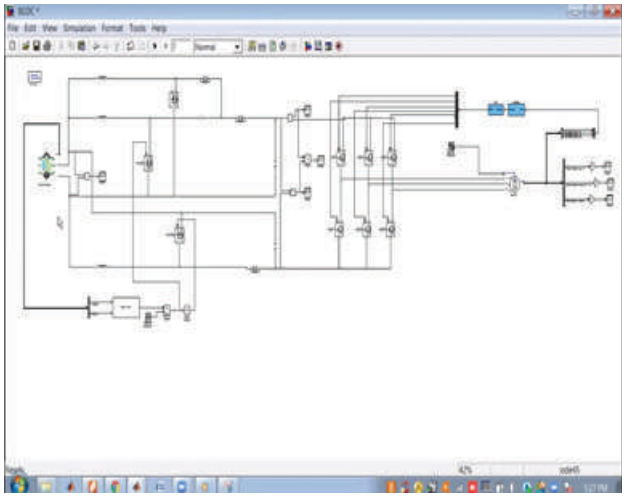

Fig 5. Simulation Architecture of proposed system

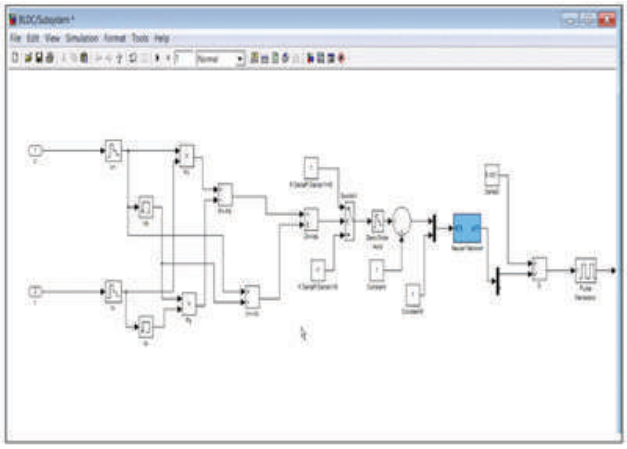

Fig 6. Neural network based MPPT Algorithm

T = 320 K for 0–0.3 sec,

T = 310 K for 0.3–0.6 sec, and

T = 330 K for 0.6–0.9 sec are the times during which these temperatures occur.

The fuel cell generates 970W over 0.3Wec to 0.6W, 0.9Wec over 1220W for 0.6 seconds, and 1080W over 0 to 0.3 seconds.

The DC Link connects voltage, power, with current via FLC based MPPT technology. It produces 1000W, 830W, or 1150W of power at 320 K, 310 K, or 330 K, respectively. Figure 8 uses the suggested RBFN-based MPPT controller to display the power, voltage, additionally power output of the DC connection. This suggested controller delivers 1200W at 330 K and 1050W at 320 K.

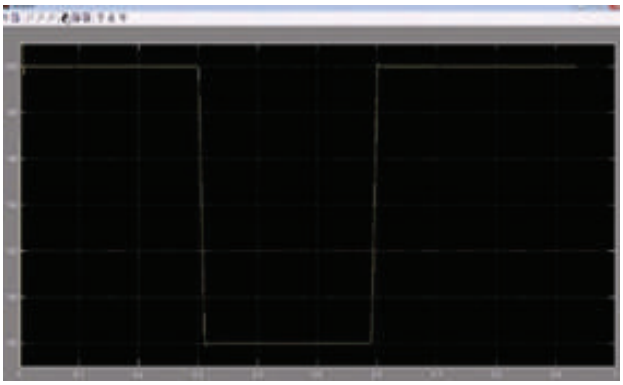

Fig. 7. Output voltage of Fuel Cell

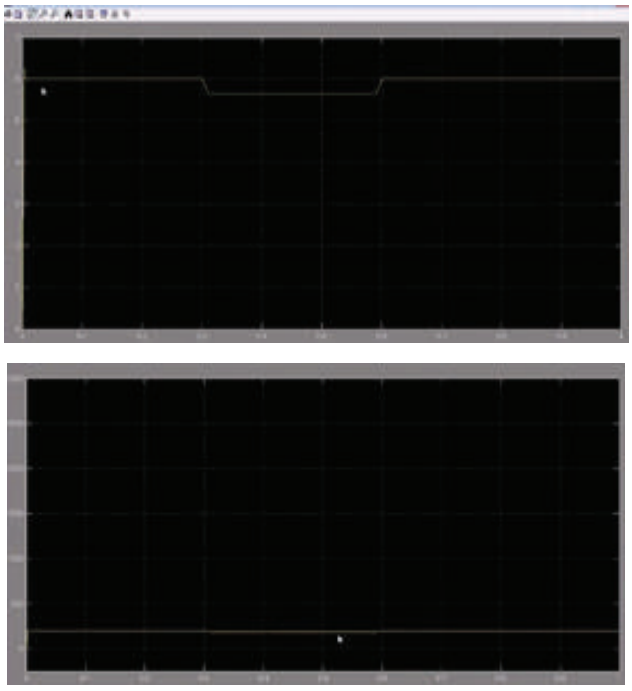

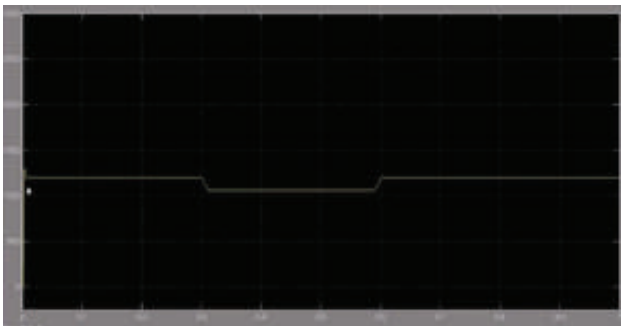

Fig. 8. Using RBFN, DC link output power, current, and voltage at various temperatures

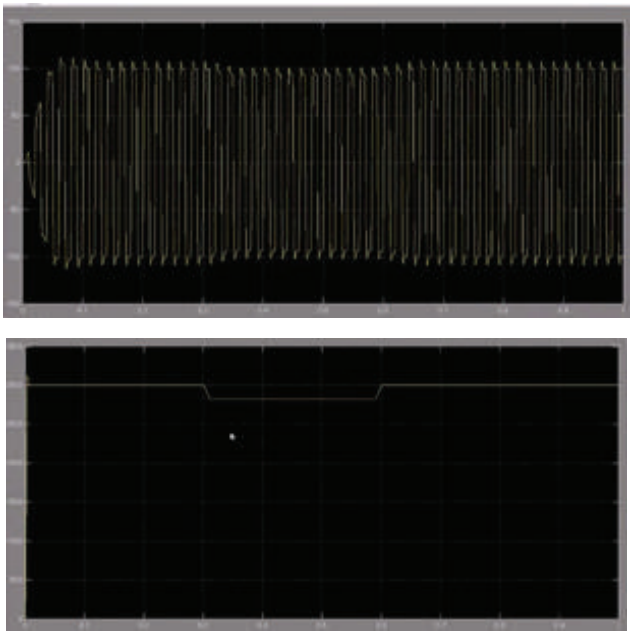

Fig. 9: BLDC motor Power, Torque, Speed parameters

The fuel cell displays the BLDC motor's temperature-dependent starting and steady-state capabilities. Figure 8 shows that the suggested controller outperforms the FLC in terms of DC link power. Additionally, a comparison of RBFN and FLC controllers is shown in the table.

Figure 9 shows motor parameters including stator power (ISA), back electrical magnetic field (E), electric torque (TE), or load force (TL) under fuel cell variable temperature settings. The BLDC motor runs in three different speeds: 0 to 0.3 seconds on 3300 rpm, 0.3 through 0.6 minutes at 2400 rpm, then 0.6 through 0.9 seconds on 3700 rpm. This variation in speed has no effect on the torque of the BLDC motor.

Parameter	1.26 kW PEMFC with fuzzy based MPPT			1.26 kW PEMFC with RBFN based MPPT		
Period (sec)	0 to 0.3	0.3 to 0.6	0.6 to 0.9	0 to 0.3	0.3 to 0.6	0.6 to 0.9
Fuel cell temperature (°K)	320	310	330	320	310	330
DC link current (A)	4.71	4.3	5.1	4.8	4.4	5.21
DC link voltage (V)	212	193	225	220	205	230
DC link power (W)	1000	830	1150	1050	900	1200

CONCLUSION

This study presents a high-gain DC for direct current (DC) with three phases of power that was specifically designed for fuel cell powered electric cars. (FCEV) software applications. Its main objectives are to reduce fuel cell current-injection implications and voltage stress for electricity semiconductor products switches. A membrane-based fuel-cell technology (PEMFC) system with a 1.26 kW proton transfer capacity is one of the configurations that is included. In particular, a Radial Basis Function Networks (RBFN)-based maximum power point tracking system (MPPT) system has been created. This MPPT technique optimizes fuel cell production of power at various operating temperatures.

We present an analysis and comparisons of the conventional Fuzzy Logic The control unit (FLC) the MPPT controller and the proposed RBFN-based MPPT controller. The simulation results demonstrate the RBFN-based MPPT device controller outperforms its FLC equivalent in terms of evaluation the maximum power limit more quickly and accurately.

Numerous performance parameters for a Brushless DC (BLDC) motor are also examined in the study, such as electromagnetic torque, speed, and the return electromotive force (EMF), across a range of operating settings that correlate to varied fuel cell system temperatures.

REFERENCES

1. Bharath.K.,Shishir K Jain, KottamVarun, Ramakrishna N. "Economic Analysis of Hyderabad Metro Rail Project". International Journal of Technology , July – December, 2015; Vol. 5: Issue 2, 297-303

2. Detailed Project Report for Pune metro, prepared by Delhi Metro Rail Corporation Ltd.,2009

3. D.Goel and S.Gupta, "The effect of metro rail on air pollution in Delhi.", Centre for Development Economics, 2014

4. J.C.Golias, "Analysis of traffic corridor impacts from the introduction of the new Athens Metro System", Journal of Transport Geography, June 2002;Vol. 10, Issue 2, 91-97.

5. K.Chakraborty and T.G.Sitharam, "A methodology to evaluate socio-economic impact of metro railway stations of Bangalore: from dwellers perspective report." IISC Bangalore (March 2013)

6. K.M. Neware (2018), "Impact of Nagpur metro on other transportation modes in terms of fuel consumption parameters." IJIES, 2018, Vol. 3, No.4, 2018

7. M.N.Murty, K.Dhavala, M.Ghosh and R.Singh,"Social Cost-Benefit Analysis of Delhi Metro", Institute of Economy Growth, Delhi, 2007, MPRA Paper No. 1658.

8. N.Sharma, A.Singh, R.Dhyani and S.Gaur), "Emission reduction from MRTS projects- A case study of Delhi metro", Atmospheric Pollution Research, 2014, Vol. 5, Issue 4, 721-728.

9. P. Chib, "Optimization of Pune Metro Rail", IJETT, 2014, Vol.17.297-304.

10. Report on Environmental impact assessment study for Ahemdabad metro rail project.

11. S. Nikfalazar, M.Amiri and H.A.Khorshidi , "Social impact assessment on metro development with a case study in Eastern District of Tehran", International Journal of Society Systems Science, 2014, Vol.6, Issue 3.

12. G.Tiwari, "Metro systems in India: Case study DMRC, promoting low carbon transport in India." UNEP, 2014.

13. W N Deulkar and A F Shaikh, " Pune metro rail project: A review", IJSCER, 2015, Vol. 4, No. 1

14. C R Kothari and G. Garg, "RESEARCH METHODOLOGY: Methods and techniques (Third edition)." New Age Internationals Publishers, 2016.

15. Lin, Boqiang, and Zhili Du. "Can urban rail transit curb automobile energy consumption?." Energy Policy 105 (2017): 120-127.

16. Shirke, Chatrali, et al. "Transit Oriented Development and Its Impact on Level of Service of Roads & METRO: A Case Study of Mumbai Metro Line-I." Transportation Research Procedia 25 (2017): 3039-3058.

17. Andrade, Carlos Eduardo Sanches de, and Márcio de Almeida D'Agosto. "The role of rail transit systems in reducing energy and carbon dioxide emissions: The case of the city of Rio de Janeiro." Sustainability 8.2 (2016): 150.

18. Doll, Christopher NH, and Osman Balaban. "A methodology for evaluating environmental co-benefits in the transport sector: application to the Delhi metro." Journal of Cleaner Production 58 (2013): 61-73.

19. Sharma, Niraj, et al. "Emission reduction from MRTS projects–a case study of Delhi metro." Atmospheric Pollution Research 5.4 (2014): 721-728.

20. Khanna, Prachi, et al. "Impact of increasing mass transit share on energy use and emissions from transport sector for National Capital Territory of Delhi." Transportation Research Part D: Transport and Environment 16.1 (2011): 65-72

Advanced Technology Strategies for Optimized Safety Management in Steel Industry

Soumendra Kumar Mishra
M. Tech Scholar
Department of Industrial Safety Engineering
Gandhi Institute For Technology (GIFT), Autonomous
Bhubaneswar, Odisha

Amar Kumar Das
Professor
Dept. of Mechanical Engineering
Gandhi Institute For Technology (GIFT), Autonomous
Bhubaneswar, Odisha
✉ amar.das120@gmail.com

S M Ali
Director, General
Solar Energy Society of India
New Delhi

ABSTRACT

The research aimed to develop and validate a system of safety management practices, assessing their impact on accident rates and exploring their effectiveness through worker engagement. Surveys of safety managers, supervisors, and employees linked safety practices, employee perceptions, and safety outcomes. Key findings include significant negative relationships between the presence of safety practices and accident rates, and between safety-focused worker engagement and accident rates. Both safety management systems and worker engagement levels independently predict accident rates, with engagement mediating the relationship between safety practices and outcomes. The study concludes that while implementing safety practices is crucial for reducing accidents, their effectiveness is greatly enhanced when combined with strategies fostering worker engagement. Data were collected using safety manager, supervisor and employee surveys designed to assess and link safety management system practices, employee perceptions resulting from existing practices, and safety performance outcomes. The study recommends the organizations to invest in safety management systems that not only establish robust practices but also actively engage workers to achieve optimal safety performance.

KEYWORDS *: Safety management practices, Steel industries, Risk assessment, Hazard identification, Safety training.*

INTRODUCTION

The steel industry is a cornerstone of industrial economies, producing essential materials for construction, automotive, and numerous other sectors. However, it is also one of the most hazardous industries due to the inherent risks associated with high-temperature operations, heavy machinery, and the handling of molten metals. Safety in the steel industry is crucial not only to protect workers but also to ensure uninterrupted production and compliance with regulatory standards [1]. Our country is the second largest manufacturer of crude steel and the manufacturer of iron all over this world. It is noted that the industries that produces steel and iron contributes about two percentage of the Gross Domestic Product (GDP) [2]. Moreover, the steel industries in our country are internationally appreciated for their superior quality.

Occupational Safety and working conditions are comparatively ignored area by the Indian industry. Iron and Steel industry in India lags its global peers on the safety performance parameter. Most of the Indian iron and steel industries do not have a correct safety management system comparable to global practices. It may be due to the fact that the nearly half of the manpower deployed in iron and steel industry are more susceptible to incidents as, they are unskilled, not so educated and unaware of the hazardous work environment.

Efforts for benchmarking by taking lessons from past failures and good practices from peer industry are limited to few organizations only. Steel manufacturing environments are hazardous, with various studies examining injury and fatality incidents and incident reporting. Krishnamurthy et al. (2017) emphasized the need for improved welfare facilities and physiological studies to protect workers from heat exposure in southern India[3]. Kim et al. (2019) highlighted that enhancing safety management systems can mitigate risks, protect workers, and improve operational efficiency and reputation[4]. Dash and Kjellstrom (2011) found that workplace heat stress poses significant health risks, decreases productivity, and reduces income[5]. Black (2012) stressed the role of healthcare professionals in occupational health through education and training[6]. Zubar et al. (2014) provided a comprehensive analysis of occupational health and safety management, focusing on protocols, accident statistics, employee motivation, leadership, training, hazard control, risk analysis, and monitoring practices[7]. Noweir et al. (2013) showed improvements in hazard exposure and medical services through walk-through surveys and detailed forms[8]. Majid et al. (2015) developed a prototype model to improve safety in process plants, particularly concerning contractor-related risks[9]. Satish et al. (2020) proposed technological strategies for achieving a zero-accident target in the steel industry [10]. Vivek et al. (2015) assessed risk mitigation in cold rolling mills, concluding that high-risk hazards can be reduced through effective safety measures [11]. Veltri et al. (2019) advocated for integrated safety, health, and environmental management systems to support lean enterprise outcomes [12].

The review highlights the use of diverse analysis techniques, from statistical analysis to case studies and thematic analysis, to study safety performance in industries. These approaches have allowed researchers to comprehensively assess safety practices, identify patterns, and understand underlying factors contributing to safety outcomes. The multidimensional nature of safety management underscores the importance of a holistic approach to address safety challenges. These analytical insights are valuable for policymakers, industry stakeholders, and safety professionals in enhancing safety practices, mitigating risks, and preventing industrial disasters.

OBJECTIVES

(i) To identify and characterize SM practices in both types of industries.

(ii) To develop and validate an instrument for measuring critical SM methods, facilitating a comprehensive assessment.

(iii) It intends to investigate the relationship between SM practices and accident rates in both certified and non-certified industries, shedding light on the effectiveness of different safety approaches.

(iv) To study the impact of system certification on SM practices specifically within steel industries, elucidating the role of certification in shaping safety protocols.

(v) To improve operational efficiency by integrating safety measures

METHODOLOGY

Approaches of Research Works

The methodology for the Steel Industry includes the following approaches;

- Exploration: Initial investigation into safety management practices across certified and non-certified sectors.
- Instrumentation: Development and validation of measurement tools for assessing critical safety methods.
- Comparative Analysis: Examination of safety practices' impact on accident rates in both certified and non-certified settings.
- Certification Influence: Evaluation of the effect of system certification on safety practices within the steel industry.
- Sub-component Identification: Identification and validation of specific elements contributing to safety performance.
- Synthesis: Integration of findings to provide comprehensive insights into safety management within the steel sector.

Stage-I

- Literature review on safety elements which are currently followed in steel industries.
- Visiting certified steel industries and studying on the various aspects of safety elements in certified steel industries.

Stage-II

- Explore the safety elements by conducting a groundwork assessment and deliberations with workers, line supervisors, safety experts and managers.
- Preparation of draft questionnaire containing 45 safety practices under 9 safety elements covering the all the aspects of safety.
- Conducting field survey in the certified and non certified steel industries located at Angul, Odisha state.

Fig. 1 Strategies for research methodology

In this work, nine major components are taken into consideration as shown in Figure 1 and each major component have five sub components that were taken into consideration. The data were collected from 200 respondents from certified and non certified steel industries.

Requirement of safety measures in different strategic points

In steel industries, safety measures are critical at various strategic points. In production areas, protective gear and regular equipment maintenance prevent accidents. In high-temperature zones, cooling systems and hydration stations are essential as shown in Figure 2. Storage areas require proper labeling and handling of hazardous materials. Transportation routes need clear signage and regular inspections. Emergency exits must be clearly marked and unobstructed. Implementing robust safety protocols, conducting regular training and continuous monitoring at these points ensure comprehensive safety, protecting workers and minimizing risks in the steel industry.

Fig. 2 (a) BOF Operation was monitored through a transparent glass window panel (b) PET strapping of coil (Source: Tataseel, Kalinganagar)

Procedures used for Collection of Data

The following procedure was used for collecting the data for the study. On site visit to each of the industries for the following purpose:

- Questionnaires were distributed to the respondents consisting of certified and non certified industries.
- Discussion was made with the line supervisors, safety officers, managers of the training departments.
- Questionnaire was distributed to the respondents of 1000 employees of certified industries and 1000 employees of non certified industries.
- The questionnaire was issued personally to all the employees.
- Data were collected from the safety departments of certified and non certified steel industries and data contains all the incidents or accident happened in the industries in the last two years. Those data were retrieved from the industries' log books, reports and safety analysis reports. Data contains type of accident, time of accident, losses due to accident, causes related to accident, degree of injury (minor / major) of injured employee and details of injured employee (skills, qualification, experience etc). In this analysis, there are two types of accidents such as minor accidents and major accidents which are classified in harmony with the degree of severity. 12 months took to collect the completed questionnaires from the respondents.

RESULTS AND DISCUSSION

Data Analysis

To analyze the safety management, the five safety management practices were considered and presented in Table 1. Table 1 shows that majority of the non certified Industries employees have opted disagree regarding safety organization. Certified industries were found to perform superior than NCI in terms of SM methods. On the other hand, external consultants and experts were not deputed to update with safety practices and protocols in certified industries. 94 employees out of 200 in certified industries, have opted disagree with respect to external consultants and experts update with safety practices and protocols. About 50% respondents are disagreeing which conveys that there seems to be a lack of safety performance in non certified industries. On the other hand only 18 % of employees have disagreed the statement in certified industries.

The results infer that there is a variation between the CI and NCI with respect to the five practices of the SM at 0.05 importance level. Hence, the null hypothesis Ho is not supported and indicates that there is variation between the groups in terms of the SM system. Thus, it can be concluded that certified industries have prominent practice of safety management system compared to non certified steel industries.

Table 1 Safety organization for non certified and certified steel industries

Sl. No.	Description	Non Certified Industries					Certified Industries				
		A	SA	N	PA	D	A	SA	N	PA	D
1	The safety organization is having well defined role and responsibilities.	12	10	14	34	131	50	20	28	48	56
2	The organization's safety initiatives are frequently updated and conveyed to employees	14	14	26	32	116	54	22	24	54	46
3	External consultants and experts update with safety practices and protocols	16	6	20	18	140	32	20	30	24	94
4	Exchange of the safety related ideas both within and between the departments	12	8	34	20	126	55	28	31	48	56
5	I personally contented with the safety act of the organization	14	10	40	35	101	78	34	22	30	36

From the survey, it can be learnt that incidents, near misses and accidents are not investigated as and when occurs to improve workplace health and safety in non certified industries. It is an important safety parameter which is area of concerned is not understood by the management of non certified industries. Moreover there is no regular meeting held among staff and administration regarding safety concerns in non certified industries. 122 respondents have denied the statement that there is periodical meeting held among staff and administration about safety related concerns in non certified industries. It implies bullying and harassment in the work place would show an impact on the safety and psychological health of the employees. This is reflected in both certified and non certified industries. Major accident is described in Table 2 as the fatality or lost time injury leading to hospitalization.

Table 2 Cause wise accident analysis

Sl. No.	Department	Incident causes	Certified Industries			
			No of Minor accidents	% of Minor accidents	No of Major accidents	% of Major accidents
1	Machine	Unguarded machinery	5	10.2	2	5.88
2	Machine	Pressed between objects	2	4.08	1	2.94

3	Material handling	Hit by falling objects	3	6.12	3	8.82
4	Casting	Hot metal burns	10	20.41	7	20.59
5	Casting	Extreme temperature	3	6.12	2	5.88

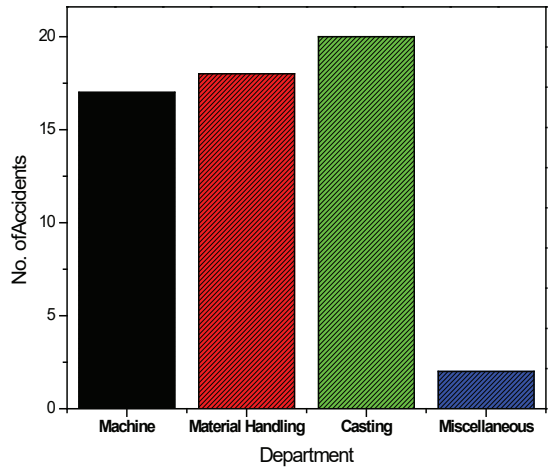

Fig. 3 Department wise Incident Statistics for Non Certified Industries

Department wise incident statistics for non certified industries is shown in Fig.3. It can be observed that 28 minor accidents occurred in machine division whereas 31 minor accidents occurred in material handling division. It can be noted that 37 number of accidents occurred in casting division in non certified industries. 9 minor accidents occurred due to the miscellaneous factors. Materials handling division is responsible for 18 major accidents. It can be observed that machine division is responsible for 17 major accidents. 20 major accidents happened in casting division. 2 major accidents occurred due to the miscellaneous factors.

CONCLUSION

This investigation on safety in steel industries yielded following several key findings;

- Certified steel industries demonstrate superior safety management practices and lower accident rates compared to their non-certified counterparts.
- Effective safety methods, including comprehensive training, clear communication, and strict enforcement of safety protocols, are essential in minimizing workplace incidents.
- A positive safety culture, supported by proactive leadership, significantly enhances safety performance. Continuous improvement through regular safety audits and feedback mechanisms is vital for maintaining high safety standards.
- Additionally, integrating advanced technologies such as real-time monitoring and virtual reality training can substantially improve safety training and management.
- It conveys that the safety rules are followed without exception in certified industries compared to non certified industries. It can be observed that the managers do not listen to the ideas and concerns of the workers in non certified 83 industries. Only 14% responders agreed in non certified industries. opportunities are not given for direct involvement in safety efforts and managers do not listen much to the ideas and concerns of the workers in non certified steel industries compared to certified industries.

REFERENCES

1. Di Benedetto, Almerinda, V. Di Sarli, and Paola Russo. "On the determination of the minimum ignition temperature for dust/air mixtures." Chemical Engineering Transactions 19 (2010): 189-194.
2. Marvel, Mary K. "Implementation and safety regulation: Variations in federal and state administration under OSHA." Administration & Society 14.1 (1982): 15-33.
3. Ardo, Shane, et al. "Pathways to electrochemical solar-hydrogen technologies." Energy & environmental science 11.10 (2018): 2768-2783.
4. Ahmed, Syed Shaheer Uddin, et al. "Harvesting solar energy: Fundamentals and applications." Sustainable utilization of natural resources. CRC Press, 2017. 381-416.
5. Margolis, Robert, et al. "Using GIS-based methods and lidar data to estimate rooftop solar technical potential in US cities." Environmental Research Letters 12.7 (2017): 074013.

6. Heylighen, F., & Joslyn, C. (2001). Cybernetics and second order cybernetics. Encyclopedia of physical science & technology, 4, 155-170.

7. Doctoral dissertation: Eindhoven University of Technology Kramer, E. H. (2007). Organizing doubt: grounded theory, army units and dealing with dynamic Complexity. Copenhagen Business School Press.

8. Kramer, E. H., de Waard, E. J., & de Graaff, M. C. (2012). Task Force Uruzgan and experimentation with organization design.

9. In R. Beeres, J. V. d. Meulen, J. M. M. L. Soeters & A. L. W. Vogelaar (Eds.), Mission Uruzgan. Amsterdam: Amsterdam University Press Kuipers, H., Amelsfoort, P., & Kramer, F. J. (2010). Het NieuweOrganiseren: alternatievenvoor de bureaucratie. The Hague: Acco. Luhmann, N. (1990). Essays on self-reference.

10. Columbia Univ Press. Luhmann, N. (1995). Social systems. Stanford University Press. Maturana, H. R. (1980). Autopoiesis and cognition: The realization of the living (Vol. 42): Springer.

11. M. Nayak, B.P. Bhol, L.K.Pani (2018). Attitude of workers towards safety management system in Rourkela Steel Plant:IJMER Vol-7,Issue10(1), 109-123

12. M. Nayak, B.P. Bhol, L.K.Pani (2017). Safety Job satisfaction of Employees working in Rourkela Steel Plant:IJMER Vol-6,Issue4(8), 34-47.

Dual Charging System for Electrical Vehicle

S N Jamadar
Assistant Professor
Yashoda Technical Campus, Satara, Maharashtra
✉ jamadarsuhani@gmail.com

ABSTRACT

This research explores the development and implementation of a dual battery electric vehicle (EV) system designed for continuous operation using both AC and solar power sources. The system automatically switches between two batteries, ensuring uninterrupted power supply while monitoring battery status. This innovative approach aims to reduce petroleum consumption and environmental pollution, providing a sustainable transportation solution. The study includes system modeling, development, and performance analysis, demonstrating the efficiency and reliability of the proposed EV system.

KEYWORDS *: Electric vehicles, Solar panel, Dual charging, BMS.*

INTRODUCTION

The transportation sector heavily relies on petroleum, contributing to environmental pollution and depleting fossil fuel reserves. Electric vehicles (EVs) offer a viable alternative, reducing greenhouse gas emissions and dependency on petroleum. However, conventional EVs face challenges such as limited battery life and long charging times. This research introduces a dual battery EV system with automatic changeover and status monitoring, utilizing solar and AC power sources. The system aims to enhance EV performance, reliability, and sustainability.

By combining the emission-free EV with the low carbon PV power generation, the problems related greenhouse gases due to the internal combustion engines can be reduced is discussed by Abdul Rauf Bhatti, Zainal Salam [1]. H.S. Das, M.M. Rahman [2] presents an evaluation on how the future EV development, such as connected vehicles, autonomous driving, and shared mobility, would affect EV grid integration as well as the development of the power grid moves toward future energy. Electric Vehicles are facing more problems due to the increased battery charging time, Jyoti M. Kharade[3]. provides the solution to reduce the charging time by incorporating a dual battery charging system. Soham Bhadra [4] proposed the charging station is powered by a combination of solar power and grid power. The system works in an integrated way to optimize the energy use from the grid. A. M. Alsomali [5] proposed a scenario of a shaded office parking with solar panels as power source is used to test the different strategy, simulation and experiment testing was successful and results showed this time-multiplexing method. Hossam A. Gabbar [6] discussed about safe BMS is the prerequisite for operating an electrical system how to be implemented. Muhammad Nizam [7] design a BMS with three main features: monitoring, balancing and protection. J. Garche and A. Jossen[8] presented at TELESCON 2000, addresses the crucial role of Battery Management Systems (BMS) in extending the operational lifespan of batteries used in various applications. Hamza Shafique[9] contributes to the field by offering a detailed analysis of EMS for BESS and providing a practical framework for its implementation. It addresses the challenges and solutions associated with integrating BESS into power systems for ancillary services, thereby supporting the transition to more sustainable and reliable energy systems. A Shahin [10] contributes to the fields of renewable energy and electric vehicle technology by providing a comprehensive framework for integrating RES with wireless charging systems. It highlights the potential benefits and addresses the technical challenges,

paving the way for more sustainable and efficient EV charging solutions.

SYSTEM MODELLING

The proposed dual battery EV system comprises several components, including batteries, a microcontroller, sensors, and a motor. The system's mathematical model is described by the following equations:

Battery Voltage Monitoring

$$V_{bat} = V_{max} - I_{load} \times R_{int} \quad (1)$$

Where

V_{bat} = the battery voltage

V_{max} = the maximum voltage

I_{load} = is the load current, and

R_{int} = the internal resistance.

This equation indicates that the battery voltage decreases as the load current increases, due to the voltage drop across the internal resistance of the battery. This helps in monitoring the battery's health and performance under different load conditions.

Battery Switching Criteria

$$\text{If } V_{bat1} < V_{threshold}, \text{ switch to battery 2} \quad (2)$$

$$\text{If } V_{bat2} < V_{threshold}, \text{ switch to battery 1} \quad (3)$$

These criteria ensure that the system switches between batteries to maintain an adequate power supply. When the voltage of the currently used battery drops below a predefined threshold ($V_{threshold}$), the system switches to the other battery. This helps in managing battery usage efficiently, preventing deep discharge and ensuring continuous operation.

Solar Power Generation

$$P_{solar} = \eta \times A \times G \quad (4)$$

Where

P_{solar} = the power generated

η = the efficiency

A = the area of the solar panel

G = the solar irradiance.

This equation calculates the power output of the solar panel based on its efficiency, area, and the available sunlight. It helps in estimating the energy that can be harnessed from the solar panel, which is crucial for planning the charging strategy and energy management.

Charging Time Calculation:

$$tcharge = Cbat/Icharge \quad (5)$$

Where

tcharget = the charging time

Cbat = the battery capacity

Icharge = the charging current.

This formula determines how long it will take to charge the battery from a given state of charge to full capacity. It helps in scheduling and managing the charging process, ensuring the batteries are charged efficiently and ready for use when needed.

The provided expressions allow for a detailed quantitative analysis of the system's performance and operational efficiency. By monitoring battery voltage, the system ensures optimal usage and longevity of the batteries. The switching criteria between batteries prevent deep discharge and maintain a continuous power supply. The solar power generation formula helps in assessing the energy contribution from renewable sources, and the charging time calculation ensures effective battery management. Together, these expressions support the design and operation of a reliable and efficient dual battery charging system, capable of leveraging both solar and AC power sources.

SYSTEM DEVELOPMENT

The system consists of two main blocks as shown in figure 1: the power generation and storage block and the control and monitoring block. The power block includes solar panels, batteries, and a DC motor. The control block features a microcontroller, sensors (voltage, temperature, humidity), and an LCD display.

The dual power source system depicted in the block diagram is designed to drive a DC motor using either solar energy or an AC supply, ensuring flexibility and reliability in power sourcing. The system begins with a solar panel that captures solar energy and converts it into electrical power. This power is regulated by a charger circuit to ensure the correct voltage and current levels

for safely charging the batteries. Alternatively, an AC supply can be used when solar power is insufficient or unavailable. The AC supply is converted to DC power by an AC/DC converter circuit, making it compatible with the battery charging system and the DC motor.

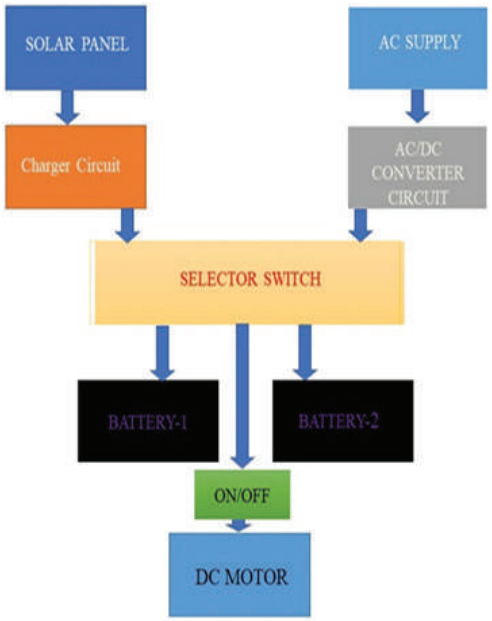

Fig. 1: Block Diagram of charging system

A selector switch plays a crucial role in this setup by allowing the user to choose between the solar panel and the AC supply for charging the batteries. This switch directs the regulated power from either source to one of two batteries, Battery-1 or Battery-2. These batteries store the electrical energy and provide a stable and continuous power supply to the DC motor. The inclusion of two batteries ensures that the system can operate continuously by allowing one battery to charge while the other is in use, thus enhancing reliability and operational efficiency. An ON/OFF switch controls the power flow from the batteries to the DC motor, enabling the user to turn the motor on or off as needed. This switch provides a straightforward means of managing the motor's operation, ensuring that power is only used when required. The DC motor then converts the electrical energy from the batteries into mechanical motion, driving the connected load.

Figure 2 shows the block diagram of microcontroller unit powered 5V DC supply. The microcontroller continuously monitors the input signals from the OP_AMP and selector switch, processes this data, and makes real-time decisions to manage the battery charging process. It directs the power from the appropriate source to the selected battery, indicates the status via an LED, and updates the 2x16 LCD with relevant system information. By controlling the ON/OFF switch, the microcontroller ensures the DC motor operates efficiently while protecting the batteries from over-discharge.

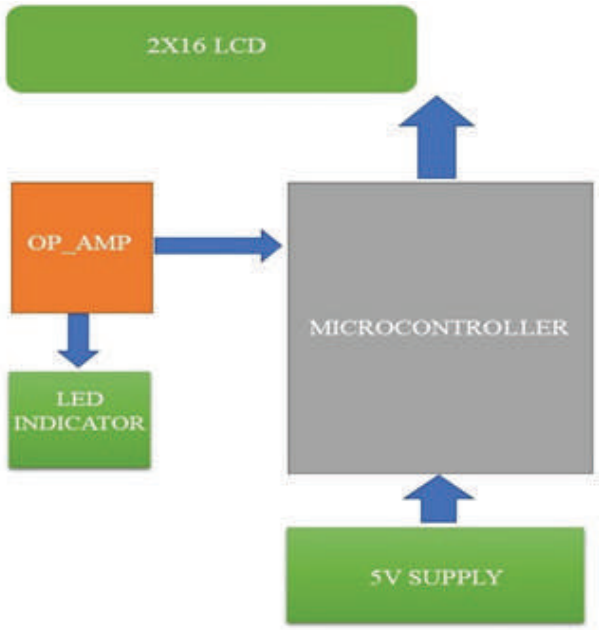

Fig. 2: Block diagram of Microcontroller unit

Flow of Operation

Solar Power Mode

Solar Panel → Charger Circuit → Selector Switch → Battery-1 or Battery-2 → ON/OFF Switch → DC Motor

AC Power Mode

AC Supply → AC/DC Converter Circuit → Selector Switch → Battery-1 or Battery-2 → ON/OFF Switch → DC Motor

The flowchart for the charging system algorithm outlines a structured process for managing the charging of a device or system is shown in figure 3. It begins with the initialization phase, where the system's parameters and initial conditions are set. This is followed by a check to determine if the device requires charging. If

charging is needed, the system proceeds to monitor the current battery level. Based on this level, the algorithm decides whether to initiate the charging process. During charging, the system continuously monitors various parameters such as temperature, voltage, and current to ensure safe and efficient operation. If any parameter exceeds safe limits, the system may pause or stop charging to prevent damage. Once the battery reaches its full charge, the algorithm stops the charging process and enters a maintenance mode to keep the battery at optimal levels. Throughout the process, the system provides status updates and logs data for further analysis and optimization. This structured approach ensures that the charging system operates safely, efficiently, and effectively.

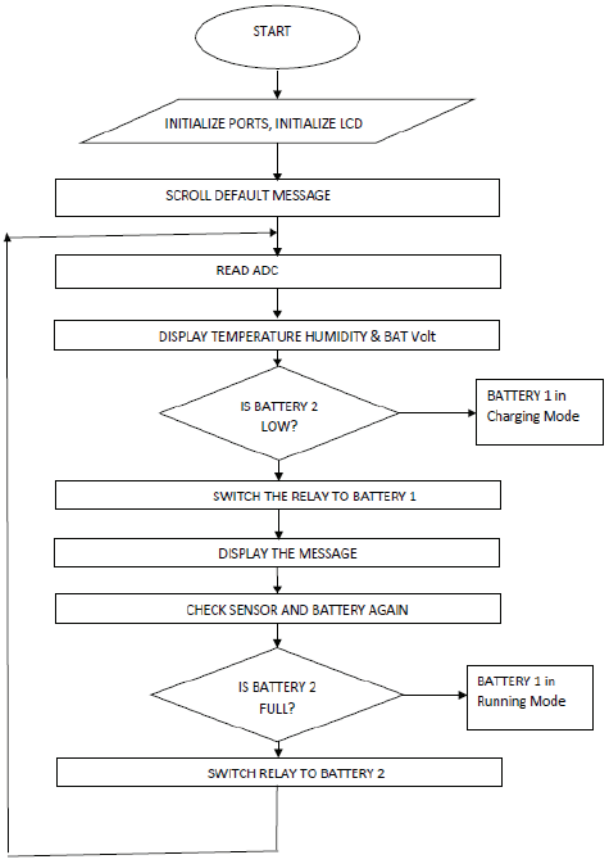

Fig. 3 Process Flowchart

RESULTS

The performance of the dual battery EV system was tested under various conditions. The results are summarized in the following table 1:

Table 1: Results

Parameter	Value
Solar Panel Specifications	12V, 5W
Motor Current Consumption	600mA
Battery Capacity	12V, 1200mAh
Full Charging Time (Sunlight)	3.75 hours
Running Time (AC)	2.5 hours
Running Time (With Sunlight)	4.5 hours
Charging Time (AC)	1.5 hours

The system demonstrated reliable operation with continuous power supply and efficient battery management, significantly enhancing the EV's operational duration. he provided parameters offer a detailed insight into the performance characteristics of the charging system. The system, primarily reliant on a 12V, 5W solar panel, showcases efficiency and sustainability in harnessing solar energy. The motor's current consumption of 600mA serves as a benchmark for power requirements and operational capabilities. The 12V, 1200mAh battery capacity ensures ample energy storage for prolonged usage. Notably, under optimal sunlight conditions, the battery achieves full charge in 3.75 hours, while runtime extends to 4.5 hours. Additionally, with AC charging, the battery attains full capacity in 1.5 hours, ensuring flexibility and reliability in power management. These results underscore the system's efficiency, resilience, and adaptability in diverse environmental conditions, catering to sustained functionality and performance.

CONCLUSION

The dual battery EV system with automatic changeover and status monitoring provides a sustainable and efficient solution for reducing petroleum consumption and environmental pollution. Utilizing solar and AC power sources, the system ensures uninterrupted operation and improved reliability. This approach contributes to the development of eco-friendly transportation, aligning with global efforts to combat climate change.

Suitability and Optimization of Retaining wall Bridge Approach System

Mohd. Zain, Rishabh Joshi
Rajendra Kumar Srivastava
Faculty of Civil Engineering
Shri Ramswaroop Memorial University
Barabanki, Uttar Pradesh
✉ mohdzain.ce@srmu.ac.in
✉ rishabhjoshi.ce@srmu.ac.in
✉ rksrivastava.ce@srmu.ac.in

Sachin R. Jambhale
Department of Civil Engineering CSMSS,
CHH. Shahu College of Engineering
Maharastra
✉ srjambhale@gmail.com

ABSTRACT

The Retaining Wall Bridge Approach System is a structural solution designed to support and protect bridges by providing a stable and secure transition from the road surface to the bridge deck. This system is specifically developed to address the challenges associated with varying ground conditions and is essential for effective erosion control. The retaining wall component of the system is designed to resist lateral earth pressure and prevent soil movement, safeguarding the stability of the bridge approach. It incorporates advanced engineering techniques and materials to withstand external loads and accommodate potential ground movement. Additionally, the bridge approach system incorporates erosion prevention techniques that lessen the consequences of water flow and prevent soil erosion. This is accomplished by using specialized erosion control mats, geotextiles, and drainage systems, which efficiently manage water runoff and safeguard the soil's integrity.

The design of the Retaining Wall Bridge Approach System emphasizes durability, cost-effectiveness, and ease of installation. It offers a versatile solution suitable for various bridge configurations and site conditions. The system's modular design allows for customization and adaptation to meet specific project requirements. Overall, the Retaining Wall Bridge Approach System provides an efficient and sustainable approach to bridge construction, enhancing safety and longevity. Its integration of retaining wall structures and erosion control measures ensures the stability and protection of the bridge approach, contributing to the long-term performance and functionality of transportation infrastructure.

In this paper, research has been conducted on cost optimization of retaining wall bridge approach system. This paper is also focused on determining that up to what height we should opt for cantilever retaining wall bridge approach system or else go for other option such counterfort retaining wall bridge approach system or reinforced earth retaining wall bridge approach system.

KEYWORDS *: Bridge approach system, Cost optimization, Cantilever retaining wall, Counterfort retaining wall, Reinforced earth retaining wall.*

INTRODUCTION

The cost optimization of Cantilever Retaining Wall bridge approach is an essential component of retaining wall design and construction, aiming to achieve an optimal balance between structural integrity and economic efficiency. This paper explores the key considerations and strategies involved in optimizing the cost of cantilever retaining walls.

The planning and building of cantilever retaining walls involve several factors that impact the overall cost, including wall height, soil conditions, loading conditions, and material selection [1-2]. Cost optimization involves

analyzing these factors and making informed decisions to achieve an economical design without compromising structural performance.

One key consideration in cost optimization is the choice of suitable materials. Different types of materials, such as concrete, masonry, or even reinforced soil, may be used for cantilever retaining walls. Evaluating the material properties, availability, and cost allows engineers to choose the best appropriate and cost-effective option for the specific project requirements [3-4].

Furthermore, efficient design practices play a vital part in cost optimization. By considering the anticipated soil pressures, wall height, and loadings, engineers can optimize the dimensions and reinforcement requirements of the retaining wall, eliminating unnecessary expenses. Advanced design methods, including computer simulations and finite element analysis, can aid in finding the most efficient design configurations [5-6].

Construction techniques also influence the cost optimization of cantilever retaining walls. Adopting techniques that reduce labour and material waste, such as precast components or modular construction, can lead to significant cost savings. Additionally, optimizing the construction sequence and scheduling can minimize downtime and enhance productivity, further reducing project costs [7-10].

Another aspect of cost optimization involves considering the long-term maintenance and resilience of the retaining wall. Implementing appropriate actions, such as providing suitable drainage systems, corrosion protection for reinforcement, and erosion control measures, can mitigate future maintenance expenses and extend the lifespan of the structure [11-14].

Ultimately, cost optimization of cantilever retaining walls needs a thorough comprehension of the project's specific requirements, along with careful analysis of material choices, design practices, construction techniques, and maintenance considerations [15-16]. By striking a balance between structural performance and cost-efficiency, engineers are able to make sure the successful implementation of cost-optimized cantilever retaining walls, delivering value for both clients and stakeholders.

METHODOLOGY

The methodology used for designing a cantilever retaining wall involves a systematic approach that takes into account various factors and considerations. While specific design procedures may vary depending on project requirements and local codes, the following general steps are commonly followed in the design process:

Preliminary Assessment

The preliminary assessment involves conducting an initial assessment of the site conditions, including soil properties, groundwater levels, and any potential external factors that may impact the wall's design. It also includes gathering necessary data through geotechnical investigations, site surveys, and geological studies.

Load Analysis

In load analysis, basically we figure out the loads and stresses that the retaining wall will be subjected to. These stresses might come from earthquake pressures, water pressure, soil pressure, and surcharge load from nearby buildings. We also need to take into consideration the soil's density, cohesiveness, and angle of friction when analyzing for active and passive soil pressures.

Structural Stability Analysis

Structural stability analysis involves analyzing the retaining wall's stability with respect to several failure modes, such as overturning, sliding, and bearing capacity. While checking the stability of structure, we also need to verify that the wall's size and reinforcement can withstand the estimated loads and maintain stability throughout time [17–19].

Wall Geometry

Wall geometry involves establishing the proper wall height, wall thickness, and base width for the cantilever retaining wall. In this, we also need to take into account the expected loads, properties of retained soil, and the amount of building area that is available.

Reinforcement Design

In reinforcement design, we need to determine the required reinforcement spacing, embedment lengths, and steel grades based on the calculated loads and design criteria.

Drainage and Erosion Control

In drainage and erosion control, we need to incorporate proper drainage systems to control water accumulation behind the wall and prevent hydrostatic pressure build-up. We also need to consider the inclusion of weep holes, gravel backfill, geotextiles, and geo-composite drains to ensure effective water management and mitigate erosion risks.

Construction Details

Construction details involves the development of detailed construction drawings and specifications, indicating dimensions, reinforcement layouts, and construction techniques. It also includes considerations related to construction joints, wall facing materials, and construction sequence considerations [20-21].

Review and Evaluation

It involves conducting a thorough review and evaluation of the design calculations, drawings, and specifications to ensure accuracy and compliance with design criteria and codes. In review and evaluation stage, we also need to seek input from relevant stakeholders, including geotechnical engineers and structural experts, to validate the design approach.

Monitoring and Maintenance

This stage involves implementing a monitoring and maintenance plan to assess the performance of the constructed retaining wall over time. Regular inspections, measurements, and assessments of wall movements and distresses helps to identify any potential issues and guide necessary maintenance or remedial actions [22-23].

It's important to note that the design methodology may vary based on specific project requirements, including the complexity of the site conditions and design constraints. Consulting with experienced geotechnical and structural engineers, and considering local design practices and codes, is essential for ensuring a safe and efficient design of a cantilever retaining wall.

In this study, we have done a thorough research on retaining wall bridge approach by designing cantilever retaining wall bridge approach for different heights of 3m, 4m, 5m, 6m, 7m, and 8m. An Excel program was made to calculate the load, moment and reinforcement details. A detailed design for 6m height retaining wall bridge approach system is as follows:

Table 1. Details of forces and moment for 6m height Retaining Wall Bridge approach

S. No.	Item	Load (kN)	Vertical Load (kN)	Horizontal load (kN)	Lever Arm (m)	Moment due to Horizontal Load (kN-m)	Moment due to Vertical Load (kN-m)
1	Live Load Surcharge	3.6X1.5X25	135		4.75		641.25
2	Foundation Slab	5.5X0.7X25	96.25		2.75		264.6875
3	Stem	7.3X0.5X25	91.25		3.75		342.1875
4	Earth Fill	7.3X1.5X18	170.1		4.75		807.975
			492.6				**2056.1**
5	Earth Pressure due to Surcharge			25.1748	3.5	88.1118	
6	Earth Pressure due to Fill			146.853	2.331	342.314343	
				172.0278		**430.426143**	
Coefficient of active earth pressure (Ka) = 0.333							
Unit weight of soil (γs) =18 kN/m^3				**x = 3.300190534 m**			
Thickness of base slab (hs) = 0.7 m							
Height of retaining wall (hf) = 7 m							
Earth pressure due to live load surcharge = 3.5964 kN/m^2							

Earth pressure due to earth fill = 41.958 kN/m²

Load due to earth pressure (p) = 172.0278 kN B = 5.5 m

e = 0.5501905 m

Maximum base pressure pmax =143.320kN / m²

Minimum base pressure pmin = 35.806 kN/m²

Factor of safety in overturning = 4.776893861 > 2 OK

Factor of safety in sliding = 1.718094401 > 1.5 OK

Table 2. Design of Stem for 6m height Retaining wall bridge approach

Height of Stem (m)	Horizontal Load		Moment			Area of Steel (mm^2)	Diameter of bar (mm)	Spacing (mm)
	Earth fill (kN)	Surcharge Live Load (kN)	Moment due to Earth fill (kN-m)	Moment due to Live Load (kN-m)	Total Moment (kN-m)			
7.3	43.8	3.6	389.017	1.2	390.217	1992.63	20	95

Percentage of steel used in stem = 0.66%

Table 3. Design of Toe of Slab for 6m height Retaining wall bridge approach

Base width of Slab (m)	Toe width of slab (m)	Moment (kN-m)	Factored moment (kN-m)	Area of Steel, A_{st} (mm^2)	Diameter of bar (mm)	Spacing c/c (mm)
5.5	3.5	738.1514	1107.22715	4295.052	25	100

Percentage of steel used in stem = 0.63%

Table 4. Design of Heel of Slab for 6m height Retaining wall bridge approach

Base width of Slab (m)	Heel width of slab (m)	Moment (kN-m)	Factored moment (kN-m)	Area of Steel, A_{st} (mm^2)	Diameter of bar (mm)	Spacing c/c (mm)
5.5	1.5	51.16428	76.7464227	840	12	100

Percentage of steel used in stem = 0.124%

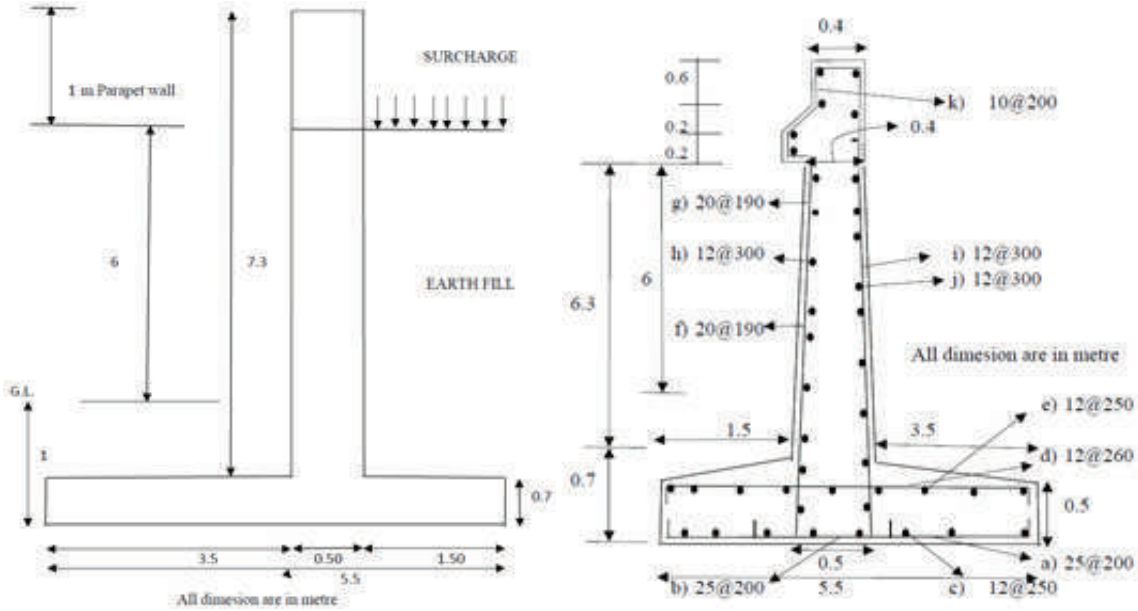

Fig 1. Retaining wall bridge approach of 6 m height

RESULTS AND DISCUSSION

The variation of stem of height, width of footing, toe width and heel width with respect to height of retaining wall is tabulated in Table 5.

Table 5. Variation of Stem height, Footing Width, Toe Width and Heel Width with height of retaining wall

Height of retaining wall (m)	Stem height (m)	Footing width (m)	Toe width (m)	Heel width (m)
3	4.7	2.5	1	1
4	5.7	3.5	1	2
5	6.7	4.5	1.25	2.75
6	7.7	5.5	1.5	3.5
7	8.7	6.5	1.75	4.25
8	9.7	7.5	1.75	5.25

The variation of maximum and minimum base pressure on base slab with respect to height of retaining wall is listed in Table 6. The maximum base pressure occurs at the toe of the wall and the minimum base pressure occurs at the heel of the slab. As the height of the retaining wall increases, the maximum base pressure at toe increases, due to the increased active earth pressure force. Similarly, the minimum base pressure at heel of slab decreases with increase in height of retaining wall.

Table 6. Variation of maximum and minimum pressure with respect to height of Retaining wall

Height of Retaining Wall (m)	Maximum pressure (Pmax)	Minimum pressure (Pmin)
3	82	65.7
4	111.4	43.2
5	124	37.4
6	143.3	35.8
7	149	34
8	142.9	41.2

Fig 2 represents the variation of maximum and minimum base pressure at toe and heel of the slab respectively, for different heights of retaining wall. It should be verified that the maximum base pressure should not be greater than bearing capacity of soil. In our study, the bearing capacity of soil is 150 kN/m2 and the maximum base pressure obtained till 8m height of retaining wall is less than the bearing capacity of soil (hence design is OK). For design purposes, it is preferred that the minimum base pressure should not be negative, otherwise heel of the slab will be in tension. Since tensile strength of the concrete is weak, hence base slab is considered to fail if minimum base pressure is negative. In our design, the minimum base pressure is always positive, hence the design criterion is satisfied.

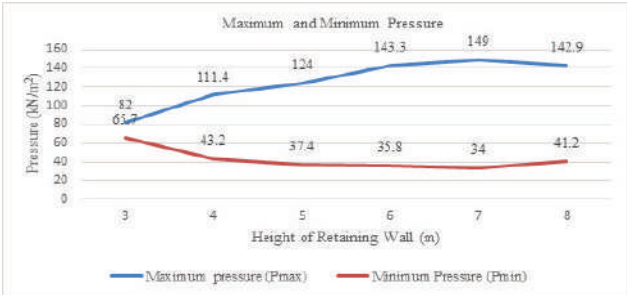

Fig 2. Maximum and minimum pressure with respect to height of retaining wall

Table 7. Variation of Sliding Force and Resisting Frictional Force with respect to height of Retaining wall

Height of Retaining Wall (m)	Sliding Force, fs (kN)	Resisting frictional force, F (kN)
3	62.3	153
4	92.9	157.68
5	129.5	213.75
6	172.1	295.6
7	220.58	362.6
8	275.1	403.29

The variation of sliding force and resisting frictional force with height of retaining wall is tabulated in Table 7. Sliding force is applied by the soil retained over the heel of the slab, whereas the resisting force is applied by the passive earth pressure force applied by the earth over toe slab and weight of the retaining wall. From the results represented in Fig 3, we can observe that the resisting friction force is greater than the sliding force, hence the factor of safety for sliding will always be greater than 1.

The variation of overturning moment and stabilizing moment about toe of the slab for different heights of retaining wall is listed in Table 8. Overturning moment on retaining wall is applied due to the moment due to

active earth pressure force applied by the earth fill, whereas the stabilizing moment about toe is applied due to the moment due to weight of the retaining wall and the passive earth pressure force applied by the earth fill.

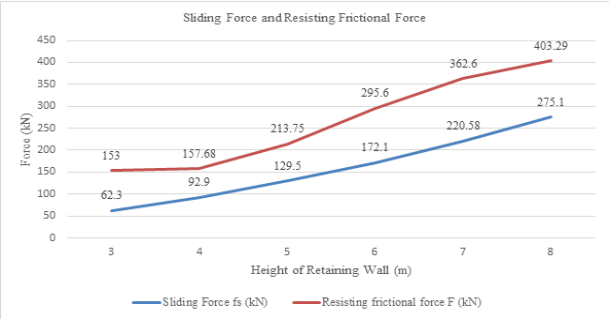

Fig 3. Sliding force and resisting frictional force

Table 8. Variation of overturning moment and stabilizing moment with respect to height of Retaining wall

Height of Retaining Wall (m)	Overturning Moment Mo (kN-m)	Stabilizing Moment Ms (kN-m)
3	92.6	295
4	169.7	682.1
5	280.3	1204.6
6	430.34	2056.1
7	626.1	3037.6
8	873.2	3777.7

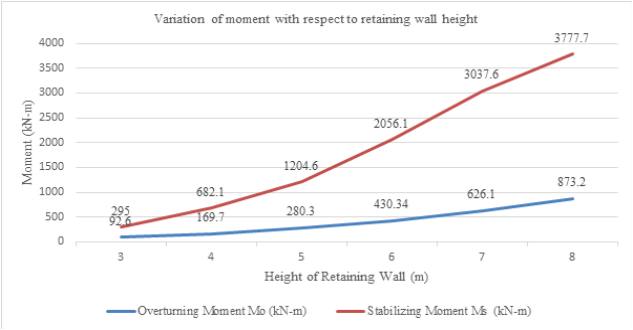

Fig 4. Variation of stabilizing and overturning moment with height of retaining wall

From the results in Fig 4, it is observed that with increase in height of retaining wall, there is an increase in overturning moment (almost linearly) and stabilizing moment (increases exponentially). The overturning moment increases almost linearly with height of retaining wall, but the stabilizing moment increases exponentially due to increased weight of individual components of retaining wall. Due to drastic increase in stabilizing moment with height of retaining wall, the factor of safety against overturning also increases.

CONCLUSION

In this study, extensive research was carried out to determine the effect of height of retaining wall on the maximum and minimum pressure on the base slab, stabilizing and overturning moments generated as well as the sliding and resisting frictional force. This study is focused on determining the effective height upto which cantilever retaining wall is most feasible option based on the factor of safety and cost optimization. From the study, it was concluded that with increase in height of retaining wall, the factor of safety in overturning increases as the increase in stabilizing moment due to weight of retaining wall is higher than the increase in overturning moment due to active earth pressure force. The retaining wall is also safe in sliding as the factor of safety is always greater than 1.5 for different heights of retaining wall. However, the maximum pressure on the toe of base slab increases with increase in height of retaining wall and it may exceed the bearing capacity of soil, hence the cantilever retaining wall should not be preferred for heights of more than 5m. Also, as the height of retaining wall increases the minimum pressure on base slab may also become negative which may induce tensile stresses on the slab. From the study, it is concluded that the cost of the retaining wall also increases drastically above 5m height of retaining wall bridge approach system. Hence, it is suggested that cantilever retaining wall bridge approach system should be adopted upto height of 5m, and other bridging options such as reinforced earth wall bridge approach system or counterfort retaining wall bridge approach system should be preferred for heights beyond 5m.

REFERENCES

1. Zain, M., Pandey, A. K., & Varma, R. Comparative analysis of T-Beam along with deck slab by Courbon's method and STAAD. Pro. Materials Today: Proceedings 2022; 56(4): 2261-2267. https://doi.org/10.1016/j.matpr.2021.11.596.

2. Patil, S. S., Bagban, A. A. R. Analysis and Design of Reinforced Concrete Stepped Cantilever retaining Wall. International Journal of Research in Engineering and Technology 2015; 4(2): 46-67.

3. Zain, M., Varma, R., & Srivastava, R. K. Cost comparison of steel plate girder and RCC Girder Bridge. Materials Today: Proceedings 2022; 56(4): 2274-2277. https://doi.org/10.1016/j.matpr.2021.11.607.

4. Zain, M., Varma, R., & Srivastava R. K. Examining the Applicability of Micro-Pile for Bridge Foundation in Difficult Terrain using Pile Load Test. Turkish Journal of Computer and mathematics Education 2021; 12(11): 6239-6245. https://doi.org/10.17762/turcomat.v12i11.6986.

5. Kapoor, K., Joshi, R., Singh, A., Resatoglu, R., & Zain, M. Calibration of FEM models of historic masonry structures and its application on a local historic structure. Materials Today: Proceedings 2023. https://doi.org/10.1016/j.matpr.2023.04.050.

6. Srivastava, V., Joshi, R., Kumar, K., Resatoglu, R., Zain, M., & Singh, A. Effect of seismic load on behaviour of RCC, composite and light steel building analysed using ETABS software: A comparative study. Materials Today: Proceedings 2023. https://doi.org/10.1016/j.matpr.2023.03.564.

7. Srivastava, S., Rao, A. K., Zain, M., & Kumar, R. Utilization of waste rubber fiber considering modification in strength reduction factor and its effect on the behavior of concrete. Materials Today: Proceedings 2020; 21(3): 1489-1495. https://doi.org/10.1016/j.matpr.2019.11.066.

8. Donkada, S., & Menon, D. Optimal design of reinforced concrete retaining walls. The Indian Concrete Journal 2012; 9-18.

9. Patil, R. B., Shahu, R., & Patil, G. Design and Detailing of Counter-Fort Retaining Walls for Construction Site. International Journal of Informative & Futuristic Research 2015; 3(1): 61-75.

10. Abood, T., Eldawi, H. E. Y., & Abdulrahim, F. R. E. Design of Cantilever Retaining Wall with 4m Height. International Journal of Civil and Structural Engineering Research 2015; 3(1):318-326.

11. Lilani, I. K., & Patel, R. Analysis of Counterfort Retaining Wall in Non over flow section of Gravity Dam. International Journal for Scientific Research & Development 2017; 5(5): 920-924.

12. Singla, S., & Gupta, S. Optimization of Reinforced Concrete Retaining Walls of Varying Heights using Relieving Platforms. International Journal of Engineering Research & Technology 2015; 4(6): 1071-1077.

13. Chaliawala, Y., Solanki, G., & Chandiwala, A. K. Comparative study of cantilever and counter fort retaining wall. International Journal of Advance Engineering and Research Development 2015; 2(12): 221-224.

14. Talatahari, S., Sheikholeslami, R., Shadfaran, M., & Pourbaba, M. Optimum Design of Gravity Retaining Walls using Charged System Search Algorithm. Mathematical Problems in Engineering 2012; 12(1). https://doi.org/10.1155/2012/301628.

15. Yang, S., Chegnizadeh, A., & Nikraz, H. Review of studies on retaining walls behavior on dynamic/seismic condition. International Journal of Engineering Research and Applications 2013; 3(6): 1012-1021. https://doi.org/10.13140/RG.2.2.14610.27843.

16. Dhamdhere, D. R., Rathi, V. R., Kolase, P. K. (2018). Design and Analysis of Retaining Wall. International Journal of Management, Technology and Engineering 2018; 8(9): 1246-1263.

17. IS 14458 (Part 1): 1998. Retaining wall for hill area-Guidelines: Part-1 Selection of type of wall. Bureau of Indian Standards, New Delhi.

18. IS 14458 (Part 2): 1997. Retaining wall for hill area-Guidelines: Part-2: Design of retaining/ breast walls. Bureau of Indian Standards, New Delhi.

19. IS 14458 (Part 3): 1998. Retaining wall for hill area-Guidelines: Part-3: Construction of dry stone walls. Bureau of Indian Standards, New Delhi.

20. Yadav, P., & Joshi, R. Effect of Height and Position of Shear Wall on G+5 Multi-Storey Building for Zone III. International Journal of Recent Technology and Engineering 2019; 8(3): 5452-5456. https://doi.org/10.35940/ijrte.C4609.098319.

21. Joshi, R., Singh, A., Resatoglu, R., Zain, M., & Singh, P. Effect of elevated temperature on Portland Pozzolona cement based concrete using Sulphonated naphthalene formaldehyde and Polycarboxylic ether as superplasticizer. Materials Today: Proceedings 2023. https://doi.org/10.1016/j.matpr.2023.03.483.

22. Joshi, R., & Burman, A. K. Effect of Periodic Loads on G+3 RCC Building. International Journal of Engineering Research & Technology 2017; 6(6): 99-102.

23. Burman, A., & Joshi, R. Effect of Impulsive Loads on G+3 RCC Building. International Journal of Modern Engineering Research 2017; 7(5): 56-62.

Effect of Population and Land use Pattern on Prediction of Black Spot

Arti Chouksey
Assistant Professor
Department of Civil Engineering
DCRUST, Murthal
✉ arti.civil@dcrustm.org

Khushboo
M.Tech Student
Department of Civil Engineering
DCRUST, Murthal
✉ arti.civil@dcrustm.org

Aman Ahlawat, Sachin Dass
Assistant Professor
Department of Civil Engineering
DCRUST, Murthal

ABSTRACT

The roads are one of the most suitable modes of transport for every person in India. Still, in this highly populated country, there are several chances of road accidents causing fatalities, injuries, and property damage. In order to minimize the risk of road accidents, it is essential to know the reasons for road factors of the stretch where accidents frequently happen and set the priority list to take the necessary actions in hazardous locations. In this paper, a detailed analysis of road accident data has been carried out for Panipat and Rohtak city, Haryana (India). The accident data accessed from the Haryana Police website have been analyzed for a 5-year period spanning 2018-2022, and then based on this data identification & representation by Arcmap10.8 of accident-prone locations, blackspots and predict the impact of Population & Land use pattern by using neural network approach has been done for the selected study area.

INTRODUCTION

The global transportation network is supported by roads. National highways (NH) facilitate the effective movement of people and goods and enhance market availability, all of which contribute significantly to the economic and social growth of the nation. They transport more than 40% of all traffic and help compensate for 2% of the entire road network .The nation's economy and population movement depend heavily on its road network. A good transport system may connect markets and provide significant economic benefits to the populace. However, out of all modes of transportation, highways are the most prone to accidents, placing the public at risk of fatalities, serious injuries, and damaging vehicles. The employment situation in India will improve promptly as a result of developed highway and road networks. It will be extremely advantageous for the expansion of the manufacturing sector across the country

Road accidents in Haryana

In 2022, the state reported 6,424 deaths from total accidents 11,875 same as in 2021, total 9,933 accidents that left 4,706 people dead and 8,121 people injured. In contrast, 9,431 accidents resulted in the death of 4,507 people in 2020. Gurugram is in first place with 871 accident. These accidents left 379 people dead and 695 people injured. Motorcyclists, pedestrians, and cyclists make up the majority of the vulnerable road users who die on the nation's roads—about half of all fatalities. [1]Day by day accidents are increasing due to so many reasons and sometimes they are very unpredictable levels of seriousness. A stretch of road that is known to have a high accident risk is commonly known as a 'black spot' or 'black zone'. The first stage in creating a safer road network is identifying the sections of highways where accidents happen often, commonly referred to as 'accident black spots.' Numerous analytical tools and methodologies have been used throughout the years to

pinpoint accident' black spots.' It might happen for a variety of reasons, such as a concealed junction on a busy route, misplaced warning signs, a sudden bend on an otherwise straight road, etc. Road engineers and highway planners have found accident prediction models to be a valuable tool for identifying causes and, as a result, suggesting solutions to increase road safety.

LITERATURE REVIEW

FIR data from police station is collected and Accident hotspot is marked based on data by various researcher for various section of NH. The collected FIR data of stretch was analysed year- wise to know the accident hotspots in by various tools and Techniques such as MS Excel, WSI (Weighted Severity Index), KDE method which allows for the overall visualization and manipulation of the accident based on density and was used to create the fundamental spatial unit for the hotspot clustering method.[2]-[12]]density-based clustering was used to figure out how severe accidents occurred in Black Spots. Results include shortest-path analysis, service-area analysis, accident-location severity, and vulnerability level. The study serves as a broad- scale representation of the clustering of traffic accidents. Some researcher also use ANN and non-linear regression approaches, Scientist has made an effort to forecast the incidence of deaths, injuries, and accidents. The ANN model was determined to be the one that performed the best overall and had the fewest errors. Stastical Methods such as ANN also used to study factors such as driver, vehicle, road, and environmental conditions for prediction of accident severity.[7], [13-19]

GIS and Remote Sensing Techniques were also used by researcher for Details about the mishap itself. Date, location, vehicle type, and casualty count, Time are only some of the details stored in the GIS database. Accident analysis research aims to identify high-accident locations and low-safety zones. GIS Techniques were used to develop map of study area with unsafe Bus stand. The 'IBM SPSS' program is used to examine accident records. GIS not only used to Identify Blackspot but also provide Solution by various alternate methods. GIS also used by author for updating Land use, Landcover Details of the area.

GIS technology used by researcher to store, query, capture, analysis, and display data and decide to improve road features, assess traffic safety, and improve.[4], [20-27]

All these literature uses latest technology and software to predict and identify blackspot taking various factors like road geometry, road condition, driver behavior, other environmental factors in to consideration. But very little or no literature are available to take landuse landcover parameter in to consideration, which may be a driving parameter influencing severity, nature and count of Accidents.[28], [29]

METHODOLOGY & STUDY AREA

In the present study the accident data of the past 3 calendar years were collected through the Haryana police website for the Panipat and Rohtak city have been identified the accident prone locations and also identified the blackspot location in both the cities on the basis of the Ministry of Road Transport and Highways (MoRTH) further created the maps through the GIS software . Using the Neutral network analysis to predict the impact of Land Use (LU) & population and compare the accident happened frequency between the study areas.

The schematic diagram of the methodology for the study is indicated in given chart:

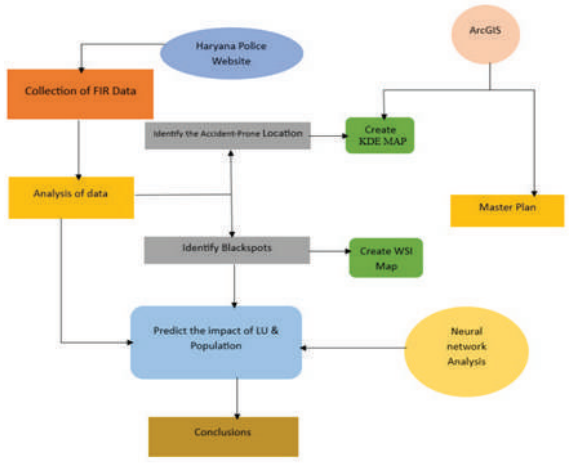

Study area: Haryana has 22 districts and 154 cities but in this research, only two cities are taken that is Panipat city and Rohtak City:

i. The historic place Panipat, often known as "The Textile City,". On (AH2 Asian Highway 2) NH-44,

it is located 169 kilometers south of Chandigarh and 95 km north of Delhi. The city of Panipat serves as the district's administrative center of Panipat district. The coordinates of Panipat are 29.3875°N, 76.9700°E. For a better understanding of the location of the study area ,Fig1 represents the map of the study area.

ii. The city of Rohtak serves as the district's administrative center of Rohtak district. It is situated on NH 9 (formerly NH 10), some 250 kilometers south of Chandigarh and 70 km northwest of New Delhi. The coordinates of Rohtak are 28.8955° N, 76.6066° E.

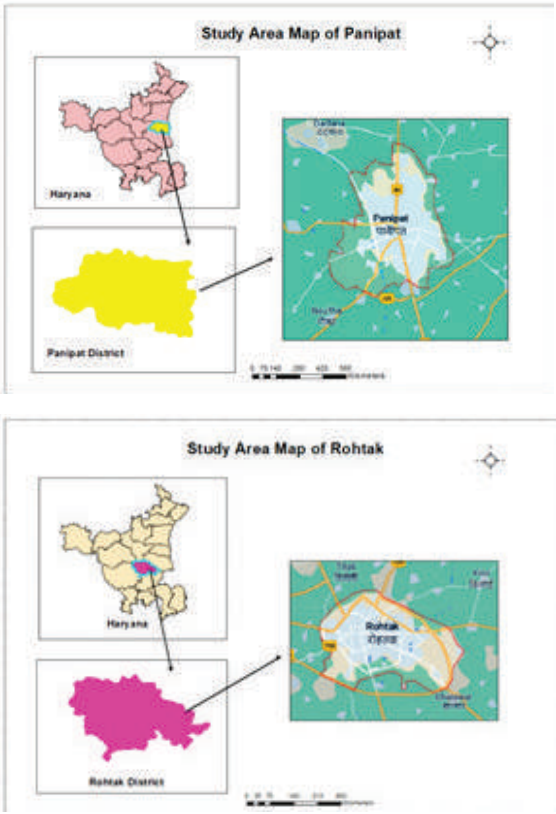

Fig. 1. The study area map for Panipat City and Rohtak City

DATA ANALYSIS

Identification of Accident-prone Locations

From the (Haryana Police FIRs)data from 2018 to 2022, the accident-prone locations where 2 or more accidents had occurred, were analysed by applying the spatial tool Kernel Density Estimation (KDE) approach in the ArcMap10.8

Kernel Density Estimation (KDE): For determining hazardous locations while taking accident severity and spatial interactions into account, Kernel density Estimation (KDE) is highly suggested. (Sanath et al.) had been applied to this approach. The bandwidth and the function K, often known as a 'Kernel,' are the two parameters that affect the form of the kernel density when using this method. When referring to risk, the terms "kernel and bandwidth" both refer to a horizontal range of accident likelihood. Consequently, bandwidth and kernel can be viewed as horizontal and vertical elements. The kernel function conceptually divides the studied area into small, user-defined cells, then calculates cell values that are highest at the locations of the points, reduce away from the points, and ultimately reach zero at the radius.

The following steps are followed for making the map of the risky locations of the study areas:

Initially, using the Digitization tool of ArcMap 10.8, create the master plans with reference from the Google Earth image for both cities (Panipat and Rohtak City).

- Digitize all the necessary features such as road network, buildings, drains, etc.
- Assign the attributes for every feature of the map by adding multiple fields such as Latitude & Longitude, names, land use, population, etc.
- Add the placemarks of the identified accident-prone locations in Google Earth Pro.
- Now, georeferenced the satellite imagery obtained from the Google Earth Pro of accident-prone locations with the master plans of the study areas by georeferencing using the four known coordinates point in the Arc GIS.
- Plotting the accident-prone locations on the master plans, the KDE tool is applied to know the accident severity in both cities, which is also represented in the given below Fig 3 & 4.

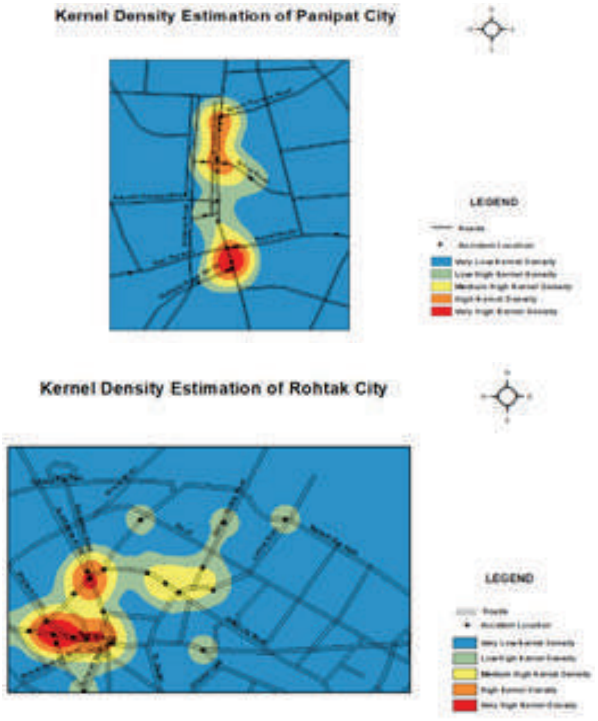

Fig. 2. Kernel Density Estimation (KDE) of the accident stretches in Panipat city and Rohtak city

From Both of the aforementioned figures illustrate a map of the Kernel Density Estimation that depicts the road network of the study areas' cities and lists the sites where two or more accidents occurred between the years of 2018 to 2022, the double-lined symbol which is mentioned in the legends of the maps also the black dots are representing the accident-prone locations. The five colour bandwidths represent the accident severity rate of the road stretch of Panipat and Rohtak city such as with red being the very high kernel density which means that the zone is highly risky, lighten the colour up to sky blue representing the very low kernel density which means that zones are low risk.

Identification & Ranking of blackspot

High-risk road stretches that have experienced a relatively large number of accidents compared to the rest throughout a given time period are known as accident blackspots. In this study, the locations showing 5 or more accidents during the 3 – year period i.e. 2020-2022 have been treated as blackspots. Accordingly, 5 blackspots have been identified in Panipat & 9 blackspots in Rohtak city.

Based on the above tables i.e. Table 1 & Table 2 the maps are generated with the help of ArcMap 10.8 of the value of the WSI (Weighted Severity Index) score of the Panipat city in which only five blackspots locations are identified during the period of the year 2020 to 2022 and Similarly, nine blackspots are identified in Rohtak city which are showing with the dots on the master plans of the study areas as per increase in WSI score the size of the dot are increasing respectively. These maps help set the priority of taking necessary steps to rectify the most hazardous location first. Fig 3 & 4 shows the map of the WSI accident venerability map of Panipat city & Rohtak city.

Table 1. Blackspot location in order of ranking for Panipat City

Sr. no.	Blackspot Location	Road Stretch	Number of accidents	Number of accidental deaths	Numbe of persons injured	Rank
1	**Red Light**	**Delhi Chandigarh Highway NH-44**	**10**	4	8	1
2	Bus stand	Delhi Chandigarh Highway NH-44	9	4	4	2
3	Sanjay Chowk	Delhi Chandigarh Highway NH-44	5	3	2	3
4	Platinum Textile World	Barast Road	5	2	3	4
5	Sky lark	Delhi Chandigarh Highway NH-44	5	2	3	5

Table 2 Blackspot location in order of ranking for Rohtak city

Sr. no.	Blackspot Location	Road Stretch	Number of accidents	Number of accidental deaths	Numbe of persons injured	Rank
1	Gohana by pass	Rohtak – Sonipat Road	20	12	7	1
2	Hisar by pass chowk	Hisar Road	18	3	15	2
3	Hisar by pass chowk	Hisar Road	18	6	13	2
4	Sukhpura Chowk	Outer City Road	15	4	15	3
5	IDC Chowk	Circular Road	9	6	3	4
6	Valmiki Chowk	Hisar - Rohtak -Sonipat Road	7	1	6	5
7	Drain no.8	Hisar Road	6	5	4	6
8	KVM School	Ladhot Road	5	1	4	7
9	Shyam Colony	Hisar Road	5	1	4	7

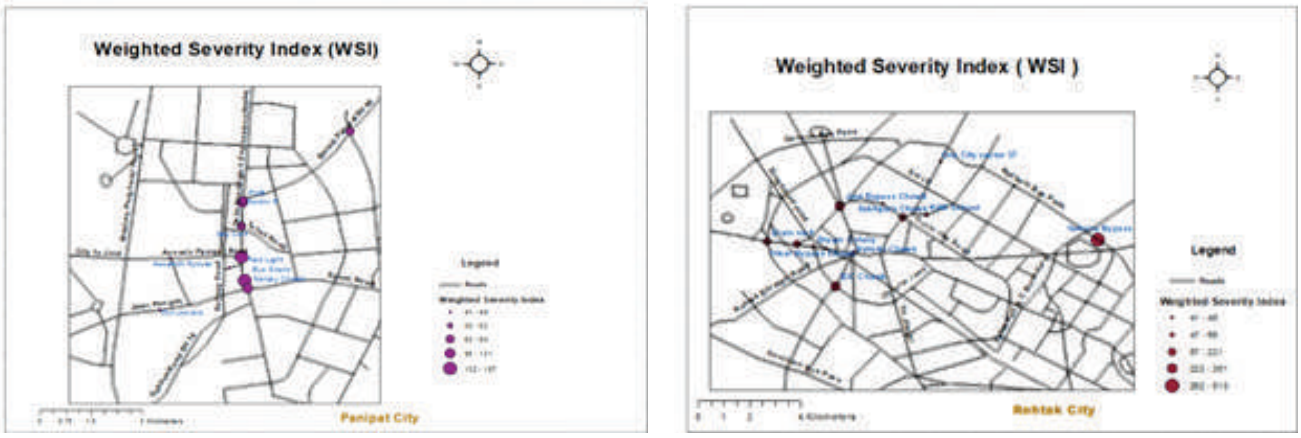

Fig 3. Weighted Severity Index (WSI) Accident Venerability Map of Panipat City and Rohtak city

The above Fig 3 shows the weighted severity index accident venerability maps of the research areas in which only those locations are considered from the master plans where the blackspots occurred. These blackspots are presented by the dot density or size increase according to their WSI value. These maps help set the priority of taking necessary steps to rectify the most hazardous location first

Implementation of neural network

Neural Networks can be defined as a system designed to establish a standard for the brain's functions and features. [32]used this approach, Neural networks are produced by connecting artificial neural cells in different configurations. Fig 4

$V=\sum xiwi + \theta, \quad y= F(v)$

Where,

W = Weight matrices of cell, V= Net input cell, Y= Output cell, X= Input vector cell,

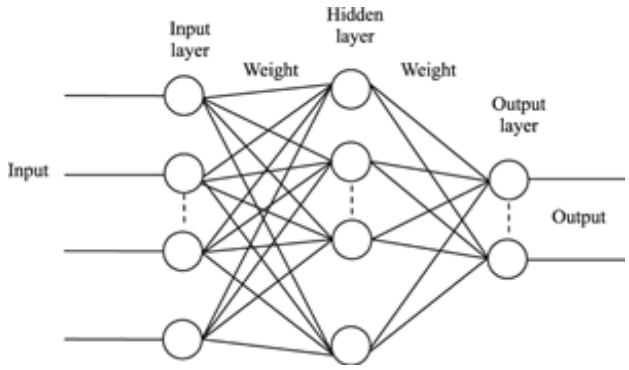

Fig. 4. Network Architecture for ANN

For carrying out the prediction, the neural network method is followed. In this method, tables of the many weighted elements that are likely to affect the frequency of accidents on the roads must be created. These criteria are given weights on a scale from 1-10, with higher weights going to those that reduce the likelihood of accidents The total weight allocated for each segment of road is found by adding the weights together, finding the mean, and then normalizing the result using the maximum weight (in this example, 90).

Table 3 Factors used in prioritization with their weights

Sr. No.	Factor Affecting Occurrence Of Accidents	Possible Variation	Weightages Assigned
1	No. of lanes in each direction	1	2
		2	4
		3	6
		4	10
2	Width of formation	>6m	1
		6m-8m	3
		8m-10m	5
		10m-12m	7
		>12m	10
3	Class of road	NH	1
		SH	4
		MDR	8
		other roads	10
4	Surface Type	Bituminous	4
		Concrete	10
5	Surface condition	Poor	1
		Fair	6
		Good	10
6	Drainage facility	Absent	2
		poor	4
		Satisfactory	6
		Good	10
7	Shoulders	Absent	4
		Unpaved	6
		Paved	10
8	Median	No	4
		Yes	10
9	Land use	Industrial	2
		Commercial/ Public use	4
		Residential / Town	8
		Open Space	10
10	Population	<5000	10
		5000-10,000	7
		10,000-15,000	4
		>15,000	1

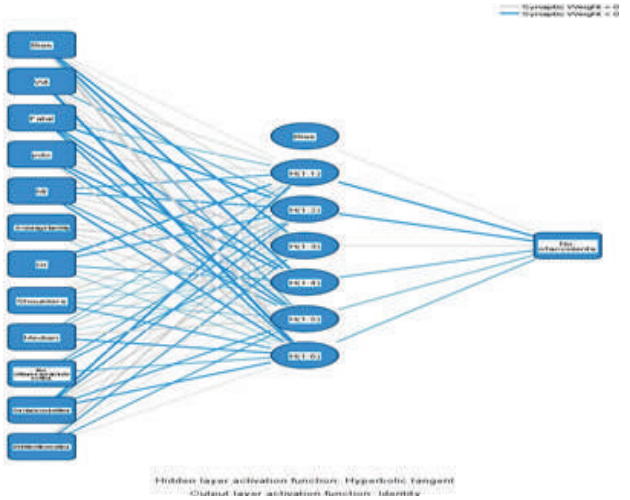

Fig. 5 Network Architecture for Panipat city by considering road factors excluding population and land use pattern

Hence,

Total Weight = (∑ Individual Weights) /90 × 100

On the bases of the final weight percent which have been calculated by the above criteria, the accident-prone level i.e. low, medium& high have been given to every location. Table 4 represents the three accident-prone levels as per final normalized weights.

The following given figures 5,6& 11 generated by the neural network which shows the network architecture for both the research cities by including and excluding population and land use pattern

Table 4 : Prioritization Table

Final Normalized Weights	Accident Prone Level
75-100	Low
40-75	Medium
0-40	High

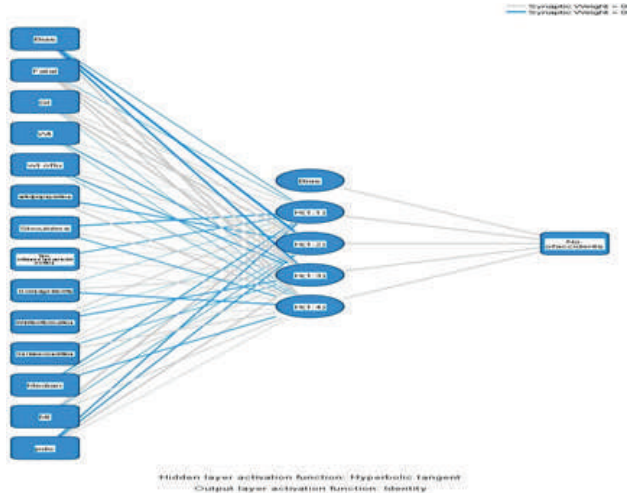

Fig. 6. Network Architecture for Panipat city by considering all road factors including population and land use pattern

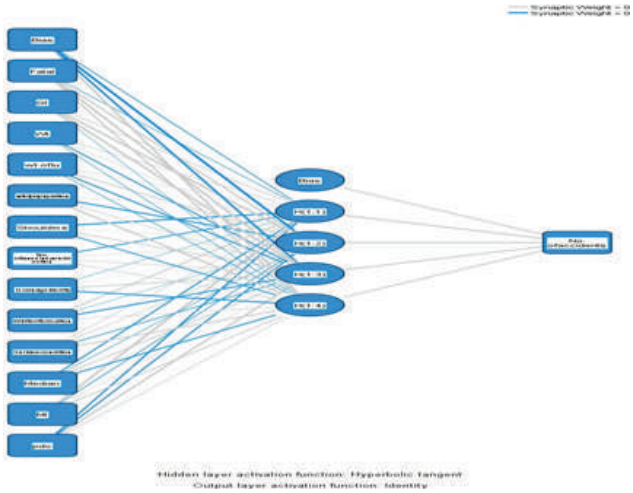

Fig. 7. Network Architecture for Rohtak city by considering road factors excluding population and land use pattern

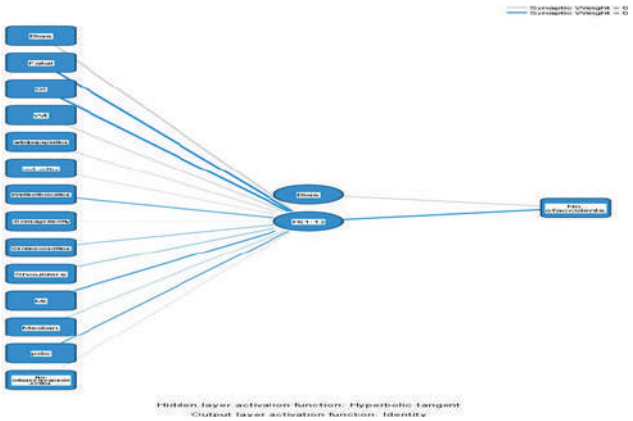

Fig. 8. Network Architecture for Rohtak city by considering all road factors including population and land use pattern

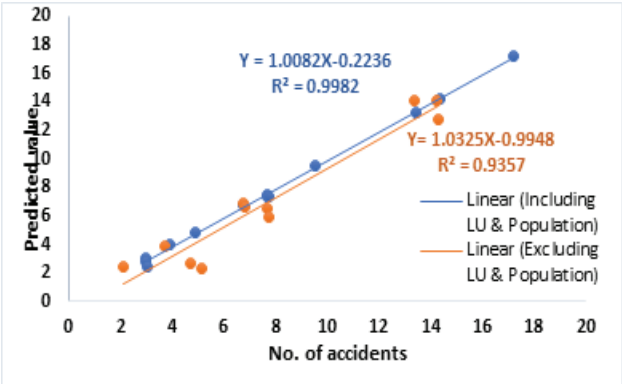

Fig. 9 Predicted value – No. of accidents relationship for Panipat city

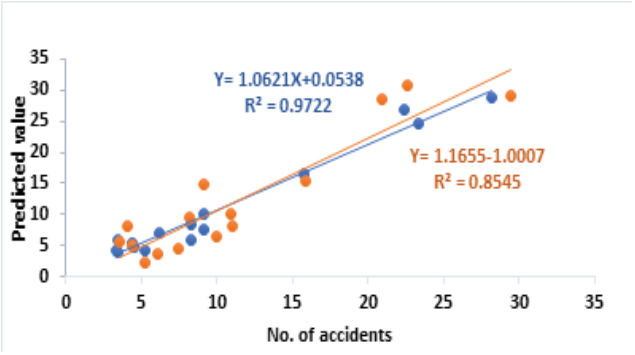

Fig. 10 Predicted value – No. of accidents relationship for Rohtak city

The above figure 12& 13 shows the comparison of regression value, R2 between the excluding and including land use & population factors for Panipat and Rohtak city.

Table 5. Predicted value – No. of accidents Equations

Sr. No.	City	Road Factor	Equation
1	Panipat	Excluding LU & Population	Y = 1.0325x - 0.9948
		Including LU & Population	Y = 1.0082x - 0.2236
2	Rohtak	Excluding LU & Population	Y = 1.1655x - 1.0007
		Including LU & Population	Y = 1.0621x + 0.0538

RESULTS AND DISCUSSION

From the detailed analysis of 5year accident data of both research area i.e Panipat and Rohtak city , total impact on the blackspots of population and land use The following observation can be drawn from the study:

1. A total of 21 accident-prone locations were found in Panipat City and 29 accident-prone locations were found in Rohtak City from 2018 to 2022.
2. In terms of the KDE (Kernel Density Estimation), the Sanjay Chowk on the stretch of Delhi Chandigarh highway NH-44 was identified as in the red zone (very high kernel density) which means the frequency of accidents was higher than the order locations, Sky lark to PVR stretch comes under the orange zone (High kernel density).
3. In Rohtak City, the Hisar bypass chowk & Jind bypass chowk have come under in red zone, where the bandwidth of the red zone in Hisar bypass chowk have higher than the Jind bypass chowk.
4. As per the MoRTH guidelines, a total of 5 and 9 blackspots have been identified in Panipat city and Rohtak city repectively.
5. As per the table 4 of the accident prone level all the selected blackspots in Rohtak lies in the medium level except Shukhpura chowk which has been in low accident prone level. Similarly, in Panipat Platinum Textile World, Assandh flyover have lies under the low accident prone level and rest eleven locations have in medium level.
6. It is observed from the relationships between predicted value – no. of accidents for Panipat, the regression value R2=0.93, by adding Population & Land use pattern the regression value R2=0.99 has increased up to 0.6 or 6 % and for Rohtak the regression value R2=0.85, by adding Population & Land use pattern the regression value R2=0.97 has increased up to 0.12 or 12%. The impact of adding two new factors i.e. Population & Land use pattern in the road prioritization weights in Rohtak almost double than the Panipat city.
7. The reason of the greater impact of LU & population has be the segregation of the data, the location of the blackspots have been distributed within the whole city , where the variation can be seen in the LU& population data, but in Panipat city, the maximum number of accidents occurred on the same stretch and lesser location of the blackspots compare as Rohtak i.e. on Delhi Chandigarh highway (NH-44), so that the data of LU & Population could not change.

CONCLUSIONS

The study presented in the dissertation is conducted to predict the impact of the LU& Population on the blackspot locations. The following main conclusions are drawn from this work:

i. The identification and analysis of accident black spots help in identifying the stretches were accidents are more and these spots reduce the road safety in general. The spot on the road were traffic accidents frequently occur is termed as black spot.

ii. Using GIS generated maps seems to be convenient for the identify the location of the accidents and also understood the land use / land lover pattern of the area.

iii. The predicted impact of the population and land use pattern on the blackspots have been increased for Rohtak city.

iv. Information derived from land use& land cover change and population can be helpful in reduce the chances of occurring the blackspots at planning stage.

REFERENCES

1. MORTH, “Road accidents in India 2022. Transport Research Wing of Ministry of Road Transport and

Highways of India. https://morth.nic.in/road-accident-in-india," 2023.

2. P. Chaudhary and G. Singh, "Analysis of Accident Data and Identification of Blackspots on National Highway 44 Between Kundli and Panipat, Haryana," International Research Journal of Engineering and Technology, vol. 09, no. 12, pp. 1255–1270, 2022, [Online]. Available: www.irjet.net

3. T. K. Anderson, "Kernel density estimation and K-means clustering to profile road accident hotspots," Accid Anal Prev, vol. 41, no. 3, pp. 359–364, 2009, doi: 10.1016/j.aap.2008.12.014.

4. P. B. Parmar, A. A. Amin, and L. B. Zala, "Black Spot Analysis Using QGIS for S.P. Ring Road, Ahmedabad," International Research Journal of Engineering and Technology (IRJET), vol. 05, no. 05, pp. 3186–3192, 2018.

5. S. Nuli, K. Rohan, and C. Joshnavi, "A Study on Road Safety Audit and Black Spot Identification," IOP Conf Ser Earth Environ Sci, vol. 1086, no. 1, 2022, doi: 10.1088/1755-1315/1086/1/012028.

6. Y. Liu, "Highway traffic accident black spot analysis of influencing factors," ICTE 2013 - Proceedings of the 4th International Conference on Transportation Engineering, pp. 2295–2300, 2013, doi: 10.1061/9780784413159.333.

7. Anusha SP, "Prioritization of Accident Black Spots in Kerala," Int J Innov Sci Res Technol, vol. 3, no. 11, pp. 210–215, 2018, [Online]. Available: www.ijisrt.com

8. A. Kumar, A. S. Chauhan, A. Thakur, K. Singh, and A. Tiwary, "Black spot analysis on NH-21A," Indian J Sci Technol, vol. 9, no. 44, 2016, doi: 10.17485/ijst/2016/v9i44/105250.

9. M. Gibin, P. Longley, and P. Atkinson, "Kernel density estimation and percent volume contours in general practice catchment area analysis in urban areas," the Proceedings of GISRUK, vol. C, no. April 2007, pp. 11–13, 2007.

10. J. Gelb, "spNetwork: A Package for Network Kernel Density Estimation," R Journal, vol. 13, no. 2, pp. 561–577, 2021, doi: 10.32614/RJ-2021-102.

11. J. Olusina and W. Ajanaku, "Spatial Analysis of Accident Spots Using Weighted Severity Index (WSI) and Density-Based Clustering Algorithm," Journal of Applied Sciences and Environmental Management, vol. 21, no. 2, p. 397, 2017, doi: 10.4314/jasem.v21i2.22.

12. I. A. Mir, A. A. Khan, G. Singh, and S. Dass, "Accident Analysis: A case study of J&K," NeuroQuantology, vol. 20, no. August, pp. 480-486 |, 2022, doi: 10.14704/nq.2022.20.9.NQ440050.

13. S. Tewatia, "Traffic Accident Data Analysis at Section from Sarai Khawaja to Old Faridabad of New Nh-44 (Old Nh-2) Including Bypass in Harayana Using GIS," Int J Sci Res Sci Technol, vol. 6, no. 3, pp. 87–96, 2019, doi: 10.32628/ijsrst196313.

14. A. P. Akgüngör and E. Doğan, "Estimating road accidents of Turkey based on regression analysis and artificial neural network approach," Advances in Transportation Studies, vol. 16, no. 16, pp. 11–22, 2008.

15. M. Y. Jamil, M. M. Rahman, and S. Sharmin, "Accident Hotspot Identification Using Geometric Problems And Characteristics In Selected Road Of The Dhaka-Aricha Highway (N5)," Journal of Transportation Engineering and Traffic Management, vol. 2, no. 3, pp. 1–17, 2021, doi: 10.5281/zenodo.5541199.

16. B. Persaud, C. Lyon, and T. Nguyen, "Empirical Bayes procedure for ranking sites for safety investigation by potential for safety improvement," Transp Res Rec, no. 1665, pp. 7–12, 1999, doi: 10.3141/1665-02.

17. T. S. L. Sowmya, A. Ramesh, B. N. M. Rao, and M. Kumar, "Black Spot Identification and Audit Analysis for Heterogeneous Traffic Conditions in Hyderabad City ◈ a Case Study," i-manager's Journal on Structural Engineering, vol. 4, no. 3, pp. 34–42, 2015, doi: 10.26634/jste.4.3.3729.

18. L. T. Truong and S. V. C. Somenahalli, "Using GIS to identify pedestrian- vehicle crash hot spots and unsafe bus stops," J Public Trans, vol. 14, no. 1, pp. 99–114, 2011, doi: 10.5038/2375-0901.14.1.6.

19. D. Delen, R. Sharda, and M. Bessonov, "Identifying significant predictors of injury severity in traffic accidents using a series of artificial neural networks," Accid Anal Prev, vol. 38, no. 3, pp. 434–444, 2006, doi: 10.1016/j.aap.2005.06.024.

20. R. and M. S. Gupta, "Accident Black-Spot Validation using GIS Abstract : About the Authors :," 2014.

21. A. H. Sanath, T. R. Nikhil, and Y. Lokesh, "Prioritization of black spots in east Bangalore & improvements of geometrics to black spot in outer ring road," International Journal of Civil Engineering and Technology, vol. 9, no. 8, pp. 1564–1574, 2018.

22. C. Zhang, Y. Shu, and L. Yan, "A Novel Identification Model for Road Traffic Accident Black Spots: A Case Study in Ningbo, China," IEEE Access, vol. 7, pp. 140197–140205, 2019, doi: 10.1109/ACCESS.2019.2942647.

23. I. Liyamol, A. Shibu, and M. S. Saran, "Identification and analysis of accident black spot using GIS," Int J Innov Res Sci Eng Technol, vol. 2, no. 1, pp. 131–140, 2013.

24. O. Kennis Verkeersonveiligheid, "Black Spot Analysis Methods: Literature Review RA-2003-07 K. Geurts, G. Wets," 2003.

25. P. R. Vyas, M. L. Honnappanavar, and B. H B, "Identification of black spots for safe commuting using weighted severity index and GIS," International Journal of Advanced Structures and Geotechnical Engineering, vol. 04, no. 01, pp. 2319–5347, 2015.

26. D. Mandloi and R. Gupta, "Evaluation of accident black spots on roads using Geographical Information Systems (GIS)," Map India, no. October, 2003.

27. L. T. Truong and S. V. C. Somenahalli, "Using GIS to identify pedestrian- vehicle crash hot spots and unsafe bus stops," J Public Trans, vol. 14, no. 1, pp. 99–114, 2011, doi: 10.5038/2375-0901.14.1.6.

28. K. Bauer and D. Harwood, "Statistical models of at-grade intersection accidents," Report No. FHWA-RD-99-094, Federal Highway Administration, no. March, p. 1996, 2000, [Online]. Available: http://trid.trb.org/view.aspx?id=478509

29. N. Deshpande and I. Chanda, "Accident Mapping And Analysis Using Geographical Information Systems," International Journal of Earth Sciences and Engineering, vol. 04, no. 06, pp. 342–345, 2011.

30. Haryana Police FIRs, "available at ." [Online]. Available: https://haryanapolice.gov.in/login

31. Y. S. Lokesh, M. A. Salim, and A. B. Siswanto, "Prioritization of black spots in east Bangalore & improvements of geometrics to black spot in outer ring road," 2018.

32. H. F. Bayata, F. Hattatoglu, and N. Karsli, "Modeling of monthly traffic accidents with the artificial neural network method," International Journal of Physical Sciences, vol. 6, no. 2, pp. 244–254, 2011, doi: 10.5897/IJPS10.606.

Exploring Properties of Porous Concrete for a Structure to Safeguard Trees and in Other Applications

Ashok B. More
HOD & Professor
Department of Civil Engineering
D.Y.Patil College of Engineering, Akurdi
Pune, Maharashtra

Neha Bagdiya
Assistant Professor
Department of Civil Engineering
D.Y.Patil College of Engineering, Akurdi
Pune, Maharashtra
✉ neha.bagdiya@gmail.com

Nitish M Sanap
Gharpure Engineering and Construction Pvt Ltd.
(GECPL)

ABSTRACT

There is currently a global trend towards the installation of 'Tree Guard' structures. This trend is impacting various aspects of society, economy, and the environment. The adoption of these precast components has led to reduced soil pollution around the base of trees, improved tree watering practices, and alleviated traffic concerns caused by trees in narrow roadways. When trees are situated near highways or in cramped road areas, water accumulation occurs, disrupting traffic and causing root damage. However, the implementation of tree guards mitigates these issues over time. These tree guards find utility in public areas such as shopping complexes, residential neighborhoods, industrial zones, and community spaces. They are manufactured using porous concrete, which facilitates water permeation, thereby enhancing water management. These precast units are robust, long-lasting, and lightweight, divided into four sections for easy placement and assembly.

The production of these tree guards involves curing 150mm x 150mm x 150mm cube-shaped porous concrete specimens in water for 7, 14, and 28 days. Subsequently, laboratory tests are conducted to assess compressive strength and permeability. It has been observed that increasing the quantity of coarse aggregate in the concrete mix leads to higher porosity but decreased compressive strength. Conversely, reducing the percentage of coarse aggregate results in a significant increase in compressive strength. These factors directly impact the strength, porosity, permeability, hydraulic efficiency, and durability of porous concrete.

KEYWORDS *: Porous concrete, Compressive strength, Permeability, Void ratio, Safeguard trees.*

INTRODUCTION

The construction sector carries substantial social, economic, and environmental consequences. Currently, the trend of erecting 'Tree Guard' structures is gaining momentum globally. The utilization of these prefabricated elements has led to reduced soil pollution in the vicinity of tree bases, improved tree hydration practices, and mitigated traffic issues caused by trees in nearby roadways. Water accumulation and congestion occur when trees are planted adjacent to highways or in narrow lanes, disrupting traffic flow and root systems. Nonetheless, the adoption of tree guards offers a solution to these challenges over time. These protective structures find applicability in various public spaces such as shopping centers, industrial complexes, residential neighborhoods, and communal areas. Additionally, these prefabricated components boast durability and resilience, ensuring prolonged effectiveness.

For controlling storm water runoff and safeguarding the environment, porous concrete is a dependable solution.

Because pervious concrete has open cell structures that allow storm water to permeate the surface and into the earth below, it reduces pollution and flooding when used for pavement. It has been discovered that enhanced porosity concrete, an alternative to conventional pervious concrete, is even more successful at managing storm water. Because of its increased porosity, storm water can seep into the concrete even more quickly. All things considered, improved porosity concrete and pervious concrete are great options for controlling storm water runoff and safeguarding the environment. Concrete's porosity does not meet our requirements if the void content is less than 15% since the voids are not connected enough to permit quick percolation. Therefore, for sufficient strength and permeability, the concrete mixture in this article has a 20% porosity. Because there is not enough connectivity between the voids to permit percolation, there is less percolation throughout the concrete for void contents less than 15%. The characteristics and ratio of the materials used, along with the compaction technique applied during the pouring process, define the density of permeable concrete. Because there isn't enough connectivity between the voids to enable quick percolation, there isn't much percolation through the concrete for void contents lower than 15%. The qualities and ratios of the materials used, along with the compaction technique utilized, affect the density of permeable concrete.

Benefits of Porous Concrete

This precast part is also used to unite trees and a sidewalk.

In accordance with the specifications of the EPA Storm Water Phase II Final Rule, pervious concrete pavement systems offer a useful storm water management tool. Phase II rules include techniques and programs to assist in reducing the quantity of pollutants in our waterways.

When it rains, oil, antifreeze, and other car fluids are collected by impermeable pavement, especially parking lots, and can end up in streams, lakes, and seas. Limits on the pollutant levels in our lakes and streams are imposed by EPA Storm

Water Rules. Two primary methods have been contemplated by local authorities to comply with these regulations. Two primary purposes for porous concrete exist.

i. Decrease an area's total runoff

ii. Lower the quantity of pollutants in runoff

Major applications of Porous Concrete

- Low-volume pavements
- Residentialroads, alleys, and driveways
- Sidewalks and pathways
- Parking areas
- Low water crossings
- Tennis courts
- Sub base for conventional concrete pavements
- Slope stabilization
- Well linings
- Hydraulic structures
- Pavement edge drains and Tree gratesin sidewalks

PROBLEM STATEMENT

The escalating need for pollution mitigation, economic stability, and water conservation has heightened awareness of the environmental impact of such endeavors. Among the methods to safeguard trees without causing harm to them or any part of their structure is the implementation of a simple, permanently installed structure at the tree base. This protective apparatus not only serves a functional purpose but also adds aesthetic appeal akin to decoration. Whether in parks, gardens, or even within agricultural estates and hospitality venues, trees can be safeguarded effectively, enhancing water management practices. These tree guards exhibit exceptional durability and are utilized to bridge gaps between footpaths and trees, further enhancing their utility.

The increasing demand for water management, tree conservation, economic stabilization, and pollution control has increased awareness of the impact these activities have on the environment. One method by which we can safeguard trees without endangering them or any of their components. It is easy to permanently settle the construction at the base of the tree. Additionally, it appears respectably decorative

on the Design and Production of Tree Guard Precast Member utilizing Porous. Hotels can successfully manage water resources and safeguard trees in parks, gardens, and even within farm buildings. Tree guards have a very long lifespan. With the help of this precast element, the spaces between the walkway and the trees are also connected.

METHODOLOGY

One of the most crucial aspects of the project is the methodology. In essence, methodology is a process that must be carried out for the project to meet its application. A flow chart is used for this project to illustrate the steps that must be carried out by carrying by taking into account a case study on a campus of an educational building. The procedures that were taken in order to design the tree guard are briefly described in the flowchart that follows. First, the residential and educational areas were where the issue was first discovered.

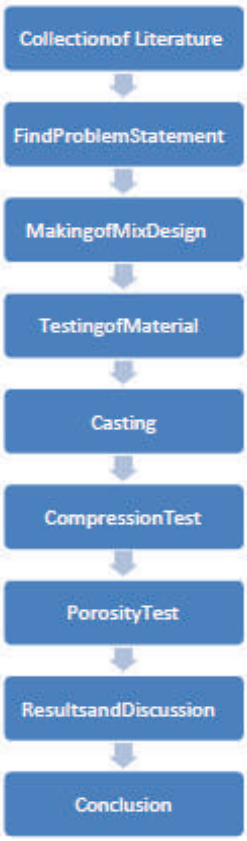

Chart 1: Flowchart for Methodology

Next, the porous concrete mix design is created so that the tree guard will both protect the tree and allow groundwater to recharge. Two mix designs, with a cement to aggregate ratio of 1:4 and 1:6, were created. To determine the concrete cubes' porosity and compressive strength, a large number of cubes and beams were cast. It was determined what the compressive strength was after 7, 14, and 28 days. To determine the porosity of concrete, a beam is casted. In this case, the porosity and compressive strength of the concrete are taken into account when creating the porous concrete mix design. The 1:4 ratio porous concrete was inserted into the tree guard mold.

MATERIALS AND METHODS

Cement

The cement used for the preparation of porous concrete is of OPC53 grade. The amount and type of cement used in porous concrete can impact its performance, including its strength, permeability, and durability. For example, the compressive strength of porous concrete can be improved by increasing the cement content, but may also reduce its permeability. Initial and final setting times, fineness, compressive strength, specific gravity, etc. are some of the tests done on cement.

Table 1. Chemical composition of Cement

Chemicalanalysis	Cement
Al_2O_3	4.53
SiO_2	18.65
MgO	0.84
Fe_2O_3	4.75
SO_3	2.8
CaO	66.74
LossofIgnition	1.05

Table 2. Chemical composition of Cement

Properties	Values
Specific gravity	3.14
Bulk density	1121kgperm3
Fineness	227sq.per kg
Initial configuration time	35Minutes
Final configuration Time	240 Minutes

Aggregates

In this paper the aggregates used for the manufacture of porous concrete is of 10 mm. The shape of coarse aggregates is crushed angular aggregates. Some general properties of coarse aggregates like bulk density, impact strength, crushing strength, void content, specific gravity etc. are described in below table no. 3

Table 3. Properties of Coarse aggregate

Properties	Values
Impact strength	26.5%
Crushing strength	25.4%
Content of voids	37.17%
Specific gravity	2.64
Bulk density	1583.34kg/m3

Table 4. Analysis of sieve for 10mm aggregates

Indian standard Sieve in mm	Passing % for single-sized aggregate of Nominal sizeas per Table 2 of IS:383
12.5	100
10	85-100
4.75	0-20
2.36	0-5

Water

The water used for casting and curing does not contain organic matter and drinking water is used according to IS 456-2000 clause 1.5.4. Amix design with too much water may lead the vacuum area to collapse and provide a nearly impenetrable concrete surface, while a mix design with insufficient water can produce a weak binder that is prone to splitting and breaking down. The ideal water cement ratio is between 0.27 and 0.30. Maximum water/cement ratio allowed for pervious concrete is 0.4.

MIX DESIGN

M30 grade Pervious Concrete mix percentage for 10 mm coarse aggregate:

- Cementtype:OPCgrade53,accordingtoIS8112
- Specific gravity of cement: 3.15
- Highest actual aggregate size:10mm
- Aggregate's specific gravity:2.65
- Coarse aggregate's water absorption:1.10
- Mix design aggregate type: Crushed angular aggregate
- Exposure condition: Severe
- Degree of supervision: Good
- Free moisture of coarse aggregate: Nil

Above mix design criteria is used for the preparation for each and every cubes. Table no.5 and table no.6 shows the proportions of materials for 1:6 and 1:4 water/ cement ratio respectively

Table 5. Typical mix design of pervious concrete for 1:6 Cement aggregate ratio

Materials	Proportions
Cement	273.6(Kg/m3)
Aggregate	1949.03(Kg/m3)
Water cement ratio	0.4

Table 6. Typical mix design of pervious concrete for 1:4 Cement aggregate ratio

Materials	Proportions
Cement	388.8(Kg/m3)
Aggregate	1814.6(Kg/m3)
Water cement ratio	0.4

RESULTS AND DISCUSSIONS

Compressive strength test

Fig. 2. Compression Test

Compression tests are used to determine performance of concrete blocks. This gives concrete block its compressive strength. Compaction is performed after

the concrete block shave been mixed, placed and cured. Below table displays the compressive strength and unit weight after 24 hours of cubes at age of 7, 14, and 28 days. An average of 3 samples is taken to calculate the final compressive strength to eliminate human or machine error.

Table no 7 Materials with their Proportions

Material	1:6	1:5	1:4	1:2
Cement	0.016416	0.0229824	0.016416	0.022982
Aggregate	0.098496	0.0919296	0.098496	0.05171
Water Cement ratio	0.0517104	0.0517104	0.0517104	0.098496

Fig. 2. Materials with their Proportions

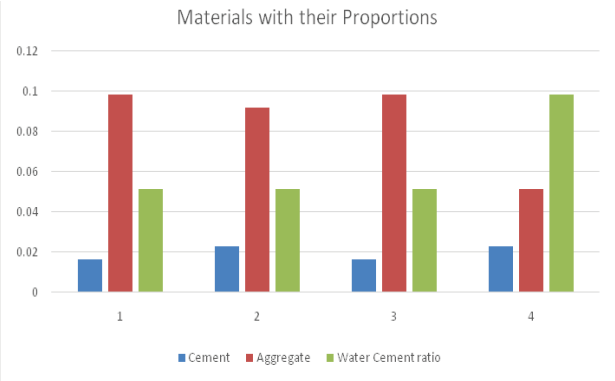

Table 8. Compressive strength and unit weight of standard porous concrete at 7 days

Age of concrete (days)	Compressive strength (MPa)
7	8.28
7	8.582
7	9.873

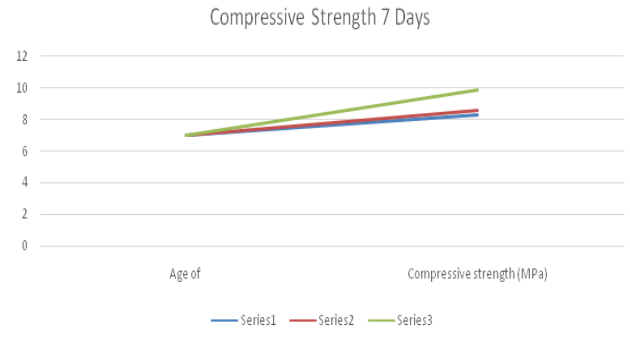

Fig 3. Compressive Strength of 7 Days

For a 1:4 mix ratio, the standard porous concrete's compressive strength after 7 days ranges from 8,280 MPa to 9,874 MPa which is shown in fig 4.

Table 9. Compressive Strength of 14 days

Age of concrete (days)	Compressive strength (MPa)
14	12.28
14	12.58
14	12.87

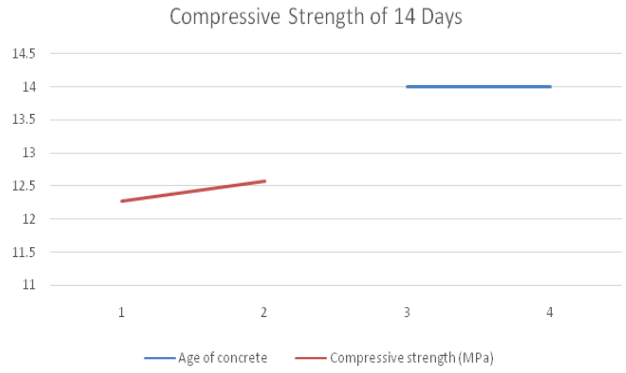

Fig 4. Compressive Strength of 14 Days

For a 1:4 mix ratio, the standard porous concrete's compressive strength after 14 days ranges from 12.28,12.58 MPa to 12.87 MPa which is shown in fig 5.

Table 10 Compressive Strength of 28 days

Age of concrete (days)	Compressive strength (MPa)
28	17.38
28	17.68
28	17.97

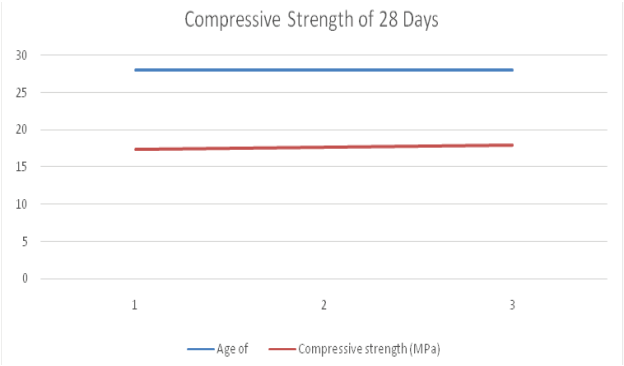

Fig 5 Compressive Strength of 28 Days

For a 1:4 mix ratio, the standard porous concrete's compressive strength after 28 days ranges from 17.38,17.68 MPa to 17.97 MPa which is shown in fig 6.

Table 7. Compressive strength and unit weight of typical porous concrete at 7 days for 1:6

Age of concrete (days)	Compressive strength (MPa)	After 24 hours, the unit weight in Kg/ m3
7	7.280	
7	6.582	1861.33
7	7.873	

Table 8. Compressive strength and unit weight of typical porous concrete at 14 days for 1:6

Age of concrete (days)	Compressive strength (MPa)	After 24 hours, the unit weight in Kg/ m3
14	10.4	
14	9.70	2026.37
14	10.84	

Table 9. Compressive strength and unit weight of typical porous concrete at 28 days for 1:6

Age of concrete (days)	Compressive strength (MPa)	After 24 hours, the unit weight in Kg/ m3
28	15.66	
28	16.03	2256.29
28	16.84	

Table 10. Compressive strength and unit weight of typical porous concrete at 7 days for 1:4

Age of concrete (days)	Compressive strength (MPa)	After 24 hours, the unit weight in Kg/ m3
7	8.280	
7	8.582	2112.34
7	9.873	

Table 11. Compressive strength and unit weight of typical porous concrete at 14 days for 1:4

Age of concrete (days)	Compressive strength (MPa)	After 24 hours, the unit weight in Kg/ m3
14	12.28	
14	12.58	2020.33
14	12.87	

Table 12. Compressive strength and unit weight of typical porous concrete at 28 days for 1:4

Age of concrete (days)	Compressive strength (MPa)	After 24 hours, the unit weight in Kg/ m3
28	17.38	
28	17.68	2181.43
28	17.97	

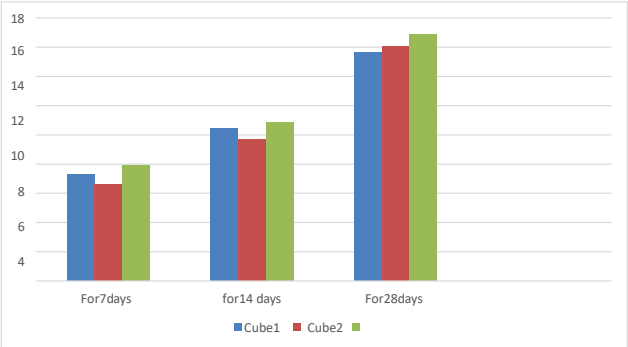

Fig.6. Compressive Strengthin MPa for 1:6

Standard compressive strength of porous concrete block is 10MPa, we got more strength for mix design of 1:6 i.e. 16.17 MPa.

Fig. 7. Compressive Strength in MPa for 1:4

Standard compressive strength of porous concrete block is 10 MPa, we got more strength for mix design of 1:4 i.e 17.67 MPa.

Table 13 Concrete in Days with their Compressive Strength

Concrete (days)	Compressive strength (MPa) (1:4) Proportion

7 Days	8.28	8.582	9.873
14 Days	12.28	12.58	12.87
28 Days	17.38	17.68	17.97

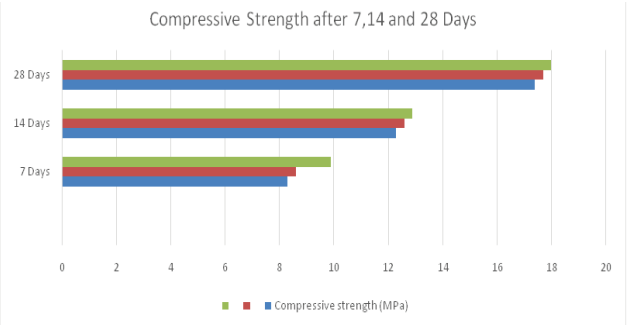

Fig. 8 Compressive Strength after 7.14 and 28 Days

From Table no 13 Concrete in 7,14 and 28 Days with their Compressive Strengths calculated and it is shown in above Figure. In 1:4 Proportion. For 7 days Compressive Strength is calculated 8.28,8.582 and 9.873 MPa.

Porositytest

Rapid Percolation - The process of flowing water through a porous media in which the infiltration rate is higher, then it is known as rapid percolation. Infiltration rate test is carried out to measure the porosity which may be defined in mm/sec.

Falling head method is used to find out porosity of concrete. Water heads of 300 mm were adopted for measuring porosity coefficient which is noted by "k", is calculated in mm/sec. Following table shows the comparison between the porosity of 1:6 and 1:4 water/ cement ratio.

Fig. 9. Porosity Test Setup

Table 13. Comparison between permeability coefficients for different mixes

Type of Mix	Permeability Coefficient mm/sec
1:6	5.4
1:5	6.04
1:4	6.2
1:3	4.6

After performing the porosity test for b1: 6,1 : 5,1 : 4 and 1:3 we calculated the values of permeability coefficient. These values are shown in above table 13.

Fig. 6. Porosity value comparison

In above graph horizontal axis shows the values of permeability coefficient and vertical axis shows the type of mix. It shows that permeability coefficient for 1:4 is more than 1:6 and 1:5.

CONCLUSION

- The water-to-cement ratio, aggregate-to-cement ratio, and size of coarse aggregate all play pivotal roles in determining the strength of permeable concrete.
- In terms of mix formulation, two critical factors for permeable concrete are void ratio and density. The compressive strength and permeability coefficient exhibit an inverse relationship.
- To enhance the compressive strength of permeable concrete, the addition of fines has demonstrated greater efficacy compared to substituting cementitious materials. Nevertheless, it's important to note that including fines and replacing cementitious materials will diminish the permeability capacity of permeable concrete.

- Density and void ratio are crucial parameters in the mix design of permeable concrete.
- Porosity is directly correlated with the void ratio, indicating that as the void ratio increases, so does porosity.
- Compressive strength and permeability share an inverse relationship, with higher porosity resulting in reduced compressive strength.
- Decreasing aggregate size results in lower porosity but can boost compressive strength.
- Due to its diminished compressive strength, permeable concrete pavement is not suitable for heavy-duty highways.
- An aggregate size ranging from 10-12.5 mm is recommended to achieve optimal compressive strength and desirable porosity in permeable concrete.
- Tree guards are highly beneficial for safeguarding trees and aiding groundwater recharge.
- There is a widespread understanding among respondents regarding the concept of tree guardians, reflecting an acknowledgment of the importance of tree protection.
- The presence of tree guards in the PCMC area varies inconsistently, with a considerable proportion of respondents seldom or never noticing them. This underscores the necessity for heightened awareness and implementation of tree guards to ensure consistent tree protection.
- The majority of respondents acknowledge the potential advantages of increased utilization of tree guards in enhancing tree health and survival rates, underscoring their significance. There exists a spectrum of opinions concerning the importance of design and aesthetics in tree guards, with some prioritizing functionality while others emphasize visually appealing designs.

REFERENCES

1. M. Uma Maguesvari, V.L. Narasimha, "Studies on Characterization of Pervious Concrete for Pavement Applications," Construction and Building Materials, vol. 136, pp. 272-282, 2017.
2. Ayyappan, A., Kumar, D.D., Sangeetha, G., Roshini, S., &Sivasangari, M. (Year). Experimental Study of Pervious Concrete. Journal Title, Volume(Issue), Page Range.
3. Chougale, M., Dehankar, S., Karmore, A., Jadhav, R., &Daingade, P. (Year). An Experimental Study on Pervious Concrete. Journal Title, Volume(Issue), Page Range.
4. Saha, S.K., Guntakalb, S.N., &Selvanc, S.S. (Year). Experimental Study on Behavior of Pervious Concrete in Strength and Permeability by Changing Different Parameters. Journal Title, Volume(Issue), Page Range.
5. Jagtap, P., Victor, O., & Verma, R. (Year). Experimental Study of Pervious Concrete. Journal Title, Volume(Issue), Page Range.Dash, S., & Kar, B. (Year). Environment-friendly Pervious Concrete for Sustainable Construction. Journal Title, Volume(Issue), Page Range.
6. Nadgouda, P.A., & Sawant, S. (Year). Experimental Studies on Pervious Concrete. Journal Title, Volume(Issue), Page Range.
7. Vijayalakshmi, R. (Year). Recent Studies on the Properties of Pervious Concrete: A Sustainable Solution for Pavements and Water Treatment. Journal Title, Volume(Issue), Page Range.
8. Panimayam, A., Chinnadurai, P., Anuradha, R., Rajalingam, M., Raj, Ajith, & Godwin. (Year). Experimental Study of Pervious Concrete using M-Sand. Journal Title, Volume(Issue), Page Range.
9. ASTM International. (2012). ASTM C1754/ C1754M-12 Standard Test Method for Density and Void Content of Hardened Pervious Concrete. USA
10. Kevern, J.T., Schaefer, V.R., Wang, K., & Suleiman, M.T. (2008). Pervious concrete mixture proportions for improved freeze-thaw durability. Journal of ASTM International, 5(2), 1-12.
11. Obla, K.H., & Sabnis, G.M. (2012). Pervious concrete for sustainable development. In G.M. Sabnis (Ed.), Green building with concrete Sustainable design and construction. CRC Press..
12. Kevern, J.T., Schaefer, V.R., & Wang, K. (2011). Mixture proportion development and performance evaluation of pervious concrete for overlay applications. ACI Material Journal, 108(4), July-August, 439-448.
13. Park, S.B., & Tia, M. (2004). An experimental study on the water-purification properties of porous concrete. Cement and Concrete Research, (34), 177-184.

Experimental Studies on High Performance Concrete Pavement Using Nano Particles and Blast Furnace Slag

Mamidi Srinivasan
Ph.D Scholar
Department of Civil Engineering
Jawaharlal Nehru Technological Univ. Coll. of Engg. Science & Technology
Hyderabad, Telangana
✉ msn9865@yahoo.co.in

P Sravana
Professor
Department of Civil Engineering
Jawaharlal Nehru Technological Univ. Coll. of Engg. Science & Technology
Hyderabad, Telangana
✉ sravana.jntu@gmail.com

ABSTRACT

This paper discusses how nanotechnology could revolutionize the infrastructure industry and enhance the performance of concrete. In particular, it looks at replacing some of the cement in High Performance Concrete (HPC) with ground-granulated blast furnace slag (GGBS) and Nano titanium dioxide (TiO2). The objective is to create concrete formulations that are more resilient, energy-efficient, and less sensitive to environmental conditions, especially for use in high-traffic areas and stiff pavements. The study looks at how different dosages of GGBS (30% and 40%) and TiO2 (0.5%, 1.0%, 1.5%, and 2%) affect the mechanical properties of M40 and M50 grade concrete. In order to determine the ideal replacement levels that produce the most desired mechanical qualities, the study will thoroughly evaluate the material's compressive, tensile, and flexural strengths at 28, 90, and 180 days after curing. The creation of long-lasting and highly effective concrete mixtures will be greatly aided by the findings of this study. The effects of GGBS and TiO2 on the characteristics of concrete allow engineers and construction professionals to choose the right materials for important infrastructure projects with knowledge. The findings also open up new avenues for study and advancement in the field of nanotechnology-enhanced concrete materials.

KEYWORDS *: Nanotechnology, High Performance Concrete (HPC), Nano Titanium Dioxide (TiO2), Ground Granulated Blast Furnace Slag (GGBS), Mechanical properties of concrete.*

INTRODUCTION

High-performance concrete (HPC) is a specialized form of concrete engineered to deliver superior strength, durability, and workability compared to conventional concrete. Its enhanced mechanical and physical properties make it well-suited for demanding applications such as high-rise buildings, bridges, tunnels and highway pavements particularly in severe environmental conditions. HPC offers significant long-term benefits. Its superior durability and resistance to degradation reduce the need for frequent maintenance and repairs, leading to substantial cost savings over the structure's lifecycle. Additionally, its increased strength allows for the use of less reinforcing steel, further optimizing construction costs.

As the world grapples with climate change and increasing infrastructure demands, HPC emerges as a crucial tool for building resilient and sustainable structures. By embracing this advanced material, we can create infrastructure that is both durable and environmentally responsible.

Study Objective

- To conduct research and offer insights into the optimal ratios of mineral additives like TiO_2 (Rutile & Anatase) and GGBS that aid in formulating concrete mixes for various construction applications such as PQC (Pavement Quality Concrete) rigid pavements for state and national highways.
- To evaluate the mechanical properties and

characteristics of conventional concrete and concrete with optimal ratios of TiO_2 and GGBS.

LITERATURE REVIEW

Nitin Kawle et al. (2023) studied the impact of Nano TiO_2 on M30 grade concrete and found that compressive strength was highest with 2% TiO_2 after seven days, 3% after 14 days, and 1% after 28 days. Flexural strength peaked at 2% TiO_2. Both strengths increased initially but decreased beyond certain limits, with 1-3% TiO_2 addition recommended for optimal strength.

Garima Rawat, Sumit Gandhi, and Yogesh Iyer Murthy (2022) assessed the effects of nano-titanium dioxide on M30-grade concrete, reducing workability, flowability, and setting times. Strength increased to a limit of 1-4%, influenced by mix proportions and other factors. Nano-titanium dioxide generally reduced water absorption and permeability, with the optimal concentration for reduced absorption being 4%, though some studies suggested lower values. The research did not explore tensile and flexural strength or other durability aspects.

Rakshak Jandial and Dr. Sanjeev Naval (2023) experimentally studied the split tensile strength of M20-grade concrete with nano-TiO_2 and fly ash using SEM analysis. They observed that split tensile strength increased with 1.5% TiO_2 replacement but decreased with further replacement. The study did not cover other mechanical properties or durability aspects.

Hilal Ahmad Wani, Sukhwinder Singh, and Tahir Mohammad Bhat (2020) investigated the flexural behavior of concrete beams with nano-TiO_2 and GGBS. Replacing cement with 1-2% TiO_2 and 10-30% GGBS increased flexural strength, with the optimum at 1% TiO2 and 10% GGBS. The study did not include compression tests, water absorption, workability, tensile strength, or durability.

Krishnan U. Ambika Kumari, Sanal Kumar, and En-Hua Yang (2021) examined the self-cleaning performance of nano-TiO_2-modified metakaolin-based geopolymers. They found that TiO_2 improved mechanical strength by 41% at 10% inclusion, enhanced density and surface properties, and increased solar reflectance and super-hydrophilicity after sunlight exposure. TiO_2 also provided photocatalytic properties, aiding dye decomposition. Specimens with 10% TiO_2 had over 80% surface reflectance recovery after UV, while 5% or more showed full recovery after sunlight. The study did not address water absorption, workability, tensile, or flexural strength.

Literature Gap

Some gaps have been identified while reviewing the above research papers.

1. There seemed to be limited research studies conducted on combining additives like TiO2 and GGBS on M40 and M50 grades of concrete. Hence, this study will try to investigate an optimum dosage of TiO_2 and GGBS and explore the workability, compressive strength, flexural strength, and split tensile strength of concrete using TiO_2 nanoparticles and GGBS at 28, 90, and 180 days.
2. Through this study, durability properties like acid resistance, sulfate attack resistance, RCPT, sorptivity, water permeability, and freeze and thaw effect of the concrete using TiO_2 nanoparticles and GGBS at 28, 90, and 180 days will also be conducted.

MATERIALS

Materials used

All the materials utilized in the present study are detailed in the table below.

Material	Description	Source
Cement	OPC 53 grade	Ultratech
Course aggregate	Zone II	Hyderabad
Fine aggregate		
TiO_2	Mineral admixtures	NCI Hyderabad
GGBS		JINDAL
SP430	Chemical admixture	FOSROC
Water	JNTUH bore well	Hyderabad

Mineral admixtures in Concrete Pavements

Admixtures are crucial additives that enhance the performance and durability of concrete used in pavements. By improving resistance to heavy traffic, extreme weather, and other environmental factors

help create more resilient and long-lasting highway pavements. These additives strengthen the concrete's structure, reducing the risk of cracking, scaling, and other forms of deterioration.

Nano Titanium Dioxide (TiO_2)

Nano-titanium dioxide (TiO_2) is a versatile material that, when incorporated into concrete, transforms it into a multifunctional material known as photocatalytic concrete. Additionally, TiO_2-enhanced concrete exhibits self-cleaning properties, reducing the need for frequent cleaning and maintenance. Research suggests that TiO_2 may also enhance the mechanical properties of concrete, potentially improving its strength, durability, and resistance to wear and tear.

Mineral admixtures in Concrete Pavements

Admixtures are crucial additives that enhance the performance and durability of concrete used in pavements. By improving resistance to heavy traffic, extreme weather, and other environmental factors help create more resilient and long-lasting highway pavements. These additives strengthen the concrete's structure, reducing the risk of cracking, scaling, and other forms of deterioration.

Nano Titanium Dioxide (TiO_2)

Nano-titanium dioxide (TiO_2) is a versatile material that, when incorporated into concrete, transforms it into a multifunctional material known as photocatalytic concrete. Additionally, TiO_2-enhanced concrete exhibits self-cleaning properties, reducing the need for frequent cleaning and maintenance. Research suggests that TiO2 may also enhance the mechanical properties of concrete, potentially improving its strength, durability, and resistance to wear and tear.

Table 1. Physical Properties of Nano Titanium Dioxide (TiO_2).

Parameter	Result	
	Rutile	Anatase
Appearance	White Powder	White Powder
Surface Area	12 m^2/g	9.21 m^2/g
Average particle size	19.6 nm	25 nm
Shape	Spherical	Spherical

Fig. 1. Titanium Dioxide (TiO_2)

Ground Granulated Blast Furnace Slag (GGBS)

Ground Granulated Blast Furnace Slag (GGBS) is a sustainable and durable construction material derived from the iron and steel industry. By partially replacing Portland cement in concrete, GGBS offers several advantages:

- Improved Durability: GGBS enhances concrete's resistance to chemical attacks, especially from sulfates and chlorides, and reduces the risk of alkali-silica reaction (ASR).
- Environmental Sustainability: GGBS reduces the demand for energy-intensive Portland cement production, lowering the overall carbon footprint of concrete.
- Green Building Certification: The use of GGBS aligns with green building standards, contributing to projects' sustainability ratings and certifications.

By incorporating GGBS into concrete, we can build a more resilient and environmentally friendly infrastructure, reducing our reliance on traditional cement-based materials.

Table 2. Physical Properties of Ground Granulated Blast Furnace Slag (GGBS)

Parameter	Result
Appearance	Light Grey to White Color Powder
Specific Gravity	2.9
Average Surface Area	9.21 m2/g
Average Particle Size	2.8 nm
Source	JSW Plant Karnataka

Fig. 2. Ground Granulated Blast Furnace Slag (GGBS).

EXPERIMENTAL INVESTIGATION

Mix Design

In the current experimental investigation, the mix proportion for M30, M40, and M50 grades of concrete has been determined per IS10262: 2019. The tables below list the amounts of each component used in M30, M40, and M50 concrete.

Table 3. M30 Grade Concrete Mix Proportions (with TiO_2 Increment only).

(NT_0 -Nano Titanium Dioxide Zero Percent &

G_0 -GGBS Zero Percent)

Mix Designation	NT_0 G_0	$NT_{0.5}$ G_0	NT_1 G_0	$NT_{1.5}$ G_0	NT_2 G_0
W/C	0.42	0.42	0.42	0.42	0.42
Cement	352	351	349	347	345
TiO_2 Kg/m^3	0	1.76	3.52	5.28	7.05
TiO_2 %	0	0.5	1	1.5	2
GGBS Kg/m^3	0	0	0	0	0
GGBS %	0	0	0	0	0
Coarse Aggregate Kg/m^3	986	986	986	986	986
Fine Aggregate Kg/m^3	924	924	924	924	924
Water (lit)	148	148	148	148	148
Admixture (lit)	2.46	2.46	2.46	2.46	2.46

Table 4. M40 Grade Concrete Mix Proportions (with Optimized TiO_2 and GGBS)

Mix Designation	NT_0 G_0	$NT_{0.5}$ G_0	NT_1 G_0	$NT_{1.5}$ G_0	NT_2 G_0	NT_1 G_{30}	NT_1 G_{40}
W/C	0.38	0.38	0.38	0.38	0.38	0.38	0.38
Cement Kg/m^3	390	388	386	384	382	270	232
TiO_2 Kg/m^3	0	1.95	3.9	5.85	7.8	2.7	2.34
TiO_2 %	0	0.5	1	1.5	2	1	1
GGBS Kg/m^3	0	0	0	0	0	117	156
GGBS %	0	0	0	0	0	30	40
Coarse Aggrega te Kg/m^3	1316	1316	1316	1316	1316	1316	1316
Fine Aggregate Kg/m^3	596	596	596	596	596	596	596
Water (lit)	148	148	148	148	148	148	148
Admixture (lit)	2.73	2.73	2.73	2.73	2.73	2.73	2.73

Table 5. M50 Grade Concrete Mix Proportions

Mix Designation	NT_0 G_0	NT_1 G_{30}	NT_1 G_{40}
W/C	0.35	0.35	0.35
Cement Kg/m^3	423	292	251
TiO_2 Kg/m^3	0	2.96	2.58
TiO_2 %	0	1	1
GGBS Kg/m^3	0	126.9	169.2
GGBS %	0	30	40
Coarse Aggregate Kg/m^3	1236	1236	1236
Fine Aggregate Kg/m^3	628	628	628
Water (lit)	148	148	148
Admixture (lit)	2.96	2.96	2.96

Casting of Specimen

The cast iron molds were cleaned thoroughly, lubricated with mineral oil, and tightened securely. Concrete was poured in three layers onto a vibrating machine, with the top surface smoothed to the mold level.

To evaluate the concrete's mechanical properties, three types of specimens were cast:

- Compressive Strength Specimens: 150mm x 150mm x 150mm cubes.
- Split Tensile Strength Specimens: Cylinders with a diameter of 150mm and a height of 300mm.
- Flexural Strength Specimens: Beams measuring 100mm x 100mm x 500mm.

RESULTS

Concrete containing 0%, 0.5%, 1%, 1.5%, and 2% Rutile TiO_2 Nanoparticles and 0% GGBS underwent compressive strength tests, accordingly.

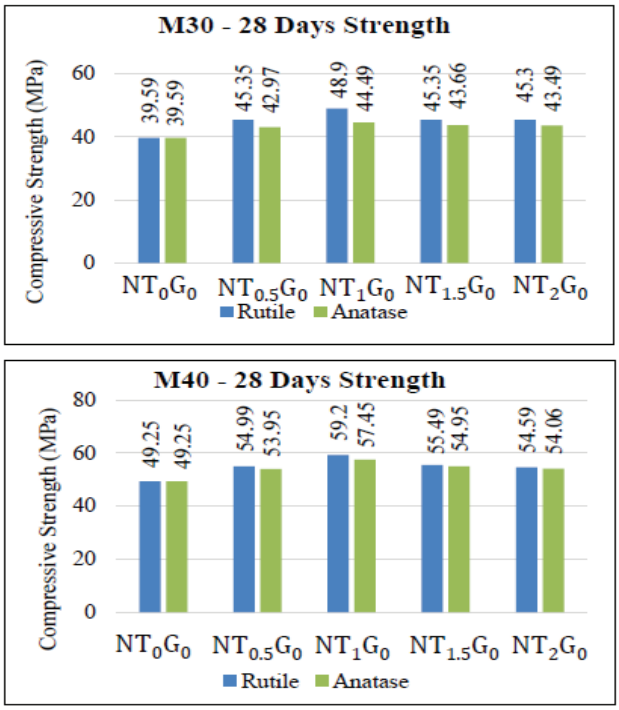

Fig. 3. Comparing Compressive Strengths of M30 and M40 for 28 Days

The M30 and M40 grades of concrete demonstrated the highest strength when 1% of the cement was replaced with TiO_2 nanoparticles. In all cases, TiO_2 (Rutile) consistently performed better than TiO_2 (Anatase). Hence, we consider that 1% of TiO_2 (Rutile) is the optimal dosage.

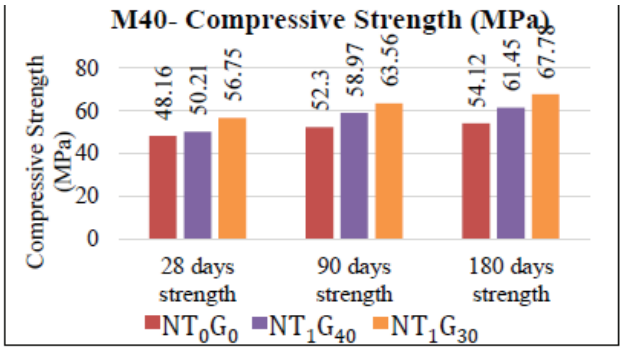

Fig 4. Comparing Compressive Strengths of M40 Grade Concrete for 28, 90, and 180 Days.

The results revealed that concrete with 30% GGBS and 1% TiO_2 performed better than concrete with 40% GGBS and 1% TiO_2.

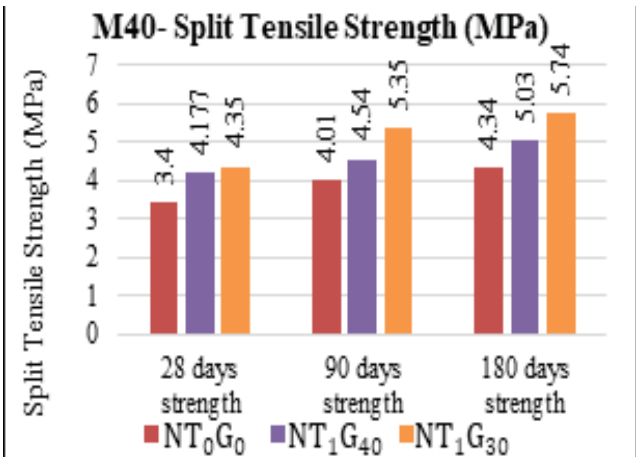

Fig. 5. Comparing Split Tensile Strength of M40 Grade Concrete for 28, 90, and 180 Days.

The finding revealed that concrete containing 30% GGBS & 1% TiO_2 had superior split tensile strength than concrete with 40% GGBS & 1% TiO_2.

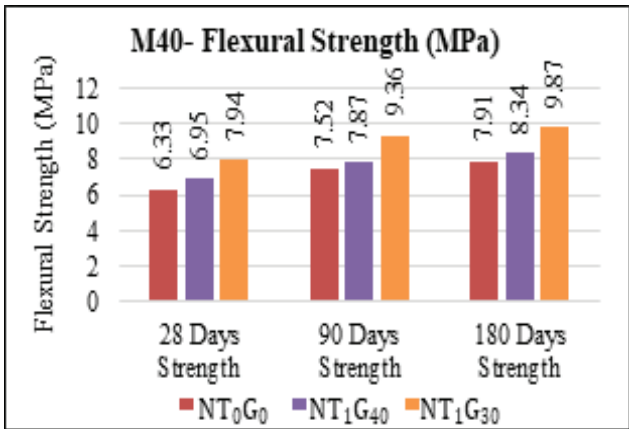

Fig. 6: Comparing Flexural Strength of M40 Grade Concrete for 28, 90, and 180 Days.

The findings revealed that concrete containing 30% GGBS & 1% TiO_2 had flexural strength compared to concrete with 40% GGBS & 1% TiO_2.

Optimal Proportion: As the results have proven that 1% TiO_2 is the optimal proportion, here we have considered doing tests for only 1% TiO_2 of cement replacement for M50 grade concrete mix.

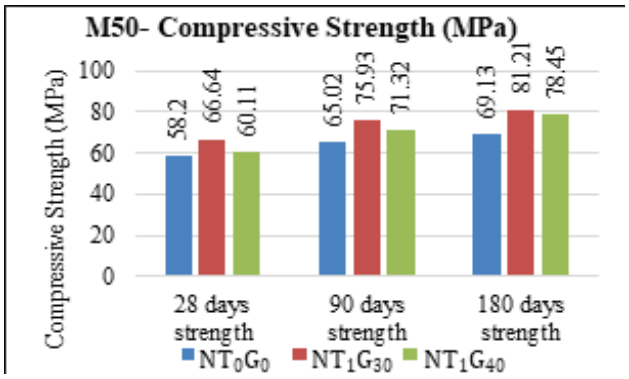

Fig. 7: Comparing Compressive Strength of M50 Grade Concrete for 28, 90, and 180 Days

The results revealed that concrete with 30% GGBS & 1% TiO_2 performed better than the concrete that contained 0% GGBS & 0% TiO_2.

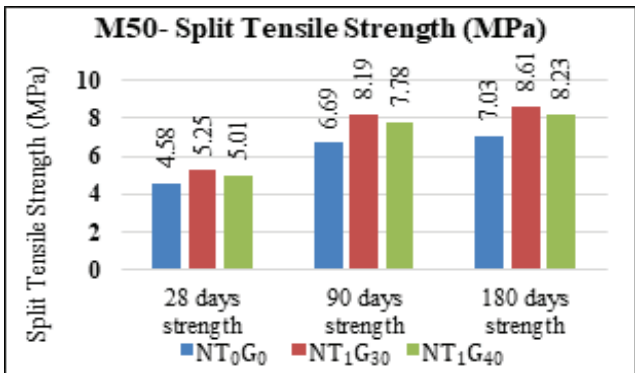

Fig. 8: Comparing Split Tensile Strength of M50 Grade Concrete for 28, 90, and 180 Days.

The findings revealed that concrete containing 30% GGBS & 1% TiO_2 had superior split tensile strength than concrete with 0% GGBS & 0% TiO_2.

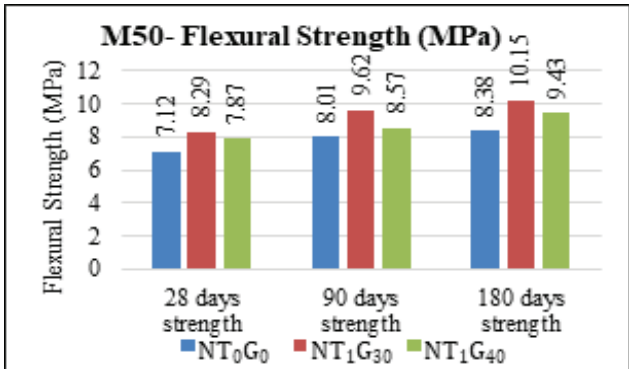

Fig. 9: Comparing Flexural Strength of M50 Grade Concrete for 28, 90, and 180 Days.

The findings revealed that concrete containing 30% GGBS & 1% TiO_2 had superior flexural strength than concrete with 0% GGBS & 0% TiO_2.

Effects of incremental and decremental dosage of mineral admixtures:

1. Initial Increase in Strength (Up to the Optimal Proportion).

Filler Effect: At low to moderate replacement levels, nanoparticles like TiO_2 and GGBS act as fillers in the concrete microstructure. They occupy the micro-pores and voids among the cement particles, creating a denser and more compact microstructure. This improved packing efficiency, thereby reducing the porosity of the concrete and increasing the material's durability and compressive strength.

Pozzolanic Reaction: GGBS and other mineral admixtures undergo a pozzolanic reaction, where they react with the calcium hydroxide (CH) produced during cement hydration to form additional calcium silicate hydrate (C-S-H). This reaction contributes to a denser matrix, improving strength and durability. By offering nucleation sites for the formation of C-S-H, TiO_2 nanoparticles can also improve hydration.

Improved Bonding: Adding nanoparticles can improve the bonding between the cement paste and aggregates. This stronger interfacial transition zone (ITZ) enhances the overall mechanical properties of the concrete.

2. Decrease in Strength Beyond the Optimal Proportion:

Excessive Admixture Disrupts Cement Hydration: When the quantity of TiO_2 nanoparticles or GGBS exceeds a certain level, it can interfere with the hydration process of the cement. High concentrations of admixtures may reduce the availability of calcium hydroxide, which is necessary for the pozzolanic reaction. As a result, there is less formation of calcium silicate hydrate (C-S-H), which is the primary source of strength in concrete.

Dilution Effect: Adding too much GGBS or other supplementary cementitious materials (SCMs) can reduce the mix's overall Ordinary Portland Cement (OPC) content. Since OPC is the primary binding agent responsible for strength development, its reduced proportion weakens the cement microstructure. This

dilution effect lowers strength as the mineral admixture percentage increases beyond the optimum level.

Evaluation of Mix Proportions

Based on the evaluation, M40 grade concrete was found to consistently outperform M50 in terms of split tensile, flexural, and compressive strength. Therefore, M40 is the recommended mix design for Pavement Quality Concrete (PQC) to ensure optimal durability and long-term performance.

Table 6. PQC MIX DESIGN for M40 Grade Concrete

Material	Mass (kg) Mix Design with Zero Replacement	Mass (kg) Mix Design with TiO_2 (1%) and GGBS (30%)
Nano TiO_2 (1%)	0	2.7
Cement	390	270
GGBS (30%)	0	117
Water (W/C = 0.38)	148	148
20mm Coarse Aggregates (CA)	790	790
10mm Coarse Aggregates (CA)	526	526
Fine Aggregates (FA)	596	596
Admixture (SP430)	3.4	3.4
Density (Kg/m3)	2453	2453
Mix Proportion	1: 1.53: 3.37	1: 2.21: 4.87

The mass of all materials (Concrete Mix Design) is shown in the table above. The mix is calculated per the IS 456:2000, IS 10262:2019, IRC 44 – 2017, IS 16714-2018 and MORTH (5th Revision).

CONCLUSION

This study involves extensive experimentation with concrete grades M30, M40, and M50 to partially replace cement with additional materials such as GGBS and Nano-TiO2 (Rutile and Anatase). The following are some critical key findings:

Optimization of TiO2 & GGBS

1. At 1% cement replacement with TiO2 nanoparticles, M30 and M40 grade concrete have exhibited maximum strength.
2. In all the cases, TiO2 Rutile consistently performed better than Anatase.
3. Concrete with 30% GGBS fared better than concrete with 40% GGBS.
4. As an optimal proportionate replacement of cement by weight, 1% TiO2 and 30% GGBS were used.

B. A detailed analysis of the mechanical properties among several mix designs was conducted.

1. M40 Grade Concrete: Refer to Table 4
2. M50 Grade Concrete: Refer to Table 5

Table 7. M40-Grade Concrete

Compressive Strength			
M40 Grade Concrete	Percentage growth over 28 days	Percentage growth over 90 days	Percentage growth over 180 days
M40- NT_0G_0	-	-	-
M40- NT_1G_{30}	**18**	**22**	**25**
M40- NT_1G_{40}	4	13	14
Split Tensile Strength			
M40- NT_0G_0	-	-	-
M40- NT_1G_{30}	**28**	**34**	**25**
M40- NT_1G_{40}	23	34	13
Flexural Strength			
M40- NT_0G_0	-	-	-
M40- NT_1G_{30}	**26**	**25**	**25**
M40- NT_1G_{40}	10	5	5

Table 8. M50-Grade Concrete

Compressive Strength			
M50 Grade Concrete	Percentage growth over 28 days	Percentage growth over 90 days	Percentage growth over 180 days
M50- NT_0G_0	-	-	-
M50- NT_1G_{30}	**14**	**16**	**17**
M50-NT_1G_{40}	3	10	14
Split Tensile Strength			
M50- NT_0G_0	-	-	-
M50- NT_1G_{30}	**15**	**23**	**23**
M50-NT_1G_{40}	10	16	17
Flexural Strength			
M50- NT_0G_0	-	-	-
M50- NT_1G_{30}	**16**	**20**	**21**
M50-NT_1G_{40}	11	7	13

From the above results, M40-grade concrete with 1% TiO2 & 30% GGBS is considered the best-performing concrete mix design.

REFERENCES

1. Nitin Kawle, Chavhan, S., Sarnaik, P Kachare, V., Pathak, S., & Khandelwal, R. (2023). https://www.jetir.org/papers/JETIR23059
2. Rawat, G., Gandhi, S., & Murthy, Y. I. (2022). https://doi.org/10.14256/jce.3291.2021
3. Jandial, R., & Naval, D. S. (2023). https://www.irjmets.com/uploadedfiles/paper/issue_3_march_2023/34117/final/fin_irjmets1678261924.pdf
4. Wani, H. A., Singh, S., & Bhat, T. M. (2020). https://www.irjmets.com/uploadedfiles/paper/volume2/issue_12._december_2020/5276/1628083212.pdf
5. Krishnan U, Ambika kumara, Sanalkumar, & Yang, E.-H. (2021). https://doi.org/10.1016/j.cemconcomp.2020.103847
6. Kaur, Inderpreet & Sharma, Sumit & Gupta, Sushant. (2019). https://www.irjet.net/archives/V6/i7/IRJET-V6I7323.pdf
7. Chandramouli, D. K., Chaitanya, J. S., Hymavathi, G., & Kumar, M. C. (2022). https://ijrpr.com/uploads/V3ISSUE7/IJRPR5843.pdf
8. Kumar, G. P., & Theja, A. R. (2023). https://doi.org/10.35940/ijrte.a1909.059120
9. Revathy, S., et al. (2019). https://troindia.in/journal/ijcesr/vol6iss3/433-448.pdf
10. Chaithra H L, Pramod K, & Dr. Chandrashekara A. (2015). https://doi.org/10.17577/ijertv4is051304
11. Liu, F., Zhang, T., Luo, T., Zhou, M., Ma, W., & Zhang, K. (2019). https://doi.org/10.3390/ma12213608
12. Ying, J., Zhou, B., & Xiao, J. (2017). https://doi.org/10.1016/j.conbuildmat.2017.05.168
13. Ambikakumari Sanalkumar, K. U., & Yang, E.-H. (2021). https://doi.org/10.1016/j.cemconcomp.2020.103847

Numerical Studies on Behavior of Strip Footing on Stabilized and Unstabilized Soil Slope under Different Soil Foundations

Rushikesh Langote
Research Scholar
Department of Civil Engineering
Government College of Engineering, Amravati
✉ rushi.langote@gmail.com

Anant I. Dhatrak
Associate Professor
Department of Civil Engineering
Government College of Engineering, Amravati

Sanket Uke
M.Tech Student
Department of Civil Engineering
Government College of Engineering, Amravati

ABSTRACT

Due to rising urbanization, unlimited land has become finite; making the availability of land for infrastructure projects a critical challenge. Foundations are frequently erected along slopes in a variety of civil engineering applications, including commercial structures, road infrastructure and bridge supports. But still, the stability and endurance of such structures at the slope edge is a difficult problem. The current work uses the finite element program MIDAS GTS NX to determine the strip footing's bearing capacity on stabilized and unstabilized soil slopes under varied soil foundations with steep soil slopes. Commercial residue, such as fly ash, is utilized to stabilize soil slope. The optimal dose of fly ash is determined based on laboratory data. Various soil models are prepared and analyzed in software to assess the influence of varied edge distances and soil foundations on the load carrying capacity of strip footings, and the outcomes are displayed using MIDAS GTS NX for stabilized and unstabilized situations. The test findings indicate that strip footing's carrying capability improves significantly with varied crest distance and for the stiff foundation conditions.

KEYWORDS *: Fly-ash, Stabilized, MIDAS-3D, Earthen slope, Embankment.*

INTRODUCTION

In a variety of civil engineering applications, foundations are frequently erected close to slopes, including structures, transmission towers, roadway pavement embankments, and bridge abutments. However, stability and long term performance of such structures near to slope facia is a difficult challenge to solve because both the long term performance and load carrying capabilities of such footings and embankments must be considered. Thus, for a long time, the idea of strengthening the earthen slope has been a primary area of study for researchers. Typical examples include applying chemical grouting, modifying the slope's surface, and employing geosynthetic layers as a kind of reinforcement, etc. The present investigation focuses on the use of waste products such as fly-ash as a stabilizing component for clay soil on various soil foundations. To improve natural soil's capacity to support more weight, fly ash is utilized as a stabilizing agent in the slope. The laboratory data is utilized to estimate the optimal fly ash dose for usage in the slope. The prototype soil model is tested for plane-strain conditions using MIDAS GTS NX, with the Non-linear Static method being employed for analysis. To provide good precision in the findings, the mesh is produced both for the soil model and the footing. Finer meshing is chosen to obtain accurate analytical results. Soil slope is built on three different soil foundations such as fly ash, clay, and sand. Analysis is performed for two distinct cases: unstabilized slope and stabilized slope. When it comes to an unstabilized soil slope, entire slope geometry is assigned with the

properties of Black cotton soil derived from laboratory testing, and in the other instance, stabilized soil properties are applied to analyze the required case. Several prototype models were examined to determine the impact of varying crest distances on load carrying capabilities. To acquire the best loading capacity value in each prototype model test, the other parameters were held constant while one parameter was changed. The spaces that exist between the slope's edge and the footing, as well as diverse soil foundations are among the several conditions investigated for load carrying capacity. Although many research projects have been conducted to investigate the behavior of slopes stabilized with different layers of geogrids as reinforcement, relatively little is known about stabilized soil slope instances.

The main objective of this study is to investigate a variety of important issues, including the effect of fly ash as a stabilizer on the bearing carrying capacity of footings, additionally the effect of various soils used in the foundation, and to recommend appropriate edge distance and type of foundation.

MATERIAL PROPERTIES

In the current investigation, the soil model is modeled using Mohr-Coulomb method and steel footing was modelled as an elastic material. Laboratory tests provide the parameters required for each analysis to establish the soil slope model, i.e., for stabilized and unstabilized soil. These are the dry unit weight (γ-dry), poisson's ratio (μ), cohesion (c), internal friction angle (ϕ), and modulus of elasticity (E).

Earthen Soil

The available literature data from Dhatrak and Langote (2024) [5] provided the properties of the clayey soil used in the prototype model test. Properties of soil are given in table no 1.

Table 1 Soft Clay Properties (Earthen Soil)

Liquid limit	47 %
Plastic limit	35.14 %
Shrinkage limit	11.18 %
Optimum water content	24 %
Dry unit weight	14.12 kN/m^3
Cohesion	46 kN/m^2
Internal friction angle	8^o

Fly Ash

Fly ash is the by-product obtained by burning of pulverised coal in thermal power plant. The parameters of fly ash used in this study are taken from the literature that is currently accessible of Langote and Dhatrak (2022) [5] which were procured from Ratan India Power Ltd. Nandgaon Peth MIDC, Amravati, and Maharashtra. India. Fly ash contains 68% silt and 28 % sand, as per the particle size distribution. The properties of fly-ash are given in table 2.

Table 2 Fly-ash Properties

Optimum water content	24 %
Dry unit weight	12.75 kN/m^3
Cohesion	3 kN/m^2
Internal friction angle	29^o

Stabilized Soil

Fly ash was used as a stabilizing material in the testing program. Series of unconfined compression strength test were carried out to find optimum percentage of fly ash in soil. After performing the test optimum content was observed to be at 25%. Table 3 shows the properties of Fly ash stabilized soil.

Table 3 Stabilized Soil Properties

Optimum water content	21.9 %
Dry unit weight	15.3 kN/m^3
Cohesion	22 kN/m^2
Internal friction angle	11^o

PROTOTYPE STUDY AND METHODOLOGY

The analytical work is carried out using MIDAS - 3D software for the unstabilized and stabilized soil slopes, and the load carrying capacity is analyzed using data received from laboratory test results. Figure 1a shows the 3D mesh generated model and 1b shows the failure of deformed slope model.

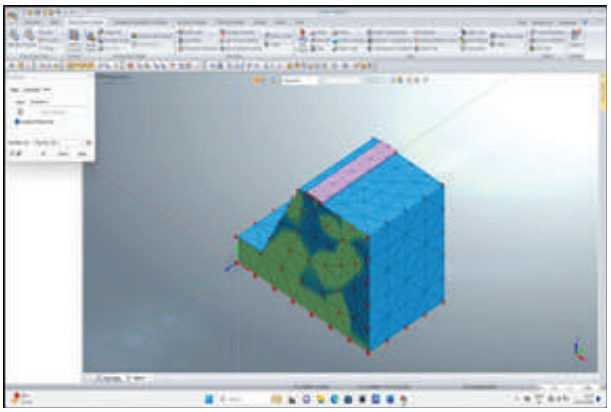

a. Generated Mesh

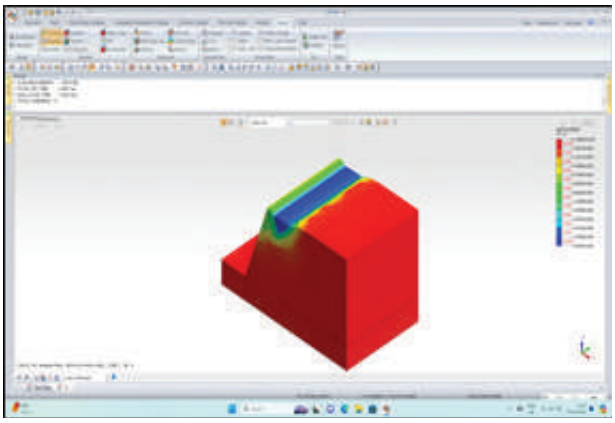

b. Failure of Footing

Fig. 1. Slope Geometry in MIDAS GTS NX

Finite Element Method

The current work aims to comprehend the load carrying capacity behavior of strip footing placed on unstabilized and stabilized soil slope by performing a series of tests using three-dimensional finite element analysis (FEA) on a prototype footing slope model using the MIDAS program. Figure 2 displays the slope geometry prototype.

A yielding base was expected to support the prototype soil model. Width and depth of soil foundation are taken as 700 mm and 100 mm respectively. Soil slope is assumed to resting on soil foundation with a steep slope angle of 70°. Height of slope is 350 mm. Soil slope is analysed for varying parameters mention in table 4. In first case unstabilized soil slope is prepared over different soil beds and tested for strip footing to determine the load carrying capacity. In the second case soil is mixed with optimum dose of fly ash to prepare stabilized soil slope. Mohr-Coulomb and plane-strain analyses can be carried out by the software.

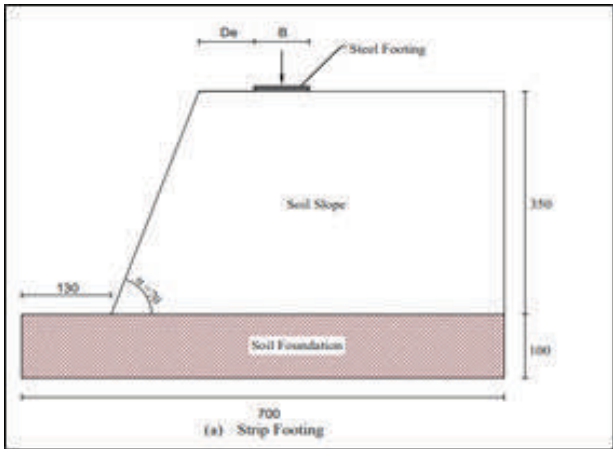

Fig. 2. Slope Model Used in MIDAS GTS NX

Table 4 Standards used for the Finite Element Method (MIDAS GTS NX)

Parameter	Clayey Soil	Stabilized Soil	Footing
Cohesion (C-kN/m²)	24	22	-
Friction angle (ϕ)°	5	11	-
Dry Unit Weight (γ-KN/m³)	14.12	15.3	-
Poisson's ratio (μ)	0.42	0.4	0.28
Modulus of Elasticity (E-KN/m²)	5000	9000	$21x10^7$
Angle of Dilatancy (ψ)	-	-	-

Table 5 Parameters used into the software model for evaluation

Test Series	Constant Parameters	Varied Parameters
1.	Unstabilized Soil Slope	
	Strip footing	De/B = 0.5, 1, 1.5,2,2.5,3,3.5,4
	Slope angle	$\alpha = 70^0$

	Slope Foundation	Fly ash, Clay and Sand
2.	Stabilized Soil Slope	
	Slope angle	$\alpha = 70^0$
	Strip footing	De/B = 0.5, 1, 1.5,2,2.5,3,3.5,4
	Slope Foundation	Fly ash, Clay and Sand

RESULTS AND DISCUSSION

The prepared slope model was analyzed to determine the ultimate bearing capacity of strip footing for various crests to width ratios corresponding to different soil foundations. Following section shows the pressure vs. settlement graphs for different conditions, the ultimate bearing capacity can be obtained by drawing tangent to the curve. Figure 3 shows pressure settlement curve for unstabilized slope for Fly ash foundation.

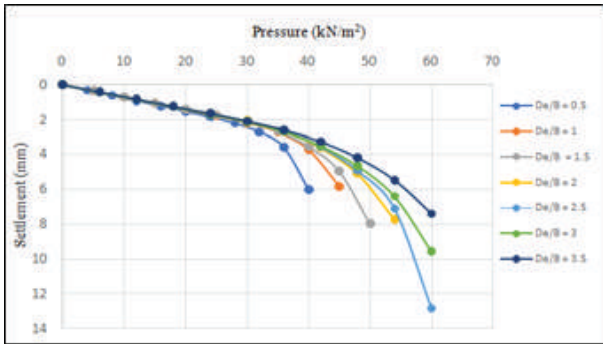

Fig. 3. Pressure against Settlement curve for Unstabilized Soil Slope for Fly ash Foundation

Figure 4 shows pressure settlement curve for unstabilized slope with clay foundation for different crest to width ratio.

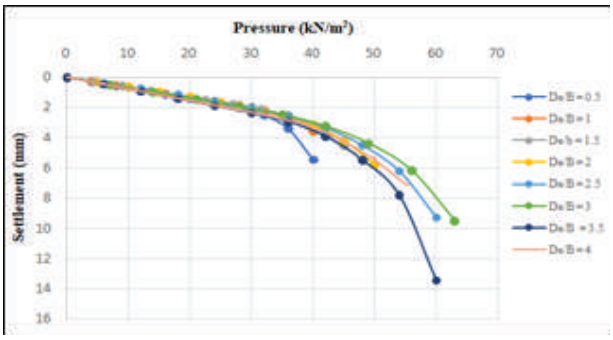

Fig. 4. Pressure against Settlement curve for Unstabilized Soil Slope for Clay Foundation

Figure 5 shows pressure settlement curve for unstabilized slope with Sand foundation for different crest to width ratio.

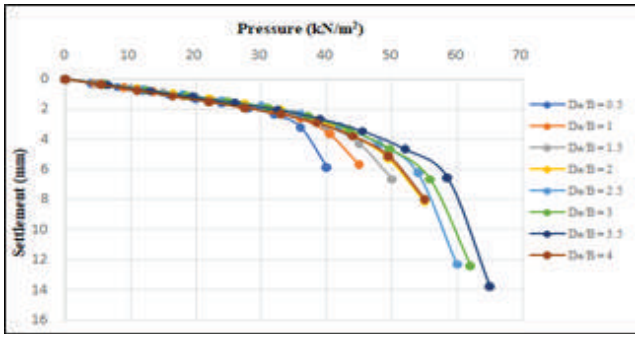

Fig. 5. Pressure against Settlement curve for Unstabilized Soil Slope for Sand Foundation

Figure 6 shows pressure settlement curve for stabilized slope with Fly ash foundation for different crest to width ratio.

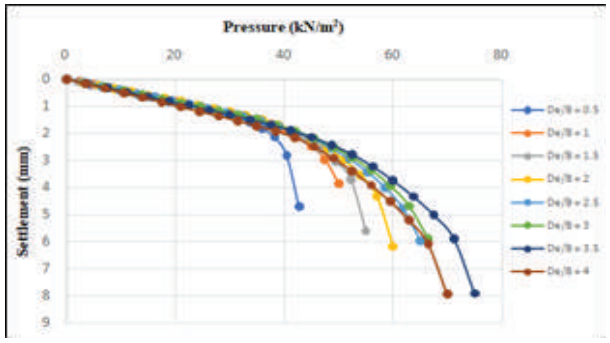

Fig. 6. Pressure Settlement curve for Stabilized Soil Slope for Fly ash Foundation

Figure 7. shows pressure settlement curve for stabilized slope with clay foundation for different crest to width ratio.

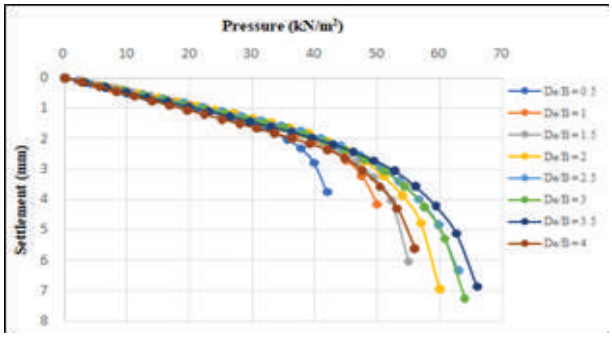

Fig. 7. Pressure Settlement curve for Stabilized Soil Slope for Clay Foundation

Figure 8 shows pressure settlement curve for stabilized slope with sand foundation for different crest to width ratio.

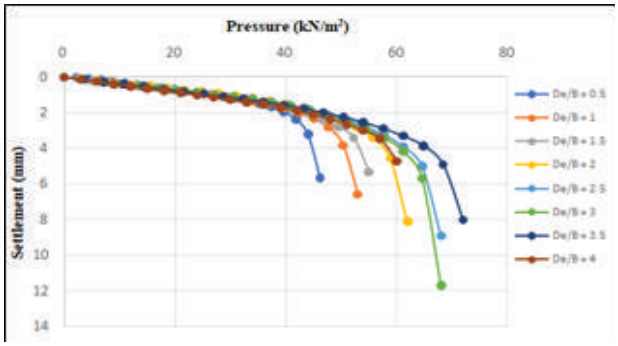

Fig. 8. Pressure Settlement curve for Stabilized Soil Slope for Sand Foundation

Effect of De/B Ratio

Crest to width distance is proven to be an important parameter as far as the performance of footing is concerned. In the present study it is evident that as De/B ratio increases, the maximum bearing capacity for different soil foundations increases upto certain limit thereafter it decreases. For unstabilized slope, the behaviour of bearing capacity of strip footing with respect to De/B ratio for various foundations is shown in figure 9.

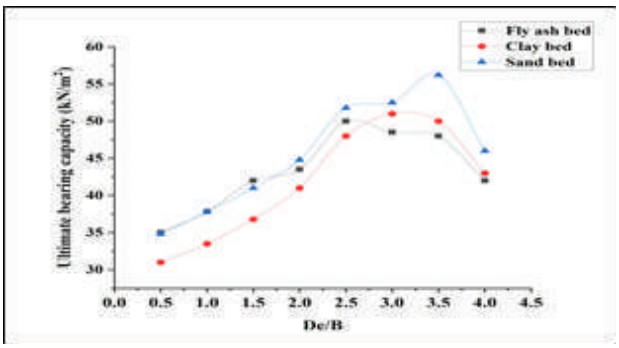

Fig. 9. Ultimate Bearing Capacity Vs De/B Ratio for Different Soil Foundations for Unstabilized Slope

Figure 9 illustrates that the maximum ultimate bearing capacity is achieved with a sand soil foundation with a de/B ratio of 3.5 further the bearing capacity falls as the crest to width ratio increases.

For stabilized soil slope, the behaviour of ultimate bearing capacity of strip footing with respect to De/B ratio for various foundations is shown in figure 10.

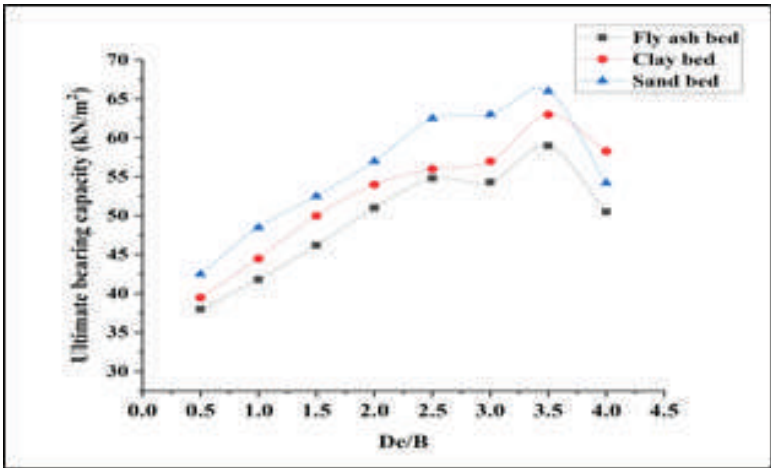

Fig. 10. Ultimate Bearing Capacity Vs De/B Ratio for Different Soil Foundations for Stabilized Slope

Figure 10 shows that the maximum ultimate bearing capacity is achieved for sand soil foundations whereas for fly ash foundation bearing capacity is on lower side for a de/B ratio of 3.5, further it can be seen that the bearing capacity falls as the crest to width ratio increases.

Table 6 shows the percentage increase in the ultimate carrying capacity of unstabilized slope with respect to the De/B ratio for different types of soil foundations.

Table 6 Percentage Increase in qu with increase in De/B ratio for Unstabilized Slope

Increase in De/B ratio		0.5-1	1-1.5	1.5-2	2-2.5	2.5-3	3-3.5	3.5-4
Percent increase in qu	Fly ash bed	8	11.11	3.57	14.94	-3.00	-1.03	-12.50
	Clay bed	8.62	8.47	9.27	15.63	1.35	7.05	-18.15
	Sand bed	8.06	9.85	11.41	17.07	6.25	-1.96	-14.00

Table 7. shows that percentage increase in the bearing capacity is maximum for De/B ratio of 2-2.5 for Fly ash bed, Clay bed and hard bed thereafter there is marginal decrement for further ratios.

Table 7. Percentage Increase in qu with increase in De/B ratio for Stabilized Slope

Increase in De/B ratio		0.5-1	1-1.5	1.5-2	2-2.5	2.5-3	3-3.5	3.5-4
Percent increase in qu	Fly ash bed	15.79	13.64	6.00	3.40	3.10	4.42	-14.41
	Clay bed	12.66	12.36	8.00	3.70	1.79	15.44	-6.08
	Sand bed	19.75	4.12	12.87	9.65	0.80	4.76	-17.88

Table 7 shows that the % increase in bearing capacity for Fly ash beds is greatest when the De/B ratio is 0.5-1 for Fly ash beds and Sand beds, while the percentage increase for Clay beds is greatest when the De/B ratio is 0.5-1.

CONCLUSIONS

After performing Finite Element Analysis for load bearing capacity of stabilized and unstabilized soil slope for different soil foundations following conclusions can be drawn,

- Bearing capacity of strip footing enhances as the crest to width ratio increases upto certain limit thereafter it reduces as the De/B ratio rises further.
- It can be evidently seen that ultimate bearing capacity is found to be optimum when crest to width ratio is 3.5 in stabilized soil slopes. This occurs as a result of soil resistance to lateral displacement increasing when the footing is positioned away from the slope's edge, which creates a wider and deeper failure zone and ultimately raises the footing's bearing capacity.
- For unstabilized case the optimum bearing capacity is observed at De/B = 3.5 for sand bed, whereas for fly ash bed, the UBC is maximum at De/B = 2.5 and that for clay bed it is 3.
- It is discovered that the footing's carrying capability on a clay soil foundation is higher than that of a fly ash soil foundation, but lower than that of a sand soil foundation. This is because the Sand bed has a higher denseness than the fly ash and clay soil foundations, which gives it more resistance to applied pressure.
- In the case of fly ash foundations, stabilized slopes have a greater ultimate bearing capacity than unstabilized slopes and similar trend is observed for clay and sand soil foundations.

The results show that stabilized slopes are more stable than unstabilized slopes, with a 17.43% increase in ultimate bearing capacity.

REFERENCES

1. Adbrabbo F., Gaaver K., Omer E. A., (2008). "Behavior of Strip Footings on Reinforced and Unreinforced Sand Slope". GeoCongress: Geosustainability and Geohazards Mitigations, 25-32
2. Altalhe E. B., Taha M. R. and Abdrabbo F. M., (2015). "Behavior of Strip Footing on Reinforced Sand Slope", Journal of Civil Engineering and Management, 21(3), 376–383
3. Bhargav Kumar K. P. and Umashankar B. (2018). "Interface Studieson Geogrid and Fly Ash" IFCEE 2018 GSP 297 ASCE. 119-129
4. Chakraborty D., Kumar J., (2013). "Bearing Capacity of Foundation on Slopes". Geomechanics and Geoengineering: An International Journal. Vol. 8 No.4, 274-285
5. Dhatrak A.I and Langote R.V., (2024). "Experimental Research on Impact of Fly Ash on Geotechnical Characteristics of Black Cotton Soil", AIP Conference Proceeding 3010, 020007-1-020007-8.

6. El. Sawwaf, (2007). "Behavior of Strip Footing on Geogrid-Reinforced Sand Over a Soft Clay Slope", Geotextiles and Geomembranes 25, 50–60

7. Li Li-Hui, Yu Chang-Dao, Xiao Heng-Lin, Feng Wei-Qiang, Ma Qiang and Yin Jian-Hua (2020). "Experimental Study on the Reinforced Fly Ash and Sand Retaining Wall under Static Load", Construction and Building Material 248 (2020) 118678

8. Nadaf M. B. and Mandal J. N. (2019). "Numerical Simulation of Cellular Reinforced Fly Ash Slopes" Geo-Congress, ASCE 2019 GSP 312, 202-211

9. Nadaf M. B. and Mandal J. N. (2016). "Model Studies on Fly Ash Slopes Reinforced with Planer Steel Grids" International Journal of Geotechnical Engineering, Vol. XX, No. X, 1-12

10. Pant A., Datta M. and Ramana G.V., (2019) "Bottom Ash as a Backfill Material in Reinforced Soil Structure" Geotextile and Geomembranes 47(2019), 514-521

11. Rui Z., Ming-xu L., Tian L., Jian-long Z. and G. Chao, (2020). "Stability Analysis Method of Geogrid Reinforced Expansive Soil Slopes and its Engineering Application", Springer Nature, J. Cent. South Univ. (2020) 27: 1965−1980

12. R. Acharyya and A. Dey, (2017). "Finite Element Investigation of the Bearing Capacity of Square Footings Resting on Sloping Ground". Indian National Academy of Engineering, Vol. 2, 97-105

13. S. Mittal, M. Shah & N. Verma, (2009). "Experimental Study of Footings on Reinforced Earth Slopes", International Journal of Geotechnical Engineering, (2009) 3: 251-260

14. Shejwal K. B. and Gaikwad A.B. (2022) "Generic Analysis of Cohesive Highway Embankment Slope with use of Fly Ash and Geogrids" International Conference on Contents, Computing & Communication (ICCCC)

15. Tahir M. B., Garg P., Grewal G. K., (2021). " Analysis of Load Carrying Capacity of Strip Footing Resting on Geogrid Reinforced Fly-Ash Over an Earthen Slope Using Plaxis2D", Journal of University of Shanghai for Science and Technology, Volume 23, Issue 2, ISSN: 1007-6735, 181-191

16. Thongpetch I. and Chimoye W., (2019). "Behavior of Reinforced Soil Slope by Finite Element Methods". International Journal of Engineering Research & Technology, ISSN: 2278-0181, Vol. 8 Issue 02, 159-163

Redefining the Street Cart Design in the Modern World A Sustainable Approach

Dharmaraj Shalini
Masters in Sustainable Design
Parul Institute of Architecture and Research
Parul University
Vadodara, Gujarat
✉ dharmarajshalini614@gmail.com

Pooja Upreti
Associate Professor
Parul Institute of Architecture and Research
Parul University
Vadodara, Gujarat
✉ pooja.upreti21233@paruluniversity.ac.in

ABSTRACT

The world of technology is advancing at an unprecedented pace. However, the question remains - is this progress sustainable and beneficial for humanity, or is it limiting opportunities for humans? If we blend technology with sustainability, it becomes efficient for both humans and the planet. Street carts are a ubiquitous sight in bustling urban areas, often serving as a hub for a range of vendors. Despite the rapid pace of modernisation and technological advancements, the design of street carts has remained remarkably consistent over the years. From the way they are constructed to the materials used. This paper proposes a redesign of street carts that incorporates technology and sustainability to improve the livelihood of local vendors considering the planet's health. The cart design has been meticulously crafted to tackle the frequent challenges faced by vendors daily. The proposed design is not only practical but also efficient in addressing vendor issues that might arise during their daily operations. The proposed prototype is designed to be as versatile as possible and can adapt to different purposes.

KEYWORDS *: Redesign, Street cart, Waste management, Recycled plastic, Vendor livelihood, Sustainable approach.*

INTRODUCTION

According to the National Policy of Urban Street Vendors, (National Policy For Urban Street Vendors)which was issued by the Government of India in 2004, a street vendor is an individual who sells goods to the public without a permanent structure. They may have a temporary setup that is either static or mobile, such as a push cart, stall, cycle, or basket on their head. They can operate in a stationary manner on pavements or other public/private areas, or they may be mobile and sell their wares in moving trains, buses, and so on. The policy encompasses all types of urban vendors, including service providers and traders, whether they are mobile or stationary, and incorporates all other local/regional terms.

For generations, the street cart method has been a tried and true approach to vending. Its long- standing success may be attributed to its inherent sustainability. Not only does it offer an economic benefit to the vendor, but it also aids in preserving the environment and provides a social benefit to the community. This approach to vending truly encompasses all three pillars (economic, environmental, and social) of sustainability, making it a valuable and enduring tradition.

Economic: The International Labour Organization (ILO) reports that approximately 100 million individuals are employed in street vending across the world. This section helps in the expansion of the informal economy, which is estimated to contribute between 25% and 40% of the Gross Domestic Product (GDP) in developing nations.

It's important to recognise that street vending plays a significant role in India's economy, with an estimated 10 million street vendors contributing to around 14 per cent of the country's urban informal employment. While many of these vendors may be informally trained

and earn low incomes, they are necessity entrepreneurs who are searching for economic opportunities. By providing a variety of goods and services, street vendors are an integral part of India's retail market. As such, it is important to support and empower these vendors, recognising the valuable contribution they make to the country's economy

Environment: Street carts are a great way to promote local crafts, fruits, vegetables, and other goods without using plastic packaging. This helps to reduce plastic waste. Additionally, street carts cut down on the long chain from the manufacturer to the customer, which in turn reduces the carbon footprint.

Social: As an Indian born in the 1990s, I have a strong emotional attachment to the concept of street carts. Whenever I hear the sound of a vegetable cart on the street, I am reminded of the times when women from the neighbourhood would gather around it and discuss household matters while buying their groceries. This activity served as a stress reliever for many women, as it allowed them to share their worries and concerns with others. Street carts also helped to promote interaction and community building among residents.

STREET VENDOR GOVERNMENT SCHEME

The PM SVANidhi Scheme, launched by the Ministry of Housing & Urban Affairs in 2020, is a Central Sector Scheme aimed at supporting street vendors nationwide. With the COVID-19 lockdown taking its toll on small businesses, the scheme's primary objective is to empower street vendors by providing them with a special micro-credit facility for their welfare. Through this scheme, the Government of India will offer short-term loans to street vendors as working capital loans, enabling them to invest in their businesses. The initial loan amount of Rs. 10,000/- will be given to street vendors for 1 year, helping them to rebuild and sustain their livelihoods.

HISTORY

In earlier civilisations, humans focused primarily on securing shelter, food, and clothing. To transport large quantities of fruits and vegetables within communities, people developed carts made of wooden planks and wheels. As civilisation progressed, trade became more common, and carts played a major role in facilitating commerce Throughout history, carts have played a significant role in our everyday lives. Whether used for transportation, hauling goods, or simply as a means of livelihood, they have been a reliable and essential part of human existence. While advancements in technology have led to the invention of vehicles that have replaced carts in many ways, it is unfortunate that these humble conveyances have not received the same level of innovation. Despite the passage of time and the progress of society, carts have remained relatively unchanged, continuing to serve their purpose in much the same way they always have.

The street cart was ingeniously designed to prioritize mobility without sacrificing space for products. A protective roof was later added to further enhance its functionality and ensure adequate shelter from the elements.

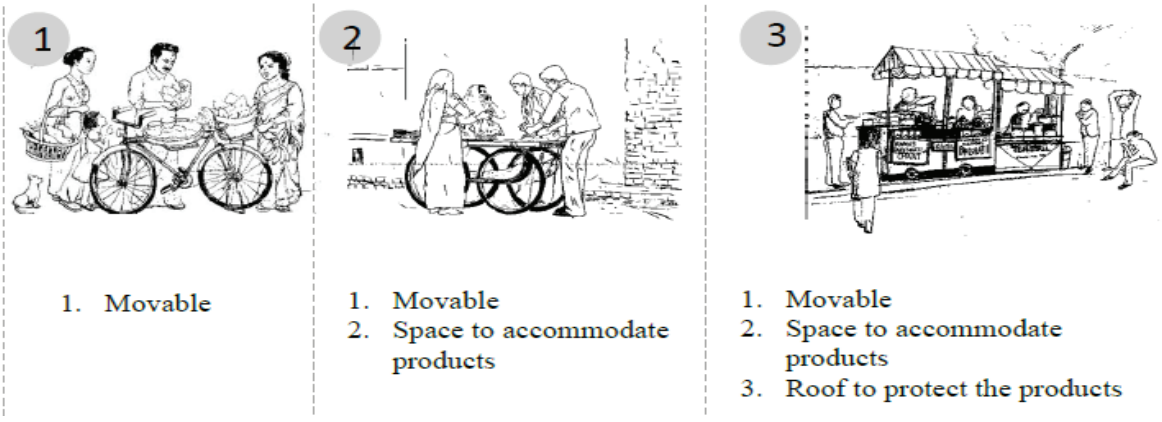

Fig. 1

LITERATURE REVIEW

"Socio-Economic View on Street Vendors: A Study of a Daily Market at Jamshedpur (Parikshit & Samarpita, 2018)" study highlights the poor working conditions of street vendors, including long working hours and unsafe working environments. The majority of vendors earn low daily wages, which reflects their low standard of living. The study also shows that vendors face poor safety and security conditions at their workplaces, as well as having to pay illegal compensation to local authorities.

A study conducted by Nidan on street vendors in Patna, Bihar, (Nidan, 2010) revealed a decrease in the proportion of female vendors over the past decade. This shift in the demographics was attributed to the harassment faced by female vendors from multiple sources, including male counterparts, police, and municipal authorities. The preferred mode of operation for female vendors was mobile vending, as it provided a safer means to avoid harassment.

"A Study on Survival of Street Vendors During the Covid-19 Pandemic with special reference to Coimbatore City" (Dr.S.Renugadevi, Dr. M. Revathy, Mrs. P.Kalaiselvi, & Mr. A. Raja, 2022)Despite challenges, street food remains popular due to its affordability, accessibility, and convenience. It is important to recognise the vital role that women play in the street food sector, both as business owners and as integral members of the supply chain. To ensure that street vendors can continue to thrive and contribute to their communities, it is necessary to address the issue of forced displacement and confiscation of merchandise by local government authorities, particularly during times of increased activity like elections or mega-events. By promoting a fair and safe environment for street vendors, we can support their livelihoods while also enjoying the delicious and diverse foods they offer.

"State of Street Vendors in India: Pre and Post COVID-19 Analysis" (Nitya Maniktala & Tanisha Jain) Street vendors are a vital part of India's urban life, contributing significantly to the economy despite operating informally. However, they face many challenges, including a lack of education and formal employment options, leading them to choose street vending as a common profession. Surrounding waste further adds to their unhygienic conditions, increasing their risk of diseases.

ARCHITECT'S ROLE IN STREET CART DESIGN

Architects play a crucial role in solving complex problems. Street vendors face a multitude of challenges daily, and these issues have been well-documented in various articles. Despite being hardworking and contributing to society, street vendors often do not receive the respect they deserve for their work. While these problems may seem to be specific to the community of street vendors, they have far-reaching effects on the entire network of the country.

Architects are professionals who specialise in designing buildings and other physical structures. Their job is to consider all aspects of the project, including the needs of the users, the client's requirements, and the surrounding environment. In the case of designing a street cart, involving an architect can be extremely beneficial. They can ensure that the design is not only functional and aesthetically pleasing but also safe, sustainable, and compliant with local regulations. An architect's expertise can be the missing piece of the puzzle that unlocks the full potential of the street cart, making it a successful and profitable venture.

The National Policy for Urban Street Vendors has proposed guidelines to improve the quality of life for street vendors. However, it seems that these guidelines have not been adequately implemented when it comes to design. Architects have a unique opportunity to contribute to the development of solutions that can address the problems faced by street vendors.

National Policy Qualitative guidelines (National Policy For Urban Street Vendors) refer to facilities to be provided at vendors' markets by the civic authorities. They would invariably include:

- Provide provisions for solid waste disposal
- Public toilets to maintain cleanliness.
- Aesthetic design of mobile stalls/ push carts
- Provision for electricity
- Provision for drinking water
- Provision for protective covers to protect their

wares as well as themselves from heat, rain, dust, etc.

- Storage facilities including cold storage

NEED FOR CART UPGRADE

The carts used are often outdated and not equipped to meet the demands of modern-day consumers. To address this issue, upgrading these carts can be a viable solution. By adding modern technology to these carts, such as digital payment options and GPS tracking, the street vendors can provide better services to their customers. This can lead to an increase in sales, which can, in turn, create more job opportunities for others. Moreover, upgrading these carts can also boost the country's GDP. Street vending is a significant contributor to the economy of India, and enhancing the capabilities of these vendors can lead to an increase in productivity and efficiency. This, in turn, can result in higher profits and a better standard of living for the vendors and their families.

DESIGN AIM

To create a cart that supports sustainability, and the livelihood of local vendors. DESIGN OBJECTIVES

- Fusing technology with design
- Easy to install and use
- Waste Management

Table 1

Street cart design proposal	Design	Foldable	
		Space effective	
	Renewable energy	Solar energy	
		Kinetic energy	
	Material	Recycle Plastic Local Waste	
	Sanitation & Necessity	In-built dust bin	Drinking water
	Technology	In-built UPI Scanner	Surveillance CAM, Robbery Alarm, Sensor Lights & GPS
	Government	Vendor schemes, Registration, Authorisation & Vendor network	

RESEARCH METHODOLOGY

- Identifying the Local Case Study
- To select the most suitable material for cart design, we will analyze the waste and waste management in that region.
- Cart design proposal

CASE STUDY – CHARMINAR

Charminar, a historic monument located in Hyderabad, is a beautiful sight to behold that is situated at the intersection of four charming streets, each with its unique character. Pathergatti Street, with its impressive heritage facade, is located on the north side of the monument. Rathkhana Street is located on the east side, while the south side is occupied by Mecca Masjid Road. On the west side lies Laad Bazaar, a bustling street named after its famous bangles.

"Street carts, roaming vendors, and people weave together, connecting all these lanes into one bustling scene."

The Charminar heritage site, unfortunately, falls short of setting an exemplary standard for cleanliness. A recent newspaper article titled "GHMC to Review Plastic Waste Situation at Charminar" (Keerthi, 2019) highlights that vendors selling a variety of items ranging from bangles to bags predominantly utilize plastic for packaging. Consequently, plastic waste is often visible on the pavements throughout the day. During the monsoon season, the situation is exacerbated as rainwater washes the plastic towards the drain outlets, creating small dumping spaces. The management of waste has become an arduous task that requires urgent attention. One possible solution to the issue is to convert plastic waste into a resource for making carts. Furthermore, reducing the number of pan shops and implementing machines that collect garbage and provide monetary incentives based on the weight of the waste could also help control waste management around Charminar.

STREET CART DESIGN PROPOSAL

"Versatility is the mother of reinvention" by Thorne The Wordsmith

An innovative street cart design has been presented, taking into account the concerns highlighted in prior

articles and national policy guidelines. The cart has been engineered to expand for use and retract when not in operation. Similar to organic elements found in nature, this cart has a distinct cycle of being activated and deactivated.

The entire design of the street cart has been thoughtfully planned and executed with a focus on addressing the various challenges faced by street vendors. Not only that, but it also takes into account the impact of these carts on the environment and the overall social impact they have on society. Each feature of the cart has been meticulously designed to ensure that it is not only functional and practical but also eco-friendly and socially responsible. From the materials used to the layout and construction, every aspect of the street cart has been considered and optimized for maximum efficiency and positive impact.

The design's versatility addresses the major issue of space efficiency in urban areas. It's important to create street carts that take up minimal space.

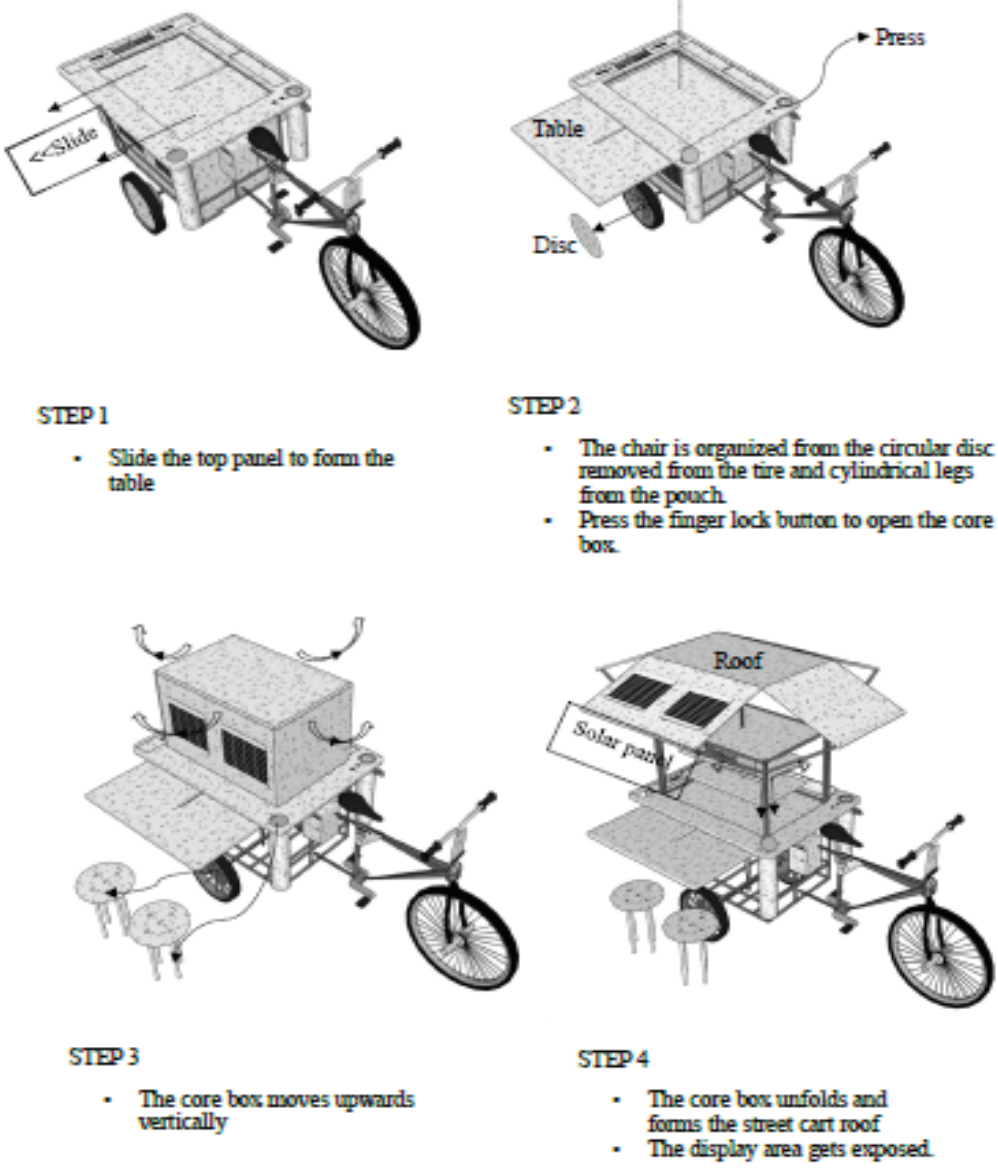

Fig. 2.

Fig. 3

Showcasing the folded and unfolded versions of the design cart.

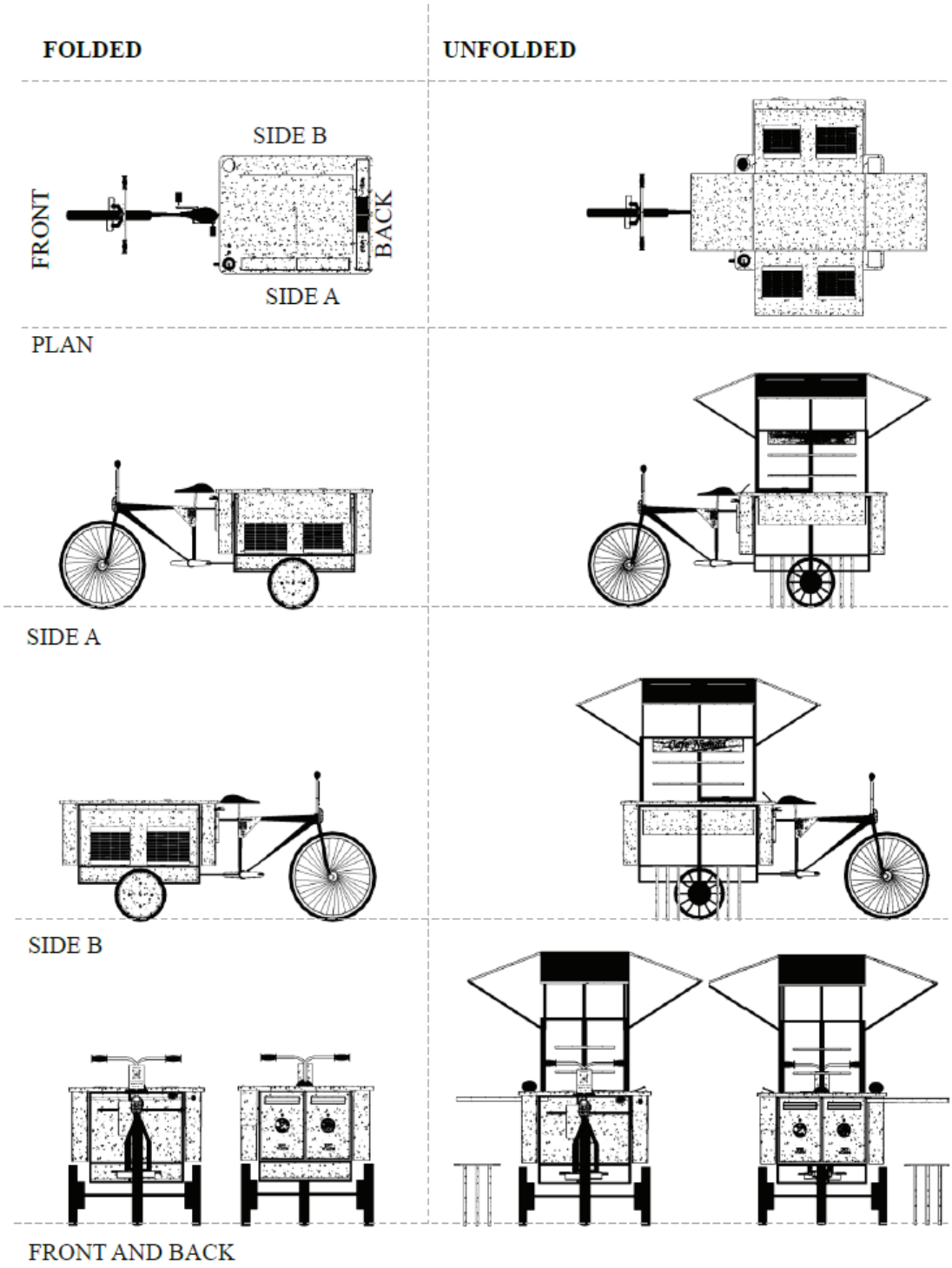

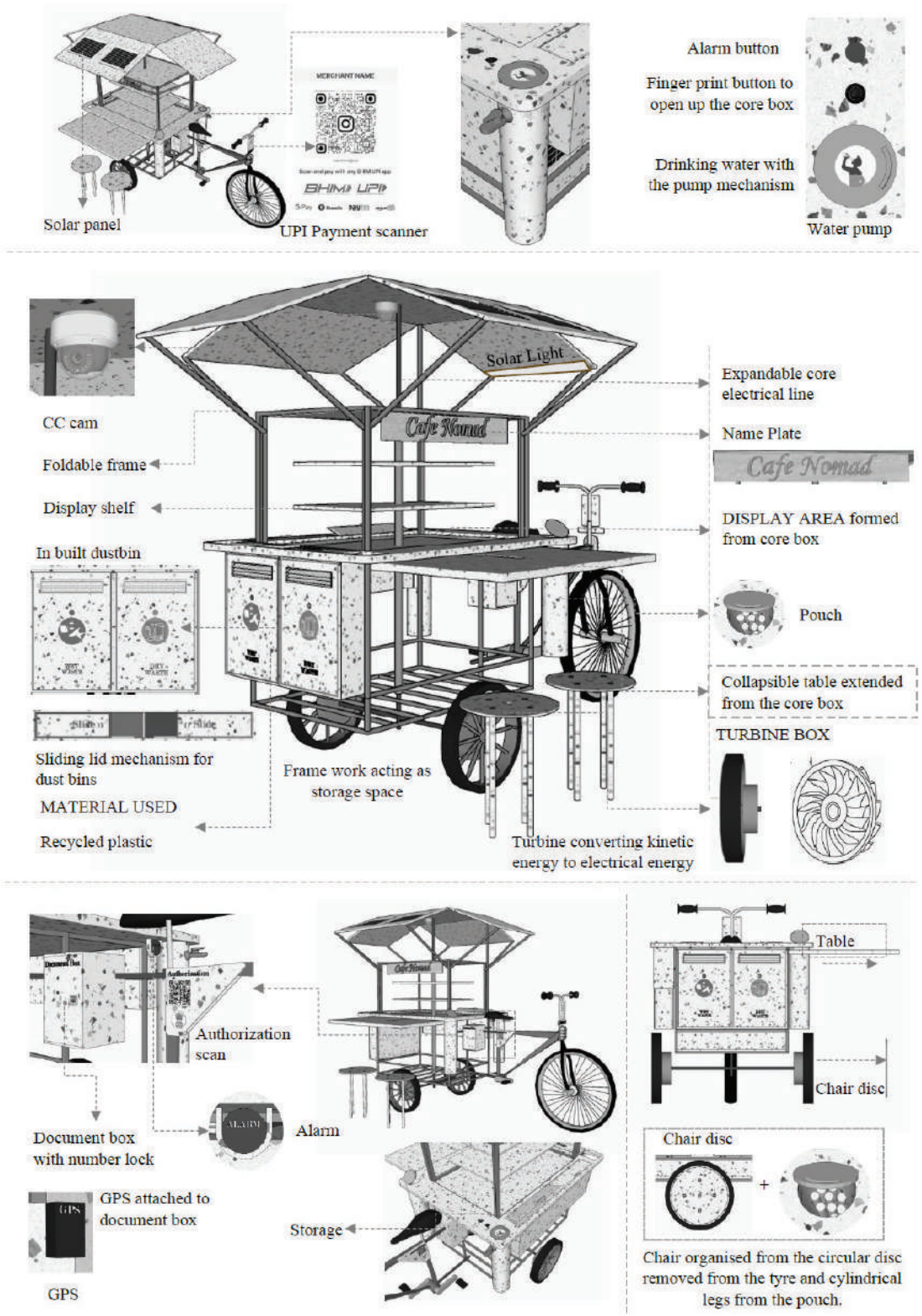
Solar panel
UPI Payment scanner
Alarm button
Finger print button to open up the core box
Drinking water with the pump mechanism
Water pump
CC cam
Foldable frame
Display shelf
In built dustbin
Sliding lid mechanism for dust bins
MATERIAL USED
Recycled plastic
Solar Light
Cafe Nomad
Frame work acting as storage space
Turbine converting kinetic energy to electrical energy
Expandable core electrical line
Name Plate
Cafe Nomad
DISPLAY AREA formed from core box
Pouch
Collapsible table extended from the core box
TURBINE BOX
Authorization scan
Document box with number lock
Alarm
GPS attached to document box
GPS
Storage
Table
Chair disc
Chair disc
Chair organised from the circular disc removed from the tyre and cylindrical legs from the pouch.

Fig. 4

FEATURES OF STREET CART

Recycled Plastic (Waste Plastics, n.d.) : Plastic waste is a significant issue that must not be ignored. Its harmful impact on the environment is undeniable and requires prompt attention. Some companies have taken the initiative to recycle plastic and make planks out of it that can be used for interiors, furniture design, and other purposes. Recycled plastic is used as the primary material source for the cart design. Different thicknesses are selected based on the intended use.

Gear Cycle: Cycling has long been associated with sustainability and health. However, for greater comfort, gear cycles are now being recommended over normal cycles. For those who prefer an alternative to cycling, electric automobiles are also an option.

Turbine fixed to cartwheels: A small attempt is made to convert kinetic energy into electrical energy, which gets stored in the cart's electrical core.

Expandable electrical core: The cart's wiring is held within a slender electrical core, which serves as the cart's heart. The core receives power from the turbine and solar panel and delivers it to the cart's solar light, CC cam, and Core uplift mechanism through a hydraulic mechanism.

UPI Scanner: UPI has become an integral part of our lives, as it has made cash and cardless transactions more feasible than ever. With UPI Scanner already in use by many vendors across India, integrating it into the design adds more practical value to the design.

Autorisation Scanner: In addition to the compassionate aspect of the street vendor industry, there exists a troubling connection to illicit networks. Certain areas may harbour vendors who engage in unlawful practices that pose a danger to the public. Therefore, implementing vendor authorisation measures can aid in monitoring and preventing such activities, ultimately promoting safety and security within the country.

Document box: It's like a safety locker with a number lock to store documents.

CC Camera & GPS: Numerous articles related to street vending have highlighted the concerns surrounding the safety and security of both the vendors and customers. One of the proposed solutions to tackle these issues is the inclusion of GPS technology and Cameras in the design of vending carts or kiosks. By incorporating GPS, vendors can keep track of their location, while authorities can monitor the movement and activities of vendors, thereby enhancing safety and security in the vending industry.

Inbuilt Drinking Water: Many major vendors are finding it challenging to obtain necessities to sustain their daily lives. One of the critical needs that they are struggling with is the availability of clean drinking water. To address this issue, it is recommended that an inbuilt water system with a hand pump be installed. Such a system will help to provide easy access to clean drinking water whenever required, thus enhancing the daily life of these vendors. Additionally, with this system in place, they will not have to worry about the availability of water and can focus on their work more effectively.

Alarm System: The design incorporates a basic alarm system to prioritize female vendor safety.

MS framework: The Framework holds the core box, the primary setup, and the cycle. After the unfold the framework acts as the storage.

Inbuilt Dustbin: Hygiene is a major concern in public areas throughout India, where street inbuilt wet and dry waste dustbins. If the government could then take care of the waste collected from the vendor network, this could benefit other sectors as well. For example, wet waste could be used to create manure, while dry waste could be recycled.

Slidable Table: The homes and streets where vendors operate aren't as spacious as public areas. Therefore, it's crucial to propose a design that can expand when in use and retract when not in use. The sliding table, which can be pulled out as needed, is the first step in the process of unfolding the cart.

DIY (Do It Yourself) Chairs: The second step is to construct chairs using the disk removed from the tyre and the cylindrical legs from the pouch.

Pouch A cylindrical storage container with the same capacity as a drinking water storage unit is integrated to hold the chair legs.

Core box: The box that encloses the display area is its

womb and the roof is its skin. As the roof unfolds, the display is revealed.

Solar panels (Jacob, 2021) : The cart is equipped with solar panels that effectively generate electricity, which is then used to power a solar light. This sustainable solution ensures that the cart's energy needs are met without relying on non-renewable sources, making it an eco- friendly alternative.

CONCLUSION

Through previous articles and case studies, an attempt has been made to analyze the problems faced by street vendors. The proposed solution is a cart design that caters to all the issues faced by vendors, including social and environmental problems. The design also includes waste management. This proposal could be a prototype for the automobile industry and allow engineers to further develop it more technically and efficiently. If implemented in the future, this design could potentially help vendors improve their livelihoods. Overall, this initiative aims to provide a safe and sustainable environment for street vendors to conduct their business.

REFERENCES

1. Consultancy, M. P. (n.d.). Meraki Portfolio Consultancy. Retrieved from https://in.pinterest.com/pin/572520171386038462/
2. Dr. S. Renugadevi, Dr. M. Revathy, Mrs. P.Kalaiselvi, & Mr. A. Raja. (2022). A STUDY ON SURVIVAL OF STREET VENDORS. International Journal of Mechanical Engineering, 1670-1677. Retrieved from https://slcs.edu.in/naac/Criterion-%202021- 22/Criterion-3%20/3.4.3%20-%20Publication%20data/SD18%20ACCA.pdf
3. Jacob, M. (2021, April). Small solar panels: What are your options? Retrieved from Energy Sage: https://www.energysage.com/solar/small-solar-panels-options/Keerthi, S. (2019, OCTOBER 19). GHMC to review plastic waste situation at Charminar. Retrieved from The New Indian Express: https://www.newindianexpress.com/cities/hyderabad/2019/Oct/19/ghmc-to-review- plastic-waste-situation-at-charminar-2049914.html
4. National Policy For Urban Street Vendors. (n.d.). Ministry of Urban Employment and Poverty Alleviation,, 1-16. Retrieved from http://muepa.nic.in/policies/index2.htm
5. Nidan. (2010). Study on Street Vendors at Patna (Bihar). Centre for Civil Society (CCS), New Delhi, 1-56. Retrieved from https://nasvinet.org/research-document/Study%20on%20Street%20Vendors%20at%20Patna.pdf
6. Nitya Maniktala, & Tanisha Jain. (n.d.). State of Street Vendors in India: Pre and Post Covid 19 Analysis. International Journal of Policy Sciences And Law, 1(2), 542-560. Retrieved from https://ijpsl.in/wp-content/uploads/2021/01/State-of-Street-Vendors- in-India-Pre-and-Post-COVID-19-Analysis_Nitya-Maniktala-Tanisha-Jain.pdf
7. P. C., & Samarpita, K. (2018). Socio-Economic View on Street Vendors: A Study of a Daily Market at Jamshedpur. Journal of Advanced Research in Humanities and Social Science, 5(1), 14-20. doi:https://doi.org/10.24321/2349.2872.201804
8. Raut, N. (n.d.). Indian street market, vegetable seller, indian people figure drawing. Retrieved from https://in.pinterest.com/pin/728527677223182229/
9. Waste Plastics. (n.d.). Retrieved from Pyrasied: https://pyrasied.com/en/material/waste- plastics/
10. YC, a. +. (n.d.). NMS Mural Sketches for Colouring. art + travel YC . National Museum of Singapore (NMS), Singapore. Retrieved from https://yipyc.com/blog/2021/02/07/nms-sketches-of-murals/

Studies on the Kinetics and Effectiveness of Natural Wetlands in Treating Municipal Wastewater in Temperate Climates

Kailash Harne
Department of Civil Engineering Department
Netaji Subhas University of Technology
New Delhi
✉ harne.kailash@nsut.ac.in

Himanshu Joshi
Department of Hydrology
IIT Roorkee
Roorkee

Padmashree Harne
Department of Civil Engineering
Anantrao Pawar College of Engineering and Research
Parvati, Pune

ABSTRACT

Natural wetlands are getting vanished day by day all over the world because of encroachment for agricultural use, urbanization, aquaculture, and many more reasons. On the other hand, natural wetlands are performing numerous functions for the betterment of human beings, it has been observed that natural wetlands play a significant role in the treatment of wastewater entering into it. Considering the magnitude of investment needed in wastewater treatment, the government and private sector would be able to mobilize funds toward the construction of conventional treatment plants in a few large towns, metropolitan areas, and industrial complexes. Natural wetlands promise to serve as an ideal alternative technology, which is simple, cost-effective, and environment-friendly. To confirm that, in a temperate environment, natural wetlands are suitable for treating municipal wastewater in a temperate climate, this study has been envisaged with the objectives to know the kinetics and performance evaluation of a natural wetland at Ganeshpur, Roorkee for the treatment of wastewater. It has been observed that the BOD5 removal rate at 20 ^{0}C is controlled by the equation $C_e/C_o = e^{-0.186x\,t}$. The rate constant Kt at ambient air temperature at 25 ^{0}C is observed to be 0.249 d^{-1}. The percent removal of various impurities like TSS, BOD, TKN, TP, and Fecal Coliforms at Ganeshpur natural wetland is observed to be 63.00 %, 49.93%, 12.5%, 11.99%, and 69.50% respectively.

KEYWORDS *: Natural wetlands, Constructed wetlands, Phragmites Australis, Typha latifolia, Hydraulic loading rate, Organic loading rate.*

INTRODUCTION

An artificial or natural, temporary or permanent area of marsh, peat land, fen, or water that has flowing or stagnant water that is fresh, brackish, or salty, including areas of marine water whose depth at low tide does not exceed six meters, is referred to as a wetland [1]. It also includes inland waters such like the reservoir, lakes, tanks, backwaters, creeks, lagoon, estuaries, manmade wetland and the zone of direct influence like drainage area or catchment region of the wetlands determined by the authority but excluding main river channels, coastal wetlands, and paddy fields.

Recent studies on wetlands observed that the freshwater biodiversity in the form of natural wetlands is the most vulnerable of all types of biodiversity [1], [2]. Twenty percent of India's biodiversity is supported by wetlands alone [3]. The spread up of wetlands in India are being observed over 58.2 million hectares of land [4].

The major reason for the loss of natural wetlands could be agricultural activities taking place in the world[5], [6], [7], [8] eventually causing serious ecological consequences, like damage of biodiversity[9], [10], [11] habitat loss [12], [13] reduction of carbon appropriation [14], [15] and deteriorations of quantity and quality of water. [16], [17]. Few more researchers also pointed out that about 7 % of the terrestrial surface is covered by wetlands all over the world providing significant and varied benefits to the human being. [18], [19], [20] However, extensive loss of wetlands

due to human activity, including construction [21], [22] agricultural [23], [24] and aquaculture [25] has been found in recent decades. Measuring the spatiotemporal patterns of agricultural infringement in the natural ecosystem is the first step in responding to these new environmental concerns. Despite initiatives to restore natural wetlands for human welfare, over half of the wetlands of world have vanished in the past century [26], [27],[28]. Wetland loss is mostly caused by agricultural encroachment, which deters natural wetlands from providing ecological services.[7], [29], [30]. For this reason, clear evaluations of the natural wetland loss brought on by agricultural adaptation are crucial for wetland transformation and fortification. Wetland ecosystem services can be divided into three categories [31], [32] by taking into account their worth at the population, ecological, and global levels of the biological hierarchy. The population is linked to the production of fish, shellfish, waterfowl, and other hunted and observed birds, the habitat of animals harvested for their pelts, the harvesting of timber and peat, and the support of vulnerable and endangered species. The entire wetland ecosystem, not just a few plant, animal, or bacterial species, is essential to ecosystem benefits that enhance water quality, mitigate the effects of storms, refill aquifers, avoid flood damage, and even sustain human societies. Global values include preserving air and water quality, which has an impact on a larger scale than the ecosystem level, particularly in regional and global carbon, nitrogen, and sulfur cycles.

Wetlands also offer significant advantages [33] by converting contaminants such nutrients, viruses, sediments, and trace metals [34], [35], [36],[37]. The organic loading rate, the hydraulic loading rate inside the wetland, the concentrations of biodegradable organic matter, the accessible surface area of plants, and other substrates for microbial development are factors that affect how effective a wetland is [38], [35]. Degradation of natural wetlands and a decrease in biodiversity can result from extreme pollutant loading to wetlands and changes in inflow rates to wetlands that were not previously affected [39], [40], and [41].

However, significant improvements to water quality, habitat variety, and ecological sustainability can all be achieved by reestablishing or improving wetlands and employing appropriate management techniques for already-existing wetlands. According to [42], [43], artificial wetlands that receive city wastewaters have average retention percentages for the following impurities: total phosphorus (34%), ortho-PO4 (41%), total nitrogen (55%), and nitrate-NO3 (51%).

MATERIAL AND METHOD

Present Study

In the absence of proper conventional methods of treatment and disposal of wastewater at present, natural wetlands are playing a vital role in the purification of wastewater in every village and most of the towns around the globe, though in an unorganized manner. The aquatic vegetation grows in natural ponds created along the course of channels carrying wastewater generated by residential, commercial, and industrial activities. The difference in these wetlands is largely related to the vegetation, which dominates the area. Grasses [44] are generally dominant in marshes, trees and shrubs characterize swamps, and sedges/ peat vegetation occurs in bogs. To the greatest extent feasible, wastewater treatment is accomplished through the removal of physicochemical and biological contaminants from wastewater through the processes of sedimentation, adsorption, microbial degradation, and plant uptake.

It has been decided to carry out the performance assessment of a natural wetland around Roorkee town. For this purpose, a survey of natural wetlands has been carried out in the vicinity of Roorkee town and a natural wetland located at Ganeshpur as shown in Fig. 1 has been selected for checking the performance of the natural wetland. The purpose of undertaking the performance study of the natural wetland at Ganeshpur is to compare the performance of this natural wetland with the constructed wetlands pilot scale plant established at Uttarakhand Jal Nigam sewage treatment plant premises at Jagjeetpur, Kankhal Haridwar but this could not possible because the constructed wetland pilot plant is yet to be matured.

Ganeshpur is a major residential part of Roorkee town located towards the west of the town. The present population of this area is about fifteen thousand people. The open drains in this area collect wastewater from individual residences and finally enter into an open channel outfall sewer. This channel traces the natural

ground slope and enters into a natural wetland formed just about two hundred meters away from the town.

The natural wetland at the site has been spread up along the drains carrying wastewater. The drain is running along a natural slope; therefore, they are rarely of regular shape and size but an irregular stomach-shaped ditch. The average dimensions of the bed as measured are given in Table 1.

The open channel outfall sewer lined with cement concrete reaches the mouth of the wetland. It enters from one side and the treated wastewater leaves the wetland bed from the opposite side. The floating impurities like vegetable dressings, plastic bottles, polyethylene bags, waste cloth pieces, etc. settles at the entrance of the bed. Valuable solid waste has been removed frequently by scavengers for recycling. The treated wastewater emanating from the wetland finally reaches a rivulet present at the downstream side of the wetland.

The vegetation available in the wetland is a mixed culture of various aquatic macrophytes. Phragmites karka and Typha latifolia were the predominant [44] vegetation profusely growing in the wetland. In addition to these, different submerged and floating vegetation like Scirpus spp., Eichhornia crassipes, Duckweed, grasses, etc. were also observed in different patches. Although the vegetation in natural wetlands does not remove all organic matter directly, however, they serve as a host for a variety of attached growth organisms, and the microbial activity is primarily responsible for the organic decomposition.

Fig. 1: Natural Wetland at Ganeshpur, Roorkee, (India)

Table 1: Average dimensions of natural wetland at Ganeshpur, Roorkee

S N (1)	Parameters (2)	Value (3)
1	Length of wetland	400 m
2	Width of wetland	40 m
3	Area of Wetland	16,000 m^2 (3.2 ha)
4	Depth of wetland	0.15 m
5	Volume of wetland	2400 m^3
6	Discharge	1800 m^3/d

Measurement of Physicochemical and Bacteriological Parameters of Wastewater

A multi-probe meter was utilized to test the electrical conductivity, pH, water temperature, and dissolved oxygen (DO). The turbidity was measured using an on-site Wag-WT3020 turbidity meter. The water samples were filtered on-site using Whatman glass micro-fiber filters (25 mm Ø) and then collected in 100 ml plastic bottles for nutritional analysis (nitrite, nitrate, ammonium, and soluble reactive phosphorus). Total nitrogen (TN), total phosphorus (TP), total suspended and dissolved solids (TSS and TDS), chloride, and alkalinity were measured in well-mixed, unfiltered water samples collected in polyethylene bottles 3. In order to collect water samples for the BOD examination, clean 1-liter polyethylene bottles were placed 30 cm below the rivers' surface, in

the opposite direction of the three current flows, and immediately sealed and reopened. The water samples were sent in a refrigerated box to the Indian Institute of Technology, Roorkee's Department of Hydrology lab for further analysis. Before the analysis, the samples were promptly placed in a cold box and stored in the freezer. In general, the samples were examined using the APHA-described standard procedures [45]. Environmental parameters such as total nitrogen (TN) and phosphorous both soluble reactive (SRP) and total (TP) have been measured using the Kjeldahl Nessler and ascorbic acid techniques, respectively. The azide adaptation of Winkler's titrimetric method was used to quantify the biochemical oxygen demand (BOD) by comparing the DO concentrations of the samples before and after five days of incubation at 20 C. The cadmium reduction method of 8039 was used to quantify nitrate in the high (0.3–30 mg/l) and low (0.01–0.5 mg/l) ranges, respectively. In accordance with the USEPA's HATCH water analysis manual, which is freely accessible online, we also employed Nessler technique 8038 to determine the ammonium-nitrogen content.

Wastewater characteristics

The wastewater entering the natural wetland under study is generated from the residential localities of Ganeshpur. As there are no major industrial and commercial activities in the area, the wastewater reaching the wetland site is primarily domestic in nature. By comparing these contaminants with the typical composition of untreated municipal wastewater [46] has been classified as weak wastewater.

RESULTS AND DISCUSSIONS

Computation of Organic Loading Rates (HLR) and Hydraulic Loading Rates (HLR) and Hydraulic Retention Time (HRT)

Although diurnal and seasonal variations were observed in the inflow, the same got dampened by several small ponds created in front of the vegetated wetland and nearly uniform flow finally has been observed to spill over these storage ponds and enter into the wetland. The average discharge passing through the wetland bed has been measured to be about 1800 m3/d. The organic loading rate, hydraulic loading rate and retention time, [35] has been estimated and summarized as below in Table 2.

$$Hydraulic\ Retention\ Time = \frac{Volume\ of\ Wetland\ (m^3)}{Discharge\ (m^3/d)} = \frac{400 \times 40 \times 0.15}{1800} = 1.33\ \text{days}$$

$$Hydraulic\ Loading\ Rate = \frac{Discharge\ (m^3/d)}{Wetland\ Area\ (m^2)} = \frac{1800}{16000} = 0.1125\ m^3/m^2.d\ (11.25\ cm/d)$$

$$Organic\ Loading\ Rate = \frac{Av.BOD\ (gm/m^3) \times Discharge\ (m^3/d)}{Wetland\ Area\ (m^2)} = \frac{126.83\ gm/m^3 \times 1800\ (m^3/d)}{16000\ (m^2)} = 14.175\ gm/m^2.d\ \ (142.68\ kg/ha.d)$$

By comparing the above parameters with the guidelines given by Central Pollution Control Board (CPCB) New Delhi, the organic loading in the present wetland is in the range prescribed for constructed wetlands (i.e.10-20 g/m2. d), but the hydraulic loading at the proposed site is more than the proposed range (4-6 cm/d). This indicates that; the natural wetland is functioning in an unorganized manner and there is no control over the discharge entering the wetland resulting in an overloading of the natural wetland.

Table 2: Hydraulic parameters of natural wetland, Ganeshpur

S N (1)	Hydraulic Parameters (2)	Value (3)
1	Discharge	1800 m^3/d
2	Hydraulic Loading	11.25 cm/d
3	Organic Loading	142.68 (kg/ha. d)
4	Hydraulic Retention Time	1.33 d

BOD Removal Kinetics at Ganeshpur Natural Wetlands

The BOD removal in the natural wetland follows the first-order plug flow model [47]. The BOD removal rate constant for different types of wetland has reportedly

given in Table 3 [47]. The average BOD removal rate constant (Kt) at 25 0C for the average inlet and outlet concentration of BOD5 and hydraulic retention time of 1.33 days at the Ganeshpur natural wetland site is estimated as 0.249 d-1 as shown in Table 4.

Table 3 : Comparison of first-order plug flow rate constant

Table 3 : Comparison of first-order plug flow rate constant

S. N. (1)	Treatment Process (2)	Rate Constant (K_t in d^{-1}) (3)
1	Subsurface Flow Wetland	1.104
2	Facultative Lagoon	0.117
3	Free Water Surface Wetland	0.501

Table 4: BOD removal rate constant at Ganeshpur natural wetlands

S. N.	Sampling Period	Effluent BOD_5 (mg/l) (C_e)	Influent BOD_5 (mg/l) (C_o)	C_e/C_o	Hydraulic Retention Time (d)	BOD Removal Rate Constant (K_t) (d^{-1})	Average BOD Removal Rate Constant a t 25 ^0C (K_t) (d^{-1})
01	Jan 2022	50	110	0.455	1.33	0.257	
02	Feb 2022	47	95	0.495	1.33	0.230	
03	Mar 2022	36	120	0.300	1.33	0.393	0.249
04	Apr 2022	72	112	0.643	1.33	0.144	
05	May 2022	80	124	0.645	1.33	0.143	
06	Jun 2022	42	115	0.365	1.33	0.329	

The value of this constant is different for different wetlands as compared by[47] and for Ganeshpur wetland is shown in the table given in Table 4.

According to reports, a number of researchers in the US, Europe, and Australia [48], [49], [50], [51] have designed subsurface flow wetland systems using a first-order plug flow model for BOD removal. The general form of the model for removal is

$$C_e/C_o = e^{-K_t \, x \, t}$$

Where,

C_e = Effluent BOD concentration (mg/l)

C_o = Influent BOD concentration (mg/l)

K_t = first order removal rate constant (d^{-1})

t = Hydraulic retention time (d)

It has been well established that the degradation of organic matter depends upon the activity of enzymes in the cell. The microorganism and its enzymes depend on their catalytic properties and temperature. According to the Arrhenius equation, the reaction rate is typically 2 to 3 times higher with each 10 0C increase in the temperature.

The value of the BOD removal rate constant (Kt) equal to 1.104 d-1 has been reportedly used by many researchers [48], [49], [52] also proposed a value of (Kt) ranging from 0.8 to 1.1 d-1 for sand and gravel. Typical detention time ranging between 2-7 days has also been given for effective removal of BOD.

After conducting the exhaustive performance studies on natural wetlands at Ganeshpur and summarized graphically from Fig 3 to 7. The BOD5 removal rate constant (Kt), the general form of the model for removal is $C_e/C_o = e^{-0.186 \, x \, t}$

Performance of Natural Wetland at the Proposed Site

The performance evaluation study of this wetland had been done over a period of six months. Wastewater samples were collected and composited hourly at the inlet and outlet of the wetland once a month. Various physical, chemical, and bacteriological analyses were performed. The concentration and percent reduction in the parameters and also the variation of these parameters with time has been shown graphically in Fig. 2 to Fig 6.

The average percentage reduction of TSS in this wetland is 63 %. Suspended solids, though, are not a limiting factor for design, but may lead to improper management of solids within the system and can result in process failure. As there has been no open space available for the growth of algae in this wetland, the suspended solids were possibly removed only because of sedimentation. Organic loading in terms of BOD5 is the limiting design parameter for a wetland system for maintaining the aerobic conditions in the upper column of the unit. The average percentage reduction of BOD in this natural wetland is found to be 49.93 %. Removal of nitrogen is caused by biological nitrification, ammonia volatilization, and plant uptake. The combined effect of these factors resulting in the reduction of TKN in the natural wetland is observed to be 12.5 %. Removal of total phosphorus in the wetland is a result of adsorption on the vegetation roots, stem, and leaflet, and also uptake by the vegetation. The removal of Total Phosphorus in the present wetland is 11.99 %. The Fecal Coliform removal has been observed to be 69.5 %.

Percent removal in these parameters has been observed to be much less than the constructed wetlands in general as given in Fig 2 to 6. This is because the natural wetlands are unorganized and uncontrolled plants and availability of less surface area for attached microbial growth for the biodegradation of pollutants present in the wastewater. Roots and submerged shoots are the only surfaces available for microbial growth in natural wetlands, in addition to the area of vegetation, a large surface area of filter media is available for microbial growth in the case of constructed wetlands.

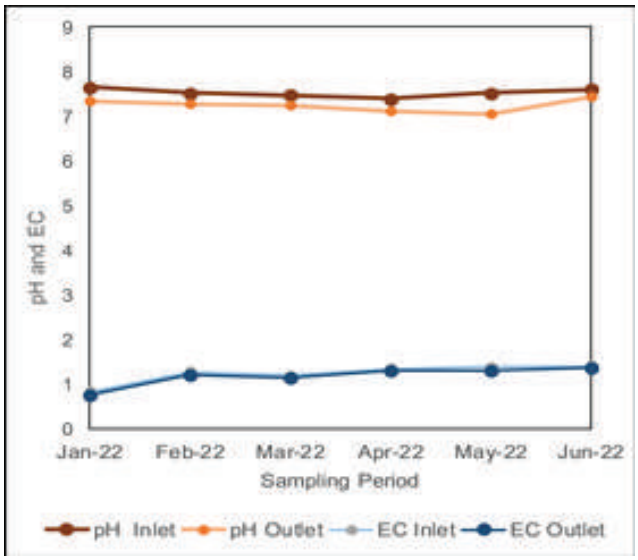

Fig. 2 Comparison of pH and EC at Inlet and Outlet

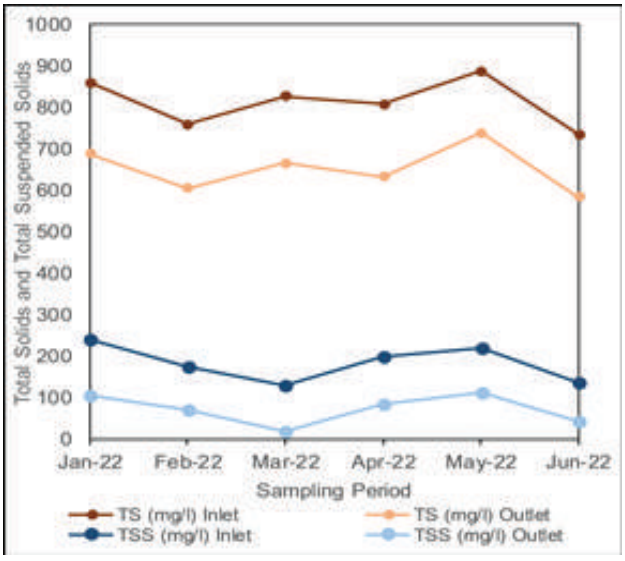

Fig. 3 Comparison of TS and TSS at Inlet and Outlet

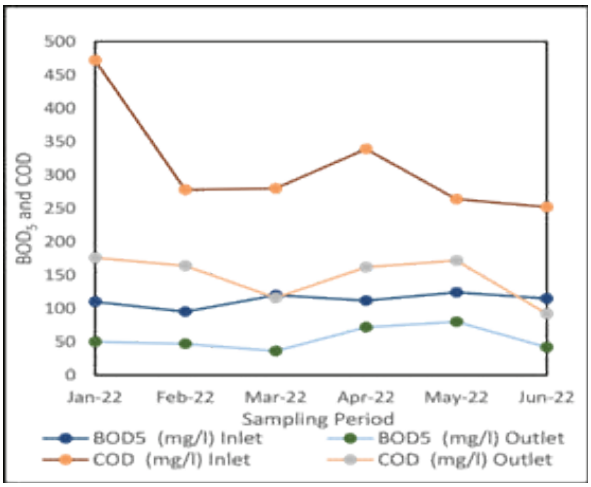

Fig. 4 Comparison of BOD5 & COD at Inlet and Outlet

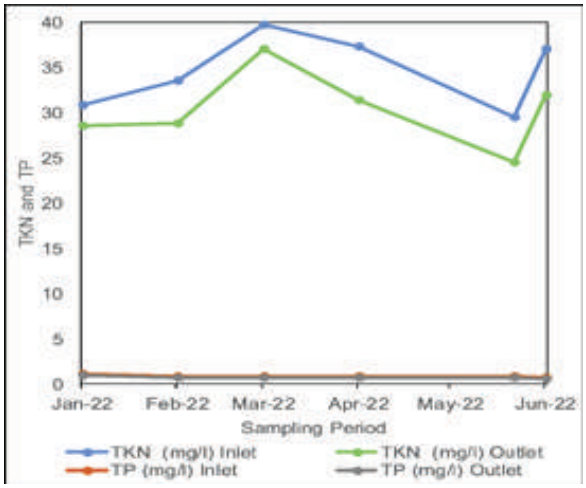

Fig. 5 Comparison of TKN and TN at Inlet & Outlet

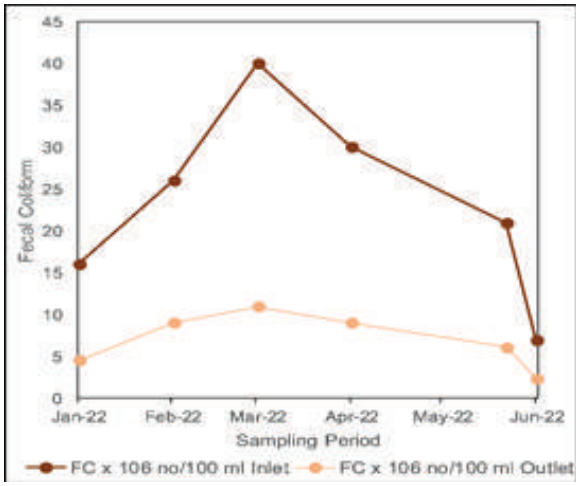

Fig. 6 Comparison of Fecal Coliform at Inlet and Outlet

CONCLUSIONS

1. The vegetation available in the natural wetland under study is a mixed culture of various aquatic macrophytes but primarily Phragmites karka and Typha latifolia are the two species predominantly growing in the wetland. The natural wetland under study is a small unit serving a population of about fifteen thousand persons and spread up over (3.2 ha) 16,000 m2 area. The discharge, organic loading rate, hydraulic loading rate and hydraulic retention time at the site were observed to be 1800 m3/d, 11.25 cm/d, 142.68 (kg/ha. d) and 1.33 d respectively. 1800 m3/d
2. After performing exhaustive studies on inlet and outlet BOD5 on natural wetlands at Ganeshpur for about six months, the BOD5 removal rate constant Kt at 200C and 250C is found to be Kt = 0.186 d-1 and Kt = 0.249 d-1 respectively. The BOD5 removal in the wetland is now controlled by the equation as

$$C_e / C_o = e^{-0.186\, x\, t}$$

3. Average percent removal of various physicochemical and bacteriological impurities like TSS, BOD, TKN, TP, and Fecal Coliforms has been achieved in the studied wetland to the extent of 63.00 %, 49.93 %, 12.5 %, 11.99 %, and 69.50 % respectively. Although this removal is less than that achieved in a conventional treatment process, the fact that no investment has been incurred on this wetland to achieve even this much purification makes this system promising.

REFERENCES

1. Wetland (Conservation and Management) Rules, (2017). Guidelines for implementing Rules and The Gazette of India, No 802, Part II, Section 3, Subsection I, September 26, 2017. Ministry of Environment, Forest and Climate Change.https://indianwetlands.in/our-work/wetlands-conservation-and-management-rules-2017/
2. Bal, R., and A., Dua. (2010). Birds of natural wetlands of north-west Punjab, India, Our Nature, 8, pp 72-81. DOI: https://doi.org/10.3126/on.v8i1.4314
3. Deepa, R.S., and T. V. Ramchandra. (1999). Impact of urbanisation on the interconnectivity of wetlands. Proceedings of ISRS National Symposium on Remote Sensing applications for natural resources, January 19-21, 343-351.https://wgbis.ces.iisc.ernet.in/energy/water/paper/imapact_of_urbanisation/Impact%20of%20Urbanisation.pdf
4. Prasad, S. N., T. V., Ramachandra, N., Ahalya, T, Sengupta., Alok, Kumar., A. K, Tiwari., V. S, Vijayan., and Lalitha, Vijayan., (2002). Conservation of wetlands of India – a review, Tropical Ecology, 43 (1), 173-186. https://wgbis.ces.iisc.ernet.in/energy/water/paper/conservation_wetlands/Conservation_of_wetlands_of_India.pdf
5. Navin, Ramankutty., and Jonathan, A. Foley, (1999). Estimating historical changes in global land cover: Croplands from 1700 to 1992, Global Biochemical Cycles 13 (4), 997-1027

   https://agupubs.onlinelibrary.wiley.com/doi/epdf/10.1029/1999GB900046
6. Qiu, J., (2011). China faces up to 'terrible' state of its ecosystems. Nature 471, 19

   https://www.nature.com/articles/471019a
7. Asselen, S., Verburg, P.H., Vermaat, J.E., Janse, J.H., (2013). Drivers of wetland conversion: a global meta-analysis. PLoS One 8, 381292.

   https://journals.plos.org/plosone/article?id=10.1371/journal.pone.0081292
8. Dehua, Mao., Ling, Luo., Zongming, Wang., Maxwell C, Wilson., Yuan, Zeng., Bingfang, Wu., Jianguo, Wu. (2018). Conversions between natural wetlands and farmland in China: A multiscale geospatial analysis. Science of The Total Environment., 634, 550-560. https://doi.org/10.1016/j.scitotenv.2018.04.009
9. An, Shuqing., Harbin, Li., Baohua, Guan., Changfang, Zhou, Zhongsheng., Wang, Zifa., Deng, Yingbiao Zhi., Yuhong, Liu., Chi, Xu., Shubo, Fang., Jinhui, Jiang., Hongli, Li. (2007). China's Natural Wetlands: Past Problems, Current Status, and Future Challenges. AMBIO: A Journal. of the Human Environment, 36(4), 335-342. https://doi.org/10.1579/0044-7447(2007)36[335:CNWPPC]2.0.CO;2
10. Cramer, Wolfgang., Emilie, Egea., Joern, Fischer., Alexandra, Lux., Jean-Michel, Salles., Josef, Settele., Muriel, Tichit. (2017). Biodiversity and food security: from trade-offs to synergies.Reg Environ Change 17:1257–1259 DOI 10.1007/s10113-017-1147-z

11. Yang, H., Ma, M., Thompson, J.R., Flower, R.J., (2017). Protect coastal wetlands in China to save endangered migratory birds. Proc. Natl. Acad. Sci. 114, E5491–E5492. https://doi.org/10.1073/pnas.1706111114. https://pubmed.ncbi.nlm.nih.gov/28626042/

12. Zhao, Shuqing., Changhui, Peng., Hong, Jiang., Dalun, Tian., Xiangdong, Lei., Xiaolu, Zhou. (2006). Land use change in Asia and the ecological consequences. Ecol Res 21, 890–896 DOI 10.1007/s11284-006-0048-2

13. Wimberly, Michael C., Diane, M. Narem., Peter, J. Bauman., Benjamin, T. Carlson., Marissa, A. Ahlering. (2018). Grassland connectivity in fragmented agricultural landscapes of the north-central United States. Biological Conservation, 217, 121-130 https://doi.org/10.1016/j.biocon.2017.10.031

14. Saunders, M.J., Kansiime, F., Jones, M. B. (2012). Agricultural encroachment: implications for carbon sequestration in tropical African wetlands. Glob. Chang. Biol. 18, 1312–1321 https://doi.org/10.1111/j.1365-2486.2011.02633.x

15. Man, W.D., Yu, H., Li, L., Liu, M.Y., Mao, D.H., Ren, C.Y., Wang, Z.M., Jia, M. M., Miao, Z.H., Lu, C.Y., Li, H. Y., (2017). Spatial expansion and soil organic carbon storage changes of croplands in the Sanjiang plain, China. Sustainability, 9 (4), 563. https://pdfs.semanticscholar.org/528b/c5e2c6ecd88cb140a59d716266879d8e6c18.pdf

16. Fang, J.Y., Rao, S., Zhao, S.Q., (2005). Human-induced long-term changes in the lakes of the Jianghan Plain, central Yangtze. Front. Ecol. Environ., 3, 186–192. https://doi.org/10.1890/1540-9295(2005)003[0186:HLCITL]2.0.CO;2

17. Scanlon, B.R., Jolly, L., Sophocleous, M., Zhang, L. (2007). Global impacts of conversions from natural to agricultural ecosystems on water resources: quantity versus quality. Water Resour. Res., 43, W03437. doi:10.1029/2006WR005486.https://www.beg.utexas.edu/files/content/beg/research/swr/pubs/Scanlon%20et%20al.%20Global%20Ag%20WRR%2007.pdf

18. MA (Assessment, Millennium Ecosystem), (2005). Ecosystems and human well-being: wetlands and water. World Resources Institute, Washington, DC, 30-33.https://www.millenniumassessment.org/documents/document.358.aspx.pdf

19. Zedler, J.B., Kercher, B., (2005). Wetland resources: status, trends, ecosystem services, and restorability. Annu. Rev. Environ. Resour. 30, 39–74. doi: 10.1146/annurev.energy.30.050504.144248

20. Keddy, P.A., (2010). Wetland ecology: principles and conservation. Cambridge University Press Cambridge.

http://assets.cambridge.org/97805217/83675/frontmatter/9780521783675_frontmatter.pdf

21. Li, Y.F., Shi, Y.L., Zhu, X.D., Cao, H.H., Yu, T., (2014). Coastal wetland loss and environmental change due to rapid urban expansion in Lianyungang, Jiangsu, China. Reg. Environ. Chang., 14, 1175–1188. https://kd.nsfc.gov.cn/paperDownload/1000015086660.pdf DOI 10.1007/s10113-013-0552-1

22. Hartig, J.H., Bennion, D., (2017). Historical loss and current rehabilitation of shoreline habitat along an urban-industrial River-Detroit River, Michigan, USA. Sustainability, 9, 828. DOI:10.3390/su9050828

https://www.researchgate.net/publication/316947523_Historical_Loss_and_Current_Rehabilitation_of_Shoreline_Habitat_along_an_Urban-Industrial_River-Detroit_River_Michigan_USA

23. Rebelo, L.M., Finlayson, C.M., Nagabhatla, N., (2009). Remote sensing and GIS for wetland inventory mapping and change analysis. J. Environ. Manag., 90, 2144–2153. https://doi.org/10.1016/j.jenvman.2007.06.027

24. Vanessa, Reis., Virgilio, Hermoso., Stephen, K, Hamilton., Douglas, Ward., Etienne, Fluet-Chouinard., Bernhard, Lehner., Simon, Linke. (2017). A global assessment of inland wetland conservation status. BioScience, Vol. 67 No. 6, 523-533.

25. Richards, D.R., Friess, D.A., (2016). Rates and drivers of mangrove deforestation in Southeast Asia, 2000–2012. PNAS 113, 344–349.

26. Wang, Zongming., Jianguo, Wu., Marguerite, Madden., Dehua, Mao., (2012). China's wetlands: conservation plans and policy impacts. AMBIO, 41, 782–786 DOI 10.1007/s13280-012-0280-7

27. MA (Assessment, Millennium Ecosystem), (2005). Ecosystems and human well-being: wetlands and water. World Resources Institute, Washington, DC, 30-33.

https://www.millenniumassessment.org/documents/document.358.aspx.pdf

28. Davidson, N.C., (2014). How much wetland has the world lost? Long-term and recent trends in global wetland area. Marine and Fresh Water Research, 65, 934–941. https://doi.org/10.1071/MF14173

29. Wang, Z.M., Mao, D.H., Li, L., Jia, M.M., Dong, Z.Y., Miao, Z.H., Ren, C.Y., Song, C.C. (2015). Quantifying changes in multiple ecosystem services during 1992–2012 in the Sanjiang Plain of China. Sci. Total Environ., 514, 119–130. DOI: 10.1016/j.scitotenv.2015.01.007

30. Sonja, Beuel., Miguel, Alvarez., Esther, Amler., Kai, Behn., Donovan, Kotze., Christine, Kreye., Constanze, Leemhuis., Katrin, Wagner., Daniel, Kyalo Willy., Susanne, Ziegler., Mathias, Becker., (2016). A rapid assessment of anthropogenic disturbances in East African wetlands. Ecological Indicators. 67, 684-692 DOI : https://doi.org/10.1016/j.ecolind.2016.03.034

31. Mitsch, W. J., Blanca, Bernal., & Maria, E. Hernandez. (2015). Ecosystem services of wetlands. International Journal of Biodiversity Science, Ecosystem Services & Management., 11(1), 1–4. http://dx.doi.org/10.1080/21513732.2015.1006250

32. Mitsch, W.J., James J. G., Gosselink. (2015). Wetlands, 5th Edition, Publisher John Wiley & Sons, Inc. ISBN: 978-1-118-67682-0 https://www.researchgate.net/publication/271643179_Wetlands_5th_edition

33. Knox, A. K., R. A., Dahlgren, K. W., Tate, and E. R., Atwill. (2008). Efficacy of natural wetlands to retain nutrient, sediment and microbial pollutants, Journal of Environmental Quality, 37, 1837–1846 DOI: 10.2134/jeq2007.0067

34. Blahnik, T., and J., Day. (2000). The effects of varied hydraulic and nutrient loading rates on water quality and hydrologic distributions in a natural forested treatment wetland. Wetlands, 20(1), 48–61. https://comiteres.com/wp-content/uploads/2018/05/Blahnik-and-Day-2000.pdf

35. Fisher, J., and M.C., Acreman. (2004). Wetland nutrient removal: A review of the evidence. Hydrol. Earth Syst. Sci., 8, 673–685. https://doi.org/10.5194/hess-8-673-2004

36. Jordan, T.E., D.F., Whigham, K.H., Hofmockel, and M.A., Pittek. (2003). Nutrient and sediment removal by a restored wetland receiving agricultural runoff. J. Environ. Qual. 32, 1534–1547. DOI:10.2134/jeq2003.1534

37. Mitsch, W.J., and J.G., Gosselink. (1993). Wetlands. Van Nostrand Reinhohld,, New York. https://doi.org/10.2134/jeq1994.00472425002300050040x

38. Phipps, R.G., and W.G., Crumpton (1994). Factors affecting nitrogen loss in experimental wetlands with different hydrologic loads. Ecol. Eng, 3, 399–408. https://doi.org/10.1016/0925-8574(94)00009-3

39. Cooke, J.G., A.B., Cooper, and N.M.U, Clunie. (1990). Changes in the water, soil, and vegetation of a wetland after a decade of receiving a sewage effluent. New Zealand Journal of Ecology, 14, 37–47. https://newzealandecology.org/nzje/1885.pdf

40. Van der Valk, A.G., and R.W., Jolly. (1992). Recommendations for research to develop guidelines for the use of wetlands to control rural nonpoint source pollution. Ecol. Eng. 1, 115–134.https://doi.org/10.1016/0925-8574(92)90028-Z

41 Gopal, B. (1999). Natural and constructed wetlands for wastewater treatment: Potentials and problems. Water Sci. Technol. 40, 27–35. https://doi.org/10.2166/wst.1999.0130

42. Zedler, J.B., (2003). Wetlands at your service: reducing impacts of agriculture at the watershed scale. Front. Ecol. Environ., 1 (2), 65–72. https://doi.org/10.1890/1540-9295(2003)001[0065:WAYSRI]2.0.CO;2

43. Kadlec, R.H., and R.L., Knight. (1996). Treatment wetlands. Second Edition. Lewis Publ., Boca Raton. https://sswm.info/sites/default/files/reference_attachments/KADLEC%20WALLACE%202009%20Treatment%20Wetlands%202nd%20Edition_0.pdf

44. Kathryn, M., Flinn, Martin., J, Lechowicz., and Marcia, J. Waterway, (2008). Plant species diversity and composition of wetlands within an upland forest. American Journal of Botany 95(10), 1216–1224.https://doi.org/10.3732/ajb.0800098

45. Standard Methods for Examination of Water and Wastewater," 20th Edition (1998). Prepared and Published Jointly by APHA, AWWA, and WPCF, Washington, D.C.,

46. Metcalf, and Eddy. (2017). Wastewater Engineering, Treatment and Reuse, Fourth Edition, Published by McGraw-Hill Education (India) Private Limited, New Delhi. http://www.mheducation.co.in

47. Reed, S.C. (1990). Natural Systems for Wastewater Treatment, MOP FD-16, Water Environment Federation, Alexandria, VA.

48. USEPA, U. S. Environmental Protection Agency. (1998). esign manual on constructed wetlands and aquatic plant systems for municipal wastewater treatment., EPA/ 625/1-88/022, U.S. EPA CERI, Cincinnati, OH.

https://www.academia.edu/33044206/Design_Manual_Constructed_Wetlands_and_Aquatic_Plant_Systems_for_Municipal_Water_Treament

49. WPCF, Water Pollution Control Federation. (1990). Natural Systems for Wastewater Treatment. Manual of Practice FD- 16, Chapter 9. Alexandria, VA.

50. Hammer, D. A. (Editor) (1989). Constructed Wetlands for Wastewater Treatment, ISBN 9781003069850 First edition, Lewis Publishers, Chelsea, Michigan, USA. https://doi.org/10.1201/9781003069850

51. Cooper, P.F., and J.A., Hobson. (1990). Sewage Treatment by Reed Bed Systems: The Present Situation in the United Kingdom In: Constructed Wetlands For Wastewater Treatment: Municipal, Industrial and Agricultural, D. Hammer Ed., 153-171, Lewis Publisher, Chelsea, MI

52. Crites, R.W., (1994). Design criteria and practices for constructed wetlands. Water Science & Technology, 29 (4), pp. 1-6.

A Study on Spin Fin Pile Under Various Loading Conditions

R. S. Bhoyar
M. Tech. Student
Department of Civil Engineering
Government College of Engineering, Amravati
✉ rugvedabhoyar@gmail.com

A. I. Dhatrak, S. W. Thakare
Associate Professor
Department of Civil Engineering
Government College of Engineering, Amravati
✉ anantdhatrak1966@gmail.com
✉ sanjay.thakare1964@gmail.com

P. P. Gawande
Research Scholar
Department of Civil Engineering
Government College of Engineering, Amravati
✉ poonamgawnd25@gmail.com

ABSTRACT

The basis of an offshore wind turbine is a spin fin pile. Due to their Omnidirectional bending resistance, substantial surface area, and ease of installation, driven pipe piles are frequently utilized near offshore buildings. Spin Fin piles are standard pipe piles with flat, steel plates ("fins") attached at a slight angle across the first few feet of the pipe. These piles achieve pile capacities that are significantly higher than ordinary piles when they are driven into the earth. It has been discovered that attaching fins or wings to the surface of monopiles is an effective way to increase the lateral load and uplift load capacities of piles. Both traditional impact and vibratory hammers, along with templates and attachments, can be used to drive these piles successfully. the determination of the maximum load carrying capacity for combined, vertical, uplift, and lateral loads.

KEYWORDS *: Spin fin pile, Ultimate load capacity, Vertical load.*

INTRODUCTION

Pile supports a wide variety of towering structures, bridges, offshore projects, and transmission towers. Strong winds and seismic activity are just two of the many loads that these structures could be exposed to. It is often modified to increase pile capacity. Steel H-heaps, bladed piles, screws, modified larger ends, and steel pipe piles are a few examples. Wind turbines, both onshore and offshore, are frequently supported by monopiles. Because of the weak soil and low overburden soil pressure in the vicinity of the pile top, large diameter piles are necessary. By adding fins to the top or bottom of the monopiles, the pile capacity can be increased. This new, modified pile is known as the Spin Fin pile. Spin fin piles are frequently utilized in piling foundations for wave barriers, docks, dolphins, retaining wall tiebacks, seismic anchors, and other applications where failure due to predicted uplift or impact load is possible. This is a unique kind of pile foundation that is resistant to considerable lateral displacement and uplift. Spin finned piles are driven heaps with welded fin attachments that change the way the pile behaves under load.

The attachment of fins on to the surface of the monopiles has been found to be a good measure to improve the lateral load and uplift load capacity of piles. Spin fin piles are a cost saving alternative for many pile foundation applications. The spin fin tip generates significantly more resistance to tensile loads than that of a conventional pile.

A standard monopile with four plates welded at a 90-degree angle to one another is an illustration of a spin fin pile. It's a stack of pipes with an outside thread that progressively forms a fin around the base of the stack. For projects requiring enhanced resistance to uplift, like seismic occurrences, or for soils with less overburden material overlaying a strong bearing layer, like glacial till over bedrock, the Spin Fin pile is especially well-

suited. The fins also increase the pile section's bearing area, which increases its resistance to compression. Figure 1 depicts an example of a typical Spin Fin pile.

Fig. 1: Typical Spin Fin pile

When observed from head to tip, the top of one fin contacts the bottom of the fin next to it, as shown in Figure 2, which illustrates the fins' 360-degree coverage. Fins are easy to install after being bought or built on-site. When connected to the pile cap and serving as an anchor, the uplift capability is much enhanced compared to a pipe alone. By expanding the gross bearing area at the pile's base, the fins also increase end-bearing capacity. Because of this, the compression and tensile capacities of Spin Fin piles are usually attained at less depths than those of straight pipe piles of comparable size. This massive project is being worked on at the moment.

Fig. 2: Cross-section view of spin fin pie

Mechanism of Spin Fin Pile Capacity

The spin fin pile rotates into the earth while driving because of its fins. With help of vibratory hammers, templates, and accessories in addition to traditional impact piles are driven. These piles have substantially higher pile capacity than conventional ones because they spin into the ground when driven. After the pile is driven, it is integrated into a pile cap. When the pile is pulled in tension, it produces a dirt cone (visible in gray), which increases the pile's capacity. The lid then limits the rotation of the pile, preventing it from twisting. This may result in a plugging effect, increasing the resistance of the pile to tension loads.

Reducing both the number and the length of piles in an application can result in significant cost savings for the building industry. Construction time is shortened by the need to drive fewer, shorter piles and by using smaller cranes and equipment. A spin fin pile costs less than a conventional pile. Figure 3 circular pile and spin fin pile comparison.

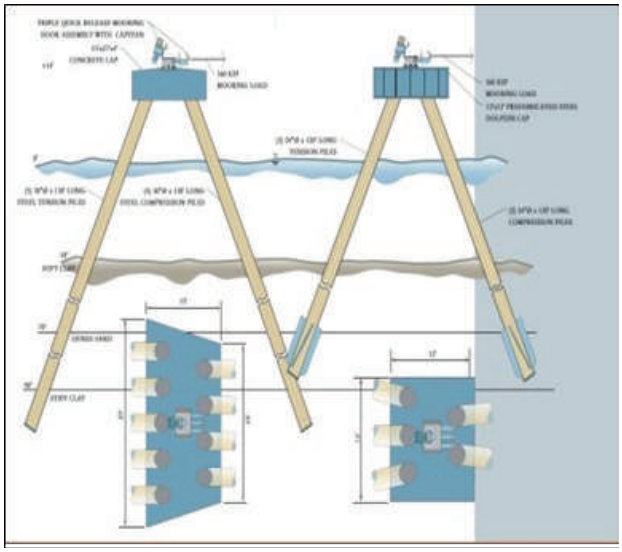

Fig. 3: Comparison between the structure with the Spin Fin pile and that of a conventional pile

The Spin Fin pile rotates into the earth while being driven by its fins. These piles can be driven successfully using templates and attachments, as well as conventional impact and vibratory hammers. These piles have a far higher pile capacity than conventional ones and rotate into the ground when pushed. After being driven, the pile is then included in a pile cap. Figure 4 illustrates a Spin Fin pile in tension and compression.

When the pile is pressed in tension, a dirt cone (which is visible in grey) is created, increasing the pile's capacity. The lid then limits the rotation of the pile to stop it from

twisting, which increases the pile's resistance to tension loads..

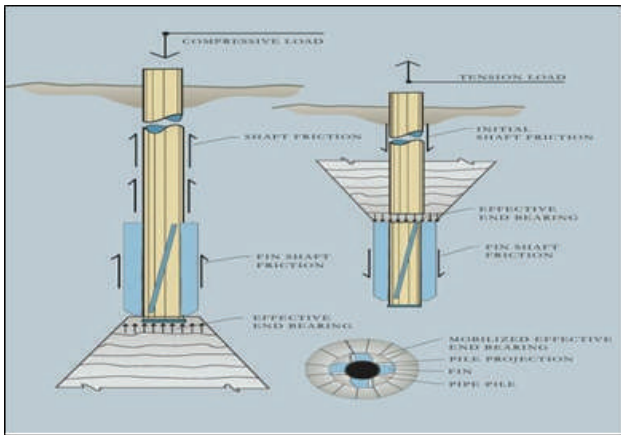

Fig. 4: Spin Fin pile load transfer mechanism

Advantges of Spin Fin pile

Following are some advantages of spin fin piles.

- In soft soil, Spin Fin piles require 50% less length than conventional piles.
- Uplift forces are produced by the rocking action of wind and earthquakes. When water levels rise beneath an ice sheet that is clinging to a building or pile, ice uplift takes place. One way to prevent uplift is to utilize spin fin piles.
- Under cyclic loading, the spin fin pile shows notable reserve strength. • This pile can take a significant amount of energy through deflection without losing strength, especially in breasting dolphin structures. This has advantages in seismic situations.
- Even after repeated loading, the deformation characteristics of Spin Fin piles permit significant pile overload deformation without catastrophic failure.
- Tests have been conducted on pile tensile capacities exceeding 800 kips with a pile embedment as short as 50 feet.
- There are major financial implications when the quantity and length of heaps are reduced.

Applications

- Many transmission towers, high-rise buildings, and bridges are supported by piles.
- Near and offshore structures such as dolphins, piers, moorings, and wind turbines are subject to severe and cyclic loading conditions

Loading Conditions of Spin Fin Pile

Spin sin pile foundation is used in offshore as well as onshore foundations.

Lateral Loading - However, offshore structure foundations must withstand substantial environmental stresses from wind, waves, and currents, which can result in lateral loads equal to or greater than one-third of the vertical loads. Structures subject to wind-earthquake loads, retaining walls, bridge abutments, and other pile foundation supporting structures may be affected by lateral loads. A recently invented kind of pile foundation that can withstand heavy lateral loads is a pile with fins.

Vertical Loading – Large vertical loads from the superstructure are typically transmitted into the underlying bearing strata via weaker subsoil using onshore piles. Since the lateral loads operating on pile foundations are sometimes much smaller than the vertical loads, they tend to be ignored.

Uplift Loading - The tensile capacity of a spin fin pile relies on both skin friction and the uplift bearing capacity of the fins, much like helical anchors. There is a strong correlation between the skin friction along the pile and the uplift bearing from the fins, therefore, if accurate skin frictional information is known, the ultimate capacity of the pile is more precisely determined. The fins also increase the gross bearing area at the bottom of the pile and improve the end bearing capacity. As a result, the compression and tensile capacity for Spin Fin piles is usually achieved at shallow depths compared to similarly sized straight pipe piles.

LITERATURE REVIEW

K.V. Babu et al. (2018) conducted an analysis of fin piles' lateral load response. The lateral load response of fin piles in sand and normal piles—piles without fins—was studied using numerical models. Fin piles and standard heaps were subjected to three-dimensional finite element analyses. In sand with varying relative densities—40%,55%, and 85%—analyses were conducted. During the analyses, regular and fin piles

with four and eight fins were taken into account. In sand, the behavior of fin heaps and regular piles with various fin orientations, numbers, and positions in relation to the sand were studied. They came to the conclusion that star fin piles, as opposed to straight and diagonal fin piles, carried a greater lateral load at higher fin lengths. Fins placed near the pile top provided more resistance than those placed near the pile bottom.

J. R. Peng et al. (2010) performed study on fin piles loaded laterally. To investigate the impact of fin diameters on their load bearing capability in sand, a three-dimensional (3D) computer simulation of laterally loaded fin piles was given. Using PLAXIS-3D software, the behavior of fin piles and the monopile was examined in order to produce pile head P-Y curves. They came to the conclusion that as fin length rose, so did lateral resistance. When the fin length is half the pile length, a fin pile has its maximum fin efficiency. Fins toward the top of the pile offered greater resistance than fins near the bottom of the pile.

S. W. Thakare et al. (2019) experimental research on rectangular spin fin piles for various loading modes. In the experimental examination, fins in the middle, bottom, and top of the spin fin pile were all taken into consideration. The results showed that spin fin piles with fins at the bottom provide substantially higher strength than traditional circular piles in both vertical and uplift capacities. Compared to conventional circular piles, spin fin piles with fins at the top have a larger lateral load capability.

N.G. Tale et al. (2019) performed a numerical analysis for a spin fin pile under various loading situations using MIDAS GTS 3D software. Studies were conducted by varying the fin placements, loading conditions, and relative densities. According to analysis, spin fin piles with fins at the bottom have a higher vertical capacity than ordinary piles.

P. Bariker et. al. (2020) carried out an experimental study to find lateral strength of a triangular fin pile's in sand. During the studies, there were variations in the relative density, pile length, number of wings, fin orientation, fin diameter, and pile type. It was determined that fin heaps offer significantly more lateral resistance than a standard circular pile. More resistance is provided by the fins at the pile head than by the pile bottom.

W. R. Azzam et al. (2017) conducted an experimental investigation of the behavior of single-finned piles under tension loads in sand. Comparative small-scale model uplift experiments were conducted on both fin-equipped and non-finned normal piles. The fin-width ratio (b/D), fin inclination angle (β), pile length-to-diameter ratio (L/D), and soil density were varied during the investigations. It was determined that in order to have the greatest positive impact, the ideal inclination angle of fins should be between (β) equal to and more than 45°. The modification of sand relative density from 50% to 85% increased the ultimate uplift load by 120% and 56% for pile L/Ds of 15 and 30, respectively, for finned piles with (b/D = 1, β = 90°).

Mohamed A. Sakr et al. (2019) conducted a study for uplift loading conditions on a single pile in sand that had wings shaped like triangles. The improved pile–soil interaction was modeled using a nonlinear 3D analysis that included interface elements, an elastic plastic soil model, and an elastic pile material. A finite element analysis PLAXIS 3D numerical research was conducted on piles with and without wings. Research was conducted by varying the number of wings (nw = 0, 2, and 4) and the wing-width ratio (Dw/dp = 2, 3, 4 and 5). We also took into account the effects of relative sand densities. The adopted wings at the pile end significantly increase the uplift capability with minimal distortion, according to the results. It has been observed that the wing efficiency for uplift capacity improves as the relative densities of sand increase, for a certain wing-width ratio (Dw/dp). For sand densities of 30%, 50%, and 80%, respectively, the improvement in the uplift capacity is determined to be (2.2, 2.33, and 2.45) times that of a conventional pile without wings for the wing-width ratio (Dw/dp of = 5) and number of wings (nw = 4). Because the soils within the wings have a considerable locking-up effect that results in higher uplift capacity, the presence of such wings at the bottom half of the piles provided an appropriate anchorage system.

Ahmed M. A. Nasr et al. (2013) conducted an experimental study using finned piles that were laterally loaded in sand. In their investigation, they assessed how a pile with fins positioned near to the

pile head improved lateral capacity. Regular piles with and without fins were subjected to model tests and numerical analysis. The sand in which the piles were placed had varying relative densities (Dr = 35% and 78%). The length, width, form, and type of pile were changed in order to conduct the testing and analysis. A comparative analysis was conducted between the model results and the prototype-scale results. When compared to a standard reference pile, they found that heaps with fins offered significantly higher ultimate lateral loads and lateral resistance.

The length of the fins had a major influence on the ultimate lateral load improvement, which increased noticeably when the length of the fin to length of pile ratio (LF/LP) reached 0.4. The ultimate lateral load of a pile enhanced by approximately 64% and 86%, respectively, when finned with triangular and rectangular fins compared to a conventional pile. Concurrently, there was a roughly 37% and 70% decrease in the lateral head deflection, respectively. Therefore, piles with rectangular fins performed better in terms of enhancing pile lateral behavior.

Shubhravi M. Akotkar, et al. (2020) A trapezoidal spin fin pile that was subjected to vertical loading was the topic of numerical study. Trapezoidal spin fin The many characteristics of the sandy soil beneath the pile foundation were investigated. Using a number of recommended parameters, an analytical model for a spin fin pile will be built in the MIDAS GTS NX 3D software to simulate the pile foundation. They came to the conclusion that a standard circular pile's vertical load-carrying capability can be doubled by adding an inclined trapezoidal spin fin pile.

P. P. Gawande, et al. (2020) A trapezoidal spin fin pile under uplift loading was the focus of a numerical investigation. The effectiveness of the trapezoidal spin fin under investigation pile foundation located in sandy soil with respect to its various characteristics. To accomplish this, an analytical model of a spin fin pile will be made utilizing a number of recommended parameters in the MIDAS GTS NX 3D software to simulate the pile foundation. They concluded that the uplift load-carrying capability of a standard circular pile is increased with the addition of a trapezoidal spin fin pile.

BEHAVIOR OF SPIN FIN PILE

Laboratory studies

A number of researchers have been utilizing small-scale laboratory testing facilities to investigate the behavior of spin fin pile under lateral loading. In 2014, Ahmed M.A. Nasr conducted research using model test studies to examine the behavior of finned piles under lateral loads in sand deposits with varying densities. The fins' length, width, form, and kind of pile were all changed during the experiments. The results show that after installing the fins near to the pile head, the piles' lateral resistance significantly increases. Up until the fin's length equals 0.4 of the pile length, the lateral resistance increases as the fins' length grows.

Ahmed M. A. Nasr4 et al. (2013) conducted an experimental study using finned piles that were laterally loaded in sand. They attempted to assess the improvement in lateral capacity of a pile with fins installed near the pile head in their study. Regular piles without (fins) and piles with fins were the subject of small-scale model experiments and a computer investigation utilizing finite element analysis. The sand in which those piles were placed had varying relative densities (Dr= 35% and 78%). The fins' length, width, form, and kind of pile were all changed during the experiments. Additionally, a comparison between the prototype-scale results and the model results was examined. Figure 5 displays a schematic elevation view of the test configuration.

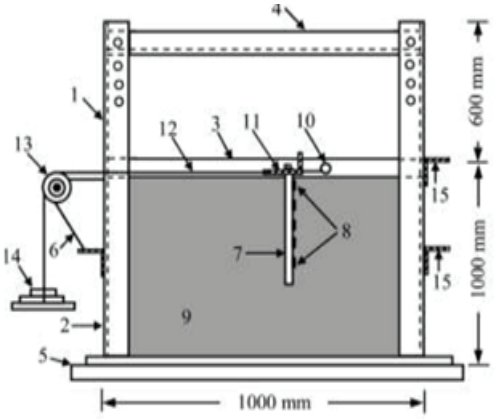

1- Loading frame; 2- Test tank; 3- Thick glass wall; 4- raining device; 5- Steel base; 6- Stiffener plate; 7- Model pile; 8- Strain gauges; 9- Sandy soil; 10- Dial gauges; 11- Model pile cap; 12- Steel wire; 13- Smooth adjust Pulley; 14- Weights; 15- Stiffener angles;

Fig. 5: Schematic Elevation View of Test Configuration (Ahmed M. A. Nasr, 2013)

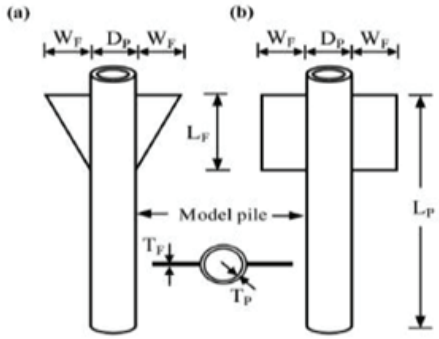

D_P = pile diameter (constant); L_P = embedded length of pile; W_F = fin width; L_F = fin length; T_P = thickness of pile wall; T_F = thickness of fin wall (constant).

Fig. 6: Different Shapes of Fins

Two distinct fin forms that were employed in the trials are depicted in Figure 6. Using steel sheets that were 2.0 mm thick, fins of two different diameters were formed into triangles and rectangles. When compared to a standard reference pile, fin-equipped piles yielded significantly greater ultimate lateral loads and lateral resistance behavior. The fins' length had a considerable impact on the ultimate lateral load improvement, which rose to a value of LF/LP = 0.4. Additional fin length increases did not have a significant impact on the pile capacity. As the fins' length increased, the lateral head deflection reduced. The fin efficiency rose as fin width grew for both short and long pilesThe ultimate lateral load of a pile enhanced by approximately 64% and 86%, respectively, when finned with triangular and rectangular fins compared to a conventional pile. Therefore, it was more successful to use rectangular fins to improve the lateral behavior of piles. Fins can be used to gain lateral resistance while reducing the length of a finned pile in comparison to a standard pile.

S. W. Thakare et al. (2019) studied performance of spin fin pile under different loading modes. The static lateral pile load test were conducted on a model pile foundation as per IS: 2911- (part 4) 1985 to evaluate the lateral pile capacity. The lateral load to the piles was applied through static loading with help of a pulley and string system as shown in Figure 7.

Fins at the bottom, middle, and top of the spin fin pile were the three placements of fins that were taken into consideration in the experimental inquiry. The ultimate capacity of the piles are contrasted with the same diameter and length of a traditional circular pile. Figure 8 displays the load vs. settlement curves for a spin fin pile with a different fin position and a regular circular pile subjected to lateral load.

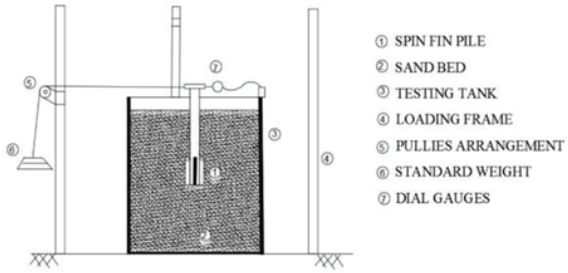

Fig. 7: The Schematic Diagram of the Test Setup for Lateral Loading used for Experimental Investigations

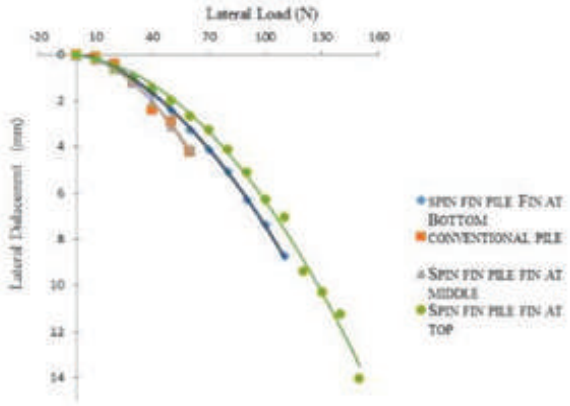

Fig. 8: Lateral load vs. lateral displacement curves for conventional circular pile and spin fin pile with different fins position.

It is observed that lateral load capacity of Spin Fin Pile with fins at top is maximum as compared to Spin Fin Pile with fins at middle and bottom and that of conventional circular pile.

Analytical Studies

K.V. Babu1 et al. (2018) conducted an analysis of fin piles' lateral load response. The lateral load response of fin piles in sand and normal piles—piles without fins—was studied using numerical models. Fin piles and standard heaps were subjected to three-dimensional finite element analyses. In sand with varying relative densities—40%,55%, and 85%—analyses were conducted. During the analyses, regular and fin piles with four and eight fins were taken into account. The impact of fins' orientation and placement on the lateral

load response of fin piles was emphasized, together with the relative density of the sand. Figure 9 show the normalized lateral load carrying capacity of regular and fin pile with various density indices having different fin orientations.

Fin direction, fin position, and relative density of the sand all affect the increase in lateral load. The total pile length and diameter were decreased with the aid of these characteristics. When compared to ordinary piles, fin piles in loose sand demonstrated a lateral load carrying capability improvement of about 60%. The lateral load carrying capacity of fin piles in medium dense sand was found to be around 65% higher than that of ordinary piles. When compared to ordinary piles, fin piles in dense sand showed an improvement in lateral load-carrying capacity of about 75%. Star fin piles, followed by straight and diagonal fin piles, carried a greater lateral strain at longer fin lengths. More resistance was offered by fins positioned close to the top of the pile than by those toward the bottom.

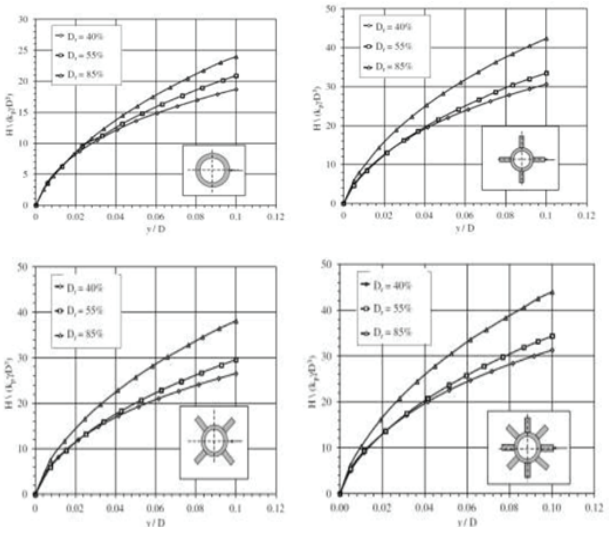

Fig. 9: Normalized lateral load-deflection curves for regular and fin piles, (a) regular pile, (b) straight fin piles, (c) diagonal fin piles, (d) star fin piles (K.V. Babu et al.,2018).

CONCLUSION

1. Spin fin piles with fins at the bottom have a far higher ultimate vertical load capacity and uplift capacity than spin fin piles with fins at the middle and top.
2. The lateral load capacity of spin fin piles with fins at the top is much higher than that of spin fin piles with fins at the bottom and center.
3. The highest vertical capacity The capacity of spin fin piles in dense sand are higher than those in loose sand.
4. The maximum vertical load capacities for both types of piles increase with pile count.

REFERENCES

1. Ahmed M.A. Nasr (2014), "Experimental and theoretical studies of laterally loaded finned piles in sand", Can. Geotech. J. 51: 381–393.
2. Azzam W. R. and Elwakilb A. Z. (2017), "Model Study on the Performance of Single Finned Pile in Sand under Tension Loads", International Journal of Geomechanics, © ASCE, ISSN 1532-3641.
3. Babu K. V., and Viswanadham B. V. S. (2018), "Numerical Investigations on Lateral Load Response of Fin Piles", Numerical Analysis of Nonlinear Coupled Problems, Sustainable Civil Infrastructures, DOI 10.1007/978-3-319-61905-7_27.
4. K. Madhusudan Reddy and R. Ayothiraman, "Experimental Studies on Behavior of Single Pile under Combined Uplift and Lateral Loading", Journal of Geotechnical and Geoenvironmental Engineering, © ASCE, ISSN 1090-0241/04015030(10).
5. Jan Duhrkop and Jurgen Grabe, (2008) "Laterally Loaded Piles With Bulge", Journal of Offshore Mechanics and Arctic Engineering NOVEMBER 2008, Vol. 130 / 041602-1 13.
6. Britta Bienen, Jan Duhrkop, Jurgen Grabe, Mark F. Randolph and David J. White (2012) "Response of Piles with Wings to Monotonicand Cyclic Lateral Loading in Sand",364 / Journal of Geotechnical and Geoenvironmental Engineering © ASCE / March 2012
7. Mohamed A. Sakr, Ashraf K. Nazir, Waseim R. Azzam and Ahmed F. Sallam, (2019) "Uplift Capacity of Single Pile with Wing in Sand-Numerical Study", International Conference on Advances in Structural and Geotechnical Engineering, ICASGE'19, 25-28 March 2019, Hurghada, Egypt.
8. J. R. Peng, M. Rouainia, and B. G. Clarke (2010), "Finite element analysis of laterally loaded fin piles", Computers and Structures 88 (2010) 1239–1247.

9. P. P. Gawande and Dr. A. I. Dhatrak (2020) "Numerical Analysis on Trapezoidal Spin Fin Pile Subjected to Uplift Loading" International Journal for Research in Applied Science & Engineering Technology (IJRASET) ISSN: 2321-9653; IC Value: 45.98; SJ Impact Factor: 7.429 Volume 8 Issue XII Dec 2020

10. Rekha Ambi, Jayashree P. K. and UnnikrishnanN (2017) "Effect of Fin Length on the Behaviour of Piles under Combined Loading Conditions", Indian Geotechnical Conference (2017).

11. Shubhravi M. Akotkar and Dr. A. I. Dhatrak (2020) "Numerical Analysis on Trapezoidal Spin Fin Pile Subjected To Vertical Loading" International Research Journal of Engineering and Technology (IRJET), Volume: 07 Issue: 12 / Dec 2020.

12. Steven Halcomb, Sean Sjostedt, and Charles Somerville (2018). "High Strain Dynamic Testing of Spin Fin Piles", IFCEE2018 GPP 11©ASCE.

13. N.G. Tale, Dr. A. I. Dhatrak and S. W. Thakare (2019), "Numerical analysis of spin fin pile under different loading conditions", International Journal of Technical Innovation in Modern Engineering & Science, e-ISSN: 2455- 2585 Volume 5, Issue 05.

14. S. W. Thakare, P. P. Wankhade and Dr. A. I. Dhatrak (2019) "Experimental investigations on performance of spin fin pile under different loading modes", International Journal of Technical Innovation in Modern Engineering & Science, e-ISSN: 2455-2585.

Developing Asbestos-free Brake Pads from Sustainable Coconut Shell Material: A Mechanical and Tribological Study

Swapnil Lokhande
Mechanical Department
Oriental University
Indore, Madhya Pradesh
✉ swapnillokhande28@gmail.com

Mohammed Ali
Mechanical Department
Oriental University
Indore, Madhya Pradesh

ABSTRACT

The current study proposes a novel coconut shell material for developing asbestos-free brake pads. The brake pads were produced from coconut shell powder of sizes 200 µm, 300 µm, 400 µm, and 500 µm. The developed brake pads are assessed for morphological, mechanical, physical, and tribological properties. Scanning electron microscopy images revealed that coconut shell powder was evenly distributed throughout the brake pad, indicating strong interfacial bonding with resin. The brake pad with a peel powder size of 300 µm was chosen as optimum because decreasing the peel powder size from 500 µm to 300 µm increased oil and water resistance, hardness, comprehensive strength, bulk density, and coefficient of friction. Furthermore, brake pads with a powdered size of 300 µm tested for smooth and hard braking exhibited uneven wear, with significant wear on the leading edge.

KEYWORDS *: Brake pads, Coconut shell, Asbestos, Wear, Coefficient of friction.*

INTRODUCTION

The braking system is a fundamental mechanical component of cars and industrial machines that converts kinetic energy into heat through friction. The disc brakes are becoming more prevalent in the vehicle industry. Disc brakes use friction material (FM) on the brake pads to stop or control motion. The FM should have a wide range of mechanical and tribological features, such as high thermal stability, low wear rate, and noise during smooth and harsh braking, a stable coefficient of friction (COF), and long-term durability. Asbestos has been widely employed in braking systems since the early twentieth century because it possesses several of the qualities required for efficient FM in brake pads. However, due to the health risks created by the carcinogenic qualities of asbestos, the Environmental Protection Agency (EPA) limited its usage. Although copper, a semi-metallic FM, has garnered significant attention in the recent two decades, developed countries have begun to impose limits on its usage, and copper as an FM is projected to be outlawed by 2025 [1]. Finding a replacement for conventional FMs is critical in the worldwide industrial sector, as FMs are at the heart of the braking system. Since the material industry has improved greatly, various research has been done in recent years to study the possibilities of using metallic, semi- or low-metallic, and composite materials as FMs. FMs contain over 15 components, including fibers, inert and functional fillers, and binders, posing a major environmental concern [2]. A feasible approach is to use sustainable natural materials as FMs in braking systems. In this regard, the current study proposed a novel coconut shell-based FM for disc brakes.

Aigbodion [3] studied the interaction of rice husk-derived carbon nanotubes with Ag nanoparticle-modified brake pads. The results demonstrate that at optimal conditions, the wear rate and COF were 2.15 mg/m and 0.42, respectively. Recently, silicon [4], bagasse [5], fine brass fibres [6], and periwinkle shell [7,8] materials were evaluated for the manufacture of asbestos-free brake pads. Chandradass et al. [9] evaluated the mechanical and tribological properties of asbestos-free carbon fiber brake pads. To maximize concentration, the carbon volume % was changed from 0 to 10. The results showed that 10-volume % carbon provided a greater COF, tensile and flexural strength,

and reduced wear rate. Sagiroglu and Akdogan [10] changed polymer-based brake pads using blast furnace slag, discovering that adding 50% slag improved the COF to 0.45. Kiehl et al. [11] studied the tribological performance of the gray cast iron brake pad coated with StelliteTM 6 for corrosion resistance. The results reveal that the StelliteTM 6 coating improves corrosion resistance by generating a passive layer of cobalt and chromium oxide. The emission of particulate matter (PM) from the brake pad has a negative impact on human health and the environment.

Carlevaris et al. [12] examined the efficacy of FM based on rice husk and rice husk ash in terms of PM emission reduction. To improve the modified FM, various weight% of rice husks were used, and it was discovered that 6-12 weight% rice husks resulted in significantly decreased PM emissions and wear rates. Singaravelu et al. [1] employed cashew friction dust as a component in FMs to manufacture copper- and asbestos-free brake pads. Five different friction modifiers were added to the FM to improve the thermal stability of the developed brake pad over time. The findings demonstrate that brake pads treated with born-graphite have superior physical, mechanical, and tribological capabilities than those modified with furfural. Singh [13] examined the tribological features of brake pads manufactured using cement by-pass dust as the filler material and barium sulfate. The results reveal that COF increased with the weight% of cement bypass dust, then reduced as the weight% increased further. To increase brake pad performance and wear, Bhakuni et al. [14] fabricated FMs from ceramic matrix composites including kaolin clay and barite powder. The findings indicated that barite-based ceramic composites had a greater COF and wear resistance. Zheng et al. [15] conducted a friction and wear investigation using iron and graphite powder-added friction material. The data showed that iron and graphite mass concentrations of 20% and 14%, respectively, resulted in the best frictional characteristics. Xu et al. [16] investigated tribological properties of copper-matrix FM incorporating mullite and kyanite. It was noted that kyanite created a tribo-film on the FM surface, protecting against wear, and 1% kyanite decreased wear by around 30%. Kalel et al. [2] developed eco-friendly brake pads from Aramid fibers/pulp and Zylon fibers. The influence of fiber aspect ratio on the tribological properties of brake pads was studied, and it was discovered that Aramid fiber/pulp-based brake pads had a greater COF than Zylon fiber-based brake pads. Jensen et al. [17] created a wear model for tribological examinations of brake pads and verified it using data from brake pads mounted on a test vehicle.

The aforementioned available literature confirms that numerous lab-synthesized friction compounds were employed to make asbestos- and copper-free brake pads. However, major disadvantage of employing modern synthetic FM is that both organic and inorganic materials endanger human health and the environment. Furthermore, the significant studies in the literature focused on the performance of brake pads on a lab scale. There have been few experimental tests on the performance of produced brake pads on test vehicles. To address these issues, the current study proposed novel coconut shell material to fabricate asbestos-free disc brake pads. The brake pads were made from coconut shell powders (200-500 µm) and examined for morphology and tribological qualities. In addition, an optimized coconut shell brake pad was physically tested on the front wheel of the test vehicle for hard and smooth braking.

MATERIAL AND METHODS

Fabrication of coconut shell (CS) brake pads

Coconut shells were purchased from local markets and washed in a fruit washer machine for 30 minutes to remove physical contaminants from the surface. To clean the sticky inner surface, coconut shells were kept in hot water (50–55 °C) for 4–5 minutes and then allowed to cool to ambient temperature. The obtained shells were dried in an electric dryer with 70°C hot air for 15 minutes. The dehydrated coconut shells were powdered in a pulverizer. The hopper in the pulverizer produced fine and coarse particles of feeding peels, which were separated using a vibrating mesh screen. To obtain various sizes of coconut shell powder, four mesh screens with sizes of 200 µm, 300 µm, 400 µm, and 500 µm were employed. Fig. 1(a-d) depicts actual photographs of different sizes of coconut shell powder prepared.

The brake pads are produced using compression molding and are made from powdered coconut shells

with sizes ranging from 200 µm to 500 µm. Due to their high viscosity, the phenolic resin, filler materials (mica and barium sulfate), and a stabilizer were combined in the Sigma mixer for 35–45 minutes. The homogeneous, viscous dough created by the mixture is left to dry in the sun for a duration of 3 hours on a sheet of paper. Following that, the dehydrated dough is subjected to compression in a compression molding machine, applying a pressure of 80 bar and a temperature of 120°C. The dough was shielded with polyvinyl chloride sheets to prevent it from adhering to the machine component. The molded material is permitted to undergo natural cooling before being precisely trimmed to the necessary dimensions and subjected to testing to ensure the absence of asbestos in brake pads. Fig. 2 illustrates the fabrication process for coconut shell brake pads.

Fig. 1 Photographs of CS powder of sizes (a) 500 µm, (b) 400 µm, (c) 300 µm, and (d) 200 µm

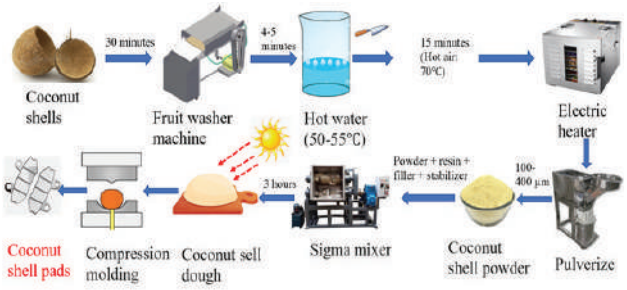

Fig. 2 Fabrication process for coconut shell brake pads

Characterization of coconut shell pads

Coconut shell pads were characterized to investigate their shape and various qualities, including mechanical, physical, and tribological. The morphology of generated pad samples is studied with an SEM (SU6600, Hitachi, Japan). Before SEM imaging, a gold sputter was used to ground extra electrons. Soak tests were performed to measure the oil and water absorption resistance of the coconut shell pads. The produced pads were soaked in SEA 20W-50 engine oil and water for48 hours at 28-32°C. The changes in the weight and size of pads before and after immersion in water and engine oil are utilized to investigate swelling. Because the shapes of the coconut shell pads were uneven, we used Archimedes' technique to compute bulk density. The pads were immersed in water, and the volume of water displaced (Vw) was estimated using Eq. 1 based on the object's weight in the water (Ww) and the actual water in the air (Wa). Finally, the pad's density (ρs) is computed using Eq. 2.

$$V_w = \frac{W_a - W_w}{g\rho_w} \quad (1)$$

$$\rho_s = \frac{\rho_w W_a}{W_a - W_w} \quad (2)$$

where g and ρ_w are the gravitational acceleration and density of water.

The hardness of the developed CS pads is determined using the Brinel-Hardness test. Pads were tested for 20 seconds under a 960-1542 N load with a 1.56 mm diameter steel indenter (harness value ~101 HRB). The Brinell hardness number is determined by precisely measuring the impression diameter using a Brinell microscope. Furthermore, the compression tests were carried out using an 11-Avery-Denison compression machine (capacity 150 kN) at a strain rate of 1.4 ms^{-1}. The brake pads were locked in a testing machine and gradually loaded until they failed.

A pin-on-disc tribometer was used to measure two-body sliding wear on produced pads in accordance with ASTM G 99-95a standards. The coconut shell pad, carved into the shape of a pin (10 mm in diameter), makes contact with a rotating cast iron disc at 1.5 m/s for 90 minutes under a force of 40-60 N without lubrication. A cast iron disk (160 HRC harness value) with a track diameter of 130 mm and thickness of 10 mm was employed. All tests were carried out at temperatures ranging from

26 to 29°C. The pad sample's initial and end weight differences were determined using a weighing scale with an accuracy of 0.0003-gram. The evaluated brake pad samples were cleaned with acetone to remove contaminants from their surfaces. The wear rate (Wr) is computed using Eq. 3 based on the sample's weight loss (WS) and sliding distance (S).

$$W_r = \frac{W_S}{S} \quad (3)$$

RESULTS AND DISCUSSION

Surface morphology of coconut shell pads

Fig. 3 shows the morphology of CS pads with powdered sizes of 200, 300, 400, and 500 µm. SEM images revealed that coconut shell powder sizes of 200 µm, 300 µm, 400 µm, and 500 µm were evenly distributed, showing strong interfacial bonding with resin. The SEM images (Fig. 3a-d) show that powdered sizes 200 µm and 300 µm have more consistent element distribution than other sizes. This could be attributed to the smaller powdered size increasing the specific surface area, resulting in stronger interfacial bonding with the resin.

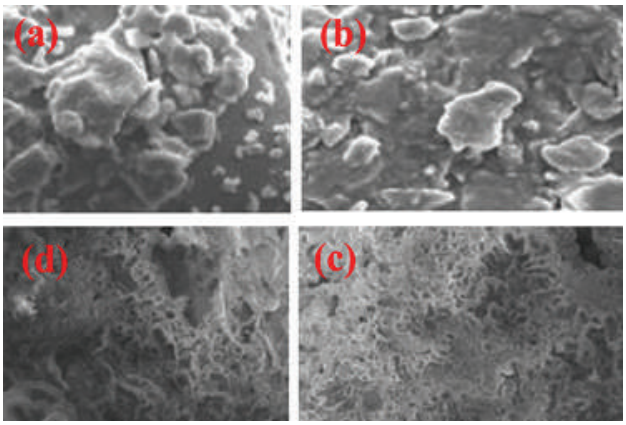

Fig. 3 SEM images of CS pads with powder sizes of (a) 500 µm, (b) 400 µm, (c) 300 µm, and 200 µm

Water and oil absorption

The absorption of oil and water by the brake pad diminishes braking effectiveness. To select an efficient brake pad, consider the amount of oil and water absorbed by the pad surface. Fig. 4 shows the thickness-swelling of coconut shell pads with different particle sizes in water and engine oil (SEA 20W-50). Reducing the peel powder size from 500 µm to 200 µm considerably decreased oil and water thickness-swelling capabilities. This may be due to greater elemental bonding and a reduction in particle size, resulting in a decrease in porosity. For optimal oil and water absorption resistance, a coconut shell pad with a peel particle size of 300 µm is recommended above a smaller size of 200 µm. The swelling of coconut shell pads during water and motor oil immersion is driven by compression forces created in compression modeling, as well as the element's hygroscopic characteristics. It is worth noting that in the water and engine oil absorption tests, the developed brake pads showed marginal swellings.

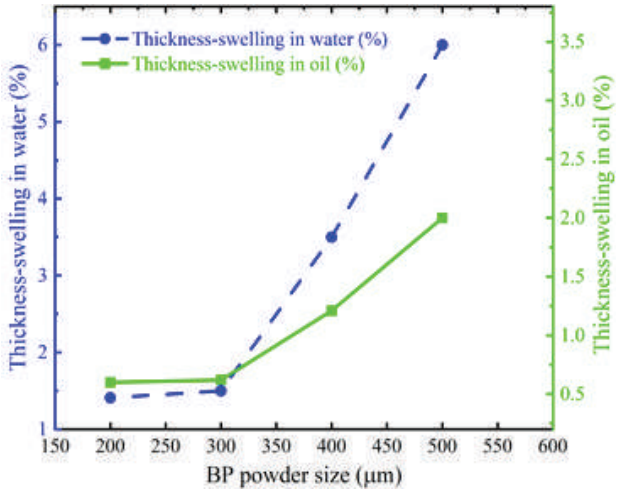

Fig. 4 Coconut shell pad thickness-swelling in water and engine oil

Hardness and compressive strength

The hardness value is an important consideration when choosing a brake pad because it depends on other properties including compressive and tensile strengths, wear resistance, stiffness, etc.. Fig. 5 shows the effect of the coconut shell powder size on the hardness and compressive strength of the pads. Reduced shell powder size from 500 µm to 300 µm led to a significant enhancement in hardness. However, further reducing the powdered size to 200 µm had only a minor effect on harness value. As the powdered size decreases, the specific surface area increases, resulting in a stronger bond with resin and an increase in hardness value. Fig. 5 shows that the CS pad sample with 300 µm powdered size has the highest hardness. Compressive strength followed a similar trend as hardness since it varies linearly with average hardness. Pads with

300 µm coconut shell powder showed the maximum compressive strength due to smaller pores, homogenous elements distribution, and improved interfacial bonding.

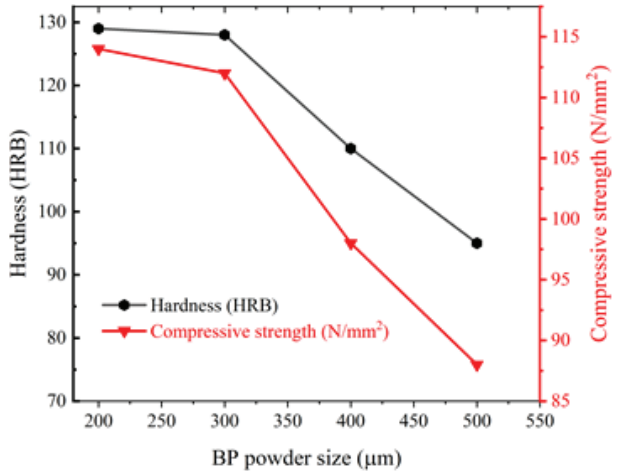

Fig. 5 Variation of hardness and compressive strength with powdered size.

Bulk density (ρ_s)

The ρ_s value affects the life and durability of brake pads since greater ρ_s brake pads handle heat more efficiently. The calculated ρ_svalues of different coconut shell brake pad samples are shown in Table 1. The average ρ_s varied marginally with powder size (~1.2%). The slight decrease in ρ_s with increasing powdered size is due to a higher fraction of coarser particles, which reduces interfacial bonding and thus ρ_s.

Table 1 Bulk density of different coconut shell brake pad

Coconut shell powder size (µm)	ρ_s (g/cm^3)
400	1.68
300	1.67
150	1.66
100	1.66

Wear rate and COF

To accomplish effective braking, the brake pads must have a greater COF and a lower wear rate. Fig. 6 depicts the variance in wear rate with load for different coconut shell brake pad samples. The pad samples were subjected to a steady sliding velocity of 1 m/s for 90 minutes. In the pin-on-disc tribometer, sliding velocity, distance, and load all contribute to wear rate and COF calculations. The current wear tests subjected coconut shell pads to stresses ranging from 40 N to 60 N. The load increased the wear rate in all pad samples. The load raises the pressure on the pad, allowing a hard-rough disc surface to plow more on the soft pad surface, resulting in increased wear mass loss and a higher wear rate. Surface wear is generally caused by the abrasive mechanism; however, the adhesive mechanism may also contribute to some wear.

It is noticed that the coconut shell brake pad with 500 µm powdered size showed significant wear, while the CS pad with 200 µm peel powdered size had low wear. This is owing to decreased particle size, higher specific surface area, and interfacial bonding with resin, all of which lead to improved hardness (see Fig. 5), resulting in a lower wear rate. The coconut shell pad with a 300 µm powdered size was selected as optimum, as the wear rate varied only slightly when the peel powdered size was reduced to 200 µm. Table 2 lists the average COF for different coconut shell brake pads. Table 2 shows that the average COF for all CS pads is comparable to commercial asbestos-based brake pads (0.3-0.5).

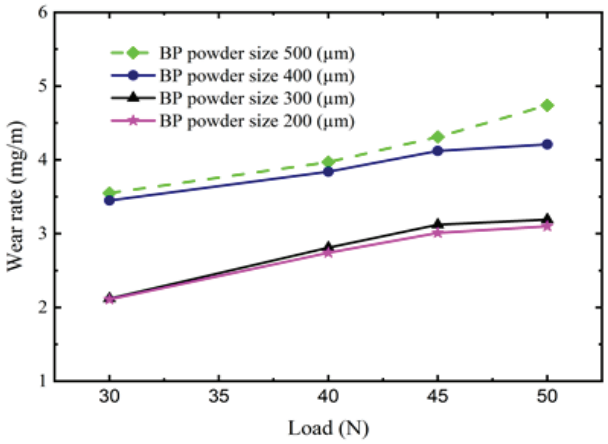

Fig. 6 Variation in wear rate with load for various coconut shell brake pads

Table 2 Average COF for different coconut shell brake pads

Brake pad of coconut shell powder size (µm)	COF
400	0.41
300	0.42
150	0.44
100	0.44

Testing of the developed CS brake pads in the test vehicle

Two 300 µm powdered coconut shell pads (CSP-300) were tested on the test vehicle's front wheels (Yamaha FZS-FI V3). The CSPs-300 were exclusively fitted on the left and right sides of the test vehicle's front wheel discs. The wear performance of the designed CSPs-300 were measured in the test vehicle under both smooth and hard braking scenarios. In the smooth braking test, the vehicle runs at a relatively constant speed on the highway with infrequent stopping over long distances, whereas in the hard braking test, the vehicle travels at a moderately varied speed on a country or dirt road with deliberate braking over shorter distances. The wear on the brake pads was tested by removing them from the vehicle after every 20 km of driving, for a total of 11 measurements over about 220 kilometers. Wear measurements were recorded at three points on the brake pad surface: the leading and trailing edges, as well as the middle. Fig. 7 depicts the various wear measurement points on both pad surfaces. Figs. 8 and 9 show the thickness variations of the left and right CSP-300 during smooth and hard braking. Wear is visible at all three measurement points on the left and right side pads during both hard and smooth braking. The leading edges of both pads were heavily worn, followed by the training edges and centers. This could be the result of faulty caliper operation. In the current test, poor operation of the guide pin may have caused the leading edge of the pads to have a greater contact angle with the disc, resulting in increased wear. Furthermore, Figs. 8 and 9 indicated that both left and right brake pad surfaces degrade much more during hard braking than smooth braking. This is largely due to frequent braking over short distances on unpaved roads.

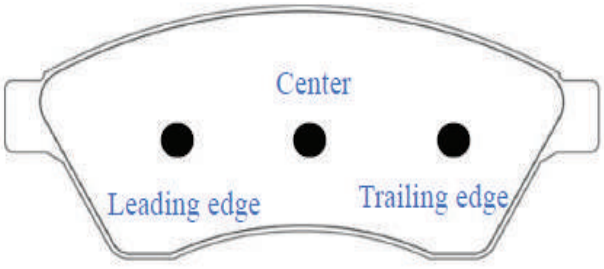

Fig. 7 Wear measurement locations on the brake pad surface

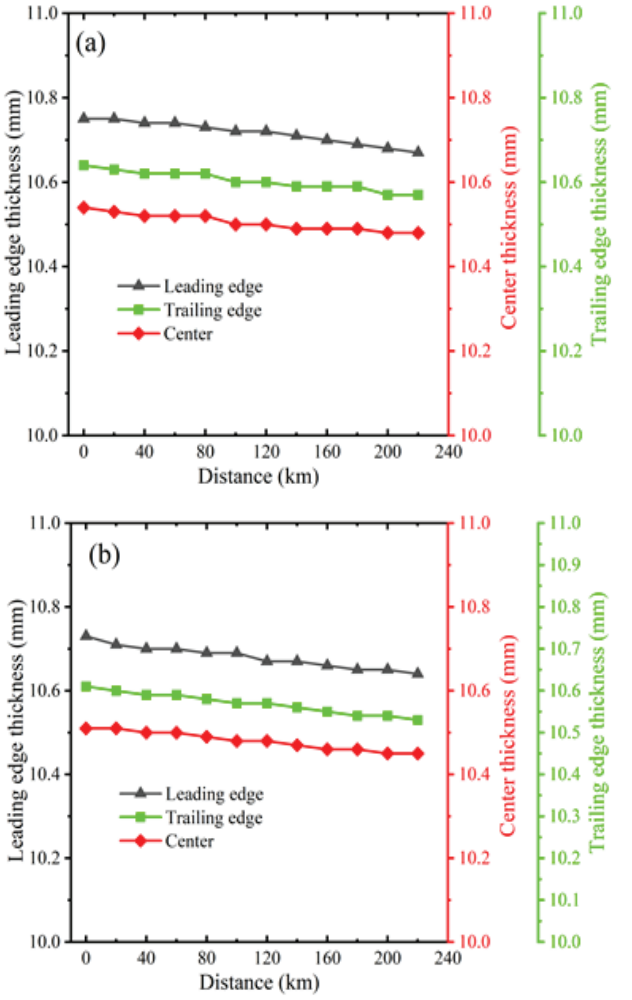

Fig. 8 Thickness variation of CSP-300 during smooth braking (a) left and (b) right side

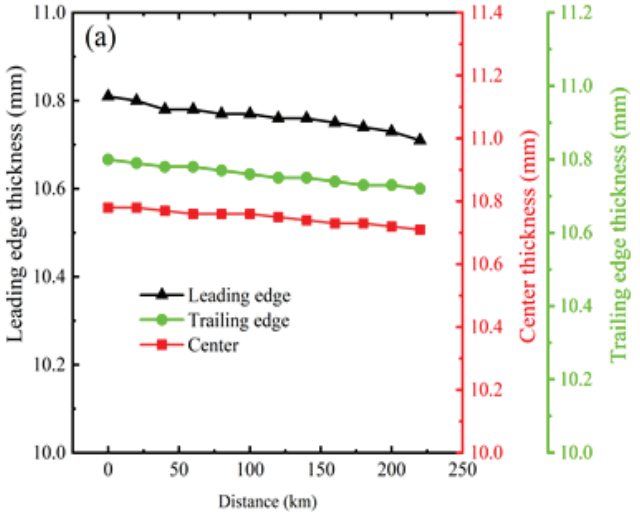

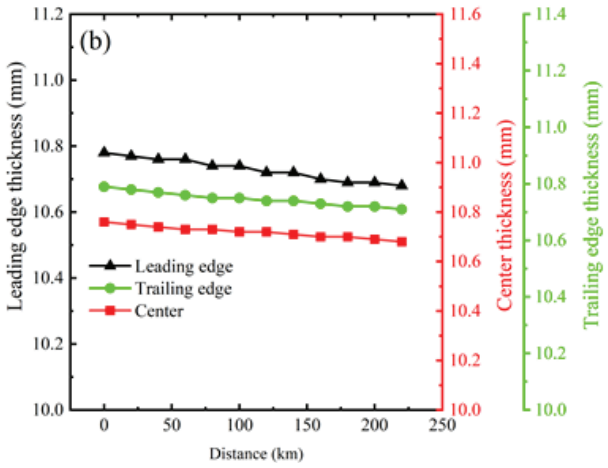

Fig. 9 Thickness variation of CSP-300 during hard braking (a) left and (b) right side

Characteristics of developed coconut shell brake pads are compared with those of commercially available asbestos-based and asbestos-free brake pads developed in recent literature.

It is noticed that wear rate COF, and hardness values of the developed CSP-300 meet accepted ISO (6312:2010) standards. Furthermore, it worth mentioning that COF of CSP-300 is relatively higher than recently studied bagasse based [5] and palm kernel fibers [18] asbestos-free brake pads. Therefore, based on the findings of the current study, CSP-300 recommended to replace conventional asbestos-based pads.

CONCLUSIONS

To address the human health and environmental issues posed by asbestos-based brake pads, the current study proposes a novel coconut shell material for asbestos-free brake pads. The brake pads were made from various coconut shell powder sizes (500–200 µm) and tested for mechanical and tribological properties. Furthermore, long- and short-term tests were conducted to assess the feasibility of the developed brake pads. Based on experimental investigation, significant findings can be summarized as follows:

- SEM images showed a homogeneous distribution of coconut shell powder within brake pads, demonstrating strong interfacial bonding with resin.
- Mechanical and tribological properties, including oil and water resistance, hardness, comprehensive strength, and bulk density, increase as the powdered size is reduced to 300 µm. The brake pad with a powdered size of 300 µm was found to be optimal.
- In pin-on-disc tribometers, wear mass loss increases with load due to increased pressure on the pad.
- The average COF for a developed coconut shell brake pad was found to be 0.41-0.44, which is comparable to conventional asbestos-based brake pads.
- During long- and short-distance vehicle testing, the leading edges of both pads were worn the most, followed by the training edges and center.

Based on the experimental findings, coconut shell brake pads are recommended to develop asbestos-free brake pads.

Design and Development of a Marker-based Augmented Reality Application for Steam Turbine Education for First-Year Engineering Students in Line with Industry 4.0

Sudhir Bharat Desai
Vaishali Prashant Bhosale
Yashwantrao Chavan School of Rural Development
Shivaji University, Kolhapur
✉ sbd.ycsrd@unishivaji.ac.in
✉ vpb.ycsrd@unishivaji.ac.in

Ajit Bhanudas Kolekar
Department of Technology
Shivaji University, Kolhapur
✉ abk_tech@unishivaji.ac.in

ABSTRACT

This research paper presents the design, development, implementation, and analysis of an augmented reality (AR) application of a steam turbine power plant to enhance the educational experience of first-year engineering students. The marker base, application is developed to enhance the learning experience. 3D modelling software Creo parametric, and 3Ds Max were used for model development and animation. Unity 3D engine, and Vuforia are used for Augmented reality application development. Students are allowed to interact with a 3D model of a steam turbine power plant and visualize it in real time. The developed application was tested and investigated the impact of the AR tool on students' understanding, engagement, and retention of complex engineering concepts related to steam turbines.

KEYWORDS *: Augmented reality, Unity, Vuforia, Marker-base, 3D models, Steam turbine power plant.*

INTRODUCTION

Education 5.0 focuses on adapting the educational system to meet the demands of the fourth industrial revolution. AR/VR technologies can be used to improve education in the context of Industry 4.0 and Education 5.0. [1-2]. Steam turbines are a fundamental topic in mechanical engineering, essential for power generation and industrial applications. Traditional teaching methods, often dependent on textbooks and static diagrams, can struggle to convey turbine operations' dynamic and complex nature. Emerging technologies like augmented reality (AR) offer innovative ways to enhance educational experiences by providing interactive and immersive learning environments. This study aims to develop an AR application for first-year engineering students, assessing its effectiveness in improving learning outcomes and engagement.

METHODOLOGY

The research follows a mixed-methods approach, combining quantitative and qualitative data collection. The development process begins with requirement analysis, involving consultations with educators and students to identify key learning objectives and features. The AR application is developed using Unity and Vuforia, incorporating 3D models of steam turbine components and interactive simulations. Testing involves iterative feedback from a pilot group of students.

AR DEVELOPMENT WITH UNITY GAME ENGINE

Unity game engine can be used to develop various applications in Augmented reality and deploy it across various platforms like Windows, android, webGL, and iOS. Unity has its own asset store that can be directly used for the development of AR applications. Unity Game Engine environment with its Panels like Hierarchy, Scene, Game, Inspector, Project, and Console plays an important role in AR application development as shown in Figure 1.

Fig. 1. Different panels in Unity

VUFORIA

Vuforia SDK is used in the Unity game engine to convert a normal Unity project into an augmented reality project. After importing Vuforia SDK the existing main camera in Unity game engine is replaced by an AR camera from the Vuforia package. Vuforia's image recognition algorithm detects unique edges or dotted lines or text on an image and generates yellow-colored feature points on top of those edges. Vuforia license key was created through the official Vuforia developer portal as shown in Figure 2 and Figure3. This key helped in unlocking the complete potential of the Vuforia SDK, allowing robust tracking and rendering of virtual objects of steam power plant.

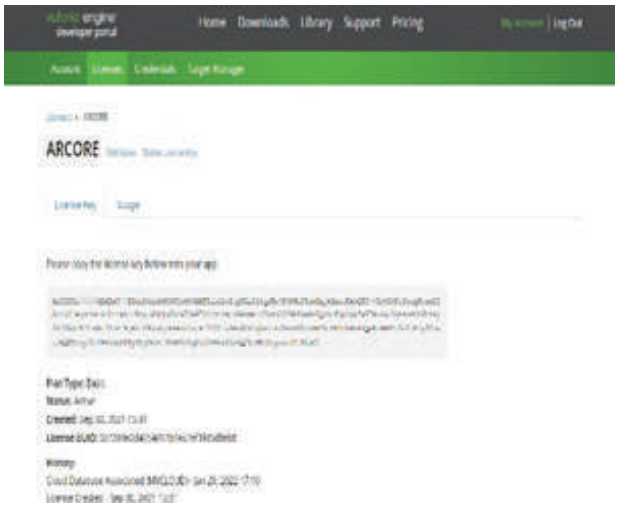

Fig. 2. Vuforia Licence Key

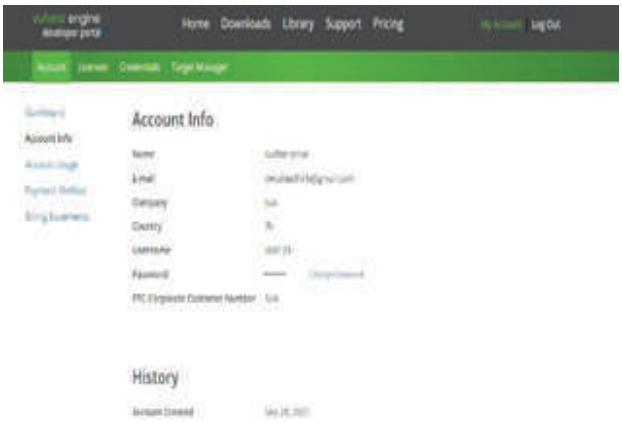

Fig. 3. Account Credentials

IMAGE TARGET

An image target is a specific image that an AR camera recognizes to display digital content in the real world. The image of a Steam power plant from a textbook is uploaded to the Vuforia database with device option as shown in Figure

4. This image is used as a marker to augment the Steam power plant over it. This image includes text for which Vuforia's algorithm generated unique feature points with a Four-star rating as shown in Figure 5, which is good for quickly recognizing the image target by the webcam or smartphone camera. Care is taken while selecting an image that it should be .jpg or .png images in RGB or greyscale. The size of the image is less than 2MB and with a minimum of 320 pixels.

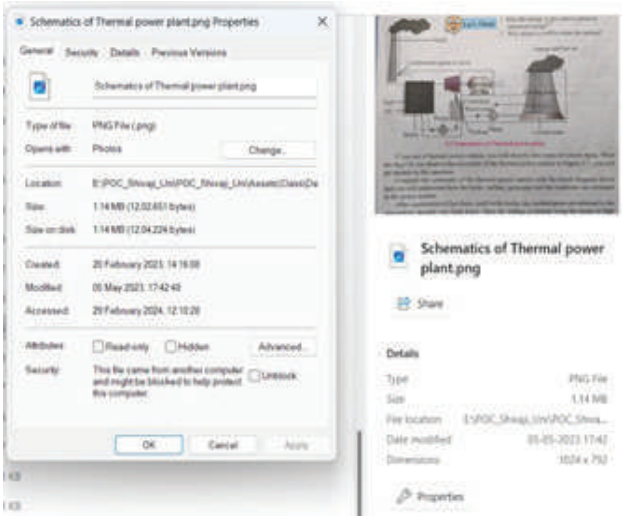

Fig. 4. Schematic of Thermal Power Plant

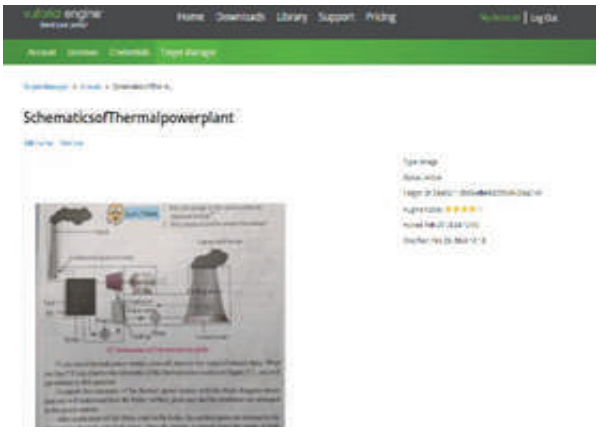

Fig. 5. Four-Star rating by Vuforia Engine

DEVELOPMENT PROCESS OF MARKER-BASED AUGMENTED REALITY APPLICATION

In AR, markers are images or objects registered with the application that act as information triggers in the application. Marker-based tracking can use various marker types, including QR codes, physical reflective markers, Image Targets, and 2D tags. The simplest and most common type of marker in game applications is an Image Target.

Development of 3D models

Creo Parametric software is used to design and development of 3D models of steam power plant as shown in Figure 6,7,8,9. The development contains, rendering, application of material, lighting effects, etc. 3Ds max is used for adding animation and texturing to 3D models. High and low poly mesh models are created using this software in AR implementation.

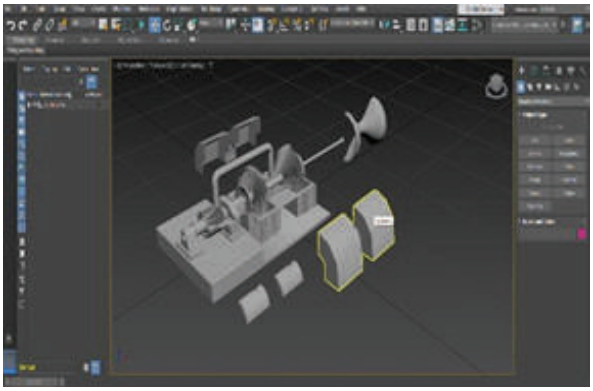

Fig. 6. 3D model of Turbine

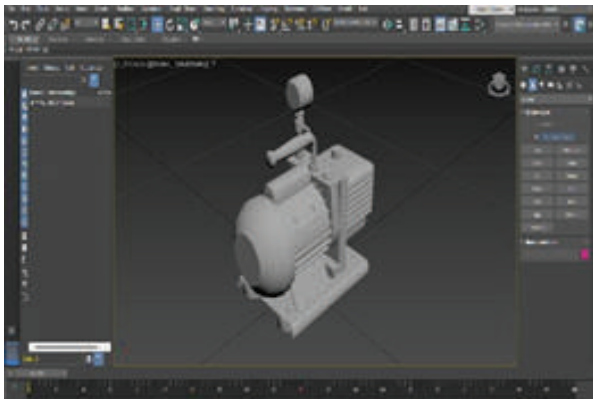

Fig. 7. 3D model of Air Compressor

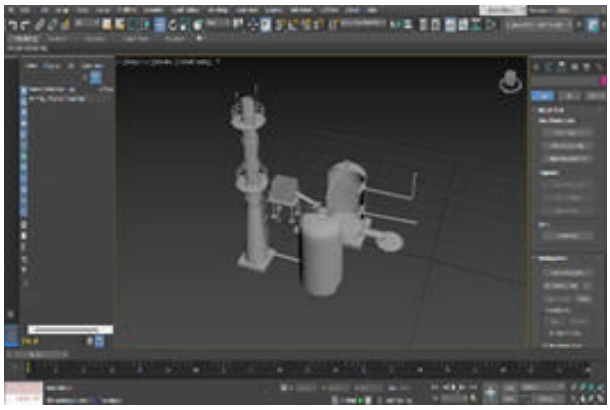

Fig. 8. 3D model of Boiler and Accessories

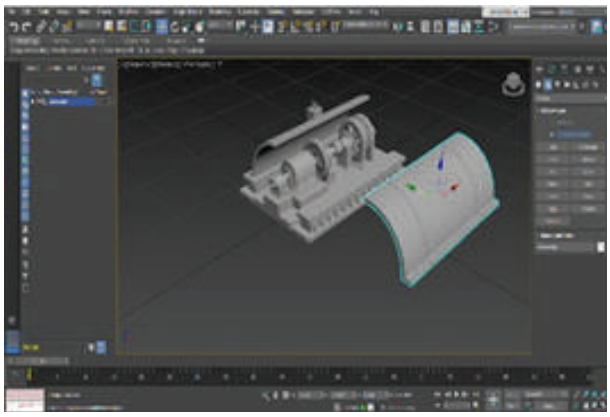

Fig. 9. 3D model of Generator

Import 3D model

3D models developed using 3Ds max software were converted to .fbx format using CAD exchanger software. The .fbx files for each component of the steam power plant were imported in the scene view of unity. The components are positioned in the desired location

for an easily navigable scene as shown in Figure 10. Parameters such as texture, material, and geometric information were organized to maintain the integrity of the 3D model. This process was critical in considering factors such as file compatibility, scale changes, and alignment to achieve a realistic AR experience for users interacting with the Steam power plant in the Unity environment.

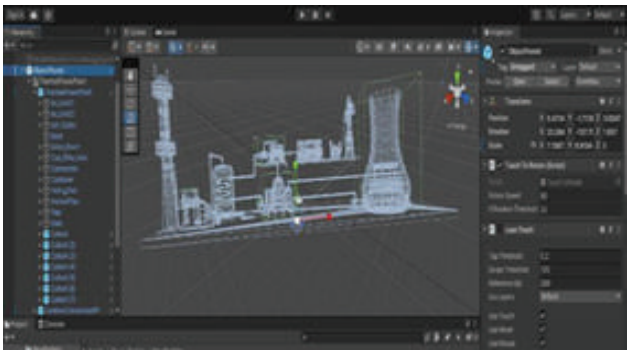

Fig. 10. Import 3D models

Adding materials and Texture to game objects inside Unity

The material components were created in the asset folder to assign colours to various parts of the steam power plant. The extension of this material is .mat. By default, the material is white coloured, using the Colour Picker option the colour of the material is changed, and applied to the game object as shown in Figure 11 in hierarchy or scene panel.

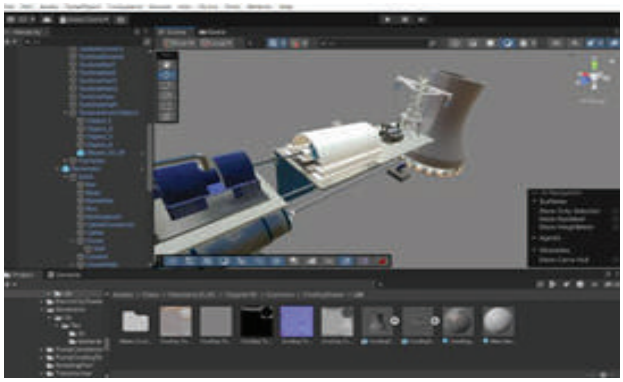

Fig. 11. Adding material to game object.

Material has a "standard" shader attached to it. For bright and clean colour effect, shader changed from standard to texture. Created realistic textures for various components of the power plant concerning metallic intensity, occlusion intensity, and smoothness as shown in Figure 12 .

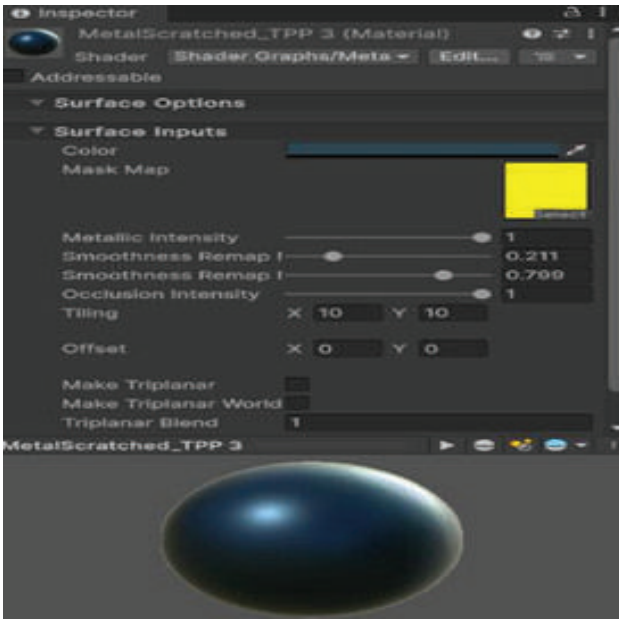

Fig. 12 Texture for Game Object

The texture overlaid on top of the material and applied to various components of steam power plant inside Unity as shown in Figure 13.

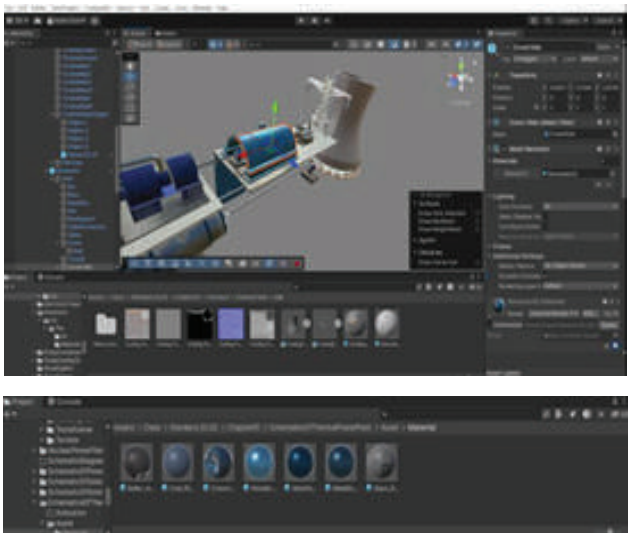

Fig. 13. Components with Texture

Animation

Animation of various parts of the steam power plant was incorporated to showcase dynamic interactions and improve the overall user experience. The animation

timelines were adjusted to ensure smooth transitions between keyframes.

Prefab

"Prefabricated objects," are created in the Unity game engine that can be saved and reused throughout a project, allowing efficient and consistent asset management as shown in Figure 14. The changes made in the prefab were automatically reflected across all game objects in the scene.

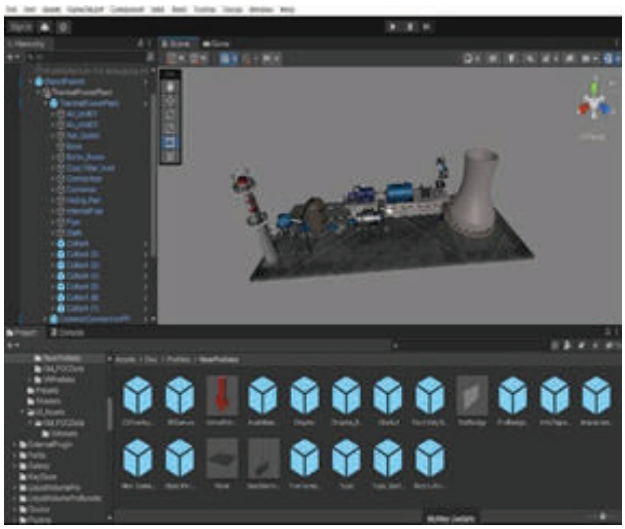

Fig. 14. Prefabs of 3D models

Import Image Target into Unity

The image target was imported in the unity scene from the downloaded Vuforia database as shown in Figure 15.

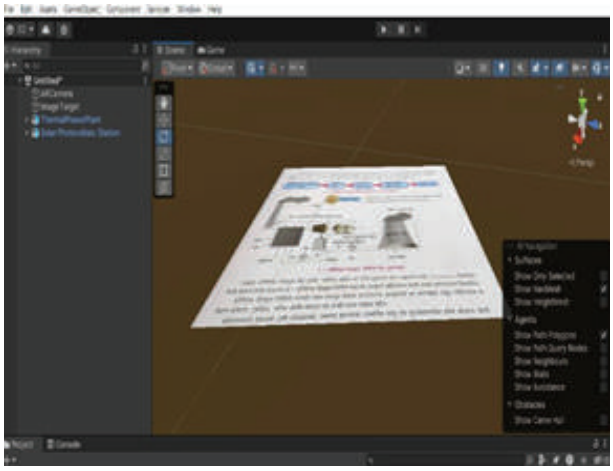

Fig. 15. Image Target

Attach 3D model to Image Target

A 3D model of the steam power plant placed on the top of image target. To achieve the desired positioning of the 3D model its scale was adjusted to the scale of the image target. The image target and 3D model bound together in parent child relationship.

Build and run AR application inside an Android Device

To build an application, first JDK and SDK modules are checked for installation and path setting inside Unity as shown in Figure 16.

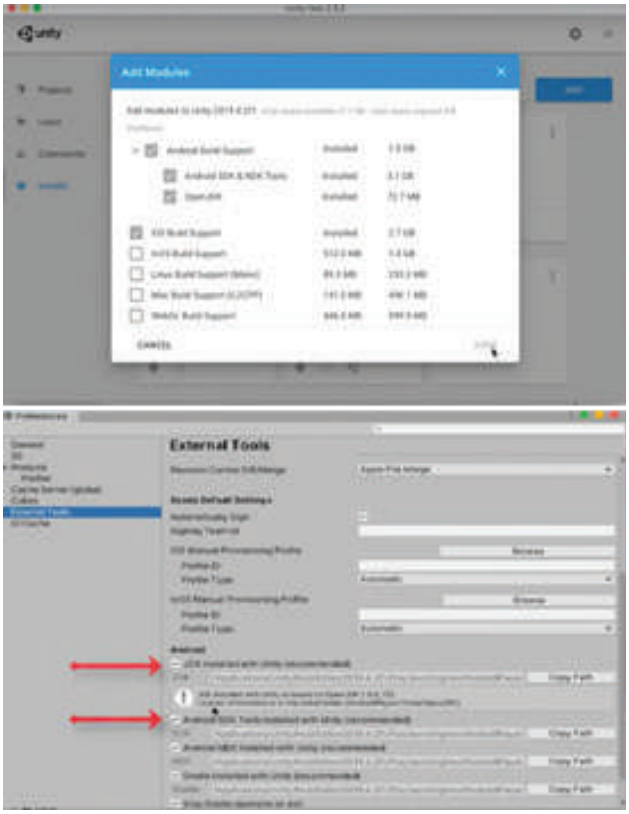

Fig. 16 JDK and SDK

The following set of steps followed to build an application for Android devices:

1. In unity build settings, selected the Android platform, then Switched the platform.

2. Added steam turbine scene and selected player settings. In the Player Settings menu various

aspects of application development are fine-tuned as shown in Figure 17.

2.1 Added product name, and icon/logo of the application.

2.2 Changed the default orientation from auto- rotation to landscape left, because many mobile devices and software adopted landscape left as the default setting. Users are familiar to this orientation, and changing it could lead to confusion.

2.3 Removed Vulkan Graphics API, because in some smartphones users have reported that black screen is the only output they observe. If Vulkan Graphics is present, users are unable to see the camera feed, and the augmented output cannot be seen. Instead, OpenGL ES 3.0 graphics API is used because it provides a powerful and efficient way to render 2D and 3D graphics for smartphones, tablets, and game consoles.

2.4 Minimum API level that is the minimum Android version which is set as Android 7.0 "Nougat" (API Level 24) and the target API level that is the maximum Android version is selected as Automatic (highest installed).

3. Build .apk file and test the output of this application on android device.

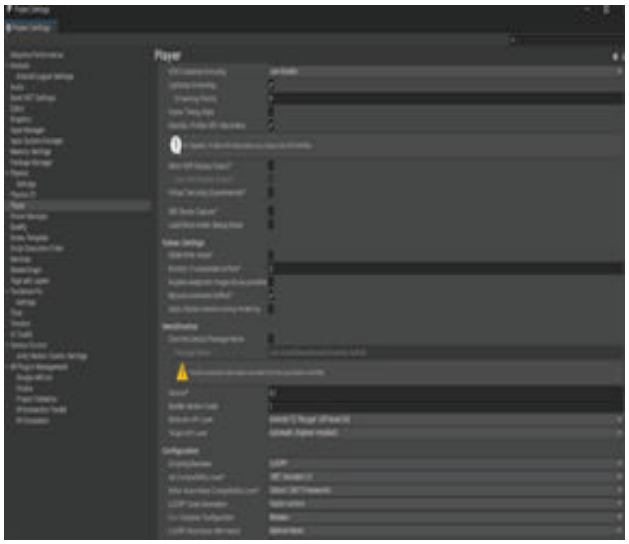

Fig. 17. Player Settings

FINAL OUTPUT

Fig. 18. Marker-Base Augmentation

CONCLUSION AND FUTURE SCOPE

The development of an AR application for steam power plant demonstrates the potential of AR to transform engineering education. By providing an immersive and interactive learning environment, the application enhances students' understanding and engagement with complex engineering concepts Recommendations for educators include integrating AR tools into curricula and providing training for effective use. Future research should explore larger-scale implementations and the integration of AR with other emerging technologies.

ACKNOWLEDGEMENT

Authors are grateful to the District Planning Commission, Collector Office Kolhapur for the financial support in the form of a "Research Fund for Innovative Plans" for the design development AR application.

REFERENCES

1. Santi, Gian Maria, Alessandro Ceruti, Alfredo Liverani, and Francesco Osti (2021). "Augmented Reality in Industry 4.0 and Future Innovation Programs" Technologies 9, no. 2: 33. https://doi.org/10.3390/technologies9020033

2. Dimitris Mourtzis, Vasilios Zogopoulos, Ekaterini Vlachou (2018) ,Augmented Reality supported Product Design towards Industry 4.0: a Teaching Factory paradigm, Procedia Manufacturing,Volume 23,2018,Pages 207-212

3. Carmigniani, J., Furht, B., Anisetti, M. et al. Augmented reality technologies, systems and applications. Multimed Tools Appl 51, 341–377,2011. https://doi.org/10.1007/s11042-010- 0660-6

4. Takrouri, Khaled & Causton, Edward & Simpson, Benjamin. (2022). AR Technologies in Engineering Education: Applications, Potential, and Limitations. Digital. 2. 171-190. 10.3390/digital2020011.

5. Heen Chen, Kaiping Feng, Chunliu Mo, Siyuan Cheng, Zhongning Guo and Yizhu Huang, "Application of Augmented Reality in Engineering Graphics Education," (2011). IEEE International Symposium on IT in Medicine and Education, 2011, pp. 362-365, doi: 10.1109/ITiME.2011.6132125.

6. Madhav Murthy, Dr.K Mallikharjuna Babu, Dr. P Martin Jebaraj et.al (2015). "Augmented Reality as a tool for teaching a course on Elements of Engineering Drawing", Journal of Engineering Education Transformations, Special Issue: Jan. 2015, eISSN 2394-1707.

7. Juhás Martin, Juhásová Bohuslava, Halenár Igor(2021). Augmented Reality in Education 4.0, IEEE CSIT 2018, 11-14 September, 2018, Lviv, Ukraine.

8. Santi, G.M.; Ceruti, A.; Liverani, A.; Osti, F (2021). Augmented Reality in Industry 4.0 and Future Innovation Programs. Technologies, 9, 33.

9. Irina Neaga, Applying Industry 4.0 And Education 4.0 To Engineering Education(2019), Proceedings 2019 Canadian Engineering Education Association (CEEA-ACEG19) Conference

10. Martin, J., Bohuslava, J., & Igor, H. (2018). Augmented Reality in Education 4.0.

11. M. F. Hossain, S. Barman and A. K. M. B. Haque (2019). "Augmented Reality for Education; AR Children's Book," TENCON 2019 - IEEE Region 10 Conference (TENCON), Kochi, India, 2019, pp. 2568-2571, doi: 10.1109/TENCON.2019.8929565

12. Takrouri, K., Causton, E., & Simpson, B. (2022). AR Technologies in Engineering Education: Applications, Potential, and Limitations. Digital, 2(2), 171–190. MDPI AG. Retrieved from http://dx.doi.org/10.3390/digital2020011

13. Kanivets, Oleksandr & Kanivets, Irina & Shmeltser, Ekaterina. (2020). Development of mobile applications of augmented reality for projects with projection drawings.

14. Kudale, Pritam & Buktar, Rajesh. (2022). Investigation of the Impact of Augmented Reality Technology on Interactive Teaching Learning Process. International Journal of Virtual and Personal Learning Environments. 12. 1-16. 10.4018/IJVPLE.285594.

Design and Development of a Sustainable Portable Noise Reduction and Amplification Device for Enhanced Auditory Experiences

Kunalsinh R. Kathia
Professor
Department of Mechanical Engineering
S.P.B. Engineering College (SIT)
Gujarat
✉ kunalsinh.kathia@saffrony.ac.in

Aksh B. Patel, Yash M. Makwana
Harsh N. Ghediya
Students
Department of Mechanical Engineering
S.P.B. Engineering College (SIT)
Gujarat
✉ akshpatel4794@gmail.com
✉ makwanayash24022003@gmail.com
✉ harshghediya16@gmail.com

ABSTRACT

This project aims to design a new portable noise reduction and amplification device for ears. A noise reduction and amplification device for ears is demonstrated in this investigation in conjunction with its computer-aided design, simulation, and sustainability analysis. In our modern society, noise pollution poses a significant threat to hearing health. According to the World Health Organization, there are currently over 466 million individuals with debilitating hearing loss, and by 2050, this figure is projected to rise to 900 million. Our device is designed to reduce noise pollution by utilizing sustainable, eco-friendly materials and technology. This project focuses on the computer-aided design (CAD) of an innovative device aimed at enhancing auditory experiences. The device integrates both noise reduction and amplification features, providing users with a versatile solution for varied environments. Using a hexagon-shaped sound module for non-electric sound modulation and pyramid-shaped plate designs for improved sound suppression, the Noise Reducing and Enhancing Headphone dramatically reduces noise. A pin shifts headphones from sound-reducing to sound-enhancing mode by matching holes on both plates and reducing them when needed. Utilizing advanced CAD design, our device optimizes noise reduction and amplification for a sophisticated and user-centric auditory experience. Employing CAD simulations, our project rigorously validates the efficacy of the noise reduction and amplification device, ensuring optimal performance. Grounded in sustainability analysis, our solution incorporates eco-friendly materials and energy-efficient design, establishing a responsible and resilient approach to auditory enhancement. Our gadget, a ground-breaking approach to improving auditory well-being, combines amplification and noise reduction to provide a flexible and long-lasting aural experience.

KEYWORDS *: Noise reduction, Auditory enhancement, Sustainable design, Solidworks, Simulation.*

INTRODUCTION

In our modern society, noise pollution is a pervasive threat to hearing health, affecting millions globally. With the increasing prevalence of hearing loss, there is a pressing need for innovative solutions to protect and enhance auditory capabilities. This paper explores various avenues, including composite earmuffs, recycled nonwoven mats, and eco-friendly materials for noise control in household appliances. The primary focus is on a novel Noise Reducing and Enhancing Headphone that introduces a sustainable and electricity-free approach to address the identified problem[1][2].

Background: The World Health Organization reports staggering statistics, with over 1.5 billion people globally experiencing some form of hearing loss. This research aims to contribute to the ongoing efforts

to combat hearing-related issues by investigating sustainable materials and designs for noise reduction and enhancement. The study encompasses composite earmuffs, recycled nonwoven mats, and the use of eco-friendly materials in household appliances.

MATERIALS & METHODS

Overview of Experiment

Designing or analyzing a device that can selectively reduce ambient noise while strengthening or amplifying appealing sounds is usually the objective of an experiment on a Noise Reduction and Amplification Device for Ears, especially in the context of communication or hearing protection.[3] An outline of one such experiment is given below. Headphones play a crucial role in the modern world, providing users with superior sound quality and immersive audio experiences.

Brief Research aims of experiment

Noise Reduction: Dislocate holes in a plate to block external noise.

Noise Enhancement: Use a cone-shaped structure to direct sound towards the user's ears.

Sustainability: Employ recycled plastics, vegan leather, acoustic cotton, and bamboo wood[4]

Product Design: Optimize materials, processes, and energy using SolidWorks' sustainability module.

Flexibility: Include adjustable features for personalized comfort.

Research based on material selection

Materials for noise reduction and amplification devices are chosen based on their noise reduction, enhancement, comfort, sustainability, and flexibility properties.

Recycled plastics: Offer excellent sound absorption, especially in hexagonal sound modules[5][6]

Vegan leather: Provide a sustainable and cruelty-free head strip coating[7]

Acoustic cotton: Offer comfort and cushioning[8]

Bamboo wood: Provide strength, sustainability, and durability for the head strip[4][9]

DESCRIPTION OF DESIGN PROCESS

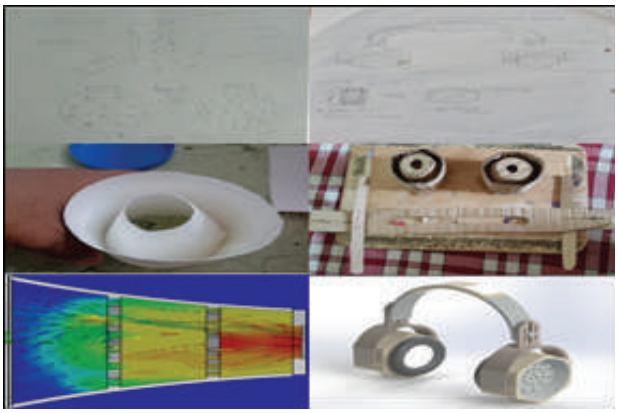

Fig. 1. Procedure overview

1. Identify the Design Domain
2. Problem Identification and Selection
3. Problem Definition
4. Ideation and Brainstorming
5. Concept Sketching (2D)
6. Concept Selection
7. Concept Direction
8. Mock-Up Model
9. Detailed 3D CAD Modeling (SolidWorks)
10. Simulation and Analysis
11. Prototyping and Testing
12. Refinement and Optimization
13. Final Design Documentation
14. Production or Implementation
15. Monitoring and Evaluation
16. Documentation and Reporting

2D CAD Design Parameters and Assemble of the Parts

Headband

Dimension parameters: The headband is the upper part of the headphone; it is in a curve type shape. It is 5 mm in thickness and 87 mm in height. Its length is 170 mm excluding outer Slider connections and its width is 24 mm. Slider connections have a 5 mm inner diameter and 10 mm outer diameter, and it is 3 mm thick. At the top portion of the headband there is lather coating to a headband, which is 9 mm thick and 97 mm long.

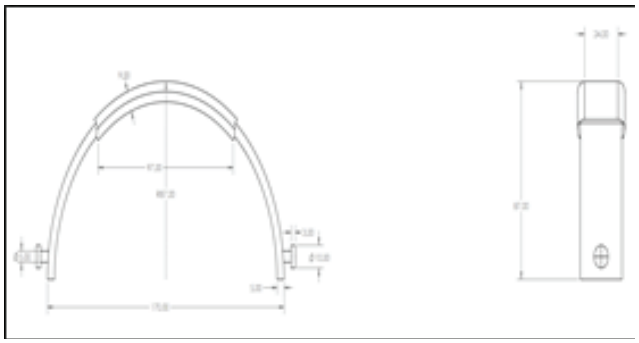

Fig. 2 Headband

Adjustability: Noise Reduction & Amplification Device For Ears have an adjustable headband to accommodate different head sizes and shapes. This adjustability is often achieved through a sliding mechanism.

Distribution of Weight: With the objective to reduce pressure on the top of the head, an efficient headband design takes weight distribution into consideration. With over-ear headphones, where the ear cushions wrap the ears, this is extremely crucial.

Headband Cushioning: For comfort, there may be extra cushioning on the headband section that makes contact with the top of the head.

Slider

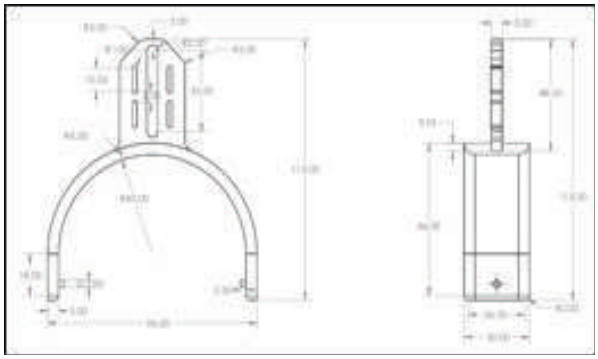

Fig. 3 Slider

Dimension parameters: The slider is a connection between the Headband and the Hexacone Sound Module. It is used to increase or decrease the length of headphones according to people's needs. Slider's total height is 113 mm, length is 96 mm and width is 30 mm. Its curved portion is up to 66 mm in height and above there is a connection and slider movement path which connects to the headband.

Adjustability: Our innovative slider mechanisms allow users to easily adjust the headphone size for a comfortable fit.

Distribution of Weight: A secure fit is ensured by the sliding mechanism, which modifies weight distribution for maximum comfort.

Hexacone Sound Module

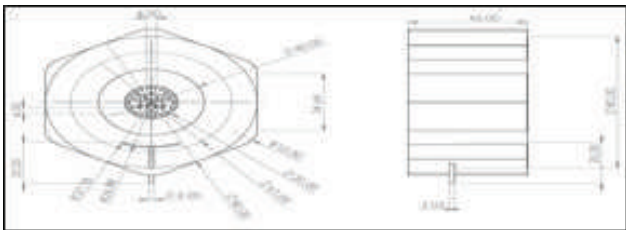

Fig. 4 Hexacone Sound Module

The Hexacone Sound Module's inner diameter can be altered from 25 mm to 6 mm. We choose the flow simulation range for our interior diameter in accordance with the research that indicates the ear tympanic cavity has a diameter of 10 mm. This is the essential part of our Headphone. It is fully designed and developed by our team, and we give it the name 'Hexacone Sound Module'. It is a type of ear cup which is used to reduce and enhance sound naturally. It is a hexagon in shape. In that there is a cone type structure which connects inner and outer openings. In that cone type structure, there are 2 plates in it. Both have different no of holes in them and when they match sound enhances and when they do not match, the sound is reduced. It also has a pyramid-type small structure on all the surfaces. So, it further reduces or enhances the sound. There is a moving key connected to the 2nd plate which is used to move it and via which the holes on both plates are matched or unmatched.

Cushion

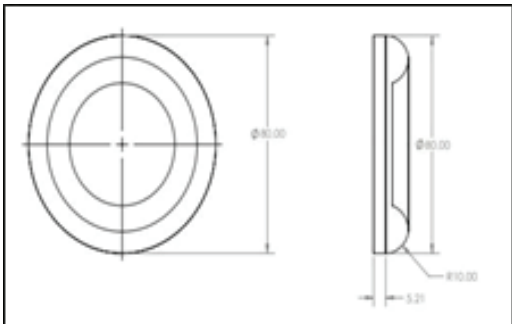

Fig. 4 Cushion

Dimension parameters: The cushion features an 80 mm outer diameter, 10 mm filet radius on both sides, and a 5 mm flat portion behind it.

The aesthetics 3D CAD model of device

Fig. 5 3D Model

The aesthetics 3D CAD model ensures precise component compatibility and functionality with an adjustable head strip, sustainable cushioning, a hexacone sound module, and a modular extension system. The Hexacone sound module features hexagonal cone-shaped chambers for optimized sound performance. It leverages advanced acoustic engineering for superior audio quality and precise frequency response[10]

The module includes Pyramid-type structure on plates for sound reduction. Adjustable pin to switch between sound-reducing and sound-enhancing modes.

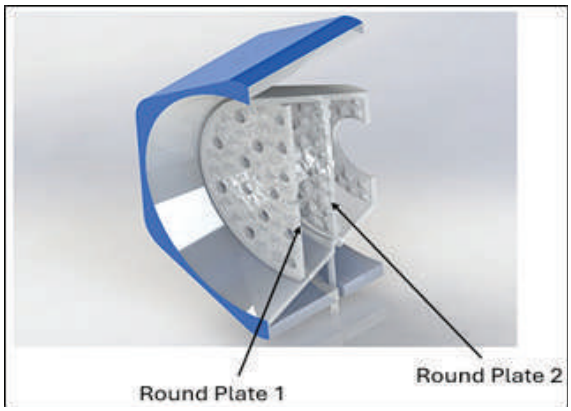

Fig. 6. Hexacone module cross section

Round Plate

Round Plate 1: The Hexacone Sound Module's first plate, a 61mm diameter, is a key component in noise reduction and enhancement in headphones, utilizing a pyramid-type structure for sound modulation. The pyramid-type structure on the first plate disrupts and redirects sound waves, reducing noise and preserving audio signals. This unique geometry enhances the headphone's ability to deliver high-quality audio experiences by selectively manipulating amplitude and frequency.

Round Plate 2: The Hexacone Sound Module's second plate enhances noise reduction and enhancement, with a 49mm diameter and pyramid-type structure, enhancing the headphone solution's overall effectiveness.

Pyramid-Shaped Absorber Plates: These plates offer efficient sound absorption,[2] reducing thickness and material usage while maintaining high performance.

Cone Shape: A wave-funneling design enhances sound quality and reduces noise by directing sound waves towards the ear canal.[11]

Lid and Insulation: A versatile lid allows for customizable configurations, while insulation prevents internal sound leakage and improves acoustic performance.

Hexagonal Shape: Hexagonal panels provide efficient coverage, aesthetic appeal, structural stability, and sound diffusion.[10]

Adjustable Pin: A simple pin mechanism switches between sound-reducing and sound-enhancing modes by aligning or misaligning holes on the plates.

Flow Simulation Analysis

The purpose of this flow simulation study is to determine different model parameters: The following are the study parameters: inlet air velocity = 2 m/s,500 Pa is the outlet air pressure.

In the first simulation the Hexacone Sound Module's inner diameter can be altered from 25 mm to 6 mm. We choose the flow simulation range for our model's inner diameter in accordance with the research that indicates the ear tympanic cavity has a diameter of 10 mm. The Solidworks Student Version 2023 is used to do the flow simulation. As shown in the figure this is a cross section of a hexacone sound module in which you can see that there are 2 plates in it placed at distance found from simulation. (refer section 4)

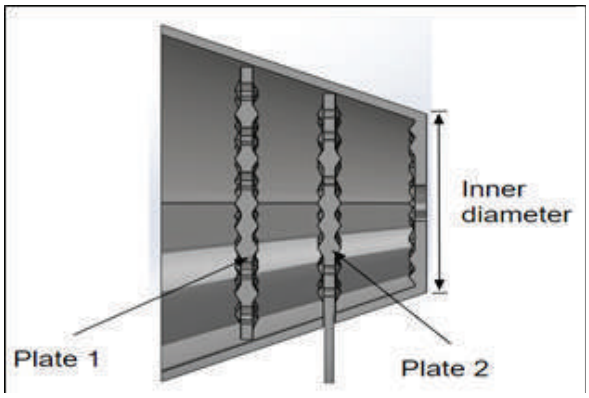

Fig. 7 Inside plates

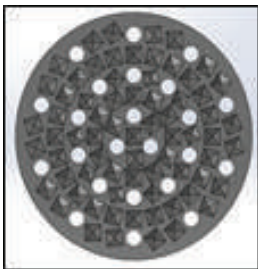

Fig. 8 Plate 1

Fig. 9 Plate 2

Above 2 figures show the design of plate 1 and plate 2. Plate 1 has this pattern of holes with hole diameter of 4 mm and plate 2 has this pattern of holes with hole diameter of 2 mm funded out from simulation. (refer section 4).

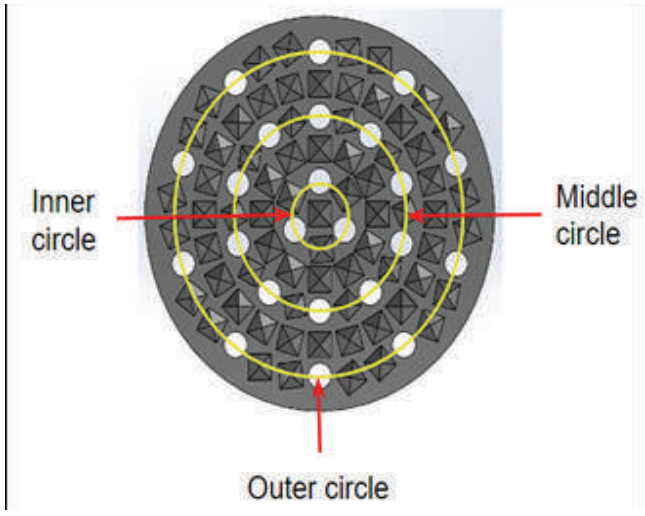

Fig. 10 Hole pattern circles

For finding the matching hole patterns we change the number of holes and for our simplicity we divide it into 3 circles inner, middle and outer as shown in figure. Inner circle connecting centers of 3 holes, middle circle connecting center of 10 holes and outer circle connecting centers of 10 holes. Same as for plate 2.

RESULTS & DISCUSSION

This research focuses on creating a passive noise reduction and amplification device. This addresses the "Earmbie" phenomenon, where headphone users may become oblivious to their surroundings, increasing the risk of accidents. Unlike active noise cancellation, it allows users to maintain some awareness of their surroundings, addressing safety concerns associated with complete noise isolation. This is particularly important in areas where auditory cues are essential, like roads with traffic. Various computational analyses are being conducted to determine the optimal parameters for the Hexacone Sound Module. First simulation is done for finding out the suitable inner cone diameter.

For Inside diameter of Hexacone Sound Module

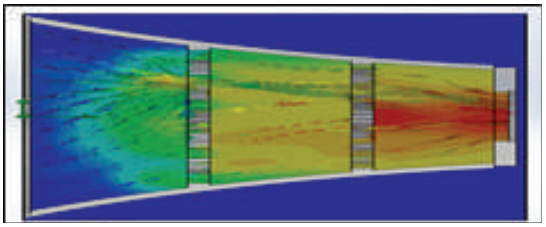

Fig. 11 Flow simulation of inside diameter of Hexacone Sound Module

The flow simulation depicted in Figure 4.1.1 illustrates the outlet acoustic power (measured in dB) and visually maps the trajectory of the passing air. The results of flow simulation for Hexacone sound module inside diameter are as Graph 4.1.

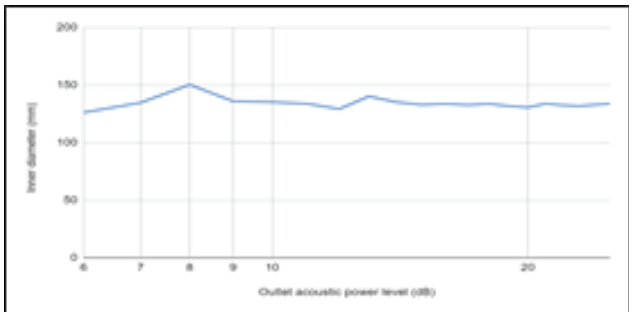

Graph 1 Result for flow simulation of inside diameter of Hexacone Sound Module

The flow simulation with an 8 mm inner diameter has the maximum acoustic power of 150.37dB.

For distance between two plates of Hexacone Sound Module

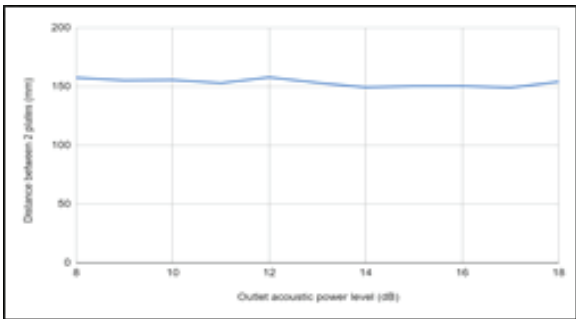

Graph 2 Result for flow simulation of distance between two plates of Hexacone Sound Module

Following the determination of the internal diameter of the Hexacone sound module, precise spacing between the two plates becomes necessary, prompting the undertaking of this study. The results regarding the distance between the plates are shown in Graph 4.2. Notably, the maximum acoustic power observed at a distance of 12 mm between the two plates reaches 157.92 dB.

Table 1 Result table for flow simulation of matching holes pattern of Hexacone Sound Module

Flow Simulation			
Sr no.	**Hole Pattern**	**Outlet velocity (m/s)**	**Outlet acoustic power level (dB)**
1	No extra holes, Matching holes 10	254.77	151.46
2	10 extra holes on both plate, Matching holes 10	299.7	147.47
3	15 extra holes on both plate, Matching holes 10	306.13	143.64
4	1st plate - 10 extra holes, 2nd plate - 15 extra holes, Matching holes 13	303.67	146.17
5	10 extra holes on both plate, Matching holes 13	299.54	153.43
6	10 extra holes on both plate, Matching holes 15	299.28	148.01

There are different holes on both plates so it must be required to find out for which holes pattern and no of matching holes gives the maximum acoustic power for that purpose this study conducted. There are hole patterns on plates like this, Inner circle consists of 3 holes, Middle circle consists of 10 holes, Outer circle consists of 15 holes. The study is conducted by changing no of holes in different circles.(refer section 3) For the holes pattern in which 13 holes are matched on both the plates and 10 holes on the outer circle we get maximum acoustic power of 153.43 dB.

Sound Reduction and Enhancement

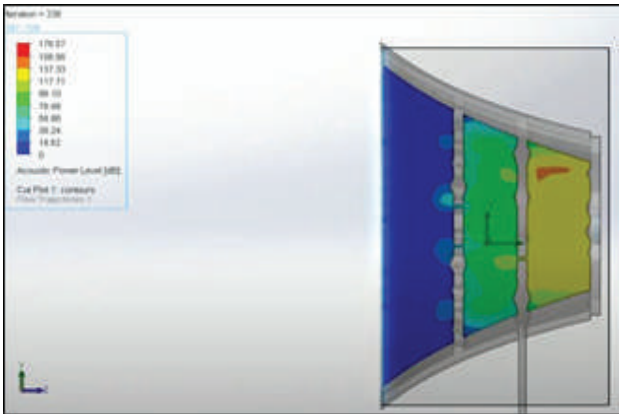

Fig. 12 Flow simulation cut plot

Figure 12 offers insight into the diverse acoustic power levels present within the Hexacone Sound Module, depicted through a spectrum of colors including blue, green, yellow, and red. In this representation, blue areas signify regions with 0 dB acoustic power, while shades of light blue represent incrementally higher levels, and green denotes medium levels. The presence of red indicates the highest acoustic power. This color gradient serves to visually demonstrate the augmentation of acoustic power as sound traverses through consecutive plates within the module[12], thereby providing evidence of sound enhancement within the module[13]

Figure 13 illustrates the flow paths observed in a flow simulation, similar to the cut plot depicted in Figure 13. The primary difference lies in the presentation of moving arrows, which outline the path of airflow around

the object. These flow paths provide valuable insights into the dynamics of airflow, highlighting areas of high density, turbulence generation, and other relevant factors. Consequently, they offer a comprehensive understanding of the airflow patterns, aiding in the identification of regions likely to experience maximum airflow.

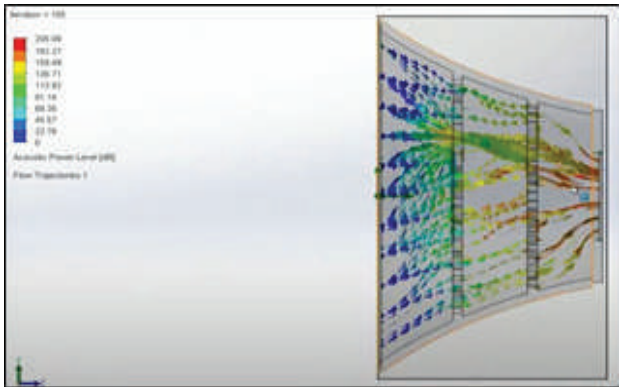

Fig. 13 Flow simulation flow trajectories

Sustainability Approach: For environmentally conscious individuals, noise-canceling headphones made from sustainable materials offer a great option. Benefits of sustainable noise canceling headphones[14] is that it reduces noise pollution, it is durable, repairable and recyclable.

Sustainability features

Reduce waste, Durability, Switch between modes, Selectable noise isolation, Ergonomic design. We develop sustainability chart using solidworks[15]

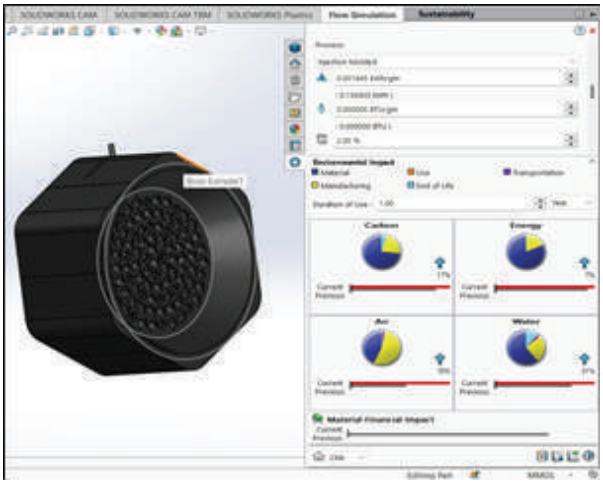

Fig. 14 Sustainability chart

Impact of our solution

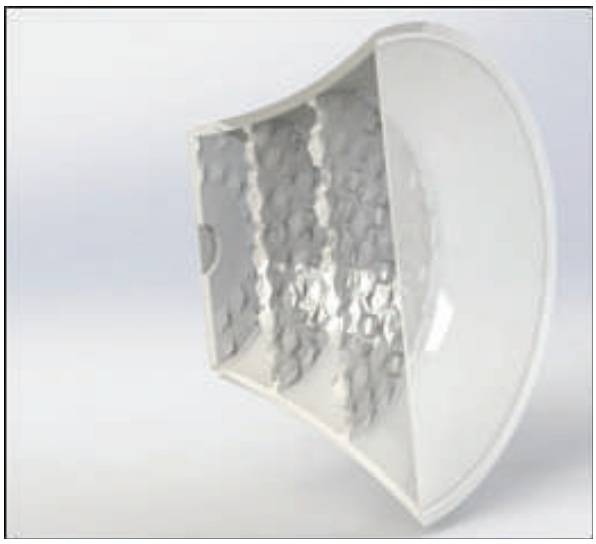

Fig. 15 Model cross section

Versatile Sound Customization: Users can easily switch between sound-enhancing and sound-reducing modes depending on their settings or personal preferences.

Selectable Noise Isolation: By dislocating holes in the plate, users can dynamically adjust the level of sound reduction, enabling them to enjoy peace and quiet or maintain situational awareness if required.

Ergonomic Design: The headphones are designed to be comfortable for extended wear, incorporating lightweight materials, adjustable headbands, and cushioned ear cups to ensure a snug fit for all users.

Premium Durability: The headphones will be constructed using high-quality sustainable materials, ensuring long-lasting performance even with regular usage.

CONCLUSION

In conclusion, this research paper provides a holistic exploration of sustainable solutions to address the urgent global issue of noise pollution. The significance lies in the development of eco-friendly alternatives, such as composite earmuffs and the Noise Reducing and Enhancing Headphone, to mitigate the impact on hearing health and the environment. By presenting innovative findings, this study contributes to the ongoing dialogue on sustainable noise control and emphasizes the importance of conscious design and material choices in creating a healthier and quieter world. As the world

grapples with the rising challenges of noise pollution and its impact on hearing health, this research presents innovative and sustainable solutions. The findings contribute to the development of composite earmuffs, recycled nonwoven mats, and eco-friendly materials for noise control. The groundbreaking Noise Reducing and Enhancing Headphone offers a unique approach to addressing the identified problem, showcasing the potential of sustainable and electricity-free solutions in the realm of auditory health.

REFERENCES

1. T. G. Hawkins, Studies and research regarding sound reduction materials with the purpose of reducing sound pollution. California Polytechnic State University, 2014.
2. M. Kaamin et al., "A Study on Sound-Absorbing Acoustic Panels from Egg Trays with Recycled Materials (Paper & Plastic).," International Journal of Nanoelectronics & Materials, vol. 13, 2020.
3. N. Ziayi Ghahnavieh, S. Pourabdian, and F. Forouharmajd, "Protective earphones and human hearing system response to the received sound frequency signals," Journal of Low Frequency Noise, Vibration and Active Control, vol. 37, no. 4, pp. 1030–1036, 2018.
4. A. R. Mohanty and S. Fatima, "Noise control using green materials," Sound and Vibration, vol. 49, no. 2, pp. 13–15, 2015.
5. M. Kolarevic, B. Radičević, V. Grković, I. Ristanović, and M. Ivanovic, "Acoustic properties of recycled plastic," 2018.
6. A. Biskupičová, M. Ledererová, S. Unčík, C. Glorieux, and M. Rychtáriková, "Sound absorption properties of materials based on recycled plastic granule mixtures," Slovak Journal of Civil Engineering, vol. 29, no. 1, pp. 15–19, 2021.
7. N. T. Minh and H. N. Ngan, "Vegan leather: An eco-friendly material for sustainable fashion towards environmental awareness," in AIP Conference Proceedings, AIP Publishing, 2021.
8. A. Putra, Y. Abdullah, H. Efendy, W. Mohamad, and N. L. Salleh, "Biomass from paddy waste fibers as sustainable acoustic material," Adv Acoust Vib, vol. 2013, no. 1, p. 605932, 2013.
9. K. Rassiah, M. M. H. M. Ahmad, and A. Ali, "Mechanical properties of laminated bamboo strips from Gigantochloa Scortechinii/polyester composites," Mater Des, vol. 57, pp. 551–559, 2014.
10. M. Coope, G. Huisman, and P. Hekkert, "Haptic aesthetics in product design: designing headphones that feel beautiful," 2023.
11. Y. Hu, X. Zhao, T. Yamaguchi, M. Sasajima, T. Sasanuma, and A. Hara, "Effects of the Cone and Edge on the Acoustic Characteristics of a Cone Loudspeaker," Adv Acoust Vib, vol. 2017, no. 1, p. 2792376, 2017.
12. F. Asdrubali, S. Schiavoni, and K. V Horoshenkov, "A review of sustainable materials for acoustic applications," Building Acoustics, vol. 19, no. 4, pp. 283–311, 2012.
13. M. E. T. Nejad, A. Loghmani, and S. Ziaei-Rad, "The effects of wedge geometrical parameters and arrangement on the sound absorption coefficient–A numerical and experimental study," Applied Acoustics, vol. 169, p. 107458, 2020.
14. S.-H. Yu and J.-S. Hu, "Controller design for active noise cancellation headphones using experimental raw data," IEEE/ASME transactions on mechatronics, vol. 6, no. 4, pp. 483–490, 2001.
15. L. I. Popa and V. N. Popa, "Products eco-sustainability analysis using CAD SolidWorks software," in MATEC Web of Conferences, EDP Sciences, 2017, p. 06002.

Design Analysis of Multi Spring Ankle Therapy Equipment

Nidhi M B
Associate Professor
Department of Mechanical Engineering
Mar Baselios College of Engineering and Technology
Trivandrum, Kerala
✉ nidhi.mb@mbcet.ac.in

Sandra Ajayan
Student
Department of Mechanical Engineering
Mar Baselios College of Engineering and Technology
Trivandrum, Kerala

ABSTRACT

Sprained ankles and weak calf muscles are very common injuries seen between the ages of 15-60. An ankle sprain occurs when the ligaments that support the ankle get overly stretched or torn. Based on the information collected from various physiotherapy clinics and studies conducted, treatment for a sprained ankle depends on the grade of the sprain. Most sprains heal with proper manual therapies and exercise under consultation, leading to the need for much advanced equipment.

Portable and feasible mechanical equipment is proposed through this project, working with multiple springs. This model consists of multiple helical compression springs of different dimensions, each serving different functions, designed considering the factors such as weight, height and foot span. The springs are incorporated with pedals over it. A resistance band element is incorporated from heels to a knee brace and from knee brace to forefeet. The knee brace is provided to ensure support and minimum movement of knee joint. When a force is applied by the forefeet on the spring, the resistance band stretches causing the lifting up of the heel on the other side. This to and fro motion of the feet ensure the required movement of the ankles hence loosening the sprain. The equipment could replace the conventional time consuming practices of physiotherapy and could be implemented in hospitals, clinics and even in gymnasiums.

KEYWORDS *: Ankle sprain, Springs, Ankle physiotherapy, Resistance band, Knee brace.*

INTRODUCTION

Sprained ankles and weak calf muscles are very common injuries seen between the ages of 15-60. From the Population based epidemiology of ankle sprains survey conducted in England during early 2000s it is observed that 53 on 10,000 individuals are affected by such ailments [1] and approximately 27,000 inversion ankle sprains occur every day in the U.S. An ankle sprain occurs when the ligaments that support the ankle get overly stretched or torn. Based on the information collected from various physiotherapy clinics and studies conducted, treatment for a sprained ankle depends on the grade of the sprain [2]. Most sprains heal with proper manual therapies and exercise under consultation, leading to the need for much advanced equipment.

Portable and feasible mechanical equipment with multiple springs is proposed through this work. It consists of multiple helical springs of different dimensions, designed considering the factors such as weight, height and foot length. The springs are incorporated with pedals over it. The wire thickness of the spring varies with varying force [3] to befit the various functions.

The most commonly deployed springs are of stainless steel or spring steel because of the very high yield strength that allows the spring to return to their original shape despite significant deflection or twisting. A resistance band component is incorporated from the heels to a knee brace and to the forefeet. The resistance band chosen are of medium tension grade. The knee brace is provided to ensure support and minimum

movement of knee joint. When a force is applied by the forefeet on the spring, the resistance band stretches causing the lifting up of the heel on the other side. This to and fro motion of the feet ensure the required movement of the ankles hence loosening the sprain.

This equipment could replace the conventional time-consuming practices of physiotherapy and could be implemented for both domestic and hospital purposes. Multiple surveys were conducted to assess the relevance of the project. A survey examined orthopedic treatments across local hospitals. The data revealed that ankle injuries are common among athletes, with rehabilitation programs emphasizing therapeutic exercise proving successful.

Notably, 60% of patients, primarily athletes, supported the proposed idea. Rehabilitation programs that emphasize the use of therapeutic exercise to restore motion, muscle strength and muscular coordination have shown to have clinical success for patients suffering various foot and ankle injuries.

A wide range of rehabilitation programs are suggested ankle sprains, plantar fasciitis and turf toe. Lateral ankle sprains are common among athletes. Figure 1 shows the two types of ankle movements; dorsiflexion which is the downward movement of the ankle and plantar flexion which is the upward movement of the ankle.

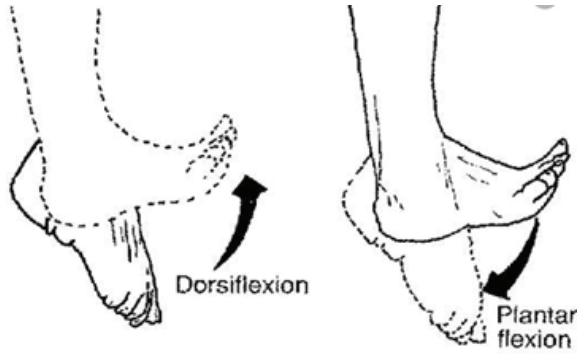

Fig. 1: Types of ankle movements

PROBLEM DEFINITION

From the surveys it was conclude, ankle sprains are very common for the ages of 15-50. Ankle sprains occur when a movement forces the ankle to budge from its original position, stretch or tear. This can be caused due to participation in sports and games, landing incorrectly on the foot after jumping, walking or running on uneven surfaces.

Damages may occur due to accidents or even due to wearing inappropriate footwear. Conventional rehabilitation exercises for an ankle sprain are towel curls, calf stretch, golf ball roll, heel cord stretch etc. Some motion exercises are shown in figure 2.

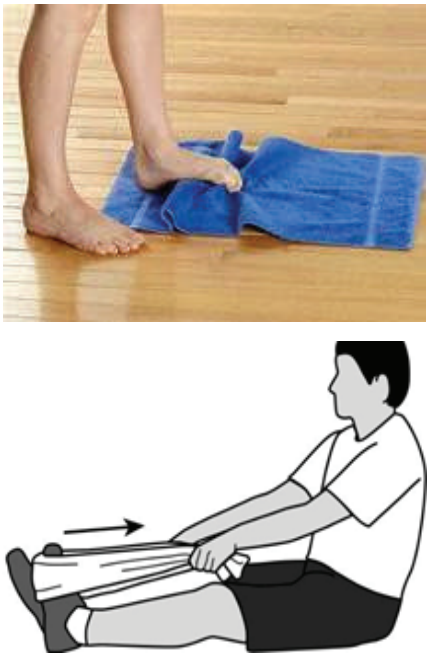

Fig. 2: Ankle Sprain relieving

This could be achieved by implementing a compact device provide better support. These provide motion of ankle in either one direction. Stability of the device must be ensured to avoid failure of the therapy process. Bulkiness of these devices makes them less user friendly. The modern effective therapy equipment's are power driven. In this scenario physiotherapy centers require a sophisticated and user friendly device for the same.

METHODOLOGY

The requirement for new equipment design was found from the data obtained from the survey, the survey details. A detailed study of existing methods and types of injuries was conducted. From the gaps identified on literature review, design of a device with three springs of varying dimensions which serves various effective physiotherapy functions is proposed.

The work focuses on addressing limitations in current ankle rehabilitation devices, such as the Calf and Foot Stretcher and the Plantar Fasciitis Night Splint, both of which have significant drawbacks. The Stretcher requires a warm-up to avoid tendon fatigue and lacks adequate support, increasing the risk of slipping and injury. The Splint, while providing passive stretching, causes shin and offers limited motion. The new model aims to improve patient comfort and effectiveness by incorporating springs of varying thicknesses for different levels of injury and athletic training. This design is expected to enhance mobility while restricting motion to the ankle, ensuring universal applicability by considering average human body measurements. The need for this device was highlighted by surveys showing a high incidence of ankle sprains and the inadequacies of current treatments, particularly for athletes.

DESIGN

Considering data collected from the studies and surveys, a design of the model was made as shown in Fig.3. The model of the base is the focus of design innovation and the device consists of a stable wooden base with three springs. Each spring is provided with a pedal on its top as shown in figure 3.

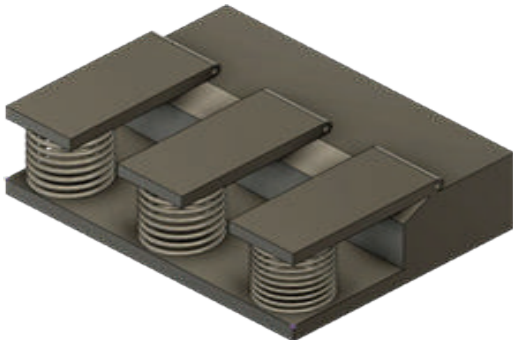

Fig. 3: Design of the Model

Person has to apply force on these pedals. The foot is kept attached to the pedal using Velcro bands. The springs are placed with a specific clearance in between. These are welded to the wooden base using intermediate metal strap. The movement of foot is monitored by the resistance band which is attached to the knee brace [6].

The displacement of spring required to produce active dorsiflexion and plantar flexion were quantitatively studied. Survey was carried out on patients and athletes Angular deflections were measured using an orthopedic joint spring Design.

COMPONENT SELECTION

The different components of the models, their specifications and calculations for selection are explained in this session. The various components of the model are; Springs,Base ,Pedals,Resistance bands,Knee brace,Velcro straps..

Spring Design

The material selection for the springs was done by considering the factors such as durability, feasibility and the tensile strength. Thus the most effective material was found to be spring steel IS 4454 grade 3, commonly known as music wire. The dimensions of the springs were calculated using the following equation;

Maximum Deflection (y),

$$y = \frac{8 F D^3 n}{G d^4} \quad (1)$$

Where, F is the load acting, D is outer diameter of the spring, n is number of turns, G is the Rigidity Modulus and d is the wire diameter of the springs.

The material selection for the springs was done by considering the factors such as durability, feasibility and the tensile strength. Thus the most effective material was found to be spring steel IS 4454 grade 3, commonly known as music wire. The dimensions of the springs were calculated using the following equation;
Maximum Deflection (y),

$$y = \frac{8 F D_3 n}{G d_4}$$

Where, F is the load acting, D is outer diameter of the spring, n is number of turns, G is the Rigidity Modulus and d is the wire diameter of the springs.

Displacement Calculation

The displacement of spring required to produce active dorsiflexion and plantar flexion were quantitatively studied. Survey was carried out on patients and athletes Angular deflections were measured using an orthopaedic joint ankle measuring scale as shown in figure 4.

Fig 4. Autodesk Fusion 360

The angular displacement (Ø) obtained in degrees are converted to radians and the corresponding linear deformation(x) were found using the formula; x = rØ eqn 3.2

Where r is length of the pedal. The measurements hence Fig 1.5. Measurement of Ankle deflection were found to be in the range of 20mm to 70mm.

Load Survey

Another survey was conducted for finding the load that could be applied the patients of different age group and gender. This was done with the aid of a weighing machine. Patients were asked to apply the maximum and minimum possible pressures on the weighing surface and the values were obtained in kilograms. The procedure was done in both sitting and standing positions.

The force values were varying with respect to age and gender in both cases. The readings hence obtained were normalized and recorded as shown in Table 1 and 2.

Table 1 Load survey while sitting

Age	Force (N)	
in yrs	Male	Female
10-20	10	8
21-30	15	13
31-45	14	12
45-55	12	9

Table 2 Load survey while standing

Age	Force (N)	
in yrs	Male	Female
10-20	18	15
21-30	25	22
31-45	28	25
45-55	33	30

For a closed end compression spring made of high carbon spring steel, G=78450 N/mm^2.

Assuming the outer diameter of the spring to be in the range of 40 to 45mm considering the size constrain, keeping the height factor in consideration assuming the no. of active turns to be 10 and applying the obtained load values into the equation 3.1, a wide range of possible values for the spring diameter were obtained. The observations are listed in table 3.

Table 3. Dimensions of spring

LOAD (N)	DEFLECTION (mm)	OUTER DIAMETER (mm)	WIRE DIAMETER (mm)
15	5	40	3.5
30	11	40	3.5
15	13	40	2.8
25	19	40	2.8
30	25	40	2.8
15	30	42	2.5
30	53	42	2.5

The following dimensions were hence obtained;

First spring

- Wirediameter = 2.5mm
- Out diameter = 42 mm
- Length: 115 mm

Second spring

- o Wirediameter =2.8mm
- o Out diameter = 40 mm
- o Length: 120 mm

Third spring

- o Wirediameter = 3.5mm
- o Out diameter = 40mm
- o Length: 120 mm

The springs were made of high carbon spring steel which has the following material properties;

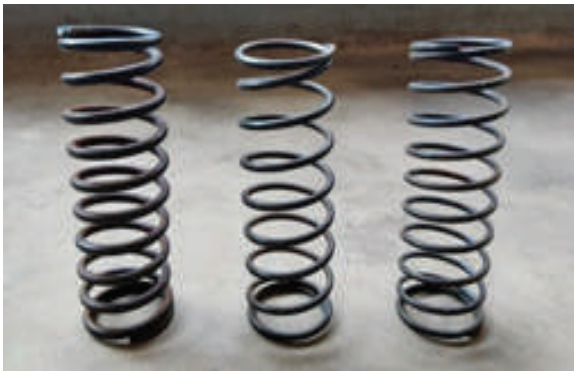

Fig 5. Manufactured springs

- Young's Modulus = 206790 N/mm^2
- Rigidity Modulus = 78450 N/mm^2
- Poisson's Ratio = .265
- Density = 7860 kg/m^3
- Ultimate Tensile Strength = 1745 N/mm^2

All three springs are of same length and has ten coil turns each, as seen in figure 6.

EXPERIMENTAL ANALYSIS

As the component selection was completed next step was to analyse the working of the selected components. The equipment is provided with 3 different springs of varying dimensions as seen in chapter 3, each serving different purposes.

The metallic pedal is attached on to the top of each spring whose other end rests on the foot resting platform. The up and down movement of the spring caused due to the load applied with the forefeet will generate the required Dorsiflexion and Plantar flexion of the ankle as shown in figure 1.1. The push-pull mechanism executed by the resistance band is provided to ensure the consecutive lifting and release of the heel. This results in motion of the ankle joint in required manner. The Velcro bands over the pedal ensure that the foot remains on the spring even during reverse action.

ANALYSIS OF SPRINGS

The mechanical analysis of the springs was carried out in with static analysis in Ansys 15 to obtain mechanical properties such as maximum and minimum possible deformation, the stress and strain developed in the springs while operating. The analysis was conducted for all three springs under the load applied during sitting and standing positions for all three springs under load applied during Sitting and standing positions.

Analysis results for loads 15N and 30N is discussed in this section. All three springs were of same material thus the Young's Modulus, Rigidity Modulus and various other factors remained constant throughout the analysis. The results obtained for the analysis of each springs 1, 2 & 3 respectively are shown in figures 8.

Fig 7. Spring Designed

Once designed its exported to ANSYS 15 software and the mechanical properties are updated. The model is messed and other parameters are uploaded. One end of the spring is fixed and load is applied on the other end. Solutions for the analysis are then obtained as shown in figure 7.

Values of stress, displacement and strain are studied for the springs. Similarly the design, as in figure 9. & 10. and the analysis for other two springs are also carried out to the study of effect of load on them.

The procedures for analysis for these two springs are identical to that of first spring. The results obtained from the analysis of all three springs under 15N and 30N are listed in Table 4 & 5 respectively.

Fig 9. CATIA drawing of spring 2

Fig 10. CATIA drawing of spring 23

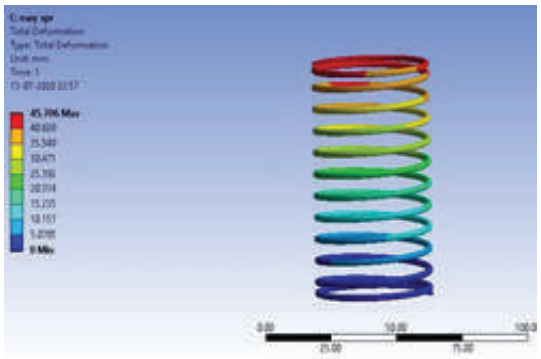

Fig. 11 a: Total deformation under 15N force

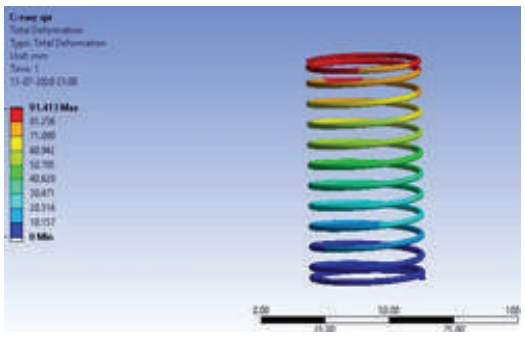

Fig 11 b: Total deformation under 30N force

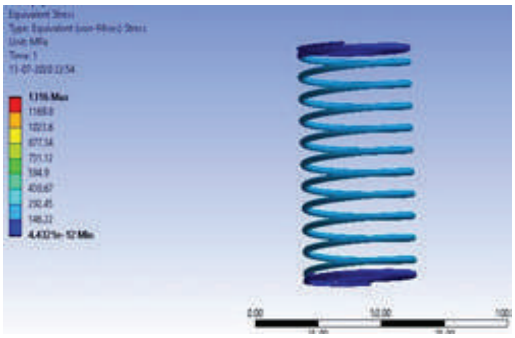

Fig 11 c: Stress developed under 15 N force

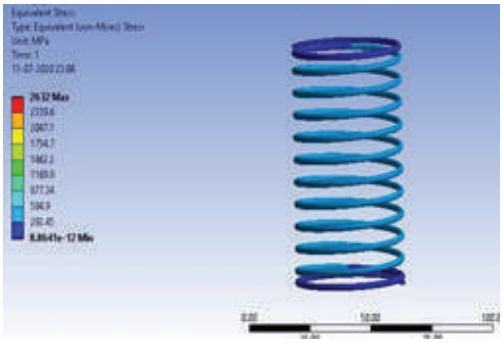

Fig 11 d: Stress developed under 30N force

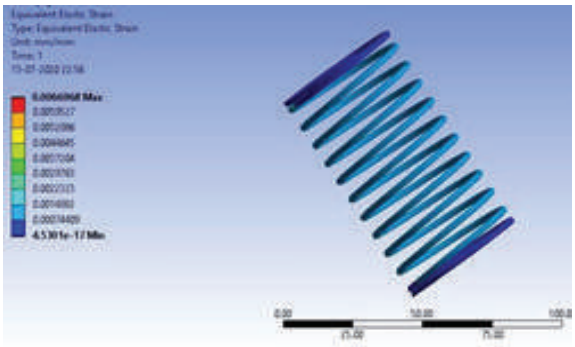

Fig 11 e: Strain under 15N force

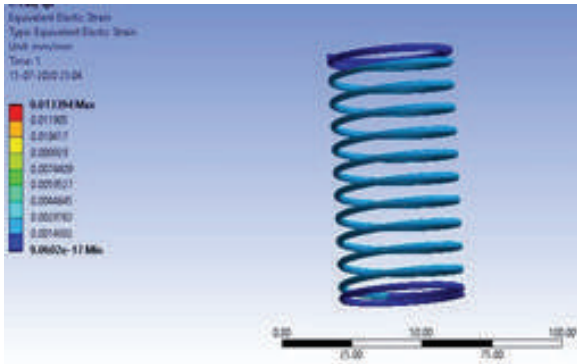

Fig 7 f: Strain under 30N force

Table 3. Analysis results under sitting condition (15N)

SPRING	Maximum Deformation (mm)	Minimum Deformation (mm)	Working stress (N/mm^2)	Elastic Strain
1	45.70	0	146.22	7.44×10^{-4}
2	20.45	0	1.28×10^{-3}	7.345×10^{-7}
3	9.30	0	1.15×10^{-4}	5.06×10^{-8}

Table 4. Analysis results for standing condition (30N)

SPRING	Maximum Deformation (mm)	Minimum Deformation (mm)	Working stress (N/mm^2)	Elastic Strain
1	91.41	0	292.45	1.48×10^{-3}
2	46.70	0	2.965×10^{-3}	3.425×10^{-6}
3	18.60	0	2.04×10^{-4}	1.023×10^{-7}

From results of the analysis, it can be concluded that for the given values of force, the deformation is maximum for the spring with least wire diameter and minimum for thickest spring. This proves that load required for the compression of spring with maximum wire thickness is much higher. Hence Spring 1 is best for weak patients and spring 3 is suitable for athletes in warming up processes.

The range of stress developed in each spring under different loads was also obtained. These values will help determining the factor of safety of each spring design under Soderberg criterion.

Testing of Springs using Soderbergs Criteria

The reliability of springs working under cyclic load can be studied with the aid of Soderberg method. Any object working under purely oscillatory load has higher chances of failure when their stresses reach the material's fatigue limit. The Soderberg Criterion provides a way to calculate a failure limit, by plotting a diagram between mean and alternating stress. Equation for Soderberg failure criterion for springs is,

$$\frac{1}{FS} = \frac{\tau_m}{\tau_Y} + \frac{\tau_a}{\tau_Y}\left(\frac{2\tau_Y}{\tau_e} - 1\right) \quad (3)$$

Where τ_e is the endurance strength, τ_y is the yield shear stress, τ_{mean} is the mean stress and τ_{alt} is the alternating stress. The shear stress in the spring alternates between its maximum and minimum values as the spring cycles. FS is the factor of safety for designing the body.

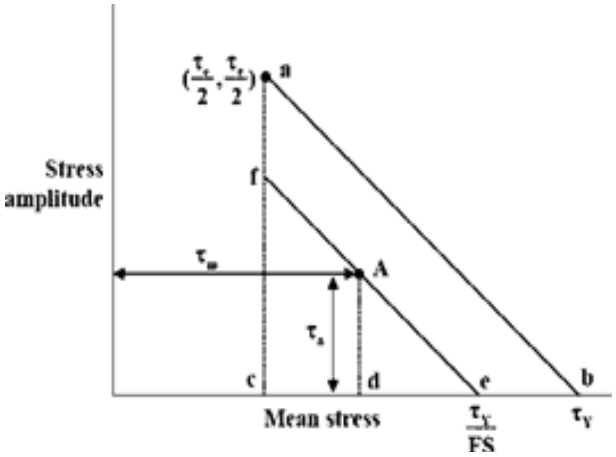

Fig. 11: Soderberg diagram for failure in springs

For safe design, the design data for the mean and average stresses, τ_a and τ_m respectively, should be below the line a-b. This line e-f in the figure is called a safe stress line and the point A is a typical safe design point. The line a-b shifts to a newer position depending on the value of factor of safety (FS). The maximum and minimum shear stress, τ on the inside surface of the spring coils are proportional to the spring forces F_{max} and F_{min}. The equations for finding τ_{max} and τ_{min} are,

$$\tau_{max} = \frac{8WD}{\pi d^3} F_{max} \quad (4)$$

$$\tau_{min} = \frac{8WD}{\pi d^3} F_{min} \quad (5)$$

W is the Wahl correction factor, D is the mean diameter and d is the wire diameter of the spring. Wahl factor for each spring was found using the following equation

Considering maximum load,

$$W = \frac{4C-1}{4C-4} + \frac{0.615}{C} \quad (6)$$

In the above equation C is the spring index. Values hence obtained for W are,

- $W_{spring\ 1} = 1.083$
- $W_{spring\ 2} = 1.107$
- $W_{spring\ 3} = 1.139$

$F_{max} = 30$ N and minimum load, $F_{min} = 8$ N. Substituting the obtained values in equations 4.2 and 4.3, τ_{max} and τ_{min} for each spring were found. Values obtained are listed in Table 7.

Table 7. Maximum and Minimum shear stress

Spring wire diameter (mm)	τ_{max} (N/mm²)	τ_{min} (N/mm²)
2.50	214.449	57.186
2.80	143.310	47.770
3.50	74.075	24.691

The mean and alternating shear stress can be now obtained by substituting τ_{max} and τ_{min} in the following equations,

$$\tau_{mean} = (\tau_{max} + \tau_{min}) /2 \quad (7)$$

$$\tau_{alternating} = (\tau_{max} - \tau_{min}) /2 \quad (8)$$

From equation 7 and 8 the mean and alternating shear stress for all three springs were found. For music wire material, endurance strength τ_e and yield shear stress τ_y can be related to its ultimate tensile strength σ_u, as given in equation 9 & 10.

$$\tau_e = .23 \times \sigma_u \quad (9)$$

$$\tau_y = .40 \times \sigma_u \quad (10)$$

Material properties of high carbon steel (Music wire) ,

- Ultimate Tensile strength $\sigma_u = 1725$ N/mm²
- Yield strength = 850 N/mm²

Substituting in equation 9 the values of τ_e and τ_y were obtained. The results hence obtained are listed in Table 8.

Table 8: Observations

SPRING	τ_{mean} (N/mm²)	τ_{alt} (N/mm²)	τ_e (N/mm²)	τ_y (N/mm²)
1	135.817	78.631	408.066	709.68
2	95.54	47.77	400.595	699.088
3	49.383	24.692	386.287	671.804

Now substituting the values of the endurance strength τ_e, yield shear stress τ_y, the mean stress τ_{mean} and alternating stress τ_{alt} in equation 1 we obtained the values of factor of safety (FS) corresponding to each spring, as follows,

- **FS spring 1 = 2.2**
- **FS spring 2 = 3.26**
- **FS spring 3 = 4.3**

RESULTS AND DISCUSSION

Once the component selection and analysis is completed and assemble the components and fabricate the model as shown in figure 3.1 was completed.. After an injury or surgery an exercise conditioning program or physiotherapy will help to return to daily activities and healthy lifestyle.

Endurance limit and fatigue strength are used to describe the range of cyclic stress that can be applied to the material without causing fatigue failure. The design will fail if the alternating stress is larger than the Soderberg stress limit. The values of working stress obtained from ANSYS analysis were found to be less than σ_y/fos. Hence the springs are safe.

CONCLUSIONS

The objective of the project was to design an effective and user friendly device for the therapeutic treatment of an ankle sprain. The following procedures were conducted;

- • Physiotherapy clinics were surveyed and the problems with existing ankle therapy methods were found. The need for a multipurpose, compact and user friendly equipment was obtained.

The developed design consists of a wooden platform, 3

springs of varying wire thickness, medium Tension resistance band elements and 3 metallic pedals.

The material selection and dimension calculations of the components were carried out considering the mechanical, economic and ergonomic factors.

The springs were customized and manufactured, pedals were fabricated and the resistance band and knee brace were purchased.

The resistance band used in the model may put forward constraints for patients suffering from calf muscle fatigue. This was not practically proven due to incompletion of fabrication of the model. Effectiveness of the device was to be tested by employing it to patients under treatment, which was a limitation due to Covid and prevailing Lockdown.

REFERENCES

1. S A Bridgman, D Clement, A Downing, G Walley, I Phair and N Maffulli "Population based epidemiology of ankle sprains attending accident and emergency units in the West Midlands of England", Emergency Medicine Journal, 2003 November, Volume 20, Issue 6
2. Lisa Chinn and Jay Hertel "Rehabilitation of Ankle and Foot Injuries in Athletes" Clinics in Sports Medicine Journal, 2010 Jan;29(1):157-67
3. Assad Al Sahlani, Mohammed K Khashan and Hayder H Khaleel "Design and analysis of Coil Spring using Finite Element Method" International Journal of Mechanical and Production Engineering Research and Development, July 2012
4. Jaqueline Santos Silva Lopes, Aryane Flauzino Machado and Carlos Marcelo Pastre "Effects of training with elastic resistance versus conventional resistance on Muscular Strength" ,SAGE Open Medicine Journal, Volume 7, February 2019
5. Jaehyun Bae, Jillian Lee, Melinda Malley, Joshua B. Gafford, Dónal Holland, Daniel Vogt and Jonathan Bean "Soft Wearable Quantitative Ankle Diagnostic Device", ASME Design of Medical Devices 9(3):030905, September 2015
6. Chuck Wolf "Functional Anatomy and Muscle Action of the Foot" Human Motion Associates, Florida, September 2005
7. Bryan J. Bergelin and Philip A. Voglewede "Design of an Ankle-Foot Prosthesis utilizing a Four-Bar Mechanism" ASME Journal of Mechanical Design 134(6):061004 June 2012
8. Doherty C, Bleakley C, Delahunt E and Holden S. "Treatment and prevention of acute and recurrent ankle sprain: an overview of systematic reviews with meta- analysis" British Journal of Sports Medicine, 51(2):113-125 October 2016
9. Xu, G.-C & Xu, D.-S & Zhao, X.-H & Bai, D.-C and Chen, J.-H. "Structure of spring steel spot welded joint and prediction for joint hardness." 41. 377-381, March 2011
10. Scott A. Paluska and Douglas B. Mckeag "Knee Braces: Current Evidence and Clinical Recommendations for Their Use" University of Pittsburgh Medical Center–Shadyside, Pittsburgh, Pennsylvania, 2000 Jan 15; 61(2):411-418.
11. Claire L Brockett and Graham J Chapman "Biomechanics of the ankle", Orthopedics and Trauma, Volume 30, Issue 3, June 2016, Pages 232-238.
12. Kyle B. Kosik, Matthew C. Hoch, Roger L. Humphries, Alejandro G. Villasante Tezanos and Phillip A.Gribble "Medications Used in U.S. Emergency Departments for an Ankle Sprain: An Analysis of the National Hospital Ambulatory Medical Care Survey" The Journal of Emergency Medicine, Vol 57, Issue 5, November 2019, Pages 662-670.

An Exploratory Research in 'Green Human Resource Management' in Automobile Sector

Anuradha
Assistant Professor
Department of Management
Bharati Vidyapeeth (Deemed to be University)
Institute of Management and Research
New Delhi
✉ anuradha.nain@bharatividyapeeth.edu

Anil Kumar Srivastav
Professor
Department of Management
Bharati Vidyapeeth (Deemed to be University)
Institute of Management and Research
New Delhi
✉ anil.kumar@bharatividyapeeth.edu

ABSTRACT

This study's objective is to investigate the factors that influence 'Green Human Resource Management'. This research focused on the statistical approach of factor analysis for developing new factors that lead to improved 'Green Human Resource Management' within the auto industry. The investigator utilized quota sampling to divide the Delhi/ NCR region into four automobile firms, each of which is a market leader in terms of market share, and purposive sampling was used in each of these sectors for the study. This method of sampling involves selecting population units that are convenient for the sampler in order to create a sample. A well-constructed questionnaire was given to the company's senior and intermediate executives in order to collect primary data for the study. (N = 423) Cronbach Alpha was used to assess the scale items' internal uniformity. The Kruskal-Wallis test was employed in conjunction with a non-parametric approach, factor analysis, and descriptive statistics. Findings revealed that 7 factors were effectively developed by means of analysis of factors and designated as elements impacting learning styles; these components are as follows: 1) Green Reward Management, 2) Green Learning & Development, 3) Eco-friendly health & safety practices and 4). Green Involvement, 5) Green Employee Relation, 6) Green Employee Discipline 7) Green Induction.

KEYWORDS *: Reward management, Learning & development, Health & safety measures, Green involvement, Green talent acquisition, Green industrial relation, Green employee discipline, Green induction.*

INTRODUCTION

Green Human Resource Management' (Green HRM) forthcoming, lately, in interest of organizations which construct positive environmental consequences within them. Green HRM is a new forthcoming set of information/issue in contemporary world. Environmental plan of actions, programs and code of conducts have become matter of deep concern for an organization in accordance with the global environment and its own development. In this upcoming area, the required study on HRM functions and its perspective is vast and unexplored. The main intent of this subsequent reading is to discover Sustainable Human Resource Management practices relying on the existent study. According to GHRM unites company's recruitment processes like appointments, selection, training & development, Performance Management & Assessment, Rewards & Recognition etc., besides environmental management aims. [1] thoroughly study on Environmental Management & Human Resource management and prepared a list of Green HRM activities. [2] describes the company receives appropriate employee environmental inputs and appropriate employee environmental work performance, it is imperative that HRM operations be changed or adjusted to be environmentally friendly.

Objective

This study's primary goal is to: Analyze the factors that lead to 'Green Human Resource Management' in Automobile sector.

Research Background

'Green Human Resource Management' (GHRM), which incorporates the maintenance of a company's business environment is one of them at solutions.

Simultaneously, other studies have discovered that companies who employ GHRM to strike a balance between preservation and industrial growth will probably yield greater profits than typical. 'Green Human Resource Management' (GHRM) was created as a result of a scholarly analysis of these environmental factors in HRM practices.

Many academics are employing various approaches to achieve a sustainable business environment and competitive edge in the GHRM studies that have emerged in the current day. Enhancing a Green HRM approaches ultimately aim to improve an organization's sustainable environmental performance. In light of this, the study's main objective is to determine how GHRM affects the automotive the capacity of the industry to keep a competitive edge.

Research gap

It is also necessary to talk about the study's shortcomings. Since In HR literature, GHRM is a relatively recent idea, this paper's subjects have limited material available. For example, [3] concurred based on the scant information currently available in the case of green pay and incentive systems. Therefore, it is advised that future study concentrate on particular green HR practices that have not received much attention.

Furthermore, as Asian nations have developing economies in which organizations play a significant role, it is advised that future research be done there. The application of GHRM in these companies may be a crucial instrument to ensure that they do not currently pollute the world to the same extent as Europe. Out of all the investigations that were covered, only the ones by Asia were the setting for [4] state that cultural values and beliefs may vary within a country cluster, which suggests that results may vary across other continents. Consequently, it is advised to repeat or carry out research on various continents.

LITERATURE REVIEW

Green HRM is used by [5] as an effort to make connections between research on 2 subjects of human resource management & environmental management in his book. Management field conceptualize the GHRM as a prominent factor quite recently. [6] states that green HRM is a component of HR improvement strategies meant to preserve and protect natural resources. Green HRM's primary goal is continuous improvement via human resource management. It replaces the traditional HRM procedures with a more ongoing and environmentally conscious set of guidelines [7].

'Green Human Resource Management' encompasses an understanding of environmental issues that support the organization's and the workers' social and economic stability [8]. It reduces costs, provide effectiveness, to reduce emission of carbon, to make green work-life balance initiatives begin [9]. [10] Green HRM practices, according to the study, give organizations a competitive advantage and help them achieve environmental and commercial sustainability. For the organization to advance consistently, it is necessary to develop the current correlation between HR policies and practices and Green HRM concepts.

Green Reward Management

Contextually, 'Green Human Resource Management' rewards & compensation work as efficient aids which support environmental activities in organizations. The claim is backed by a UK survey by CIPD/KPMG, which found that 8% of UK businesses polled offered financial incentives or other awards for their green efforts [11]. These techniques can be helpful in motivating employees to develop eco-initiatives [12]. The culture to establish Pay and Reward Systems in Work organizations ideally benefit for waste reduction practices developed by the team. For example, in the U.S., DuPont identifies employees winning performances related to environment. Such procured employees get honored with Environmental Respect Awards.

Green Training & Development

The objectives of green training and development are to raise employees' understanding of environmental issues, cultivate a positive outlook, and adopt a daring and creative approach to environmental concerns, and cultivate the virtuosity to recycle garbage and reprocess energy [13]. Social and environmental topics are added

to employee training and development programs at all levels, from shop floor safety deliberations to strategic affairs for continually using an item for a period of time under the executive management's wider concept of sustainability.

Various studies have shown that in-house training works as an intent involvement of an organization to manage waste (in terms of both prevention and reduction).

Green Health and Safety Management

Environment friendly health and safety is genuinely not covered by the typical HRM health and safety management position. Actually, it incorporates not just the traditional health and safety practices but also other aspects of an organization. Because of this, many businesses are reconsidering the role of "health and safety manager" in favour of "health, safety and environmental manager" in the modern era.

This job has a wider scope than the typical health and safety management position within a business. It includes, for instance, initiatives to preserve biodiversity and assist local populations. Green health and safety's key duty is to guarantee a green working place for all. An ecologically sensitive, resource-conscious, and socially conscious working place is referred to as a "green workplace" [14].

Green Induction

It seems that new personnel need to undergo induction to ensure that employee should know the importance and take the environment friendly practices earnestly. [15] Employers need to make sure that newly recruited employees are aware about environmental responsibilities, health and safety procedures, value the culture, and hold the eco-friendly policy and practices of the business.

Green Employee Discipline

Discipline and Grief Regarding grievances and discipline in EM, few companies have generally encouraged internal "whistleblowing" over environmental violations, imitating the British company National Westminster Bank. Grievances must be filed in high-risk enterprises (due to their safety record), and it makes sense that disciplinary actions be linked to environmental regulations and obligations in cases where not complying with law and rules happens [16]. According to professional judgment on legal concerns, some businesses may take steps after all to guarantee that responsibilities concerning environment met by putting provisions in employee bound contracts that state, among other things, that engaging in being ecologically irresponsible could be grounds for contract termination as a breach [17].

Green Employee Relation

Many hypothetical employers use 'Employee Involvement' (EI) teams in Environment Management as understand that their employees could reduce wastage. According to them, their staff have the most practical understanding of the related job procedures and end products. Work procedures are altered, and worker health and safety are enhanced when EI is used in the EM domain. For instance, Tennant Company and other American businesses have utilized EI to create new dry-abrasive systems that replace the outdated method for stripping and recoating industrial concrete floors. 2. According to [18], The UK government is considering legislation aimed at combating climate change which, in conjunction with municipal rules, could compel businesses to adopt environmentally friendly practices in their operations.

RESEARCH METHODOLOGY

Green human resource management is the basis of this empirical research. The two components that make up the entire study are the pilot research and study based on questionnaire. Pilot study of selected formations is done to find the factors of 'Green human resource management'.

The organization is the study's unit of analysis. Using factor analysis, seven new components were successfully generated based on the findings. This study uses an Empirical Cum Descriptive Research Design to discover the problem's solution by gathering both primary and secondary data. Data from 500 respondents were collected using both judgmental and purposeful methods for the pilot survey. It signifies that the questionnaire was filled out with the help of references from the automotive industry. The number of factors extracted was determined using EFA (Exploratory Factor Analysis).

Based on data illustrating the automobile share in India during the year 2019, the population of this study consists of companies that are leaders in the Delhi-NCR region's automotive market. The Society of Indian Automobile Sectors (SIAM) is the source. This is a reference to the site where the sample will be collected. The study's participants comprised firms located in Delhi/NCR, India. The partakers had been chosen constructed on Vijay Sathe's theory (2005), which considers share in the market and presentation in the auto sector, such as sales turnover, profitability, and so on. (SIAM- Society of Indian Automobile Sector.) Hyundai Motors, Maruti Suzuki, Mahindra and Mahindra, and TATA were chosen as the four major players. Non-random Purposive/Judgmental sampling was used in this study and Random Snowball Sampling was employed. It's an inspection technique where the most beneficial population units are chosen to obtain a sample.

All the data of importance and relevance was collected using of a routinely created Questionnaire distributed to employees in the chosen organizations in order to meet the research's final goal. Furthermore, the Judgmental or Purposive Inspecting approach was adopted since it was assumed that the participants' selection would have sufficient broad knowledge of green resource management because they apply a variety of sustainable practices in the organizations.

For the aim of the study, more than 400 to be precise 432 top level and mid executives from different automotive companies had been chosen. A sample size of 330 is sufficient for factor analysis [19]. After the affirmation portion of the questionnaire was finished, it was tested in a pilot study with a small sample size (100 participants). The universe from which the primary survey surveys, which employ questionnaires, are performed is the pool from which test participants are selected [20].

Pilot Study

The goal of questionnaire analyzing had been to ensure that questionnaire remains straightforward for participants to understand and acknowledge, as well as to eliminate the risk of misinterpretation, distraction, and partiality. The questionnaire was given to 100 individuals during the testing phase. As a result, all the partakers were asked questions from the questionnaire, with the goal of identifying the questionnaire's vulnerable regions. Each participant was asked to describe the difficulties they encountered while writing the questionnaire, as well as proposed improvements that could make it easier for the participants to accept it. The instructions for dialectics, questioning, organizing, and arranging, among other things, were witnessed.

Reliability Analysis

According to [21], reliability is measured through examining the organized variation's amount in the measuring scale. Reliability is defined as the degree to which replicating data gathering would produce results that are comparable for a set of quantifiable variables. The most often used indicator of internal resemblance is the measurement of a measurement scale's Cronbach alpha coefficient, which is over 0.7 in a fair sense [22]. [23]. Internal similarity reliability is defined as a value of less than 0.7. [24]. Cronbach's coefficient alpha for the 9 constructs with 32 statements used in the pilot study is being concise in the below table.

Table 1: Table 1 summarizes the pilot study's overall and individual construct reliability analysis

Cronbach's Alpha		No. of the Items
0.905		32
Constructs	**Items**	**Cronbach Alpha**
Green Reward Management	5	0.711
Green Training and Development	5	0.859
Green Health and Safety	6	0.884
Green Involvement	4	0.911
Green Employee Relation	3	0.736
Green Employee Discipline	5	0.708
Green induction	4	0.715

All of the components had Cronbach alpha values more than 0.7, which is considered fair and appropriate. This indicates that each item has a high level of internal consistency.

Interpretation and Analysis: Data analysis would be the assessment of its applicability in the Exploratory Factor Analysis (EFA). Factorability The factorability of the data can be investigated using two statistical

tests: the Kaiser-Meyer-Olkin Measure of Sampling Adequacy (KMO) and the Bartlett's Test of Sphericity. The importance of Bartlett's Test of Sphericity is appropriate, and the study's KMO sample adequacy score is higher, at 0.761. Consequently, the evaluation results offer adequate proof to supervise the proper use of factor analysis on the quantifiable effects of "Green Human Resource Management."

Table 2. Kaiser-Meyer-Olkin and Bartlett's Test

KMO Measure of Sampling Adequacy.		.761
'Bartlett's Test of Sphericity'		17395.719
		496
		.000

Interpretation of Factors

For the sake of identification and clarification, every construct requires a label or logo [25] Every component of product innovation discovered by Principle Component Analysis in this study's EFA process is displayed. Each construct's labels are determined by the explanation of its 'Green Human Resource Management' construct scale factors, and they are discussed in the sections following

'Green Reward Management'

The first construct, which has the highest percentage of Total Variance Explained (9.862%) was explained as 'Green Reward Management' because it incorporates scale variables that have been searched for and accepted from prior researches regarding the effect of GHRM associated with the features of 'Green Reward Management'. Scale variables that load into the construct 1 is listed in table number 3.

Table 3: An overview of Variance, and Rotated Component Matrix of Factor number 1

Variables	Percentage of Variance Explained		Loadings of factor
	Sums of extraction for squared loadings	summation of rotations for squared loads	
Give "long-term" recognition—that is, consistent exceptional performance over an extended period of time—special financial bonuses	26.742	9.862	0.753
Reward with letter of appreciation			0.662
Granting recognition for innovative recommendations that enhance performance is necessary.			0.693

'Green Training and Development': 'Green Training and Development' was identified as the component with the highest value of Total Variance Explained (9.772%), because it includes scale variables that were previously looked up and taken from research on how "green human resource management" affects the relational component of "green training and development." Table 4 below displays the scale variables that load into the construct 2

Table 4: An overview of Variance, and Rotated Component Matrix of Factor number 2

Variables	Percentage of Variance Explained		Factor Loadings
	Extraction sums of squared loadings	Rotation sums of squared loadings	
Employees have known the objective of the training	7.058	9.772	0.635
Training increase employee's motivation to the job you do			0.73

Training improve employee's skills, knowledge, attitude change, new capability			0.658
Training lead you to be satisfied with employee's job			0.667

'Green Health and Safety' 'Green Health and Safety' has been described as 3rd component having highest Total Variance Explained value which is 7.858 %, because it included scale variables that were looked up and included from earlier research on the effects of the environment. The scale variables that load onto the construct 3 are shown in Table 5 below.

Table 5: Variance, and Summary of the Rotated Component Matrix of factor number 3

Variables	Percentage of Variance Explained		Factor Loadings
	Extraction sums of squared loadings	Rotation sums of squared loadings	
Organization provides green workplaces for all.	4.652	7.858	0.654
The organization implements eco-friendly measures to decrease stresses on workers & work-related illnesses because of by dangerous working environments.			0.78
Employees at the company are given the chance to participate in environmental management initiatives.			0.644

'Green Involvement'

Due to the combination of scale variables that were looked up and used from earlier research on the effect of GHRM on relationship scale factors that were looked up and used from earlier research on how GHRM affected the relational component of I, the fourth factor with the largest Total Variance The 7.440 percent explained number has been explained as Green Involvement. Green Participation, the conduct of businesses is based on organizational brilliance, which includes the brilliance of employees Table 6 below displays the scale factor that load into the construct 4.

Table 6: Variance, and Summary of the Rotated Component Matrix of factor number 4

Variables	Percentage of Variance Explained		Factor Loadings
	Extraction sums of squared loadings	Rotation sums of squared loadings	
Organisation established a focused communication structure, which permits workers to share ideas on worker skills and motivations	4.457	7.44	0.744
The company provides a common learning culture for environmentally conscious thinking and conduct.			0.648
Employees at the company are given the chance to participate in environmental management initiatives.			0.644

Green Employee Relation

The explanation for the fifth factor, which has the highest Total Variance Explained value of 5.012 percent, is Green Employee Relation because it incorporates scale variables that were searched for and taken from prior studies regarding the effects of GHRM pertaining to the feature of Green Employee Relation. Table 7 below displays the scale factor that load into the construct 5.

Table 7: Cronbach's Alpha, Variance, and Summary of the Rotated Component Matrix

Variables	Percentage of Variance Explained		Loadings of factors
	Extraction sums of squared loadings	Rotation sums of squared loadings	
What work activities (i.e. trips) the worker would perform	4.167	5.012	0.649
How the work was to be performed?			0.771

Green Employee Discipline

Because it included scale factors that were looked up and taken from earlier studies on the impact of Green HRM on relational component of Green Employee Discipline, Green employee discipline has been cited as the explanation for the sixth element, which has the largest Total Variance Explained value (4.410 percent).

Green Induction: The seventh component having biggest Total Variance Explained value i.e.. 4.047 %, was described as green induction because it combines scale factors that have been looked for and accepted from the prior researches regarding the effects of GHRM pertaining to element of Green induction.

CONCLUSION

The research discovered that 'Green Reward Management', 'Green Training and Development', 'Green Health and Safety', 'Green Involvement', 'Green Recruitment and selection', 'Green Employee Relation', 'Green Employee Discipline', and 'Green Induction' are the most important variables in 'Green Human Resource Management'.

The conclusions of the study on organisational structure will aid managers in the creation of a right structure for employing 'Green Human Resource Management'. The numerous processes and practices that aid implementation of sustainable and green practices at human resource department of an organisation would guide managers in designing the appropriate systems to GHRM. Following a discussion of numerous organisational characteristics found in the literature, empirical research has been done to learn the effects of GHRM. The findings of this study show that, in the face of rapidly changing environment, implementation of 'Green Human Resource Management' practices in automobile organisation is quite high.

REFERENCES

1. Renwick, D. W., Redman, T., & Maguire, S. (2013). Green human resource management: A review and research agenda. International journal of management reviews, 15(1), 1-14.
2. Opatha, H. H. P. (2013). Green human resource management a simplified introduction.
3. Hiba A.Masri, Ayham A.M Jaaron, Assessing Green human resource management practices in Palestinian manufacturing context: An empirical study, Joournal of cleaner production, Volume 143, P,474-489
4. Woods, (1993), In Milliman, J., and Clair, J. (1996), "Best Environmental HRM Practices in the USA", In Wehrmeyer, W., (eds), (1996), Greening People - Human Resources and Environmental Management, First Edition, Sheffield, England: Greenleaf Publishing.
5. Patil, V., Wadhwa, C., Bhalerao, K., Nair, D., & Khandare, D. M. (2022). Green human resource management enabled business sustainability. Journal of Information and Optimization Sciences, 43(7), 1635–1650. https://doi.org/10.1080/02522667.2022.2128521
6. Beard, C., & Rees, S. (2000). Green teams and the management of environmental change in a UK county council. Environmental Management and Health, 11(1), 27-38.
7. Clarke, E. (2006). Power brokers. People Management, 18, 40-42.

8. Clement, K. (1997). Multi-disciplinary teams and environmental integration: European programmes. Team Performance Management: An International Journal, 3(4), 261-269.

9. Cook, J., & Seith, B. J. (1992). Designing an effective environmental training program. Journal of Environmental Regulation, 2(1), 53-62.

10. Farrell, K. (2015). Work-life balance practices among Irish Hotel Employees and Implications for HRM. Level 3, 12(2), 4.

11. Charles Jr, O. H., Schmidheiny, S., & Watts, P. (2017). Walking the talk: The business case for sustainable development. Routledge.

12. Epstein, M. J. (2018). Making sustainability work: Best practices in managing and measuring corporate social, environmental and economic impacts. Routledge.

13. Frey, C. B., & Osborne, M. A. (2017). The future of employment: How susceptible are jobs to computerisation?. Technological forecasting and social change, 114, 254-280.

14. Glendon, A. I., Clarke, S., & McKenna, E. (2016

15. Unnikrishnan, S., & Hegde, D. S. (2007). Environmental training and cleaner production in Indian industry—A micro-level study. Resources, conservation and recycling, 50(4), 427-441.

16. Halawi, A., & Zaraket, W. (2018). Impact of green human resource management on employee behaviour. SBS Journal of Applied Business Research (SBS-JABR), 6, 18-34.

17. Govindan, K., Kaliyan, M., Kannan, D., & Haq, A. N. (2014). Barriers analysis for green supply chain management implementation in Indian industries using analytic hierarchy process. International journal of production economics, 147, 555-568.

18. Govindan, K., Khodaverdi, R., & Vafadarnikjoo, A. (2015). Intuitionistic fuzzy based DEMATEL method for developing green practices and performances in a green supply chain. Expert Systems with Applications, 42(20), 7207-7220.

19. Govindan, K., Muduli, K., Devika, K., & Barve, A. (2016). Investigation of the influential strength of factors on adoption of green supply chain management practices: An Indian mining scenario. Resources, Conservation and Recycling, 107, 185-194.

20. Kossek, E. E., & Michel, J. S. (2011). Flexible work schedules.

21. Kramar, R. (2014). Beyond strategic human resource management: is sustainable human resource management the next approach? The international journal of human resource management, 25(8), 1069-1089.

22. Leigh, N. G., & Blakely, E. J. (2016). Planning local economic development: Theory and practice. SAGE publications.

23. Luthra, S., Garg, D., & Haleem, A. (2015). An analysis of interactions among critical success factors to implement green supply chain management towards sustainability: An Indian perspective. Resources Policy, 46, 37-50.

24. Rafiei, N., & Davari, F. (2015). The role of human resources management on enhancing the teaching skills of faculty members. Materia socio-medica, 27(1), 35.

25. Rothenberg, S., Hull, C. E., & Tang, Z. (2017). The impact of human resource management on corporate social performance strengths and concerns. Business & Society, 56(3), 391-418.

The Effectiveness of Naukri Platform in Candidate Sourcing: A Case Study

R. Padmaja
Associate Professor
Department of Business Management
Krishna University, Rudravaram
Machilipatnam, Andhra Pradesh
✉ padmajapeddireddi@rediffmail.com

ABSTRACT

The study examines the effectiveness of Naukri, an online recruiting platform in sourcing candidates within selected Information Technology (IT) organizations in Vijayawada. The study aims to comprehensively assess Naukri's impact on candidate sourcing effectiveness within this specialized industry context. Given the rapid growth of the IT industry in Vijayawada, there is a greater need for highly competent people. This highlights the importance of having effective methods for finding and attracting qualified candidates. The study employs a quantitative methodology, using structured questionnaires to collect data from recruiters at specific IT organizations. The research assesses the efficacy of Naukri as a platform for sourcing, its dependability in delivering candidates of high quality, and its relationship with the success of sourcing strategies. The results emphasise the perceived efficacy and dependability of Naukri among recruiters, demonstrating favourable connections between the frequency of Naukri's use and several measures of sourcing strategy success.These insights offer practical implications and recommendations for refining candidate sourcing practices within Vijayawada's IT landscape.

KEYWORDS *: Candidate sourcing, Effectiveness, Information technology, Recruiter, Naukri.*

INTRODUCTION

Recruitment stands as a pivotal process, crucial for organizations striving to achieve their objectives by acquiring individuals who drive expansion, innovation, and progress. The intricacy of identifying the right candidate influences not just productivity but also shapes an organization's culture and trajectory, demanding meticulous analysis and integration of candidates' profiles.

In today's competitive landscape, job portals like Naukri play a pivotal role in assisting HR professionals (Recruiters) faced with the daunting task of finding the perfect candidate. Naukri, a prominent player in online recruitment, is lauded for its ability to optimize the recruiting procedure. However, its effectiveness in candidate sourcing, particularly within the intricate domain of Information Technology (IT) organizations, remains a subject ripe for further investigation.

Naukri's networking platform has revolutionized the job search process, seamlessly connecting job seekers and recruiters. This user-friendly interface provides an extensive exploration of job opportunities, benefiting both candidates in finding the right fit and recruiters in reaching suitable candidates. Additionally, Naukri's job posting services and AI tools further enhance candidate sourcing and response management, streamlining the recruitment process.

With its array of services and cutting-edge technology, Naukri emerges as a premier job portal for effective candidate sourcing, serving the needs of job seekers and recruiters alike, solidifying its integral role in India's employment landscape.

The selection of Information Technology (IT) organizations in Vijayawada as the focal point of this study stems from several strategic considerations. Vijayawada has witnessed a significant surge in its IT

sector in recent years, emerging as a burgeoning hub for technological innovation and business growth. This rapid expansion has underscored the critical need for skilled professionals, intensifying the importance of effective candidate sourcing mechanisms within this specialized industry.

By focusing on Vijayawada's IT sector, this research seeks to contribute valuable insights and empirical evidence specific to this regional IT landscape. The findings aim to offer practical recommendations and strategies tailored to the needs of IT organizations in Vijayawada, enriching the discourse on effective candidate sourcing practices within this specific geographical domain.

PURPOSE OF THE STUDY

This study endeavors to rigorously assess the effectiveness of Naukri as a candidate sourcing platform within selected IT organizations in Vijayawada. Through meticulous examination, this study aims to illuminate the nuanced leveraging of Naukri's capabilities in sourcing qualified talent, thereby contributing to a deeper understanding of its impact within the specific context of Vijayawada's IT sector.

OBJECTIVES OF THE STUDY

The objectives of this research are formulated to comprehensively assess and understand the effectiveness of Naukri as a candidate sourcing platform within the context of Information Technology (IT) organizations in Vijayawada. The specific aims of this study include:

a. To evaluate the efficiency of Naukri as a candidate sourcing platform within selected IT organizations in Vijayawada.

b. To assess the reliability of Naukri in the candidate sourcing process, considering its impact on the quality of recruited candidates within the IT sector.

c. To analyze the correlation between the utilization of Naukri and the effectiveness of candidate sourcing strategies adopted by IT organizations in Vijayawada.

REVIEW OF LITERATURE

Malvania and Doshi (2022) emphasised the significance of firms adopting online recruiting and screening procedures, particularly in light of technological improvements and the post-COVID age. The study suggests that while the majority of IT recruiters are knowledgeable about different recruiting tools, there is still a lack of information about selection tools such as psychometric tools, reference check tools, and application tracking systems. In addition, the analysis indicates that although recruiters are familiar with these technologies, they mostly utilise them on well-known sites such as Naukri, LinkedIn and job portals. Furthermore, Skype is often used for selection reasons. The analysis recommends that recruiters should consider transitioning the whole recruiting and selection process to an online platform, since this may result in savings in terms of time and money.

Banerjee and Gupta (2019) studied HR managers' talent acquisition issues in contemporary labour markets. It emphasises the time required to identify qualified candidates and the rise in applicant volume resulting from the implementation of online recruitment channels. The study discusses how podcasts, blogs, and online employee testimonials may boost an employer's brand. A multi-group mediated mediation analysis was done with 361 online recruiting platform-using professionals. The results imply that video podcasts and realistic employee testimonials on third-party blogs improve job-seekers' opinion of the employer's quality and trustworthiness, increasing their attractiveness and desire to apply.

Kamalasaravanan (2019) concentrated on the efficacy of private organisations' utilisation of employment portals and networking sites for recruitment purposes. The objective of the study is to ascertain the job portal that employees prefer, evaluate the effectiveness of recruitment strategies, and determine the level of convenience associated with portal usage. Naukri is the job portal of choice for candidate procurement, and the majority of respondents concur that the recruitment strategy is successful. In addition, employee shift preferences, candidate selection methods, remuneration considerations, and the practicality of networking sites are assessed in the review. In general, the research indicates that networking sites and job portals are both efficacious in the realm of recruitment. The One-Way Anova and Chi-Square tests are utilised to examine the correlation between various variables.

Punn et al. (2018) studied the efficacy of using social media platforms for recruiting purposes in Indian IT firms. The study examines the viewpoints of individuals seeking employment and those responsible for hiring, with a specific emphasis on the utilisation of social networking platforms as a method for enhancing the promotion of abilities and establishing connections with prospective applicants.

Venaik and Sinha (2018) conducted an investigation on the perspective of job searchers from the millennial generation in Delhi which revealed that elements such as utility, user-friendliness, additional services, potential career prospects, and the quality of the system had a substantial impact on their view of job portals. These elements enhance the expeditious and effective job search process for millennials.

Uzair et al. (2017) focused on examination of the recruitment applications of social media in Pakistan. The purpose of the study is to ascertain whether social media recruitment has had an effect on assortment levels in the Pakistani services division. The research inquiries concern candidate screening in relation to their social media profiles, as well as the motivations and approaches employers employ when utilising social media for recruitment purposes. The research findings indicate that social networking sites have a substantial impact on the recruitment process in Pakistan. HR departments are advised to acquaint themselves with these platforms. In general, while social media has increased the accessibility and autonomy of the recruitment process, industry analysis and personal social connections remain indispensable in assessing an individual's suitability for a particular position.

METHODOLOGY

Research Design: The research has adopted a quantitative approach utilizing structured questionnaires to evaluate the effectiveness of Naukri as a candidate sourcing platform within Vijayawada's IT organizations.

Participants and Sampling: Recruiters directly involved in the hiring process from five selected IT organizations in Vijayawada are the target population. Convenience sampling is used to select five recruiters from each organization, totaling 25 recruiters for the study.

The choice of convenience sampling stems from practical constraints inherent in accessing recruiters directly engaged in the hiring process within Vijayawada's limited pool of IT organizations. Given the time-sensitive nature of this research and the need for swift data collection, convenience sampling provides an expedient means to gather insights from key stakeholders. While acknowledging its limitations in representation and potential bias, this method remains appropriate for the study's localized focus, aiming to derive context-specific conclusions pertinent to the nuances of candidate sourcing within Vijayawada's IT sector. This approach strikes a balance between practicality and relevance, facilitating the acquisition of valuable insights despite its restricted scope.

Data Collection Method: Structured questionnaires are designed to gather quantitative data from the recruiters. The questionnaire will focus on assessing the efficiency of Naukri in sourcing candidates, gauging the reliability of Naukri in providing quality candidates, understanding the recruiters' perceptions and experiences with Naukri's effectiveness.

Data Analysis: Python programming is utilized for data analysis. The survey instrument's reliability was evaluated using Cronbach's alpha to assess the internal consistency of the questionnaire items related to Naukri's effectiveness as a candidate sourcing platform. The collected survey data has undergone descriptive statistical analysis using Python libraries to derive measures of central tendency and correlations between variables.

Ethical Considerations: The anonymity of organizations and participants will be ensured in the study and questionnaire responses. Informed consent is sought from each participating recruiter, clarifying the study's purpose and their voluntary participation.

LIMITATIONS

a. The study's results may be constrained by the limited sample size and potential lack of universal generalizability.

b. Convenience sampling, chosen due to practicality, may introduce biases by selecting participants based on accessibility rather than random sampling.

RESULTS AND DISCUSSION

Internal Consistency Test

A Cronbach's alpha coefficient (α) is 0.8431783536585368 ≅ 0.843 was obtained, indicating a good level of internal consistency among the questionnaire items. This suggests that the items within the survey demonstrated a relatively high degree of agreement in measuring the intended construct, reinforcing the reliability of the questionnaire used in this study.

Evaluating the Efficiency of Naukri as a Candidate Sourcing Platform

The assessment of Naukri's efficiency as a candidate sourcing platform involved a thorough examination of respondents' ratings. As shown in the Figure 1, the mean efficiency rating derived from the survey data was approximately 3.96, with a median efficiency rating of 4.0 on a 5-point scale. These scores capture the aggregated perceptions of recruiters concerning Naukri's efficacy in matching job descriptions with candidate profiles.

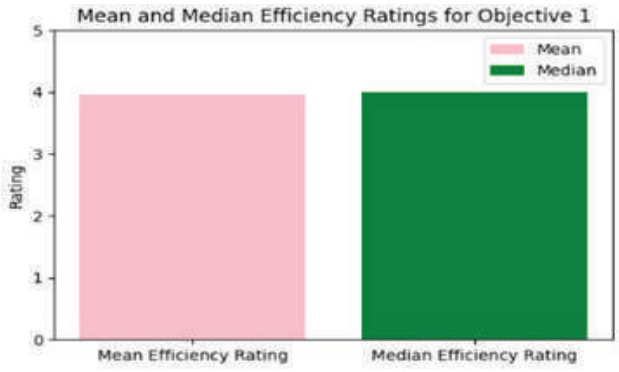

Fig. 1. Mean and Median Efficiency Ratings Output

The obtained ratings suggest a moderately positive sentiment among respondents towards Naukri's efficiency, positioned close to the upper end of the 5-point scale. The proximity of the mean and median scores to 4 signifies a generally favorable perception among the surveyed recruiters regarding Naukri's ability to effectively align job roles with candidate qualifications. This analysis implies that, on average, respondents viewed Naukri as a candidate sourcing platform exhibiting commendable efficiency in aligning job descriptions with candidate profiles.

Assessing Naukri's Reliability in Candidate Sourcing

As shown in the Figure 2, the mean quality rating provided by respondents for candidates recruited from Naukri compared to other methods is approximately 3.84 on a 5-point scale. The median quality rating aligns with a score of 4, indicating a consistent perception among respondents with the middlemost value of the ratings. The mean and median ratings suggest an overall positive perception of candidate quality sourced via Naukri, indicating that, on average, respondents perceived candidates recruited through Naukri to be of reasonably good quality compared to other recruitment methods.

Fig. 2. Mean and Median Quality Ratings Output

Analysing the Correlation between the Utilization of Naukri and the Effectiveness of Candidate Sourcing Strategies

The correlation matrix illustrates the relationships between the frequency of Naukri utilization for candidate sourcing and various metrics associated with sourcing strategy effectiveness within IT organizations in Vijayawada. The results are shown in Figure 3.

Strong Positive Correlations (Values Close to 1.0)

Utilization Frequency vs. Efficiency Rating (0.961): The high positive correlation indicates that as the frequency of Naukri usage increases, there is a substantial increase in the efficiency rating provided by recruiters, suggesting a direct association between higher Naukri utilization and perceived efficiency in the sourcing process.

Utilization Frequency vs. Overall Satisfaction (0.911): A robust positive correlation denotes that increased

utilization of Naukri is closely linked to higher levels of overall satisfaction among recruiters, implying that more frequent usage tends to correspond with greater satisfaction regarding candidate sourcing.

Integration Level vs. Sourcing Strategy Success (0.964): This strong positive correlation suggests that a well-integrated utilization of Naukri within sourcing strategies significantly aligns with higher overall success in sourcing strategies, emphasizing the importance of seamless integration for better outcomes.

Other Significant Correlations

Quality Rating with Other Metrics (Range: 0.708 - 0.957): The positive correlations between quality rating and metrics like efficiency, integration level, and sourcing strategy success imply that perceived candidate quality sourced from Naukri is associated with various aspects of sourcing strategy effectiveness.

Moderate Correlation (0.708 - 0.791)

Job Fit & Retention with Utilization Frequency and Integration Level: These moderate correlations suggest a moderate association between job fit & retention and the frequency of Naukri utilization, as well as its integration level within sourcing strategies.

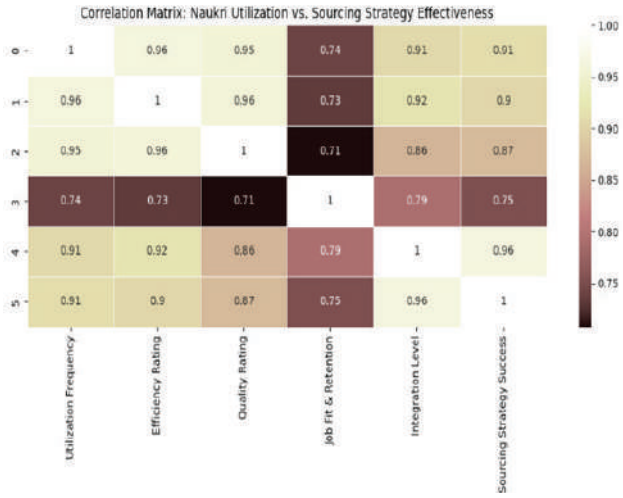

Fig. 3. Correlation Matrix Output

The observed correlations highlight the significant relationship between Naukri utilization and various dimensions of sourcing strategy effectiveness within IT organizations in Vijayawada. The findings emphasize the potential impact of increased Naukri utilization on enhancing efficiency, satisfaction, quality, and overall success in sourcing strategies.

RECOMMENDATIONS

a. Maximize Utilization Frequency for Improved Efficiency: The recruiters within IT organizations should be encouraged to increase the frequency of utilizing Naukri. The study revealed a strong positive correlation between higher Naukri usage and increased efficiency ratings. By utilizing the platform more frequently, organizations can potentially enhance their sourcing process efficiency.

b. Emphasize Integration for Enhanced Success: The study showed a strong correlation between integration levels and sourcing strategy success. IT organizations should focus on effectively embedding Naukri within their recruitment procedures to achieve better overall success in candidate sourcing.

c. Quality Enhancement Initiatives: While respondents perceived candidates sourced via Naukri to be of reasonably good quality, continuous efforts should be made to ensure consistent quality improvements. Organizations could explore refining search filters, optimizing job postings and mass mailings, showcasing the company brand, leveraging RMS, and other features provided by Naukri to attract higher-quality candidates.

d. Job Fit and Retention Focus: Given the moderate correlations found between job fit, retention, and Naukri utilization, IT organizations should focus on leveraging Naukri to find candidates with better job fit. Additionally, monitoring the retention rate of candidates sourced via Naukri can provide insights into the platform's long-term impact on employee stability.

e. Expand Research and Collaboration: Encouraging further research collaborations between academia and industry is beneficial. Exploring partnerships with Naukri or similar platforms to analyze trends, share insights, and co-create solutions to optimize candidate sourcing processes further would add great value.

CONCLUSION

The research explored into assessing Naukri's impact on candidate sourcing within selected Vijayawada's Information Technology (IT) organizations, highlighting its critical role in sourcing highly skilled professionals. Leveraging structured questionnaires and a quantitative approach, the study revealed positive perceptions among recruiters regarding Naukri's effectiveness and its correlation with sourcing strategy success. Despite acknowledging limitations like sample size and potential biases, the study's findings emphasize the need to optimize Naukri's usage frequency, integration, and continuous quality enhancement to further refine candidate sourcing practices within IT landscape of Vijayawada.

REFERENCES

1. Ghodasara, J. (2023, November 9). Candidate Sourcing: Secrets to Find & Attract Hidden Gems|iSmartRecruit. iSmartRecruit. https://www.ismartrecruit.com/blog-ways-recruiters-source-the-candidates
2. Shah, M. (2022, September 1). Here Is How Naukri Portal & Naukri Blog Can Guide You to a Successful Career. Naukri's Official Blog. https://www.naukri.com/blog/here-is-how-naukri-portal-can-guide-you-to-a-succesful-career/
3. Malvania, V., & Doshi, V. (2022). An Exploratory Study on awareness of different online tools and technologies used in Recruitment and Selection Process among Recruiters in IT Companies.
4. Pal, A., Kundu, A., Polley, S., Chatterjee, S., & Chakraborty, S. (2021). A Study on Finding the Most Effective Social Media Platform for E-Recruitment Process. Interdisciplinary Research in Technology and Management, 451-455.
5. Kamalasaravanan, S. (2019). A Study on the Effectiveness of Job Portal and Networking Sites Recruitment. IJEMR, 9(1). https://ijemr.in/wp-content/uploads/2019/01/A-Study-on-the-Effectiveness-of-Job-Portal-and-Networking-Sites-Recruitment-4.pdf
6. Banerjee, P., & Gupta, R. (2019). Talent attraction through online recruitment websites: Application of web 2.0 technologies. Australasian Journal of Information Systems, 23.
7. Punn, M., & Chaudhuri, M. (2018). Impact of Social Media Usage on Recruitment in the Indian IT Industry. Amity Business Review, 19(2).
8. Venaik, A., & Sinha, S. (2018). Factors affecting students perception towards E-recruitment: A study of Naukri. Com. Journal of Global Information and Business Strategy, 10(1), 44-48.
9. Uzair, S., Kanwal, S., & Haleem, R. (2017). The use of social media in the recruitment process: A study on Karachi. International Journal of Multidisciplinary and Current Research, 5, 360-364.
10. Team, D. (2015, October 30). CASE STUDY:How Naukri.com Became #no1 Indian Job Portal When The Internet Was In Its Infancy? DSIM. dsim.in. https://dsim.in/blog/case-studyhow-naukri-com-became-no1-indian-job-portal-when-the-internet-was-in-its-infancy/

A Descriptive Study of Knowledge Management for Industry Chain

Muktak Vyas
Professor
Department of Management
Poornima University
Jaipur
✉ muktak.vyas@poornima.edu.in

ABSTRACT

Knowledge management (KM) plays a crucial role in improving the efficiency, innovation, and competitiveness of organizations across diverse industry chains. This study delves into the implementation of KM strategies tailored specifically for industry chains, with the goal of optimizing information flow, promoting collaboration, and capitalizing on intellectual assets within the intricate network of interconnected businesses. The paper thoroughly examines key concepts in knowledge management and their adaptation to the dynamics of industry chains. It underscores the significance of identifying, acquiring, storing, disseminating, and applying knowledge throughout the value chain. Additionally, the study investigates the transformative role of emerging technologies like artificial intelligence, big data analytics, and block chain in reshaping knowledge management practices within industry chains.

INTRODUCTION

Industry chains, encompassing diverse stakeholders from raw material suppliers to end consumers, operate in a landscape marked by rapid technological advancements, global competition, and ever-evolving market demands. In such a context, the ability to effectively harness and capitalize on the wealth of knowledge distributed across the entire value chain becomes paramount. This paper explores the nuanced dimensions of knowledge management tailored to the intricacies of industry chains, shedding light on the challenges, opportunities, and best practices associated with implementing effective KM strategies. The overarching objective of this research is to underscore the significance of knowledge management in optimizing industry chain operations. As organizations navigate through the stages of production, distribution, and consumption, they encounter various knowledge-related challenges – from ensuring the quality and timeliness of information exchange to promoting a culture of collaboration and continuous learning. By examining the specific needs of industry chains, this study aims to offer insights that can inform and guide organizations in developing robust knowledge management frameworks aligned with the unique demands of their respective value chains. Throughout this exploration, we will delve into key components of knowledge management, covering aspects from knowledge creation and acquisition to dissemination and application. Additionally, we will scrutinize the role of cutting-edge technologies in transforming knowledge management practices within industry chains and explore the organizational and leadership elements essential for fostering a culture of knowledge-sharing. Through these efforts, we seek to contribute to the ongoing discourse on knowledge management for industry chains and provide a foundational resource for organizations navigating the complexities of today's interconnected business ecosystems.

FUTURE USES

Academic Databases

These databases contain a diverse collection of scholarly articles spanning various fields. To find articles related

to knowledge management in industry chains, utilize keywords such as "knowledge management," "industry chain," "supply chain," and other relevant terms during your search. Employ Boolean operators such as AND, OR, and NOT to fine-tune your search, enabling a more targeted exploration of scholarly literature.

Journal In Knowledge Management

Explore specialized journals in knowledge management to access in-depth articles and research papers. Consistently monitor these journals for the most recent publications on strategies for knowledge management within industry chains.

Research Organization

Investigate reports on industry trends from research organizations and think tanks, as they frequently publish valuable insights. Explore publications from these reputable sources to gain a deeper understanding of knowledge management practices within industry chains.

Conference Proceeding

Participate in conferences focused on knowledge management, supply chain management, and industrial practices to showcase cutting-edge research. Stay informed by reviewing conference proceedings, including those from events like the International Conference on Knowledge Management or Supply Chain Management conferences, to access the latest research findings.

Books And Book Chapters

Books and book chapters authored by experts can provide comprehensive coverage of the subject. Search platforms like Google Books or Amazon for titles related to knowledge management in industry chains.

IMPLEMENTING KNOWLEDGE MANAGEMENT

Conduct a Knowledge Assessment

Start by assessing the existing knowledge assets, both explicit and tacit, within the industry chain. Identify critical knowledge areas, key stakeholders, and potential knowledge gaps.

Define Objectives and Goals

Clearly articulate the objectives and goals of implementing knowledge management. Determine what the organization aims to achieve through effective knowledge management within the industry chain, such as improved collaboration, innovation, and operational efficiency.

Develop a Knowledge Management Strategy

Formulate a comprehensive KM strategy that aligns with the specific needs and characteristics of the industry chain. Consider the unique challenges and opportunities presented at different stages, from raw material suppliers to end consumers.

Establish Governance and Leadership

Appoint leaders and establish governance structures to oversee the knowledge management initiative. Assign responsibilities for knowledge stewardship, ensuring that there is accountability for the success of KM practices throughout the industry chain.

Create a Knowledge Sharing Culture

Foster a culture that encourages knowledge sharing and collaboration. Implement incentives, recognition programs, and communication strategies to promote the value of sharing insights and expertise across stakeholders.

Implement Technology Solutions

Leverage technology to facilitate knowledge management processes. Implement collaborative platforms, document management systems, and other tools that enable seamless sharing and retrieval of information within the industry chain.

Capture and Codify Knowledge

Develop processes for capturing tacit knowledge and converting it into explicit forms. Create knowledge repositories, databases, or wikis to store and organize information relevant to different stages of the industry chain.

Provide Training and Support

Offer training programs to educate stakeholders on the importance of knowledge management and how to use the implemented tools effectively. Provide ongoing support to address any challenges and ensure the continuous adoption of KM practices.

Encourage Cross-Functional Collaboration

Facilitate collaboration among different functions and entities within the industry chain. Promote cross-functional teams and collaborative projects to enhance knowledge exchange and problem-solving.

Measure and Evaluate

Establish key performance indicators (KPIs) to measure the success of knowledge management initiatives. Regularly evaluate the impact on efficiency, innovation, and overall performance within the industry chain.

Iterate and Improve

Knowledge management is an evolving process. Continuously gather feedback, learn from experiences, and iterate on the KM strategy to address changing dynamics and emerging challenges within the industry chain.

Document Best Practices

Document successful knowledge management practices and lessons learned. Share these insights across the industry chain to encourage the replication of effective strategies and processes.

EXPECTED BARRIERS OF THE PROPOSAL MODEL

Resistance to Change

Employees at various stages of the industry chain may resist changes in their established workflows and practices. A cultural shift towards knowledge sharing and collaboration may face resistance, particularly if employees perceive it as disrupting their routine or job security.

Lack of Leadership Buy-In

Without strong support from leadership and a clear commitment to knowledge management principles, the initiative may lack the necessary resources, visibility, and influence to succeed. Leaders must actively champion the importance of KM and integrate it into the organization's strategic goals.

Technology Adoption Challenges

Implementing new technologies for knowledge management can be met with challenges, including technical complexities, integration issues with existing systems, and a learning curve for users. Ensuring user-friendly interfaces and providing comprehensive training can help mitigate these challenges.

Data Security and Privacy Concerns

The sharing of knowledge often involves sensitive information. Concerns about data security, privacy, and intellectual property protection may arise. Establishing robust security measures and clear policies is crucial to address these concerns and build trust among stakeholders.

CONCLUSION

In summary, integrating knowledge management (KM) into an industry chain is a strategic necessity for organizations aiming to excel in the contemporary and interconnected business landscape. The diverse network of stakeholders, spanning from raw material suppliers to end consumers, calls for a comprehensive approach to knowledge management that encompasses the entire value chain. Throughout this extensive study, we have delved into crucial considerations and steps essential for effectively harnessing and leveraging knowledge to optimize the operations of industry chains. The study consistently underscores the significance of knowledge identification, acquisition, storage, dissemination, and application. Recognizing the distinctive challenges and opportunities at each stage of the industry chain, organizations must tailor their KM strategies to address specific needs and complexities. Whether the focus is on enhancing collaboration, fostering innovation, or improving operational efficiency, KM emerges as the pivotal factor in unlocking the untapped potential inherent in the collective intelligence of the industry chain.

REFERENCES

1. https://ied.eu/blog/importance-of-knowledge-management-in-supply-chain-management/
2. https://www.sciencedirect.com/science/article/abs/pii/S0957417411015788
3. https://www.getguru.com/reference/knowledge-management-supply-chain-management
4. https://www.iese.edu/media/research/pdfs/DI-0900-E.pdf
5. https://scholarspace.manoa.hawaii.edu/server/api/core/bitstreams/0ef0aaf9-0a2d-44a4-abad-d5748c8d57e8/content

Comparative Predictive Modeling of Bankruptcy in India's Real Estate and Construction Sector: A Machine Learning vs. Traditional Approach

Sakshi Sharma
Research Scholar
University School of Management
Kurukshetra University
Kurukshetra, Haryana
✉ sakshi.usm@kuk.ac.in

Bhag Singh Bodla
Retired Professor
University School of Management
Kurukshetra University
Kurukshetra, Haryana
✉ bsbkuk@gmail.com

Anil Kumar Mittal
Professor
University School of Management
Kurukshetra University
Kurukshetra, Haryana
✉ Anilmittalkuk@gmail.com

ABSTRACT

This study aims to perform the comparative analysis of seven different predictive models which includes Multiple Discriminant Analysis (MDA), Logistic Regression (LR), Decision Trees (DT), Support Vector Machine (SVM), Artificial Neural Network (ANN), Random Forest (RF), and Gradient Boosting Method to predict the bankruptcy of companies in the Indian real estate and construction sector. This dataset covers the period from the year 2017 to the year 2022 with 12 different financial ratios and 2 non-financial variables of 94 bankrupt and 94 non-bankrupt firms. The models were assessed with accuracy, Precision, F1 score, and the Area Under the Curve (AUC) based on the results. This study shows that machine learning models outperform statistical models. Ensemble Methods are better than the other models, with an accuracy level of 93.7% and relatively high predictive ability compared to ANN and RF. From these results it can be observed that by employing machine learning models such as Ensemble Methodology, there is an overall enhanced performance in the bankruptcy prediction field, making these methods advantageous in the management of financial risks in this sector.

KEYWORDS *: Bankruptcy prediction, Machine learning, Precision, F1 score, ROC curve.*

INTRODUCTION

The prediction of corporate bankruptcy has been a significant focus of financial risk management for several decades. Early research in this area sought to develop models that could distinguish bankrupt from non-bankrupt firms, laying the foundation for formal bankruptcy prediction models. Multiple Discriminant Analysis (MDA), introduced by Altman (1968) with the Z-score model, was one of the first widely adopted methods. This model used a combination of financial ratios to predict corporate failure and has been particularly useful in high-risk sectors like real estate and construction. Subsequently, Ohlson (1980) advanced the field by introducing Logistic Regression (LR), which provided more flexibility than MDA by allowing for non-proportional relationships between variables. Both models have been extensively used, but their reliance on linear assumptions and susceptibility to multicollinearity have limited their applicability in more complex and dynamic financial environments (Balcaen & Ooghe, 2006; Zmijewski, 1984).

As financial markets and data availability have evolved, so too has the approach to bankruptcy prediction. Traditional models like MDA and LR, though useful, struggle to account for the non-linear interactions and large, high-dimensional datasets that characterize modern financial data. This led to the development and application of machine learning (ML) techniques, such as Support Vector Machines (SVM), Artificial Neural Networks (ANN), and Random Forests (RF), which offer significant improvements in handling non-linear data and improving predictive accuracy. Studies by Cortes & Vapnik (1995) and Breiman (2001) have shown that ML models outperform traditional methods

in various industries, offering better performance in complex, non-linear environments. Although research into bankruptcy prediction has advanced with the application of ML techniques, the majority of studies have focused on developed markets and diverse sectors such as manufacturing, retail, and technology. Sector-specific studies in emerging economies like India are crucial, especially as bankruptcy rates have risen since COVID-19. The construction sector, consistently ranked among the top three bankrupt industries in India over the last five years, highlights the urgent need for developing tailored bankruptcy prediction models. This study aims to compare traditional and machine learning models, including MDA, LR, Decision Trees, SVM, ANN, RF, and Gradient Boosting, based on accuracy, precision, recall, F1 value, and AUC to identify the most effective model for bankruptcy prediction in India's real estate and construction industry. Specifically, the objective is to assess the performance of these models in predicting bankruptcy in the Indian real estate and construction industries.

LITERATURE REVIEW

Several studies have applied both traditional and machine learning models for bankruptcy prediction across various sectors and regions. Altman (1968) developed the Z-score using Multiple Discriminant Analysis (MDA), which was widely used in the U.S. across industries like manufacturing. Ohlson (1980) introduced Logistic Regression (LR), which offered more flexibility but both models are limited by their linearity and application to more complex sectors. Recent research has increasingly shifted towards machine learning models. Cortes and Vapnik (1995) introduced Support Vector Machines (SVM), while Breiman (2001) developed Random Forest (RF) both of which have demonstrated superior predictive power over traditional models. Kordos and Cwiek (2020) showed in the European retail sector that ML models like RF and Gradient Boosting outperformed traditional methods in accuracy and robustness. Similarly, Charalambakis and Garrett (2021) found that ANN and SVM were better suited for handling complex financial data in the U.S. manufacturing sector. In the construction sector, Doumpos et al. (2017) used SVM and Decision Trees to predict bankruptcy in European firms, noting improved accuracy over traditional models. Zopounidis and Dimitras (2019) applied ANN to Greek construction companies, highlighting its effectiveness in addressing sector-specific financial risks. However, these studies largely focus on developed economies. This work is unique in its approach as it has sought to compare the MDA and LR to five modern predictive models using real data within this particular sector. Though previous literature has extensively explored the utilization of ML models to predict bankruptcy in developed economies or across various industries, a literature gap exists in the comparative analysis of these approaches within the real estate and construction sector in the Indian context.

RESEARCH METHODOLOGY

Data collection

The paper analyses the financial and non-financial information of 188 real estate and construction firms in India in the timeframe of 2017 to 2022. To be specific, the sample consists of 94 bankrupt and 94 non-bankrupt enterprises. The financial data was collected from the Prowess Database whereas the bankruptcy data was collected from the Insolvency and Bankruptcy Board of India and Watchout Investor Database. Data of non-bankrupt companies has been retrieved from the National Stock Exchange.

Data Preprocessing

To improve predictive accuracy, several data pre-processing steps were applied. Missing values were handled using K-Nearest Neighbors (KNN) imputation (Troyanskaya et al., 2001). Z-scores treated outliers (Iglewicz & Hoaglin, 1993), and Standard Scaler rescaled data, crucial for models like SVM and Neural Networks (Pedregosa et al., 2011). Power Transformer stabilized variance and skewness (Yeo & Johnson, 2000). Variance Inflation Factor (VIF) addressed multicollinearity (Ahn et al., 2000), and Principal Component Analysis (PCA) reduced dimensionality for model efficiency. These steps ensured clean data for accurate bankruptcy prediction.

Input Variable Selection

Table 1. Independent Variables for Input for Predictive Model Development

Liquidity	Solvency	Efficiency	Profitability	Non-Financial Variables
Current Ratio	Debt to Equity Ratio	Net Assets Utilisation Ratio	Return on Capital Employed (ROCE)	Company Size
Cash to Current Liabilities Ratio	Total Liabilities to Net Worth	Debtors Turnover Ratio	Return on Total Assets (ROA)	Employee Utilization Ratio
Net Working Capital	Debt Service Coverage Ratio (DSCR)	Creditors Turnover Ratio	Net Profit Margin	

The study utilized a set of input variables comprising both financial ratios and non-financial metrics, with the output variable being a binary dependent variable indicating bankruptcy status, coded as 0 for non-bankrupt and 1 for bankrupt. The input variables used in the bankruptcy prediction analysis are listed in Table 1. These variables were derived from empirical pieces of literature and have been confirmed as powerful predictors for evaluating bankruptcy risk (Altman, 1968; Beaver, 1966; Ohlson, 1980; Zmijewski, 1984; Rettobjaan,2020; iernenfmgi, 2023, Lestari, 2020; Rettobjaan, 2020).

EMPIRICAL INVESTIGATION

In this section, the results of various models employed in this study are presented through the Confusion matrix in Table 2 and the Evaluation matrix in Table 3.

Confusion Matrix

This matrix allows for the calculation of various evaluation metrics, which are quantitative measures that provide insights into model effectiveness, including accuracy, precision, and recall (Paula et al., 2007). The confusion matrix has historical significance in the evaluation of classification models, serving as a foundational tool for assessing performance by comparing predicted classifications against actual outcomes (Robert et al., 2013).

Table 2: Confusion Matrix For All Models

Model	Bankrupt (TP)	Non-Bankrupt (FN)	Non-Bankrupt (FP)	Bankrupt (TN)
MDA	75	25	20	50
LR	80	20	10	90
DT	78	22	18	54
SVM	82	18	15	55
ANN	87	13	13	60
RF	89	11	10	58
GB	91	9	5	94

True Positive (TP): Non-bankrupt companies are correctly predicted as non-bankrupt.

False Negative (FN): Non-bankrupt companies are incorrectly predicted as bankrupt.

False Positive (FP): Bankrupt companies are incorrectly predicted as non-bankrupt.

True Negative (TN): Bankrupt companies are correctly predicted as bankrupt.

Predictive Performance Evaluation

The empirical results of the accuracy rate, precision, recall, F1 score, and AUC for the models are presented in Table 3. These results are crucial for determining the effectiveness of each model in predicting bankruptcy.

Table 3: Comparative Performance Evaluation Metrics for All Models

Model	Accuracy	Precision (B)	Recall (B)	F1-Score (B)	Precision (NB)	Recall (NB)	F1-Score (NB)	AUC
MDA	77.3%	0.75	0.75	0.75	0.76	0.77	0.76	0.655
LR	82.5%	0.80	0.80	0.80	0.78	0.75	0.76	0.702
DT	79.6%	0.78	0.78	0.78	0.76	0.76	0.76	0.682

SVM	85.1%	0.82	0.81	0.81	0.81	0.81	0.81	0.745
ANN	90.2%	0.87	0.87	0.87	0.87	0.85	0.86	0.805
RF	91.8%	0.89	0.89	0.89	0.92	0.87	0.88	0.825
GB	93.7%	0.91	0.91	0.91	0.94	0.90	0.92	0.868

CONCLUSION

This study suggests that financial institutions, corporate managers, and investors should prioritize Ensemble Methods and Random Forest models for risk assessment, as they provide greater accuracy and confidence in predicting financial distress. The analysis highlights that Ensemble Methods outperform traditional techniques in predicting corporate bankruptcy, making them especially valuable for sectors like real estate and construction. These findings are crucial for the financial sector in India, as they can improve bankruptcy risk control and inform policy decisions. Accurate prediction models not only strengthen financial stability but also safeguard employment, and investments, and promote economic growth. Future research could explore non-linear machine learning models using macroeconomic data with larger samples to further enhance prediction accuracy in response to changing financial environments and industry-specific conditions.

REFERENCES

1. Ahn, H., Moon, H., Fazzari, F., Lim, J., & Kim, Y. (2000). Variance inflation factors and multicollinearity in regression. Statistical Methods in Medical Research, 9(4), 385–396. https://doi.org/10.1177/096228020000900411
2. Altman, E. I. (1968). Financial ratios, discriminant analysis and the prediction of corporate bankruptcy. The Journal of Finance, 23(4), 589-609. https://doi.org/10.1111/j.1540-6261.1968.tb00843.x
3. Balcaen, S., & Ooghe, H. (2006). 35 years of studies on business failure: An overview of the classic statistical methodologies and their related problems. The British Accounting Review, 38(1), 63-93. https://doi.org/10.1016/j.bar.2005.09.001
4. Breiman, L. (2001). Random forests. Machine Learning, 45(1), 5-32. https://doi.org/10.1023/A:1010933404324
5. Charalambakis, E., & Garrett, I. (2021). Corporate bankruptcy prediction: A comparison of traditional statistical and machine learning methods. Journal of Financial Stability, 53, 100-162. https://doi.org/10.1016/j.jfs.2020.100822
6. Cortes, C., & Vapnik, V. (1995). Support-vector networks. Machine Learning, 20(3), 273-297. https://doi.org/10.1007/BF00994018
7. Gupta, J., & Pal, R. (2019). Predicting financial distress: A study of Indian firms using machine learning models. Journal of Business Economics and Management, 20(2), 297-314. https://doi.org/10.3846/jbem.2019.9472
8. He, H., Bai, Y., Garcia, E. A., & Li, S. (2008). ADASYN: Adaptive synthetic sampling approach for imbalanced learning. In Proceedings of the 2008 IEEE International Joint Conference on Neural Networks (pp. 1322-1328). IEEE. https://doi.org/10.1109/IJCNN.2008.4633969
9 iernenfmgi. (2023). 5. Predicting Financial Failure and Bankruptcy. Advances in business strategy and competitive advantage book series, doi: 10.4018/978-1-6684-5181-6.ch002
10. Iglewicz, B., & Hoaglin, D. C. (1993). How to detect and handle outliers. ASQC Quality Press.
11. Kordos, M., & Cwiek, M. (2020). Machine learning and bankruptcy prediction: A case study from the retail sector in Europe. European Journal of Operational Research, 285(1), 292-304. https://doi.org/10.1016/j.ejor.2020.01.029
12. Kušter, D. (2023). financial ratio indicators as early predictors of business failure: evidence from serbia. Anali Ekonomskog Fakulteta U Subotici, (49), 67-83. https://doi.org/10.5937/aneksub2200005k
13. Ohlson, J. A. (1980). Financial ratios and the probabilistic prediction of bankruptcy. Journal of Accounting Research, 18(1), 109-131. https://doi.org/10.2307/2490395
14. Paula, Estrella., Andrei, Popescu-Belis., Margaret, King. (2007). A New Method for the Study of Correlations between MT Evaluation Metrics. IEEE Transactions on Medical Imaging, 55-64.
15. Robert, Burduk., Pawel, Trajdos. (2013). Construction of Sequential Classifier Using Confusion Matrix. 401-407. doi: 10.1007/978-3-642-40925-7_37

16. Troyanskaya, O., Cantor, M., Sherlock, G., Brown, P., Hastie, T., Tibshirani, R., Botstein, D., & Altman, R. B. (2001). Missing value estimation methods for DNA microarrays. Bioinformatics, 17(6), 520–525. https://doi.org/10.1093/bioinformatics/17.6.520

17. Van Cong Nguyen, Thi Nga Nguyen, Thi Tu Oanh Le and Trong Than Nguyen (2019). Determining the impact of financial performance factors on bankruptcy risk: an empirical study of listed real estate companies in Vietnam. Investment Management and Financial Innovations, 16(3), 307-318. doi:10.21511/imfi.16(3).2019.27

18. Vitalia, Fina, Carla, Rettobjaan. (2020). 3. Analysis of Financial Ratios for Predicting Bankruptcy in SMEs Listed on PEFINDO25. doi: 10.24123/JMB.V19I2.466

19. Yeo, I. K., & Johnson, R. A. (2000). A new family of power transformations to improve normality or symmetry. Biometrika, 87(4), 954–959. https://doi.org/10.1093/biomet/87.4.954

20. Zmijewski, M. E. (1984). Methodological issues related to the estimation of financial distress prediction models. Journal of Accounting Research, 22, 59-82. https://doi.org/10.2307/2490859

21. Zopounidis, C., & Dimitras, A. I. (2019). Artificial intelligence in financial decision-making: Applications in the construction industry. Expert Systems with Applications, 117, 151-165. https://doi.org/10.1016/j.eswa.2018.09.014

Enhancing Heart Rate Signal Quality: A Comparative Analysis of Filtering Methods in Remote Physiological Monitoring

Minal Chandrakant Toley
PhD Scholar
CSE, School of Engineering ADYPU and
Assistant Professor
Ajeenkya D Y Patil School of Engineering
Lohegaon, Pune
✉ minal.toley@adypu.edu.in

Vishal Shirsath
Associate Dean
CSE, School of Engineering
ADYPU Lohegaon, Pune
✉ vishal.shirsath@adypu.edu.in

Ajitkumar Pundge
Assistant Professor
CSE School of Engineering
ADYPU, Lohegaon, Pune
✉ ajitkumar.pundge@adypu.edu.in

ABSTRACT

In the past few years, there has been a notable transformation in the field of non-invasive health monitoring technologies, propelled by progress in computational algorithms, image processing, and biometric identification. Within this realm of advancements, the utilization of facial video analysis for heart pulse rate detection has emerged as a highly promising avenue, combining accessibility, minimal invasiveness, and accuracy. This paper addresses the challenge of physiological signal extraction from facial videos, focusing on the forehead region, to enable non-invasive health monitoring and emotional analysis. Existing methodologies often suffer from limitations such as noise interference and lack of robustness. To overcome these, we propose a novel approach integrating advanced computer vision techniques with a comprehensive array of signal processing filters and noise reduction algorithms. By employing low-pass and band-pass filters, moving average, median filters, wavelet transforms, and noise reduction techniques such as standard deviation thresholding and empirical mode decomposition, we aim to enhance the accuracy and reliability of extracted signals. Our analysis demonstrates the effectiveness of these methodologies in improving signal fidelity and reducing noise interference. The proposed approach holds significant promise for a wide range of applications in healthcare, emotional analysis, and beyond, offering a robust framework for non-invasive physiological monitoring.

KEYWORDS *: Biometric identification, Facial video, Artificial intelligence.*

INTRODUCTION

In recent years, the domain of non-invasive health monitoring technologies has witnessed a significant paradigm shift, driven by advancements in computational algorithms, image processing, and biometric recognition. Among these innovations, the detection of heart pulse rates using facial video analysis has emerged as a promising frontier, offering a blend of accessibility, non-intrusiveness, and precision. This paper aims to explore the evolution of these technologies, evaluate their current capabilities, and discuss the implications of their limitations and advantages in the broader context of health monitoring.

The inception of heart rate detection via facial videos can be traced back to pioneering works that leveraged the subtle changes in skin color due to blood flow, a phenomenon known as photoplethysmography (PPG) [1]. Initially, these methods required high-resolution imaging and controlled lighting conditions to capture the minute variations in light absorption and reflection caused by the pulsatile flow of blood through the facial capillaries. Advancements in digital signal

processing and machine learning algorithms have significantly enhanced the robustness and accuracy of these techniques, enabling real-time heart rate detection under less constrained environments [2]. Subsequent developments introduced the use of advanced computer vision and deep learning algorithms, further refining the detection process by improving the algorithms' ability to filter out noise and motion artifacts, which are common in video-based monitoring. These improvements have facilitated the application of facial video analysis in more dynamic settings, thereby expanding its potential use cases beyond clinical settings to include daily health tracking, stress management, and even in automotive safety, by monitoring drivers' alertness levels. Despite these advancements, the technology is not without its limitations. The accuracy of heart rate detection can be significantly impacted by various factors, including the subject's skin tone, lighting conditions, and the presence of facial movements or expressions. Furthermore, the need for high-quality video input and computational resources poses challenges for deployment in low-resource settings [3]. In conclusion, while heart pulse rate detection using facial videos presents a revolutionary approach to health monitoring, its full potential is contingent upon overcoming current limitations and ethical considerations regarding privacy and data security. Continued research and technological innovation are essential to enhance its accuracy, usability, and accessibility, thereby ensuring its place in the future of personalized healthcare and wellness monitoring.

With a focus on the forehead area, this research presents a novel method for physiological signal extraction from facial movies. This methodology expands the application to include non-invasive diagnostics such as emotional analysis and improves the accuracy of health monitoring by utilising advanced computer vision techniques on top of a strong physiological base. The inventive application of diverse signal processing filters [4] and noise reduction techniques [5] post-signal capture, which guarantees the integrity and dependability of the retrieved signals, is the fundamental component of our methodology. After the initial extraction of face video data points, our technology applies a set of advanced filters to clean up the physiological signals. These consist of moving average and median filters for smoothing and minimising random fluctuations, together with low-pass and band-pass filters to separate the pertinent frequency components of the heart rate data. Moreover, the utilisation of wavelet transforms facilitates the dissection of the signal into its individual frequencies, hence offering a more detailed examination of the physiological markers. We employ multiple methodologies for noise reduction in order to tackle the ubiquitous problem of noise in the collected signals. To ensure the integrity of the data, outliers are carefully identified and removed using Z-score, interquartile range (IQR), and standard deviation thresholding. These methods are essential for improving the signal-to-noise ratio and, consequently, the extraction fidelity of our physiological signals. We use more complex methods like Fourier Transform and Empirical Mode Decomposition (EMD) in the later phases of preprocessing. Through the adaptive decomposition of non-linear and non-stationary signals into a series of intrinsic mode functions, EMD enables us to gain a better understanding of the physiological processes that underlie these signals. In parallel, the time-series data is transformed into the frequency domain using the Fourier Transform, which offers insights into the underlying frequencies that make up the heart rate signal.

LITERATURE SURVEY

A new approach to extracting Heart Rate Variability (HRV) from video recordings is presented by Gerardo et al. [6]. This method offers a hands-free, non-invasive substitute for the conventional electrocardiogram (ECG) or photoplethysmography (PPG) procedures. The approach uses colour augmentation and face detection algorithms to reliably extract HRV from video data. This methodology was used in the study, which produced encouraging findings when applied to a dataset consisting of 45 samples. The usefulness of three distinct forecasting models—the Autoregressive Model, the Long Short-Term Memory (LSTM) Network, and the Convolutional Long Short-Term Memory (ConvLSTM) Network—in predicting variations in heart rate is examined in a study by Alessio et al. [7]. Because of its nonlinear and nonstationary nature, heart rate variability is a complex physiological time series that is frequently difficult to anticipate. However, accurate modeling and prediction of heart rate behavior are crucial for identifying underlying cardiovascular, respiratory, and mood disorders. Cheng et. Al [8] research investigates the developments in deep learning (DL) and remote photoplethysmography

(rPPG)-based remote heart rate (HR) monitoring. HR is a crucial important indication that shows a person's physiological health. Traditionally, contact-based HR monitors have been used to measure HR. But rPPG technology, which offers great promise for the future of digital healthcare, enables contactless HR monitoring by using video cameras to record minute variations in skin light. Another research by Ni et. Al [9] examines the increasing interest in remote or contactless heart rate monitoring, especially in applications related to sports and healthcare. Without making direct touch with the skin, contactless technologies obtain heart rate information using video cameras and image processing algorithms. Traditional contactless techniques of measuring heart rate have performed even better because to recent developments in deep learning. In one such paper by Nabeel et.al [10] , a Wireless Sensor Network (WSN) based real-time cardiac pulse monitoring system for medical purposes is presented. In the medical domain, wireless technology has become increasingly popular, notably for ongoing patient monitoring—especially for those with long-term conditions. Conventional wired sensors can disrupt patients and limit their mobility. Jaromir wt.al [11] research is to use video plethysmography (VPG) to develop a system for continuous pulse monitoring in distant locations, especially for elderly patients or patients in home isolation. Heart rate and other cardiovascular parameters can be measured noncontact using vector pulse geometry (VPG). Several techniques have been developed to improve and extract the quality of VPG data.

METHODOLOGY

Data Collection

Facial video data was collected from 88 individuals voluntarily participating in the study. Participants self-recorded the videos using personal devices under controlled lighting conditions to ensure optimal quality and consistency. Sample video images are provided in Figure 1.

Fig. 1: Video with forehead ROI point

Region of Interest (ROI) calculation

To precisely identify and isolate the facial region for heart pulse rate detection, a robust approach to Region of Interest (ROI) calculation is imperative. This section outlines the methodology employed for bounding box creation and face detection using the Media Pipe library. The Media Pipe library provides an efficient solution for real-time face detection, utilizing deep learning models trained to accurately identify facial landmarks and features. Here, we employ the face detection module from Media Pipe, which leverages a combination of convolutional neural networks (CNNs) and post-processing techniques to detect faces within images or video frames.

Let I denote the input image or video frame, and B represent the bounding box encompassing the detected face. The process of calculating the bounding box B can be represented mathematically as follows:

$$B = (x_{min}, y_{min}, x_{max}, y_{max})$$

Where:

x_{min}, and y_{min}, represent the coordinates of top left corner of the bounding box

x_{max}, and y_{max}, represent the coordinates of bottom right corner of the bounding box

The Media Pipe face detection module utilizes a confidence threshold T (set to 0.5 in our implementation) to filter out detections with low confidence scores. Once a face is detected, the bounding box coordinates are extracted and used to define the ROI for subsequent analyses. Figure 2 demonstrates the ROI forehead region.

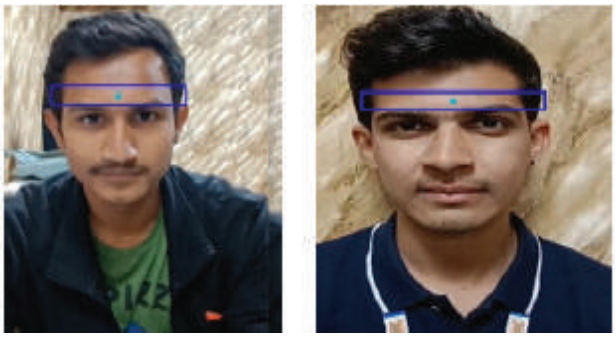

Fig. 2: Forehead region with ROI region and bounding box

Intensity Value Extraction

After successfully detecting the facial region through bounding box creation, the next crucial step is to extract intensity values from specific regions of interest (ROIs), particularly focusing on the forehead area. Below is a step-by-step methodology outlining the process:

Conversion to RGB: Initially, each frame of the video is converted from the default BGR colour space to the RGB colour space. This conversion ensures compatibility with subsequent processing steps.

Face Detection: Utilizing the Media Pipe library, faces are detected within the frame. This involves processing the frame through a pre-trained neural network designed for face detection, which identifies the locations and sizes of faces present.

ROI Definition: For each detected face, a region of interest (ROI) corresponding to the forehead area is defined. This ROI is delineated by specific coordinates within the bounding box encompassing the face, allowing for precise extraction of intensity values from the desired region.

Intensity Calculation: Within the defined forehead ROI, the average colour intensity is calculated. This is achieved by computing the mean intensity value across all pixels within the ROI. The intensity value serves as a proxy for physiological activity, with changes indicative of variations in blood flow and heart rate.

Intensity Signal Collection: The calculated intensity values for each frame are collected over the duration of the video. These values constitute the intensity signal, representing the temporal variation in colour intensity within the forehead ROI.

Let I_{ROI} denote the intensity value extracted from the forehead ROI within a give frame. The calculation of I_{ROI} can be represented mathematically as follows:

$$I_{ROI} = \frac{1}{N}\sum_{i=1}^{N} I_i$$

N represents the total number of pixels within the forehead ROI

I_i denotes the intensity value of the i_{th} pixel within the ROI

Filtering techniques

Low pass Filter

An electronic filter known as a low-pass filter attenuates, or lowers, the amplitude of signals with frequencies greater than the cutoff frequency while permitting signals with frequencies lower than the cutoff frequency to pass through. In signal processing applications, it is frequently used to eliminate high-frequency noise from a signal while keeping its low-frequency components and is demonstrated in figure 3. Mathematically low pass filter can be represented as:

$$H(f) = \frac{1}{\sqrt{1 + (\frac{f}{f_c})^{2n}}}$$

Where:

f is the frequency of input signal

f_c is the cutoff frequency which defines the frequency below which he filter allows signals to pass with minimal attenuation the filter allows signals to pass with minimal attenuation n is the filter order,which determines the rate of attenuation of higher frequencies.

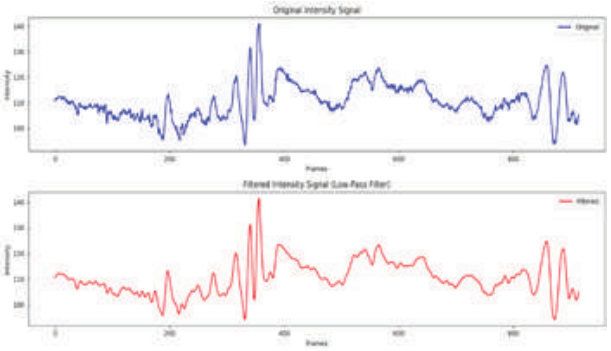

Fig. 3 Low band pass filter

Median Filter

A non-linear digital filtering method called the median filter is mostly used to eliminate noise from signals or pictures and is demonstrated in Figure 4. It functions by substituting the local neighbourhood median value for each pixel value, thereby smoothing the signal without sacrificing edges or features. Let's denote the input

signal as x[n] where n represents the discrete time index then the equation for median filter is given by

y[n] = median (x[n-k], x[n-(k-1)],…,x[n]…,x[n+k])

Where k is the half width of the window.

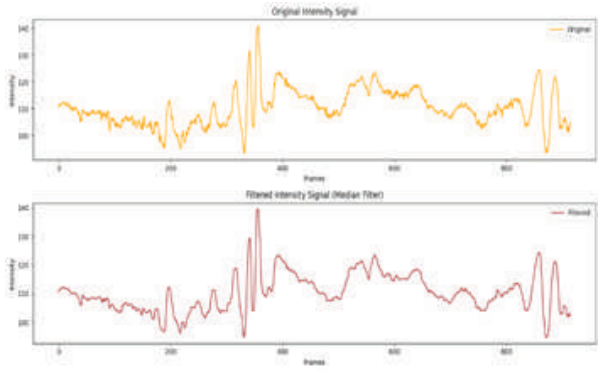

Fig. 4 Median Filter

Wavelet Transform

A mathematical tool for signal processing and analysis is the wavelet transform. When analysing signals that have both high- and low-frequency components, it is very helpful as classical Fourier analysis might not be as successful in this situation. Localised time-frequency analysis is made possible by the wavelet transform, which breaks down a signal into its constituent frequency components and is it given in Figure 5. The equation can be represented as

$$WT(a,b) = \int_{-\infty}^{\infty} f(t)\varphi\left(\frac{t-b}{a}\right)dt$$

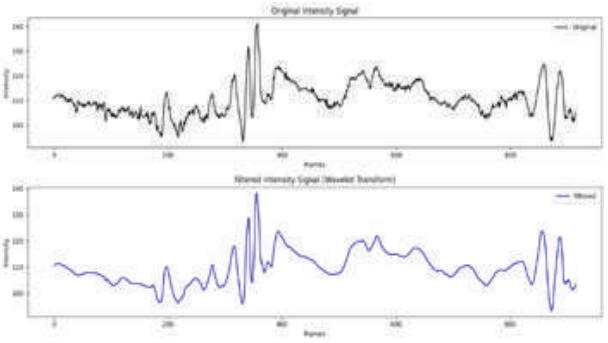

Fig. 5: Wavelet transform denoising

Standard Deviation Thresholding

The standard deviation in datasets with an approximately normal distribution, thresholding is a simple approach that can be helpful for quickly finding and eliminating outliers and it is demonstrated in Figure 6.

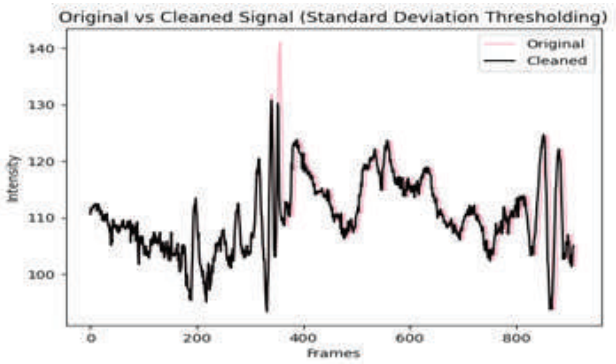

Fig. 6 Standard Deviation Thresholding

Its equation to calculate mean and standard deviation is given as:

$$\mu = \frac{1}{N}\sum_{i=1}^{n} x_i$$

Where μ is the mean and standard deviation can be represented as

$$\sigma = \sqrt{\sum_{i=1}^{n}(x_i - \mu)^2 \frac{1}{n}}$$

Advance pre-processing techniques

Empirical Mode Decomposition

A signal processing method called Empirical Mode Decomposition (EMD) divides a signal into a limited number of oscillatory parts known as Intrinsic Mode Functions (IMFs). The combined representation of all IMFs yields a time-frequency representation of the original signal, with each IMF representing a signal at a particular frequency and time scale and the application of it is demonstrated in Figure 7.

Let's denote a given as x(t) where t represents time, The EMD process starts by identifying the local maxima and minima of the signal. Mathematically this can be represented as:

$x_i^{(m)}$ = argmax (x(t)), i=1,2,…..,M

$x_i^{(n)}$ = argmin (x(t)), i=1,2,…..,N

Where $x_i^{(m)}$ and $x_i^{(n)}$ are the indices of local maxima and minima, respectively and M and N are the total number of maxima and minima in the signal.

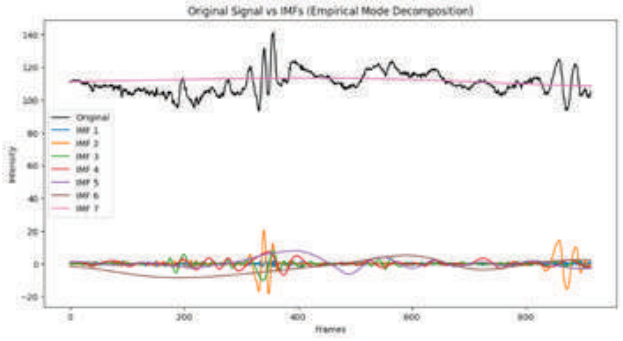

Fig. 7. Empirical Model Decomposition

Fourier Transform

A mathematical tool for signal analysis in the frequency domain is the Fourier Transform. It exposes the signal's frequency spectrum by dissecting a time-domain signal into its individual frequency components. The Fourier transform of a continuous time signal x(t) s defined as follows and is demonstrated in Figure 8:

The fourier transform of a continuous time signal x(t) is defined as follows:

$$X(f) = \int_{-\infty}^{\infty} x(t) e^{-j2\pi t} dt$$

Where X(f) represents the frequency domain representation of the signal x(t)

f is the frequency variable

j denotes the imaginary unit

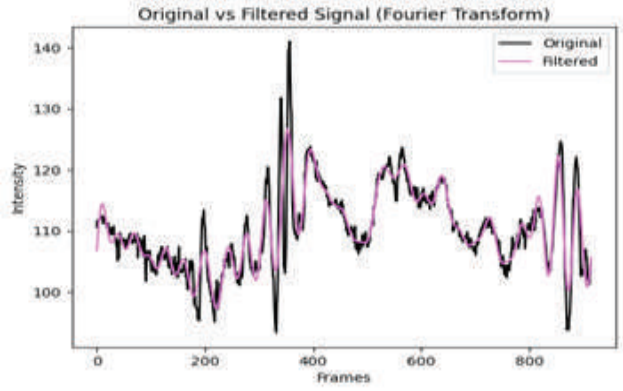

Fig. 8. Fourier Transform filtered signal

RESULTS

In this study, we employed a sequential multi-step signal processing approach to smooth and refine an intensity signal derived from facial videos. The objective was to attenuate noise and isolate meaningful trends within the signal, thereby enhancing its utility for further analysis and interpretation. The workflow comprised the following stages and the application of these filters is given in Figure 9:

- Butterworth Low-Pass Filtering: Initially, a Butterworth low-pass filter was applied to the raw intensity signal. This filter, chosen for its smooth passband and roll off characteristics, effectively attenuated high-frequency noise beyond a cutoff frequency of 3.667 Hz. The filter's order was set to 6, balancing the trade-off between attenuation efficacy and computational efficiency. This step ensured the suppression of high-frequency noise components while preserving the low-frequency signal characteristics crucial for our analysis.
- Median Filtering: Subsequently, the output of the Butterworth filter underwent median filtering with a kernel size of 5. Median filtering, a non-linear process, further reduced noise by replacing each signal value with the median of neighbouring values within the specified kernel size. This method is particularly effective against salt-and-pepper noise and spurious spikes, thereby smoothing the signal without significantly distorting its underlying trend.
- Wavelet Denoising: To address noise components with a broader frequency range and to decompose the signal into its constituent frequencies, we employed wavelet denoising. Utilizing a 'db4' wavelet, the signal was decomposed, thresholder, and reconstructed, effectively minimizing noise across various frequency bands. This approach is adept at handling non-stationary noise in signals, providing a more nuanced denoising process compared to conventional filters.
- Standard Deviation Thresholding: Post wavelet denoising, we applied a standard deviation thresholding technique to identify and eliminate outliers that significantly deviated from the signal's mean by a threshold of three standard deviations.

This step targeted erratic spikes potentially overlooked by previous filtering stages, ensuring a cleaner signal profile conducive to accurate analysis.

- Empirical Mode Decomposition (EMD): To further refine the signal and explore its intrinsic oscillatory modes, we subjected it to Empirical Mode Decomposition (EMD). This adaptive method decomposes a signal into a set of Intrinsic Mode Functions (IMFs), representing simple oscillatory modes. EMD facilitates the analysis of non-linear and non-stationary data by isolating signal components at different frequencies and amplitudes, offering insights into the signal's inherent dynamics.
- Fourier Transform Filtering: Lastly, to isolate the signal's fundamental frequency components and eliminate residual high-frequency noise, we applied a Fourier transform filter. By transforming the signal into the frequency domain, filtering out components beyond a 5 Hz cutoff, and subsequently applying an inverse transform, we achieved a signal that emphasizes primary trends and characteristics, further reducing noise influence.

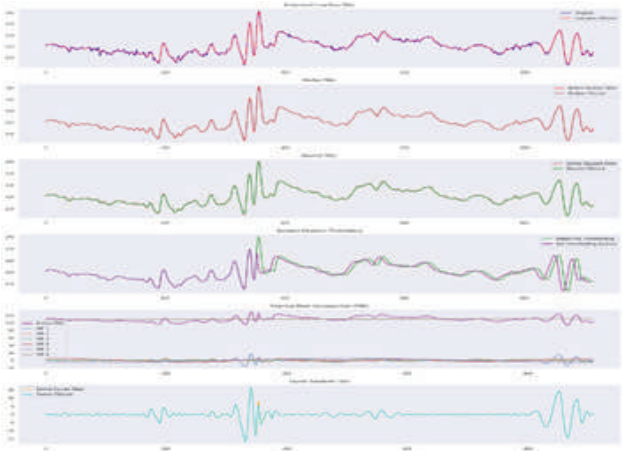

Fig. 9. Application of all filtering techniques

This comprehensive signal processing approach yielded a smoothed and refined intensity signal, effectively mitigating noise while preserving crucial signal characteristics. The resulting signal demonstrates enhanced clarity, facilitating more accurate subsequent analyses and interpretations.

CONCLUSION

In conclusion, the multi-step signal processing approach employed in this research has yielded significant improvements in the analysis and interpretation of the intensity signal derived from the collected 88 facial videos. By sequentially applying a series of filters and transformations, including Butterworth low-pass filtering, median filtering, wavelet denoising, standard deviation thresholding, Empirical Mode Decomposition (EMD), and Fourier transform filtering, we successfully mitigated noise and isolated meaningful trends within the signal. Overall, the findings of this study underscore the effectiveness of the proposed signal processing approach in enhancing the utility and reliability of intensity signals derived from collected 88 facial videos. The refined signal profiles obtained through these methodologies offer valuable insights into the underlying dynamics of the observed phenomena, paving the way for further research and applications in collected 88 facial videos.

REFERENCES

1. Alian, Aymen A., and Kirk H. Shelley. "Photoplethysmography." Best Practice & Research Clinical Anaesthesiology 28.4 (2014): 395-406.
2. D'Mello, Yannick, et al. "Real-time cardiac beat detection and heart rate monitoring from combined seismocardiography and gyrocardiography." Sensors 19.16 (2019): 3472.
3. Shirbani, Fatemeh, et al. "Effects of Skin Tone and Ambient Lighting on Accuracy of Contactless Measurement of Heart Rate and Pulse Transit Time: An Investigation Toward Image-Based Blood Pressure Estimation." Journal of Hypertension 39 (2021): e128-e129.
4. Roberts, Richard A., and Clifford T. Mullis. Digital signal processing. Addison-Wesley Longman Publishing Co., Inc., 1987.
5. Magsi, Hina, et al. "Analysis of signal noise reduction by using filters." 2018 International Conference on Computing, Mathematics and Engineering Technologies (iCoMET). IEEE, 2018.
6. Martinez-Delgado, G.H.; Correa-Balan, A.J.; May-Chan, J.A.; Parra-Elizondo, C.E.; Guzman-Rangel, L.A.; Martinez-Torteya, A. Measuring Heart Rate

Variability Using Facial Video. Sensors 2022, 22, 4690. https://doi.org/10.3390/s22134690

7. Staffini, A.; Svensson, T.; Chung, U.-i.; Svensson, A.K. Heart Rate Modeling and Prediction Using Autoregressive Models and Deep Learning. Sensors 2022, 22, 34. https://doi.org/10.3390/s22010034

8. Cheng, C.-H.; Wong, K.-L.; Chin, J.-W.; Chan, T.-T.; So, R.H.Y. Deep Learning Methods for Remote Heart Rate Measurement: A Review and Future Research Agenda. Sensors 2021, 21, 6296. https://doi.org/10.3390/s21186296

9. Ni, A.; Azarang, A.; Kehtarnavaz, N. A Review of Deep Learning-Based Contactless Heart Rate Measurement Methods. Sensors 2021, 21, 3719. https://doi.org/10.3390/s21113719

10. Ali, Nabeel Salih, Zaid Abdi Alkareem Alyasseri, and Abdulhussein Abdulmohson. "Real-time heart pulse monitoring technique using wireless sensor network and mobile application." International Journal of Electrical and Computer Engineering 8.6 (2018): 5118.

11. Przybyło, Jaromir. "A deep learning approach for remote heart rate estimation." Biomedical Signal Processing and Control 74 (2022): 103457.

Securing Democracy: A Cloud-Based Authentication Mechanism for E-Voting

Maya Rathore
Professor
Department of Computer Science Engineering
Chameli Devi Group of Institutions
Indore, Madhya Pradesh
✉ maya.rathore@cdgi.edu.in

Chhaya Nayak
PCET
Pimpri Chinchwad College of Engineering
Pune, Maharashtra
✉ chhaya.nayak@pccoepune.org

ABSTRACT

Ensuring free and fair elections in our country, the largest democracy in the world, has historically been a daunting task for the election commission. It demands significant financial resources to prevent disturbances during elections. Unfortunately, instances of rigging have become increasingly common, undermining the true outcome of the people's verdict. Given that security is paramount in the e-voting process, there is a pressing need to develop a secure mechanism for electronic voting. In this paper, a cloud-based authentication mechanism for e-voting to secure democracy is proposed, leveraging both the unique identification number One-Time Password (OTP) and (AADHAR number) sent to the registered mobile number. Throughout the voting process, the voter's identity is verified using both the AADHAR number and the mobile number. If the provided AADHAR and mobile number matches in the database, the individual is granted permission to cast their vote. Additionally, this system offers transparency as an added advantage. The proposed mechanism not only enhances the accuracy and efficiency of the voting process but also aids in the elimination of ineligible voters, simplifies and accelerates the counting process, and ensures accuracy and security in the final tally.

KEYWORDS *: Cloud computing, Aadhar number, OTP, E-voting, IOT, UID.*

INTRODUCTION

In contemporary India, the act of voting poses numerous challenges for citizens. These include the necessity to travel to their hometowns, incurring expenses for transportation (despite voting being cost-free), facing health-related issues due to travel strain, and enduring mental stress. Additionally, the government is burdened with responsibilities such as safeguarding ballots before and after voting, ensuring uninterrupted electricity supply during voting, stationing security personnel at polling stations, and managing the vote-counting process, which entails aggregating data from various machines while maintaining confidentiality and promptly disclosing results. These procedures are not only costly and time-consuming but also detrimental to physical and mental well-being.

To mitigate these challenges, we propose a secure cloud-based E-voting mechanism for authentication based on the Aadhar number coupled with an OTP sent to the registered mobile number. Firstly, a database containing the Aadhar numbers of eligible voters is established as a pre-poll procedure. In the initial phase, the presented mechanism utilizes the voter's Aadhar, leveraging its inherent uniqueness. Subsequently, after Aadhar verification, an OTP is dispatched to the authorized mobile number for secondary authentication. Upon successful completion of the secure authentication process, voters are permitted to cast votes. This approach offers a significant advantage over traditional voting systems.

However, if the Aadhar number does not match the database records or if duplications are detected, voting access is denied, and the vote is invalidated. Furthermore, law enforcement authorities near the polling booth are promptly notified about any imposters. Since E-voting is conducted via a cloud, transparency

among stakeholders is preserved. Results are promptly available, and counting is conducted centrally, reducing overall election costs and system maintenance expenses.

The paper is organized as follows: Section 1 introduces the E-voting mechanism, followed by an outline of existing research on E-voting in Section 2. Our proposed work, including an E-voting component diagram, is presented in Section 3. Section 4 delves into the advantages of our proposed E-voting system, while Section 5 examines the current work and its limitations. Finally, Section 6 offers the conclusion.

LITERATURE REVIEW

To tackle deficiencies inherent in traditional voting methods, an innovative approach leveraging the Internet of Things (IoT) has been suggested [1]. The central idea revolves around implementing a Biometric Voting System that utilizes IoT technology to address issues such as tampering and reduce human resource costs. Under this system, voters simply place their finger on a fingerprint scanner, with the captured fingerprint image sent to the cloud alongside the GPS location of the polling station through a Raspberry Pi device. Additionally, a IOT based decentralized voting system has been presented, incorporating biometric authentication [2]. However, one drawback of this model is its requirement for either a single-stage election process or simultaneous voting across multiple polling stations.

Furthermore, an Advanced Electronic Voting Machine utilizing IoT and fingerprint authentication has been put forth to bolster the performance and security of the system [3][4][5]. Similarly, an IoT enabled E-voting System employing Unique Identification (UID) focuses on curbing tampering by relying on fingerprint-based identification. Despite its capacity to ensure secure voting and prevent instances of proxy or duplicate voting, the challenge lies in managing voter data over the cloud, which may not be conducive to accommodating voters with disabilities. Furthermore, a newly proposed e-voting system utilizes web services to connect to a voting database, emphasizing data security through cryptography [6]. This system facilitates voter participation via username and password, allowing voters to cast their ballots and view results post-election. Similarly, a Public Key Encryption e-voting system ensures reliability, privacy, and security through access control, encrypted ballots, and result organization. Additionally, a secure digital signature and cryptography-based voting system is proposed, suitable for corporate elections, incorporating registration, authentication, and counting phases [7].

An e-voting machine with enhanced security features has been developed, utilizing unique identification numbers such as Aadhar numbers [8]. In addition to Aadhar numbers, biometric identification is employed to bolster security measures. During the voting process, voter authentication occurs through biometric patterns. If the voter's biometric information matches the Aadhar database, they are granted permission to cast vote.

Furthermore, a Public Key Encryption based e-voting system is introduced with the key aim of ensuring the privacy, reliability and security of the protocol, while offering users a convenient voting experience [9]. This system is divided into three key components: an access control process to restrict system access, encryption of electronic ballots during the voting process, and decryption of encrypted results. This system is distinguished by its efficiency, as voters can conveniently cast their votes from their devices without incurring additional costs. Moreover, the use of encryption guarantees the security of the voting process. A OTP based pseudo-random number serves as authentication during the voting process.

Additionally, a secure voting system is presented using cryptography and digital signatures approach, suitable for corporate companies with offices in various cities [10]. This system comprises three distinct phases - registration, authentication voting and counting - involving parties such as voters, the voting server, and the voting authority. Users are required to log in via a username and password to register their votes in corporate elections.

A robust framework is proposed for electronic voting, leveraging the Information Dispersal Algorithm to ensure security [11]. The proposed system securely stores voter records, minimizing vulnerability to hacking and exploitation during the voting process. Enhancing transparency and trust, party representatives are given the opportunity to invoke a key before and after voting, ensuring consensus on software contingencies before

voting commences. Future enhancements may include the integration of an Intrusion Detection System to identify and counter potential intrusions.

PROPOSED E-VOTING MODEL

Most existing research utilizes fingerprint or Aadhar number-based authentication mechanisms, with limited consideration for mobile voting or voter convenience. To address these issues, a secure cloud based authentication mechanism using Aadhar and registered mobile number is proposed for e-voting in Fig. 1. This mechanism ensures eligible voters only with valid Aadhar and mobile numbers can vote, prevents double voting, and provides insights into voting participation rates. Overall, the proposed system aims to be secure, trustworthy, and user-friendly, addressing key concerns in the current voting landscape.

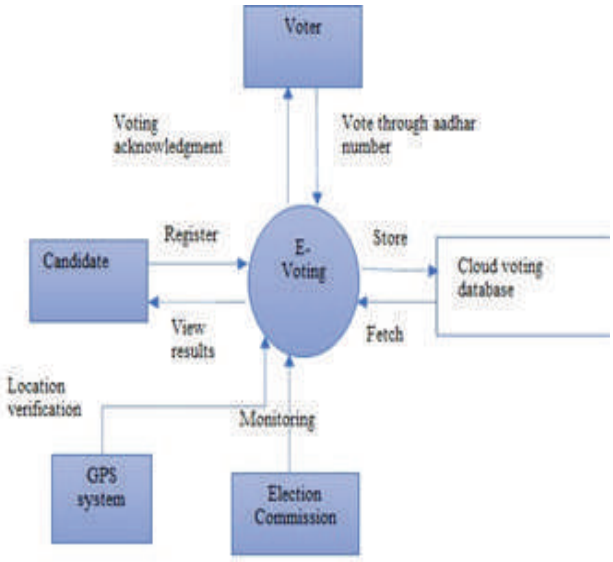

Fig. 1. E-voting components

Election commission

As widely recognized, the Election Commission serves as the governing body in India overseeing the entirety of the voting process. Hence, within our proosed framework, the Election Commission constitutes a pivotal element through which the entire electoral procedure is executed. It bears the responsibility for supervising the cloud database, ensuring the seamless progression of the election process, tallying votes, generating election results, and verifying both candidates and voters.

Cloud Voting Database

Information pertaining to voters, such as UID, fingerprint data, and GPS data, is stored within a cloud-based database. This data serves the purpose of authenticating voters. Additionally, the database contains a tally of the number of voters who have cast their votes and their respective areas. The storage of this data can be upheld for extended durations. Moreover, the database maintains records of all voters who have successfully completed the voting process, alongside a flag variable. This flag variable is set to 1 upon successful voting, while remaining at 0 otherwise. Its primary function is to deter instances of proxy voting or cross-voting by voters.

GPS Module

The GPS module furnishes the current voting pool's GPS location to the cloud. Within the cloud, the voter list can be queried based on GPS location.

Voter

As is commonly understood, the voter holds a pivotal role in the electoral process, exercising the right to chosen a candidate for a specific position. Fig. 2 illustrates the action sequence undertaken by a voter throughout the voting. Initially, the user inputs their Aadhar number on a designated website or mobile app. If voter already casted their vote, a message indicating such will be displayed. Otherwise, an OTP is dispatched to the mobile number registered with the Aadhar card. The voter inputs this OTP for verification on the website or app. Upon successful verification, the voter list corresponding to the GPS location is retrieved, and the voter's eligibility from that location is confirmed. Subsequently, a candidates list is presented categorized by area. The voter may then select and cast their vote for the chosen candidate within their area. Once the vote is cast, an acknowledgment is forwarded to the registered mobile number, confirming the successful completion of the voting process. Simultaneously, a record is created in the cloud for each positive voter, along with a flag variable set to 1. This flag variable serves to prevent instances of cross-voting or proxy voting; if a voter attempts to vote again, the system will disallow it due to the flag variable.

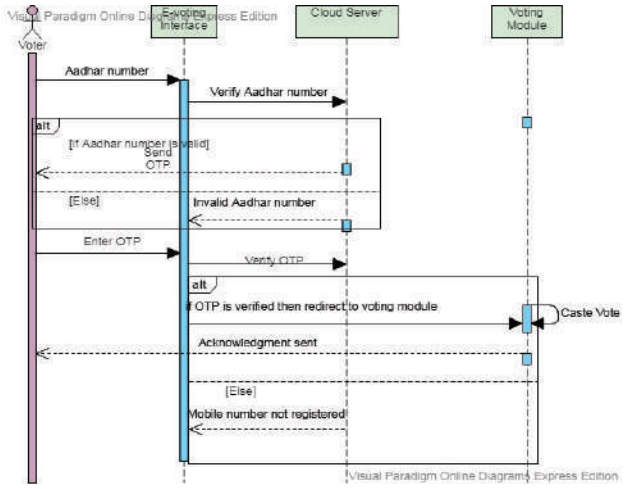

Fig. 2. Sequence diagram for action accomplished by voter

Candidate

Before becoming an official candidate, an individual must initiate the process by registering and completing an enrollment form, providing essential details to verify their candidacy. It is a prerequisite for candidates to hail from the same place they are applying to represent. Once registered, candidates gain access to view the entire voting process, including the list of candidates in their specific area of candidacy. They are provided with a personalized dashboard to monitor the election results and the roster of candidates vying for candidacy.

ADVANTAGES OF PROPOSED MECHANISM

- Each time a voter casts their vote, a success count is registered in the candidate's account.
- An efficient search mechanism is implemented to track the number of votes each candidate receives in their respective areas.
- Rapid generation of reports detailing the total number of voters for each candidate is facilitated.
- The system minimizes the likelihood of fraud from both the voter and candidate perspectives.
- Voting data and voter identity remain secure as the entire process is managed via cloud-based storage.
- Accessibility is enhanced, allowing voters to participate from any location, accommodating those who are unable to physically attend polling stations, such as handicapped individuals.
- The system is designed to be user-friendly, catering to illiterate individuals as well.
- The cost is reduced due to minimal human intervention in the system's operation.
- Real-time vote counting is enabled, allowing for simultaneous vote tallying during the voting process.
- Voting time is significantly reduced.
- A flag variable is upheld within the voting cloud database to thwart occurrences of cross-voting.
- The deployment process for the overall system is straightforward.
- The system contributes to an increase in overall voting turnout.
- Manpower requirements are reduced.
- It lowers costs for voters who would otherwise need to travel to their native polling stations if residing elsewhere.

DISCUSSION

In the current Indian electoral process, several shortcomings persist, such as the necessity for voters to physically visit polling booths and the absence of voting acknowledgment. Much of the process still relies on manual operations, resulting in numerous challenges for voters. Therefore, this paper aims to address these issues by introducing a cloud based authentication mechanism for E-voting using registered mobile and Aadhar number. Despite the numerous advantages offered by this presented mechanism, certain dependencies exist. One major limitation is the requirement for high-speed internet connectivity for successful implementation. Lower internet speeds can impede the voting process and potentially frustrate voters, leading to disengagement from the voting process. Additionally, the system heavily relies on the use of smartphones or keypad phones for receiving OTPs to facilitate e-voting. Without access to such devices, voters would be unable to cast votes.

CONCLUSION

A cloud-based voting authentication system is introduced for e-voting to secure democracy leveraging both the Aadhar number and registered mobile number. It enables voters across India to cast their votes online, mitigating risks associated with proxy voting or double voting. By addressing the limitations of manual voting systems such as ropes, fraudulent votes, and voter authentication errors, the proposed mechanism ensures the integrity of the electoral process. Leveraging the uniqueness of Aadhar numbers, this system significantly reduces the likelihood of invalid votes, making it accessible even to illiterate individuals. Additionally, it enhances security by allowing each voter to cast only one vote, using a combination of unique identification and registered mobile numbers. The inclusion of a flag variable further prevents instances of dual or cross voting by the same individual, thus safeguarding against fraudulent practices common in manual voting systems. This system also enhances transparency in the vote count process and offers numerous benefits including economic efficiency, faster result tabulation, enhanced accessibility, heightened accuracy, and reduced risks of human as well as mechanical errors. To ensure the system's effectiveness, it is imperative to update the database with details such as age and biometrics prior to each election. Moreover, voters can receive information about their casted votes through messaging systems, enhancing transparency and accountability. By combining Aadhar numbers with registered mobile numbers, the system minimizes human errors and ensures reliability. Future endeavors aim to enhance user-friendliness, security and transparency by incorporating audio output features to cater to illiterate voters and use of blockchain technology.

REFERENCES

1. Pavan Yejare et al.,"IOT : A novel strategy for Biometric Voting system," International Journal of Electrical, Electronics and Computer Systems (IJEECS), 2017, Vol. 5, Issue 2, ISSN (Online): 2347-2820.
2. Channakeshava RN, "Distributed Voting System Using IOT," International Journal of Innovative Research in Computer and Communication Engineering, 2017, Vol.5, Special Issue 2.
3. Ms S. & Mr.Ashwin C., "Advanced Secure Voting System with IoT," International Journal Of Engineering And Computer Science, 2016.
4. Shubham J. Devgirikar j et al., "Advanced Electronic Voting Machine using Internet of Things (IOT)," 2nd National Conference Recent Innovations in Science and Engineering (NC-RISE17), 2017, Vol. 5, Issue 9, pp. 83-85, ISSN: 2321-8169.
5. Prof. Swati Gawhale et al., "IOT Based E-Voting System," International Journal for Research in Applied Science & Engineering Technology (IJRASET), 2017, Vol. 5 Issue 5, pp. 1064-1067, ISSN: 2321-9653.
6. Feras A. Haziemeh, Mutaz Kh. Khazaaleh And Khairall M. Al-Talafha ,"New applied e-Voting system," Journal of Theoretical and Applied Information Technology, 2011, Vol. 25, No. 2, pp. 88-97.
7. J. Deepika, S. Kalaiselvi, S. Mahalakshmi and S. A. Shifani, "Smart electronic voting system based on biometrie identification-survey," Third International Conference on Science Technology Engineering & Management (ICONSTEM), Chennai, 2017, pp. 939-942.
8. Miss. Nikalje Dipti et al., "Iot Based Advanced E-Voting System," International Journal for Research Trends and Innovation (IJRTI), 2019, Vol 4, Issue 4, ISSN: 2456-3315.
9. V. Sahaya Sakila, Debin Jose, Abhijith K P, Adith R Babu, "Secure Online E-voting Protocol Based on Voters Authentication," International Journal of Innovative Technology and Exploring Engineering (IJITEE), Volume 9, No. 1, November 2019, ISSN: 2278-3075.
10. Jagdish B. Chakole, P. R. Pardhi, "The Design of Web Based Secure Internet Voting System for Corporate Election," International Journal of Science and Research (IJSR), India, Volume 2, No. 7, July 2013, Online ISSN: 2319-7064.
11. John Kingsley Arthur et al., "A Secured Cloud-based E-voting System using Information Dispersal Algorithm", International Journal of Computer Applications (0975 – 8887), Volume 175, No.20, September 2020.

GENERAL GUIDELINES FOR PREPARING AND SUBMITTING PAPERS

First Author*, Second Author†
*Institution and Country of first author's affiliation
†Institution and Country of second author's affiliation

Abstract

It should consist of a concise summary of the material discussed in the article below. It is preferable not to use footnotes in the abstract or the title. The acknowledgement for funding organizations etc. is placed in a separate section at the end of the text.

Keywords

Maximum 3 keywords may be placed after the abstract.

Introduction

Provide a historical perspective regarding the subject of your paper.

Background

Provide broad definitions and discussions of the topic and incorporate views of others (literature review) into the discussion to support, refute or demonstrate your position on the topic.

Main Thrust of the Paper

Present your perspective on the issues, controversies, problems, etc., as they relate to theme and arguments supporting your position. Compare and contrast with what has been, or is currently being done as it relates to your specific topic and the main theme of the volume.

Future Trends

Discuss future and emerging trends. Provide insight about the future of the topic from the perspective of published research on the topic. If appropriate, suggest future research opportunities within the domain of the topic.

Conclusion

Provide discussion of the overall coverage of the topic in your manuscript and conclusion should include key findings of the paper & concluding remarks.

References

References should follow the conclusions. The references should be listed in numerical order with the corresponding number cited inside the printed manuscript within square brackets at appropriate places [1, 2].

For example:

1. Hake, Richard R. 1998. Interactive-engagement versus traditional methods. A six-thousand student survey of mechanics test data for introductory physics courses. American Journal of Physics 66(1): 64-74
2. Steif, Paul S., and Anna dollar, 2003. A new approach to teaching and learning statics. In Proceedings of the ASEE Annual Conference and Exposition. Nashville, TN

GENERAL GUIDELINES FOR PREPARING AND SUBMITTING PAPERS

Acknowledgement

The acknowledgement for funding organizations etc. should be placed in a separate section at the end of the text.

Biodata

Please include brief bio data of the author (s) within 300 words and also attached a scanned copy of the latest passport size colour photograph of author (s)

Style

Manuscript should be printed on A4 size good white paper. Papers must be typed in English using MS Word. Kindly follow the instructions given below for all the pages

Margins:	:	Top	1.2”
		Bottom	1.2”
		Left	1.2”
		Right	1.2”
Orientation:	:	Portrait	
Font	:	Arial / 12 pt	
Heading	:	14 point	
Sub Heading	:	13 pt	
Spacing	:	Single line spacing	
Para Indent	:	6 point	

Length of Paper

The length of manuscript should not exceed 15 pages, including, figures/ photographs and references. The minimum number of pages should be 7 pages

Figures

All figures should be captioned and printed / pasted in appropriate place of the paper. Caption for the figures should be printed below the figures and numbered consecutively throughout the text. Tables should be placed closest to the text of citation and the title of the table to be printed on top of the table.

All figures, tables, drawings, screen shots are to be sent in a separate file preferably in an editable form.

Submission of the full paper

The final paper(s) may kindly be submitted to at the following address by post or to email : **editor@isteonline.org**

The Editor
(Indian Journal of Technical Education)
Indian Society for Technical Education
IIT Campus, Shaheed Jeet Singh Marg,
Near Katwaria Saria, New Delhi - 110 016
Phone : +91-11-26963542,26963431

Subscription details:

For subscribing the IJTE kindly visit our website www.isteonline.in and download the necessary forms.

ABOUT THE JOURNAL

Periodicity : Quarterly **Subject :** Multidisciplinary

Indexed in the UGC-Care Journal list

The Indian Journal of Technical Education is published by the Indian Society for Technical Education on quarterly basis with the aim to provide an appropriate platform presenting well considered, meaningful, constructively thought provoking, non-political and non-controversial but critically analyzing and synthesizing present and future aspects of Technical Education System with particular reference to our country. The contributors are expected to highlight various issues of Technical Education (a broad outline of the journal objective is to promote the theory and practice of Engineering, Science & Technology, Management and Computer Applications) along with meaningful suggestions for solution, refinement and innovations.

The following guidelines must be carefully followed.

1. IJTE is a peer reviewed Journal.

2. Manuscripts submitted to the journal will be initially screened by the editors. Those considered inappropriate will be returned to the sender.

3. The Authors are fully responsible for the contributions.

4. The Authors should be the Life Member of ISTE, if not, while submitting the paper they can apply for the membership by clicking https://membership.isteonline.in

5. The Copyright clearance will be the sole responsibility of authors for their papers. Enough precaution should be taken to make the manuscript error free.

6. Upon acceptance of a paper, the author(s) will be requested to provide an electronic copy of the paper, compatible with Microsoft Word.

7. The selection of papers for publication will be based on their relevance, clarity, topicality and originality.

8. The manuscript should be submitted and author's details should be mentioned in the beginning. The author should not be identified anywhere else in the article. The authors details should include full name, affiliation, e-mail address etc.

9. **Manuscripts should not exceed 7 pages A-4 size with fonts size 11 points in Times New Roman only with one and half line space in MS Word format.** .

10. Submit an abstract of about 200 words. The articles should be in clear, coherent and concise English language. Author/s should upload manuscript in MS-Word,

11. Tables should be numbered and referred to in the text as Table 1, Table 2, etc. Tables should not duplicate results in graphs. The minimum amount of descriptive text should be used on graphs and drawings (label curves, points, etc. with single letter symbols). The tables and figures should be clearly visible, readable and monochromatic in nature. Avoid inserting pictures of tables and figures in the manuscript.

12. In view of the large responses from Technical Education fraternity and limited space available in the Journal, the publication may take usually 3 months to 6 months from the date of receipt of the manuscript subject to approval by the reviewers.

13. All contributors are requested to please co-operate by observing the above mentioned Guidelines strictly while sending the paper for publication in the Indian Journal of Technical Education.

Note : Articles will be selected by the Editorial Board and are subject to editorial modification, if necessary

Volume 47 • No 3 • July-September 2024
Periodicity: Quarterly • Subject: Multidiciplinary

ISSN 0971-3034

PUBLISHED BY
INDIAN SOCIETY FOR TECHNICAL EDUCATION
Near Katwaria Sarai, Shaheed Jeet Singh Marg,
New Delhi - 110 016

Printed at: Compuprint, Flat C, Aristo, 9, Second Street, Gopalapuram, Chennai 600 086.
Phone : +91 44 2811 6768 • www.compuprint.in